1 September 2006 | $10

Science

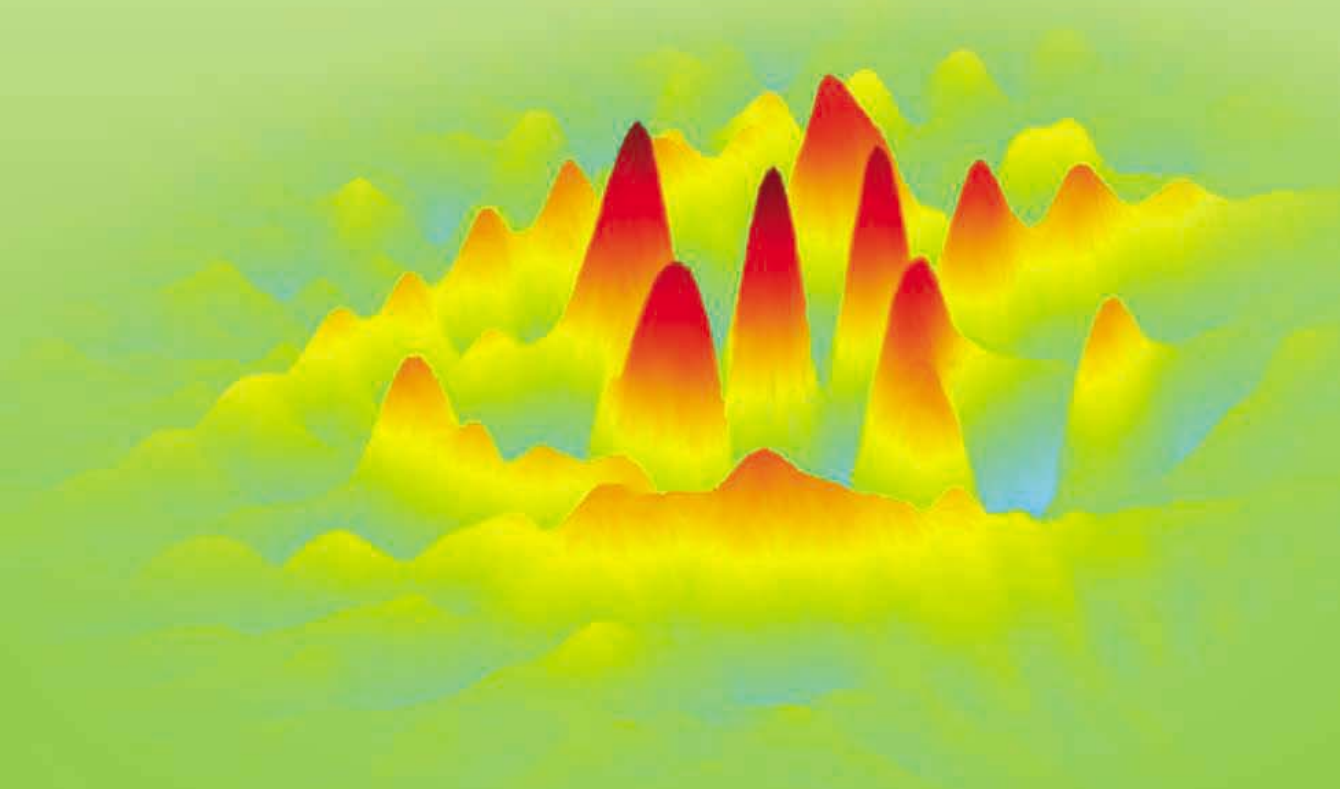

AAAS

Volume 313, Issue 5791

COVER

Three-dimensional Wigner plot (where *x* is time, *y* is wavelength, and *z* is amplitude of the electrical field) of the specific laser pulse found to enhance the photoisomerization quantum yield of retinal in bacteriorhodopsin in the weak excitation limit. The complex periodic pattern induces coherent nuclear motions that are specific to the isomerization reaction. See page 1257.

***Image:* Helena V. Prokhorenko**

DEPARTMENTS

EDITORIAL

NEWS OF THE WEEK

NEWS FOCUS

LETTERS

BOOKS *ET AL.*

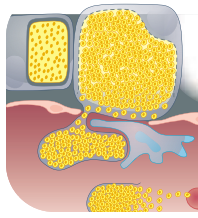

1245 & 1287

POLICY FORUM

PERSPECTIVES

CONTENTS continued **>>**

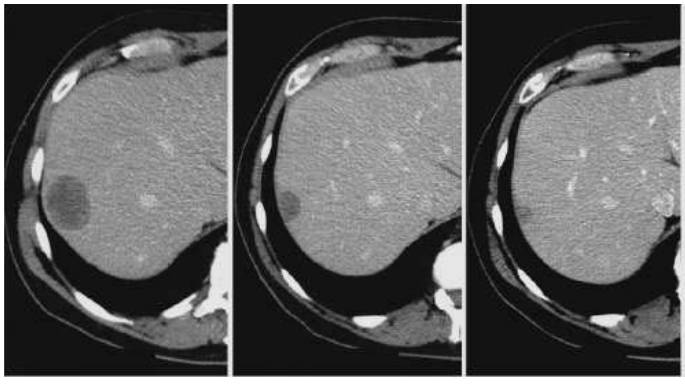

SCIENCE EXPRESS

www.sciencexpress.org

MEDICINE

Cancer Regression in Patients After Transfer of Genetically Engineered Lymphocytes
R. A. Morgan et al.
Immune cells of cancer patients are induced to carry genes that help destroy tumors.
10.1126/science.1129003

ATMOSPHERIC SCIENCE

Solid Ammonium Sulfate Aerosols as Ice Nuclei: A Pathway for Cirrus Cloud Formation
J. P. D. Abbatt, S. Benz, D. J. Cziczo, Z. Kanji, U. Lohmann, O. Möhler
Solid ammonium sulfate can form ice particles in cirrus clouds through heterogeneous processes not previously suspected.
10.1126/science.1129726

GENETICS

Global Genetic Change Tracks Global Climate Warming in *Drosophila subobscura*
J. Balanyá, J. M. Oller, R. B. Huey, G. W. Gilchrist, L. Serra
On three continents, a low-latitude, natural genetic variant of the fruit fly is increasingly found at higher latitudes, paralleling climate warming over the past 25 years.
10.1126/science.1131002

CHEMISTRY

Irreversible Organic Crystalline Chemistry Monitored in Real Time
P. R. Poulin and K. A. Nelson
A single-femtosecond laser pulse, rather than the usual destructive multiple pulses, yields the dissociation dynamics of delicate molecules such as crystalline I_3^- over time.
10.1126/science.1127826

PERSPECTIVE: A Pixellated Window on Chemistry in Solids
V. A. Apkarian
10.1126/science.1133024

TECHNICAL COMMENT ABSTRACTS

BREVIA

RESEARCH ARTICLES

REPORTS

CONTENTS continued **>>**

Science

REPORTS *CONTINUED...*

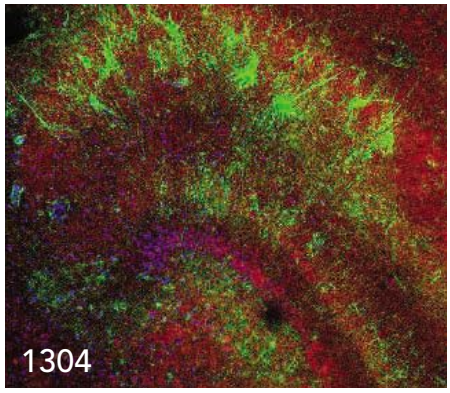

AAAS
ADVANCING SCIENCE, SERVING SOCIETY

SCIENCE (ISSN 0036-8075) is published weekly on Friday, except the last week in December, by the American Association for the Advancement of Science, 1200 New York Avenue, NW, Washington, DC 20005. Periodicals Mail postage (publication No. 484460) paid at Washington, DC, and additional mailing offices. Domestic individual membership and subscription (51 issues): $139 ($74 allocated to subscription). Domestic institutional subscription (51 issues): $650; Foreign postage extra: Mexico, Caribbean (surface mail) $55; other countries (air assist delivery) $85. First class, airmail, student, and emeritus rates on request. Canadian rates with GST available upon request, GST #1254 88122. Publications Mail Agreement Number 1069624. **Printed in the U.S.A.**

Change of address: Allow 4 weeks, giving old and new addresses and 8-digit account number. **Postmaster:** Send change of address to AAAS, P.O. Box 96178, Washington, DC 20090–6178. **Single-copy sales:** $10.00 current issue, $15.00 back issue prepaid includes surface postage; bulk rates on request. The identification code for *Science* is 0036-8075. *Science* is indexed in the *Reader's Guide to Periodical Literature* and in several specialized indexes.

CONTENTS continued **>>**

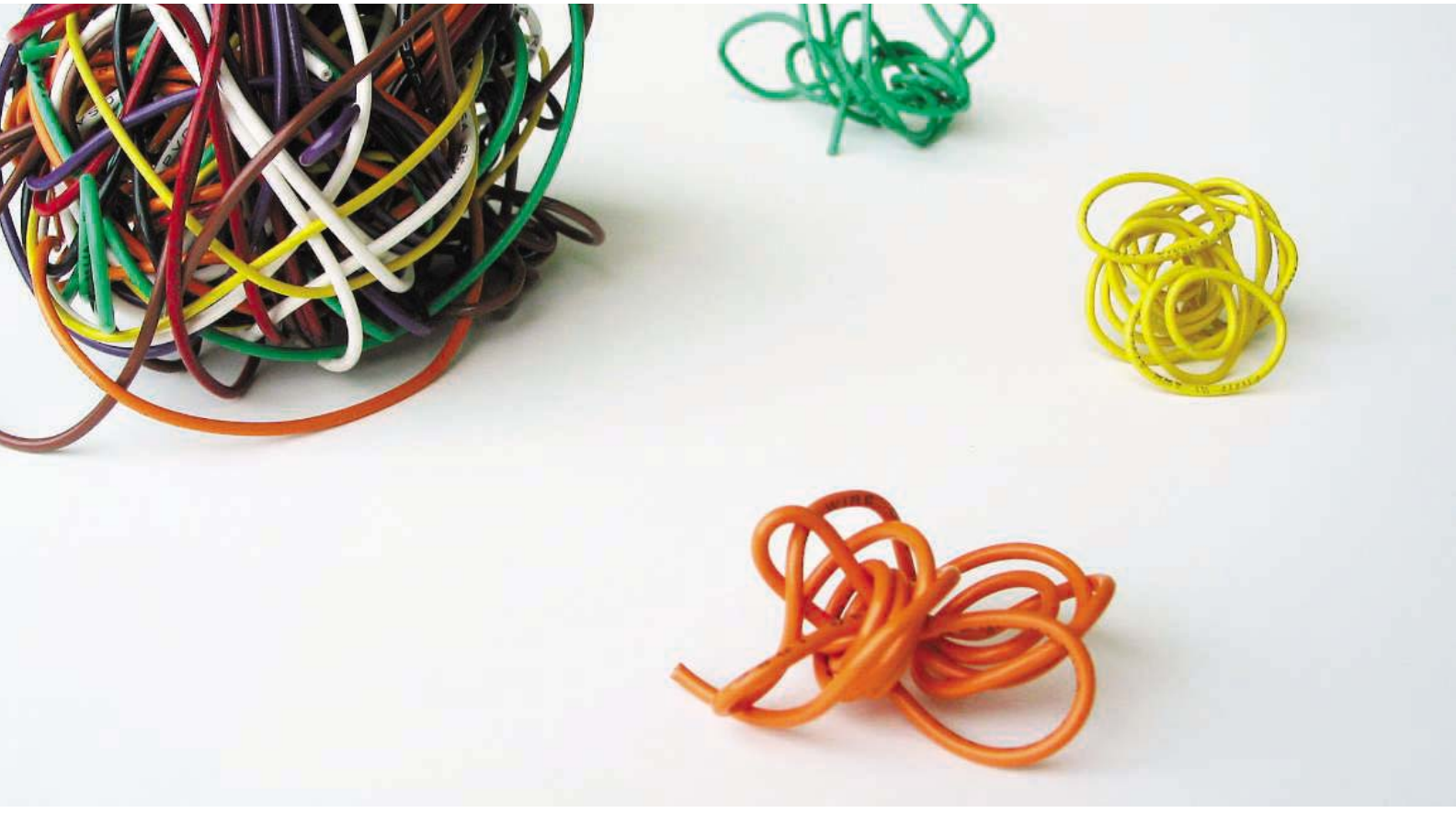

Fractionation made simple.

Reduce the complexity of your protein sample with the MicroRotofor™ system.

Fractionation is an essential step for increasing protein resolution in proteomics workflows. By fractionating, you reduce your sample complexity and enrich low-abundance proteins, both of which are central to biomarker discovery. Bio-Rad offers the MicroRotofor system for fractionation of proteins prior to most downstream proteomics applications, including 2-D gel electrophoresis and LC-MS/MS analysis.

The MicroRotofor system

The MicroRotofor system:

- Handles small volumes (~2.5 ml) of precious samples
- Is compact and easy to use
- Separates proteins by liquid-phase isoelectric focusing
- Fractionates complex protein mixtures under native and denaturing conditions
- Offers customizable pH gradients to further enhance resolution of proteins of interest

For more information, visit us on the Web at **www.bio-rad.com/microrotofor/**

Visit us on the Web at **discover.bio-rad.com**
Call toll free at 1-800-4BIORAD (1-800-424-6723);
outside the US, contact your local sales office.

BIO-RAD

SCIENCE**NOW**

www.sciencenow.org DAILY NEWS COVERAGE

Marine Methane Heats Things Up
Undersea deposits of greenhouse gas may have played larger role in global warming than thought.

City Rat, Country Rat
Researchers solve mystery of why leptospirosis is more widespread—and deadly—in urban areas.

Take a Load Off
Treatment that relieves stress in cellular organelle reverses type 2 diabetes in mice.

SCIENCE**PODCAST**

Listen to the 1 September *Science* Podcast to hear about reducing the racial achievement gap, the science of the Web, maintaining freshwater resources, and more.
www.sciencemag.org/about/podcast.dtl

Hanging in as a scientist and mom.

SCIENCE **CAREERS**

www.sciencecareers.org CAREER RESOURCES FOR SCIENTISTS

GLOBAL: Canopy Meg—A Case Study of a Mom-Scientist
I. Levine
Biologist Margaret Lowman is a single mom who involves her two sons in her career.

US: Postdoc Unionization Drive Reaches a Climax in California
B. Benderly
Pro- and anti-union sides exchange accusations of unfairness in California's labor dispute.

GLOBAL: Reversing the Brain Drain
J. Kling
Foreign governments and United States funding organizations build research expertise in foreign countries.

GRANTSNET: September 2006 Funding News
J. Fernandez
Learn about the latest research funding, scholarships, fellowships, and internships.

Back to school.

SCIENCE'S **STKE**

www.stke.org SIGNAL TRANSDUCTION KNOWLEDGE ENVIRONMENT

TEACHING RESOURCE: Assessing Undergraduate Laboratory Performance
E. M. Adler and N. R. Gough
Teach students how to effectively collect and present scientific information.

TEACHING RESOURCE: Differentiation of PC12 Cells
E. M. Adler, N. R. Gough, J. A. Blundon
Students will explore the signaling pathways that lead to neuronal differentiation of a cultured cell line.

FORUM: Teaching Cell Signaling
Share experiences and tips with others who teach lectures and courses in cell signaling.

Separate individual or institutional subscriptions to these products may be required for full-text access.

What if staying up to date with the latest technology published in journals and patents were as easy as pushing a button?

It is.

With the "Keep Me Posted" alerting feature, SciFinder sends you automatic updates on areas you—and your competitors—are interested in.

You can monitor specific research topics, companies, authors, substances, or sequences, and choose how frequently you receive notifications: daily, monthly, or weekly.

The service isn't just convenient, it's incredibly current. Journal article records often appear in SciFinder before they're even in print. New references, substances, and sequences are added daily. Patents from all the major offices are added within two days of issuance.

As with all SciFinder features, Keep Me Posted is integrated with your workflow. At any point in a search (including the beginning), simply click on the Keep Me Posted button. SciFinder tracks your steps and will generate the appropriate alert—even for complex topics. When you receive a notification, you can follow each reference as you would in a search: find citing or cited articles (with links to the electronic full text), and follow referenced substances and reactions for further information.

Comprehensive, intuitive, seamless—SciFinder doesn't just alert you, it's part of the process. To find out more, call us at 800-753-4227 (North America) or 614-447-3700 (worldwide) or visit www.cas.org/SCIFINDER.

SciFinder®

Part of the process.™

EDITED BY STELLA HURTLEY AND PHIL SZUROMI

Corridor Confirmation

Although "corridors" connecting patches of habitat are proposed to be beneficial in terms of preserving biodiversity, this theory has never been tested experimentally at large scales. Using replicated experimental 50-hectare landscapes consisting of open patches in longleaf pine forest connected by similarly open corridors, **Damschen *et al.*** (p. 1284) show that corridors increase the species richness of herbaceous plants. These findings confirm the validity of corridors as a tool for conservation and landscape managers.

Steering Retinal

Because of the wave-particle duality inherent in quantum mechanics, different states along the pathway of a molecular rearrangement can interfere with each other like vibrations on a string. The phases and amplitudes of spectral components in light pulses that initiate photochemical reactions can now be created that can steer small molecules along distinct reaction trajectories by inducing constructive or destructive wave interference among states. **Prokhorenko *et al.*** (p. 1257; see the Perspective by **Chergui**) show that this approach can modulate the efficiency of retinal isomerization in the protein bacteriorhodopsin (a rearrangement closely related to the vision response) by as much as 20% in either direction. The extent of modulation is remarkable in light of the many degrees of freedom in the protein environment that might be expected to randomize the wave phases.

P_2 Gently Generated

Although elemental nitrogen and oxygen are most stable as diatomic molecules, their heavier congeners, such as phosphorus and sulfur, are inhibited from multiple bonding by core electron repulsion, and so tend to exist as polyatomic clusters instead. **Piro *et al.*** (p. 1276) have prepared a niobium precursor that releases P_2 at 65°C, and thereby facilitates exploration of the solution-phase chemistry of this unusual molecule, which is otherwise only accessible through decomposition of the P_4 cluster above 1000°C. The authors show that P_2 can be trapped by successive Diels-Alder coupling to two cyclohexadiene molecules, which is consistent with the presence of a reactive triple bond.

Snapshots of Working Catalysts

Vanadium phosphates (VPOs) are used industrially to catalyze the partial oxidation of *n*-butane to maleic anhydride, which is then used as a starting material for products such as resins and lubricants. However, the reaction proceeds at elevated temperatures (in excess of 400°C), and VPO phases stable under those conditions will transform to other phases at ambient conditions, so an understanding of this catalyst demands that it be studied near its working conditions. **Conte *et al.*** (p. 1270) have used powder x-ray diffraction, as well as laser Raman spectroscopy and electron paramagnetic resonance spectroscopy, to determine the transformation of VPO phases as a function of temperature and with various reactants and products present over the catalyst. They conclude that the presence of the reactants rapidly converts ω-$VOPO_4$ to δ-$VOPO_4$, but that the initial formation of the ω phase may create the V^{5+} sites associated with increased catalytic activity.

Tiny Fluorous Flasks

Fluorocarbons have been increasingly applied as media for chemical reactions and separations because their solubilizing properties are distinct from those of both water and traditional organic solvents. **Sato *et al.*** (p. 1273; see the Perspective by **Gladysz**) have created a nanometer-scale fluorous environment within a polar organic solvent. Arrow-shaped ligands with perfluoroalkyl tails self-assemble with palladium ions in dimethyl sulfoxide to form a shell in which the fluorinated chains are directed inward toward the center. By varying the lengths of these chains, the shell size could be tuned to encapsulate a liquid-like, disordered phase of ~2 to ~6 perfluorooctane molecules, which were characterized spectroscopically and crystallographically.

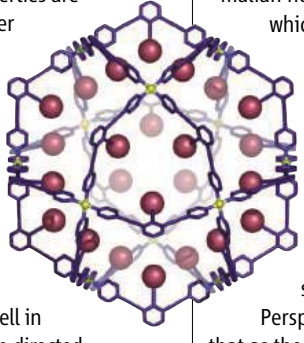

Round the Bend

The Hawaiian Islands chain of volcanoes sits within a long line of seamounts stretching 6000 km across the Pacific. The Hawaiian volcanoes had been considered to be produced by the relative motion of the Pacific plate over a southward drifting locus of melting in the mantle. About 3500 kilometers west of Kilauea, there is a sharp bend in the chain. **Sharp and Clague** (p. 1281; see the Perspective by **Stock**) inferred a time line for the formation of the Hawaiian-Emperor seamount chain by measuring $^{40}Ar/^{39}Ar$ ages for eight volcanoes. They give an average age for the bend of about 50 ± 1 Ma, older than previous estimates. The ages, increasing to the north, imply that rates of migration have varied considerably. These results imply the plate motion must have changed at this time, which coincides with the development of subduction zones around the Pacific plate boundary.

Direct Delivery

The life cycle of the malaria parasite in its mammalian host begins with a liver-specific stage, in which sporozoites delivered by the mosquito invade hepatocytes, where they develop into merozoites that invade red blood cells. Merozoites must enter the bloodstream, although precisely how they move from hepatocyte to the lumen of the liver sinusoid has remained a matter of speculation. In a study of a rodent form of the parasite, **Sturm *et al.*** (p. 1287; see the Perspective by **Cowman and Kappe**) reveal that as the merozoites induce death of the hepatocyte, they simultaneously hold in check the normal cues that would signal phagocytosis of the dying cell. This alteration allows membrane-bound extensions of the infected cells, which the authors term merosomes, to bud off and shuttle the merozoites directly into the bloodstream. Thus, the parasites modify the host response to dying infected cells to ensure better survival and replication.

Continued on page 1199

CREDITS (TOP TO BOTTOM): ELLEN DAMSCHEN AND THE U.S. FOREST SERVICE; SATO *ET AL.*

Fastest Sample Prep System
FastPrep®-24

Lyse Any Tough Tissue or Cells in 40 Seconds or Less!

- ***> 24 samples homogenized simultaneously***
- ***> Lyse efficiently:***

  plants, seeds, gram+ bacteria, spores, bones, animal tissue, swabs, soil, feces, forensic samples, etc...
- ***> Preserves integrity of DNA, RNA and proteins***
- ***> Removable sample holder***
- ***> Easy to clean/decontaminate***

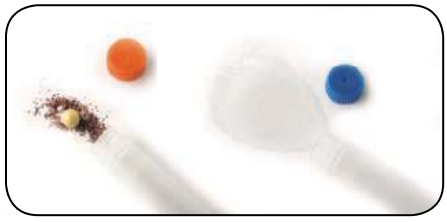

Optimized Lysing Matrix and Complete Extraction Kits for All Your Needs

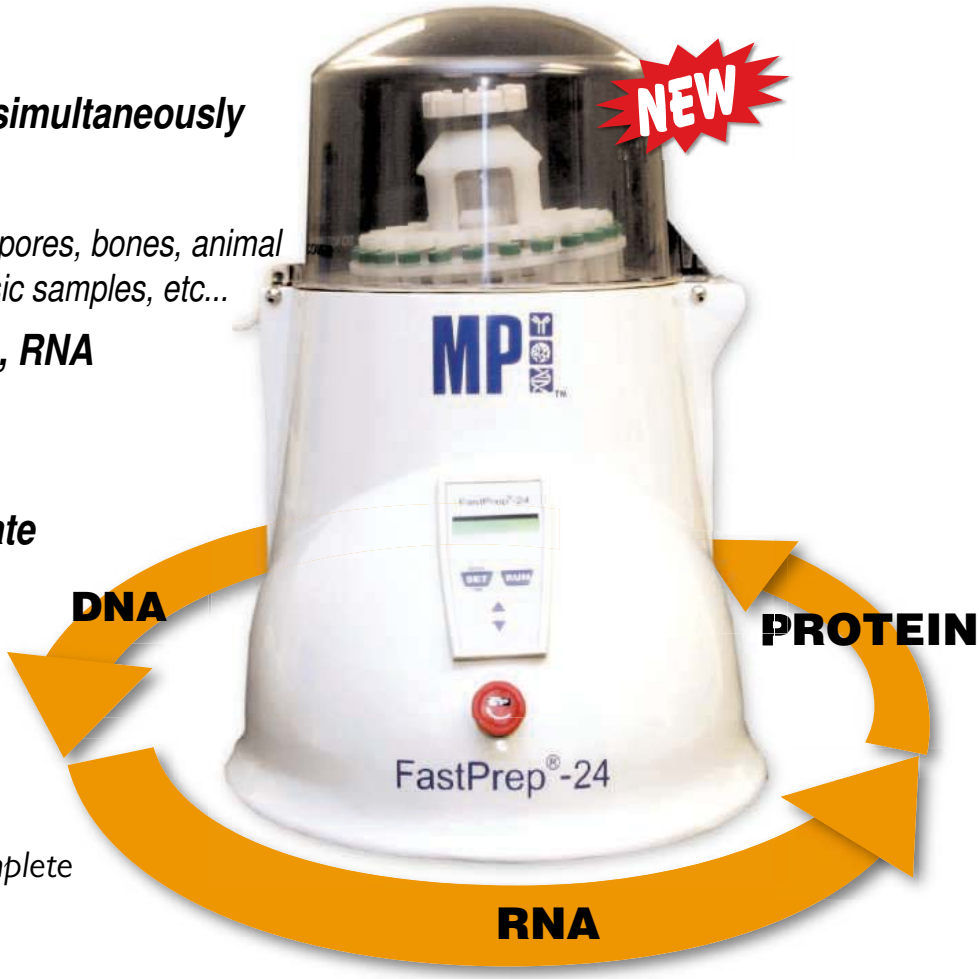

The newest generation of the proven Bio101® FastPrep System, 5000+ users worldwide

Order the FastPrep® - 24 by October 31st and receive a **FREE** FastPrep® kit of your choice!
Request a trial today! Product number - 6002500!
Use promo code FPSCI2006

www.mpbio.com

MP Biomedicals • 29525 Fountain Parkway • Solon, OH 44139 • tel: **1.800.854.0530** • fax: 1.800.334.6999

MP™

Q·BIOgene
An MP company

Continued from page 1197

A Tale of Two Spirals

A facile route to crystal growth is for atoms to attach to a surface at a screw dislocation. **Hannon *et al.*** (p. 1266; see the Perspective by **Voorhees**) studied atomic growth of two silicon surfaces, the (111) and (001) faces, at 1100°C with low-energy electron microscopy. On the (111) surface, growth proceeded smoothly with a spiral pattern, in accord with the classic model. However, on the (001) surface, growth occurred along a spiral with an S-shaped undulating profile, and the step edges rotated with an almost ratchet-like motion. The origin of this difference is attributed to the nonuniform strain field created by the two possible surface terminations of the (001) surface, and the growth profiles were analyzed in detail with a continuum step model.

Out of the Shadows

Phytophthora species are oömycetes and belong to the kingdom Stramenopila, which is evolutionarily distant from plants, animals, and fungi. Importantly, nonphotosynthetic stramenopiles, including the oömycetes, are believed to have lost their plastids at some point in evolution. The two *Phytophthora* genome sequences presented by **Tyler *et al.*** (p. 1261) provide compelling evidence that their ancestor indeed harbored a photosynthetic endosymbiont. The genomes also show a striking diversification of infection-associated genes, which consists of about 350 genes in each genome and reflects intense coevolutionary processes occurring between these parasitic species and their hosts.

Genetic Measures of Human Evolutionary Proximity

Gene sequences that show a pronounced human lineage–specific increase in copy number and that also encode multiple copies of a domain of unknown function (DUF1220) have been identified by **Popesco *et al.*** (p. 1304). These domains show significant hyperamplification in the human lineage and generally increase in copy number as a function of a primate species' evolutionary proximity to humans. Antibody studies indicated that DUF1220 sequences are abundantly expressed in structures of the neocortex and in particular subsets of neurons. These sequences might be important to cognitive pathways and synaptic function.

An Ounce of Prevention

Members of groups subject to stereotyping are more likely to behave in a fashion that conforms to the stereotype when the stereotype is made salient; for instance, women score lower than men on tests when the tests are identified as math as opposed to problem-solving. **Cohen *et al.*** (p. 1307; see the Perspective by **Wilson**) report the results of two field studies in which a brief, value-affirmation intervention at the beginning of the school year appeared to buffer the effects of a stereotype threat on 7th-grade African Americans such that they maintained their achievement levels (as did European American students) throughout the remainder of the school year, in comparison to African American students in the control condition.

Brain Regions and Social Organization

There is general agreement that humans can represent the mental states of others (theory of mind), and the current consensus appears to be that we are unique in this respect. Nevertheless, other animals have been shown to possess some aspects of social intellect, but precisely who knows what is unclear. **Rudebeck *et al.*** (p. 1310) have carried out a lesion study in monkeys to examine the differential contributions of two neighboring cortical areas, the anterior cingulate and the orbitofrontal region. They find that the gyrus of the anterior cingulate is needed in order to orient toward a specifically social stimulus, such as the face of another monkey, in contrast to other potent stimuli, such as a moving snake, which are processing in the orbitofrontal cortex.

CREDIT: ALEX MOLNAR/AGRICULTURE AND AGRI-FOOD CANADA

Bibliographies made tra easy.

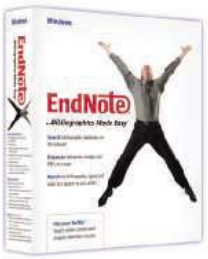

For over two decades, EndNote® has been the industry standard software tool for creating and managing bibliographies. With EndNote X, we're creating a new standard for ease-of-use. And that has students, researchers, writers and librarians jumping for joy.

Expanded PDF management lets you drag and drop PDF files for auto-linking and storage. An enhanced reference list display lets you see more information. More options make it easier to search EndNote libraries. And increased flexibility gives you more ways to enter and edit references—and create bibliographies in over 2,300 publishing styles.

EndNote X is compatible with Microsoft® Word for Windows® and Mac® OS X, and EndNote libraries can easily be shared across platforms. That makes it not only Xtra easy to use, but also Xtra easy to work with throughout your organization—and all over the world.

Download your Free demo or buy online today. www.endnote.com

EndNote®
...Bibliographies Made Easy™

THOMSON™

800-722-1227 • 760-438-5526
rs.info@thomson.com

Discover RefViz®
Search online content and analyze references visually

Iwao Matsuda is the Minister of State for Science and Technology Policy of Japan.

Boosting S&T Innovation in Japan

JAPAN'S ECONOMY IS FINALLY EMERGING FROM A LOST DECADE. ECONOMIC DATA CONTINUE to suggest that the recovery this time around is real. But before celebrating, Japan's policy-makers must recognize that the key to Japan's future lies in science and technology (S&T) and do some serious rethinking of our economic strategy.

Fortunately, the importance of S&T has not escaped the attention of policy-makers in Japan. Even during the stagnated economic growth of the 1990s, and despite severe general government spending cuts, the rate of government investment in S&T has consistently increased. But because the need to raise productivity is paramount, we will require more major breakthroughs in S&T than we have accomplished at any other time in our history. How will we achieve that? The Third Basic Science and Technology Plan, approved by the Cabinet this past March, lays out government policy guidelines for the next 5 years and projects a total budget of some 25 trillion yen for S&T investment during that time. This is a clear indication that Japan is committed to pursuing future excellence in S&T. As the minister presiding over that decision, I think this course is the correct one for Japan and for our future generations.

So everything is peachy, right? Well, not quite. It is true that Japan's persistent investment efforts have begun to bear fruit. The recent economic recovery has been supported by such science-based innovations as electrically conductive plastic, now widely used in high-tech equipment such as mobile phones. But there are challenges that Japan faces, including the country's declining birth rate and aging population, and we will require much more of this kind of success. The key word is innovation. In both private and public sectors, we should ask ourselves whether Japan's traditional self-contained approach, endemic in many research institutions, has tended to suppress the flourishing of new ideas. Improving the mobility of researchers will create many more opportunities for them to explore new ideas and projects. In the private sector, venture businesses must be encouraged.

It is often asserted that innovation is hard to achieve unless it is supported by strong basic science. More and more, universities play a central role as the primary source of innovation. Many of the universities in Japan are national and have recently been made into corporate entities. But reforming higher education is still a work in progress. One major challenge is to eliminate such rigidities as seniority-based pay for researchers. To accelerate this change, the Third Basic Plan intends to create 30 world-class research centers and actively attract the best researchers from all over the world. The centers will have budgetary priority and a merit system with attractive pay packages. And a targeted reform of immigration control will facilitate the entry of foreign researchers into Japan and will also support them.

We also need structural reform in government processes. To clarify investment priorities and policy goals, we have worked hard to identify targets in each of eight S&T areas for the next 5 years. Under this framework, the Council for Science and Technology Policy (CSTP), chaired by the prime minister, should strengthen the coordination of various ministries toward policy goals. In addition to setting priorities for S&T resource allocation, the CSTP will address the need for regulatory and institutional reform. For example, current regulations regarding clinical research should be thoroughly reviewed and reformed, so that research can be carried out more transparently, with measures to protect participants in clinical tests. Another example is the reform of government procurement to expand new technology products and services.

If this new innovation-friendly strategy is successful, I am certain that the international scientific community will witness the beginning of a new growth era for Japan in the 21st century. My concluding message to that community is both enthusiastic and direct: "Researchers of the world, come to Japan to work with us. We will wholeheartedly welcome you!"

– Iwao Matsuda

10.1126/science.1133128

Introducing Rosetta Elucidator® system. It's a flexible, scalable solution for managing and analyzing large volumes of proteomics data. Powerful and reliable algorithms enable differential protein expression analysis so you can identify and validate potential biomarkers during drug development. Industry-leading tools manage terabytes of data and workflows improve productivity and focus research efforts. The result is an integrated bioinformatics platform that helps you optimize your organization's drug discovery and development process.

Find what you're looking for today.
Go to WWW.ROSETTABIO.COM/ELUCIDATOR for more details.

ROSETTA
BIOSOFTWARE

Trying to stay warm.

PHYSIOLOGY

Pigs in Blankets

Human infants, like other newborn animals and hibernating rodents, are endowed with a built-in central heating system: Mitochondrial proton gradients are uncoupled from ATP production in brown adipose tissue, so chemical energy is converted directly into heat, which protects against the vicissitudes of an uncertain environment. Uncoupling protein 1 (UCP1), which is present only in brown adipose tissue, is critical for thermogenesis. Piglets, though, are unusual in this regard, as they lack this kind of fat and rely instead on shivering as a way to stay warm.

Berg *et al.* looked for and, surprisingly, found *UCP1* sequences in preliminary pig genome data. But closer examination revealed that the gene is peppered with small errors and is missing exons 3 to 5, a deletion that they also found in other species of pig, wild boar, and hog, and that almost certainly renders the gene useless. The pig *UCP1* sequences have randomly drifted away from those of other closely related animals, further evidence that the gene is nonfunctional and that this drift has been going on for some 20 million years, implying that the gene has been out of commission for the same period. Many pig species hail from relatively balmy environments, where such a heat-generating system would not have been needed for survival. Not so for the wild boar, which thrives in colder climes, partly because of the evolution of a nest-building behavior that compensates for the ancient loss of *UCP1* and brown adipose tissue. — GR

PLoS Genet. **2**, e129 (2006).

MICROBIOLOGY

Pleiotropic Tensegrity

Systems biology has popularized the view of metabolic and regulatory pathways as networks, and experimental and bioinformatics studies of protein-protein interactions have codified these networks as centralized hubs and radiating spokes. One somewhat deceptive implication inherent in these representations is the static character of these linkages.

Knight *et al.* provide a comprehensive proteomic analysis of *Pseudomonas fluorescens* SBW25, where spontaneous adaptive mutations in the *wspF* gene result in the ability to grow at the air/liquid interface (as opposed to within broth). Although the genetic difference between the parental SM (smooth morphology) and evolved LSWS (Large Spreading Wrinkly Spreader) strains corresponds to the replacement of a serine with an arginine in a single component of the Wsp chemotaxis pathway, there are significant differences in the amounts of 46 proteins (identified by mass spectrometry and recourse to the draft genome), primarily with functions in amino acid uptake and catabolism. Mapping the variation in the amounts of these proteins across independent replicate cultures revealed that the LSWS strain, in comparison to the original SM strain, exhibits a distinct network of covariation. These distributed, yet coordinated, changes in protein levels suggest that understanding network dynamics will be key to explaining pleiotropy. — GJC

Nat. Genet. **38**, 10.1038/ng1867 (2006).

GEOPHYSICS

The Big Dig

By analyzing aerial photographs of the M_w 7.6 Kashmir earthquake that struck northern Pakistan on 8 October 2005, Avouac *et al.* show that, unusually for this area, the rupture broke through to the surface. Displacements are evident in ASTER images of the region taken just weeks after the event when these are compared to images of the same area from 5 years earlier. The surface rupture was confined to a strip a few hundred meters wide. Horizontal slip along the fault measured ~4 m on average, but offsets as large as 7 m were seen north of Muzaffarabad. Because the earthquake was shallow and compact, it caused intense but localized destruction. This pronounced movement along the fault suggests that adjacent regions may be soon be prone to large earthquakes. — JB

Tracing the fault.

Earth Planet. Sci. Lett. 10.1016/j.epsl.2006.06.025 (2006).

MICROBIOLOGY

More A's than B's

In contrast to eukaryotes and bacteria, archaea have only recently become the objects of study, and then primarily as hardy denizens of extreme environments, such as hot springs or acid mines. However, as analytical techniques for detecting trace amounts of archaeal components in unpurified samples have been refined and more widely applied, evidence has been accumulating that these species are likely to participate in biogeochemical cycles that affect all spheres of life.

Wuchter *et al.* and Leininger *et al.* have looked at the archaea-based oxidation of ammonia in North Sea waters and in northern European soil, respectively. They have measured the amounts of the gene encoding ammonia monooxygenase, the first enzyme in the nitrification pathway, and correlated these data with the presence of Crenarchaeota-specific lipids. Quantitation of ammonia monooxygenase genes in the upper 1000 m of the North Atlantic and across pristine and fertilized soils revealed that the archaeal version was generally several orders of magnitude more abundant than the bacterial enzyme. Incubation of the marine sample and estimates of the rates of Crenarchaea growth and production of nitrite yielded an oxidation flux of about 3 fmol of

Continued on page 1205

Success is based on knowledge, not chance

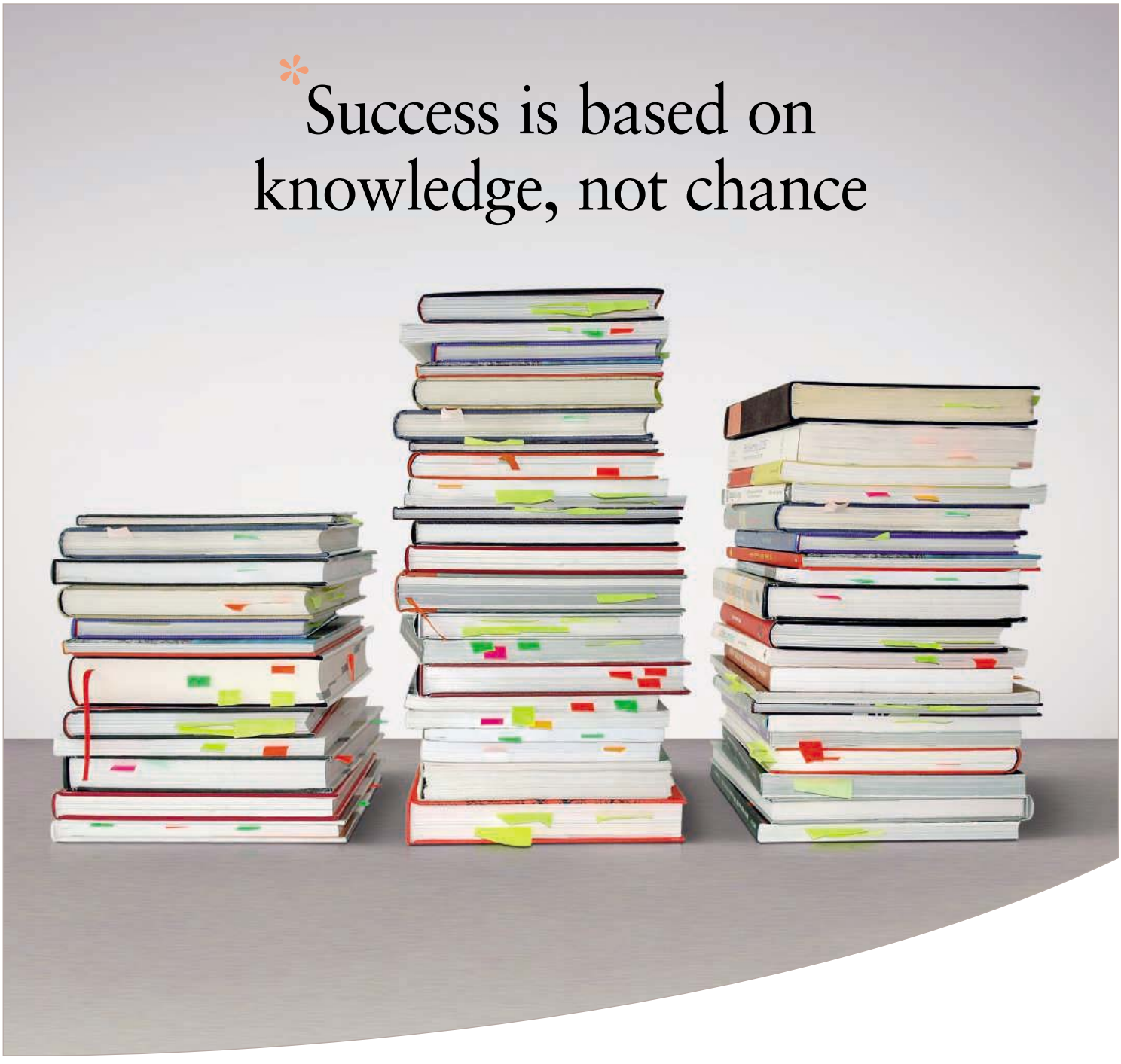

A system for success

Making the right decision at the right time is the key to success, from basic research through drug discovery and development, to manufacturing and QC.

More than 15 years of knowledge and experience in protein interaction analysis support every Biacore® system. Whatever your field, highest quality, information-rich data will enable you to make critical decisions with confidence.

Select the perfect system for your application requirements – from the company that sets the standards for label-free protein interaction analysis.

Define · Decide

BIACORE

www.biacore.com

Continued from page 1203

NH_3 per cell per day, which could be extrapolated to a global inorganic carbon fixation rate of 4 x 10^{13} mol of C per year. — GJC

Proc. Natl. Acad. Sci. U.S.A. 103, 12317 (2006); *Nat.* **442**, 806 (2006).

MATERIALS SCIENCE

Mining for Crystals

Predicting the crystal structure of an alloy is challenging, because even small changes in composition can lead to large changes in the way the atoms prefer to coordinate. Fischer *et al.* have developed a technique that mines the existing crystal database to determine top candidate structures, which are then evaluated using quantum mechanical calculations. The model determines correlations for structural motifs that jointly appear in a single alloy system at different compositions, and thereby assigns probabilities to candidate structures, given those already known in the system. In one test, the authors considered the Ag-Mg alloy with 75% Mg content, for which the exact crystal structure is undetermined. The top candidate highlighted by their model was the $Cu_{2.82}P$ structure, an uncommon motif that nonetheless was computed to have the lowest ground-state energy.

They also tested the model by selectively removing specific compositions from the database to see if the remaining data could be successfully used to predict the correct structures; this approach succeeded 90% of the time in placing the true missing structure among the top five candidates. — MSL

Nat. Mater. **5**, 641 (2006).

CHEMISTRY

Microscale Origami

Recent advances in lithography and other surface-patterning techniques have fostered construction of a wide range of microfluidic devices that offer precise control over chemical and biochemical reactions and separations at or below microliter volume scales. However, one limitation of this fabrication technology is its inherent restriction to two-dimensional device geometries.

Leong *et al.* overcome this limitation by patterning flat wafers with solder deposited along hinge lines. When heat is applied to melt the solder, the wafers fold spontaneously along the hinges to form cubic or pyramidal boxes, with volumes ranging from ~0.2 to 8 nl. The authors use photolithography to imprint distinct pore arrangements into the surfaces set to become the box faces. As a result, they can inject chemical reagents embedded in polymeric gels and control the rate and orientation of their release. The fabrication process is high-yielding, and when nickel is used as the substrate, the corresponding box can be manipulated with an external magnet to release its chemical cargo in a spatially selective manner. — JSY

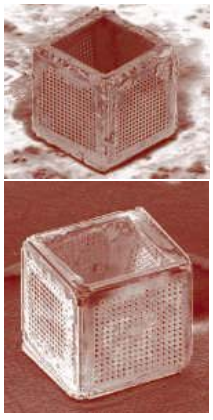

Nanoliter boxes.

J. Am. Chem. Soc. **128**, 10.1021/ja063100z (2006).

<< Waking Stem Cells

Hematopoietic stem cells (HSCs) reside in bone marrow in a nondividing state from which they can be roused to enter the cell cycle. Noting the similarity of HSC dormancy to mammalian hibernation and *Caenorhabditis elegans* dauer formation, Yamazaki *et al*. looked at the PI3K (phosphatidylinositol 3-kinase)–Akt–FOXO signaling pathway. In quiescent cells freshly isolated from mouse bone marrow, no phosphorylated (activated) Akt was apparent and its downstream target FOXO3a was found in the nucleus; in contrast, phosphorylated Akt and FOXO3a were found in the cytoplasm of cycling progenitor cells. Cytokine treatment of quiescent cells led to polarization of the lipid raft marker GM1 ganglioside as well as phosphorylation of Akt and relocation of FOXO3a to the cytoplasm. Depleting cholesterol with β-cyclodextrin (MβCD) in order to inhibit lipid raft clustering suppressed Akt activation and FOXO3a relocation. When single HSCs that had survived without dividing for several days in the presence of MβCD, stem cell factor, and thrombopoietin were placed in MβCD-free medium, they proliferated and differentiated along various myeloid lineages in vitro and could repopulate the hematopoietic system of lethally irradiated mice. Thus, lipid raft clustering may mediate HSC emergence from dormancy via signaling pathways resembling those involved in the dauer stage. — EMA

EMBO J. **25**, 3515 (2006).

JOIN THE ACS CYCLE OF EXCELLENCE

contribute | *publish* | *review*

The Most Cited Journals in the Chemical & Related Sciences

The peer-reviewed journals of the ACS rank #1 in citations and/or ISI® Impact Factor in the seven ISI® core chemistry categories and seven additional ISI® categories ranging from agriculture to polymer science to the new category of nanoscience & nanotechnology. ACS Journals exceeded 1.13 million total citations in 2005, an increase of 13% over 2004. With a collection of over 600,000 original research articles spanning over 125 years of science, the American Chemical Society publishes the world's most respected journals in the chemical and related sciences.

#1 in citations or ISI® impact factor in the 7 ISI® core chemistry categories:

CHEMISTRY, MULTIDISCIPLINARY – ACS Journals account for 25% of articles and 49% of total citations

Journal of the American Chemical Society – #1 in total citations (257,810) • 11% increase in citations • High ISI® Impact Factor (7.419) • #1 in articles published (3,391)

Chemical Reviews – #1 in ISI® Impact Factor (20.869) • #4 in citations (51,878)

Accounts of Chemical Research – #3 in ISI® Impact Factor (13.141) • 13% increase in citations (21,293)

CHEMISTRY, INORGANIC & NUCLEAR – ACS Journals account for 19% of articles and 34% of total citations

Inorganic Chemistry – #1 in citations (56,284) • #1 in articles published (1,273) • #6 in ISI® Impact Factor (3.851)

Organometallics – #2 in citations (28,985) • #2 in articles published (849) • High ISI® Impact Factor (3.473)

CHEMISTRY, MEDICINAL – ACS Journals account for 22% of articles and 37% of total citations

Journal of Medicinal Chemistry – #1 in citations (35,053) • High ISI® Impact Factor (4.926)

Journal of Combinatorial Chemistry – 17% increase in citations (1,977) • High ISI® Impact Factor (3.459)

Journal of Natural Products – #4 in citations (9,928) • Increase in ISI® Impact Factor (2.267)

Chemical Research in Toxicology – #7 in citations (7,302) • High ISI® Impact Factor (3.339)

CHEMISTRY, APPLIED – ACS Journals account for 24% of articles and 32% of total citations

Journal of Agricultural and Food Chemistry – #1 in total citations (32,470) • High ISI® Impact Factor (2.507)

Organic Process Research & Development – Increase in ISI® Impact Factor (1.749) • 22% increase in citations

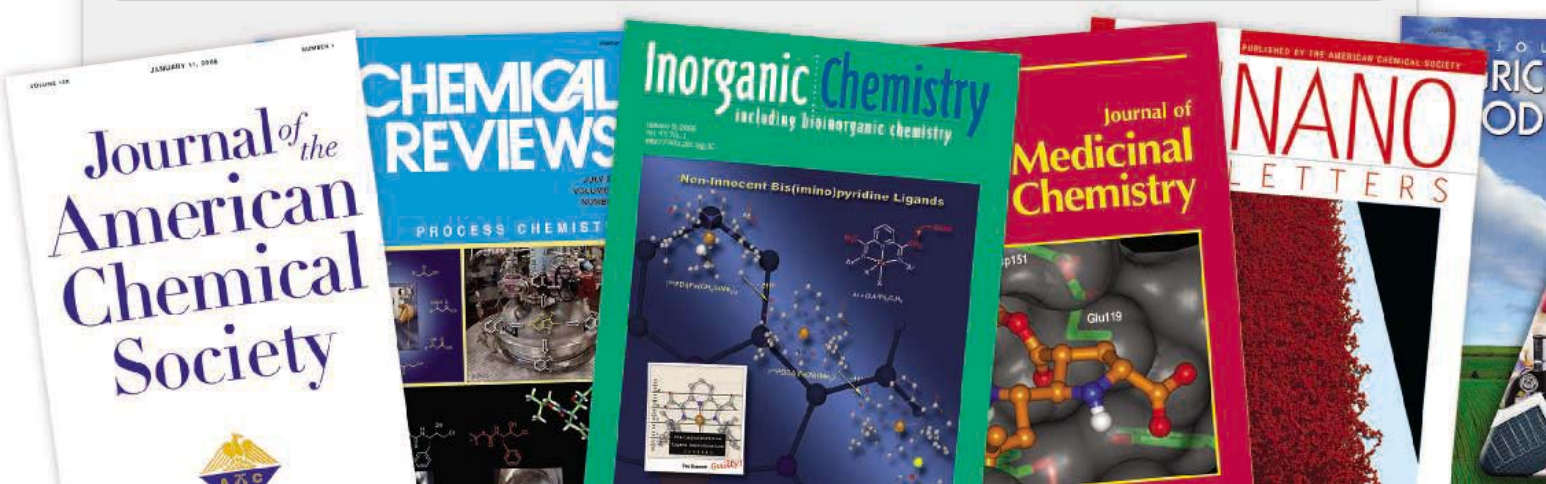

CHEMISTRY, PHYSICAL – ACS Journals account for 24% of articles and 28% of total citations

The Journal of Physical Chemistry B – #1 in citations (59,826) • #1 in articles published (3,121) • High ISI® Impact Factor (4.033)

The Journal of Physical Chemistry A – #5 in citations (32,086)• High ISI® Impact Factor (2.898) • #3 in articles published (1,455)

Langmuir – #2 in citations (55,025) • High ISI® Impact Factor (3.705) • #2 in articles published (1,777)

CHEMISTRY, ORGANIC – ACS Journals account for 26% of articles and 35% of total citations

The Journal of Organic Chemistry – #1 in citations (79,573) • High ISI® Impact Factor (3.675)

Organic Letters – Highest ISI® Impact Factor communications journal (4.368) • #5 in citations (27,569)

Bioconjugate Chemistry – #6 in ISI® Impact Factor (3.943) • 19% increase in citations (5,620)

CHEMISTRY, ANALYTICAL – ACS Journals account for 7% of articles and 18% of total citations

Analytical Chemistry – #1 in total citations (64,301) • #1 in ISI® Impact Factor (5.635)

#1 in citations or ISI® impact factor in 7 additional categories:

AGRICULTURE – *Journal of Agricultural and Food Chemistry* – #1 in total citations (32,470) • #1 in ISI® Impact Factor (2.507) • #1 in articles published (1,521)

ENGINEERING, ENVIRONMENTAL – *Environmental Science & Technology* – #1 in citations (39,785) • #1 in ISI® Impact Factor (4.054) • #1 in articles published (1,282)

ENVIRONMENTAL SCIENCES – *Environmental Science & Technology* – #1 in citations (39,785) • #1 in articles published (1,282)

FOOD SCIENCE & TECHNOLOGY – *Journal of Agriculture and Food Chemistry* – #1 in citations (32,470) • #1 in articles published (1,521) • #2 in ISI® Impact Factor (2.507)

MATERIALS SCIENCE, MULTIDISCIPLINARY – *Chemistry of Materials* – #1 in citations (33,648) • 27% increase in citations • #9 in ISI® Impact Factor (4.818)

POLYMER SCIENCE – *Macromolecules* – #1 in citations (71,840) • #3 in ISI® Impact Factor (4.024) • #1 in articles published (1,415)

NEW CATEGORY

NANOSCIENCE & NANOTECHNOLOGY – *Nano Letters* – #1 in ISI® Impact Factor (9.847) • #2 in citations (13,040) • 77% increase in citations

Also highly ranked in these 10 additional categories:

- Biochemical Research Methods
- Biochemistry & Molecular Biology
- Biotechnology & Applied Microbiology
- Computer Science, Information Systems
- Crystallography
- Energy & Fuels
- Engineering, Chemical
- Pharmacology & Pharmacy
- Physics, Atomic, Molecular & Chemical
- Toxicology

HIGHLY RANKED

BIOCHEMISTRY & MOLECULAR BIOLOGY – *Biochemistry* – #3 out of 261 journals in citations (95,172) • High ISI® Impact Factor (3.848) • 2nd most cited ACS Journal

Visit our Web site for more information: http://pubs.acs.org

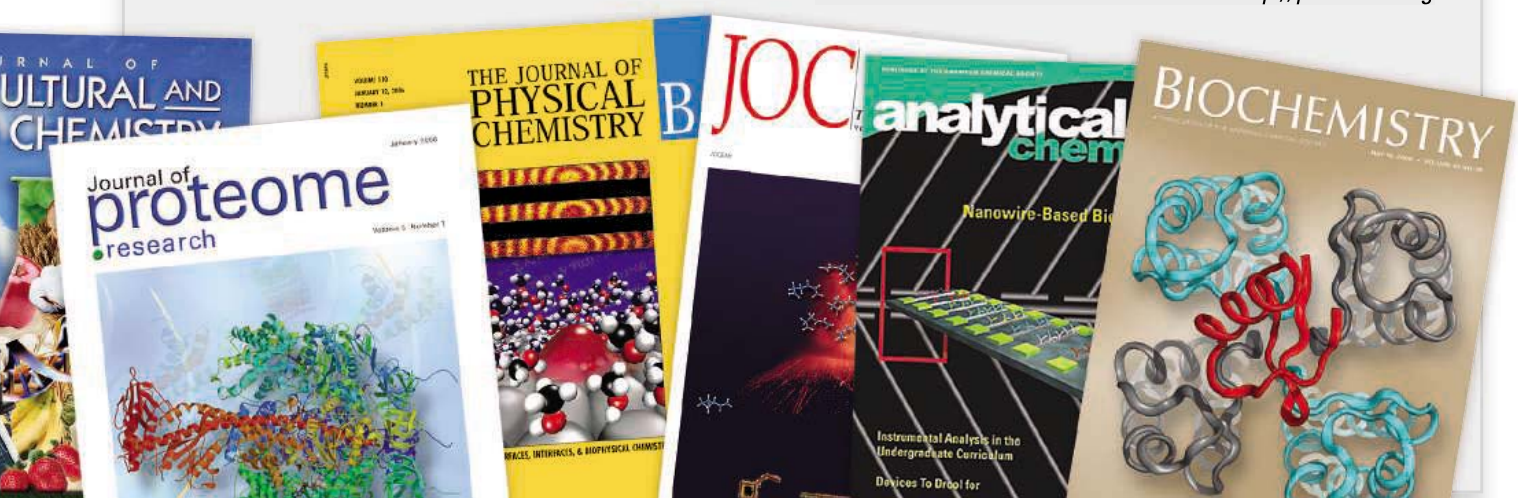

www.sciencemag.org

Science

1200 New York Avenue, NW
Washington, DC 20005
Editorial: 202-326-6550, FAX 202-289-7562
News: 202-326-6500, FAX 202-371-9227

Bateman House, 82-88 Hills Road
Cambridge, UK CB2 1LQ
+44 (0) 1223 326500, FAX +44 (0) 1223 326501

Subscription Services For change of address, missing issues, new orders and renewals, and payment questions: 866-434-AAAS (2227) or 202-326-6417, FAX 202-842-1065. Mailing addresses: AAAS, P.O. Box 96178, Washington, DC 20090-6178 or AAAS Member Services, 1200 New York Avenue, NW, Washington, DC 20005

Institutional Site Licenses please call 202-326-6755 for any questions or information

Reprints: Author Inquiries 800-635-7181
Commercial Inquiries 803-359-4578
Corrections 202-326-6501

Permissions 202-326-7074, FAX 202-682-0816

Member Benefits Bookstore: AAAS/BarnesandNoble.com bookstore www.aaas.org/bn; Car purchase discount: Subaru VIP Program 202-326-6417; Credit Card: MBNA 800-847-7378; Car Rentals: Hertz 800-654-2200 CDP#343457, Dollar 800-800-4000 #AA1115; AAAS Travels: Betchart Expeditions 800-252-4910; Life Insurance: Seabury & Smith 800-424-9883; Other Benefits: AAAS Member Services 202-326-6417 or www.aaasmember.org.

science_editors@aaas.org	(for general editorial queries)
science_letters@aaas.org	(for queries about letters)
science_reviews@aaas.org	(for returning manuscript reviews)
science_bookrevs@aaas.org	(for book review queries)

Published by the American Association for the Advancement of Science (AAAS), *Science* serves its readers as a forum for the presentation and discussion of important issues related to the advancement of science, including the presentation of minority or conflicting points of view, rather than by publishing only material on which a consensus has been reached. Accordingly, all articles published in *Science*—including editorials, news and comment, and book reviews—are signed and reflect the individual views of the authors and not official points of view adopted by the AAAS or the institutions with which the authors are affiliated.

AAAS was founded in 1848 and incorporated in 1874. Its mission is to advance science and innovation throughout the world for the benefit of all people. The goals of the association are to: foster communication among scientists, engineers and the public; enhance international cooperation in science and its applications; promote the responsible conduct and use of science and technology; foster education in science and technology for everyone; enhance the science and technology workforce and infrastructure; increase public understanding and appreciation of science and technology; and strengthen support for the science and technology enterprise.

Information for Contributors

See pages 102 and 103 of the 6 January 2006 issue or access www.sciencemag.org/feature/contribinfo/home.shtml

Be More Specific.

TaqMan MicroRNA Assays—the miRNA quantitation solution.

TaqMan® MicroRNA Assays are exactly what's needed for high-quality gene expression quantitation results in miRNA research. Whether profiling miRNA or monitoring specific miRNA genes, you'll get the gold standard in sensitivity, specificity, and ease of use that only real-time PCR TaqMan® assays can provide. The TaqMan MicroRNA Assay specifically measures the biologically active mature form—not the inactive precursor miRNA transcript. And since the assays are functionally validated, you can be confident they will work for your target of interest. TaqMan® chemistry provides the single-base specificity to differentiate between closely related sequences, and unparalleled sensitivity to help conserve your precious samples.

The rapidly growing TaqMan® MicroRNA Assays portfolio includes assays for human, mouse, rat, *C. elegans*, *Drosophila*, and *Arabidopsis*.

Get all the specifics at mirna.appliedbiosystems.com

Applied Biosystems

25 YEARS ADVANCING SCIENCE

RESOURCES

Dragons of the Ancient Sea

Dinosaurs weren't the only charismatic reptiles alive during the Mesozoic Era from 245 million years ago to 65 million years ago. Plying the oceans were plesiosaurs such as the snake-necked *Elasmosaurus* (left), which could reach 14 meters in length. Get a close look at these aquatic creatures at the growing Plesiosaur Directory. The not-so-invisible hand behind the site is grad student Adam Smith of University College Dublin in Ireland. A taxonomic listing describes more than a dozen plesiosaur genera and includes images, details of fossil discoveries, and distribution information. Pages on the creatures' biology delve into their anatomy and dining habits and offer animations depicting how their flattened limbs might have moved during swimming. The directory also showcases some plesiosaur appearances on TV and in films, none of which was Oscar-worthy. >>
www.plesiosauria.com

COMMUNITY SITE

Recipe Swap

A few tips from a veteran cook can ensure that your first soufflé comes out fluffy instead of leaden. The same principle motivates the SyntheticPages, hosted by the University of Warwick in the U.K. Midway between a journal and a user-written wiki, the site allows researchers to share not just the procedure for making a compound, but also pointers and common problems. So far, contributors have submitted 220 protocols for synthesizing everything from quinoline to substituted flavones. In contrast to wiki-style sites, editors vet the procedures before they're posted. The site's goal isn't to replace traditional publications but to allow researchers to pass on their experience with a reaction. Visitors can also have their say, adding clarifications and refinements. >>
www.syntheticpages.org

EDUCATION

On-Screen Physics >>

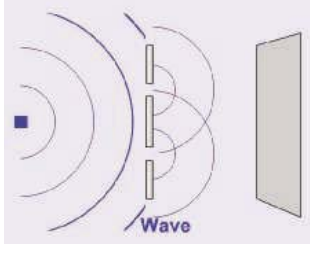

Physics topics such as kinematics and traveling waves are obvious subjects for teaching animations. But plenty of other ideas become clearer if they're put in motion, as shown by this collection of Flash animations from physicist David Harrison of the University of Toronto in Canada. Harrison's 87 creations will help introductory students follow the dynamics of a projectile, for example, or understand the time-dilation effect predicted by Einstein's special theory of relativity. Above, the double-slit experiment illustrating the wave-particle nature of electrons. >>
www.upscale.utoronto.ca/GeneralInterest/Harrison/Flash

LINKS

Bypass the Bookstore

The Textbook Revolution offers college students something almost as welcome as cheap beer: free textbooks. The site from undergrad Jason Turgeon of Boston University links to a library's worth of texts and other educational materials that users can read online or download as PDFs. If you're looking for an advanced treatise on electromagnetic field theory or an introduction to physical geography, you'll find them among the site's more than 150 science titles. >>
textbookrevolution.org

EXHIBIT

The Nation's Photo Album

The Smithsonian Institution in Washington, D.C., has been amassing photographs such as this 1890 shot of a snowflake (above) almost since the medium was invented. Now you can check out highlights from the museum's more than 13 million images at the new Smithsonian Photography Initiative Web site. Visitors can flip through about 1800 photos, some of which date back to the 1840s. The subjects of the nearly 600 entries on science and nature range from a water-scarred martian crater to native seal hunters in Glacier Bay, Alaska. Some of the images are historically important. The snowflake shot, for instance, is part of a collection from Wilson Bentley (1865–1931), a Vermont farmer and self-tutored scientist who was the first to photograph an individual snowflake. >>
www.spi.si.edu

Send site suggestions to >> netwatch@aaas.org
Archive: www.sciencemag.org/netwatch

CREDITS (TOP TO BOTTOM): CHRIS BUTLER/PHOTO RESEARCHERS INC.; SMITHSONIAN INSTITUTION; DAVID HARRISON

17,520 HOURS OF WORK. CONSECUTIVELY.

NO VACATIONS. NO BREAKS. NO EXCUSES.

Meet your new co-worker, the NanoLC-2D™ proteomics system from Eksigent. It will work hard for you. It is dependable. It delivers quality results. And, if you want it to help you identify proteins for 17, 520 hours straight (2 years) it can.

That's why we're offering an additional one-year warranty to those who add a NanoLC system to their staff before the end of 2006.

a reliable worker
- Proven direct pumping technology lets you identify peptides and proteins 24/7
- Fewer moving parts means dependable, worry free operation

easy to work with
- Set up a 2D method in seconds
- Eksigent Control Software gives you complete control of pumps, valves and autosampler
- Reduce solvent waste by 99%
- Integrates seamlessly with your MS data system

delivers quality results
- Precise and immediate flow rate control
- Reproducible gradients result in high quality LC/MS data

for more on our two-year warranty offer visit:
www.eksigent.com/2-yr

eksigent
rethinkHPLC

tel: 925 560 2600
web: www.eksigent.com

MEGAPODE MAY FOLLOW DODO

The Nicobar megapode, a ground-dwelling bird in some ways resembling the ill-fated dodo, has had a tough decade—and the Asian tsunami of 2004 has made matters worse. The Wildlife Institute of India has surveyed the bird's habitat and found that the population has declined by about 70% over the past dozen years.

The reddish-brown megapode lays its eggs in large mounds of sand, loam, coral bits, and rotting vegetation. Once two to four eggs have been laid, the parents cover the nest with plant debris, which generates enough heat to incubate the eggs. Incubation mounds can reach heights of 3.5 meters.

Earlier this year, India's premier wildlife institute conducted a status survey of endangered species in the Nicobar Islands east of Sri Lanka, which were severely affected by the tsunami. The researchers found evidence of only 800 breeding pairs of the megapode. Worse, says institute scientist K. Sivakumar, Megapode Island, which was declared a wildlife sanctuary for the birds, has been totally submerged. Sivakumar believes that if local tribes can be made aware of the problem, the bird population, which is mainly threatened by habitat destruction, could bounce back.

STRIKE OUT? >>

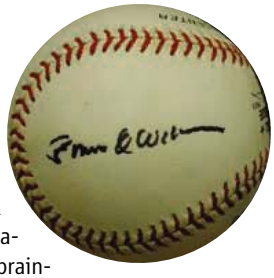

Scientists need $1.3 million to buy a piece of tropical forest in Costa Rica. They're hoping to raise it by selling a baseball on eBay. Not just some Babe Ruth memento, but a ball signed by "the four greatest conservationists on Earth." The idea was the brainchild of Norman Gershenz, director of the San Francisco, California–based Center for Ecosystem Survival. The ball, with a starting bid of $2500, has been signed by Harvard's E. O. Wilson, Paul Ehrlich of Stanford University, Peter Raven of the Missouri Botanical Garden, and Daniel Janzen of the University of Pennsylvania.

Janzen explains that the center wants to buy a strategically located 1600-hectare piece of land owned by the Del Oro orange plantations. The purchase would join Pacific dry forest to Atlantic rainforest in the Área de Conservación Guanacaste in northwestern Costa Rica.

"Getting one signature from any of the individuals in this esteemed group would be a coup; getting four together on one item is priceless," says Gershenz. It's not clear whether anyone agrees. As of 25 August, the ball, which went on sale on 21 August for a week, had received no bids.

A Prematurity Gene

African-American women are two to three times as likely to give birth prematurely as women of European origin. Scientists have now identified a possible genetic contributor to the difference: a gene variant that affects the strength and resilience of the amniotic sac.

Preterm premature rupture of membranes (PPROM)—the term for when a woman's "water breaks" prematurely—accounts for one-third of premature births, and a black woman's risk of PPROM is more than twice that of a Caucasian woman. Scientists led by physician Jerome Strauss of Virginia Commonwealth University in Richmond now say a gene that helps boost collagen levels in fetal membranes could explain the disparity.

The gene, which encodes heat shock protein 47, has a variant that is less active in collagen production and is present in 12% of African Americans but only 4% of Caucasians.

The team collected genetic data on infants delivered by 602 black mothers in four U.S. cities. Among the fetuses of the 244 mothers who had PPROM, 11.5% had this variant, whereas it was present in only 4.5% of the infants delivered at term, the researchers reported online last week in the *Proceedings of the National Academy of Sciences*. This is the first example of an "ancestry-informative" marker for pregnancy complications in African Americans, the authors claim.

The study is "potentially important," says physician Richard Cooper of Loyola University in Maywood, Illinois. But he contends that the black-white gap in premature births has been narrowed by better care in recent years, so the mutation would only explain a "small proportion" of the difference.

AMAZONIAN AMBER

This tiny fly is is one of a variety of bug and plant fossils recently found in amber desposits on the banks of the Amazon in northeastern Peru. John J. Flynn of the American Museum of Natural History in New York City, with colleagues from France and Peru, has been plying the river in search of 15-million-year-old Miocene outcroppings that would reveal the history of the region. "The discovery virtually instantaneously opens a window to the Amazon," he says. There have been only three other finds of amber-encased fossils in Latin America covering the past 65 million years, he says. The abundance of species—13 arthropods and some 30 plant, fungus, and bacterium types—confirms that a rich tropical rainforest thrived even then, the scientists report in this week's *Proceedings of the National Academy of Sciences*.

CREDITS (TOP TO BOTTOM): K. SIVAKUMAR/WII; ANNIE GRIFFITHS BELT/CORBIS; NORMAN GERSHENZ; ANDRÉ NEL/MUSÉUM NATIONAL D'HISTOIRE NATURELLE, PARIS

Unwelcome traveler
1218

Intense debate
1221

PLUTO

Underworld Character Kicked Out of Planetary Family

PRAGUE, CZECH REPUBLIC—The debate wasn't even supposed to be about Pluto. Last week's vote by the International Astronomical Union (IAU) to define the term "planet" was intended to set rules for the classification of new discoveries in the outer solar system. Instead—in a pair of votes that made headlines around the world—IAU not only dropped the small, distant ice ball from the roster of planets but also all but guaranteed that no more planets would be discovered in the solar system in the future.

The decision, made here at the closing session of the IAU's triennial meeting,* reclassifies Pluto as a "dwarf planet"—but not a planet. That is "patently incorrect," says astronomer and Pluto buff Alan Stern of the Southwest Research Institute in Boulder, Colorado, who heads the New Horizons mission that set off last January to explore the tiny ex-planet in 2015. "If the IAU wants to proclaim that the sky is green, that doesn't make it so." But other astronomers and planetary scientists—including some who supported Pluto's planetary status—say it's time to move on.

* 26th General Assembly, International Astronomical Union, 14–25 August, Prague.

Pluto has always been an oddball. Smaller than Earth's moon, it follows a skewed, elongated orbit into a region known as the Kuiper belt, home to a population of countless "ice dwarfs": rubble left over from the baby days of the solar system. After Pluto was discovered in 1930, IAU declared it a planet by fiat but never clearly defined what a planet is.

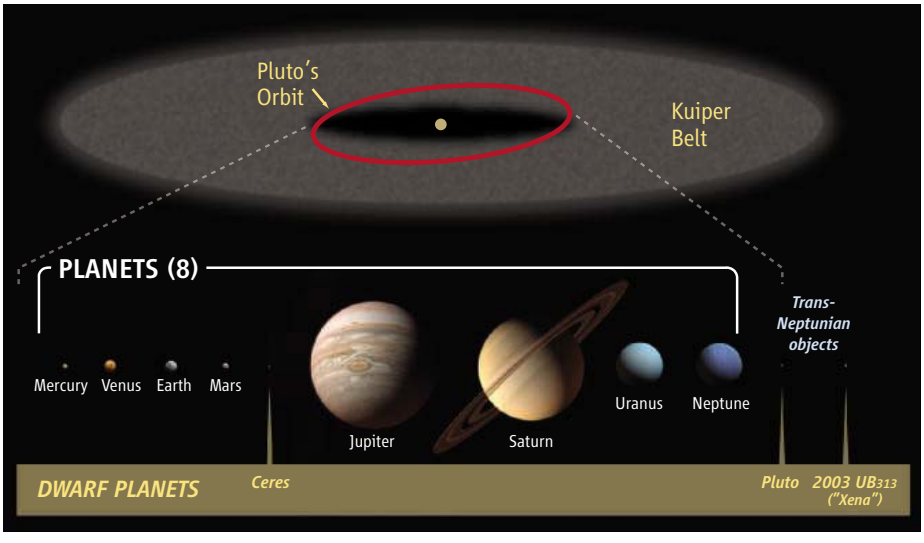

Reclassified. Under new rules adopted by the International Astronomical Union, Pluto becomes one of three "dwarf planets" as well as the innermost member of a still-unnamed class of Kuiper belt objects.

The question became impossible to ignore in the summer of 2005, when Michael Brown, a planetary scientist at the California Institute of Technology in Pasadena, announced the discovery of 2003 UB_{313} (nicknamed "Xena"), an icy world farther from the sun than Pluto and some 10% larger. Had Brown discovered the 10th planet? Without a formal definition, there was no way to tell. So earlier this year, the IAU Executive Committee asked seven people (including award-winning science writer Dava Sobel) to write one.

Chaired by Owen Gingerich, a professor of astronomical history at the Harvard-Smithsonian Center for Astrophysics in Cambridge, Massachusetts, the committee met in Paris on 30 June and 1 July and unanimously agreed that planet club membership would be open to any sun-circling body big and massive enough to become spherical under its own self-gravity. That would include not only Pluto and "Xena" but also Ceres, the largest member of the rocky asteroid belt between the orbits of Mars and Jupiter. The definition also opened the door for scores of yet-to-be-discovered Kuiper belt planets. In addition, the committee proposed that Pluto's large moon Charon should be considered a planet in its own right and that Pluto-like objects in the Kuiper belt should be called "plutons."

IAU presented the resolution to its General Assembly on 16 August, giving the roughly 2500 attendees more than a week to discuss it. But the committee expected clear sailing. "We felt we had a resolution that anybody could love," Sobel says.

Instead, the "12-planet proposal" went down in flames. Critics objected that planets should also be defined by their orbital dynamics, not just their size and shape. All eight "major" planets, they pointed out, were massive enough to sweep up, fling away, or gravitationally control all the debris in their parts of the early solar system, but Ceres and Pluto—and a host of other candidate "planets"—were not.

Many astronomers lambasted the resolution during a tumultuous lunchtime meeting on 22 August. To Gingerich's argument that the proposal rested on physical criteria, asteroid researcher Andrea Milani of the University of Pisa in Italy, literally screamed, "Dynamics is not physics?" Other astronomers protested the committee's neglect of extrasolar planets, only to be angrily silenced by outgoing IAU President Ronald D. Ekers, who declared such issues to be "out of order!" Some in the audience expressed chagrin. "It should never have become this emotional," says astronomer George Miley of Leiden University in the Netherlands.

On the morning of 24 August—the day of the vote—IAU issued a revised resolution (5A) adding gravitational dominance to the requirements for planethood and omitting any reference to Charon or "plutons." Ceres, Pluto, "Xena," and other spherical sun-circling bodies were labeled "dwarf planets." But to the surprise of many, IAU added an optional amendment (resolution 5B) that would have changed the term "planet" in ▶

SOURCES: INTERNATIONAL ASTRONOMICAL UNION AND JPL/NASA

Blowing the whistle on a mentor
1222

Big-game protector
1226

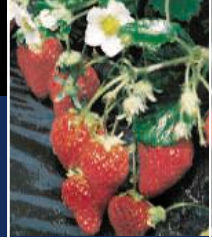

Ripening knowledge
1230

resolution 5A into "classical planet." By restricting the new definition to the eight existing "classical planets," the second resolution implied that dwarf planets were a subcategory of planets, too. To "Pluto-bashing" planetary scientists, it looked as if the committee had made a final attempt to keep the small balls in the planet league.

As it turned out, resolution 5A (including the dynamical criterion) passed by a margin so wide that no formal count was deemed necessary, and its sibling 5B was soundly defeated. At 3:32 p.m. European time, Pluto ceased to be a planet.

The Plutonic wars aren't over yet. "This is a sloppy, bad example of how science should be done," says Stern, who was not at the meeting. In protest, he and others have already withdrawn articles from an upcoming edition of a professional solar system encyclopedia after the editor requested them to change Pluto's status in the articles. A petition against the accepted planet definition is already circulating among planetary scientists.

But 2003 UB_{313}'s discoverer Michael Brown (who is not an IAU member and thus had no say in the matter) urges peace. "It was the right scientific choice. As scientists, we should say, 'It's fine. Let's let it go and get on with the business.' "

The business includes coining a word for dwarf planets beyond Neptune, of which Pluto has been designated as the prototype, and setting an official name for dwarf planet 2003 UB_{313}. Planetary scientists must also decide whether dwarf planets belong in their large and steadily growing list of minor planets or in a new catalog.

And of course, schoolbooks have to be rewritten. Despite the flood of news stories speculating about the effect of the IAU vote on students' fragile psyches, Brown predicts that children will adapt easily to the revised solar system. "People are not as upset about schoolkids as they think they are," he asserts. "They're actually upset about their memories of themselves as schoolkids. The kids will be fine." **–GOVERT SCHILLING**

Govert Schilling is an astronomy writer in Amersfoort, the Netherlands. With additional reporting by John Bohannon and Robert Coontz.

SCHOLARLY PUBLISHING

Particle Physicists Want to Expand Open Access

Particle physicists have come up with a novel way to promote free, immediate access to journal articles. Led by CERN, the giant lab near Geneva, Switzerland, they want to raise at least $6 million a year to begin buying open access to all published papers in their field.

The proposal adds fuel to the ongoing debate about public access to research results. Some private biomedical funding groups, such as the U.K.'s Wellcome Trust, now pay the author fees required for their grantees to publish in open-access journals. CERN's announcement goes further, say observers. "Across a discipline is new," says Peter Suber, a philosophy professor at Earlham College in Richmond, Indiana, who closely follows open-access developments for the Scholarly Publishing and Academic Resources Coalition.

CERN organizers cite next year's start-up of the Large Hadron Collider (LHC), the most powerful accelerator ever, as the proposal's motivation. That will be "a unique opportunity to reform the publishing paradigm of the particle physics community to ensure the widest, most efficient dissemination of results from this unique facility," a task force of CERN, other particle physics funders, and scientific publishers concluded in a report issued in June.*

To accomplish this goal, the task force proposed that a consortium of labs and funding agencies pay publication costs for particle physics papers. It would cost $6 million or more a year to include all the journals willing to offer an open-access option, the group estimated. That would cover up to half of the 6000 or so original theory and experimental papers published each year.

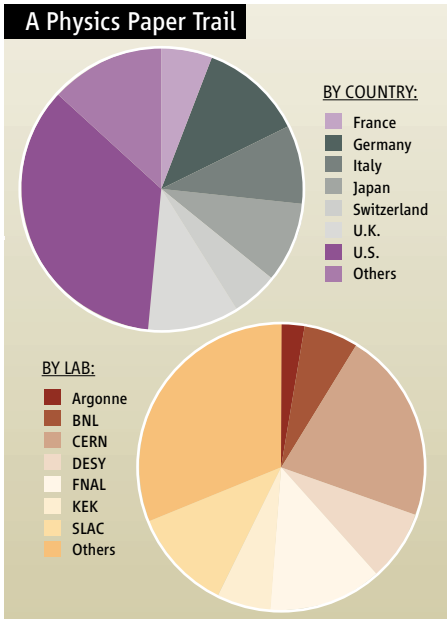

Knowledge glut. The 5-year totals for 17,995 theoretical (*top*) and 2618 experimental (*above*) papers in open-access-ready journals.

SOURCE: CERN

The task force hopes to start with $3 million to implement the policy at a few major journals. The practice would begin with the first LHC technical papers next year, says CERN's Rüdiger Voss.

Last week, the American Physical Society announced that a $975 to $1300 payment to its two main journals would make an article available to all readers (*Science*, 25 August, p. 1031). Elsevier, the other major particle physics publisher, recently announced an open-access option for $3000, an amount not included in the task force's cost estimate. CERN's plan to sponsor journals would not be permanent: "We see it primarily as a transition scenario," Voss says, after which funders would pay author fees for individual grantees.

Nearly all particle physicists already share preprints of their articles on free servers such as arXiv.org at Cornell University Library. Voss, however, argues that the final, vetted article is still what academia values most and that physicists are losing access as budget-strapped libraries cut back on journal subscriptions. Paul Ginsparg, who runs arXiv.org, adds that journals serve as stable, long-term archives and offer extras such as searching for related papers in other journals.

–JOCELYN KAISER

* library.cern.ch/OATaskForce_public.pdf

K. lactis Protein Expression Kit from New England Biolabs

YEAST PROTEIN EXPRESSION MADE EASY

The *K. lactis* Protein Expression Kit provides a simple method to clone and express your gene of interest in the yeast *Kluyveromyces lactis*. This system offers many advantages over bacterial systems and eliminates the methanol containing medium and antibiotic requirements of *Pichia pastoris*. With easy-to-use protocols and highly competent *K. lactis* cells included, this system can take you from bench top to large scale production with ease.

Advantages:

- High yield protein expression
- Rapid high cell density growth
- Methanol-free growth media
- Plasmid integration enhances stability
- Acetamide selection enriches for multi-copy integrants, enhancing yield
- Tight control of gene expression enables expression of toxic genes
- Access to eukaryotic protein folding and glycosylation machinery
- Simultaneous expression of multiple proteins
- Ease-of-use for those inexperienced with yeast systems
- Yeast competent cells included
- No license required for research use

***K. lactis* Protein Expression Kit** **E1000**

Kit components sold separately

***K. lactis* GG799 Competent Cells** **C1001**

pKLAC1 Vector **N3740**

	K. lactis	*P. pastoris*
High yield expression	✓	✓
Rapid high cell density growth	✓	✓
Yeast Competent Cells Included	✓	
Methanol-free growth media	✓	
Antibiotic-free Selection	✓	
Enhanced multi-copy integration	✓	
Protein folding and glycosylation	✓	✓
Expression of genes toxic to *E. coli*	✓	✓

Quick comparison of *K. lactis* and *P. pastoris* expression systems.

For more information and international distribution network, please visit www.neb.com

- **New England Biolabs Inc.** 240 County Road, Ipswich, MA 01938 USA 1-800-NEB-LABS Tel. (978) 927-5054 Fax (978) 921-1350 info@neb.com
- **Canada** Tel. (800) 387-1095 info@ca.neb.com
- **Germany** Tel. 0800/246 5227 info@de.neb.com
- **UK** Tel. (0800) 318486 info@uk.neb.com
- **China** Tel. 010-82378266 beijing@neb-china.com

NEW ENGLAND BioLabs® Inc.

the leader in enzyme technology

GENETICS

Genomes Highlight Plant Pathogens' Powerful Arsenal

For farmers and botanists, *Phytophthora* unfortunately lives up to its name, which is Greek for "plant destroyer." The 70-odd species of this eukaryotic genus include the pathogens behind root rot in soybeans, sudden oak death, and potato blight, which still causes upward of $5 billion of damage across the world. Just about all broadleaf plants suffer to some extent from *Phytophthora*, a distant relative of kelp and diatoms. "They've been terrifically successful as plant pathogens," says Brett Tyler of Virginia Polytechnic Institute and State University in Blacksburg.

On page 1261, a large team led by Tyler and Jeffrey Boore of the Joint Genome Institute in Walnut Creek, California, describes the first two genomes of this genus. The sequences reveal that *P. sojae* and *P. ramorum*, which cause soybean root rot and sudden oak death respectively, have a diverse array of proteins with which to attack their hosts. Plant pathologists are eager to learn more about such attacks and how to prevent the damage they cause. The sequences "open so many doors that we can now investigate; I'm very excited," says William Fry of Cornell University.

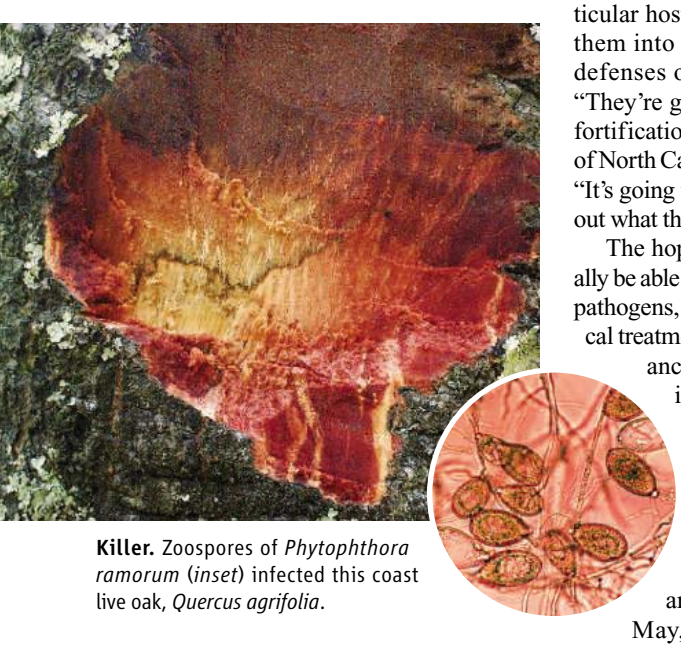

Killer. Zoospores of *Phytophthora ramorum* (*inset*) infected this coast live oak, *Quercus agrifolia*.

CREDITS: DOUG SCHMIDT

Tyler and Boore's team began sequencing the two genomes in 2002. The team has so far identified 19,027 likely genes in *P. sojae* and 15,743 in *P. ramorum*. Fungal pathogens, in comparison, typically have 10,000 to 12,000 genes.

One reason for the surfeit is that the two species have diversified their genetic repertoire for making substances that attack plants, such as toxins and enzymes to break down cell walls. In particular, the secretome—those genes that make proteins to be secreted—is evolving much more rapidly in each species than are the overall collection of protein-encoding genes. In *P. sojae*, for example, 17% of the 1464 genes for secreted proteins are at least 30% distinct from their peers; overall, it's just 9%. "It tells us that secreted proteins are diverging more rapidly," Tyler says.

Both species have about 350 genes that resemble so-called avirulence genes seen in bacterial plant pathogens. But such bacteria typically have only 20 to 30 of these genes. Avirulence proteins are highly targeted to particular hosts, and bacterial pathogens inject them into plant cells, lowering the plant's defenses or exploiting other weaknesses. "They're going after the generals inside the fortifications," says genomicist Ralph Dean of North Carolina State University in Raleigh. "It's going to be absolutely amazing to figure out what these do" in *Phytophthora*.

The hope is that researchers will eventually be able to slow the assault of *Phytophthora* pathogens, either by designing better chemical treatments or engineering stronger resistance into plants. Neither prospect is imminent. The genomes appear to contain complex arrays of genes with overlapping or redundant functions, making it difficult to find a single approach that will deliver a knockout blow. Nonetheless, the genome sequences are already proving their worth. In May, two team members used gene markers from the sequences to show that diversity of *P. ramorum* is much higher in nurseries than in forests, which further demonstrated the role of plant nurseries in the spread of the pathogen.

Other findings reported in the *Science* paper include hundreds of *Phytophthora* genes apparently derived from red algae or cyanobacteria, bolstering a hypothesis that several kingdoms evolved from a photosynthetic ancestor. Meanwhile, researchers at the Broad Institute in Cambridge, Massachusetts, released a preliminary assembly in July of half of the much larger genome of *P. infestans*, the cause of potato blight. **–ERIK STOKSTAD**

No Messing With the Margins

Seeking brevity, the National Institutes of Health (NIH) aims to shorten grant applications. Reviewers of NIH's standard R01 application must currently wade through 25 pages with unlimited appendices—longer than at any other major funding agency. At a meeting of the NIH Center for Scientific Review's advisory council this week, NIH staff said they were considering a limit of 15 pages with no appendices. Biologist Keith Yamamoto of the University of California, San Francisco, suggested seven pages with emphasis on innovation instead of preliminary results. NIH will request input on the issue this fall.

–JOCELYN KAISER

Sanguine in Japan

Last year, Japan's Ministry of Education asked for a 9.5% increase in science and technology spending; it ended up with a 0.1% cut, leaving the budget at $19.7 billion. Ever optimistic, this year the ministry's spending wish list, announced this week, would boost spending 20%. Officials acknowledge that budget-cutting fever could dampen their hopes, but they feel lucky. "Compared to other budget categories, science spending could rise, but we don't know just how much," says Kazuo Todani, head of the Education Ministry's budget department. Projects likely to receive sustaining funds include a 10-petaflops supercomputer, expected to cost $1 billion over 7 years, and a $365 million x-ray free electron laser. **–DENNIS NORMILE**

Singing Singh's Praises

Soothing words from Prime Minister Manmohan Singh last week appear to have headed off a move by leading retired Indian nuclear scientists to publicly object to the U.S.-India nuclear agreement. Eight dissenters—including three former chairs of India's Atomic Energy Commission (AEC)—wrote an open letter to the Indian Parliament last month saying that limitations in the proposed pact with the United States would endanger the "independence" of India's nuclear research and possibly impose a bomb test ban (*Science*, 5 May, p. 679).

Supporters of the deal feared that the influential researchers could have raised a public outcry. But after a 1.5-hour private conference with the leader, says former AEC chair M. R. Srinivasan, Singh "assured and reiterated that the past gains made in the nuclear program will be consolidated." The group has declared its concerns addressed.

–PALLAVA BAGLA

EMERGING INFECTIOUS DISEASES

During a Hot Summer, Bluetongue Virus Invades Northern Europe

In a striking example of pathogens hopscotching the globe, a livestock virus originating in Africa appears to have hit three countries in northern Europe since 14 August. More than 70 farms in the Netherlands, Germany, and Belgium have been affected by bluetongue disease, an insect-borne infection of ruminants such as cows, sheep, goats, and deer. Scientists are trying to discover how the virus traveled and how far it might spread, while the European Union (E.U.) has implemented control measures, including some exports.

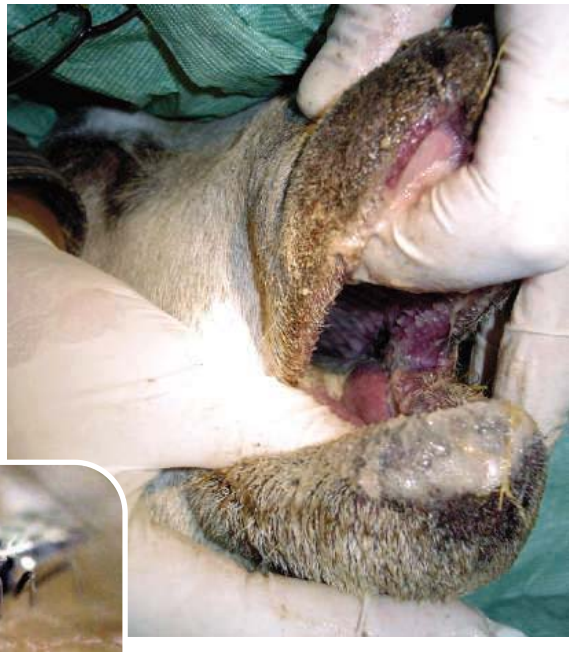

Pestilence. Tiny *Culicoides* midges can carry a virus harmful to sheep and other ruminants.

The bluetongue virus, carried by tiny insects called *Culicoides*, or biting midges, is harmless to humans but causes a severe and sometimes fatal disease—symptoms include a blue tongue, a result of bleeding—in sheep and goats. Cows are reservoirs but usually don't get sick. The virus, for which 24 serotypes are known, occurs in many parts of the world, but until recently it was almost never seen in Europe. Since 1998, however, some serotypes have made dramatic incursions into Greece, Italy, Spain, Portugal, and the Balkan countries, a trend some scientists blame on climate change.

When the virus first turned up in the Netherlands on 14 August—much farther north than it had ever been seen—researchers assumed one of the southern European strains had taken another major leap, which in itself would have been "very surprising" given *Culicoides*'s limited flying abilities, says bluetongue epidemiologist Bethan Purse of the University of Oxford. But a genetic analysis completed last weekend at the Institute for Animal Health (IAH) in Pirbright, U.K., revealed the virus to be of serotype 8, previously known to occur sporadically in sub-Saharan Africa, South America, and the Indian subcontinent. Its genetic fingerprint is closest to that of a Nigerian strain, which strongly suggests an African source, says IAH virologist Peter Mertens.

It's a mystery how this strain reached northern Europe, because there is very little traffic of ruminants between Africa and Europe, says epidemiologist Aline de Koeijer of the Central Institute for Animal Disease Control (CIDC) in Lelystad, the Netherlands. Perhaps an imported zoo animal was infected, she suggests, or an infected midge may have hitched a ride on an airplane. The current outbreak is unusual in that some cows have gotten sick, but it's unclear whether this is typical ▶

COMPUTER SECURITY

DOE Tightens Monitoring of Lab Collaborators

In an effort to safeguard sensitive and classified information, the U.S. Department of Energy has decided that anyone who wants to access the agency's computers must first give DOE written permission to do some electronic snooping. Managers at DOE national labs say that the new rule could hinder collaborations between lab scientists and academic researchers and, at a minimum, be an administrative nightmare. But agency officials say researchers shouldn't worry because the rule won't be implemented as written.

The rule, which builds on the National Defense Authorization Act of 2000, was published in the *Federal Register* on 19 July and went into effect 18 August. It mandates that anybody accessing information on computers owned by DOE and its contractors first provide the agency with "written consent" for investigators to check any DOE computer accessed by the individual for up to 3 years in the future. Currently, a warning banner appears whenever somebody logs on to a DOE computer—be it an employee at a national lab or an academic researcher logging on remotely from a university campus—asserting DOE's right to monitor the user's computer habits.

With the new regulation in place, thousands of university researchers around the world—in addition to DOE and national lab employees—would need to agree in advance to those conditions in writing rather than electronically. The regulation "is not well suited to the collaborations we do at our lab," says Dwayne Ramsey, computer protection program manager at Lawrence Berkeley National Lab in California. He adds that complying with the rule will be nearly impossible for grid computing projects, which often involve a fluid cast of users and computing resources. "Large international scientific collaborations increasingly depend on the trust of domains, not just people," he says.

Physicist James Shank of Boston University, who heads the U.S. grid computing effort for Atlas—an international particle physics experiment at CERN partly underwritten by DOE—says complying with the rule will also pose an unnecessary financial burden. "We will likely have to redirect somebody from the project or hire somebody to take care of the paperwork," says Shank, who along with hundreds of academic colleagues routinely logs on to computers at DOE's Brookhaven National Laboratory in Upton, New York, in order to work on Atlas.

A DOE spokesperson told *Science* that the agency plans to implement the rule in a way that will address these concerns. One possibility is for DOE to interpret "written consent" broadly so as to accept electronic signatures, which would enable users to click "I agree" on a consent form on the Web. One lab official calls that "a graceful way not to admit that the regulation is flawed."

–YUDHIJIT BHATTACHARJEE

CREDITS: R. VROUENRAETS/GD DEVENTER AND DAC HEERLEN; (INSET) RUBEN SMIT/WAGENINGEN UR

of the little-studied serotype 8, says CIDC virologist Eugène van Rooij.

In southern Europe, bluetongue's main vector is a species called *C. imicola*, which doesn't occur in the newly affected countries. Around stricken farms, a team led by medical and veterinary entomologist Willem Takken of Wageningen University in the Netherlands has found predominantly *C. obsoletus*—which lab studies have shown to be a potential vector for bluetongue—as well as eight other *Culicoides* species, Takken says. All will be tested for the presence of the virus.

Once introduced, the virus may have benefited from the warm weather, which speeds up its life cycle; July was the hottest month on record in the Netherlands. Scientists are hoping that the northern European winter will kill off all infected midges and prevent a 2007 sequel. **–MARTIN ENSERINK**

ACADEMIC CAREERS

USC Hires Prepackaged Team

Academic departments typically grow in the way that crystals do, by adding faculty to their existing lattices one member at a time. But in a bold experiment that begins this fall, the University of Southern California (USC) in Los Angeles has hired seven scientists who pitched themselves to the institution as a package.

The appointments by the Wrigley Institute for Environmental Studies (WIES) are part of the university's push to add 100 faculty members to its College of Letters, Arts, and Sciences. Three of the seven WIES hires are genomics experts; the rest specialize in marine biogeochemistry. Together, the septet plans to use gene sequencing as a tool to explore the dynamic relationship between microbial colonies and the ocean's chemical environment. The 11-year-old institute has some 30 faculty members and includes a marine biology station on Catalina Island.

"By hiring researchers who are already organized into a team, we're starting out with a very strong basis for interdisciplinary scholarship," says institute director Anthony Michaels, who sold the idea to the university. Michael Quick, dean of the college, says administrators felt that the concept fit USC's strategy of creating "niches within fields in which we can be leaders."

The process began last year with ads for "an integrated group, a mix of Full, Associate, and Assistant Professors, who are innovative, entrepreneurial, interdisciplinary leaders." Michaels says he wanted to invite big, novel ideas "to break the limits of our own imagination." Another goal, he says, was "to achieve economies of scale. We thought that members of a group applying together would be much more willing to share resources than individuals hired separately."

Of the 100 applications, the search committee ended up liking three groups, all of whom shared an interest in applying genomic analysis to understanding marine geochemistry. At the committee's prodding, the three clusters merged and presented their work last fall at a seminar. "We knew they were going to get along," says Michaels.

"Working within such a group will allow us to focus on a range of big questions," says John Heidelberg, who comes to the cluster from The Institute for Genomic Research in Rockville, Maryland. Another genomics expert in the cluster is his wife Karla, formerly at the neighboring J. Craig Venter Institute. Three members come from the Woods Hole Oceanographic Institution in Massachusetts: geobiologist Katrina Edwards; her husband Eric Webb, who specializes in cyanobacterial physiology and genomics; and James Moffett, an expert in trace metal ocean biochemistry. The team also includes oceanographer David Hutchins of the University of Delaware, Lewes, and trace metal biochemist Sergio Sañudo-Wilhelmy of Stony Brook University in New York. **–YUDHIJIT BHATTACHARJEE**

All for one. USC's Anthony Michaels sees faculty strength in numbers.

CREDIT: PHIL CHANNING

Flap Claims Journal Editor

The editor of *Neuropsychopharmacology* will relinquish his post following a stir over his failure to list commercial ties in a July article about a new treatment for depression on which he was primary author (*Science*, 4 August, p. 598). Charles Nemeroff, chair of the psychiatry department at Emory University in Atlanta, Georgia, last week notified the American College of Neuropsychopharmacology (ACNP), the journal's publisher, that he would step down when his 3-year term ends in December. "The controversy … continues to detract from our basic mission," says Nemeroff, who was offered a second term in May. "I cannot recall another time where there has been so much concern among the membership," wrote ACNP president Kenneth Davis in a 27 August letter to members.

Last week, the ACNP Council, which oversees the journal, approved a series of measures to address the issue. These include disclosure by all council members and their spouses of recent relationships with industry. "Our College … sits on the fault line between academia and industry," wrote Davis, who said he hopes the new editor will be "relatively free of industry relationships."

–CONSTANCE HOLDEN

Tooooooooooot

All aboard the Florida gravy train. The Scripps Research Institute in San Diego, California, was the first to climb on in 2003, when it inked a deal to open a brand-new East Coast branch in Palm Beach County—greased with $510 million from state and local governments. Last week, the Burnham Institute, also in San Diego, got aboard as well. Burnham pledged to bring as many as 300 well-paying biomedical research jobs to Orlando in exchange for a package of $310 million from Florida, the city of Orlando, the surrounding county, regional universities, developers, and philanthropies.

The dealmaking likely isn't done yet. A third San Diego–based research outfit—The Torrey Pines Institute for Molecular Studies—is being wooed by the cities of Port St. Lucie and Boca Raton with a package of incentives valued at $93 million. And the Silicon Valley–based SRI International is in negotiations as well.

Diabetes researcher Mark Atkinson of the University of Florida, Gainesville, says he expects the Burnham deal to be a boon for local science. He doesn't know how Florida Governor Jeb Bush keeps snagging California institutes, he adds, "but it seems to be working."

–ROBERT F. SERVICE

- Mastercycler ep® *realplex* real-time PCR System

- epMotion® 5070 automated pipetting system

- Highly precise pipetting tools

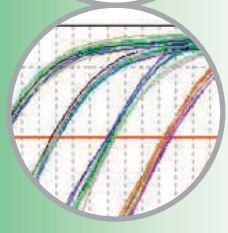

- Comprehensive software for optimized data analysis

licensed for real-time PCR

Automated real-time PCR that pays for itself

Precision pipetting · Reproducible results · Affordable automation

Eppendorf Automation and real-time Systems (ARTS™) combine the most accurate and reproducible pipetting with the fastest and most sensitive real-time cycling.

That means you get highly consistent and reproducible results within and across experiments. You can even perform reactions in lower volumes—and with fewer replicates, so you will also save significantly on reagents!

Visit: **www.epMotion.info** or **www.realplex.com**

Mastercycler ep *realplex*:
- Real-time PCR in less than 30 minutes
- User-friendly software
- Highly sensitive optical system

epMotion 5070 automated pipetting system
- Easy operation via control panel or PC
- Preinstalled, validated applications/consumables
- High-precision pipetting from 1 µl to 1.000 µl

eppendorf

In touch with life

www.eppendorf.com · Email: info@eppendorf.com · Application support: 516-515-2258
In the U.S.: Eppendorf North America, Inc. 800-645-3050 · In Canada: Eppendorf Canada Ltd. 800-263-8715
Your local distributor: www.eppendorf.com/worldwide · Application support: Phone +49 180 366 67 89

METEOROLOGY

A Hurricane's Punch Still Knocks Out Forecasters

A day and a half before Hurricane Charley hit Florida on 13 August 2004, the National Oceanic and Atmospheric Administration (NOAA) predicted it would probably be a Category 2 storm, "just shy of major hurricane status" and with maximum winds of 177 kilometers per hour. But the storm made landfall as a Category 4—with 241-km/h winds that killed 10 people and left billions of dollars of damage.

Decades of federally funded research have led to impressive gains in predicting where a hurricane will strike. But although forecasting a storm's track is largely influenced by nearby weather, sea, or land features, scientists say that knowing a storm's intensity also depends on the internal dynamics of a chaotic system. That's a much harder challenge and one that NOAA scientists admit they haven't solved. "We don't even know why [Charley] intensified," confesses meteorologist Morris Bender of NOAA's Geophysical Fluid Dynamics Laboratory (GFDL) in Princeton, New Jersey. Nor, for that matter, do scientists know why Katrina dipped in intensity before it pounded the Louisiana coast 1 year ago this week.

As the 2006 hurricane season unfolds, the best way to improve NOAA's ability to forecast storm strength is a pressing—and controversial—question. Agency officials say that a current $4 million project to create a new computational model is sufficient. But a recent report by a NOAA advisory panel disagrees and calls for massive new investment, research initiatives, and sharing arrangements. "NOAA's current program is moving in the right direction," says meteorologist John Snow of the University of Oklahoma, Norman, who chaired the panel. "We think they can move much more aggressively."

NOAA's best current prediction tool is a statistical model that uses data from previous hurricanes to give a probable outcome of a storm given its initial conditions. But the agency would prefer to develop a computational model that dynamically approximates the behavior of local weather and sea conditions, as a particular storm may not match a historical situation. Last year, its current computational model, named for the New Jersey lab, only just matched the mediocre performance of its statistical competitor—a result GFDL developer Robert Tuleya, now a NOAA contractor, called "quite frankly … embarrassing." After all, a computational model, if it accurately mimics a real system, should beat what amounts to a statistical guess. (The model gets good marks for predicting a hurricane's track.) Along with the new model, which will be made more realistic by including aspects of ocean behavior and cloud ice, the agency plans by 2009 to outfit hurricane-hunter planes with a $13 million storm-imaging radar system to supplement satellite data.

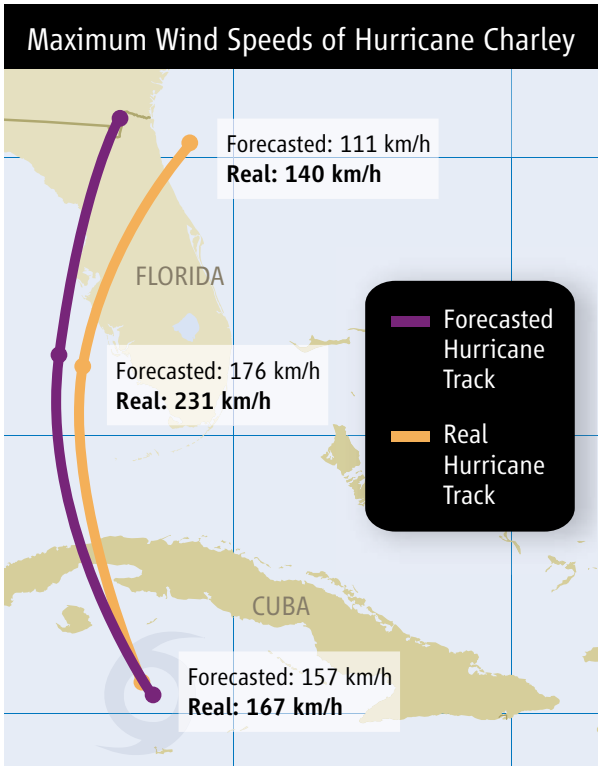

Blown away. Hurricane Charley in 2004 turned out to be much more powerful than forecasters predicted 18 hours before Florida landfall.

But Snow and others question whether those efforts will be enough to solve the intensity riddle. NOAA's new modeling effort will image features on a 9-kilometer-square grid. But that's much too crude to detect clues about a key phenomenon called a "replacement cycle"—in which outer rainbands can dissipate or later strengthen the storm's most intense inner winds. Those events occur on scales as small as 1 kilometer, Snow says, adding that NOAA will be "consistently underestimating storms" unless it can image such features.

Some scientists also feel that nascent efforts by NOAA to link ocean conditions and hurricane intensity are going too slowly. The modeling community and NOAA have available only a half-dozen data sets that relate ocean currents to hurricane strength, a situation physical oceanographer Lynn Shay of the University of Miami in Florida calls "pathetic." The same shortcoming exists for ocean waves, says Shay, adding that "you can't do coupled models without having ocean and atmospheric data."

Shay would like NOAA to ask academic scientists to help it design buoys or probes to generate more data. Snow's group also proposed a new advisory board on hurricane modeling, drawn from the wider academic community, as well as a new, bolstered hurricane center that would include NOAA's applied research.

NOAA, which received $3 million of supplemental funding this year to speed modeling efforts, defends its current intensity approach. The agency already spends $26 million a year for computing needs in weather, climate, and ocean prediction, and Louis Uccellini, head of NOAA's prediction operations in Camp Springs, Maryland, fears that focusing efforts on resolution alone would overshadow efforts to integrate data, study storm dynamics, or link atmospheric effects with the ocean. "There are no silver bullets," he says. A model with finer resolution could also eat up the limited computing time the agency has to model a storm as it approaches. In fact, some scientists say it's impossible to know whether a 1-km-resolution model would actually lead to better intensity forecasting because the eye-replacement cycle is only one of a number of factors that might lead to better forecasts.

Officials say recent practice runs using a GFDL model souped up with code for cloud physics and other phenomena were on average 20% more accurate in predicting the intensity of major storms in the past 3 years. And the developers of the next-generation model should reap the benefits, says Bender: "We're making great strides."

–ELI KINTISCH

SOURCE: NOAA

After making the difficult decision to turn in their adviser for scientific misconduct, a group of graduate students is trying to recover from the resulting damage to their careers

Truth and Consequences

MADISON, WISCONSIN—In those first disorienting months, as fall last year turned to winter and the sailboats were hauled out of nearby lakes, the graduate students sometimes gathered at the Union Terrace, a popular student hangout. There, they clumped together at one of the brightly colored tables that look north over Lake Mendota, drinking beer and circling endlessly around one agonizing question: What do you do when your professor apparently fakes data, and you are the only ones who know?

Chantal Ly, 32, had already waded through 7 years of a Ph.D. program at the University of Wisconsin (UW), Madison. Turning in her mentor, Ly was certain, meant that "something bad was going to happen to the lab." Another of the six students felt that their adviser, geneticist Elizabeth Goodwin, deserved a second chance and wasn't certain the university would provide it. A third was unable for weeks to believe Goodwin had done anything wrong and was so distressed by the possibility that she refused to examine available evidence.

Two days before winter break, as the moral compass of all six swung in the same direction, they shared their concerns with a university administrator. In late May, a UW investigation reported data falsification in Goodwin's past grant applications and raised questions about some of her papers. The case has since been referred to the federal Office of Research Integrity (ORI) in Washington, D.C. Goodwin, maintaining her innocence, resigned from the university at the end of February. (Through her attorney, Goodwin declined to comment for this story.)

Although the university handled the case by the book, the graduate students caught in the middle have found that for all the talk about honesty's place in science, little good has come to them. Three of the students, who had invested a combined 16 years in obtaining their Ph.D.s, have quit school. Two others are starting over, one moving to a lab at the University of Colorado, extending the amount of time it will take them to get their doctorates by years. The five graduate students who spoke with *Science* also described discouraging encounters with other faculty members, whom they say sided with Goodwin before all the facts became available.

> **"Here I am, I've invested so much time in grad school,** and this happens. If we let someone know …"
>
> —Chantal Ly

Fraud investigators acknowledge that outcomes like these are typical. "My feeling is it's never a good career move to become a whistleblower," says Kay Fields, a scientific investigator for ORI, who depends on precisely this occurrence for misconduct cases to come to light. ORI officials estimate that between a third and half of nonclinical misconduct cases—those involving basic scientific research—are brought by postdoctoral fellows or graduate students like those in Goodwin's lab. And the ones who come forward, admits ORI's John Dahlberg, often suffer a "loss of time, loss of prestige, [and a] loss of credibility of your publications."

Indeed, Goodwin's graduate students spent long hours debating how a decision to alert administrators might unravel. Sarah LaMartina, 29, who gravitated to biology after its appeal outshone her childhood plan to become a veterinarian, had already spent 6 years in graduate school and worried whether all that time and effort would go to waste. "We kept thinking, 'Are we just stupid [to turn Goodwin in]?' " says LaMartina, whose midwestern accent reflects her Wisconsin roots. "Sure, it's the right thing to do, but right for who? … Who is going to benefit from this? Nobody."

Shock waves

Goodwin, in her late 40s, had come to the University of Wisconsin in 2000 from Northwestern University in Chicago, Illinois, and was awarded tenure by UW soon after. Landing in Wisconsin was something of a homecoming for her; she had done a postdoc under Judith Kimble, a prominent developmental geneticist in the same department.

CREDIT: GREG ANDERSON/GETTY IMAGES

Career conundrum. Chantal Ly, in her adviser's now-vacant lab, faced wrenching choices after she and fellow graduate students began questioning the contents of their boss's grant application.

Goodwin studied sex determination in worms during their early development and has published more than 20 papers on that and other subjects in various prominent journals (including, in 2003, *Science*). Goodwin was also the oldest of a crop of female faculty members hired in recent years by genetics department chair Michael Culbertson. "She was the role model," he says.

In the beginning, the Goodwin lab had a spark. Students recall being swept up in its leader's enthusiasm when, seeking a lab in which to settle, they rotated through for a month during their first year of graduate school. Goodwin pushed her students to believe that compelling scientific results were always possible, boosting their spirits during the low points that invariably strike Ph.D. hopefuls. She held annual Christmas parties at her home west of Madison. Once, she took the entire lab on a horseback-riding trip.

Then, last October, everything changed. One afternoon, in the conference room down the hall from the lab, Ly told Goodwin she was concerned about her progress: The project she'd been working on, Ly felt, wasn't yielding usable results. Despite months of effort, Ly was unable to replicate earlier observations from the lab.

"At that time, she gave me three pages of a grant [application]," Ly recalled recently. The proposal, which was under review at the National Institutes of Health (NIH), sought to broaden a worm genetics project that another student, third-year Garett Padilla, had begun. Goodwin, Ly says, told her that the project, on a new, developmentally important worm gene, was "really promising, but there's so many aspects of it there's no way he can work on everything." Goodwin urged Ly to peruse the pages and see whether the gene might interest her as a new project.

Reading the grant application set off alarm bells for Ly. One figure, she quickly noticed, was represented as unpublished data even though it had appeared in a 2004 paper published by Goodwin's lab.

Ly and Padilla sat back to back at desks in the corridor outside the lab. When she showed him the pages from the grant application, he too was shaken. "There was one experiment that I had just not done," as well as several published and unpublished figures that seemed to have been manipulated, he says. Two images apparently identical to those already published were presented as unpublished and as representing proteins different from the published versions. "I remember being overwhelmed and not being able to deal with it at that moment," says Padilla.

A bearish 25-year-old with a closely cropped beard and wire-rimmed glasses, Padilla speaks softly, with deliberation. Bored by bench work, he was considering leaving biology research for law school and had discussed the possibility with Goodwin. She had urged him to "stick it out," he says. "Everybody goes through a phase where they don't want to be here," he recalls Goodwin telling him.

Happier times. The lab poses for a group shot, including (*front row*) Professor Elizabeth Goodwin in blue, Sarah LaMartina in white, Chantal Ly in gray, (*back row*) Garett Padilla in red, postdoc Scott Kuersten in black, and Mary Allen in green.

At a loss after seeing the grant application, Padilla consulted two scientists for advice: his fiancée's adviser, a physiology professor at the university, and Scott Kuersten, a former postdoc in Goodwin's lab who had been dating LaMartina for several years and who happened to be in town. Kuersten and Padilla talked for about an hour and together examined the papers cited in the proposal. Kuersten, now at Ambion, a biotechnology company in Austin, Texas, advised Padilla to ask Goodwin for an explanation, as did the physiologist.

Padilla steeled himself for a confrontation. On Halloween day, he paced nervously outside Goodwin's office, summoning the courage to knock. The conversation did not go well, says Padilla.

In a computer log of events he had begun to keep at Kuersten's urging, which he shared with *Science*, Padilla wrote that Goodwin denied lifting a Western blot image from a published paper and presenting it as unpublished work, although, he added in the log, "She became extremely nervous and repeatedly said, 'I fucked up.' " Padilla also noted: "I left feeling that no issues were resolved." His confusion deepened when Goodwin later that day blamed the problem on a computer file mix-up.

Meanwhile, word was leaking out to others in the lab that something was terribly wrong. Two days later, Padilla called a meeting of all current lab members: six graduate students and the lab technician. To ensure privacy, the group, minus Ly, who had recently had a baby girl, convened in the nearby engineering library. Padilla laid out the grant papers for all to see.

In that meeting, ensconced in the library, the grad students hesitated at the thought of speaking with the administration. "We had no idea what would happen to us, we had no idea what would happen to Betsy, we had no idea how the university would react," says LaMartina, who admits to some distrust of authority and also a belief that people who err deserve a second chance.

Ly felt less charitable toward Goodwin but confesses that at first she considered only her own predicament. In many ways, just reaching graduate school was a triumph for Ly, and she badly wanted that doctorate. In 1981, when Ly was 8 years old, her family fled Cambodia for the Chicago suburbs. Around Ly's neck hangs a gold-plated French coin, a 20-franc piece her curator father had collected before he was killed in his country's civil war.

In Chicago, Ly's mother worked long hours and put her daughter through Wellesley College in Massachusetts. When Ly moved to Madison, so did her husband, now an anesthesia resident, and her mother, who speaks little English and cannot drive. "Here I am, I've invested so much time in grad

CREDIT: COURTESY OF MARY ALLEN

school, and this happens. If we let someone know …" she says, her voice trailing off.

The students decided that Padilla needed to speak with Goodwin a second time, in hope of extracting a clear account of what went wrong or even a retraction of the grant application. Four days after his first nerve-wracking encounter, Padilla was in Goodwin's office again. This time, the conversation put him at ease. Padilla says Goodwin asked for forgiveness and praised him for, as he wrote in the log, "pushing this issue." She told him that the grant application was unlikely to be funded—an assertion that turned out to be untrue given that NIH approved it—but offered to e-mail her NIH contact citing some of the problems in the application. Goodwin subsequently sent that e-mail, on which Padilla was copied. He left the encounter relieved.

"At that point, I was pretty content to leave it alone," he says. "I felt like we had compromised on a resolution."

A wrenching choice

Another student, however, was finding little peace. Mary Allen, 25 and in her fourth year of graduate school, couldn't shake a sense of torment about what her mentor might have done. A bookworm who squeezed 3 years of high school into one and entered college at age 15, Allen is guided by unambiguous morals and deep religious convictions, attending a local church regularly and leading a youth group there. She could not fathom that Goodwin had falsified data; at one point, Allen refused even to examine another suspect grant application. But, concerned because Goodwin seemed to have admitted to some wrongdoing, Allen felt she needed to switch labs.

Allen alerted Goodwin that she would likely be moving on. Their mentor then began offering additional explanations for the grant application, say Allen and the others. Goodwin told them that she had mixed up some files and asserted that the files had come to her unlabeled. In a private conversation with Allen, she adamantly denied faking data.

As November wore on, the lab's atmosphere grew ever more stressful and surreal. When Goodwin was present, she chatted with the students about their worm experiments and their families—the same conversations they'd always had.

> **"I remember being overwhelmed** and not being able to deal with it at that moment."
>
> —Garett Padilla

Yet the strain was taking its toll. LaMartina's appetite declined, and she began losing weight, shedding 15 pounds before the ordeal was over. Padilla called former postdoc Kuersten nearly weekly for advice, and the students talked obsessively with one another. Careful to maintain confidentiality, "the only people we could bounce ideas and solutions off of were each other," says Padilla. The tension even penetrated Goodwin's annual Christmas party. For the first time, several lab members didn't show up.

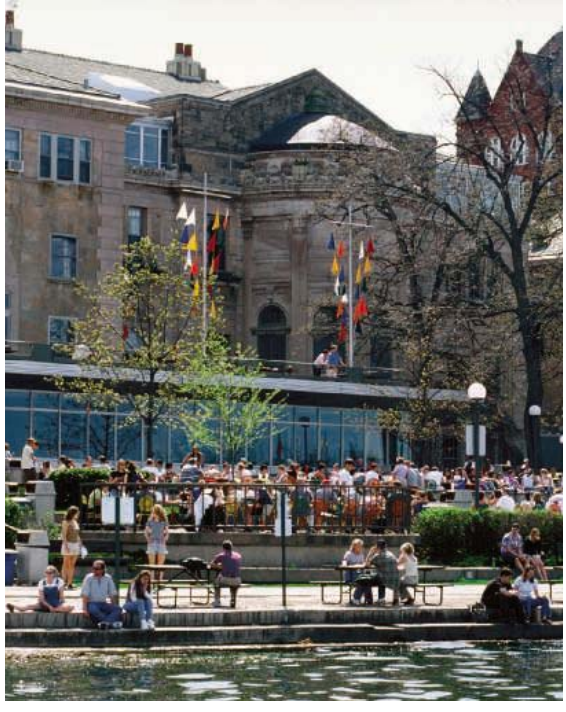

Gathering place. Most students in Madison hit the Union Terrace for fun and food, but the lab's graduate students had weightier issues on their minds.

Deeply worried about how speaking with administrators might impact the more senior students, lab members chose not to alert the university unless the desire to do so was unanimous. Gradually all, including Ly and LaMartina, the most senior among them, agreed that their mentor's denials left them uncomfortable and concerned that she might falsify data in the future. "My biggest worry was what if we didn't turn her in … and different grad students got stuck in our position," says Allen.

Two days before exams ended, on 21 December, Ly and Padilla met together with Culbertson and showed him the suspect grant pages. Culbertson didn't know what to think at first, he says, but "when somebody comes to me with something like that, I have to investigate."

A surprise resignation

Culbertson quickly referred the matter to two university deans, who launched an informal inquiry to determine whether a more formal investigation was warranted. As is customary, Goodwin remained on staff at the university during this time. She vigorously denied the charges against her, telling Culbertson and the students in a joint meeting that the figures in question were placeholders she had forgotten to swap out. According to Padilla's log of that meeting, Goodwin explained that she "was juggling too many commitments at once" when the proposal was submitted.

Two biology professors ran the informal inquiry, conducting interviews with Goodwin and her students. One of the two, Irwin Goldman, was also a dean, and he became the students' unofficial therapist and news source. At their first meeting in January, Goldman reassured the six that their salaries would continue uninterrupted.

The informal inquiry wrapped up a few weeks later, endorsing a more formal investigation. Three university deans, including Goldman, appointed three faculty scientists to the task.

At about this time, says Goldman, the university grew uneasy about possible fraud not only in the first grant application that the students had seen but also in two others that had garnered funding, from NIH and the U.S. Department of Agriculture. The school canceled all three grants. After a panicky 2 weeks during which the lab went unfunded, Goldman drew on money from both the college of agricultural and life sciences and the medical school. (Goodwin had a joint appointment at the two.) The students peppered Goldman regularly with questions, seeking advice on whether to talk to a local reporter or how their funding might shake out.

Still, because privacy rules prevented sharing the details, "we felt isolated up on our floor," says Padilla. "There were faculty nearby, but they didn't really know what was going on." Goodwin, meanwhile, all but disappeared from the lab, appearing only once or twice after the investigation began. The students tried to keep up with their projects as they'd always done. They held lab meetings

CREDIT: JEFF MILLER/UNIVERSITY OF WISCONSIN, MADISON

alone before being invited to weekly gatherings with geneticist Philip Anderson's lab.

Most faculty members were aware that an investigation had been launched, and some had heard that Goodwin's students were the informers. That led to disheartening exchanges. A faculty member, asked by one of the students whether they'd done the right thing, told her he didn't know. Rumors reached the students that Goodwin had had "to fake something because her students couldn't produce enough data," says Ly.

In late February, Goodwin resigned. The students say they learned of her departure from a biologist who worked in a neighboring lab.

Three months later, the university released its investigation report, which described "evidence of deliberate falsification" in the three applications for the cancelled grants, totaling $1.8 million in federal funds. In the school's report, which university officials shared with *Science*, investigators also raised questions about three published papers, in *Nature Structural and Molecular Biology*, *Developmental Biology*, and *Molecular Cell*.

None has been retracted or corrected so far. "We are considering the implications" of the university report, said Lynne Herndon, president and CEO of Cell Press, which publishes *Molecular Cell*, in a statement. The editor of *Nature Structural and Molecular Biology* said she was awaiting the results of the ORI investigation, and the other authors of the *Developmental Biology* paper are reviewing the relevant data, says the journal's editor in chief, Robb Krumlauf of the Stowers Institute for Medical Research in Kansas City, Missouri.

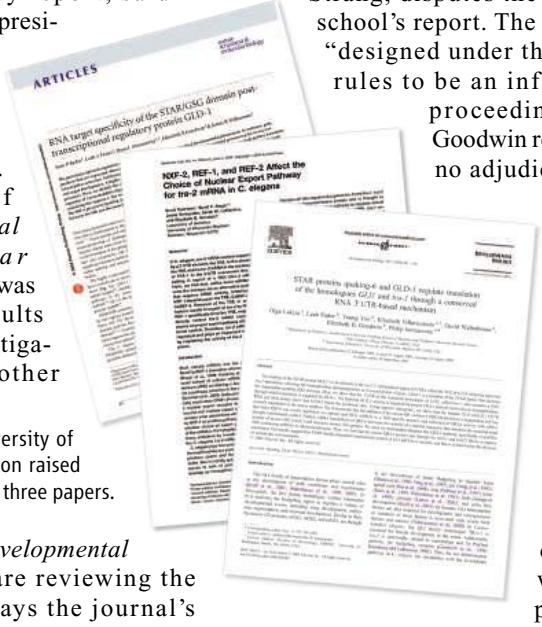

Questioned. A University of Wisconsin investigation raised concerns about these three papers.

The university investigators also noted other problems in the Goodwin lab. "It appears from the testimony of her graduate students that Dr. Goodwin's mentoring of her graduate students included behaviors that could be considered scientific misconduct—namely, pressuring students to conceal research results that disagreed with desired outcomes and urging them to over-interpret data that the students themselves considered to be preliminary and weak," they wrote in their report.

Goodwin's lawyer in Madison, Dean Strang, disputes the reliability of the school's report. The investigation was "designed under the applicable UW rules to be an informal screening proceeding," and, because Goodwin resigned, "there was no adjudicative proceeding at the administrative level or elsewhere," Strang wrote in an e-mail message. He added that "there are no problems with the three published papers cited in the report (or any others)." Strang declined to address whether Goodwin pressed students to overinterpret data. "Dr. Goodwin will not respond at all to assertions of students in this forum," he wrote.

Seeking a new start. The possibility that her mentor had faked data left grad student Mary Allen determined to switch labs.

Uncertain future

Culbertson distributed the investigating committee's report to all department faculty members; it even appeared on Madison's evening news. Still, the rapprochement some of the students had hoped for never materialized. "No one ever came up and said, 'I'm sorry,' " Padilla says.

As the graduate students contemplated their futures this spring, they did have one point in their favor: Ironically enough, the sluggish pace of their projects meant that almost none had co-authored papers with Goodwin. But when several of them sat down with their thesis committees to assess their futures, the prognosis was grim. Only one student of the six, who did not reply to *Science*'s request for an interview, was permitted to continue with her original project. She has moved to another Wisconsin lab and hopes to complete her Ph.D. within about a year, according to the others.

Thesis committees and faculty members told Ly, LaMartina, and fourth-year Jacque Baca, 27, that much of their work from Goodwin's lab was not usable and recommended that they start over with a new doctoral project. The reason wasn't necessarily data fraud, the students say, but rather Goodwin's relentless optimism that some now believe kept them clinging to questionable results. Allen, for example, says she sometimes argued but gave in to Goodwin's suggestions that she stick with molecular data Allen considered of dubious quality or steer clear of performing studies that might guard against bias. Ly, on her third, floundering project, says, "I thought I was doing something wrong experimentally that I couldn't repeat these things."

Despite her setback, Baca has chosen to stay at Wisconsin. "It's kind of hard to say" how much time she'll lose, says Baca, who notes that her thesis committee was supportive in helping her find a new lab.

CREDIT (TOP): KIM COOK/GETTY IMAGES

The other four—Ly, LaMartina, Padilla, and Allen—have scattered. Only Allen plans on finishing her Ph.D. Determined to leave Wisconsin behind, she relocated in late March to the University of Colorado, Boulder, where she hopes to start fresh. Members of her church, her husband, and her parents persuaded her to stay in science, which she adores, but she still wonders about the future. "We unintentionally suffer the consequences" of turning Goodwin in, Allen says, noting that it will now take her 8 or 9 years in all to finish graduate school. To her husband's disappointment, their plans for having children have been deferred, as Allen always wanted to wait until she had completed her degree.

For Padilla, the experience cemented the pull of the law. In late July, a month after his wedding, he and his wife moved to Minneapolis-St. Paul, Minnesota, not far from where Padilla grew up, because his wife's adviser, the physiologist, had shifted his lab there. Padilla began law school in the city last week.

LaMartina spent 2 months in a different Wisconsin genetics lab, laboring over a new worm project she'd recently started under Goodwin. That project, however, fell apart in June. She then spent 3 weeks in Seattle and Alaska with Kuersten. During the trip, LaMartina abandoned her Ph.D. plans, and in July, she left Wisconsin for Texas, joining Kuersten at Ambion as a lab technician.

"Sure it's the right thing to do, but right for who?"
—Sarah LaMartina

When Ly learned from her thesis committee that her years in the Goodwin lab had come to naught, she left the program and, as a stopgap, joined a cancer lab as a technician. "I decided that I had put my life on hold long enough," Ly says. She intends to leave science altogether and is considering business school.

For Goldman, the dean who supported the graduate students, the experience was bittersweet. Impressed by the students' professionalism and grace under trying circumstances, he came to believe strongly that science needs individuals like them. And although he admits that it's "horrible" that so many of the students were told to start over, "I don't see us changing our standards in terms of what a Ph.D. means," he says.

Still, Goldman does plan to craft formal policies for students who might encounter this situation in the future. The policies, he says, would guarantee that the university protects students from retribution and that their funding remains secure. He hopes that codifying such safeguards will offer potential whistleblowers peace of mind.

In a building with a lobby graced by a fountain shaped like DNA, the Goodwin lab now sits deserted on the second floor. Incubators, pipettes, and empty plastic shoeboxes that once held worms litter its counters. Ly's original fear months before, that something bad would happen to the lab, had proved more prescient than she had imagined.

–JENNIFER COUZIN

PROFILE: THOMAS KAPLAN

From Making a Killing to Saving a Species

A retired financier turned philanthropist is making an unprecedented investment in conservation science to help save the big cats

Thomas Kaplan was a long way from his usual Wall Street habitat. The wealthy financier spent 4 days last year tracking a 3-year-old leopard named Ngoye in the humid woodlands of northern KwaZulu-Natal Province in South Africa. Along with Luke Hunter, a wildlife biologist for the New York–based Wildlife Conservation Society (WCS), and Guy Balme, a graduate student at the University of KwaZulu-Natal, Durban, Kaplan was silently willing Ngoye to cross from private lands, which were off-limits to the trio, into the Phinda Game Reserve so they could replace her radio collar. Just as they were about to give up and head back to Cape Town, Ngoye finally entered the reserve. Balme quickly tranquilized her and replaced her collar.

The trek turned out to be a pivotal experience—and not just for the 43-year-old Kaplan, who was fulfilling a lifelong dream to study big cats. After he learned that Balme was struggling to find the money to complete his master's degree, Kaplan wrote a $20,000 check to cover Balme's expenses for 2 years. That philanthropic act was just the start: Kaplan decided there and then to launch a grants program with WCS for graduate students working on cat conservation. So far, he has given $307,000 to 20 students at institutions all over the world, with a goal of spending $500,000 a year. Balme says he now plans to pursue a Ph.D. in zoology.

On the move. Biologist Alan Rabinowitz searches for tigers in Laos.

CREDIT: SALISA RABINOWITZ

Graduate students aren't the only beneficiaries of Kaplan's largess. Since his trek, Kaplan has pledged $13 million over 10 years for a variety of cat-related conservation efforts, making him quite possibly the largest individual source of research support for such efforts around the world. Conservation scientists say that his long-term philanthropic commitment promises not only to give them more tools with which to save these magnificent beasts but also to nurture the next generation of conservationists. "I don't think anyone else is in this bracket," says conservation

biologist John Seidensticker of the Smithsonian Institution's National Zoo in Washington, D.C.

Cat lover

Kaplan, who grew up in New York City, says books such as Jim Corbett's *The Man-Eating Leopard of Rudraprayag* fueled his passion for big cats. By the age of 11, he had tracked bobcats in Florida, sighted a panther, and searched for jaguars in the Amazon. "Their gait is self-assured, their bearing confident, their coats are brilliant and practically glow with the richest hues," he enthuses.

Despite his interest in animals, Kaplan decided to make his mark in the financial world. After finishing a Ph.D. in history from Oxford University, Kaplan managed hedge funds before founding Apex Silver Mines in 1993. Helped by an investment from the Soros family, Apex became one of the world's largest silver-mining companies; *Forbes* magazine estimated that Kaplan's 20% stake in the company was worth $70 million in 2000. In late 2004, Kaplan retired from Apex; since then, he has founded an energy company and another firm that explores for precious metals around the world.

However, those interests leave him plenty of time for philanthropy. He endowed The Lillian Jean Kaplan Renal Transplantation Center at the University of Miami, Florida, after his mother died of kidney disease in 2002 and helped set up a prize for research on the disease.

Kaplan was introduced to modern conservation efforts through reading *Jaguar*, a book by WCS wildlife biologist Alan Rabinowitz about setting up the world's first jaguar preserve in Belize. "I felt an immediate, indeed, filial, affection for the man and a knowing connection to the depth of his passion," Kaplan says. "I resolved one day to help him fulfill his biggest ambitions in the way that he had unknowingly lived all of mine."

After leaving Apex, Kaplan called Rabinowitz, who suggested that Kaplan familiarize himself with WCS by visiting Hunter's project in South Africa. "I've dealt with donors since 1978 … I could tell he was real," Rabinowitz says. "It's very rare for someone to say big cats have been a lifelong passion."

Setting targets

Experts warmly welcome Kaplan's decision to continue supporting the work of students he has funded. Explains Seidensticker: "The problem for many graduate students is that they get a degree, go back to their countries, and there are no support bases. They get drawn away from the field." The 20 graduate students currently receiving funding are conducting research on wild cats in Africa, Asia, Central and South America, and elsewhere. Their projects include a conservation plan for the 15 remaining Armenian leopards and a study of how young cougars disperse through developed lands around Yellowstone National Park.

The scholarships are funded through Panthera, a foundation Kaplan created that is also contributing $10 million (half of it from Michael Cline, a venture capitalist in Greenwich, Connecticut) toward a conservation project in Asia called Tigers Forever. The project works with local governments and landowners to address conservation issues and is modeled after Rabinowitz's jaguar conservation program in Latin America. (In April, Rabinowitz helped persuade eight governments in the region to incorporate a jaguar corridor within the ongoing Mesoamerican Biological Corridor initiative, running from Mexico to Panama.)

The novelty of Tigers Forever, Rabinowitz says, is the setting of specific recovery targets—an average 50% increase over 10 years across the nine sites at which WCS works. "It holds our feet to the fire and makes us more accountable than anything ever done in conservation before," Rabinowitz says. "That's an extraordinary thing to do," says Seidensticker.

Two months ago, Kaplan finalized plans with WCS for Project Leonardo, which will evaluate the status of lions in Africa and plan for their conservation. Kaplan and WCS have each committed $750,000 over 3 years for the effort, named for Kaplan's 4-year-old son, and he anticipates extending his commitment if the project meets its goals.

This fall, he plans to start an annual $50,000 lifetime achievement award for big cat conservation, joined next year by a $25,000 young scientist award in the field. With other projects in mind, Kaplan expects his commitment to top $20 million within 5 years. "I hope to collaborate with like-minded people who have passion for big cats," he says. "I'm willing to put serious money to get this done."

–DIANE GARCIA AND ERIK STOKSTAD

CREDIT: LUKE HUNTER/WCS

Radio contact. Tom Kaplan (*left*) helps Guy Balme change Ngoye's radio collar after sedating the leopard inside the Phinda Game Reserve in South Africa.

Open to anything

The Agilent DNA Microarray Platform enables research on your own terms

As a genomics researcher, you need tools that empower rather than impede. Whether you're searching for low-abundance gene expression targets, performing genome-wide scans on whole blood samples or adopting emerging applications such as oligo array CGH or ChIP-on-chip, you need a microarray platform that has the flexibility, sensitivity and genome coverage that your research requires. A platform that will keep your research moving forward, wherever it takes you.

To hear from researchers who are charting their own course in Genomics **visit www.OpenGenomics.com**

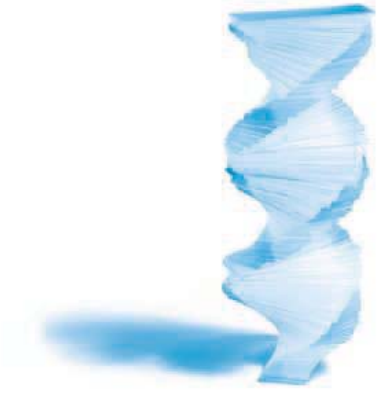

Agilent Technologies

ECOLOGY

Plant Wannabes

Sea slugs that take in chloroplasts or algae make the photosynthesizers feel right at home

VIENNA, AUSTRIA—Some sea slugs have figured out how to act like plants or at least like coral. Several species of these shell-less mollusks carry algae or chloroplasts in cells of their digestive glands. The slugs acquire the algae or the organelles from their diet and harvest the carbohydrates or lipids the chloroplasts produce by photosynthesis.

Researchers have known for decades about these partnerships, but only through histological studies. Now, they are watching them in action. In presentations here last month at the International Symbiosis Society Congress, two research teams described how they have brought sea slugs into the lab and begun to use the latest molecular techniques to reveal the secrets of the symbiotic relationships.

They reported that algae and even naked chloroplasts can function for months inside a slug and that one sea slug species has acquired algal genes to help such a partnership thrive. The discoveries are "nice examples of coevolution," says Jörg Ott, a marine biologist at the University of Vienna.

Ingo Burghardt, a zoologist at Ruhr University in Bochum, Germany, has focused on *Phyllodesmium*, a sea slug genus with species that salvage algae from the soft corals they eat. Working with Heike Wägele of the University of Bonn, Burghardt has demonstrated that slugs hosting microscopic algae called zooanthellae can last without food for up to 260 days, thanks to contributions from the algae. The longevity of the zooanthellae—and the sea slug's ability to withstand starvation—seems tied in part to the slug's evolution of a complex midgut that houses the algae, Burghardt reported.

Dietary supplements. The flowing branches of this sea slug house photosynthesizing algae (brown) taken from the soft coral it eats.

To understand how sea slug–zooanthellae partnerships arose, Burghardt has been working out the *Phyllodesmium* family tree by comparing each species' ribosomal DNA. At the same time, he has been examining the digestive systems of slugs within this group. He uses a fluorometer, which measures energy released in the form of fluorescence during photosynthetic reactions, to monitor the efficiency of photosynthetic activity when the slugs are given no access to food.

So far, he's found that various sea slug species differ in the complexity of their digestive gland, the size of dorsal appendages that contain these branches, and their ability to keep zooanthellae. When such features are overlaid onto the slug family tree, "you can see that species that have similar digestive-gland structures group together," he said. Moreover, there is a correlation between a species' success at keeping zooanthellae—and itself—alive and the degree of branching in its digestive gland. "Species with highly branched glands hold on to their zooanthellae a longer time," he reported.

The algae turn *Phyllodesmium* slugs the same color as the soft corals they eat, and Burghardt suspects that this camouflaging originally prompted the evolution of a relationship between the two. Only later, he surmises, did the slugs evolve the ability to use the zooanthellae's photosynthesizing as a food source. And as it did, it made more room by adding on to its digestive glands. "What we see," says Ott, "is an interplay between dependence on symbiosis and the development of special organs."

Mary Rumpho, a biochemist at the University of Maine, Orono, and her colleagues have been studying an even more intriguing relationship: the sea slug *Elysia chlorotica*'s dependence on chloroplasts. They found that *Elysia* eggs hatch into free-floating larvae that harbor no chloroplasts, but when University of Maine colleague Mary Tyler filmed juvenile sea slugs munching on their favorite seaweed, *Vaucheria litorea*, "we could literally watch the sea slug suck the chloroplasts out of the alga," says Rumpho. The ability to harness chloroplasts is critical: If the juveniles don't have access to this organelle, "they don't make it," Rumpho reported. Moreover, despite being removed from its normal algal home, the chloroplasts can continue to photosynthesize within the sea slug for most of the animal's 10-month life. "That's pretty spectacular," says Margaret McFall-Ngai of the University of Wisconsin, Madison.

Leaves of the sea. This sea slug harvests chloroplasts from its seaweed meals and depends on them for some of its energy needs.

It's perhaps not too surprising that sea slugs can house zooanthellae: These algae can survive on their own if they have to. But chloroplasts are dependent on proteins that are typically provided by the plant's nuclear genome. *Elysia*, it turns out, has what it takes to make the slug-chloroplast partnership work. At the meeting, Rumpho's graduate student Jared Worful described his discovery of large parts of two plant genes in the sea slug's DNA. "When [the sea slug] takes in the chloroplast, it has the machinery to keep the chloroplast active and happy," says David Richardson, a lichenologist at Saint Mary's University in Halifax, Canada.

Because these genes are not normally found in animals, Rumpho is convinced they originally came from ingested algae. "We're seeing the evolution of photosynthesis in an animal," says Rumpho.

–ELIZABETH PENNISI

CREDITS (TOP TO BOTTOM): M. E. RUMPHO *ET AL.*, *PLANT PHYSIOLOGY* **123** (MAY 2000); MICHAEL SCHROEDL

Sweet effects. Auxin helps prompt the growth and maturation of strawberries and other fruits.

PLANT SCIENCE

Auxin Begins to Give Up Its Secrets

Auxin controls the growth of plants and their interactions with their environment, but only now are researchers understanding the basics of this hormone

Next time you bite into a deliciously juicy strawberry or tomato, thank the seeds. As a fruit forms, its seeds produce a plant hormone called auxin, prompting the fruit to grow and ripen. Without seeds—and without auxin—fruit stays shrunken on the stem.

The wonders auxin works on strawberries and tomatoes are just the start. The hormone controls almost every aspect of plant growth, from putting down roots to determining where to start a new stem or leaf. It allows plants to react to their environment, shaping the response to signals such as light, gravity, and even the presence of bacteria. Auxin is so fundamental that one leading researcher has called it the brains of the plant world. "I got in a fair amount of trouble for saying that" in a radio interview, Ottoline Leyser of the University of York in the United Kingdom ruefully admits, cautioning that the comparison can be taken too far. "But the useful analogy is that it's an information-processing system."

Auxin has fascinated and puzzled plant scientists for more than 100 years. In 1880, Charles Darwin and his son Francis wrote in *The Power of Movement in Plants* about a substance that seemed to be produced at the tip of growing plant shoots, prompting them to bend toward light. It was one of the first scientific descriptions of the action of auxin. (There are several closely related hormones known collectively as auxin.) But it wasn't until the 1930s that scientists identified the chemical structure of the most common plant auxin, indole-3-acetic acid (IAA). Since then, auxins and their synthetic cousins have been used to boost plant growth—and to kill weeds. Too much auxin is actually deadly to plants; the herbicide 2,4-D is a synthetic auxin, and Agent Orange contains a combination of synthetic auxins.

Several recent advances have helped give scientists a better picture of this multitalented hormone. They have finally identified the receptor that senses auxin's presence, and the transport system that plants use to control levels of the hormone is becoming clearer. Researchers have also found clues to the fundamental mystery of how plants make auxin—still a surprisingly difficult question. They are even unearthing new roles for auxin in plants' defenses against pathogens. To tackle such complexities, several groups are developing computer models that can keep track of dozens of genes that control or respond to auxin in growing roots or new branches.

All of this is helping to explain how a relatively simple molecule such as auxin can perform such versatile tasks. "It's a very general signaling system," says Leyser.

Target found

Last year, scientists solved one of the biggest outstanding questions in plant biology when two groups reported that they had finally identified the auxin receptor (*Science*, 27 May 2005, p. 1240). It turns out that the long-sought protein was hidden in plain sight.

In papers published simultaneously in *Nature*, Leyser and her colleagues and Mark Estelle of Indiana University, Bloomington, and his research group showed that auxin binds directly to a protein called TIR1. Scientists already knew that the hormone's presence in plant cells triggers TIR1 to bind to a class of proteins called Aux/IAA, which repress genes known to be triggered by auxin. But most people assumed that auxin turned on such genes by setting off a long signaling cascade, involving numerous proteins and feedback loops.

In fact, the cascade is just a few steps: Auxin binds to TIR1, which is part of a molecular complex that attaches the cell's garbage tag, ubiquitin, to proteins destined to be recycled. Auxin, by glomming onto TIR1, helps the complex ubiquitinate Aux/IAA proteins. When the Aux/IAA proteins are broken down, the genes they had repressed turn on. The find "has really simplified things," Estelle says. Adds Leyser: "I'm just massively relieved that we have a signal-transduction pathway that starts at auxin and ends at gene expression, and that all the parts are there."

The find also triggered interest beyond the auxin field. TIR1 is one of roughly 700 so-called F-box proteins already identified in plants and long suspected of playing a role in ubiquitination. The auxin connection suggests that similar small molecules in plants might join with these F-box proteins to direct the breakdown of proteins, Estelle says. Animals, too, have hundreds of F-box proteins.

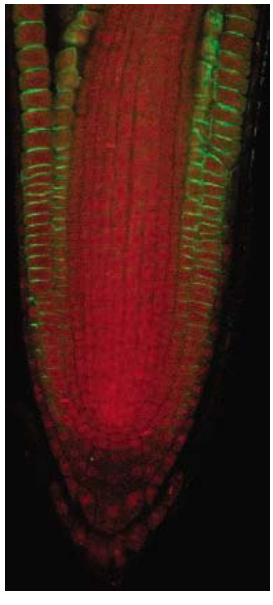

One way. Auxin transporters such as PIN2 (green) help determine which way the hormone flows in growing root tissues.

A deeper look at the auxin-TIR1 interaction has turned up a surprise. Estelle and structural biologist Ning Zheng of the University of Washington, Seattle, have teamed up to solve the crystal structure of TIR1—both with and without auxin. Small molecules that interact with proteins such as TIR1 often change the shape of the target protein. But, as Estelle and Zheng have described at meetings this summer, TIR1 keeps its shape when united with auxin. Auxin, Zheng says, appears to act as "a molecular glue," helping TIR1 bind to the Aux/IAA proteins. Zheng, who works in a pharmacology department, says this discovery serves as a reminder for drug developers: Instead of just seeking molecules that disrupt binding, it might be useful to also search for those that encourage binding.

CREDITS (TOP TO BOTTOM): PHOTOS.COM; RANJAN SWARUP

Transport streams

Before auxin can interact with TIR1 to unleash gene activity, it needs to get to the right place in the right amount. A picture is gradually emerging, says Leyser, of a system of checks and balances that provide stable yet flexible auxin signals for plant growth and development. A plant regulates auxin levels in its cells by manipulating auxin production, making use of specialized transporters that either allow auxin into a cell or pump it out, and adjusting how quickly cells break down the molecule.

One key to this tight control of auxin is a family of proteins called PIN-FORMED or PINs, named for the pin-shaped, flowerless shoots grown by *Arabidopsis* mutants lacking the proteins. In May, Eva Zazimalova of the Institute of Experimental Botany in Prague, Czech Republic, and her colleagues confirmed suspicions that this growth defect was due to an auxin dysfunction. They showed that PIN proteins can transport the hormone between cells and that they are distinct from a second group of well-known auxin transport proteins, called the PGPs (*Science*, 12 May, p. 914). In the same issue of *Science*, Jiri Friml of the University of Tübingen, Germany, and his colleagues report that the specific type and combination of different members of the PIN family, which localize to different sides of a plant cell, determine which direction auxin flows.

Other clues about auxin are coming from computer models that can begin to weave together the effects of dozens of genes. Several groups, including Elliot Meyerowitz of the California Institute of Technology in Pasadena and his colleagues, have developed transgenic *Arabidopsis* plants in which the PIN genes, among others, glow green during plant growth. The scientists film the plants' growth and use the digitized images to build models of the roles and reactions of key development genes in response to auxin. They can then use such a "virtual plant" to better understand how changing levels of the hormone affect different cells and tissues.

Illustrating the complexity of the task, Gerd Jürgens and his colleagues at the University of Tübingen have shown in several recent papers that, among other factors, specific combinations of the 29 different Aux/IAA proteins and 22 so-called auxin response factors control a plant cell's response to the hormone.

A strategic defense

Growing evidence suggests that RNA strands also play an important role in the auxin story. In April, for example, Jonathan Jones of the John Innes Centre in Norwich, U.K., and his colleagues revealed that RNAs appear to dampen auxin signaling when a plant is infected with certain bacteria. Plants can sense the presence of bacterial flagella and turn various genes on and off in response. And Jones's team showed that when a plant senses the bacteria, it ramps up production of certain microRNAs (miRNAs), short stretches of RNA that can interfere with the manufacture of specific proteins. They also showed that the miRNAs thwart the production of TIR1 and several related proteins.

Why would a plant interrupt its own auxin response? Perhaps to control plant-dwelling bacteria that also make auxin, says Estelle. Such bacteria, he speculates, use the hormone as part of their colonizing strategy. Extra auxin can trigger growth of new leaves, which might give the bacteria more living space. Indeed, says Estelle, there seems to be a sort of battle to control auxin between plant and pathogen. When the scientists disrupted the miRNA's ability to work, plants more easily succumbed to bacterial infection (*Science*, 21 April, p. 436).

The microbe-induced response isn't the first to implicate RNA interference in auxin signaling. Bonnie Bartel of Rice University in Houston, Texas, and her colleagues have found that miRNAs interfere with the expression of several auxin-responsive genes. She predicts that such interactions may be a common way plants regulate auxin's powers. Plant miRNAs "seem to have an overabundance of auxin-implicated genes in their repertoire of clearer control," says Bartel.

Although the regulation and effects of auxin are coming into focus, plant biologists have a somewhat embarrassing problem: They still do not know exactly how plants make the hormone. Researchers have worked out how bacteria produce auxin, but the technique used by plants has remained a mystery because it's not just complex but also multiplex. The hormone is so crucial to plant development that a nearly fail-safe system of backup production has evolved. If scientists try to knock out a gene that plays a role in the hormone's synthesis, another is available to jump in and take its place, thus obscuring the initial gene's importance.

A recent paper in *Genes and Development*, however, may have broken the impasse. Yunde Zhao and his colleagues at the University of California, San Diego, showed that a family of genes named after a growth-defective *Arabidopsis* mutant called *yucca* seems to play a key role in producing auxin during development. Although knocking out a single member of the gene family left the mustard plant's growth unperturbed, knocking out three or four at once generated severely misshapen leaves and flowers. Adding auxin back through the stem didn't rescue the plants, but by inserting a bacterial auxin-producing gene attached to a *yucca* promoter, the scientists produced nearly normal-looking plants.

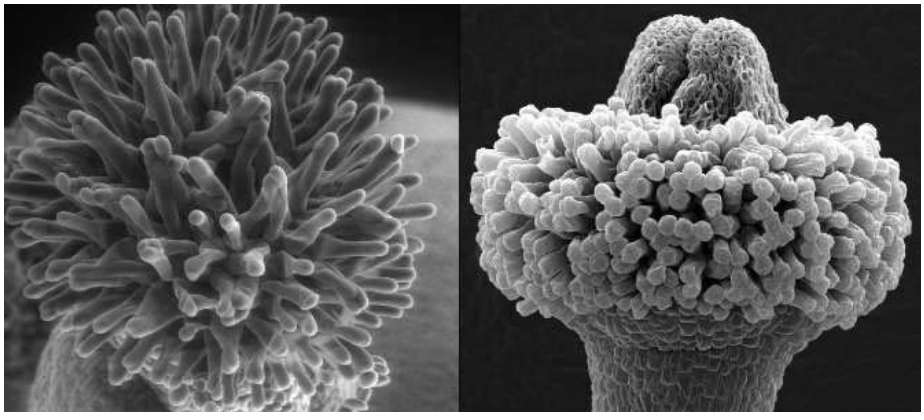

Misdirected development. Unlike a normal *Arabidopsis* (*left*), plants lacking several genes involved in auxin synthesis have flowers that fail to form properly (*right*).

CREDIT: YUNDE ZHAO/UCSD

The paper "is a huge step forward" in understanding the specific genes involved in plant auxin production, Estelle says. But Jerry Cohen of the University of Minnesota, Twin Cities, cautions that the story is far from solved: "Nothing has gotten to the point that you can say, 'This is how it's made.' "

As scientists sort out the pieces of how auxin is produced, moved, and blocked and broken down, it becomes clearer, says Leyser, that all the processes "interact and intertwine and interreact in horribly complicated feedback mechanisms." That makes any one part of the auxin system difficult to understand on its own. "It's necessary to think about it as an integrated system," she says. "It's hard science. You have to be moderately obsessed to stick with it. But that's also why it's so exciting."

–GRETCHEN VOGEL

EDITED BY YUDHIJIT BHATTACHARJEE

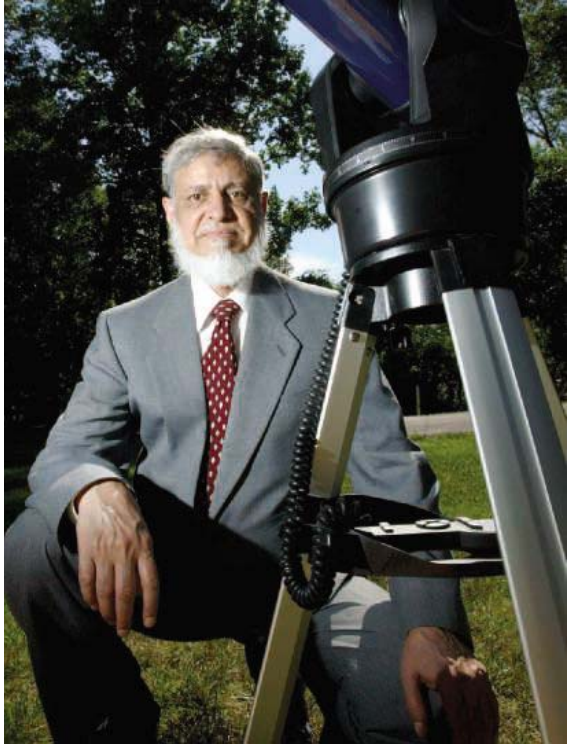

Pioneers

LET THE FEAST BEGIN. Thanks to Khalid Shaukat, Muslims in North America will no longer have to wait until the last moment to know when to begin Eid al-Fitr, the festival marking the end of the month-long Ramadan fast.

The holiday starts the morning after a new moon (approximately 23 October this year), and for 1400 years, Muslims have used moon sightings to determine that date and others in the Islamic calendar. But that practice has sparked disputes and made precise planning impossible. So for the past 20 years, Shaukat, 63 and a research engineer at the U.S. Nuclear Regulatory Commission in Silver Spring, Maryland, has used astronomical calculations to predict the dates when it should be possible to sight the new moon after sundown from somewhere on the earth. Now, a committee of Islamic jurists has adopted Shaukat's calculations as the basis for its calendar. Shaukat says he hopes "to make people understand that this is nothing new and is not against the jurisprudence of Qu'ran and Hadith."

Sayyid Syeed of the Islamic Society of North America thinks that the prophet Mohammed would have approved of this technical adjustment. "If it had been possible to do such exact calculations," Syeed says, "the Prophet would have said, 'You don't have to look for the new moon—just calculate it.' "

TWO CULTURES

ATOMIC VOICE. Nobelist Frank Wilczek of the Massachusetts Institute of Technology in Cambridge is a bonafide scientific star. But last week, the 55- year-old particle physicist experienced the tremulousness of a novice as the hero of the opera *Atom & Eve*.

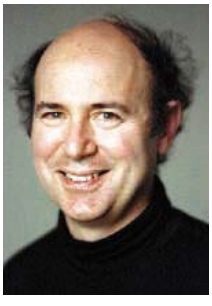

Wilczek had initially agreed to play the piano in the opera, to be performed in Alpbach, Austria, as part of the 2006 Alpbach Technology Conference. But instead of singing "some little ditty in the chorus," Wilczek wound up cast in the title role. "I kind of got leveraged into it," he laughs.

The opera portrays the story of Atom, a young oxygen atom, and Eve, a beautiful young chemist. The lovelorn couple is separated by Eve's microscope and their massive size difference. Science brings them together in the endwith laser beams that make a "single gigantic atom" out of many atoms.

Despite months of practice, Wilczek admitted that he was "a little anxious" about his 25 August performance. *Science* went to press before any reviews were in.

MISCONDUCT

VERBATIM. Call it a Himalayan-sized case of plagiarism. After reading an article on ocular cancer in the December 2003 issue of the *Indian Journal of Ophthalmology*, retinal cell biologist Gail Seigel compared it to her 2002 review paper in the *Digital Journal of Ophthalmology*. They were virtually identical, right down to the opening quote from an early 20th century ophthalmologist and the images of ocular melanoma.

"I was just in shock," recalls Seigel, a professor at the Ross Eye Institute at the University of Buffalo in New York, who immediately notified the editors of both journals. In June, the Indian journal retracted the article, and its editor, Barun K. Nayak, wrote in the journal that the four authors of the article had been banned from appearing in the journal again "till further notice."

Three of them apologized to Seigel in an e-mail message, noting that the complaint "was a great surprise to us." The fourth and primary author, Sunil Chaturvedi, could not be located by *Science*. All four are identified as working at the Himalayan Institute of Medical Sciences in Uttaranchal, India.

Got a tip for this page? E-mail people@aaas.org

Movers >>

A SECOND CHANCE. The disgraced stem cell scientist Woo Suk Hwang is back at work, but not on anything involving human embryonic stem cells.

Hwang, who was fired from Seoul National University's (SNU's) Veterinary College in December 2005, is awaiting trial on fraud and embezzlement charges. On 19 August, the Science Ministry officially confirmed that Hwang has opened a private laboratory in Guro. According to his colleagues, the cloner and his team of 20-some scientists moved into their new laboratory in late July and are "just getting started." The research team includes 15 graduate students in addition to four research assistants who used to work with Hwang.

The laboratory is part of the newly established Suam Bioengineering Research Institute, which is funded with $2.6 million from the Suam Scholarship Foundation. The institute's mission statement, presented to the Science Ministry, says Hwang and his team will study animal cloning, animal stem cells, research on production of animal organs, and biological textile products.

CREDITS (TOP TO BOTTOM): MATT HOUSTON/AP PHOTO; DONNA COVENEY/MIT; AHN YOUNG-JOON/AP PHOTO

Because you have more important things to do

Find Lab Equipment Online

We save you time so you can focus on your research. Search over 300,000 products from hundreds of vendors, organized and catalogued according to specialty ... free, online, and all in one place.

- Detailed Product Descriptions and Specifications
- Product Reviews
- No Registration Required
- E-mail Newsletters
- Direct Links to Supplier Product Pages

biocompare®

The Buyer's Guide for Life Scientists™

www.biocompare.com

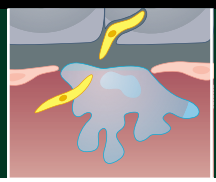

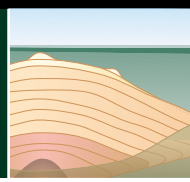

LETTERS

edited by Etta Kavanagh

Other Nations Catching Up to United States

CORPORATIONS AND NATIONS ARE IN A RACE TO MAKE THE NEXT MAJOR SCIENTIFIC BREAKthroughs that will transform society and enhance our everyday lives. As Intel's lead technologist who oversees research labs across the globe, I spend a lot of time looking over my shoulder, wondering who will move a new concept more quickly to the marketplace or create a breakthrough that will eclipse even our most ambitious research efforts.

What I see in the rear view is a cause for concern and action. Unless steps are taken now, the advantage the United States enjoys could be over within the next 10 years. India and China have built first-rate higher education systems and are churning out 10 times the number of engineers that we are in the United States. The Chinese government has created an entirely new degree program in software engineering, providing these new departments with bright young faculty members and new facilities.

While enrollments in scientific and engineering disciplines swell in China and India, they are falling across the United States, and the quality of the students in the pipeline is declining as well. The most recent Nation's Report Card for science found that 41% of 8th graders and 46% of 12th graders performed below the basic level (*1*). The study revealed that although science achievement has improved for elementary school students over the last decade, it has remained flat for middle school students and declined among high schoolers. These results are similar to those of international studies (*2*).

"We need to move further and faster to strengthen science and mathematics education if we want the United States to continue to lead the world in scientific breakthroughs and technical innovations."

—Rattner

We need to move further and faster to strengthen science and mathematics education if we want the United States to continue to lead the world in scientific breakthroughs and technical innovations.

As a junior high school student in the early 1960s, I had the opportunity as part of a special summer science program to visit the Hughes Research Laboratory in Malibu, California. There I saw the first ruby laser in development and was able to watch some of the finest scientists in the world growing the synthetic ruby that became the heart of the laser's intense beam of light. The visit inspired me so much that a few years later, I took up the study of applied physics at Cornell.

We need to develop programs that bring young students into our top laboratories to see researchers at work first-hand. There is nothing like experiencing scientific discovery to excite someone about a career in science and technology.

We also must pay more for quality teachers who understand the research process and can use that knowledge to instill a deep interest in science and mathematics in their students.

Finally, the time is long past for a new national mission in science and engineering to capture the imagination of our youth the way the space program did following the launch of Sputnik. There is no doubt that we face challenges to our country that are every bit as great as those during the Cold War. Unfortunately, landing humans on Mars is not what we need and is only of interest to those inside the Beltway. Instead, energy independence and health care are prime examples of critical missions we must embrace at the national level. Where is our national leadership when the country needs a new mission that will ensure not only our security or health, but also our continued leadership in science and technology?

JUSTIN RATTNER

Chief technology officer, Intel Corporation, 2200 Mission Boulevard, Santa Clara, CA 95052, USA.

References

1. The Nation's Report Card: Science 2005, see www.nationsreportcard.gov.
2. Results from the Trends in International Mathematics and Science Study 1995, 1999 and 2003, see http://timss.bc.edu/.

Why Academic Drug Discovery Makes Sense

CONTRARY TO THE OPINIONS EXPRESSED BY J. Erickson in his Letter "Translation research and drug development" (19 May, p. 997), we strongly believe that investing in academic drug discovery makes good financial and scientific sense.

Erickson presents alarming data on the rising costs and dwindling efficiency of the industrial drug discovery process as a main impediment to academic drug discovery. We believe that these costs are largely associated with failed paradigms (*1*) and with marketing costs hidden under the guise of pre- and postmarketing trials (*2*). Moreover, because "big pharma" is solely profit-driven, there is no willingness to reinvigorate cheaper off-patent versions of approved medications for common diseases or to invent new drugs for the neglected diseases of developing-world countries (*3*).

Indeed, because of these failed paradigms, big pharma is dependent on universities and small biotechnology companies to fill the drug pipeline. NIH and several nonprofit foundations (e.g., Stanley Foundation, High Q Foundation, and Gates Foundation) have made substantial resources available to move compounds along in the drug development process.

What is missing at the academic level is a network of medicinal chemists who can

devote themselves to translating promising "hits" into lead compounds and, ultimately, into drug candidates. The Molecular Library Screening Centers Network (MLSCN) is currently generating large numbers of promising hits (*4*), but without substantial optimization of drug leads, these hits will lie fallow and the promise of the MLSCN to provide novel small-molecule–based tools for medical research will remain unfulfilled.

One way to bridge the gap between hits and drugs would be to develop National Medicinal Chemistry Resource Centers. Such centers would naturally feed the most promising drug candidates into the industrial drug discovery pipeline through appropriate licensing agreements. In this way, NIH, academia, and industry could become partners in the ongoing quest for better treatments for diseases.

ALAN P. KOZIKOWSKI,[1] BRYAN ROTH,[2] ALEXANDER TROPSHA[3]

[1]Drug Discovery Program and Department of Medicinal Chemistry and Pharmacognosy, University of Illinois at Chicago, 833 South Wood Street, Chicago, IL 60612, USA. E-mail: kozikowa@uic.edu. [2]National Institute of Mental Health Psychoactive Drug Screening Program and Departments of Biochemistry, Psychiatry, Neurosciences, and Oncology, Case Western Reserve University Medical School, 2109 Adelbert Road, SOM W441, Cleveland, OH 44106, USA. E-mail: bryan.roth@case.edu. [3]Medicinal Chemistry and Natural Products, University of North Carolina School of Pharmacy, Campus Box 7360, Beard Hall, Room 327A, Chapel Hill, NC 27599–7360, USA. E-mail: alex_tropsha@unc.edu

References

1. S. Frantz, *Nature* **437**, 942 (2005).
2. M. Angell, *CMAJ* **171**, 1451 (2004).
3. K. A. O'Connor, B. L. Roth, *Nat. Rev. Drug Discov.* **4**, 1005 (2005).
4. C. G. Bologa *et al.*, *Nat. Chem. Biol.* **2**, 207 (2006).

Propagation of Errors in Review Articles

SCIENCE HAS DONE AN EXCELLENT JOB OF sensitizing us to issues of fabricated data. Nevertheless, there is a related issue that also deserves discussion: sham publication in the secondary literature. It is important because scientists rely on the authors of reviews to gather and analyze the unwieldy primary literature. Inasmuch as the secondary literature is a major driver of science, propagation of errors in it should elicit concern. Often it doesn't.

The following example epitomizes the issue: An article in a recent issue of a chemical education journal (*1*) described a metal-carbene–initiated olefin metathesis reported in 1980 as the first example of its kind and a major breakthrough. Indeed, olefin metathesis is a significant chemical transformation, whose development was recognized by the latest Nobel Prize in Chemistry, but this experiment could not have been a major breakthrough because no such experiment has ever been published (*2*). This and other information in the article appears to have been taken from an earlier review, which, in turn, seemingly contained information from seven previous erroneous reviews by others (*2*), but cited as a source an article in which the experiment cannot be found.

Frequent repetition can turn fictional breakthroughs into common lore. The one above is well on its way and, after its appearance as fact in a journal directed toward teachers, could move to textbooks and chemistry courses. Corrections might lead readers to examine the original literature, but journals are sometimes reluctant to publicize mistakes (*3*). The fact is that science does not always self-correct; it has to be corrected. And for that to happen, the principles of accountability that apply to fabrication in experiments should apply to fabrication in reviews.

THOMAS J. KATZ

Department of Chemistry, Columbia University, New York, NY 10027, USA. E-mail: tjk1@columbia.edu

References

1. C. P. Casey, *J. Chem. Educ.* **83**, 192 (2006).
2. Summarized in T. J. Katz, *Angew. Chem. Int. Ed.* **44**, 3010 (2005).
3. J. Couzin, K. Unger, *Science* **312**, 38 (2006).

Role of Leucine in Regulating Food Intake

IN THEIR RECENT REPORT "HYPOTHALAMIC mTOR signaling regulates food intake" (12 May, p. 927), D. Cota *et al.* detail the metabolic mechanisms controlling food intake and show that increased hypothalamic availability of the branched-chain amino acid (BCAA) leucine acts as a potent signal that reduces food intake by promoting mTOR signaling in rats. Cota *et al.* further suggest that low leucine levels in peripheral tissues may curtail protein synthesis while stimulating food intake in the brain.

Although very interesting, these experimental data appear to conflict with clinical data. The amino acid leucine has been used for decades to treat hepatic encephalopathy, to increase muscle protein synthesis, and to improve appetite (*1*). Although usually supplemented with the other BCAAs (valine and isoleucine), leucine typically accounts for about 50% of the given dose of BCAAs. When supplemented, leucine effectively competes with the neutral amino acids for crossing the blood-brain barrier, and its supplementation in humans yields increased leucine brain levels and reduced concentrations of the competitors. These changes in brain neurochemistry are not associated with reduced food intake, but rather with enhanced appetite and protein synthesis. In cancer patients, BCAA supplementation that provides 7 g/day of leucine rapidly improves food intake (*2*) and enhances protein synthesis (*3*). Similar results are seen in malnourished uremic patients undergoing hemodialysis (*4*) and in patients with liver cirrhosis (*5*). We therefore believe that BCAA, particularly leucine supplementation, remains a useful and clinically relevant tool to improve food intake and enhance protein synthesis in patients suffering from chronic diseases, at least at the doses used in clinical trials. It remains to be ascertained whether higher leucine doses that have not been given in clinical trials would be perceived by the brain as toxic, thus prompting a reduction of food intake by means of increased mTOR signaling.

ALESSANDRO LAVIANO,[1] MICHAEL M. MEGUID,[2] AKIO INUI,[3] FILIPPO ROSSI-FANELLI[1]

[1]Department of Clinical Medicine, University La Sapienza, 00185 Rome, Italy. [2]Department of Surgery, SUNY Upstate Medical University, Syracuse, NY 13210, USA. [3]Department of Behavioral Medicine, Kagoshima University, Kagoshima 890-8544, Japan.

References

1. A. Laviano *et al.*, *Curr. Opin. Clin. Nutr. Metab. Care* **8**, 408 (2005).
2. C. Cangiano *et al.*, *J. Natl. Cancer Inst.* **88**, 550 (1996).
3. G. Biolo *et al.*, *Nutrition* **22**, 475 (2006).
4. K. Hiroshige *et al.*, *Nephrol. Dial. Transplant.* **16**, 1856 (2001).
5. G. Marchesini *et al.*, *Gastroenterology* **124**, 1792 (2003).

Response

LAVIANO AND COLLEAGUES QUESTION WHETHER the mTOR system that we describe in the hypothalamus is sensitive to nutrient supplementation of the diet, and they cite examples in which leucine has supplemented the diet to encourage weight gain during pathological conditions. We used healthy rats of normal weight to investigate the physiological role of hypothalamic mTOR in the regulation of food intake. Thus, our model does not address the role that central nervous system (CNS)

Letters to the Editor

Letters (~300 words) discuss material published in *Science* in the previous 6 months or issues of general interest. They can be submitted through the Web (www.submit2science.org) or by regular mail (1200 New York Ave., NW, Washington, DC 20005, USA). Letters are not acknowledged upon receipt, nor are authors generally consulted before publication. Whether published in full or in part, letters are subject to editing for clarity and space.

INNOVATION @ WORK

Everybody wants it. Every company strives for it.

Sigma has it.

Take a close look at some of Sigma's Best-in-Class technologies and innovative products to enable your next discovery breakthrough:

- **RNAi** with our MISSION™ TRC shRNA products and our partnership with Rosetta Inpharmatics for Sigma-Proligo® siRNA
- **Whole genome amplification** with our GenomePlex® Whole Genome Amplification, now for single cell genomic amplification
- **Protein depletion** with our ProteoPrep®20 Plasma Immunodepletion product that specifically removes 20 of the most abundant proteins from human plasma or serum
- **Protein microarrays** for rapid multiplex profiling in one day with our unique Panorama® Functional and Antibody Arrays
- **Cell signaling** with thousands of high quality antibodies and bioactive small molecules to support key areas of disease research

Learn more about Sigma's innovative solutions at **sigma.com**

Genomics
GenomePlex® Whole Genome Amplification
sigma.com/wga

Functional Genomics
MISSION™ TRC shRNA
sigma.com/rnai

Genosys-Proligo siRNA
sigma.com/sigmagenosys

Proteomics
ProteoPrep® 20 Plasma Immunodepletion Kit
sigma.com/proteoprep20

Panorama® Functional Protein Arrays and Antibody Arrays
sigma.com/arrays

Cell Biology
Cell Signaling and Neuroscience
sigma.com/cellsignaling

SIGMA®

Accelerating Customers' Success through Leadership in Life Science, High Technology and Service
SIGMA-ALDRICH CORPORATION • BOX 14508 • ST. LOUIS • MISSOURI 63178 • USA

mTOR may play in chronic diseases associated with malnutrition and weight loss.

The contradiction between evidence that supplemental leucine in the diet causes weight gain and our findings that CNS administration causes weight loss raises three key issues. First, there is a difference between adipose and lean tissue mass. The cited examples are clinical syndromes associated with substantial loss of muscle mass, and the supplementation is designed to promote muscle gain. Whether such manipulations increase appetite and independently increase adipose mass is less clear. Second, mTOR activity is regulated in numerous cell types in the periphery and is associated with numerous aspects of cellular function, including cell growth (*1*, *2*). Consequently, it is not surprising that leucine supplementation increases peripheral mTOR activity and leads to an overall anabolic action. Indeed, mice deficient in the downstream target of mTOR, S6K1, are smaller overall than their wild-type controls (*3*). This is not the only example of a system that is anabolic in its peripheral action and catabolic in its CNS action. Insulin administration in the periphery can produce rapid increases in adipose mass, given that available fuel is sequestered in adipose tissue (*4*, *5*). Conversely, CNS insulin administration reduces food intake and leads to adipose tissue depletion (*6*, *7*). Third, although it is clear that branched-chain amino acids such as leucine can enter the CNS, the determinants of their levels in the specific circuits we describe is unclear. Furthermore, these amino acids are critical to the synthesis of a number of important neurotransmitters, and altering their rate of entry may complicate their effect on food intake and body weight.

All three of these issues provide notable barriers to the rapid application of our findings to the treatment of obesity. Our work represents the initial steps of a lengthy process whereby fuel-sensitive pathways in neurons that contribute to the regulation of energy balance might be therapeutically exploited. Dietary changes may ultimately provide a way to manipulate these hypothalamic circuits for therapeutic benefit, but much more work is necessary to identify specific means to do so.

DANIELA COTA, KARINE PROULX, STEPHEN C. WOODS, RANDY J. SEELEY

Department of Psychiatry, University of Cincinnati, Cincinnati, OH 45237, USA.

References

1. E. Jacinto, M. N. Hall, *Nat. Rev. Mol. Cell. Biol.* **4**, 117 (2003).
2. S. Wullschleger, R. Loewith, M. N. Hall, *Cell* **124**, 471 (2006).
3. M. Pende *et al.*, *Mol. Cell. Biol.* **24**, 3112 (2004).
4. E. M. MacKay, J. W. Calloway, R. H. Barnes, *J. Nutr.* **20**, 59 (1940).
5. M. W. Schwartz, D. Porte Jr., *Science* **307**, 375 (2005).
6. S. C. Woods, E. C. Lotter, L. D. McKay, D. Porte Jr., *Nature* **282**, 503 (1979).
7. M. W. Schwartz, D. P. Figlewicz, D. G. Baskin, S. C. Woods, D. Porte Jr., *Endocr. Rev.* **13**, 387 (1992).

CORRECTIONS AND CLARIFICATIONS

Reports: "Electric fields at the active site of an enzyme: direct comparison of experiment with theory" by I. T. Suydam *et al.* (14 July, p. 200). Due to a printer error, symbols were set incorrectly in the PDF and HTML online versions. The revised Report with corrected symbols was posted on 18 July 2006 and can be found at www.sciencemag.org/cgi/content/full/313/5784/200.

Reports: "Impaired control of IRES-mediated translation in X-linked dyskeratosis congenita" by A. Yoon *et al*. (12 May, p. 902). The third author's name was spelled incorrectly; it should be Yves Brandenburger.

TECHNICAL COMMENT ABSTRACTS

COMMENT ON "A Well-Preserved *Archaeopteryx* Specimen with Theropod Features"

Ian J. Corfe and Richard J. Butler

On the basis of new information from the tenth specimen of *Archaeopteryx*, Mayr *et al*. (Reports, 2 December 2005, p. 1483) suggested that birds, or avian flight, originated twice. We investigate the statistical support for this phylogenetic hypothesis and show that it is no better supported by available morphological character data than the hypothesis of a single avian origin.

Full text at www.sciencemag.org/cgi/content/full/313/5791/1238b

RESPONSE TO COMMENT ON "A Well-Preserved *Archaeopteryx* Specimen with Theropod Features"

Gerald Mayr and D. Stefan Peters

We agree that statistical support for our proposed phylogeny is weak, but the monophyly of Aves favored by most current researchers is also weakly supported. In the absence of unambiguous apomorphies of a clade including *Archaeopteryx* and *Confuciusornis*, but not deinonychosaurs, we do not believe that the statistical comparisons made by Corfe and Butler challenge our hypothesis regarding the ancestry of birds.

Full text at www.sciencemag.org/cgi/content/full/313/5791/1238c

Discover!

INNOVATION @ WORK

With Sigma, reveal more unique protein data

Until now, discovering protein biomarkers has felt like searching for a needle in a haystack.

Introducing the **ProteoPrep® 20 Plasma Immunodepletion Kit...**

- See proteins previously masked
- Visualize low abundance proteins
- Discover biomarkers quickly and accurately

Visit sigma.com/prot20new

Accelerating Customers' Success through **Leadership** in **Life Science, High Technology** and **Service**
SIGMA-ALDRICH CORPORATION • BOX 14508 • ST. LOUIS • MISSOURI 63178 • USA

SIGMA®

GEOSCIENCE

Heating Up the Hotspot Debates

Paul Tackley

The theory of plate tectonics has been extraordinarily successful in explaining the first-order behavior of our planet's rocky outer layer and the location of most volcanoes and earthquakes—they occur at plate boundaries. Many volcanoes do not, however, fit this framework. Some of these are characterized as "hotspots" and commonly thought to be caused by hot, columnar plumes upwelling from deep within Earth's 2900-km-thick rocky mantle, perhaps from its base where the mantle meets the liquid iron outer core. A plume impinging on a rapidly moving plate might explain long chains of volcanoes such as the Hawaiian-Emperor chain, a 4000-km-long procession of seamounts and volcanoes that extends west and north from the Hawaiian Islands to the Aleutian Islands at the edge of the Pacific plate. Plumes that initially develop with a large, rounded head might explain flood basalts—immense, rapid outpourings of magma that have covered large areas of continent or ocean floor and often exist at the start of hotspot tracks. The observed geochemical differences between magmas erupted at hotspots and those erupted at mid-ocean ridges could be explained by plumes sampling the deep mantle while midocean ridges sample the shallow mantle.

Plates, Plumes, and Paradigms

Gillian R. Foulger, James H. Natland, Dean C. Presnall, and Don L. Anderson, Eds.

Geological Society of America, Boulder, CO, 2005. 893 pp. Paper, $180. ISBN 0-8137-2388-4. Special Paper 388.

Despite these apparent successes of plume theory, some are skeptical. *Plates, Plumes, and Paradigms* has been compiled and edited by geoscientists who believe that hotspots and flood basalts are not caused by plumes but have other, shallow causes. Although this view is at one end of the spectrum, there has always been a debate even among plume advocates about which hotspots are caused by deep-seated plumes—for example, one recent survey identified only seven hotspots that originate from the deepest part of the mantle (*1*). The volume contains an interesting mixture of 47 peer-reviewed chapters, which range from reviews and historical perspectives to presentations of new scientific findings and cover a wide range of scientific subdisciplines including geology, petrology, geochemistry, seismology, tectonics, geomagnetism, and planetary science. Even though this compendium is not intended to present a balanced debate on the merits of plume theory—there are no contributions from major plume proponents, and the majority of chapters focus on problems with the theory and favor alternative explanations—it includes several chapters that offer useful neutral surveys of findings from seismology and other fields and a few that argue in support of plumes.

What is wrong with the idea that plumes cause hotspots and flood basalts? Several authors document ways in which, for some such features, inferences they make from observations are in conflict with a plume cause. Various chapters argue, for example, that the sources of some hotspot magmas were not hot (inferred from petrology or subsidence rates), the 1- to 4-km uplift expected should a buoyant plume head reach a plate is not observed for many flood basalts, there is a lack of a clear signal indicating enhanced heat flux, some hotspot chains show inconsistencies in the progression of their ages, and there are some problems with spatial relations between hotspot chains and supposedly related flood basalts.

If plumes are not the answer, what is? Here the arguments presented by the contributors sometimes get awkward. Often a different detailed explanation seems to be required for each case. Most proposals, however, fall under one or both of two themes: shallow processes related to plates and a shallow mantle that is laterally heterogeneous in both composition and temperature. One frequent topic is the relationship of flood basalts or hotspots to preexisting plate structures such as cratons (the old, strong parts of continents) and oceanic fracture zones and to changes in plate motions (including extension, continental breakups or collisions, and movements of triple junctions) or changes in plate stress. The volume contains arguments that, for example, hotspot chains may be caused by propagating cracks and flood basalts may be caused by tectonic events that trigger delamination of the lower part of the plate or by local convection driven by lateral variations in plate thickness. Lateral variations in composition, such as enrichment in volatiles or subducted crust, could also lead to high melt production in localized areas. Some chapters invoke asteroid impacts.

Such alternative explanations raise many issues that will need to be resolved before they become widely accepted. For example, the Pacific hotspots exhibit little relative motion as the plate moves over them. If they are caused by propagating cracks, why do all the cracks propagate at the same rate? Plate boundaries tend to be linear. Why then are flood basalts, and hotspots that occur at spreading centers, not linear, following the plate boundary? With some notable exceptions (delamination, "edge-driven" convection, impact volcanism), we currently lack quantitative modeling that demonstrates the feasibility of alternative mechanisms.

In conclusion, despite its strong emphasis on the skeptic side of the plume debate, *Plates, Plumes, and Paradigms* is a stimulating and useful reference for observations and arguments. The volume contains several

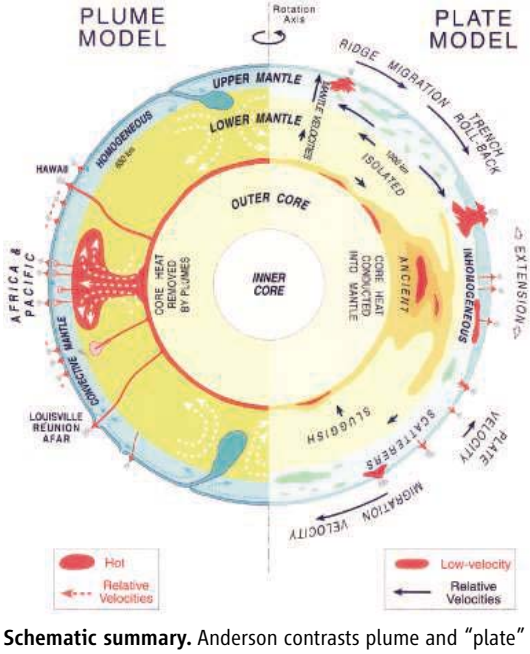

Schematic summary. Anderson contrasts plume and "plate" (or "shallow") models.

CREDIT: FIG. 1 FROM D. L. ANDERSON, IN *PLATES, PLUMES, AND PARADIGMS*, CHAP. 4

The reviewer is at the Institute of Geophysics, Swiss Federal Institute of Technology, ETH Hönggerberg, CH-8093 Zürich, Switzerland. E-mail: ptackley@ethz.ch

valuable contributions that plume proponents will need to pay attention to. Most geoscientists agree that plate structure does exert a major influence on volcanism (for example, all continental flood basalts occur at the edge of cratons). Determining the relative importance of deep plumes versus plate dynamics in causing flood basalts and hotspots will not be straightforward. Resolving the issue will require much interdisciplinary research, integrating observational and theoretical constraints from geology, geophysics, geochemistry, petrology, and several other fields. Such future work may well demonstrate that the formation of hotspots requires a combination of both deep plumes and plate dynamics.

Reference

1. V. Courtillot, A. Davaille, J. Besse, J. Stoack, *Earth Planet. Sci. Lett.* **205**, 295 (2003).

10.1126/science.1130117

GEOSCIENCE

Charting Earth's Activities

Peter Crowley

Maps have been a mainstay of geologists since at least the publication of William Smith's geological map of England in 1815. Unfortunately, in recent years the paper map has almost disappeared; currently, most new maps are released instead as electronic databases. Although this development has produced a wealth of information for the specialist, it has made it harder to disseminate that information to the interested nonspecialist.

Maps, such as Bruce Heezen and Marie Tharp's shaded relief maps of the ocean floor (from the 1970s), have been instrumental in conveying complex geological ideas to broad audiences. By clearly showing the complicated topography of the ocean floor, the Heezen and Tharp maps made plate tectonics seem real and changed the way that many viewed our planet. In many ways, *This Dynamic Planet* (like its earlier, 1989 and 1994, versions) is an update of these now-classic maps. The front side of the sheet is dominated by the colored and shaded relief map of the world on which the locations of earthquakes, volcanoes, plate boundaries, and impact craters are plotted. The 1:30 million map uses a variety of symbols to depict earthquake magnitudes and focal depths, the size of impact craters, and the age of volcanic eruptions as well as absolute and relative plate motion vectors. The reverse side of the map provides a heavily illustrated explanation of plate tectonics.

Although the topography of the ocean floor on *This Dynamic Planet* is much less exaggerated than it was on the Heezen and Tharp maps, important features of the deep ocean such as trenches, fracture zones, and seamounts are distinctly depicted, as are the large-scale features of the continents. The overlay of plate boundaries, volcanoes, and earthquakes on the topography very clearly demonstrates the importance of plate boundary processes. The explanation of plate tectonics given on the back of the map (which occupies the spatial equivalent of approximately 25 printed pages) is beautifully illustrated and extraordinarily detailed. That detail proves to be both the strength and the weakness of the map's reverse side. The quite complete but sometimes nuanced explanations make for good reference material, but they may prove a hard read for anyone who is not already familiar with the basics of plate tectonics.

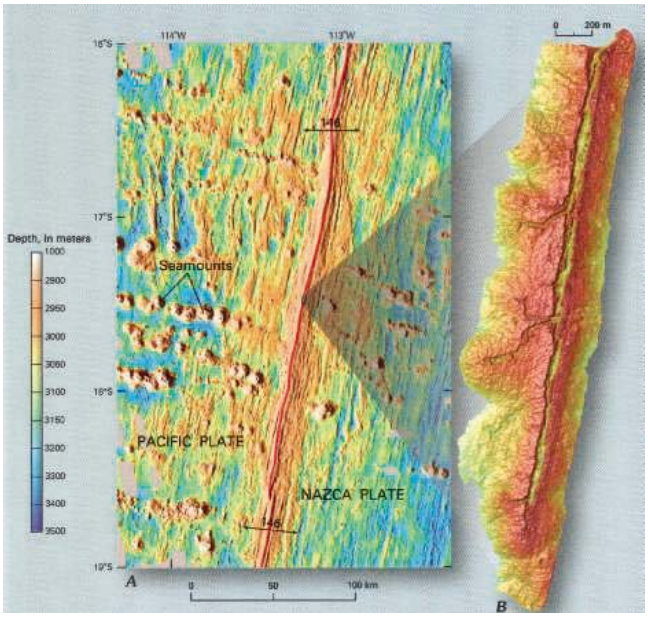

Topography of a fast-spreading ridge. Here on the East Pacific Rise, the Pacific and Nazca plates are separating at 146 mm/year.

This Dynamic Planet
World Map of Volcanoes, Earthquakes, Impact Craters, and Plate Tectonics

by Tom Simkin, Robert I. Tilling, Peter R. Vogt, Stephen H. Kirby, Paul Kimberly, and David B. Stewart

U.S. Geological Survey, Smithsonian Institution, and U.S. Naval Research Laboratory, Washington, DC, 2006. $14. U.S.G.S. Geologic Investigations Series Map I-2800.
www.minerals.si.edu/tdpmap/index.htm

For educators, the uses of this map are far from clear. Although the map is large (1.5 m by 1 m), it is nonetheless too small and detailed for use during lectures. The details that make the map so informative (e.g., plate boundaries and earthquake locations) become difficult to discern at distances greater than just a few meters. Thus educators may find the companion Web site (www.minerals.si.edu/tdpmap/index.htm) very helpful. The Web site offers an interactive version of the map that allows the viewer to examine any or all of 18 different layers of information as well as PDF versions of the map and its explanatory text and figures. Images from the Web site could be projected so that both the big picture and its details are evident to a class.

Overall, the map is extremely useful, and my complaints are fairly minor. Divergent and transform plate boundaries are shown on the main map, but convergent boundaries are, for some reason, omitted. This is an unfortunate oversight, particularly since they are depicted on the PDF version and are available as a layer on the interactive map. Even though the shallow ocean topography is more exaggerated than that of the deep ocean, details of continental margins such as submarine canyons remain hard to see. The Web site allows users to create a wide array of interesting and revealing maps and to save images of those maps. These images would be ideal for classroom projection if only the resolution was a bit higher.

In an era when new maps are commonly released as geographic information systems databases, it is refreshing that a hard-copy version of the U.S. Geological Survey's best-selling *This Dynamic Planet* has been updated and re-released. My copy is already up on the wall, where it will serve as a valuable reference tool.

10.1126/science.1132757

The reviewer is at the Department of Geology and the Museum of Natural History, Amherst College, Amherst, MA 01002, USA. E-mail: pdcrowley@amherst.edu

CREDIT: FIG. 8 FROM INSET 1 ("DIVERGENT BOUNDARIES"), *THIS DYNAMIC PLANET*

International Society for Stem Cell Research

5th ISSCR Annual Meeting

The world's premier stem cell research event

June 17 – 21, 2007

Cairns Convention Centre
Cairns, Queensland, Australia

www.isscr.org

Junior Investigator Travel Awards will be available for this meeting. Check www.isscr.org for updates.

Supported by the Australian Stem Cell Centre

Important Dates

Junior Investigator Travel Award applications accepted with abstract submission — **Opens October/November 2006**

Abstract submission — **Opens October/November 2006**

Exhibit space contracts — **Due April 2007**

Annual meeting support contracts — **Due April 2007**

Hotel reservation discount — **May 2007**

Online registration — **Opens November/December 2006**

For more information e-mail isscr@isscr.org or go to www.isscr.org.

ENERGY

A Road Map to U.S. Decarbonization

Alternative energy sources could replace 70% of fossil fuels in America within 30 years at a cost of $200 billion per year.

Reuel Shinnar* and Francesco Citro

Today, 85% of the United States' energy mix comes from carbon-rich fossil fuels: oil, natural gas, and coal (*1*). With demand increasing worldwide, existing oil reserves could peak within 20 years (*2*), followed by natural gas and coal. Growing fuel use is increasing CO_2 and CH_4 emissions and the risk of global warming. The United States has responded by sponsoring research into alternative energy (*3*). However, because research success is not predictable, an effective plan must be based on proven technologies. We propose to switch our economy slowly (over 30 to 50 or more years) to nonfossil energy sources by using proven technologies and available, expandable distribution systems.

Enhanced online at www.sciencemag.org/cgi/content/full/313/5791/1243

Available Methods

Because all available energy technologies have limitations (see table, above right), a comprehensive plan should include several options:

1. Concentrated solar thermal (CST) energy with storage, a proven technology for electricity generation (*4*), can provide variable energy, to compensate for fluctuations in demand, for a large fraction of U.S. energy needs.

2. Nuclear energy. New and safer designs, not yet built on a commercial scale, merit construction. The implementation of a large nuclear capacity [1000 gigawatts (GW)] requires study regarding the long-range availability of nuclear fuel and the disposal of accumulated waste. Present nuclear plants are used for base power, only 40% of our electricity needs.

3. Geothermal and hydroelectric plants. However, their total output is limited.

4. Wind. The amount of uncontrollable electricity the grid can accept from this highly variable source is limited.

5. Solar cells. Sunlight is available for only part of the day. Like wind power generators, solar cells lack storage capacity. However, unlike CST, solar cells can be widely distributed.

The authors are with the Clean Fuels Institute, City College of New York, New York, NY 11031, USA.

*Author for correspondence. E-mail: shinnar@ccny.cuny.edu

Potential for fossil fuel replacement and CO_2 reduction

Fossil fuel use	Fossil fuel replaced (%)	CO_2 emissions reduction (%)
Replaced by electricity from alternative sources		
All coal for electricity	25	33
All natural gas and petroleum for electricity	7	6
All fossil fuels for residential and commercial	13	11
65% of petroleum for transportation	20	21
70% of natural gas used in industry	7	5
Replaced by syngas processes from biomass		
All petroleum + 30% of natural gas used in industry	14	9
35% of petroleum for transportation	12	12
Total	**98**	**97**

[Source (*4*)]

6. Biomass. The only renewable source of industrial petrochemical feedstocks and fuels for trucks and aviation that cannot be provided by electricity is biomass, but only a limited amount can be grown. Proven technologies for generating syngas by combining carbon oxides (from partial oxidation of biomass) with H_2 (from electrolysis) can currently generate three to four times the product yield obtainable by fermentation (*5*).

A discussion of decarbonization should also include CO_2 sequestration, a technology available only for new coal power plants (*6*). This technology depletes valuable fossil fuel resources and is more expensive than CST and nuclear (*4*). It is doubtful that it will play a major role in the near to midterm future.

Alternative Energy Sources

The magnitude of our energy problem is illustrated in the figure (below); our plan is outlined in the table on page 1244. Electricity from alternative sources could replace all fossil fuel power plants and all residential and commercial uses with available technology and distribution systems, as well as 70% of the natural gas used for industrial furnaces, steam generation, and H_2 production (*1*, *7*).

Of the gasoline used for private cars and light trucks, 80% can be replaced by hybrid cars with plug-in batteries (*8*), the cheapest way to reduce oil consumption. Railroads driven by electricity could probably assume 50 to 60% of long-distance hauling. Therefore, 72% of the current use of fossil fuels can be replaced by electricity from alternative sources and 26% by combined biomass and H_2, whereas 2% cannot be replaced at all.

Concentrated Solar Thermal Energy

CST technology utilizes solar collectors that concentrate solar rays on a heat-transfer fluid able to sustain high temperatures (>800°F) (*4*) and raise steam for driving turbines. This technology has been demonstrated in a 354-MW modular plant running in the Mojave Desert for the past 20 years (*4*). On rainy days, the steam power plant consumes fossil fuel, but it could use fuels made from biomass and H_2.

For CST, the collectors and storage (90% of the investment) are comparable to the fuel plant for a conventional steam power plant (10% of the investment). By doubling the capacity of the steam power plant, a solar plant designed for 1-kW capacity or 24 kW hours (kWh)/day continuous production (base load) can supply 2 kWh for 12 hours with only a 10% incremental investment or 4 kWh for 6 hours with a 30% incremental investment, by quadrupling the capacity of the steam plant. For coal or nuclear plants, the increase in investment is 100 and 300%, respectively. Investment and electricity costs for CST are given in the table (page 1244) and compared with costs for nuclear and various versions of coal power (*6*, *9*,

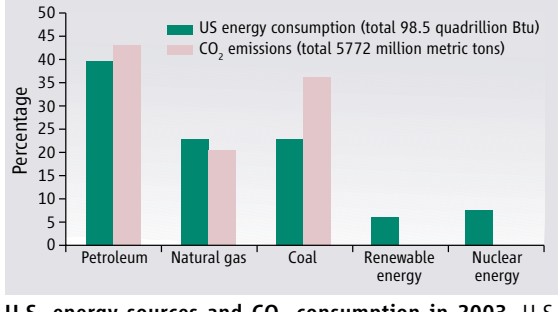

U.S. energy sources and CO_2 consumption in 2003. U.S. energy consumption (total, 98.5 quadrillion Btu) (white bars) and CO_2 consumption (total 5772 million metric tons) (black bars). [Source (*1*)]

Electricity costs for solar thermal compared with conventional energy sources

	Investment ($/kW installed)	Cost (cents/kWh)		
		Base	Intermediate	Load following
Solar thermal: near term (*10*)	4000*	8.0†	8.0	10.4‡
Solar thermal: future (*10*)	3220	6.2†	6.2	8.6‡
Conventional coal power plant (with scrubbers) (*6*)	1200	4.5§	8.0	13.5‖
Clean coal (*6*)	1550	5.6§	10	Cannot supply it
Clean coal (*6*) (with CO_2 sequestration)	2000	10–11	14–15	Cannot supply it
Nuclear (*9*)	2200	6.0§	10–11	Cannot supply it

[Source (*4*)] *Explanation of estimate (*4*). †Operated 4900 hours/year. ‡A power plant designed to supply, for each kW installed, 12 kWh/day of variable electricity at instantaneous maximum rate of 4 kWh. §Operated 6500 hours/year. ‖Designed for the same load-following capability as in ‡.

10). CST is not competitive yet with nuclear or coal for continuous production (base load). However, it is more flexible in adjusting to changing needs, potentially switching off in periods of low demand, such as at night (intermediate load). Power can be produced according to demand almost instantaneously (load following), which makes it cheaper than other sources of power. CST is cheaper than new coal power plants with CO_2 sequestration, even for base power.

CST load-following capabilities enable it to be the anchor of an alternative energy grid that can compensate for the variable output of wind and solar cells. An area of the desert Southwest of 15,000 square miles is sufficient to supply 50% of our total present energy requirements (*2*). The transmission lines of the national grid would have to be 100% larger at a cost of about $250 billion to $300 billion (*11*). The cost of the local distribution lines, independent of the location of the power plants, would add another $850 billion to $1000 billion (*11*). The nationwide power losses in transmission and distribution, with present technology, are less than 7% (*1*).

Role of Biomass and H_2

Of the fossil fuels we currently use, 28% cannot be replaced by electricity but can be replaced by hydrocarbons produced from biomass in combination with H_2. Efforts now focus on ethanol, but we prefer biomass from less–energy-intensive agriculture such as fast-growing trees, grass, and agricultural waste. Biomass is used to generate syngas to produce methanol or liquid hydrocarbons (*12*, *13*). Available technologies can produce any fuel or petrochemical from these two ingredients. The syngas for these two processes can be made from H_2 and CO or CO_2. H_2 can be generated on location by electrolysis using alternative electricity (*14*), and the O_2 coproduced can be used to partially oxidize the biomass. This method produces three to four times as many hydrocarbons as by fermentation to ethanol (*5*), which is an advantage as there are limits to the amount of biomass that can be grown. In our plan, biomass is converted on location in small plants, and the methanol produced is transported to a biorefinery or to existing petrochemical plants. Further investigation is needed to determine how much biomass can be produced and the optimal technologies for its utilization.

H_2 is not available in nature; energy is required to generate it. Were we to generate sufficient H_2 from natural gas to fuel our cars, we would double our natural gas consumption. To produce H_2 from alternative sources (by electrolysis) is an expensive process. As the direct use of electricity is cheaper by a factor of 3, our plan minimizes the use of H_2 to uses for which electricity cannot be substituted. We eliminate the problems of safety and transportation (*14*) by generating H_2 on location and converting it on site in a controlled industrial environment to conventional hydrocarbons.

Conclusions

Except for H_2, all the technologies we consider could become competitive with crude oil at $70 per barrel. Our main objective, however, should be to implement the best technology for eliminating dependency on fossil fuels rather than to compete with coal or cheap oil. Investment in demonstration plants and in large-scale implementations will be required.

Approximate cost estimates (*4*, *7*) to replace 70% of our fossil fuel use (including most coal) are about $170 to $200 billion per year over 30 years. At current levels of CO_2 emission, a tax of $45 to $50 per ton of CO_2 would pay for the whole investment and provide incentives for implementing renewable technologies (*5*).

We must start now, as our country does not have the resources to complete this switch within a few years. The United States must create long-range incentives (such as a CO_2 tax or tax credits) large enough to induce companies and utilities to implement proven technologies and to provide the required infrastructure. A successful U.S. program can set an example for the rest of the world, as many of the key technologies are well suited to developing countries. Once the technologies are established on a large scale and are mass-produced, these costs should go down by a factor of 2, making them competitive and reducing the need for subsidies. The required increase in the electric distribution system poses problems, such as obtaining rights of way for new distribution lines, that only the federal government can handle. There are political hurdles, but we believe they can be overcome.

References and Notes

1. Energy Information Administration (www.eia.doe.gov).
2. National Research Council (NRC), *Trends in Oil Supply and Demand, the Potential for Peaking of Conventional Oil Production, and Possible Mitigation Options: A Summary Report of the Workshop*, Washington, DC, 20 and 21 October 2005 (National Academies Press, Washington, DC, 2006).
3. G. W. Bush, State of the Union address, 20 January 2003.
4. R. Shinnar, F. Citro, "Solar thermal energy: The forgotten energy source," presented at the American Institute of Chemical Engineers, annual meeting, Cincinnati, OH, 30 October to 4 November 2005 (*IEEE Technol. Soc.*, in press) (www1.ccny.cuny.edu/ci/cleanfuels/publications. cfm).
5. Supplemental calculations are available as supporting material on *Science* Online.
6. N. Holt, *Gasification Process Selection—Trade-offs and Ironies* [Electric Power Research Institute (EPRI), Palo Alto, CA, 2004] (www.gasification.org/Docs/2004_Papers/30HOLT_Paper.pdf).
7. R. Shinnar, F. Citro, "Decarbonization of the U.S. energy mix," presented at the AAAS Annual Meeting, St. Louis, MO, 16 to 20 February 2006 (www.nrel.gov/ncpv/thin_film/docs/decarbonization-02-24-06.doc); updated at (www1.ccny.cuny.edu/ci/cleanfuels/publications.cfm).
8. S. C. Davis, S. W. Diegel, *Transportation Energy Data Book* (Oak Ridge National Laboratory, Oak Ridge, TN, prepared for the U.S. Department of Energy, Washington, DC, ed. 25, 2006) (http://cta.ornl.gov/data/index.shtml).
9. *Projected Costs of Generating Electricity: Update for 1998* (Nuclear Energy Agency, International Energy Agency, and Organization for Economic Cooperation and Development, Paris, 1998) (www.iea.org/textbase/nppdf/free/1990/projected1998.pdf).
10. *Assessment of Parabolic Trough and Power Tower Solar Technology Cost and Performance Forecasts* (Sargent & Lundy Consulting Group, Chicago, for the National Renewable Energy Laboratory, Golden, CO, 2003) (www.nrel.gov/docs/fy04osti/34440.pdf).
11. *Power Delivery System of the Future: A Preliminary Estimate of Costs and Benefits* (EPRI, Palo Alto, CA, 2004).
12. R. B. Anderson, *The Fischer-Tropsch Synthesis* (Academic Press, Orlando, FL, 1984).
13. C. D. Chang, *Hydrocarbons from Methanol* (Marcel Dekker, New York, 1983).
14. NRC and National Academy of Engineering, *The Hydrogen Economy: Opportunities, Costs, Barriers, and R&D Need* (National Academy Press, Washington, DC, 2004) (www.nap.edu/books/0309091632/html).

15. The authors thank M. Green Shinnar for editing.

Supporting Online Material
www.sciencemag.org/cgi/content/full/313/5791/1243/DC1

10.1126/science.1130338

MICROBIOLOGY

Malaria's Stealth Shuttle

Membranous vesicles shuttle malaria parasites from liver to blood cells during infection, ensuring protection against the host's defenses.

Alan F. Cowman and Stefan H. I. Kappe

In the arms race between pathogens and their hosts, suicide of infected cells is a prominent defense mechanism used by the host to protect against establishment of further infection. Not surprisingly, some pathogens have evolved mechanisms to interfere with host cell death. *Plasmodium* parasites that cause malaria are among the most successful and deadly pathogens of vertebrates, yet the manipulation of molecular pathways responsible for host cell death has only recently emerged as part of their survival toolbox (*1*). On page 1287 of this issue, Sturm *et al.* (*2*) report a major twist to this story during the liver stage of malaria infection. Using *Plasmodium berghei*, a mouse model of malaria, they show that the liver-stage parasite keeps its host hepatocyte alive long enough to complete development but allows it to then commit an unusual form of suicide that helps the parasite evade host defenses and deposit new invasive forms into the bloodstream.

Plasmodium parasites are transmitted to a host organism by the bite of a female *Anopheles* mosquito. The sporozoite form rapidly invades liver hepatocytes (*3*, *4*) and over a number of days, matures as a liver-stage parasite within a membrane-bound vacuolar compartment, shielded from the intracellular milieu of the host cell (see the figure). The liver-stage parasites differentiate into many thousands of merozoites that, when released into the bloodstream, invade erythrocytes, initiating the blood-stage cycle that causes the pathophysiology of malaria.

For liver-stage merozoites to access the bloodstream, they must leave their host cells and cross both an extracellular matrix-filled space and the endothelium of liver blood vessels (sinusoid). Merozoites also must avoid phagocytes in the liver, such as Kupffer cells and dendritic cells, which are eager to attack any foreign invader. Exactly how they overcome these hurdles for release into the bloodstream has been unknown. Using cultured hepatocytes and histological analysis of infected mouse livers, Sturm *et al.* show that late liver-stage parasites dissolve their surrounding vacuolar compartment, thereby gaining access to the hepatocyte cytoplasm. Subsequently, the infected hepatocytes detach from the extracellular substrate and other cells. The authors also identify membrane-enclosed structures—merosomes—that are extruded from the infected cell. In cultured liver cells, merosomes clearly contained merozoites. Real-time intravital imaging of infected mice also revealed merosomes emerging from parasite-infected hepatocytes and entering the sinusoid lumen. The merosomes appear to act as shuttles, allowing safe passage of the parasite into the bloodstream. However, low resolution of the live imaging did not allow the authors to demonstrate unequivocally the presence of fully formed merozoites within merosomes in vivo. Merosome-like structures released into the sinusoids have also been reported recently in the related rodent malaria parasite *Plasmodium yoelii* by intravital imaging (*5*), indicating that these putative shuttles are not a species-specific feature.

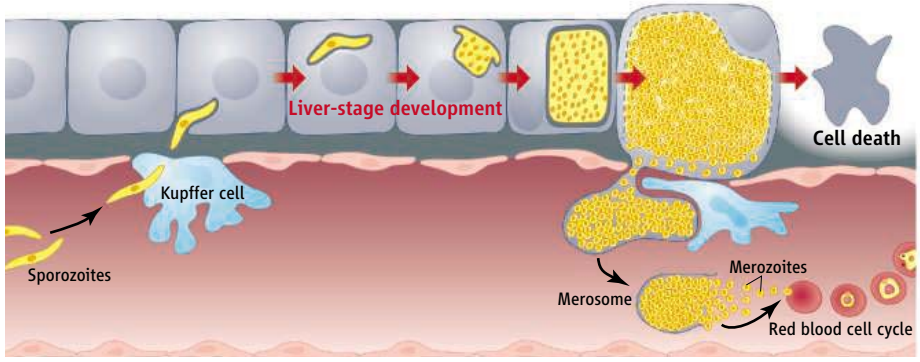

Liver to blood transit. The malaria parasite rapidly grows in liver hepatocytes, producing thousands of merozoites that are competent to infect red blood cells. These liver-stage parasites inhibit hepatocyte cell death during most of their development. When ready to leave hepatocytes, the parasite induces cell death, and causes the release of merozoites in merosomes, thus avoiding host cell defense mechanisms. Merozoites eventually escape from merosomes and infect red blood cells.

What is the benefit to the parasite in packaging liver-stage merozoites into merosomes for delivery to the bloodstream instead of releasing them individually or in one big burst? Sturm *et al.* determined that loss of hepatocyte adhesiveness is associated with host cell death. Although the observed cell death had the hallmarks of classic apoptosis, such as loss of mitochondrial membrane potential and mitochondrial release of cytochrome c, host cell DNA was not characteristically fragmented. Cell death also occurred independent of caspases, proteolytic enzymes whose activity is associated with apoptosis (*6*). However, other cysteine proteases appear to be involved.

Inducing the death of a cell infected with a pathogen seems counterintuitive to providing an advantage for successful infection. In addition to killing the parasite, apoptotic infected cells are also red flags for the immune system. Indeed, *P. berghei* inhibits hepatocyte cell death during most of liver-stage development (*1*). A possible explanation for this twist was found by analyzing the amount of phosphatidylserine in the plasma membrane of infected hepatocytes. In an apoptotic cell, the release of Ca^{2+} from intracellular stores into the cytoplasm causes the amount of phosphatidylserine in the outer leaflet of the plasma membrane to increase substantially. This phosphatidylserine serves as an attraction signal for phagocytic cells (*7*). Sturm *et al.* show that phosphatidylserine is absent in the outer membrane leaflet of dying, infected hepatocytes, thus allowing the hepatocytes to avoid recognition by phagocytic cells. Furthermore, the amount of Ca^{2+} in infected hepatocytes is low, whereas in merozoites it is high, suggesting that the parasite may absorb released Ca^{2+} and thereby suppress exposure of phosphatidylserine on the cell surface. Consistent with this finding, the Ca^{2+} ionophore ionomycin induced phosphatidylserine exposure in infected hepatocytes, and these cells were indeed more frequently phagocytosed compared to untreated infected hepatocytes.

Although the study by Sturm *et al.* provides some answers about the delivery of liver-stage

A. F. Cowman is at The Walter and Eliza Hall Institute of Medical Research, Melbourne, Victoria 3050, Australia. S. H. I. Kappe is at the Seattle Biomedical Research Institute, Seattle, WA 98109–5219, USA. E-mail: cowman@wehi.edu.au (A.F.C.); stefan.kappe@sbri.org (S.H.I.K.)

merozoites to the bloodstream, there are still many issues to be addressed. How do merosomes, which are large and presumably not motile, pass through the extracellular matrix and sinusoid endothelium? How do merozoites burst out of the merosome once it reaches the bloodstream? How does a liver-stage parasite inhibit the death of the host cell for most of its life but then allow death to occur in a manner that guarantees merozoite progression to blood-stage infection? It is of great interest to determine the molecules and mechanisms that mediate these processes. This is particularly true for *P. falciparum*, which causes the most severe form of malaria and most mortality in humans, because it may reveal potential avenues for the development of novel treatments that block the onset of disease.

References

1. C. van de Sand *et al.*, *Mol. Microbiol.* **58**, 731 (2005).
2. A. Sturm *et al.*, *Science* **313**, 1287 (2006); published online 3 August 2006 (10.1126/science.1129720).
3. U. Frevert *et al.*, *PLoS Biol.* **3**, e192 (2005).
4. R. Amino *et al.*, *Nat. Med.* **12**, 220 (2006).
5. A. S. Tarun *et al.*, *Int. J. Parasitol.* doi10.1016/j.ijpara.2006.06.009 (12 July 2006).
6. N. N. Danial, S. J. Korsmeyer, *Cell* **116**, 205 (2004).
7. V. A. Fadok *et al.*, *Nature* **405**, 85 (2000).

10.1126/science.1132940

CHEMISTRY

Controlling Biological Functions

Manipulation of the quantum properties of matter can influence the course of biochemical reactions.

Majed Chergui

Can biological functions, such as vision or photosynthesis, that are driven by incoherent phenomena have anything to do with quantum mechanics, where the wave properties of matter play a key role? The answer is yes, and on page 1257 of this issue (*1*), Prokhorenko *et al.* show that biological processes can be manipulated by means of coherent control (*2*).

Coherent control refers to experiments that make explicit use of the wavelike nature of matter to direct the behavior of atomic and molecular systems, often to alter the likelihood of a particular chemical reaction. An analogy with Young's double-slit experiment is useful: Light passes through both slits at the same time and interferes with itself at a distant screen to produce dark and bright fringes. To achieve complex interference patterns, however, one needs to control the number, widths, and positions of the slits.

For a quantum mechanical object, one can arrange interference of several "paths" to create constructive interference that selects one state and destructive interference that blocks the others. This is achieved with a pulse of light whose spectral components are controlled in phase and amplitude. This is accomplished by dispersing the different frequency components of the pulse spatially with a diffraction grating, manipulating their phase and amplitude with a spatial mask, and then recombining them to produce a short pulse of well-defined shape. Because adjustment of the relative phases of the components modifies the pulse temporal structure, coherent control can be seen in the time domain as control over a quantum system through manipulation of the temporal structure of the laser field.

The ideal pulse shape is not known a priori, however. In their experiment, Prokhorenko *et al.* used a well-established genetic algorithm inside a feedback loop (*2*) (see the figure). Successful control schemes have previously been demonstrated for specific molecular product channels and states in the gas phase. But most chemical and biological reactions and important physical processes occur in the condensed phase, where interactions of the system with the fluctuating environment may lead to the destruction of the coherence imparted to the system.

Although coherent control has been demonstrated in a variety of condensed-phase systems, including proteins (*3*, *4*), the work of Prokhorenko *et al*. on bacteriorhodopsin contains important novel aspects. First, in all previous coherent control experiments, the shaped laser pulse suppressed unwanted pathways and therefore merely acted as a filter. Examples where the desired target is reached with higher efficiency than with symmetrically shaped pulses are lacking, but Prokhorenko *et al.* were able to increase or decrease the absolute quantum yield of isomerization of the 13-cis retinal isomer in bacteriorhodopsin by as much as 20%, as compared to excitation with symmetric pulses. Second, they used intensities of the exciting light comparable to that of sunshine, relevant to photobiological processes. This is important for controlling the actual reaction coordinate rather than the excited-state population (*4*), and in interpreting the correlation of the shaped pulses to the molecular processes. And third, at the end of the optimization (or antioptimization) control loop, their pulse shapes capture the underlying molecular dynamics driving the process, and show a selective coherent excitation of precisely those torsional modes responsible for isomerization.

But why perform coherent control in bio-

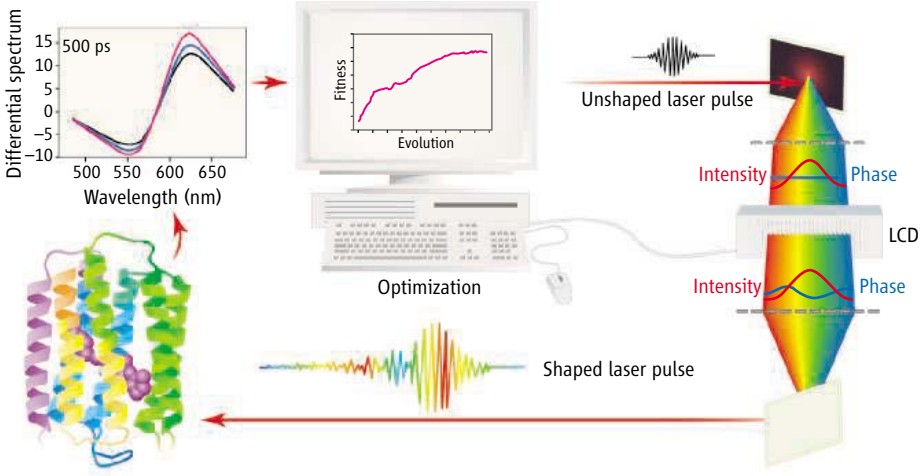

In the loop. A feedback loop is used to control isomerization of bacteriorhodopsin. An initial laser control field is created with a pulse shaper (on the right) and is then applied to the protein sample. The action of the control pulse, measured as the difference spectrum of the sample, is used by a learning algorithm to produce an improved field. Repeated excursions around the loop result in an optimum control.

The author is at the Laboratoire de Spectroscopie Ultrarapide, Ecole Polytechnique Fédérale de Lausanne, CH-1015 Lausanne-Dorigny, Switzerland. E-mail: majed.chergui@epfl.ch

logical systems, as these often already carry out their functions with unsurpassed selectivity and efficiency? The work of Prokhorenko *et al.* goes beyond the specifics of biological systems: It shows that for a quantum system in a fluctuating bath, one can manipulate the outcome of the reaction by creating constructive or destructive interferences along the reaction coordinate. Their investigation of the phase dependence of isomerization is quite revealing of the coherent nature of their control, and it is hoped that future studies will demonstrate the phase sensitivity of coherent control for molecules in liquids as well.

Further work with these coherent tools may allow the exploration of systems considered intractable on an ab initio quantum mechanical level. As such, coherent control experiments represent a new type of "active" spectroscopy for the investigation of dynamics in complex systems. Although any single experimental spectroscopic observation may unambiguously identify a local region in the dynamics, it would be useful to develop methods where the genetic algorithm uses a "movie" of atomic motion obtained from ultrafast imaging techniques, such as those achieved by x-ray methods (*5*, *6*).

References

1. V. I. Prokhorenko *et al.*, *Science* **313**, 1257 (2006).
2. H. Rabitz, R. de Vivie-Riedle, M. Motzkus, K. Kompa, *Science* **288**, 824 (2000).
3. C. J. Bardeen, V. V. Yakovlev, J. A. Squier, K. R. Wilson, *J. Am. Chem. Soc.* **120**, 13023 (1998).
4. J. L. Herek, W. Wohlleben, R. J. Cogdell, D. Zeidler, M. Motzkus, *Nature* **417**, 533 (2002).
5. G. Hummer, F. Schotte, P. A. Anfinrud, *Proc. Natl. Acad. Sci. U.S.A.* **101**, 15330 (2004).
6. W. Gawelda *et al.*, *J. Am. Chem. Soc.* **128**, 5001 (2006).

10.1126/science.1132749

MATERIALS SCIENCE

Step Dances on Silicon

Atomic structures grow differently on different crystal surfaces of silicon. Low-energy electron microscope images now explain why.

Peter W. Voorhees

Dislocations are one-dimensional or line imperfections in the structure of a crystal that result from missing or irregularly positioned atoms. In addition to their central role in setting the mechanical properties of crystalline materials, nearly every textbook on crystal growth discusses their role in the motion of a crystal-vapor or crystal-liquid interface. In 1949, Frank postulated that a particular type of dislocation, called a screw dislocation, provides an unending source of steps on a crystal surface (*1*). Because the core of the dislocation is fixed, as the atoms coming from the vapor or liquid attach to the step, the step winds around the core, producing a beautiful spiral-shaped step pattern on the surface of the crystal. On page 1266 of this issue, Hannon *et al.* (*2*) show that, whereas crystal growth via a screw dislocation intersecting one type of silicon surface [Si(111), where the indices denote the crystallographic plane that is exposed at the surface and hence the arrangement of the surface atoms] does exhibit the classic spiral pattern predicted by Burton, Cabrera, and Frank (*3*), far more complicated step motion occurs on a different silicon surface [Si(001)]. These complicated patterns clearly show that the textbook description of dislocation-mediated crystal growth requires modification.

The difference in the atomic structure of the Si(111) and Si(001) surfaces is one of the causes of this behavior. To reduce the number of dangling surface bonds, the atoms on the Si(001) surface rebond to form dimer pairs in which two surface atoms are connected by a single bond. These dimer pairs then align to form rows along the <110> directions of the crystal. As might be expected from this highly anisotropic atomic structure, elastically straining the silicon crystal in a direction parallel to the dimer row leads to a different change in the energy of the surface compared to that when it is strained perpendicular to the row. Another unique aspect of the Si(001) surface follows from the diamond crystal structure of silicon. At a Si(001) surface, a step of size equal to the silicon lattice parameter, a double step, can dissociate into two single-height atomic steps (see the figure). Unlike double-height steps, the orientation of the dimer rows changes by 90° across the step. This change in orientation, when coupled with the manner in which the direction of the applied strain affects the surface energy, forms the basis of the novel step patterns observed during growth in the presence of dislocations.

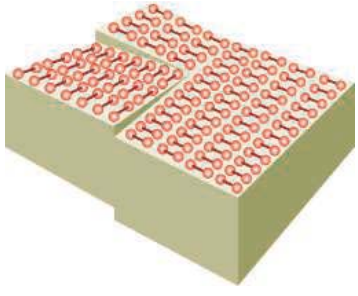

A different kind of surface motion. An idealized Si(001) surface showing the two single-height atomic steps that emanate from the dislocation core and the dimer rows. Note that the orientation of the dimer rows changes on crossing a step.

Only recently has it been possible to explore the structure and dynamics of crystalline surfaces. Scanning tunneling microscopy (STM) studies of Si(001) surfaces have revealed the presence of dimer rows on the surface (*4*) and the anisotropy of the strain dependence of the surface energy (*5*). But the essence of the work of Hannon *et al.* lies in the dynamical behavior of the surface. To observe step motion at over 1000°C, they used low-energy electron microscopy (LEEM). Although lacking the atomic resolution of STM, LEEM provides a real-time picture of the motion of steps on the surface. Others have used LEEM to identify properties of steps on Si(001) such as the step mobility and the step energy (stiffness) (*6*). These past experiments make the Si(001) surface one of the most fully characterized surfaces known and allows for the careful comparison between theory and experiment evident in the work of Hannon *et al.*

Burton, Cabrera, and Frank (*3*) showed that the chemical potential of an atom at a step is the key to understanding what controls the step motion. When the step chemical potential is a function of the curvature of the step, during growth or sublimation the step obtains an Archimedean spiral shape as the step spins around the core of the dislocation. In the case of growth on Si(111) at the relatively high temperatures used in the experiment of Hannon *et al.*, the chemical potential is, in fact, a function only of the curvature of the step and the difference in chemical potential of an atom on the surface and at the step, and thus such spiral shapes are observed.

The absence of spiral-shaped step patterns on Si(001) indicates that an essential piece of physics is missing from the classical description: the coupling of the chemical potential of a

The author is in the Department of Materials Science and Engineering, Northwestern University, Evanston, IL 60208–3108, USA. E-mail: p-voorhees@northwestern.edu

For news and research with impact, turn to *Science*

There's only one source for news and research with the greatest impact – *Science*. With over 700,000 weekly print readers, and millions more online, *Science* ranks as one of the most highly read multidisciplinary journals in the world. And for impact, *Science* can't be beat. According to the recently released Thomson ISI Journal Citation Report 2005, *Science* ranked as the No. 1 most-cited multidisciplinary journal with a citation factor of 31. Founded in 1880 by inventor Thomas Edison, and published by the nonprofit AAAS, *Science*'s reputation as the leading source for news, research, and leading edge presentation of content continues to grow. Looking for news and research that will impact the world tomorrow? Then look in *Science*.

www.sciencemag.org

To join AAAS and receive your own personal copy of *Science* every week go to **www.aaas.org/join**

Science
AAAS

step to the elastic energy. In this case, the elastic energy is a result of the stain dependence of the (100) surface energy (surface stress) and the strain field induced on the surface by the presence of the dislocation. Because the dimer rows change orientation as a step is traversed, the surface energy on the upper side of a step is different from that on the lower side. As a result, there is an elastic energy driving force for step motion. Because the strain due to a dislocation is a complicated function of position along the surface, the difference in surface energy across a step changes with the location of the step and the classic Archimedean spiral step pattern is not observed. The experiments are performed in a parameter range where the double-height step dissociates into two single-height atomic steps. Thus, the LEEM results show that these two single-height steps engage in a complicated dance as they rotate about the dislocation core.

Although such a qualitative description captures the basic cause of the novel step patterns, the distinguishing aspect of this work is that all the parameters needed to make a comparison between theory and experiment—such as step mobility, step stiffness, and anisotropy in the surface stress—are known. With these data and a numerical solution to the variation in the velocity of a step as a function of position along the surface, it is possible to confirm that the strain field of the dislocation and the surface structure of Si(001) are responsible for the observed novel step motion.

This work shows that the dynamics of step motion on semiconductor surfaces still holds many surprises and that much remains to be discovered. For example, at lower temperatures step energies become more anisotropic. This would alter the step patterns and might affect the manner in which the steps move. Another extension of this work is to study step motion under growth with different atomic species. For example, when germanium is deposited on silicon, the difference in lattice parameter between the two materials yields another source of stress. This stress would then couple to the stress generated by the dislocation and, potentially, alter the manner in which the steps move. Yet more complex step dances wait to be discovered.

References

1. F. C. Frank, *Disc. Faraday Soc*. **5**, 48 (1949).
2. J. B. Hannon, V. B. Shenoy, K. W. Schwarz, *Science* **313**, 1266 (2006).
3. W. K. Burton, N. Cabrera, F. C. Frank, *Proc. R. Soc. A* **243**, 299 (1950).
4. R. J. Hamers, R. M. Tromp, J. E. Demuth, *Phys. Rev. B* **34**, 5343 (1986).
5. M. B. Webb, F. K. Men, B. S. Swartzentruber, R. Kariotis, M. G. Lagally, *Surf. Sci*. **242**, 23 (1991).
6. N. C. Bartelt, R. M. Tromp, E. D. Williams, *Phys. Rev. Lett*. **73**, 1656 (1994).

10.1126/science.1131892

CHEMISTRY

Fluorous to the Core

Molecular cages with highly fluorinated cores can easily take up suitable guest molecules.

John A. Gladysz

Fluorous molecules—which are fluorine-rich and based on saturated carbon (*1*)—commonly separate from aqueous and organic phases. This "molecular xenophobia," which is often reversible at elevated temperatures, is caused not by repulsive forces but rather by the much greater attractions between water molecules or organic molecules. Fluorous molecules have been widely used to separate products and catalysts or products and reagents, purify mixtures, and control reactions. Many fluorous microenvironments have been created, including micelles, vesicles, microbubbles, tubules, and hollow fibers (*2*), dendrimers (*3*, *4*), nanoparticles (*5*), and modified solid phases (*6*, *7*). They have been exploited as contrast agents for ultrasound imaging, drug delivery, and oxygen transport.

However, none of these assemblies feature the elegant design elements and the degree of molecular control that characterize the complexes reported by Sato *et al.* on page 1273 of this issue (*8*). The authors use coordination-driven self-assembly to generate a polycationic cage consisting of 12 palladium atoms and 24 bent pyridine-based linkers (see the figure). Attached to the concave side of the linkers are ponytails of the formula $–OCH_2CH_2X$, where X is a completely fluorinated chain of six to nine saturated carbon atoms. These chains reside in the cage, creating fluorous environments. Nuclear magnetic resonance (NMR) data support the proposed structures, which might be viewed as prototypes for "inverse dendrimers," with branches in a converging region of space.

Models suggest that if X is a six-carbon fluorinated chain, the chains do not completely fill the cage, leaving a void space. The fluorous guest molecule perfluoro-*n*-octane can then be incorporated in the cage from a surrounding dimethyl sulfoxide suspension. NMR data indicate that an average of 5.8 molecules of perfluoro-*n*-octane can be accommodated. Single crystals of the inclusion complex can be grown. Synchroton x-ray studies of these crystals indicate a slightly oval geometry (4.9 nm by 4.2 nm); the fluorinated segments are disordered, suggesting a fluidlike or "nano-droplet" environment.

Other experiments support this host/guest model. For example, complexes with longer

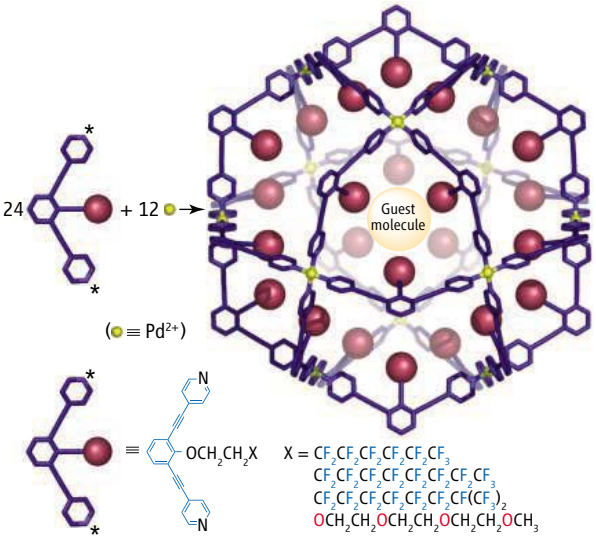

Self-assembly and guest incorporation. Cages containing 12 positively charged palladium atoms (yellow) are generated using banana-shaped linkers (dark blue) with fluorous or polyether substituents (red spheres). Void spaces in the core of the fluorinated cages allow the selective incorporation of fluorous molecules. Nonfluorous molecules such as hexafluorobenzene do not function as guests, but smaller gas molecules such as O_2 and CH_4 might have appreciable solubilities in fluorocarbons. The polyether cages reversibly bind metal ions.

CREDIT: ADAPTED FROM (*8*)

The author is at the Institut für Organische Chemie, Friedrich-Alexander-Universität, 91054 Erlangen, Germany. E-mail: gladysz@chemie.uni-erlangen.de

fluorinated carbon chains should have less interior void space. When these are similarly treated with perfluoro-*n*-octane, fewer molecules are incorporated. For the nonfluorous hexafluorobenzene molecule, no host/guest complex can be detected.

Thus, in contrast to the inaccessible interiors of large fullerenes, the cages reported by *Sato et al.* can readily take up suitable guests. It remains unclear, however, how the guests gain access. Dissociation of linkers from the cages would generate transient channels or pores, but this process is known to be slow. Hence, transport probably occurs through one of the existing large portals.

The same research team has previously reported closely related complexes with other types of interior functionality (*9*). For example, when X is a polyether segment, the core of the cage complex features a dense array of oxygen donor atoms that should be able to bind metal ions. Indeed, when acetonitrile solutions of this complex were treated with sources of La^{3+} ions, about 20 ions were incorporated. When dimethyl sulfoxide (which strongly solvates many metal cations) was added, the La^{3+} ions were extracted, demonstrating that the formation of host/guest complexes is reversible.

How might such assemblies be exploited in future work? One major impetus for the industrial development of fluorous chemistry during the 1990s was the hope that fluorous media might be used in the selective oxidation of methane to methanol (*10*). Small gaseous molecules such as methane and oxygen are usually highly soluble in fluorous phases. Methanol, because of its much greater polarity, might be rapidly scavenged by a nonfluorous phase before further oxidation could occur. Reactions of such guest molecules with the fluorous cages reported by Sato *et al.* are therefore of particular interest. The next logical step would be to immobilize a fluorous oxidation catalyst in the cage interior and treat the system with a mixture of methane and oxygen.

The highly positively charged cages might also be attractive for anionic fluorous guests. Because of toxicity concerns and environmental persistence, several commercial fluorous carboxylates and sulfonates have been removed from the market in recent years (*11*, *12*). It is possible that they could be scavenged by the fluorous cages or by second-generation derivatives.

The results reported by Sato *et al.* are likely to inspire many more ideas for applications. Given that such assemblies can be prepared from a variety of linkers, that guests can easily be incorporated, and that more voluminous analogs are likely to be available soon, this initial study is certain to be followed by many exciting discoveries.

References and Notes

1. I. T. Horváth, D. P. Curran, J. A. Gladysz, in *Handbook of Fluorous Chemistry*, J. A. Gladysz, D. P. Curran, I. T. Horváth, Eds. (Wiley/VCH, Weinheim, Germany, 2004), pp. 1–4.
2. M. P. Krafft, in *Handbook of Fluorous Chemistry*, J. A. Gladysz, D. P. Curran, I. T. Horváth, Eds. (Wiley/VCH, Weinheim, Germany, 2004), pp. 478–490.
3. A. Garcia-Bernabé, M. Krämer, B. Olàh, R. Haag, *Chem. Eur. J.* **10**, 2822 (2004).
4. V. Perec *et al.*, *Angew. Chem. Int. Ed.* **44**, 4739 (2005).
5. M. Moreno-Mañas, R. Pleixats, in *Handbook of Fluorous Chemistry*, J. A. Gladysz, D. P. Curran, I. T. Horváth, Eds. (Wiley/VCH, Weinheim, Germany, 2004), pp. 491–507.
6. D. P. Curran, in *Handbook of Fluorous Chemistry*, J. A. Gladysz, D. P. Curran, I. T. Horváth, Eds. (Wiley/VCH, Weinheim, Germany, 2004), pp. 101–127.
7. L. V. Dinh, J. A. Gladysz, *Angew. Chem., Int. Ed.* **44**, 4095 (2005).
8. S. Sato, J. Iida, K. Suzuki, M. Kawano, T. Ozeki, M. Fujita, *Science* **313**, 1273 (2006).
9. M. Tominaga *et al.*, *J. Am. Chem. Soc.* **127**, 11950 (2005).
10. I. T. Horváth, in *Handbook of Fluorous Chemistry*, J. A. Gladysz, D. P. Curran, I. T. Horváth, Eds. (Wiley/VCH, Weinheim, Germany, 2004), pp. 5–10.
11. C. Hogue, *Chem. Eng. News* **83**, 5 (4 July 2005).
12. S. K. Ritter, *Chem. Eng. News* **84**, 37 (30 January 2006).
13. I thank the Deutsche Forschungsgemeinschaft (grant GL 300/3-3) for support.

10.1126/science.1131944

GEOCHEMISTRY

The Hawaiian-Emperor Bend: Older Than Expected

The kink in the Hawaiian-Emperor seamount chain in the Pacific Ocean was initiated ~50 million years ago, at a time when major plate motion changes occurred.

Joann M. Stock

One of the most stunning features of the Pacific Ocean floor is the Emperor-Hawaiian volcanic seamount chain, which stretches for 6000 km from the vicinity of the Kamchatka peninsula to the modern volcanic island of Hawaii, with a 60° kink in the middle (the "Hawaiian-Emperor Bend"). The seamounts and islands get progressively younger from north to south; the oldest mounts in the north were active ~80 million years ago, whereas Hawaii is still an active volcano today.

This age progression has been attributed to the relative motion between the Pacific lithospheric plate and a deeper source of the volcanism (the Hawaiian hot spot source). However, it has been difficult to explain the bend in the chain, because its age of 43 million years (*1*, *2*) did not correspond to any known change in the motion of the Pacific plate with respect to adjacent plates (*3*, *4*). On page 1281 of this issue, Sharp and Clague (*5*) provide new dates for the volcanic rocks that push the age of the bend back to ~50 million years—a time when major plate motion changes occurred. The result has important implications for studies of drift among hot spots, mantle flow fields, and the initiation of subduction.

How could the age of these seamounts have been underestimated by so much? At any volcano, the youngest eruptive products overlie the older ones and are therefore most accessible to seafloor sampling, coring, and dredging. Rocks that erupted during the major shield-building phase—the main phase of eruption of the volcano, during which it is centered over the hot spot source and 90 to 95% of the lavas are erupted—often can only be retrieved by drilling holes in the ocean floor. As more sampling has been done, the multimillion-year life span of the Hawaiian and Emperor volcanoes has become apparent (*6*, *7*). Furthermore, age dating, paleomagnetic studies, and geochemical studies have shown that many previously dated samples postdate the main shield-building events at these volcanoes (*5*) (see the figure). Improvements in isotopic dating techniques have allowed more precise dating of samples, and reevaluation of past results indicates that the ages of some samples reflected not the time of the original eruption but that of a later reheating event (*5*, *8*).

The Hawaiian-Emperor bend is the most widely cited example of a change in the velocity of a tectonic plate relative to an underlying volcanic source. The origin of the volcanism is controversial, but the erup-

The author is in the Division of Geological and Planetary Sciences, California Institute of Technology, Pasadena, CA 91125, USA. E-mail: jstock@gps.caltech.edu

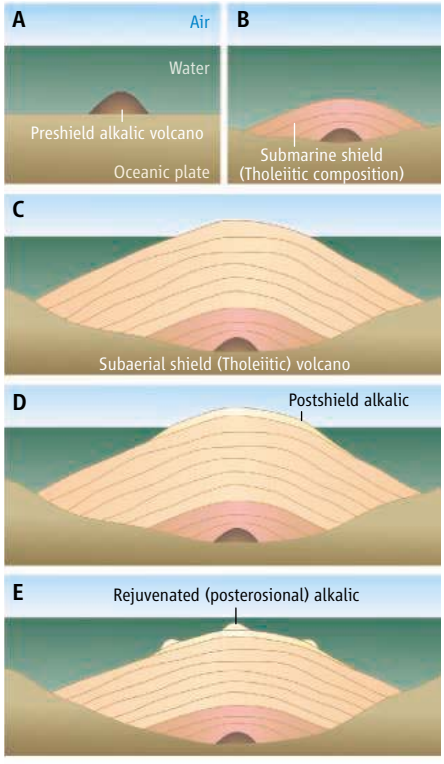

A typical ocean island volcano. These cross sections of an ocean island volcano such as a Hawaiian seamount illustrate the main stages of its evolution: preshield alkalic stage (**A**), main shield-building stage (**B** and **C**), postshield alkalic stage (**D**), and rejuvenated stage (**E**). The rocks most easily sampled or dredged on the volcano's surface can be considerably younger than the major phase of volcanism that built the volcano.

tion source clearly has not been stationary with respect to Earth's spin axis, because the latitude of the Emperor seamount eruptions decreased with time until roughly the time of the Hawaiian-Emperor bend (*9*). Duncan and Keller (*8*) recently showed that the rate of propagation of volcanism along the Emperor section of the seamount chain varied considerably, first speeding up and then slowing down. Sharp and Clague now show that the change in orientation of the seamount chain was not abrupt: The change started 50 million years ago and took more than 8 million years to complete.

The revision of the age of such a tectonic feature by 7 million years has far-reaching consequences. Studies of plate motions and mantle dynamics that assumed a younger age of the bend will have to be adjusted (*10*, *11*). Plate reconstructions based only on marine magnetic anomalies from seafloor spreading centers are not affected, but the exact rates of relative hot spot drift calculated from these reconstructions (*12*) may have to be adjusted in light of the new ages assigned to the Hawaiian-Emperor volcanism. There will be better agreement between two different methods for determining the northward motion of the Pacific plate—one based on sedimentation patterns that show when locations on the Pacific plate crossed the equator (*13*), the other based on the age progression of the Hawaiian seamounts.

The new ages for the Hawaiian-Emperor bend and seamount chain help to clarify the connections among mantle dynamics, Pacific plate motion, and major reorganizations of plate boundaries in the western Pacific Ocean. The Aleutian, Izu-Bonin-Marianas, and Tonga-Kermadec subduction zones, which all started between 55 and 45 million years ago, involved major changes in the geometry and forces at the boundaries of the Pacific plate (*14*, *15*). None of these geometric changes could have occurred unless there had already been a change in the relative velocity of the Pacific plate with respect to adjacent plates. The time lag between these changes and the occurrence of the Hawaiian-Emperor bend was a major conundrum; the problem has now been removed by Sharp and Clague. Their results will spur new efforts to model mantle dynamics and plate kinematics through times of major changes in plate configuration, as well as additional data collection efforts.

More details of the spatial variation in paleolatitude and in volcanic propagation rates for the Hawaiian-Emperor volcanic seamount chain remain to be identified, and the published age progressions of other volcanic seamount chains will need to be scrutinized. The results of Sharp and Clague highlight the key role played by ocean drilling on this and many other seamount chains.

References

1. D. A. Clague, G. B. Dalrymple, *USGS Prof. Pap. 1350*, 5 (1987).
2. G. B. Dalrymple, D. A. Clague, *Earth Planet. Sci. Lett.* **31**, 313 (1976).
3. T. Atwater, in *The Geology of North America, The Eastern Pacific Ocean and Hawaii*, E. Winterer, D. M. Hussong, R. W. Decker, Eds. (Geological Society of America, Boulder, CO, 1989), vol. N, p. 21–72.
4. I. O. Norton, *Tectonics* **14**, 1080 (1995).
5. W. D. Sharp, D. A. Clague, *Science* **313**, 1281 (2006).
6. B. C. Kerr, D. W. Scholl, S. L. Klemperer, *Geochem. Geophys. Geosyst.* **6**, 10.1029/2004GC000705 (2005).
7. T. A. Bianco, G. Ito, J. M. Becker, M. O. Garcia, *Geochem. Geophys. Geosyst.* **6**, 10.1029/2005GC000945 (2005).
8. R. A. Duncan, R. A. Keller, *Geochem. Geophys. Geosyst.* **5**, 10.1029/2004GC000704 (2004).
9. J. A. Tarduno *et al.*, *Science* **301**, 1064 (2003); published online 24 July 2003 (10.1126/science.1086442).
10. M. A. Richards, C. Lithgow-Bertelloni, *Earth Planet. Sci. Lett.* **137**, 19 (1996).
11. B. Steinberger, R. Sutherland, R. J. O'Connell, *Nature* **430**, 167 (2004).
12. C. A. Raymond, J. M. Stock, S. C. Cande, *AGU Geophys. Monogr.* **121**, 359 (2000).
13. J. M. Parés, T. C. Moore, *Earth Planet. Sci. Lett.* **237**, 951 (2005).
14. M. A. Cosca, R. J. Arculus, J. A. Pearce, J. G. Mitchell, E. J. Essene, *Island Arc* **7**, 579 (1998).
15. M. G. Gurnis, C. Hall, L. Lavier, *Geochem. Geophys. Geosyst.* **5**, 10.1029/2003GC000681 (2004).

10.1126/science.1131789

BEHAVIOR

The Power of Social Psychological Interventions

Timothy D. Wilson

Brief social psychological interventions that focus on people's perceptions of themselves and their environment have been shown to increase academic performance.

Some readers will undoubtedly be surprised, or even incredulous, that a 15-min intervention can reduce the racial achievement gap by 40%. Yet this is precisely what Cohen *et al.* (*1*) report on page 1307 of this issue. African American seventh graders randomly assigned to write about their most important values achieved significantly better end-of-semester grades than students in a control condition. How can this be?

As the authors note, these results are not unprecedented. Previous studies have found results of similar magnitude in samples of United States college students (see the table) (*2*–*4*). These studies share important features: Each drew on social psychological theories to change people's self- and social perceptions (i.e., people's explanations for their poor performance, their views of the malleability of their own intelligence, or their sense of social connectedness). Each did so with brief, inexpensive interventions. In each study, people in the treatment conditions achieved better grades than people in the control conditions. These increases were

The author is in the Department of Psychology, University of Virginia, Charlottesville, VA 22904–4400, tdw@virginia.edu

modest, averaging .29 on a grade-point average (GPA) scale (where A = 4, B = 3, and so on; see the table). Nonetheless, these gains are impressive, given that grades were assessed from several weeks to several months after the interventions.

The Cohen *et al*. study adds substantially to this earlier work. They used an intervention tailored to help African Americans, a group that has underperformed in American educational settings (*5*). Students in the treatment condition spent 15 min writing about why certain values, such as relationships with other people, were important to them. Students in the control condition wrote about why specific values were important to other people. African American students in the treatment condition achieved better end-of-semester grades than did African American students in the control condition. These results are especially encouraging given how intractable a problem the racial achievement gap has appeared to be (*6*).

Social psychological interventions

Participants	Intervention	Increase in GPA
African American 7th graders (*1*)	Students wrote about why a selected value was important to them	0.30
First year college students (*2*)	Information that grades improve after the first year	0.27
College students (*3*)	Information that intelligence is malleable	0.23
African American college students (*4*)	Information that worries about social belonging lessen over time	0.34

Better grades. Brief theory-based interventions improved students' grades [increases shown on a four-point grade point average (GPA) scale, relative to randomly assigned control groups].

The Cohen *et al.* study and the others like it illustrate key social psychological points. It can be as important to change people's "construals"—their interpretations of the social world and their place in it—as it is to change the objective environment. In none of the studies, for example, was there an effort to change the quality of the instruction students received, the clarity of the texts they read, or any other objective feature of the educational environment. Instead, the researchers attempted to change students' construals of themselves or how other people viewed them, with promising results. The objective environment is obviously important as well; as Cohen *et al*. note, the success of their intervention depended on students being in a supportive environment. How people perceive that environment, however, can be key to bringing about lasting change.

Brief theory-based interventions that focus on people's construals can reap large benefits. Kurt Lewin, the founder of modern social psychology, noted that many behavioral patterns are the result of a complex interplay of opposing social forces, resulting in a "tension system" (*7*, *8*). Sometimes these opposing forces exist in a delicate state of equilibrium, such that small interventions can set in motion processes that change the entire system. Altering people's views of themselves, or how they think others view them, can lead to cascading changes in motivation and performance. For example, students can be caught in a self-perpetuating "exacerbation cycle," whereby poor academic performance confirms their worst fears about themselves, which increases their anxiety, which hampers their subsequent performance, which further confirms their worst fears, and so on (*9*, *10*). Giving people nonpejorative explanations for poor performance (e.g., everyone has to "learn the ropes" at college) can interrupt this cycle and prevent its spiraling consequences (*2*, *11*).

The success of such interventions—indeed, of any intervention—is best tested with experimental designs in which people are randomly assigned to treatment and control conditions. As obvious as this point is in some settings (e.g., tests of medical treatments), it is not fully appreciated in others (e.g., educational settings, in which new programs are frequently implemented without being evaluated experimentally) (*12*). There are a number of reasons for this, such as people's reliance on common sense to judge the effectiveness of interventions in familiar domains (e.g., the classroom). A lesson of the studies reviewed here is that common sense is sometimes wrong. Without the experimental results presented by Cohen *et al*., who would have thought that a 15-min exercise would have had such long-lasting effects?

Social psychological theories, based on carefully conducted laboratory experiments, generate (often nonobvious) predictions about human behavior. Dozens of experiments, conducted primarily with college students in laboratory settings, have documented the damaging effects that stereotypes about one's group can have on individuals' performance (known as stereotype threat), as well as relatively simple ways of avoiding this damage (*13*–*15*). The Cohen *et al*. intervention follows directly from this basic research.

The fact that small, theory-based interventions can have large effects should not be taken as a criticism of large-scale attempts at social change. As important as people's construals of their environment are, often the environment itself needs changing. The achievement gap is surely caused by multiple factors, including poverty, racism, and lack of parental involvement (*6*). Findings such as Cohen *et al*.'s should not divert our attention from these critical problems. By the same token, the fact that large-scale societal factors need changing should not prevent us from seeking proximate solutions that are easy to implement.

There are, of course, limitations to the findings from these studies, as well as many unanswered questions. It is not clear why students in the Cohen *et al*. sample failed to self-affirm on their own. Why did it take an in-class essay to focus students' attention on values that were important to them? Issues of generalizability also arise, such as whether the self-affirmation exercise would work with younger age groups. These questions can be answered only with additional experiments, ideally ones as well conducted as the Cohen *et al*. studies.

References

1. G. L. Cohen, J. Garcia, N. Apfel, A. Master, *Science* **313**, 1307 (2006).
2. T. D. Wilson, P. W. Linville. *J. Pers. Soc. Psychol.* **49**, 287 (1985).
3. J. Aronson, C. B. Fried, C. Good. *J. Exper. Soc. Psychol.* **38**, 113 (2002).
4. G. M. Walton, G. L. Cohen *J. Pers. Soc. Psychol.,* in press.
5. C. M. Steele, *Amer. Psych.* **52**, 613 (1997).
6. R. Rothstein, *Class and Schools* (Teachers College Press, New York, 2004).
7. K. Lewin, *Field Theory in Social Science* (Harper, New York, 1951).
8. L. Ross, R. E. Nisbett, *The Person and the Situation* (McGraw Hill, New York, 1991).
9. S. Valins, R. E. Nisbett, in *Attribution: Perceiving the Causes of Behavior*, E. E. Jones *et al*., Eds. (General Learning Press, Morristown, NJ, 1972), pp. 137–150.
10. M. D. Storms, K. D. McCaul, in *New Directions in Attribution Research,* J. H. Harvey *et al.*, Eds. (Erlbaum, Hillsdale, NJ, 1976), vol. 1, pp. 143–164.
11. T. D. Wilson, M. Damiani, N. Shelton, in *Improving Academic Achievement,* J. Aronson, Ed. (Academic Press, San Diego, CA, 2002), pp. 89–108.
12. T. D. Wilson. *Psychol. Inq.* **16**, 185 (2005).
13. C. M. Steele, in *Advances in Experimental Social Psychology*, L. Berkowitz, Ed. (Academic Press, San Diego, CA, 1988), pp. 261–302.
14. C. M. Steele, S. J. Spencer, J. Aronson, in *Advances in Experimental Social Psychology*, M. P. Zanna, Ed. (Academic Press, San Diego, CA, 2002), pp. 379–440.
15. D. K. Sherman, G. L. Cohen, in *Advances in Experimental Social Psychology*, M. P. Zanna, Ed. (Academic Press, San Diego, CA, 2006), pp. 183–242.

10.1126/science.1133017

Legal Notice

UNITED STATES DISTRICT COURT
FOR THE DISTRICT OF COLUMBIA

MOLECULAR DIAGNOSTICS LABORATORIES, Plaintiff, v. HOFFMANN-LA ROCHE INC., ROCHE MOLECULAR SYSTEMS, INC., ROCHE DIAGNOSTICS CORPORATION, PE CORPORATION, PE BIOSYSTEMS GROUP, THE PERKIN-ELMER CORPORATION, PE APPLIED BIOSYSTEMS, and APPLERA CORPORATION, Defendants.	: Civil Action No. 1:04CV01649 (HHK) : CLASS ACTION

TO: ALL PERSONS OR ENTITIES WHO PURCHASED CERTAIN *TAQ* PRODUCTS DIRECTLY FROM DEFENDANTS DURING THE PERIOD OF SEPTEMBER 23, 2000 TO THE PRESENT.

YOU ARE HEREBY NOTIFIED, pursuant to an Order of the United States District Court for the District of Columbia, that a class of purchasers of certain *Taq* products has been certified by the Court, pursuant to an Order of the Court dated July 5, 2006.

The Class is defined as:

> All persons or entities who purchased certain *Taq* products directly from Defendants during the period of September 23, 2000 to the present. Excluded from the class are Defendants, their officers, directors, management, employees, subsidiaries, or affiliates, and the federal government.

Your rights may be affected by this litigation if you directly purchased the *Taq* products at issue from a defendant from September 23, 2000 to the present. For a list of the *Taq* products at issue, please refer to www.completeclaimsolutions.com/taq/.

If you have not received a printed Notice of Class Certification ("Notice"), you may obtain a copy by writing to *Taq Antitrust Litigation* c/o Complete Claim Solutions, LLC, P.O. Box 24652, West Palm Beach, Florida 33416, by calling the Claims Administrator's *Taq* Hotline at 1-877-884-5903, or by accessing those documents at www.completeclaimsolutions.com/taq/. The Notice contains further information regarding the rights of Class Members.

PLEASE DO NOT CONTACT THE COURT OR THE CLERK'S OFFICE REGARDING THIS NOTICE.

Dated: August 4, 2006

Henry H. Kennedy
United States District Judge

Microarthropods Mediate Sperm Transfer in Mosses

Nils Cronberg,[1]* Rayna Natcheva,[1,2] Katarina Hedlund[1]

The algal ancestors to all land plants were fertilized by sperm, which could freely swim between male and female structures in the aquatic environment. Some extant land plants, such as ferns, lycopods, horsetails, and bryophytes (mosses, liverworts, and hornworts), are still fertilized by sperm, whereas gymnosperms and angiosperms are fertilized by pollen, which is drought resistant and dispersed by wind or animals. Sperm are usually considered inefficient and poorly adapted to terrestrial conditions because of their dependency on a continuous water layer for dispersal.

We designed a greenhouse experiment to test whether springtails or mites could mediate fertilization between spatially separated male and female mosses. Patches of male and female plants of a cosmopolitan unisexual moss (*Bryum argenteum* Hedwig) were positioned at three different distances, 0 cm (i.e., united), 2 cm, and 4 cm apart, in separate transparent plastic vials (Fig. 1A). A bottom layer of water-absorbing plaster of Paris served as a physical barrier for sperm. This design was replicated (n = 7) for three different treatments: (i) with actively moving springtails (*Isotoma caerulea* Bourlet), (ii) with slower moving oribatid mites [*Scutovertex minutus* (C. L. Koch) and *S. sculptus* Michael], and (iii) without animals. Successful fertilization was expected to result in production of sporophytes physically attached to the mother shoots.

After 3 months, abundant sporophytes were found in vials in which male and female patches were united, where sperm could swim freely (Fig. 1B). No fertilization was observed in the treatment without animals and where the sexes were kept apart at 2 and 4 cm, confirming that sperm were unable to disperse on their own. Numerous sporophytes were produced when animals were present and when moss patches were spatially separated, demonstrating that both springtails and mites were capable of transporting sperm across both distances. The means of this transport is an open question, but presumably the sperm adhere to arthropod cuticle somehow. The results also confirm that distances of sperm transfer between mosses are related to the mobility of the animals, because the test with the more-mobile springtails gave a higher fertilization success at a greater distance.

These observations raise the question of whether animal-mediated fertilization results from passive random movements or active visits to fertile structures, similar to visits of pollinators to flowers. To test this, we conducted a series of preference experiments. In separate sets of vials, we allowed animals to choose between male fertile versus sterile shoots, between female fertile versus sterile shoots, and also between fertile shoots of both genders. Both springtails and mites preferred fertile to sterile shoots (Fig. 1C). We do not know the reason for the attraction, but it may be because fertile shoots are a source of food, because they not only secrete sucrose (*1*) but also starch, fatty acids, and mucilage (*2*–*4*).

Our results suggest that a mutualistic relationship exists between bryophytes and microarthropods. About 50% of moss species are unisexual, having male and female structures on different individuals, which means that fertilization success is distance-dependent and often limited by the availability of mates. When water is scarce and a continuous water film is lacking, animal-mediated sperm transfer seems to be the only possible mode of fertilization, even in bisexual and potentially self-compatible species.

The origin of animal-mediated fertilization has been assumed to involve angiosperms and insects (insect pollination), although angiosperms first emerged during the early Cretaceous (circa 140 million years ago), and some of the insect groups involved in pollination appear to have radiated well before this period (*5*). It is hypothesized that insect pollination started as pollinivory (pollen consumption) and then evolved toward more-complex mutualistic relationships (*6*). Mosses, springtails, and mites are extant representatives of taxa that originated after the early phase of land colonization (circa 440 to 470 million years ago). Animal-mediated fertilization in mosses therefore potentially antedates similar syndromes in other plant groups.

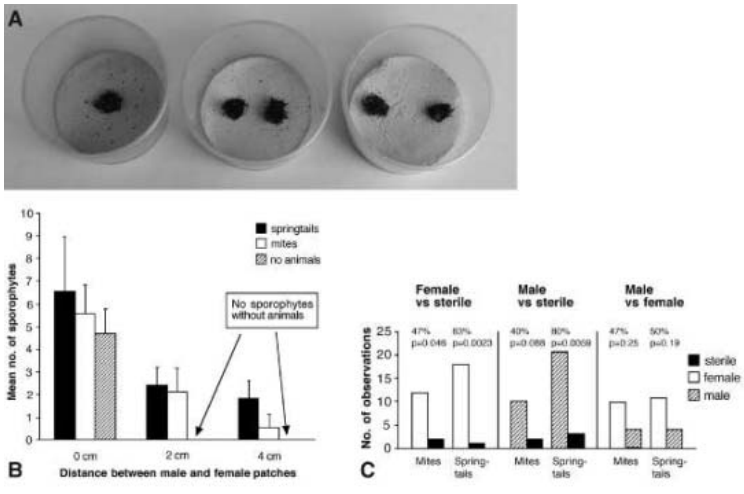

Fig. 1. Fertilization of moss shoots by mites and springtails. (**A**) Vials with male and female moss patches united or separated by 2 and 4 cm. (**B**) Sporophyte production in female moss patches in presence versus absence of springtails or mites. Fertilization was achieved when patches of different sexes were united and, when spatially separated, exclusively in the presence of animals. Each bar represents the mean number of sporophytes in seven replicates (error bars represent one standard error). (**C**) Preference experiment (two-choice test) in which mites and springtails were allowed to choose between fertile and sterile moss shoots. Percentages represent the proportion of 30 replicates in which animals were present on the moss shoots. Bars show the numbers of animals present on fertile or sterile shoots. Significance levels of G tests are also given.

References and Notes

1. W. Pfeffer, *Untersuchungen aus dem botanischen Institut in Tübingen* 1, 363 (1884).
2. R. J. Harvey-Gibson, D. Miller-Brown, *Ann. Bot.* (London) **41**, 190 (1927).
3. D. J. Paolillo, *Bryologist* **82**, 93 (1979).
4. K. Renzaglia, D. J. Garbary, *Crit. Rev. Plant Sci.* **20**, 107 (2001).
5. K. J. Willis, J. C. McElwain, *The Evolution of Plants* (Oxford Univ. Press, Oxford, 2002).
6. C. C. Labandeira, *Science* **280**, 57 (1998).
7. We thank S. Andersson, W. van der Putten, and R. Wyatt for helpful comments on the manuscript. N.C. acknowledges support from the Swedish Research Council for Environment, Agricultural Sciences, and Spatial Planning (FORMAS).

Supporting Online Material

www.sciencemag.org/cgi/content/full/313/5791/1255/DC1
Materials and Methods
Tables S1 and S2

13 April 2006; accepted 12 July 2006
10.1126/science.1128707

[1]Department of Ecology, Lund University, S-223 62 Lund, Sweden. [2]Bulgarian Academy of Sciences, 23 G. Bonchev Street, 1113 Sofia, Bulgaria.

*To whom correspondence should be addressed. E-mail: Nils.Cronberg@ekol.lu.se

What are viewers saying about *Science* Online Seminars?

"Fabulous...Fantastic...Terrific idea!"

"It is a wonderful mode of education in this age of interdisciplinary science. Thank you for launching this series."

"This is a FANTASTIC new offering by *Science*! Congratulations!"

"This is a very neat series, and I would love to be able to use this as a resource for my undergraduate teaching."

"I am introducing it to many of my colleagues."

"This feature alone is worth the subscription, very cool. Thank you!"

"This is absolutely fantastic!"

See them for yourself at:

www.sciencemag.org/onlineseminars

Science
AAAS

Coherent Control of Retinal Isomerization in Bacteriorhodopsin

Valentyn I. Prokhorenko,[1] Andrea M. Nagy,[1] Stephen A. Waschuk,[2] Leonid S. Brown,[2] Robert R. Birge,[3] R. J. Dwayne Miller[1]*

Optical control of the primary step of photoisomerization of the retinal molecule in bacteriorhodopsin from the all-trans to the 13-cis state was demonstrated under weak field conditions (where only 1 of 300 retinal molecules absorbs a photon during the excitation cycle) that are relevant to understanding biological processes. By modulating the phases and amplitudes of the spectral components in the photoexcitation pulse, we showed that the absolute quantity of 13-cis retinal formed upon excitation can be enhanced or suppressed by ±20% of the yield observed using a short transform-limited pulse having the same actinic energy. The shaped pulses were shown to be phase-sensitive at intensities too low to access different higher electronic states, and so these pulses apparently steer the isomerization through constructive and destructive interference effects, a mechanism supported by observed signatures of vibrational coherence. These results show that the wave properties of matter can be observed and even manipulated in a system as large and complex as a protein.

Quantum mechanics dictates that all matter has an inherent wave property. On a molecular scale, this property can lead to destructive and constructive interferences that have a pronounced effect on transmission probabilities along reaction coordinates. Modern spectroscopic techniques have afforded direct evidence of such interferences and even exploited interference of the underlying wave properties to steer chemical reactions one way or another (*1*). For the most part, however, these studies have focused on small molecules and ions. In a protein, random fluctuations among the enormous number of degrees of freedom might be expected to cancel any interference effects. At the same time, proteins are highly evolved structures, and the question arises whether the phases of the underlying matter waves could play a role or even be manipulated in directing biological processes. This question can be addressed by determining the degree of conserved phase relationships, or quantum coherence, involved in a chemical process occurring within the confines of the protein environment. Experimental tests for coherence, as for any wave phenomena, must be able to demonstrate the creation of both constructive and destructive interference pathways, a process termed coherent control for molecular systems (*1*, *2*).

Tests of quantum coherence are most readily accomplished for photoactive processes in which short, specifically shaped excitation pulses can be used to manipulate the process on a time scale faster than random thermal motions act to scramble phase relationships (cause decoherence). In this regard, one of the fastest biological processes is the photoisomerization of the retinal molecule in rhodopsin proteins. This relatively simple photochemical reaction is the primary event for vision in higher organisms, photoreceptor response, and energy conversion in halobacteria. As such, the reaction has been subject to intense experimental and theoretical investigation (*3*–*11*). The possibility of manipulating the isomerization efficiency by excitation with tailored excitation light pulses has also been discussed from a theoretical standpoint in which a small subset of the total number of coupled motions is treated (*12*, *13*). However, the full problem is computationally intractable and so requires direct experimental investigation for resolution.

Experimental manipulation of the relative photoisomerization yield of a molecule was recently reported for the cyanine dye NK88 in solution (*14*). These studies were conducted using excitation energies near saturation level for the absorption in question (1.5 μJ per pulse); the primary action of the shaped light fields may have been to control the excited-state population (*15*) rather than the reaction coordinate itself. Under strong field excitation conditions, multiphoton processes inevitably access higher-lying excited states and so substantially perturb the state of interest. These issues are irrelevant if the objective is to induce a particular reaction outcome, but they become important in interpreting the correlation of the pulse shapes with the molecular processes.

Previous pulse-shaping studies of biological systems (*16*) were also performed under relatively strong excitation conditions and demonstrated the quenching of energy transfer from the carotenoids in light-harvesting systems. This effect was attributed to enhanced nonradiative relaxation of the carotenoid excited state; it was not possible to control the converse pathway to increase energy transfer. Our goal in the present study was to control the absolute isomerization yield of the 13-cis retinal isomer in bacteriorhodopsin (bR). We sought specifically to control the degree of coherence in the protein environment in the weak field regime so as to ensure that the resultant dynamics would pertain to the protein's behavior under normal functional conditions. In this context, we report the manipulation of the absolute yield of 13-cis retinal over a 40% range, clearly demonstrating that a protein can manifest coherent interference effects. Through feedback-controlled amplitude and phase variation of the spectral components composing the excitation pulse, we could selectively enhance or suppress the isomerization yield by 20% in either direction.

Optimization of the isomerization yield. Photoisomerization of the retinal chromophore in bR (Fig. 1) occurs with a relatively high quantum yield (≈65%) (*17*, *18*) of the 13-cis isomer. Prior work has shown that the isomerization is complete within ≈3 ps (*6*), and the product, termed the K intermediate, has a well-resolved positive differential absorption (ΔA) band in the 630- to 640-nm range (*19*, *20*). To ensure adequate vibrational cooling, we chose a 20-ps delay after the actinic pulse before targeting the 630-nm absorption feature for optimization (a detailed description of the materials and methods is given in the supporting online material). At this delay, the magnitude of measured signal ΔA, weighted by actinic excitation energy (the amount of photons absorbed in a sample), directly reflects the isomerization

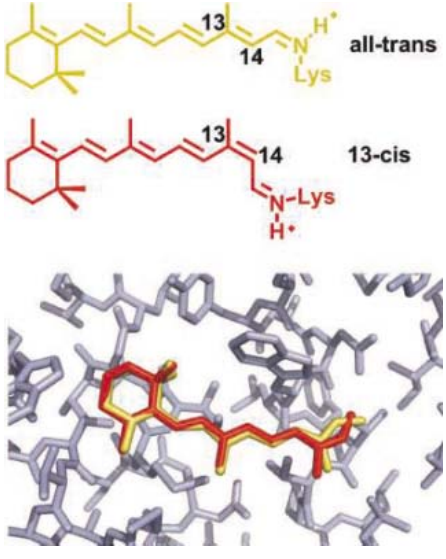

Fig. 1. Configurations of the retinal molecule (**top**) in bacteriorhodopsin (**bottom**) in the ground state (all-trans, yellow), and after isomerization (13-cis K form, red). [The bottom image is from the Protein Data Bank; identification numbers 1QHJ and 1QKP (*39*).] The photoisomerization process requires a torsional motion and bond stretching along the C13-C14 axis. The motion through the transition-state region connecting the excited reactant and product surfaces will involve a superposition of vibrations to give this localized displacement (*11*, *12*).

[1]Institute for Optical Sciences, Departments of Chemistry and Physics, University of Toronto, 80 St. George Street, M5S3H6, Toronto, Ontario, Canada. [2]Department of Physics, University of Guelph, N1G2W1, Guelph, Ontario, Canada. [3]Department of Chemistry, University of Connecticut, Storrs, CT, USA.

*To whom correspondence should be addressed. E-mail: dmiller@lphys.chem.utoronto.ca.

yield. We then used a well-established genetic algorithm and feedback approach to solve a multivariable problem to converge toward tailored pulses that would either maximize or minimize the 630-nm induced absorption, corresponding to the respective enhancement or suppression of the isomerization yield (Fig. 2). The different excitation pulse shapes were generated by appropriate manipulation of incoming transform-limited pulses [19 fs full width at half maximum (FWHM), centered at 565 nm with a bandwidth of 60 nm] in both frequency and phase domains (*21*). Using only phase manipulation would substantially restrict the control space. In accordance with certain properties of the Fourier transform, frequency amplitude modulation is necessary to produce, for example, a comb of temporally spaced subpulses, a prominent feature of the optimal pulses derived in recent coherent control experiments (*16*, *22*).

We applied the optimization algorithm to a starting set of 30 pulses with randomly distributed spectral phases and amplitudes (pulse energies were 16 to 17 nJ, corresponding to a fluence E_{exc} = 2.7 × 10^{14} photons/cm^2); the growth of ΔA consistently saturates after 30 to 40 generations (600 to 800 shaping cycles) at a level ~23% higher than that induced by the excitation with the transform-limited pulse. The spectrum of the optimal excitation pulse (Fig. 3A) has a gravity center at ~557 nm and a regular structure composed of several peaks spaced ~6 nm apart (both of these features have been reproduced in more than 20 optimization experiments). The anti-optimization experiment (Fig. 2B) also converged after ~30 generations under the same conditions, to yield a pulse that suppresses isomerization efficiency by ~24%. The spectrum of the anti-optimal pulse (Fig. 3D) was relatively broad and redshifted to ~577 nm. The isomerization quantum yield of 13-cis retinal in bR has been shown experimentally to be wavelength-independent across the full 500- to 670-nm absorption band. This spectral insensitivity was confirmed at different temperatures, using different light sources and methods (*23*–*26*). Nevertheless, we performed an additional check by irradiating our bR samples with tunable 120- to 140-fs excitation pulses of relatively narrow spectral width (8 nm FWHM), and found the yield to be wavelength-independent within a 535- to 610-nm window (fig. S2). The optimization has to be ascribed to the specific shapes of the excitation pulses.

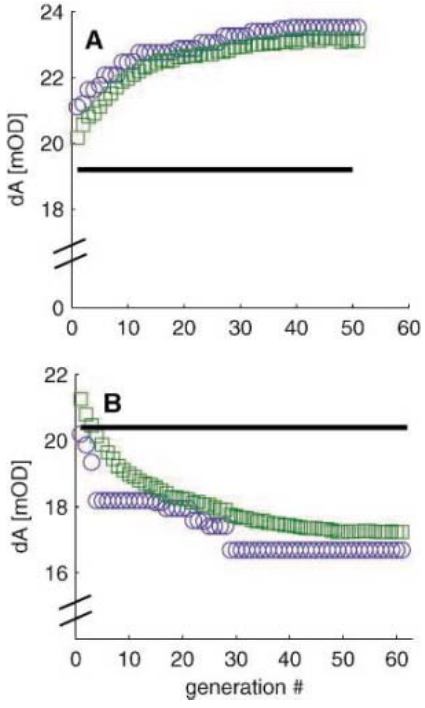

Fig. 2. Effect of evolving pulse shapes on the isomerization yield of retinal in bR, measured at 630 nm delayed 20 ps after excitation. In (**A**) maximization and (**B**) minimization experiments, green squares correspond to averaged values of the differential absorbance ΔA (over the whole population), and blue circles correspond to the most effective pulses [for enhancement in (A) or suppression in (B)] within the current population. The solid horizontal lines correspond to the ΔA measured by excitation with the transform-limited pulse (19 fs FWHM) as a baseline for comparison.

For determining the temporal profiles of the optimized pulses, we used frequency-resolved optically gated (FROG) measurements (Fig. 3). Both optimal and anti-optimal pulses displayed regular and periodic modulations. The retrieved intensity profile of the optimal pulse showed a comb of ~eight subpulses (Fig. 3C). In contrast, energy in the anti-optimal pulse was mostly concentrated in a single feature ~80 fs (FWHM) in duration (Fig. 3F), with smaller-amplitude subpulses. These intensity profiles were independently examined by recording the cross-correlation functions between the investigated pulses and a compressed white-light pulse (harmonic sum generation, with detection corresponding to the doubled frequency of the pulses) and were in good agreement with the retrieved pulse profiles from the FROG measurements.

Regarding frequency distributions over time, distinct spectral components in the optimal pulse had different magnitudes (and signs) of chirp (Fig. 3C), whereas the main peak in the anti-optimal pulse was not chirped (Fig. 3F). In our previous studies of the population transfer in solvated molecules, an anti-optimal pulse that suppressed the excited-state population had a clear, strong, negative chirp (*22*). Lack of this feature in the present case implies that suppression of the isomerization yield in bR is caused not by lowering of the excited-state population but by some process that affects the reaction probability; namely, destructive interference effects in the excited vibrational modes. This interpretation was independently confirmed by measuring the number of absorbed photons directly (the absorbed energy was measured as the difference between incoming and outgoing pulse energies, using a power meter with a corresponding correction for wavelength). To an accuracy of ±1%, the number of absorbed photons was found to be the same for the optimal, transform-limited, and anti-optimal pulses at low excitations, where the response of the bR is linear with respect to absorbed energy. Because the number of absorbed photons exactly corresponds to the number of excited molecules in this low excitation limit, we therefore conclude that the observed changes in isomerization yield, in both the optimization and anti-optimization experiments, were due to control of the intrinsic isomerization efficiency rather than to modulation of the excited-state population. Selective coupling of the applied electric field to vibrational modes appears to be involved in controlling the reaction.

From the time profiles of the shaped pulses, one can get an appreciation of the driving force provided by the applied electric field to gain insight into the mechanism. In order to better elucidate the details of the underlying shaped electric fields that drive the molecular coherences, we used a Wigner transform (*27*) to uncover the instantaneous frequency profile of the pulse shape

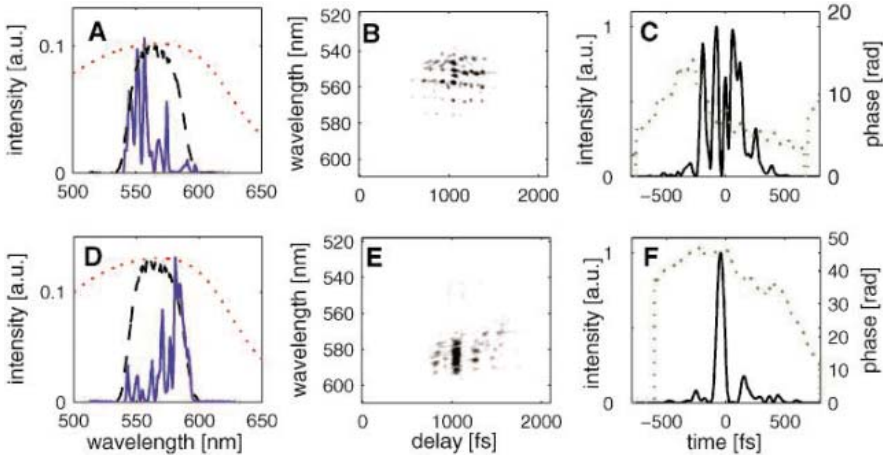

Fig. 3. (**A**) Spectral profile of the optimal excitation pulse (solid blue line), the transform-limited (19 fs FWHM) pulse (black dashed line), and bR transmittance spectrum (red dotted line). (**B**) Measured FROG trace for the optimal pulse. (**C**) Retrieved intensity (solid line) and phase profile (dashed line) from the FROG trace. (**D** to **F**) Corresponding data for the anti-optimal pulse. a.u., arbitrary units; rad, radians.

(fig. S3). According to these plots, the optimal pulse has a main temporal modulation with a period of 145 fs (230 ± 14 cm^{-1}), whereas the anti-optimal pulse is modulated by a period of approximately 215 fs (155 cm^{-1}). The optimal pulse has a modulation period that is resonant with the low-frequency torsional motions (and harmonics) in the excited state that are thought to be the key modes involved in the isomerization process, whereas the anti-optimal pulse is off resonance and thereby out of phase with this period. The exact modulation is more complex, involving different spectral components in the laser pulse that may be related to the non-Markovian dynamics of the involved vibrational modes. The most distinctive feature is the correspondence of the laser field modulation to one of the key modes involved in the reaction.

In the initial phase of the optimization experiments, we found that ΔA and thus the isomerization efficiency were slightly higher when the excitation pulse had randomly distributed phases and amplitudes than when it was transform-limited. This observation is very unusual and surprising (more than 20 optimization experiments were carried out in order to confirm this effect). No such effect has been observed in solvated organic molecules (*22*). In this regard, the photoisomerization process involves the displacement of more than one vibrational mode of retinal along the reaction coordinate (predominantly torsional and bond stretching character between C13 and C14), but not all vibrational modes uniformly; and this process is in strong competition with very fast nonradiative relaxation back to the ground state. We speculate that the protein structure may be biased to the displacement of the reactive modes preferentially along the reaction coordinate, in which case, sparse excitation to populate these modes may be favored over excitation of single vibrations or many unreactive modes that would steer the system away from the conical intersection or barrier crossing for reaction. In any case, this observation explains how the pulse optimization process avoided simple control of the excited-state population. There is a strong built-in bias for the photoreaction.

Transient kinetics. Transient kinetics (Figs. 4 and 5) were measured at the sample at variable delay times (within a 5- to 600-ps window) after excitation with the transform-limited, optimal, and anti-optimal pulses (all with equivalent actinic energies of 15.1 nJ ± 1%). The changes in isomerization efficiency had a stationary character (the absorption changes were constant within the 20- to 600-ps delay window), and the differences in the magnitudes of ΔA were ~20% (500-ps delay at 630 nm) relative to the difference spectrum observed upon excitation with the transform-limited pulse (Fig. 5). These magnitudes are smaller than those obtained during the optimization experiments (most likely because of differences in the samples used); however, they are still within the absolute accuracy of measurements. The distinction in pump-probe kinetics within the first ~5 ps after the excitation pulses is noteworthy, especially with excitation using the anti-optimal pulse. The difference in the population kinetics across the three pulses is present not only in the traces displayed in Fig. 5A, but in the whole investigated spectral range. In the delay window corresponding to the overlap of the probe pulse (~30 fs FWHM) with the excitation pulses, we clearly detected the presence of specific periodic modulations in pump-probe signals driven by the optimal and anti-optimal pulses (Fig. 4, B and C). Coupling of the optimal light pulse to specific vibrational modes resulted in the appearance of 195 ± 15 cm^{-1} oscillations with substantial amplitude (±30% of the maximal bleaching) in pump-probe kinetics (Fig. 4, B1 and B2). In contrast, in the pump-probe kinetics driven by the anti-optimal pulse, the observed oscillation had an aperiodic character (Fig. 4, C1 and C2) and strong positive chirp. The manifestation of strong oscillations in the pump-probe kinetics (quantum beats) clearly indicates a coherent excitation of the vibrational states (*28*) by the optimal pulse. Taking into account the results of previous studies of the retinal and bR vibrational structure (*29*, *30*), we posit that such an excitation pulse selectively and efficiently drives the ~200 cm^{-1} torsional mode in retinal by keeping the corresponding molecular vibrational mode in a coherent state during the excitation cycle (~300 fs) of the shaped pulse, and thus enhances the isomerization yield. We are effectively creating a specific superposition of vibrational modes (the so-called vibrational wave packet) on the excited-state surface that then propagates to the reactive crossing and is better tuned to the reaction. This enhancement of specific Raman-active modes has recently been experimentally demonstrated (*31*), using "open-loop" control to generate temporally periodic pulses that were resonant with the vibrational period of the desired mode (a train of several pulses spaced apart in time and frequency domains to be in resonance with this mode).

We emphasize the similarity between the temporal/spectral profile of the oscillations derived from the two-dimensional (2D) transient

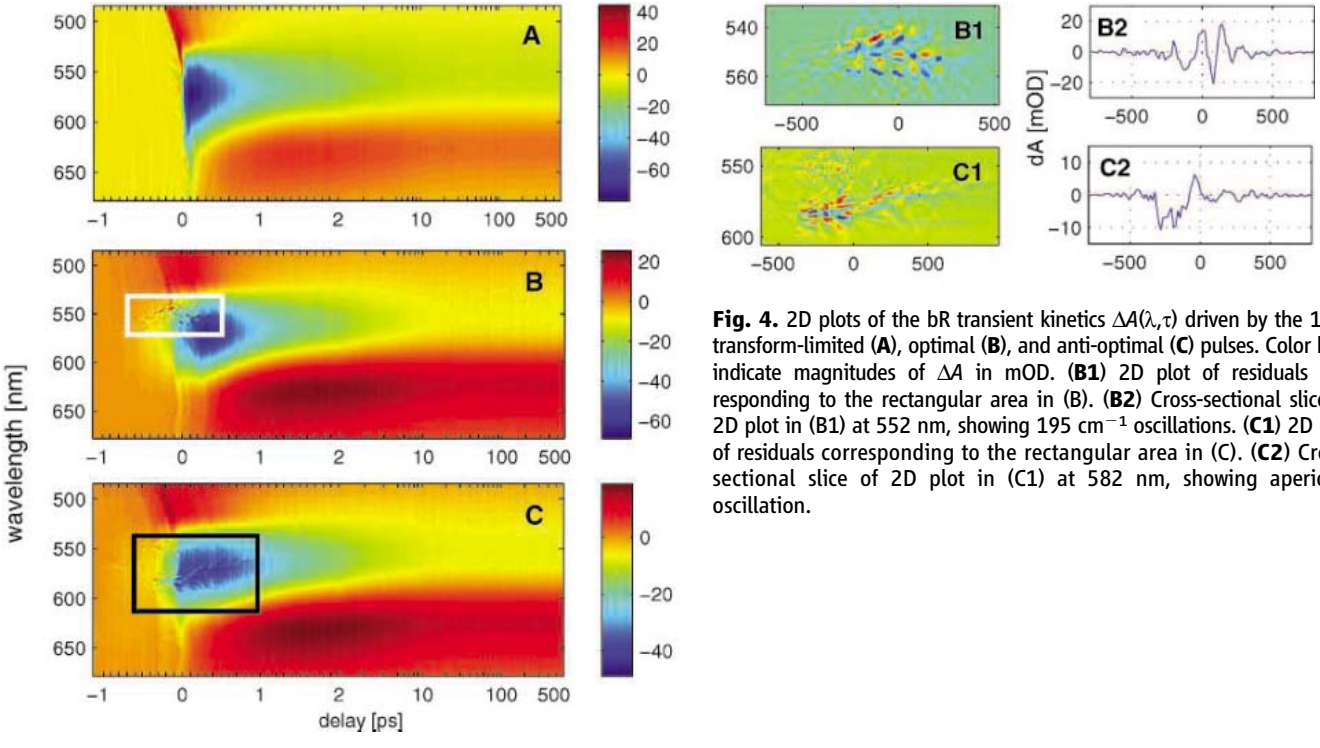

Fig. 4. 2D plots of the bR transient kinetics $\Delta A(\lambda,\tau)$ driven by the 19-fs transform-limited (**A**), optimal (**B**), and anti-optimal (**C**) pulses. Color bars indicate magnitudes of ΔA in mOD. (**B1**) 2D plot of residuals corresponding to the rectangular area in (B). (**B2**) Cross-sectional slice of 2D plot in (B1) at 552 nm, showing 195 cm^{-1} oscillations. (**C1**) 2D plot of residuals corresponding to the rectangular area in (C). (**C2**) Cross-sectional slice of 2D plot in (C1) at 582 nm, showing aperiodic oscillation.

kinetics (Fig. 4, B1 and C1) and the Wigner plots of the optimized pulses (*21*). The latter projections provide a visual portrayal of these key features of the shaped excitation fields.

Isomerization efficiency. At probe delays long enough to ensure completion of the K-intermediate buildup and full relaxation of unreacted all-trans retinal molecules to the ground state, the differential absorption spectrum was determined by absorption cross sections of the product isomer $\sigma_{cis}(\lambda)$ and the initial reactant $\sigma_{trans}(\lambda)$

$$\Delta A(\lambda) \propto \eta_{IY}[\sigma_{cis}(\lambda) - \sigma_{trans}(\lambda)]A_0 \quad (1)$$

where η_{IY} is the isomerization efficiency. A_0 is proportional to the number of initially excited all-trans retinal molecules and can be determined from the pump-probe kinetics driven by an impulsive excitation from the initial bleaching at zero delay [the absorption and excited-state emission spectra in bR are well separated (*10*), and thus the transient kinetics in the 540- to 600-nm window are not affected by stimulated emission]. Using the measured in situ absorption cross section $\sigma_{trans}(\lambda)$, the K-intermediate spectra can be straightforwardly derived from the ΔA spectra measured at a delay of 500 ps (Fig. 5B) by applying Eq. 1. Such decomposition (initial bleaching A_0 = –78 milli–optical density (mOD), using the19-fs pulse excitation) reproduces, within experimental accuracy, identical spectral shapes for the K intermediate and equal ratios [$\max(\sigma_{cis})/\max(\sigma_{trans})$ = 0.91 ± 0.01] if the isomerization yields η_{IY} are input as 78, 65, and 52% for the optimal, transform-limited, and anti-optimal pulses, respectively (fig. S4). Thus, the control of the absolute isomerization yield in bR using tailored excitation pulses is achieved over an absolute range of (78 – 52)/65 = 40%. The ratio between the maxima of the absorption cross sections for all-trans and 13-cis bR forms, as well as the position (585 nm) and shape of the band with $\max(\sigma_{cis})$, are in good agreement with the previously resolved transient spectra for these states (*19*).

Energy dependence of isomerization and phase sensitivity. Our experiments were designed to test for quantum interference effects within biological systems. These studies must be conducted under weak field conditions in order to ensure that the same electronic levels are probed as in the actual biological processes. Ideally, these experiments should be conducted within the linear response with respect to the excitation energy to avoid any possible multiphoton processes. In the low–excitation energy limit, an isolated quantum system with a finite number of eigenstates, such as a small molecule in vacuum, should generally be insensitive to the phase information contained in the excitation light (*1*). Such a "closed" quantum system is always in a pure state (a coherent superposition of eigenstates) that can be described using the Schrödinger equation and wave function formalism (*32*). The retinal molecule in a protein environment belongs to the class of "open" systems, wherein the molecule/environment (system/bath) interaction leads to dephasing of the system states and energy redistribution among them, creating mixed states. Coherent control of such open systems is a difficult problem to treat theoretically because it requires specific information about the bath interactions that is generally not known. However, very recently the manipulation of the excited-state population in an open system (a molecule in a solvent) was experimentally demonstrated, and the phase sensitivity in the weak excitation limit (only 1 molecule in ~500 absorbing a photon during the excitation cycle) was revealed (*22*). The phase sensitivity of the excited-state population in dissipative systems was further modeled numerically (*33*), and the selective excitation of Raman active modes in the excited state in this regime has also been demonstrated (*34*). These recent developments are consistent with our interpretation of exciting specific vibrations in the excited state that interfere at the reaction crossing point. However, the energy dependence and coherent nature of the excited modes need to be determined to ensure that the experiments are in the weak field limit for coherent control.

The fluence in the optimization experiments E_{exc} = 2.7 × 10^{14} photons/cm^2 was approximately 20 times lower than the level necessary to saturate the retinal $S_0 \rightarrow S_1$ transition in the protein environment, which can be estimated, using the known extinction coefficient (*35*) ε(560 nm) = 54000 M^{-1} cm^{-1}, to be E_s = 4.8 × 10^{15} photons/cm^2 (*36*). At this relatively low fluence, the ratio between excited and nonexcited molecules (per laser shot) can be estimated, using the Poisson distribution, to be 1:40, and ~1% of the measured signal can arise from two-photon processes such as cascaded absorption $S_1 \rightarrow S_n$ (*37*). Therefore, the influence of actinic pulse energy on the isomerization control efficiency was checked independently by measuring ΔA (630 nm) at a delay of 20 ps for a wide range of pulse energies (Fig. 6A). Coherent control of the isomerization efficiency is clearly operative at the lower energies. Figure 6B shows the corresponding isomerization yield dependencies, defined as $IY(E_{exc}) \propto \Delta A/E_{exc}$. There is a slight nonlinearity to the dependence at a high actinic energy level. However, the isomerization efficiency depends strongly on the excitation pulse shape even for a pulse energy less than 1 nJ, which corresponds to the excitation of 1 bR out of ~300 per laser shot. Another order-of-magnitude reduction in actinic excitation energy with an improvement in signal-to-noise ratio (which is physically limited by

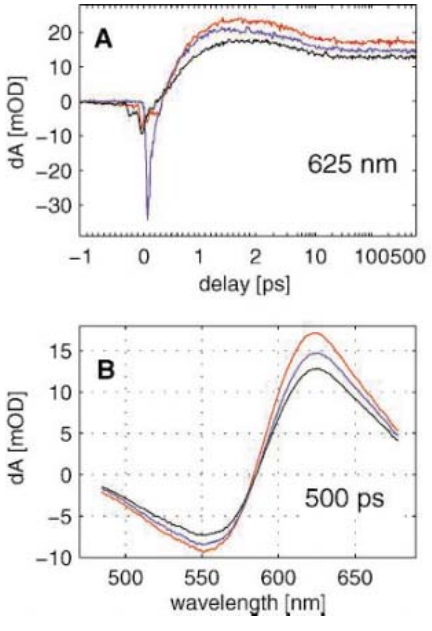

Fig. 5. (**A**) Decay traces at 625 nm measured in a 600-ps delay window after excitation with the optimal (red), transform-limited 19-fs FWHM (blue), and anti-optimal (black) pulses. (**B**) Differential absorption spectra $\Delta A(\lambda)$ acquired 500 ps after excitation [color scheme is as in (A)].

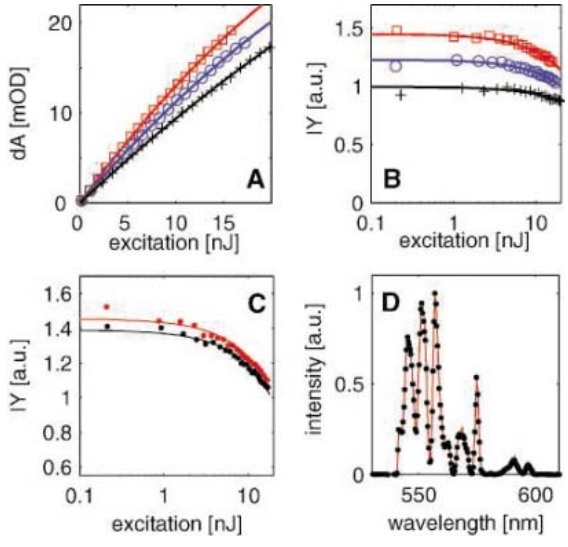

Fig. 6. Energy dependence of (**A**) the ΔA signal, measured at 630 nm 20 ps after excitation, and (**B**) the corresponding isomerization yields. Both plots show results for the optimal (red), anti-optimal (black), and transform-limited (blue) pulses. A quadratic fit (solid lines) shows the energy dependence to be essentially linear at low energies, with a small deviation (due to saturation of the absorbance) of less than 18% at the highest excitation energy. (**C**) Isomerization yields versus excitation energy for the optimal pulse with the phase modulation (red points) and without it (black points), showing a phase sensitivity of isomerization. Lines are quadratic fits. (**D**) Comparison of the spectral profiles of the optimal pulse with (red line) and without (black points) phase modulation. Spectral shapes are essentially identical, and thus the fluence dependencies $\Delta A(E_{exc})$ can be compared directly.

intrinsic light scattering in bR) will help establish the exact nature of the field interaction. The main conclusion is that the experiment is clearly in the weak field limit and the laser field is not strongly perturbing the underlying thermally populated modes, but rather inducing their interference in the excited-state surface. Isomerization yields were also compared with and without phase control (Fig. 6C), keeping spectral amplitudes constant (Fig. 6D; spectral profiles were confirmed using a tunable monochromator with 0.2-nm spectral resolution). The data show a clear phase dependence indicative of coherent control.

Pure amplitude modulation alters the temporal profile of the pulse (fig. S5); therefore, removing the phase modulation affects the isomerization yield by only 5 to 7%. The phase sensitivity of the control efficiency further illustrates the coherent nature of the state preparation.

The temporal profiles of the shaped optimal and anti-optimal pulses and the observed degree of the isomerization yield control are consistent with the known fast electronic dephasing of bR (*10*, *38*). The largest field amplitudes are confined to approximately 300-fs widths to yield 20% control. In the case of transform-limited pulses, all the vibrational levels within the excitation bandwidth are excited in phase and there is a fast decoherence in the initial electronic polarization (*38*). However, with the phase-selective restricted bandwidths in the shaped pulses, there is an opportunity to manipulate different vibrational states with much longer coherence times than the electronic polarization. The resultant constructive and destructive interference effects involving vibrational modes displaced along the reaction coordinate offer the possibility of controlling isomerization. Experimental observations presented here show that the wave properties of matter can play a role in biological processes, to the point that they can even be manipulated.

References and Notes

1. M. Shapiro, P. Brumer, *Rep. Prog. Phys.* **66**, 859 (2003).
2. S. H. Shi, H. Rabitz, *J. Chem. Phys.* **92**, 364 (1990).
3. W. T. Pollard, S. Y. Lee, R. A. Mathies, *J. Chem. Phys.* **92**, 4012 (1990).
4. Q. Wang, R. W. Schoenlein, L. A. Peteanu, R. A. Mathies, C. V. Shank, *Science* **266**, 422 (1994).
5. K. C. Hasson, F. Gai, P. A. Anfinrud, *Proc. Natl. Acad. Sci. U.S.A.* **93**, 15124 (1996).
6. T. Ye *et al.*, *J. Phys. Chem. B* **103**, 5122 (1999).
7. R. Gonzalez-Luque *et al.*, *Proc. Natl. Acad. Sci. U.S.A.* **97**, 9379 (2000).
8. T. Kobayashi, T. Saito, H. Ohtani, *Nature* **414**, 531 (2001).
9. J. Herbst, K. Heyne, R. Diller, *Science* **297**, 822 (2002).
10. J. T. M. Kennis *et al.*, *J. Phys. Chem. B* **106**, 6067 (2002).
11. S. Hayashi, E. Tajkhorshid, K. Schulten, *Biophys. J.* **85**, 1440 (2003).
12. S. C. Flores, V. S. Batista, *J. Phys. Chem. B* **108**, 6745 (2004).
13. Y. Ohtsuki, K. Ohara, M. Abe, K. Nakagami, Y. Fujimura, *Chem. Phys. Lett.* **369**, 525 (2003).
14. G. Vogt, G. Krampert, P. Niklaus, P. Nuernberger, G. Gerber, *Phys. Rev. Lett.* **94**, 068305 (2005).
15. K. Hoki, P. Brumer, *Phys. Rev. Lett.* **95**, 168305 (2005).
16. J. L. Herek, W. Wohlleben, R. J. Cogdell, D. Zeidler, M. Motzkus, *Nature* **417**, 533 (2002).
17. J. Tittor, D. Oesterhelt, *FEBS Lett.* **263**, 269 (1990).
18. S. L. Logunov, M. A. El-Sayed, *J. Phys. Chem. B* **101**, 6629 (1997).
19. H. J. Polland *et al.*, *Biophys. J.* **49**, 651 (1986).
20. F. Gai, K. C. Hasson, J. C. McDonald, P. A. Anfinrud, *Science* **279**, 1886 (1998).
21. See supporting data on *Science* Online.
22. V. I. Prokhorenko, A. M. Nagy, R. J. D. Miller, *J. Chem. Phys.* **122**, 184502 (2005).
23. A. K. Dioumaev, V. V. Savransky, N. V. Tkachenko, V. I. Chukharev, *J. Photochem. Photobiol. B Biol.* **3**, 397 (1989).
24. G. Schneider, R. Diller, M. Stockburger, *Chem. Phys.* **131**, 17 (1989).
25. A. Xie, *Biophys. J.* **58**, 1127 (1990).
26. S. P. Balashov, E. S. Imasheva, R. Govindjee, T. G. Ebrey, *Photochem. Photobiol.* **54**, 955 (1991).
27. J. Paye, *IEEE J. Quant. Electron.* **28**, 2262 (1992).
28. H. L. Fragnito, J.-Y. Bigot, P. C. Becker, C. V. Shank, *Chem. Phys. Lett.* **160**, 101 (1989).
29. A. B. Myers, R. A. Harris, R. A. Mathies, *J. Chem. Phys.* **79**, 603 (1983).
30. B. X. Hou, N. Friedman, M. Ottolenghi, M. Sheves, S. Ruhman, *Chem. Phys. Lett.* **381**, 549 (2003).
31. R. Morita, M. Yamashita, A. Suguro, H. Shigekawa, *Opt. Commun.* **197**, 73 (2001).
32. K. Blum, *Density Matrix Theory and Applications* (Plenum, New York, 1981).
33. D. Gelman, R. Kosloff, *J. Chem. Phys.* **123**, 234506 (2005).
34. J. Hauer, H. Skenderovic, K.-L. Kompa, M. Motzkus, *Chem. Phys. Lett.* **421**, 523 (2006).
35. D. Oesterhelt, W. Stoeckenius, in *Methods in Enzymology*, vol. 31 of *Biomembranes* (Academic Press, New York, 1974), pp. 667–678.
36. The saturation energy is related to the absorption cross section σ as $E_s = 1/\sigma_{trans}$ (for a negligibly small contribution of the excited-state emission), and σ is related to the extinction coefficient ε as $\sigma = [\log(10)/N_A]\varepsilon = 3.86 \times 10^{-21}\varepsilon$, where N_A is Avogadro's number.
37. The fraction of excited molecules can be estimated as a ratio between the number of absorbed photons $n_p = E_{exc} \times \pi d_0^2/4$ and the number of retinal molecules $N_m = C \times V$ in an excited volume $V_0 \cong l_0 \times \pi d_0^2/4$, where the concentration is $C = 2.303A_0/\sigma_{trans}$, A_0 is OD at 565 nm (0.9), $l_0 = 0.04$ cm is the path length in the cell used, and $d_0 = 0.015$ cm is the beam diameter in the sample. This gives a fraction of excited molecules of 0.0236 (that is, 1 out of 42.3 molecules will be excited during the excitation pulse at a given fluence). The fraction of double-excited molecules can be estimated from the Poisson distribution $f(k) = e^{-\lambda}(\lambda)^k/k!$, where $\lambda = 0.0236$, and k is the number of occurrences ($k = 1$ for the single excitation, $k = 2$ for the double excitation, etc.). Thus, the fraction of double-excited molecules $f(2)/f(1) = \lambda/2$; that is, 1.18%.
38. V. F. Kamalov, T. M. Masciangioli, M. A. El-Sayed, *J. Phys. Chem.* **100**, 2762 (1996).
39. K. Edman *et al.*, *Nature* **401**, 822 (1999).

40. This work was supported by the National Sciences and Engineering Research Council of Canada. The authors thank J.T.M. Kennis, Vrije Universiteit Amsterdam, for helpful discussions of preliminary results.

Supporting Online Material

www.sciencemag.org/cgi/content/full/313/5791/1257/DC1
Materials and Methods
Figs. S1 to S5
References

1 June 2006; accepted 10 August 2006
10.1126/science.1130747

Phytophthora Genome Sequences Uncover Evolutionary Origins and Mechanisms of Pathogenesis

Brett M. Tyler,[1*] Sucheta Tripathy,[1] Xuemin Zhang,[1] Paramvir Dehal,[2,3] Rays H. Y. Jiang,[1,4] Andrea Aerts,[2,3] Felipe D. Arredondo,[1] Laura Baxter,[5] Douda Bensasson,[2,3,6] Jim L. Beynon,[5] Jarrod Chapman,[2,3,7] Cynthia M. B. Damasceno,[8] Anne E. Dorrance,[9] Daolong Dou,[1] Allan W. Dickerman,[1] Inna L. Dubchak,[2,3] Matteo Garbelotto,[10] Mark Gijzen,[11] Stuart G. Gordon,[9] Francine Govers,[4] Niklaus J. Grunwald,[12] Wayne Huang,[2,14] Kelly L. Ivors,[10,15] Richard W. Jones,[16] Sophien Kamoun,[9] Konstantinos Krampis,[1] Kurt H. Lamour,[17] Mi-Kyung Lee,[18] W. Hayes McDonald,[19] Mónica Medina,[20] Harold J. G. Meijer,[4] Eric K. Nordberg,[1] Donald J. Maclean,[21] Manuel D. Ospina-Giraldo,[22] Paul F. Morris,[23] Vipaporn Phuntumart,[23] Nicholas H. Putnam,[2,3] Sam Rash,[2,13] Jocelyn K. C. Rose,[24] Yasuko Sakihama,[25] Asaf A. Salamov,[2,3] Alon Savidor,[17] Chantel F. Scheuring,[18] Brian M. Smith,[1] Bruno W. S. Sobral,[1] Astrid Terry,[2,13] Trudy A. Torto-Alalibo,[1] Joe Win,[9] Zhanyou Xu,[18] Hongbin Zhang,[18] Igor V. Grigoriev,[2,3] Daniel S. Rokhsar,[2,7] Jeffrey L. Boore[2,3,26,27]

Draft genome sequences have been determined for the soybean pathogen *Phytophthora sojae* and the sudden oak death pathogen *Phytophthora ramorum*. Oömycetes such as these *Phytophthora* species share the kingdom Stramenopila with photosynthetic algae such as diatoms, and the presence of many *Phytophthora* genes of probable phototroph origin supports a photosynthetic ancestry for the stramenopiles. Comparison of the two species' genomes reveals a rapid expansion and diversification of many protein families associated with plant infection such as hydrolases, ABC transporters, protein toxins, proteinase inhibitors, and, in particular, a superfamily of 700 proteins with similarity to known oömycete avirulence genes.

Phytophthora plant pathogens attack a wide range of agriculturally and ornamentally important plants (*1*). Late blight of potato caused by *Phytophthora infestans* resulted in the Irish potato famine in the 19th century, and *P. sojae* costs the soybean industry millions of dollars each year. In California and Oregon, a newly emerged *Phytophthora* species, *P. ramorum*, is responsible for a disease called sudden oak death (*2*) that affects not only the live

oaks that are the keystone species of the ecosystem but also a large variety of woody shrubs that inhabit the oak ecosystems, such as bay laurel and viburnum (*2*). Many other members of the oömycete phylum are plant or animal pathogens, and some pose biosecurity threats such as the maize downy mildews *Peronosclerospora philippinesis* and *Sclerophthora rayssiae*. Extensive classical and molecular genetic tools and genomics resources have been developed for *P. sojae* and *P. infestans* (*3*, *4*).

Oömycetes fall within the kingdom Stramenopila (*5*, *6*), which also includes golden-brown algae, diatoms, and brown algae such as kelp (Fig. 1A). The algal stramenopiles are secondarily photosynthetic, having engulfed a red alga and adopted its plastid approximately 1,300 million years ago (*6*). However, nonphotosynthetic stramenopiles, such as the oömycetes, do not even have the vestigial plastids found in apicomplexan and euglenoid parasites that originate from phototrophs. Therefore, an important evolutionary question is whether the kingdom Stramenopila was founded by a photosynthetic or nonphotosynthetic organism and, more generally, whether a much larger group of secondarily photosynthetic organisms, called the chromalveolates (*6*), was founded by a single photosynthetic ancestor.

We report here the draft genome sequences of *P. sojae* and *P. ramorum*. The sequences, a nine-fold coverage of the 95 Mb *P. sojae* genome and a seven-fold coverage of the 65 Mb *P. ramorum* genome, were produced using a whole-genome shotgun approach (*7*). We constructed a physical map of *P. sojae* to aid the sequence assembly by using restriction enzyme fingerprinting of bacterial artificial chromosome (BAC) clones from two libraries (*7*). We identified 19,027 predicted genes (gene models) in the genome of *P. sojae* and 15,743 in the genome of *P. ramorum*, supported in part by expressed sequence tags (ESTs) from *P. sojae* and proteomic surveys in *P. ramorum* (*7*). Of these, 9768 pairs of gene models could be identified as putative orthologs (*7*). There are 1755 gene models in *P. sojae* and 624 in *P. ramorum* encoding unique proteins that do not have a homolog in the other genome at a significance threshold of 10^{-8}. The overall higher number of predicted genes in *P. sojae* results from a greater size of many gene families within the species.

There is extensive colinearity of orthologs between the two genomes. One colinear block, illustrated in Fig. 2, spans 1.8 Mb of *P. sojae* sequence and 0.8 Mb of *P. ramorum* sequence and contains 425 *P. sojae* and 265 *P. ramorum* genes, respectively, of which 170 are orthologous (*7*). The longest colinear block spans an estimated 4.8 Mb in *P. sojae* and 2.9 Mb in *P. ramorum* and contains 1129 *P. sojae* and 793 *P. ramorum* gene models, respectively, of which 463 are orthologous. The long-range colinearity between the two genomes is preserved despite the presence of many local rearrangements and many nonorthologous genes. Local disruptions of the gene colinearity are particularly common in the vicinity of genes associated with plant infection such as *P. sojae Avr1b*-1 (*8*) (Fig. 2B).

The genome sequences of *P. sojae* and *P. ramorum* imply several metabolic idiosyncrasies. For example, the CYP51 group of cytochrome P450 enzymes are considered necessary for sterol biosynthesis (*9*). Consistent with *Phytophthora* being sterol auxotrophs, none of these genes could be identified in either *Phytophthora* genome, although most other sterol biosynthetic genes could be recognized. More unexpectedly, neither genome appears to contain any gene for phospholipase C (PLC), an enzyme present in all eukaryotes sequenced so far (*10*), nor are PLC sequences present in a collection of 75,757 ESTs from *Phytophthora infestans* (*11*). In contrast, the diatom *Thalassiosira pseudonana* has three PLC genes. No other highly conserved genes were identified as missing from both the *P. sojae* and *P. ramorum* genomes.

Because *P. ramorum* has recently appeared in California and Europe, an important priority is the development of genetic markers for population genetics and strain tracking of the pathogen. Through sequencing the *P. ramorum* genome, we identified ~13,643 single nucleotide polymorphisms (SNPs) (*7*) and numerous simple sequence repeats useful for this purpose. The *P. sojae* genome sequence contains only 499 SNPs, probably because *P. sojae* is homothallic (inbreeding), whereas *P. ramorum* is heterothallic (outcrossing).

To address whether the kingdom Stramenopila might have been founded by a photosynthetic ancestor (*6*), we searched for *Phytophthora* genes that had especially strong similarities to genes of photosynthetic organisms (*7*). We identified 855 genes with a putative heritage from a red alga or cyanobacterium (fig. S2), of which 30 are detailed in table S4. Some of the most striking examples of the putative acquisition of genes from a photosynthetic ancestor are provided by genes encoding biosynthetic enzymes targeted to the chloroplasts of photosynthetic organisms and to the mitochondria of nonphotosynthetic organisms. Table S4 includes 12 genes whose protein product has a predicted mitochondrial location in *Phytophthora* and a predicted plastid location in plants and/or algae. One example, the gene for 2-isopropylmalate synthase (functioning in leucine biosynthesis), is shown in Fig. 1B. Although a few details of this tree appear to be anomalous, owing perhaps to the ancient separation of these lineages and sparse taxon sampling, there are clearly two major phylogenetic groups of this gene: one acquired in fungi by transfer from an α-proteobacterium, presumably the endosymbiont that gave rise to mitochondria, and the other acquired in algae, plants, and stramenopiles from a cyanobacterium, presumably the endosymbiont that originally gave rise to plastids. It is further interesting that this gene in the diatom *Thalassiosira pseudonana* groups with those of green plants rather than red algae, perhaps indicating a separate ancestry, as has been suggested for some other chromalveolates (*12*, *13*), although this could alternatively be an artifact due to incomplete sampling of lineages or of the genes within them. Figure 1C shows a more unusual example, from the sixth step of purine biosynthesis. The two *Phytophthora* species, together with the diatom *Thalassiosira pseudonana* and the green alga *Chlamydomonas reinhardtii*, are unique among eukaryotes because they have a prokaryotic, organelle-targeted N-phosphoribosyl-carboxy-aminoimidazole (NCAIR) mutase homolog closely resembling that of cyanobacteria (*14*), in addition to a conventional eukaryotic, cytoplasmic-targeted 1-(5-phosphoribosyl)-5-amino-4-imidazole (AIR) carboxylase (Fig. 1C). The presence of numerous genes of putative phototroph origin in the *Phytophthora* genomes lends support to the hypothesis that the stramenopile ancestor was photosynthetic, which is consistent with the chromalveolate hypothesis.

Genes involved in the interactions of *P. sojae* and *P. ramorum* with their hosts are of central interest. Motile *Phytophthora* zoospores exhibit

[1]Virginia Bioinformatics Institute, Virginia Polytechnic Institute and State University, Blacksburg, VA 24061, USA. [2]Department of Energy Joint Genome Institute, Walnut Creek, CA 94598, USA. [3]Genomics Division, Ernest Orlando Lawrence Berkeley National Laboratory, Berkeley, CA 94720, USA. [4]Laboratory of Phytopathology, Wageningen University, NL-6709 PD Wageningen, Netherlands. [5]Horticulture Research International, Wellesbourne, Warwick CV35 9EF, United Kingdom. [6]Department of Biological Sciences, Imperial College, London SL5 7PY, United Kingdom. [7]Center for Integrative Genomics, University of California, Berkeley, CA 94720, USA. [8]Department of Plant Pathology, Cornell University, Ithaca, NY 14853, USA. [9]Department of Plant Pathology, Ohio Agricultural Research and Development Center, The Ohio State University, Wooster, OH 44691, USA. [10]Department of Environmental Science, Policy, and Management, Ecosystem Sciences Division, University of California, Berkeley, CA 94720, USA. [11]Agriculture and Agri-Food Canada, London, ON, Canada, N5V 4T3. [12]Horticultural Crops Research Laboratory, USDA Agricultural Research Service, Corvallis, OR 97330, USA. [13]Biosciences Directorate, [14]Computation Directorate, Lawrence Livermore National Laboratory, Livermore, CA 94550, USA. [15]North Carolina State University Mountain Horticultural Crops Research and Extension Center, Fletcher, NC 28732, USA. [16]Vegetable Laboratory, Henry Wallace Beltsville Agriculture Research Center, USDA Agricultural Research Service, Beltsville, MD 20705, USA. [17]Department of Entomology and Plant Pathology, University of Tennessee, Knoxville, TN 37996, USA. [18]Department of Soil and Crop Sciences, Texas A&M University, College Station, TX 77843, USA. [19]Chemical Sciences Division, Oak Ridge National Laboratory, Oak Ridge, TN 37831, USA. [20]School of Natural Sciences, University of California, Merced, CA 95344, USA. [21]Department of Biochemistry & Molecular Biology, University of Queensland, St. Lucia, Queensland 4072, Australia. [22]Department of Biology, Wilkes University, Wilkes-Barre, PA 18766, USA. [23]Department of Biological Sciences, Bowling Green State University, Bowling Green, OH 43402, USA. [24]Department of Plant Biology, Cornell University, Ithaca, NY 14853, USA. [25]Laboratory of Ecological Chemistry, Hokkaido University, Sapporo 060-8589, Japan. [26]Department of Integrative Biology, University of California, Berkeley, CA 94720, USA. [27]Genome Project Solutions, Hercules, CA 94547, USA.

*To whom correspondence should be addressed. E-mail: bmtyler@vt.edu

chemotaxis toward signals from host tissue such as isoflavones (*15*). In other eukaryotes, chemotaxis reception is mediated by G protein–coupled receptors (GPCRs) (*16*). *P. sojae* and *P. ramorum* each have 24 GPCRs, four of which show a top match to the *Dictyostelium* cyclic adenosine monophosphate chemotaxis receptor. Another 12 GPCRs have a C-terminal intracellular phosphatidylinositol-4-phosphate 5-kinase domain similar to the RpkA gene of *Dictyostelium* (*17*); this domain would enable signaling to bypass the heterotrimeric G proteins, perhaps explaining why the *Phytophthora* genomes contain only single genes for G-α and G-β subunits (*17*).

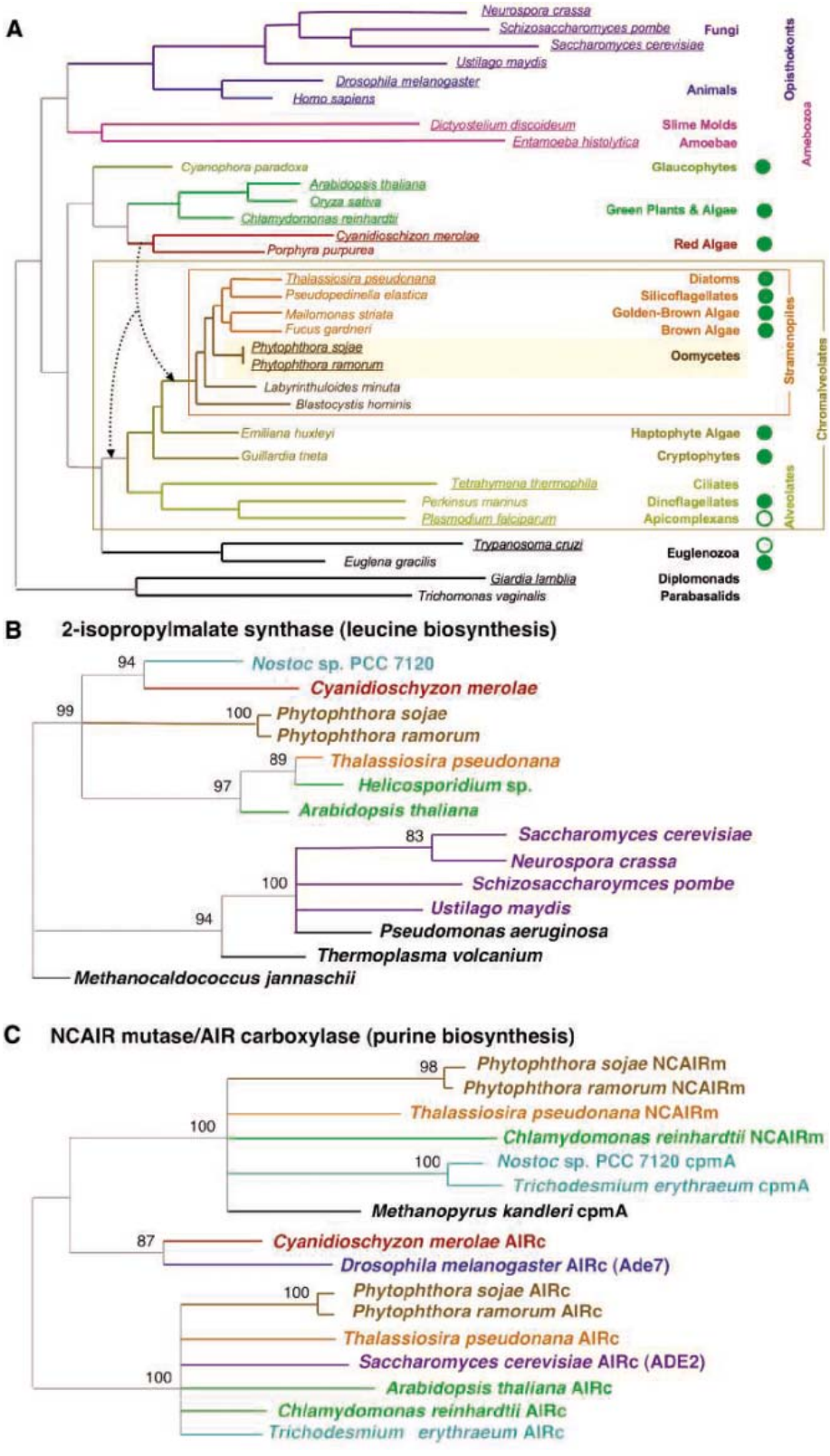

Fig. 1. Identification of genes potentially originating from a photosynthetic endosymbiont. (**A**) Schematic phylogenetic tree of the eukaryotes. The tree is adapted from that of Baldauf *et al*. (*5*) that is based on a concatenation of six highly conserved proteins. Filled green circles on the right indicate photosynthetic species, open green circles indicate species with vestigial plastids of photosynthetic origin. The dotted arrows indicate hypothetical events in which an ancient red algal endosymbiont might have been acquired by an ancestor of the chromalveolates (left arrow) or of the stramenopiles alone (right arrow). (**B** and **C**) Phylogenetic trees produced using maximum parsimony (with the branch and bound algorithm) of amino acid sequences with the computer program PAUP 4.0b10 (*32*). Inferred amino acid sequences were aligned using ClustalW, and these were manually trimmed at each end to a position of confident alignment. (B) and (C) show strict consensus trees for two and three equally parsimonious trees, respectively. In both cases, numerals indicate bootstrap support values, and any with less than 80% have been collapsed. Branch lengths are proportional to sequence change using the accelerated transformation mode for character state reconstruction. Trees were rooted by specifying *Methanocaldococcus jannaschii* and the NCAIR mutase/cpmA cluster of genes as outgroups for (B) and (C), respectively. Taxonomic affinities of the organisms listed are as in (A), with the following additions: green plants, *Helicosporidium* sp.; cyanobacteria, *Nostoc* sp., *Trichodesmium erythraeum*, and *Synechocystis* sp.; other eubacteria, *Pseudomonas aeruginosa*, *Bacillus halodurans*, and *Clostridium acetylbutylicum*; archaebacteria, *Thermoplasma volcanium, M. jannaschii*, and *Methanopyrus kandleri*. In (C), NCAIRm, AIRc, and cpmA denote, respectively, N-phosphoribosylcarboxy-aminoimidazole (NCAIR) mutase, 1-(5-phosphoribosyl)-5-amino-4-imidazole (AIR) carboxylase, and the circadian modifer gene cpmA that is a member of the NCAIR mutase family (*14*).

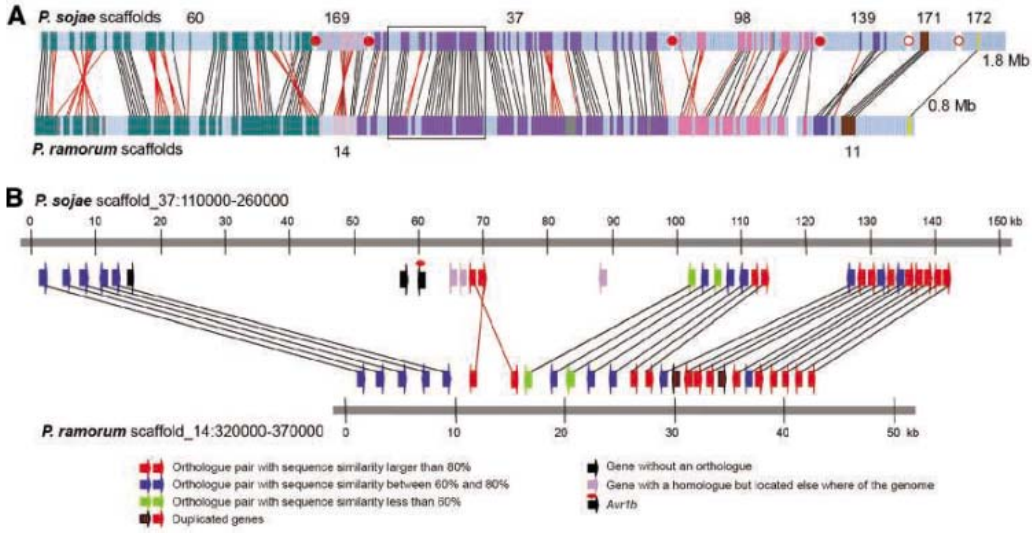

Fig. 2. Long-range gene colinearity between the genomes of *P. sojae* and *P. ramorum*. In (**A**) and (**B**), black and red lines link orthologs of like and reversed orientation, respectively. In (A), colored bars indicate orthologs located in different *P. sojae* sequence scaffolds. Gray bars indicate genes without orthologs. Filled red circles indicate scaffolds linked by a single end-sequenced BAC, and open red circles indicate scaffolds linked by end-sequenced BAC contigs. The boxed area in (A) is enlarged in (B).

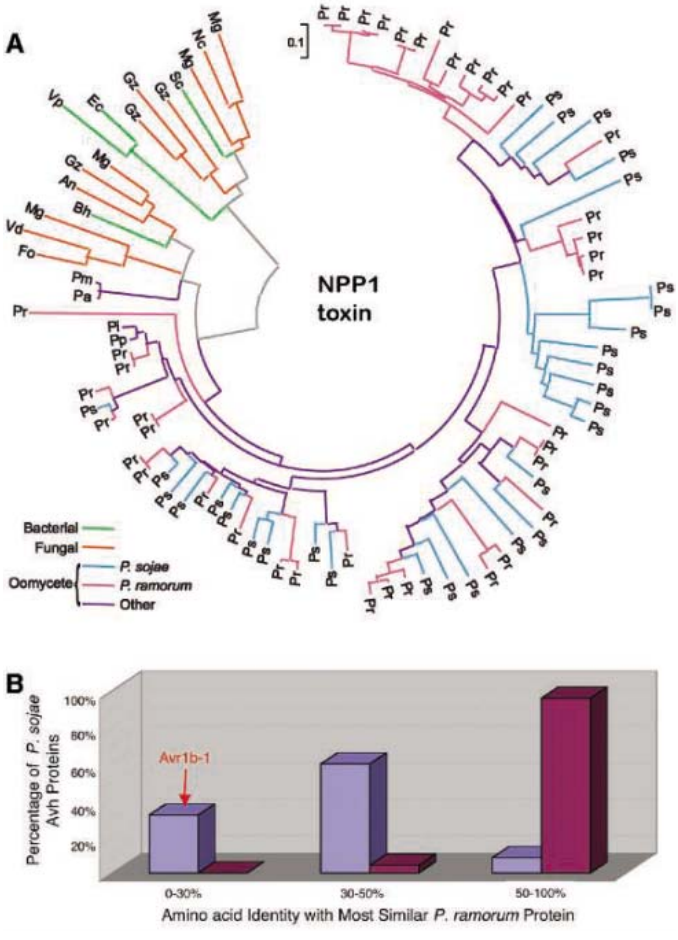

Fig. 3. Sequence divergence of two potential families of pathogenicity genes. (**A**) NPP1 or Nep1-like (NLP) protein sequences. A total of 89 sequences were used to construct this phylogram, including 40 *P. ramorum* and 29 *P. sojae* sequences. The remaining sequences were retrieved from GenBank. Protein sequences were edited to remove signal peptides and other domains and were aligned using ClustalW, and the unrooted phylogram was made using the neighbor-joining method (MEGA 3.1). The scale bar represents 10% weighted sequence divergence. Species of origin are abbreviated as follows: An, *Aspergillus nidulans*; Bh, *Bacillus halodurans*; Ec, *Erwinia caratovora*; Fo, *Fusarium oxysporum*; Gz, *Giberella zeae*; Mg, *Magnaporthe grisea*; Nc, *Neurospora crassa*; Pa, *Pythium aphanidermatum*; Pi, *Phytophthora infestans*; Pm, *Pythium monospermum*; Pp, *Phytophthora parasitica*; Ps, *Phytophthora sojae*; Pr, *Phytophthora ramorum*; Sc, *Streptomyces coelicolor*; Vd, *Verticillium dahlia*; Vp, *Vibrio pommerensis*. (**B**) Similarity of *P. sojae* Avh genes to *P. ramorum*. Purple indicates Avh genes, and crimson indicates a set of randomly chosen *P. sojae* genes having a functional annotation. The red arrow indicates the class that contains the *Avr1b*-1 gene itself.

Because *P. sojae* and *P. ramorum* have very different host ranges, it is expected that some of their genes involved in host interactions will have rapidly diverged between the two species as a result of strong selection for effective pathogenesis. Because *Phytophthora* species are cellular pathogens, secreted proteins are prime candidates for mediators of host interactions (*18*). The predicted secretomes (*7*) of the two species (1464 and 1188 proteins, respectively) are evolving significantly more rapidly than the overall proteome. For example, 17% and 11% of the secreted *P. sojae* and *P. ramorum* proteins, respectively, are unique at the 30% identify level, whereas only 9% and 4%, respectively, of the overall proteomes are unique. The relatively rapid diversification of the secretomes is also evident in the number of multigene families encoding these proteins: 77% of the proteins belong to families of two or more members, and 30% belong to families of 10 or more members.

Both *P. sojae* and *P. ramorum* derive their nutrition biotrophically from living plant tissue during the initial hours of infection, but they switch to necrotrophic growth once the infection has been established, deriving their nutrition from killed plant tissue. As hemibiotrophs, the two species are expected to produce gene products that enable them to evade or suppress the plant's defense responses during early biotrophic infection and to produce gene products that kill and destroy plant tissue during later necrotrophic growth. Table 1 summarizes a wide variety of hydrolytic enzymes encoded by the genomes of the two species in comparison with the genome of the diatom *Thalassiosira pseudonana*, an autotroph. These destructive enzymes potentially could be associated with the necrotrophic phase. The two *Phytophthora* genomes encode large numbers of secreted proteases in contrast to the diatom and also encode the pectinases and cutinases required for hydrolyzing plant cell wall and cuticular material. The number of proteinase inhibitor genes required to protect the pathogens from plant proteases is also expanded in the *Phytophthora* genomes.

Gene families encoding proteins previously demonstrated to be toxic to plants show striking diversification; fewer than 25% of the genes remain identifiably orthologous between the two

Table 1. Potential infection-related genes in the *P. sojae* and *P. ramorum* genome sequences.

Gene product	Numbers of genes			
	P. sojae	*P. ramorum*	Orthologs*	Diatom
Hydrolases				
Proteases, all	282	311	221	314
Extracellular	47	48	38	8
Serine proteases	119	127	86	123
Metalloproteases	71	86	62	84
Cysteine proteases	67	74	52	63
Glycosyl hydrolases	125	114	54	n.d.†
Secreted	56	37	23	n.d.
Pectinases				
Pectinesterases	19	15	n.d.	0
Pectate lyases	43	41	n.d.	0
Cutinases	16	4	1	0
Chitinases	5	2	2	49
Lipases	171	154	n.d.	n.d.
Phospholipases	>50	>50	n.d.	23
Phospholipase C	0	0	0	3
Phospholipase D	18	18	18	3
Protease inhibitors, all	22	19	13	9
Kazal	15	12	8	2
Cystatin	4	4	4	0
Protein toxins				
NPP family‡	29	40	7	0
PcF family§				
Six Cys family	2	4	0	0
Eight Cys family	17	0	0	0
Crn family‖	40	8	2	0
Secondary metabolite biosynthesis				
Nonribosomal peptide synthetases	4	4	4	16
Polyketide synthases	0	0	0	0
Cytochrome P450's	30	24	21	10
CYP51 clan	0	0	0	1
ABC transporters	134	135	105	63
PDR¶ (ABCG-full)	45	46	30	3
ABCG-half	23	22	19	6
MDR# (ABCB)	7	7	4	3
MRP** (ABCC)	23	22	19	6
Effectors				
Elicitins	18	17	13	0
Elicitin-like	39	31	22	0
Avh (RXLR) family	350	350	83 (21)††	0

*Genes orthologous between *P. sojae* and *P. ramorum* were estimated based on bidirectional best BLAST hits and/or using similarity trees created by ClustalW. †n.d., not determined ‡Necrosis and ethylene-inducing protein family (*19*, *20*). §(*18*, *21*). ‖Crinkling and necrosis-inducing protein family (*22*). ¶Pleiotropic drug resistance transporters. #Multi-drug resistance transporters. **Multi-drug resistance–associated transporters. ††For the Avh family, the estimations of orthology are uncertain due to the rapid divergence of this family. The number in parentheses refers to orthologs that are syntenic and hence most likely to be correct.

species, and in several cases there are no identifiable orthologs (Table 1). There are also substantial differences in sizes of the gene families. The NPP1 family (*19*, *20*) is more expanded and diversified in *P. ramorum*, whereas the PcF (*18*, *21*) and crn (*22*) toxin families are more expanded in *P. sojae*. Figure 3A illustrates the explosive diversification of the NPP1 toxin family in the genus *Phytophthora*. This toxin family is interesting because several fungal plant pathogens also contain NPP1 toxin genes (*19*, *20*), but they contain only two to four genes, whereas the *Phytophthora* species contain 29 or 40 (Fig. 3A).

The largest and most diverse family of infection-associated genes identified in the *P. sojae* and *P. ramorum* genomes is a superfamily with ~350 genes in each genome (*7*) that are similar to four oömycete genes identified as "avirulence" or "effector" genes, namely *Avr1b*-1 of *P. sojae* (*8*), *Avr3a* of *P. infestans* (*23*), and *Atr*1 (*24*) and *Atr*13 (*25*) of *Hyaloperonospora parasitica*. We have termed these Avh (avirulence homolog) genes. Avirulence genes were historically identified by their genetic interaction with plant disease resistance genes that encode defense receptors (*26*). In bacterial plant pathogens, some avirulence proteins function to promote infection by suppressing the plant defense response—hence their renaming as "effector" proteins (*26*). Many of these bacterial effector proteins are injected into host cells by the type III secretion machinery (*26*), which explains the intracellular location of many resistance gene–encoded plant defense receptors. Intriguingly, the plant defense receptors that interact with the four cloned oömycete avirulence proteins also have a predicted intracellular location (*8*, *23*–*25*, *27*). However, the mechanisms by which the oömycete proteins may enter the plant cell are unknown. The four oömycete avirulence proteins share only very modest sequence similarity, but they do share two motifs, named RXLR and dEER, near the N terminus (*24*, *28*) which are also shared by all of the 700 Avh gene products. Comparison of the 700 Avh sequences reveals a nonrandom distribution of amino acid residues surrounding each motif (*7*), which could potentially contribute to the their functions. Similarity of the RXLR motif to a motif used by the malaria parasite to transport proteins across the membrane of the parasitiphorous vacuole into the cytoplasm of human erythrocytes (*29*, *30*) suggests that the RXLR motif may function to transport oömycete effector proteins into the plant cytoplasm. Figure 3B shows that the Avh gene family has undergone extensive diversification in comparison with a random set of *P. sojae* and *P. ramorum* genes. The diversification of the Avh family, driven presumably by selection pressure from the host defense machinery, underlines the potential importance of this superfamily for infection by these pathogens. Further characterization of these genomes will be published elsewhere (*31*).

References and Notes

1. D. C. Erwin, O. K. Ribiero, *Phytophthora Diseases Worldwide* (APS Press, St. Paul, MN, 1996).
2. D. M. Rizzo, M. Garbelotto, E. M. Hansen, *Annu. Rev. Phytopathol.* **43**, 309 (2005).
3. S. Kamoun, *Eukaryot. Cell* **2**, 191 (2003).
4. B. M. Tyler, *Trends Genet.* **17**, 611 (2001).
5. S. L. Baldauf, A. J. Roger, I. Wenk-Siefert, W. F. Doolittle, *Science* **290**, 972 (2000).
6. H. S. Yoon, J. D. Hackett, G. Pinto, D. Bhattacharya, *Proc. Natl. Acad. Sci. U.S.A.* **99**, 15507 (2002).
7. Materials and methods are available as supporting material on *Science* Online.
8. W. Shan, M. Cao, D. Leung, B. M. Tyler, *Mol. Plant Microbe Interact.* **17**, 394 (2004).
9. S. L. Kelly *et al.*, *Biochem. Soc. Trans.* **29**, 122 (2001).
10. M. J. Rebecchi, S. N. Pentyala, *Physiol. Rev.* **80**, 1291 (2000).
11. T. A. Randall *et al.*, *Mol. Plant Microbe Interact.* **18**, 229 (2005).
12. J. D. Hackett *et al.*, *Curr. Biol.* **14**, 213 (2004).
13. S. Li, T. Nosenko, J. D. Hackett, D. Bhattacharya, *Mol. Biol. Evol.* **23**, 663 (2006).
14. V. Dvornyk, *Microbiol.* **152**, 75 (2006).
15. P. F. Morris, E. W. B. Ward, *Physiol. Mol. Plant Pathol.* **40**, 17 (1992).
16. M. J. Caterina, P. N. Devreotes, *FASEB J.* **5**, 3078 (1991).
17. D. Bakthavatsalam, H. J. G. Meijer, A. A. Noegel, F. Govers, *Trends Microbiol.*, in press, doi: 10.1016/j.tim.2006.07.006.
18. S. Kamoun, *Annu. Rev. Phytopathol.* **44**, 41 (2006).

19. G. Fellbrich *et al.*, *Plant J.* **32**, 375 (2002).
20. D. Qutob, S. Kamoun, M. Gijzen, *Plant J.* **32**, 361 (2002).
21. G. Orsomando *et al.*, *J. Biol. Chem.* **276**, 21578 (2001).
22. T. A. Torto *et al.*, *Genome Res.* **13**, 1675 (2003).
23. M. R. Armstrong *et al.*, *Proc. Natl. Acad. Sci. U.S.A.* **102**, 7766 (2005).
24. A. P. Rehmany *et al.*, *Plant Cell* **17**, 1839 (2005).
25. R. L. Allen *et al.*, *Science* **306**, 1957 (2004).
26. J. H. Chang, A. K. Goel, S. R. Grant, J. L. Dangl, *Curr. Opin. Microbiol.* **7**, 11 (2004).
27. H. Gao, N. N. Narayanan, L. Ellison, M. K. Bhattacharyya, *Mol. Plant Microbe Interact.* **18**, 1035 (2005).
28. P. R. Birch, A. P. Rehmany, L. Pritchard, S. Kamoun, J. L. Beynon, *Trends Microbiol.* **14**, 8 (2006).
29. M. Marti, R. T. Good, M. Rug, E. Knuepfer, A. F. Cowman, *Science* **306**, 1930 (2004).
30. N. L. Hiller *et al.*, *Science* **306**, 1934 (2004).
31. A series of papers describing detailed analyses of the *P. sojae* and *P. ramorum* genome sequences will be published in a special issue of *Molecular Plant-Microbe Interactions* in December 2006.
32. D. Swofford, *PAUP*: Phylogenetic Analysis Using Parsimony* (and other methods)*, 4.0b7 beta version (Sinauer Associates Sunderland, MA, 2002).
33. We thank M. Arnaud, G. Cai, S. Constanzo, M. DiLeo, S. Doyle, C. Paeper, L. Waller, and L. Zhou for their contributions to the annotation of the *P. sojae* and *P. ramorum* sequences; C. Volker and M. Chibucos for manuscript preparation; and J. Mullins for preparation of illustrations. This work was supported by grants to B.M.T. from the National Research Initiative of the USDA Cooperative State Research, Education, and Extension Service, grant numbers 00-52100-9684, 2001-35319-14251, and 2002-35600-12747; from the U.S. National Science Foundation, grant numbers MCB-0242131 and EF-0130263; and by funds from the U.S. Department of Energy Joint Genome Institute and the Virginia Bioinformatics Institute. Much of this work was performed under the auspices of the U.S. Department of Energy's Office of Science, Biological, and Environmental Research Program and by University of California, Lawrence Livermore National Laboratory under contract no. W-7405-Eng-48; Lawrence Berkeley National Laboratory under contract no. DE-AC02-05CH11231; and Los Alamos National Laboratory under contract no. W-7405-ENG-36. R.H.Y.J. was supported by Aspasia grant no. 015.000.057 from the Netherlands Science Foundation and fellowship NGI 050-72-404 from Netherlands Genomics Initiative. The *P. sojae* and *P. ramorum* whole-genome shotgun projects have been deposited at DDBJ/EMBL/GenBank under the project accessions AAQY00000000 and AAQX00000000, respectively. The versions described in this paper are the first versions, AAQY01000000 and AAQX01000000, respectively.

Supporting Online Material

www.sciencemag.org/cgi/content/full/313/5791/1261/DC1
Materials and Methods
SOM Text
Figs. S1 to S3
Tables S1 to S5

17 April 2006; accepted 18 July 2006
10.1126/science.1128796

REPORTS

Anomalous Spiral Motion of Steps Near Dislocations on Silicon Surfaces

J. B. Hannon,[1]* V. B. Shenoy,[2] K. W. Schwarz[1]

We have used low-energy electron microscopy to measure step motion on Si(111) and Si(001) near dislocations during growth and sublimation. Steps on Si(111) exhibit the classic rotating Archimedean spiral motion, as predicted by Burton, Cabrera, and Frank. Steps on Si(001), however, move in a strikingly different manner. The anomalous behavior can be understood in detail by considering how the local step velocity is affected by the nonuniform strain field arising from the dislocation. We show how the dynamic step-flow pattern is related to the dislocation slip system.

Dislocations strongly influence both the mechanical and electrical properties of solids, and have been investigated in detail for more than 50 years. Although most investigations have focused on bulk properties, dislocations also influence surface processes. Perhaps the most striking example is the realization by Frank (*1*) that dislocations mediate crystal growth under conditions of low supersaturation and provide the surface steps required to capture deposited atoms. On a low-index surface without dislocations, islands must spontaneously nucleate before such growth can occur.

More recently, there has been interest in exploiting the strain field of bulk dislocations to tailor surface properties. For example, periodic arrays of dislocations have been used to engineer the strain at the surface of a thin Si(001) film. The strain pattern can be used to preferentially nucleate Ge quantum dots at specific locations on a surface (*2*, *3*). Here, we describe how the dislocation strain fields influence step motion during growth. By imaging the Si(001) surface in real-time at 1100°C, during growth and sublimation, we show that step motion near the dislocation core is inconsistent with classic models that predict rotating spiral step profiles (*4*). We find instead that the step velocity can be interpreted directly in terms of the surface strain field generated by a bulk dislocation.

Images of a step on Si(111) emerging from a screw dislocation (Fig. 1A) were obtained using low-energy electron microscopy (LEEM) (*5*) during sublimation at elevated temperatures ($T \approx 1100$°C). Si atoms evaporated from the terrace are replenished by atoms detaching from steps, causing the steps to retract. Burton, Cabrera, and Frank (BCF) (*4*) developed a simple theory of step motion near a dislocation

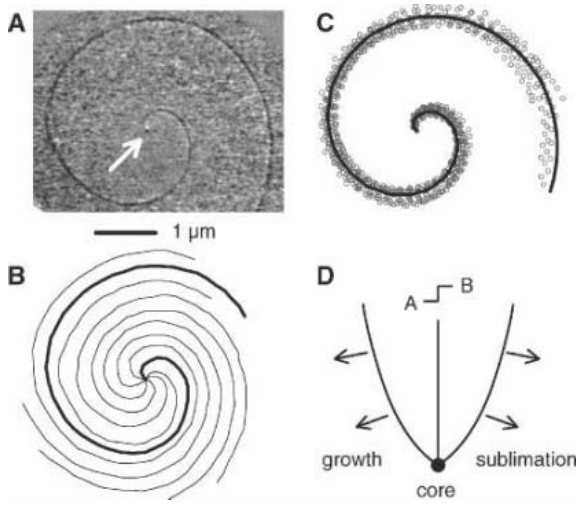

Fig. 1. (A to C) Step motion near a dislocation core on Si(111) during sublimation. (**A**) 40 eV LEEM image of a step emerging from a dislocation core measured at time t_1. The step curvature decreases monotonically away from the core (indicated by an arrow). (**B**) Position of the step at 5-s intervals as it winds (counterclockwise) about the core during sublimation. The curve corresponding to (A) is shown in bold. (**C**) Measured step profiles, each rotated by an angle $(t - t_1)/t_0$, where $t_0 = 36$ s is the period of the step motion and t is the time the profile was measured. The solid curve shows the prediction of the BCF model with $r_c = 93$ nm. (**D**) Spiral onset from growth and sublimation of a surface step emerging from a dislocation. The step separates two surface phases: *A* on the lower side of the step and *B* on the upper side. If the step direction is reversed, so is the direction of motion.

[1]IBM Research Division, T. J. Watson Research Center, Yorktown Heights, NY 10598, USA. [2]Division of Engineering, Brown University, Providence, RI 02912, USA.

*To whom correspondence should be addressed. E-mail: jbhannon@us.ibm.com

core during growth or sublimation, the basic features of which have been confirmed experimentally in a number of systems using surface microscopy (*6*–*9*). BCF considered the case of diffusion-limited growth in equilibrium with the vapor, but the results apply equally well to sublimation and to cases in which the growth is limited by the attachment and detachment of atoms to steps [e.g., Si(001) (*10*)]. Specifically, BCF showed that during growth the normal velocity of a step, v_n, is given by

$$v_n = v_\infty(1 - \rho_c/\rho) \quad (1)$$

where ρ is the local radius of curvature of the step, ρ_c is the critical nucleus size, and v_∞ is the velocity of a straight step. The two free parameters, v_∞ and ρ_c, of the model are functions of the supersaturation. BCF showed that the steady-state step profile corresponding to Eq. 1 has the classic Archimedes spiral shape, $r(\theta) \approx 2\rho_c\,\theta$, that rotates about the core with a constant angular velocity $\omega \approx v_\infty/3\rho_c$. For later reference, Fig. 1D illustrates how the direction of the spiral motion depends both on the step direction and on whether the crystal is growing or sublimating.

On Si(111), the spiral profile predicted by the BCF model is clear (Fig. 1A). A key feature of this shape is that the curvature is large near the core but decreases monotonically with distance from the core. Step profiles measured at 5-s intervals during sublimation on Si(111) are shown in Fig. 1B. If the profile does not change as the step moves, the curves can be collapsed onto each other by a suitable rotation about the core. The results of this procedure (Fig. 1C) show that the profile is essentially constant and rotates about the core with a constant angular velocity. The solid curve is a fit to the BCF prediction, $r(\theta) \approx 2\rho_c\,\theta$, with $\rho_c = -93$ nm. Clearly, the BCF theory successfully describes step motion on Si(111) during sublimation.

Step motion on Si(001) is qualitatively different. A sequence of LEEM images were recorded during sublimation at elevated temperature (1100 ± 50°C) (Fig. 2). The dimer-row reconstruction results in two equivalent surface terminations, (2 × 1) and (1 × 2); the atomic structure of the two phases is identical, but the dimer rows are rotated with respect to each other by 90°. Our LEEM images were formed from the half-order diffraction spot belonging to the (2 × 1) phase. Under these dark-field (*5*) imaging conditions, the (2 × 1) phase (with dimer axes parallel to [110]) appears bright, whereas the (1 × 2) phase (with dimer axes parallel to $[\bar{1}10]$) appears dark (*11*). At an atomic step, the surface termination changes, e.g., from (2 × 1) to (1 × 2), a consequence of the diamond crystal structure of Si. Thus, the change of contrast in the LEEM image from bright to dark indicates the position of an atomic step on the surface. The screw component of the Burgers vector corresponds to two atomic-height steps. Because this is unstable, it breaks up into two steps (indicated in blue and red in Fig. 3) that meet at the intersection of the core with the surface. Arrows at the step indicate the "step up" direction. During the sublimation, the two steps rotate clockwise about the core with a period of 77 s.

The steps clearly do not have the simple spiral shape predicted by the BCF model. For example, the S-shaped red step at t = 39 s has a large positive curvature near the core but a negative curvature further from the core. Furthermore, although the step motion about the core is periodic, the steps do not move with a constant angular velocity. Between t = 48 s and t = 58 s, the red step near the core moves through an angle of almost 270°, whereas it takes nearly 70 s to rotate through the remaining 90°. Movie S1 is a video sequence of motion near the core (*12*).

The anomalous step motion must arise from energetic or kinetic factors not accounted for in the BCF expression for the step velocity given in Eq. 1. In terms of the thermodynamic step properties—the stiffness $\tilde{\beta}$, and the mobility Γ (*13*)—the Gibbs-Thomson relation can be invoked to write Eq. 1 in the form

$$v_n = \frac{\Gamma}{k_B T}\left(\Delta\mu - \frac{\tilde{\beta}}{\rho}\right) \quad (2)$$

where $\Delta\mu$ is the Si adatom chemical potential at the steps (per unit area) relative to that of a

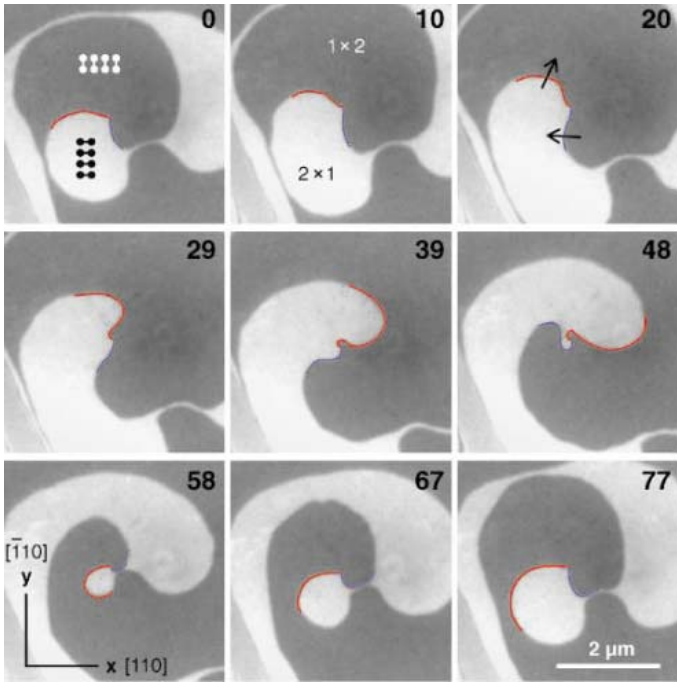

Fig. 2. Sequence of 2.5 eV dark-field LEEM images of steps emerging from a dislocation on Si(001) during sublimation at ~1100°C. The images are labeled by the acquisition time in seconds. The dimer axis of the (2 × 1) (bright) phase is parallel to [110]; that of the (1 × 2) (dark) phase is parallel to $[\bar{1}10]$. Two steps emerge from the core. The leading step is indicated in red and the trailing step in blue. The steps "unwind" clockwise about the core. Arrows indicate the "step up" direction.

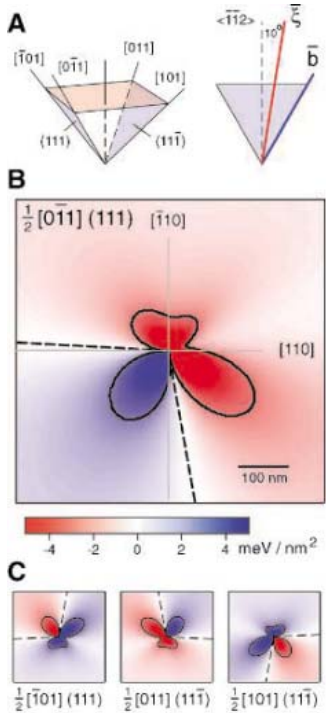

Fig. 3. (**A**) 60° slip systems in Si. The triangular sides define the allowed glide planes, the triangle edges are parallel to the allowed Burgers vectors for that glide plane. The right panel shows the equilibrium line direction ξ, representing a compromise between lowering the dislocation energy by shortening its length or by aligning it with the Burgers vector ***b***. (**B**) Computed surface energy difference, $\Delta\gamma = \gamma_{1\times2} - \gamma_{2\times1}$, near a dislocation on Si(001) for the $\frac{1}{2}[0\bar{1}1](111)$ slip system. The contour indicates $|\Delta\gamma| = 2$ meV/nm². The dashed lines correspond to $\Delta\gamma = 0$. (**C**) Calculations for the three other possible slip systems.

straight step, T is the temperature, and k_B is Boltzmann's constant. With this growth law, the curvature of the step need not be a monotonic function of the distance from the dislocation core, but it should not switch its sign at any point along the step. That is, even if $\tilde{\beta}$ is anisotropic, the sign of the curvature never changes along the step during growth. We therefore rule out anisotropy in the step stiffness as the source of the anomalous behavior.

The key difference between Si(001) and Si(111) is the existence of the two surface terminations on Si(001) with different surface stress tensors. In each phase, the surface stress parallel to the dimer axis, $\sigma_{\parallel}$, is more tensile than that normal to the dimer axis, $\sigma_{\perp}$ (*14*, *15*, *16*). In the absence of strain, the surface energies of the two phases are the same, $\Delta\gamma = \gamma_{1\times2} - \gamma_{2\times1} = 0$. However, as Men *et al*. showed (*14*), an applied strain breaks this symmetry and makes one domain energetically more favorable. LEEM investigations have shown that the strain due to bulk dislocations can also lead to asymmetric domain populations (*17*). The asymmetry in the surface energy results in a force on the step, which tends to increase the area of the favored domain at the expense of the unfavorable one. By measuring the relative fraction of each phase in equilibrium as a function of applied strain, Webb *et al*. determined the stress anisotropy, $\sigma_{\parallel} - \sigma_{\perp} = 7$ eV/nm^2 (*16*).

During sublimation, the surface is not in fact in equilibrium; the steps are always in motion. The force on the steps caused by the dislocation now leads to an additional term in Eq. 2.

$$v_n = \frac{\Gamma}{k_B T}\left(\Delta\mu - \frac{\tilde{\beta}}{\rho} \pm \Delta\gamma\right) \qquad (3)$$

with the difference in surface energy between the phases given by (*15*)

$$\Delta\gamma = \gamma_{1\times2} - \gamma_{2\times1} = (\sigma_{\parallel} - \sigma_{\perp})(\varepsilon_{yy} - \varepsilon_{xx}) \quad (4)$$

where ε_{xx} and ε_{yy} are the diagonal components of strain tensor. In principle, the strain tensor includes contributions from the dislocation, from the steps themselves, and from external sources (e.g., the sample holder). However, it is expected that the dislocation field will become more and more dominant as the core is approached. Thus, it will be useful to think in terms of a region at (or very near to) the core where the dislocation field is the only contribution that matters, a region near the core where the curvature term in Eq. 3 is also important, and an outer region where external strains and other experimental effects can strongly influence $\Delta\gamma$, and thus modify the step-flow pattern. We choose the x axis parallel to [110] and the y axis parallel to $[\bar{1}10]$, as shown in Fig. 2. The sign that must precede $\Delta\gamma$ in Eq. 3 can then easily be sorted out for each step by referring to Fig. 1D. If the surface energy of the upper side (B phase) is increased relative to that of the lower side (A phase), energy minimization will favor the conversion of the B phase to the A phase. During sublimation, an $A \rightarrow B$ step front will then be consumed more rapidly, while a $B \rightarrow A$ front will be slowed. For the data shown in Fig. 2, the plus sign in Eq. 3 refers to the $2\times1 \rightarrow 1\times2$ (bright to dark, or red) step fronts, whereas the minus sign refers to the $1\times2 \rightarrow 2\times1$ (dark to bright, or blue) step fronts.

We computed the surface strain field assuming a straight dislocation intersecting the surface at the equilibrium angle. The lowest energy dislocation in the diamond crystal has a Burgers vector in the [110] direction with {111} glide planes. In the absence of extraneous bulk stresses, the equilibrium configuration for the dislocation is a straight line (*18*) with a fixed angle between the normal and the Burgers vector (Fig. 3A). Our dynamically computed (*19*) angle of 9.880° agrees with the theoretical value of 9.887° to within 0.1%, establishing the accuracy of the calculation (*20*). The specific slip system of the dislocation is not known a priori but, as we show below, it can readily be deduced from the step-flow behavior.

The strain-relieving slip systems for the coordinate system shown in Fig. 2 are shown in Fig. 3A. The {111} glide planes form a pyramid, the edges of which correspond to the allowed $\frac{1}{2}[110]$ Burgers vectors. In our experiments, we often see the dislocations glide, especially if the temperature is changed suddenly. For the dislocation shown in Fig. 2, we observed the point of intersection of the core with the surface moving in the $[\bar{1}10]$ direction, implying that the dislocation glide plane is either (111) or $(11\bar{1})$ (shaded blue in Fig. 3A). We have used Eq. 4 to compute $\Delta\gamma$ for the four possible slip systems compatible with these glide planes (*21*) (Fig. 3, B and C). Red areas indicate where the (1×2) (dark) phase is favored, whereas blue areas indicate where the (2×1) (bright) phase is favored. The $\frac{1}{2}[0\bar{1}1](111)$ slip system is most consistent with step motion shown in Fig. 2, especially near the core: The (1×2) phase is favored in the first, second, and fourth quadrants, whereas the (2×1) is favored only in the third quadrant.

The identification of the slip system can be done very convincingly when the supersaturation is small and $\Delta\mu \ll \Delta\gamma$. In this case, steps near the core are essentially straight, and Eq. 3 simplifies to $v_n = \Gamma\Delta\gamma / k_B T$. In fact, for low enough supersaturation (or for distances close enough to the core), the steps will become trapped in regions where the magnitude of the $\Delta\gamma$ is small. We have created this situation experimentally by depositing Si during sublimation. We adjust the incident Si flux so that step motion on the surface is minimized and the amount of Si evaporating is roughly equal to that deposited. The steps near the core become trapped at 177° and –80°, as shown in Fig. 4. It is seen that this corresponds well to the $\Delta\gamma = 0$ contour for the $\frac{1}{2}[0\bar{1}1](111)$ slip system (Fig. 3B). This procedure provides a direct method of experimentally determining the contours on which $\varepsilon_{yy} - \varepsilon_{xx} = 0$, and of differentiating between the possible slip systems.

At the core, where the dislocation field dominates, the steps are pinned in the pattern shown in Fig. 4. However, the computed values of $\Delta\gamma$ shown in Fig. 3 can be used to interpret the more interesting step dynamics in the region near the core (Fig. 2). The domain configuration at $t = 0$ has a relatively low energy: The (2×1) phase is found in the third quadrant (where it is favored), and the (1×2) in the other three. As the leading (red) step retracts into the second quadrant, conversion of the (1×2) phase to (2×1) is no longer favorable, and the motion of the red step is retarded. Near the core, where $\Delta\gamma$ is largest, the red step actually becomes pinned, although further from the core it continues to unwind.

At $t = 20$ s, the leading step moves into the first quadrant, converting the locally favorable (1×2) phase into the unfavorable (2×1) phase. Far from the core, this simply slows the advance of the leading step, but near the core (for $r < 200$ nm), $\Delta\gamma$ is so large that the step does not initially advance. As a result, a large positive curvature develops near the core ($t =$ 29 to 48 s), whereas far from the core, the curvature is negative. The trailing (blue) step shows the same behavior as it enters the third quadrant [i.e., $t = 39$ s, where the (1×2) phase is unfavorable].

An interesting instability develops after $t =$ 48 s. When the trailing step enters the second quadrant, it speeds up, converting the un-

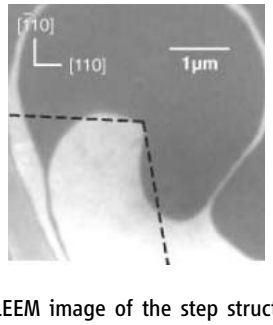

Fig. 4. LEEM image of the step structure near the core in a background pressure of 3.5×10^{-7} Torr disilane. Under these conditions, the incident Si flux nearly cancels the sublimation rate, and steps near the core are static. Dashed lines indicate the contour $\Delta\gamma = 0$ for the $\frac{1}{2}[0\bar{1}1](111)$ slip system.

favorable (2 × 1) surface into the favorable (1 × 2). Simultaneously, the leading step slows. Near the core, the trailing step essentially collides with the leading step, pushing it ahead through the first and fourth quadrants in a matter of seconds. When the step pair reaches the boundary between the fourth and second quadrants, the energetics flip; now the trailing step slows and the leading step accelerates. At $t = 77$ s, one unwinding cycle is complete, and the step structure near the core is the same as that at $t = 0$.

The magnitude of $\Delta\gamma$ near the core can be estimated from an analysis of the pinned step profile. During the interval from 29 to 48 s, both steps develop an S-shaped profile because the steps become pinned. Near the core, the supersaturation and curvature forces are balanced by the force arising from the dislocation strain field and $v_n = 0$. Equation 3 can be used to estimate the magnitude of $\Delta\gamma$. Far from the core, straight steps move with a speed of about -30 nm/s, corresponding to $\Delta\mu = -0.7$ meV/nm^2, using measured values of Γ and $\tilde{\beta}$ (*22*). The radius of curvature is about $\rho \approx -90$ nm. For v_n to vanish, $\Delta\gamma \approx 1.5$ meV/nm^2. As the calculations show, 100 nm from the core, $\Delta\gamma$ is indeed on the order of 1 to 2 meV/nm^2 (Fig. 3).

Given the experimental difficulty of resolving what is happening very near the core, the above interpretation is not obvious and was in fact obtained by directly computing how steps will move in the dislocation strain field. We chose an arbitrary initial profile for the leading and trailing steps. We then used Eq. 3 to compute the normal velocity at each point on the steps, using the values for $\Delta\gamma$ shown in Fig. 3B. For simplicity, we assumed that both $\tilde{\beta}$ and Γ are isotropic. Measurements of Si(001) step dynamics suggest that, at 1100°C, Γ is indeed isotropic (*23*) and that the anisotropy in β is about 25% (*24*). We also took $\Delta\mu$ to be constant. Island-coarsening studies have shown that steps on Si(001) are permeable (*25*) and that surface diffusion is fast compared with the attachment rate at steps (*10*), suggesting that spatial variations in $\Delta\mu$ are small for our experimental conditions. After computing the velocity of each point on the step, the step positions were updated. The process was repeated to compute the step motion about the core. After one or two revolutions, the transients have decayed and the computed step motion becomes periodic. In our calculations, we included the elastic interaction between the leading and trailing steps. This interaction, which prevents the steps from crossing, is important only when the step separation is small. In the simulation we used the measured values for Γ and $\tilde{\beta}$ (*22*) and the stress anisotropy $\Delta\sigma = 7$ eV/nm^2, measured by Webb *et al.* (*16*, *24*). We chose the supersaturation $\Delta\mu = -0.96$ meV/nm^2 to give a period comparable to that seen in the experiment (100 s). Finally, far from the core, the LEEM images show that the (1 × 2) phase is favored over the (2 × 1) because of a residual external strain. To account for this effect in the simulation (Fig. 5), we added a constant offset to $\Delta\gamma$ corresponding to a uniform, external strain of 0.0025%, or approximately 0.17 meV/nm^2. Movie S2 is an animation of the computed step motion through the dislocation strain field (*12*). The simulation reproduces all of the features seen in the experiment. As the leading step moves into the second quadrant, it becomes pinned near the core and continues moving clockwise away from the core. Similarly, the trailing step gets pinned near the core as it enters the third quadrant. As in the experiment, both shapes develop the characteristic S profile (e.g., at $t = 63$ s). Between $t = 70$ and $t = 87$ s the trailing step accelerates, driving the leading step forward by step-step repulsion through the first and fourth quadrants.

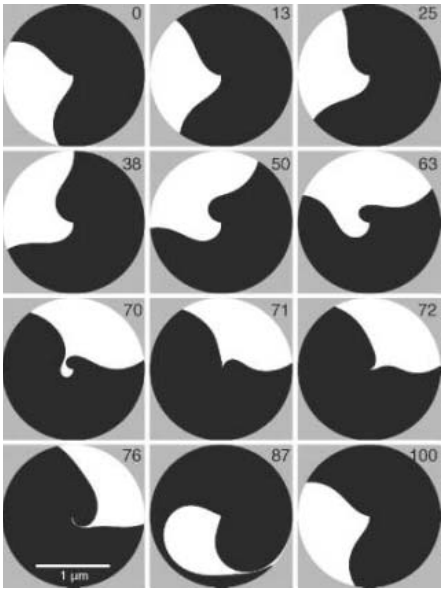

Fig. 5. Calculated step motion through the strain field corresponding to Fig. 3B. Each image is labeled by the time in seconds.

We have shown that the surface strain field of a dislocation fundamentally influences how surface steps move. Although the motion about the core is periodic, the step profile no longer has the simple spiral shape predicted by the BCF model. The demonstration that this behavior can be understood in quantitative detail validates our understanding of surface-step dynamics at a new level. Nearly all investigations of surface strain fields have focused on static equilibrium step structures. Here, we have extended this analysis to step flow by explicitly considering how step velocities are influenced by surface strain. This approach allows us to understand how strain fields arising from dislocations or other localized stress sources can affect the details of crystal growth.

References and Notes

1. F. C. Frank, *Disc. Faraday Soc.* **5**, 48 (1949).
2. S. Y. Shiryaev, F. Jensen, J. Lundsgaard Hansen, J. Wulff Pedersen, A. Nylandsted Larsen, *Phys. Rev. Lett.* **78**, 503 (1998).
3. F. Leroy, J. Eymery, P. Gentile, F. Fournel, *Appl. Phys. Lett.* **80**, 3078 (2002).
4. W. K. Burton, N. Cabrera, F. C. Frank, *Proc. R. Soc. A* **243**, 299 (1950).
5. E. Bauer, *Rep. Prog. Phys.* **57**, 895 (1994).
6. C. Hsu, Y. C. Lu, J. Xu, I. Wilson, *Appl. Phys. Lett.* **64**, 1959 (1994).
7. Y. Kim, L. Jiang, T. Iyoda, K. Hashimoto, A. Fujishima, *Appl. Phys. Lett.* **71**, 3489 (1997).
8. H. H. Teng, P. M. Dove, C. A. Orme, J. J. De Yoreo, *Science* **282**, 724 (1998).
9. S. Kodambaka *et al.*, *Nature* **429**, 49 (2004).
10. N. C. Bartelt, W. Theis, R. M. Tromp, *Phys. Rev. B* **54**, 11741 (1996).
11. The orientations of the bright and dark phases were determined by growing islands at lower temperatures, where step energy anisotropy leads to elliptical islands. The short axis of the ellipse is parallel to the dimer axis.
12. Movie files are available as supporting material on *Science Online*.
13. N. C. Bartelt, J. L. Goldberg, T. L. Einstein, E. D. Williams, *Surf. Sci.* **273**, 252 (1992).
14. F. K. Men, W. E. Packard, M. B. Webb, *Phys. Rev. Lett.* **61**, 2469 (1988).
15. O. L. Alerhand, D. Vanderbilt, R. D. Meade, J. D. Joannopoulos, *Phys. Rev. Lett.* **61**, 1973 (1988).
16. M. B. Webb, F. K. Men, B. S. Swartzentruber, R. Kariotis, M. G. Lagally, *Surf. Sci.* **242**, 23 (1991).
17. P. Sutter, M. G. Lagally, *Phys. Rev. Lett.* **82**, 1490 (1999).
18. J. Lothe, *Fundamental Aspects of Dislocation Theory*, J. A. Simons, R. deWit, R. Bullough, Eds., Spec. Pub. 317 (National Bureau of Standards, Washington, DC, 1970), pp. 11–22.
19. X. H. Liu, K. W. Schwarz, *Model. Simul. Mater. Sci. Eng.* **13**, 1233 (2005).
20. The material parameters used in the calculations were those appropriate to silicon: $c_{11} = 187.7$ GPa, $c_{12} = 52.3$ GPa, $c_{44} = 67.7$ GPa, and unit-cell dimension = 0.5433 nm. The core rationalization procedure used was equivalent to assuming a core cutoff radius of b/e, where b is the length of the Burgers vector.
21. Without loss of generality, we take the z component of the Burgers vector to be positive. We then choose the sign of the dislocation line direction, ξ, to give the correct step configuration at the surface, that is, so the "step up" direction is the clockwise direction. This choice corresponds to ξ directed outward from the surface ($\xi \cdot \boldsymbol{b} > 0$).
22. Following the work of Bartelt *et al.* (*24*), we choose $\Gamma = 5000$ nm^3/s and $\beta = \tilde{\beta} = 45$ meV/nm for $k_BT = 100$ meV. With these values, $v_\infty = -30$ nm/s corresponds to $\Delta\mu = -0.7$ meV/nm^2.
23. N. C. Bartelt, R. M. Tromp, *Phys. Rev. B* **54**, 11731 (1996).
24. N. C. Bartelt, R. M. Tromp, E. D. Williams, *Phys. Rev. Lett.* **73**, 1656 (1994).
25. S. Tanaka, N. C. Bartelt, C. C. Umbach, R. M. Tromp, J. M. Blakely, *Phys. Rev. Lett.* **78**, 334 (1997).

26. We gratefully acknowledge the research support of the National Science Foundation through grants CMS-0093714 and CMS-0210095 and the Brown University Materials Research Science and Engineering Center program.

Supporting Online Material

www.sciencemag.org/cgi/content/full/313/5791/1266/DC1
Movies S1 and S2

1 May 2006; accepted 15 June 2006
10.1126/science.1129342

Chemically Induced Fast Solid-State Transitions of ω-$VOPO_4$ in Vanadium Phosphate Catalysts

Marco Conte,[1] Gerolamo Budroni,[1] Jonathan K. Bartley,[1] Stuart H. Taylor,[1] Albert F. Carley,[1] Andi Schmidt,[1] Damien M. Murphy,[1] Frank Girgsdies,[2] Thorsten Ressler,[2] Robert Schlögl,[2] Graham J. Hutchings[1]*

Vanadium phosphates are important catalysts for the oxidation of alkanes, and commercial catalysts comprise a complex range of V^{4+} and V^{5+} phosphates. We used three complementary in situ characterization methodologies—powder x-ray diffraction and laser Raman and electron paramagnetic resonance spectroscopies—to show that the metastable phase ω-$VOPO_4$ is very sensitive to many of the reactants and products of butane oxidation. A rapid transformation from ω-$VOPO_4$ to δ-$VOPO_4$ occurs on exposure to butane at the reaction temperature, and hence the metastable ω-$VOPO_4$ may play a role in the formation of commercial catalysts.

Vanadium phosphates (VPOs) (*1*) exhibit interesting magnetochemical properties (*2*) and are catalysts for a number of reactions, particularly maleic anhydride production (*3*, *4*). The exact nature of the active components remains a matter of debate (*5*), partly because of the structural complexity of VPOs, which display many possible phases, both crystalline and disordered, that can be involved at the elevated temperatures of the catalytic process (*6*).

[1]School of Chemistry, Cardiff University, Main Building, Park Place, Cardiff CF10 3AT, UK. [2]Department of Inorganic Chemistry, Fritz-Haber-Institut der Max-Planck Gesellschaft, Faradayweg 4-6, D-14195, Berlin, Germany.

*To whom correspondence should be addressed. E-mail: hutch@cf.ac.uk

To date, there have been few in situ studies, and these have shown the importance of both V^{4+} and V^{5+} phases (*7*, *8*). One relevant VPO, ω-$VOPO_4$, has received limited attention because it is stable only at elevated temperatures, although its stability region (*9*, *10*) encompasses the conditions used in commercial oxidation reactors (*6*). We carried out a detailed in situ study using three complementary diffraction and spectroscopic techniques and showed that ω-$VOPO_4$ undergoes fast transitions in its bulk structure and is particularly sensitive to many reaction components. This observation is relevant to current commercial VPO catalysts for the oxidation of *n*-butane and has potential applications in magnetochemistry or sensors.

VPO catalysts have been extensively studied (*3*, *4*, *11*), and commercial catalysts are typically prepared from $VOHPO_4{\cdot}0.5H_2O$. In many cases, this material is precalcined at high temperatures before being loaded into the reactor and exposed at elevated temperature, typically ~400°C, to reactants [either ~1.5% butane in air for fixed bed reactors, ~4 to 5% butane in air for fluidized bed reactors, or 100% butane for the riser reactor (*12*–*14*)]. The resulting catalyst comprises a complex mixture of $(VO)_2P_2O_7$ in combination with the α_{II}-$VOPO_4$ and δ-$VOPO_4$ phases (*7*). Coulston *et al.* (*8*) have shown that the presence of V^{5+} appears to be essential for the initial activation of *n*-butane, an observation that is essentially in agreement with earlier temporal analysis of products–pulse reactor experiments (*15*). To some extent, the debate concerning the involvement of specific VPO phases is complicated by the observation that many VPO catalysts contain substantial amounts of disordered material (*5*–*7*). All of these factors combine to make the VPO system one of the most challenging to study. However, most of these studies have used ex situ analysis, and it has been difficult to gain an understanding of the nature of the VPO structure under realistic reaction conditions. Our in situ study of metastable ω-$VOPO_4$, which used techniques that explored the nature of the structure of the solid phases rather than the surface structure, shows that this VPO displays marked sensitivity to the reactants and products of the reaction and may play a role in the formation of active VPO catalysts.

Our initial experiments were focused on the synthesis of ω-$VOPO_4$ from $VOHPO_4{\cdot}0.5H_2O$,

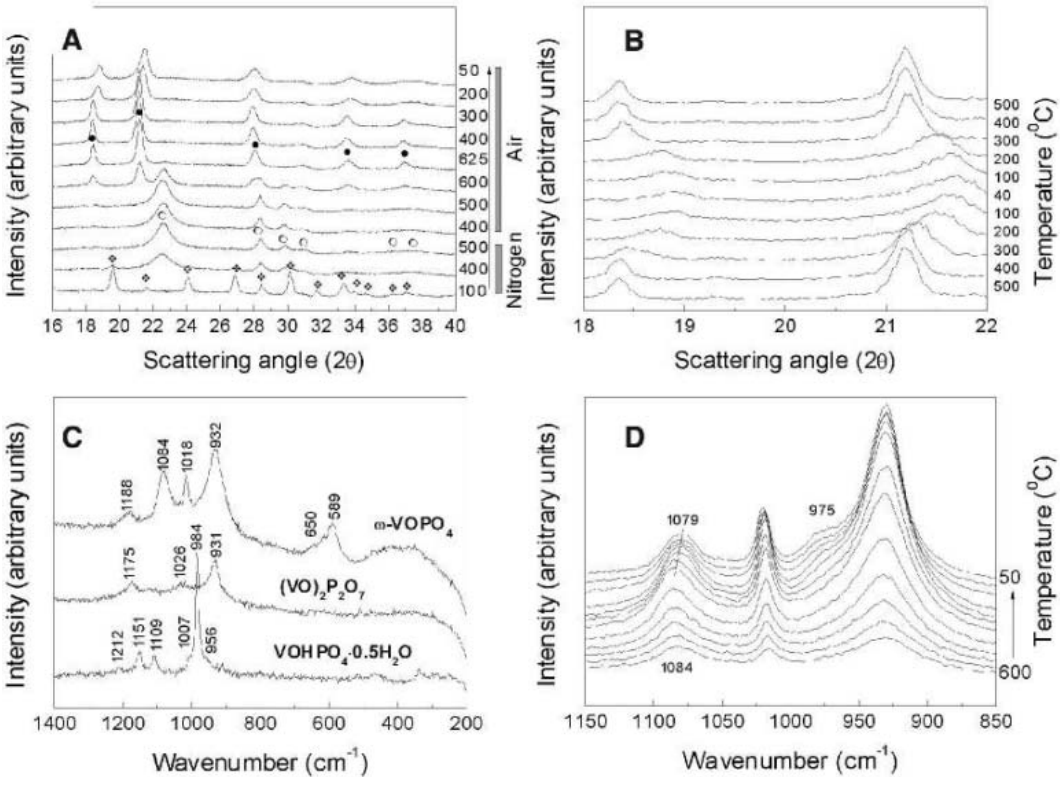

Fig. 1. (**A**) In situ powder XRD patterns recorded at different temperatures during the preparation of $(VO)_2P_2O_7$ (open circles) from VPO hemihydrate (multidiamond shapes) in N_2. The sample, cooled at 400°C and subsequently calcined in air at 625°C, transforms completely to ω-$VOPO_4$ (solid circles). (**B**) In situ XRD patterns of ω-$VOPO_4$ during a temperature cycle performed by acquiring patterns between 18° and 22° 2θ every 100°C, covering the region with the two most intense ω-$VOPO_4$ reflections. (**C**) In situ laser Raman spectra of $VOHPO_4{\cdot}0.5H_2O$ heated at 550°C in N_2 and subsequently cooled to room temperature and calcined at 625°C. As in the XRD experiment, $VOHPO_4{\cdot}0.5H_2O$ transforms into a poorly crystalline $(VO)_2P_2O_7$ and the calcination of $(VO)_2P_2O_7$ leads to ω-$VOPO_4$. (**D**) Enlargement of the in situ Raman spectra of ω-$VOPO_4$, collected at every 25°C interval between 600° and 50°C.

which is the standard precursor for the current commercial VPO catalyst for the oxidation of *n*-butane. We prepared $VOHPO_4 \cdot 0.5H_2O$ using standard preparation methods (*14*), which are known to form very active catalysts for butane oxidation (*16*). The $VOHPO_4 \cdot 0.5H_2O$ was heated in dry N_2 (500° to 750°C for 3 hours) and the transformation to $(VO)_2P_2O_7$ was monitored by means of in situ powder x-ray diffraction (XRD) [Fig. 1A and fig. S1 (*17*)]. The $(VO)_2P_2O_7$ was cooled to 400°C and then heated in air to 625°C at 10°C/min, and XRD patterns were recorded at 100°C intervals. Under these conditions, ω-$VOPO_4$ was formed and remained stable after cooling to 400°C. The diffraction pattern for ω-$VOPO_4$ (Fig. 1A) was in agreement with that previously observed (*9*, *10*).

ω-$VOPO_4$ is known to be thermally unstable at temperatures below 350°C (*10*), and we investigated this transition by cycling the temperature between 400° and 25°C several times (Fig. 1B and figs. S1 and S2) in air and N_2 environments. In both cases, ω-$VOPO_4$ could be reversibly formed. We believe that the structure at temperatures below 400°C can be induced by the twisting of the phosphate groups to form a less symmetrical structure, together with increasing disorder as the temperature decreases; in the XRD pattern, this change appears as a broadening and decreasing of the peak intensity. Although the phase at room temperature resembles δ-$VOPO_4$, the XRD patterns of δ-$VOPO_4$ and ω-$VOPO_4$ at room temperature have small appreciable differences that are preserved at different temperatures (fig. S3); for example, note the position of the most intense reflection at 21.5° 2θ for ω-$VOPO_4$ and the absence of the reflection at 23.8° 2θ. Concerning the structure of ω-$VOPO_4$ and δ-$VOPO_4$, recent results (*18*) have shown that δ-$VOPO_4$ is closely related to ω-$VOPO_4$. Both structures share the same three-dimensional arrangement of infinite chains of distorted trans-corner sharing VO_6 octahedra. The distortion of the octahedra is much more pronounced than in other $VOPO_4$ polymorphs, because the V···O distance is much longer in comparison. The most notable difference between ω-$VOPO_4$ and δ-$VOPO_4$ is that the ω-$VOPO_4$ structure is disordered with respect to both the orientation of the phosphate groups and the direction of the V=O bonds within the chains (*10*), whereas the δ-$VOPO_4$ structure is ordered. The difference in ordering may be related to the chains being straight in the ω-$VOPO_4$ phase but having a zigzag shape in the δ-$VOPO_4$ phase.

These initial observations confirm the metastable nature of ω-$VOPO_4$, as well as providing insights into the reactivity of this material. Indeed, if ω-$VOPO_4$ is formed in commercial catalysts during the initial precalcination, then it may be reformed upon heating once it is loaded into a commercial reactor. This concern is not trivial; the catalytic performance that we measured for a material formed from ω-$VOPO_4$ as a catalyst precursor for *n*-butane oxidation (fig. S4, A and B) was poor. Thus, the best industrial conditions also discourage ω-$VOPO_4$ formation.

For this reason, we studied the sensitivity of the long-range ordering of ω-$VOPO_4$ at 400°C under a number of chemical environments that would be expected during *n*-butane oxidation. Initially, we tested the stability of ω-$VOPO_4$ in air with and without added water vapor, because water is formed in the selective oxidation of *n*-butane to maleic anhydride. In both cases, ω-$VOPO_4$ was stable at 400°C and no hydration was observed (fig. S5). Next, we exposed ω-$VOPO_4$ to three different *n*-butane environments: 1.5% *n*-butane in air (Fig. 2A and fig. S6A), 3% *n*-butane in air (fig. S6B), and 5% *n*-butane in N_2 (Fig. 2B). In all of these experiments, we first stabilized ω-$VOPO_4$ in the in situ diffraction cell in air or N_2 at 400°C before adding the *n*-butane at the specified concentration. In the 1.5% concentration of *n*-butane in air, ω-$VOPO_4$ transformed rapidly to δ-$VOPO_4$. This result confirms that, under our experimental conditions, δ-$VOPO_4$ can be obtained only by the effect of a reactant. Moreover, the transformation is very rapid; it occurred on the same time scale needed to fill the reaction cell and was complete within minutes. Because XRD examines the bulk structure, these experiments suggest a close structural correlation between ω-$VOPO_4$ and δ-$VOPO_4$. This observation is important because, although a single previous example of a rapid transformation of the bulk structure by exposure to a surface treatment has

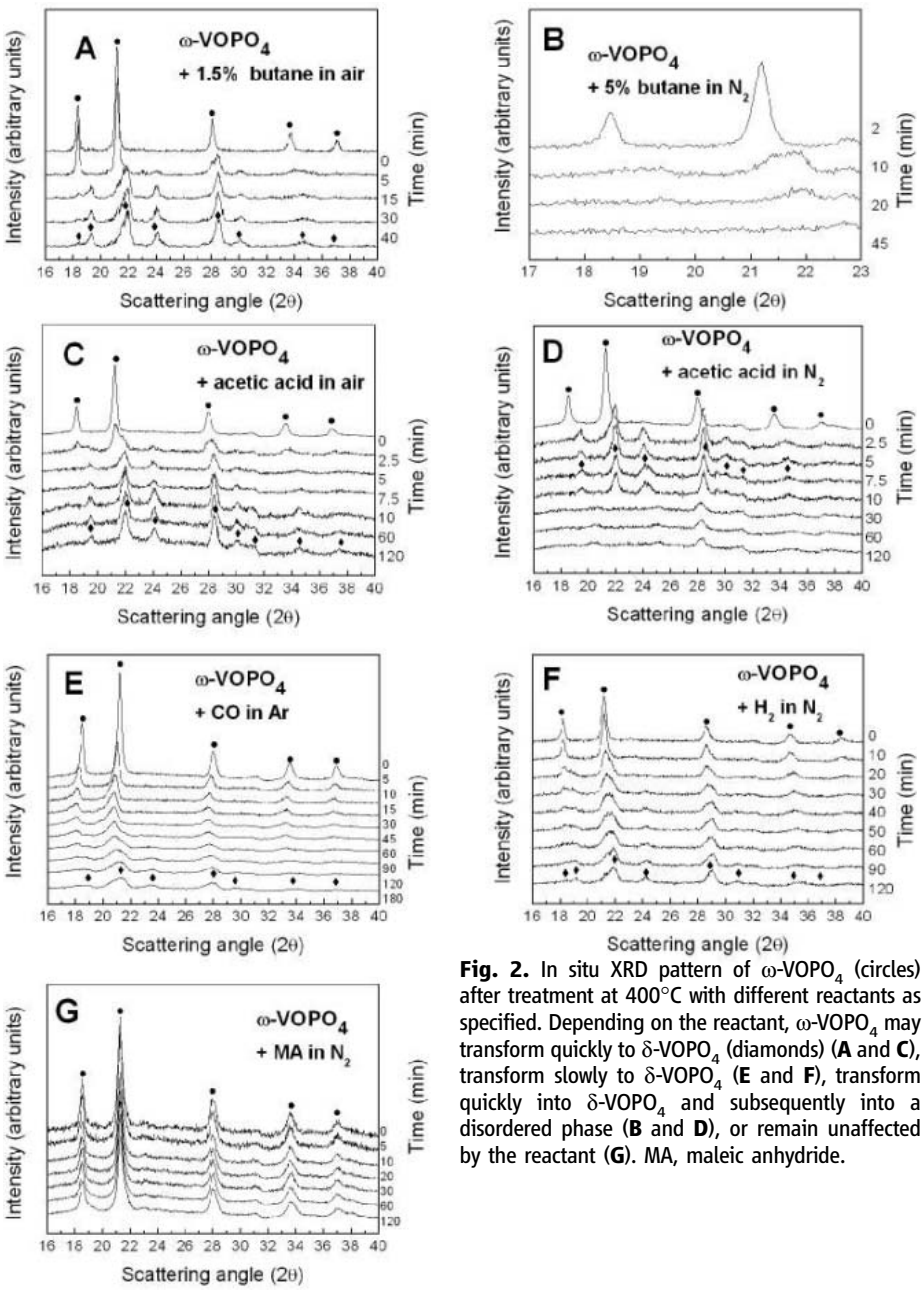

Fig. 2. In situ XRD pattern of ω-$VOPO_4$ (circles) after treatment at 400°C with different reactants as specified. Depending on the reactant, ω-$VOPO_4$ may transform quickly to δ-$VOPO_4$ (diamonds) (**A** and **C**), transform slowly to δ-$VOPO_4$ (**E** and **F**), transform quickly into δ-$VOPO_4$ and subsequently into a disordered phase (**B** and **D**), or remain unaffected by the reactant (**G**). MA, maleic anhydride.

been reported (*19*), the change in oxidation state in our case can be assumed to be present only on the surface, thereby preserving the polymorphic nature of ω-$VOPO_4$ and δ-$VOPO_4$. Moreover, these data help to clarify how the metastable transformations of ω-$VOPO_4$ occur.

When the amount of *n*-butane was increased to 3% in air, the same effects were observed, and a rapid transformation to δ-$VOPO_4$ occurred. However, if the reaction was carried out in the absence of air, ω-$VOPO_4$ initially transformed into δ-$VOPO_4$ and then rapidly converted into a largely disordered material (Fig. 2B). This transformation was accompanied by a chemical reduction, as confirmed by x-ray photoelectron spectroscopy (XPS), electron paramagnetic resonance (EPR), and experiments that used a pulse flow reactor (*17*), which showed that, when ω-$VOPO_4$ reacts with *n*-butane under these conditions, CO_2 (23%), CO (13%), and maleic anhydride (64%) were observed at low conversion (2.2%). This evidence supports the proposal that the initial trigger for the structural change is the removal of surface lattice oxygen, which is replaced from the bulk structure and leads to a disordered material [see scheme S1 for the proposed transformations]. Indeed, δ-$VOPO_4$ and the disordered material could be transformed back to ω-$VOPO_4$ on heating in air at 600°C.

To establish whether the observed phase transitions involved interaction with reaction products (*7*), we performed further in situ powder XRD studies (Fig. 2, C and E). During maleic anhydride production, CO and CO_2 are often formed as nonselective byproducts, and acetic acid is often observed in trace amounts (*11*). Treating ω-$VOPO_4$ with CO_2 in N_2 had no effect (fig. S7), but CO treatment in N_2 or CO treatment in Ar led to a slow transformation to δ-$VOPO_4$ (Fig. 2E); the transformation commenced at ~15 min and was completed after >2 hours. Nevertheless, when acetic acid in air was used, the transformation was again rapid, being essentially complete after 5 min (Fig. 2C), and the resultant δ-$VOPO_4$ could be transformed back to ω-$VOPO_4$ on heating in air at 600°C. In the absence of air, treatment with acetic acid again led to a rapid transformation to δ-$VOPO_4$ (Fig. 2D), but this material transformed into a largely disordered material from which ω-$VOPO_4$ could not be reformed by subsequent heating. We propose that the inability to reform ω-$VOPO_4$ under these conditions is due to a loss of lattice oxygen.

We next investigated the stability of ω-$VOPO_4$ toward H_2 and maleic anhydride. The treatment of ω-$VOPO_4$ at 400°C in 5% H_2 in N_2 led to a slower transformation to δ-$VOPO_4$ with a similar time scale to that observed for CO (Fig. 2F), but no phase transition occurred when maleic anhydride was used (Fig. 2G). The reactivity of ω-$VOPO_4$ versus different reactants (*n*-butane, CO, and acetic acid) and its nonsensitivity to maleic anhydride (structural transformations of ω-$VOPO_4$ are shown schematically in Fig. 3) indicate that the effects observed were not due to interactions with the maleic anhydride product.

We also used in situ laser Raman spectroscopy and EPR spectroscopy to study the transformations of ω-$VOPO_4$ under reaction conditions. The laser Raman spectrum of ω-$VOPO_4$, formed by heating the $VOHPO_4 \cdot 0.5H_2O$ precursor in the same way as described for the in situ powder XRD experiments, is shown in Fig. 1C. The Raman spectrum is similar to that of δ-$VOPO_4$, except that the 1084 cm^{-1} signal substitutes for the 1075 and 1090 cm^{-1} signals (*16*). The effects of cooling and heating ω-$VOPO_4$ in air on the laser Raman spectrum are shown in Fig. 1D. Although there are differences in the powder XRD pattern for a similar set of treatments, only subtle changes in the Raman spectra were detected (a slight but detectable shift in the band at 1084 to 1079 cm^{-1}). This result suggests that only the local V=O structure was affected by cooling. Similar effects on the Raman spectra were observed when ω-$VOPO_4$ was treated with *n*-butane in air, although, in the in situ powder XRD experiments, the material transformed again to δ-$VOPO_4$, which suggests a close structural correlation between δ-$VOPO_4$ and ω-$VOPO_4$ (fig. S8, A and B). However, after the sample was cooled to 25°C in air, the Raman band at 1079 cm^{-1} clearly split into a doublet (Fig. 4A), which is characteristic of δ-$VOPO_4$, confirming that this phase is formed under these conditions.

To investigate the effects of reactants on the vanadium oxidation state, two samples of ω-$VOPO_4$, derived from precursors prepared by different routes, that had been cooled in air to 25°C were investigated by XPS (fig. S9). The V($2p_{3/2}$) peaks for both samples show the presence of V^{5+} and V^{4+} components, as deduced from a comparison with reference binding-energy values. The surfaces of the two samples

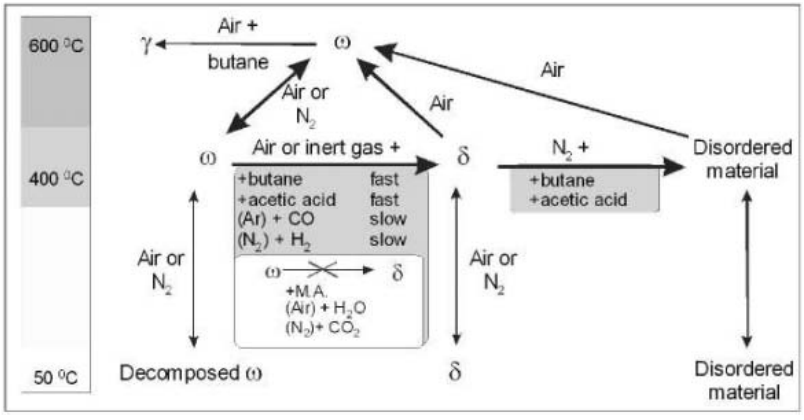

Fig. 3. Summary of ω-$VOPO_4$ transformations observed between 50° and 600°C. ω-$VOPO_4$ transforms to δ-$VOPO_4$ when exposed to a variety of reactants at 400°C. A further transformation of δ-$VOPO_4$ into a disordered material was observed when butane or acetic acid was added in the absence of oxygen. δ-$VOPO_4$ recrystallized to ω-$VOPO_4$ when calcined at 600°C in air. The disordered material obtained in the butane experiment recrystallized to ω-$VOPO_4$ when calcined at 600°C in air. ω-$VOPO_4$ transforms irreversibly to γ-$VOPO_4$ when exposed to butane in air at 600°C.

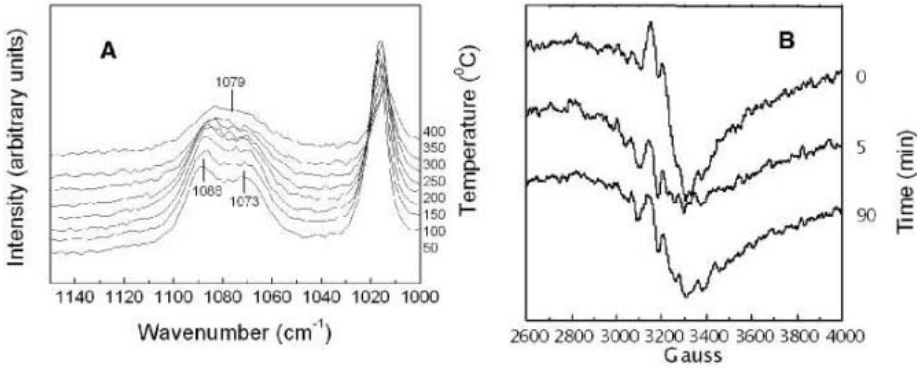

Fig. 4. (**A**) Enlargement of the Raman spectra of ω-$VOPO_4$ collected during the cooling of the sample after exposure for 2 hours to butane in air at 400°C. During the butane treatment, only a small shift (to lower wave numbers) of the signal at 1084 cm^{-1} was observed (fig. S8B). However, when the sample was cooled at room temperature, the signal split in two parts, and a δ-$VOPO_4$ spectrum was obtained. (**B**) In situ EPR spectra of ω-$VOPO_4$ at 400°C in air and the effect of 1.5% butane (0-, 5-, and 90-min exposures). Initial ω-$VOPO_4$ (0 min) underwent a fast transition (5 min), which then stabilized over the next 90 min.

consist of similar amounts of V^{4+} (24 and 29%), with the remainder being V^{5+}. Samples derived from the VPO hemihydrate that were heated in N_2 to temperatures in the range from 550° to 750°C and cooled in N_2 contained no surface V^{5+} species.

Because the sample of ω-$VOPO_4$ that was cooled to room temperature was found to have surface V^{4+}, we investigated the transformation of ω-$VOPO_4$ using in situ EPR spectroscopy (Fig. 4B). The ω-$VOPO_4$ was reformed in the EPR cell at 400°C in the presence of air. *n*-Butane was then added to the cell/catalyst, and the spectra were collected continuously. The results showed an immediate, albeit small, change in the X-band EPR spectrum (Fig. 4B) after exposure to *n*-butane. This change occurred within the first 5 min after *n*-butane addition. After 90 min, no further change occurred in the spectra. This result supports the fast transformation observed in the XRD experiments. Because of the poor resolution of the high-temperature EPR spectra, the room-temperature spectra of ω-$VOPO_4$ and δ-$VOPO_4$ were also recorded at higher Q-band frequencies, in order to obtain more accurate spin Hamiltonian parameters (fig. S10). Analysis of these parameters revealed slight differences in the crystal field parameters α and Δ (*17*), indicating an increased extent of tetragonal distortion in the VO_6 units for the δ-$VOPO_4$ sample, as would be expected from the removal of lattice oxygen. Furthermore, an increased V^{4+} signal intensity was observed for δ-$VOPO_4$ as compared to ω-$VOPO_4$ (from 1.0 to 1.2 arbitrary units), which is in agreement with the XPS observation (24 to 29%, respectively).

Based on these complementary in situ experiments, we conclude that the phase transition from ω-$VOPO_4$ to δ-$VOPO_4$ appears to be directly connected with the oxidizing action of the catalyst and its reactivity toward the gas-phase components. For example, *n*-butane and acetic acid rapidly induce a phase change, and it is known that VPOs are very reactive toward these materials. The effect is less pronounced with CO and H_2, which are less potent reducing agents for VPOs, and maleic anhydride does not display any effect.

We propose that the transition from ω-$VOPO_4$ to δ-$VOPO_4$ is only possible with a certain minimum concentration of surface oxygen vacancies, in order to facilitate the oxygen mobility necessary to rearrange the structure. Overall, this transition is clearly a reduction process, but it has to be considered as too small a degree of reduction to be a bulk process; otherwise, ω-$VOPO_4$ and δ-$VOPO_4$ could not be considered as polymorphs because there would have to be a change in stoichiometry. The experimental evidence (that in the absence of air, δ-$VOPO_4$ evolves to a disordered material in which it is possible to regenerate to ω-$VOPO_4$ only if air is used) can be explained by the formation of a large number of oxygen vacancies involving bulk reduction (scheme S1). δ-$VOPO_4$ can be recrystallized to ω-$VOPO_4$ when the sample is heated at 600°C in air, and the formation of δ-$VOPO_4$ from ω-$VOPO_4$ occurs only with a suitable reducing agent at 400°C; although at 600°C, no reaction occurs in the absence of O_2. These are indications of the metastability of the ω-$VOPO_4$ phase, with ω-$VOPO_4$ being more stable than δ-$VOPO_4$ at high temperatures, whereas the opposite is true at 400°C. The disordered material can also be fully recrystallized to ω-$VOPO_4$ when the oxygen is replaced at 600°C.

The observation that the Raman spectrum of ω-$VOPO_4$ is very similar to that of δ-$VOPO_4$ is relevant to previous in situ spectroscopic studies of VPO catalysts. In previous studies, the assignment of the presence of δ-$VOPO_4$ was often based on Raman spectroscopy. Thus, the formation of ω-$VOPO_4$ during the industrial process can be considered possible, particularly during the formation of the calcined catalyst precursor. Obviously, ω-$VOPO_4$ cannot be involved in the main catalytic process because we observed its rapid transformation to δ-$VOPO_4$ in the presence of the reactants, but the ω-$VOPO_4$ phase could play an important role in the activation of the catalyst. For example, ω-$VOPO_4$ could be involved in the formation of a certain amount of V^{5+} (*7*, *8*), which is recognized to be important for improving the catalyst performance (*10*).

References and Notes

1. P. Amorós, D. Marcos, A. Beltrán-Porter, D. Beltrán-Porter, *Curr. Opin. Solid State Mater. Sci.* **4**, 123 (1999).
2. G. Villeneuve, K. S. Suh, P. Amorós, N. Casañ-Pastor, D. Beltrán, *Chem. Mater.* **4**, 108 (1992).
3. G. Centi, Ed., vol. 16 of *Catalysis Today* (Elsevier, Amsterdam, 1993), part 1.
4. E. Bordes, *Catal. Today* **1**, 499 (1987).
5. G. J. Hutchings *et al.*, *J. Catal.* **208**, 197 (2002).
6. G. J. Hutchings, *J. Mater. Chem.* **14**, 3385 (2004).
7. G. J. Hutchings, A. Desmartin Chomel, R. Olier, J. C. Volta, *Nature* **368**, 41 (1994).
8. G. W. Coulston *et al.*, *Science* **275**, 191 (1997).
9. H. Wibbeke, International Centre for Diffraction Data, Powder Diffraction File, Entry 37-809 (1996).
10. P. Amorós *et al.*, *J. Phys. Chem. Solids* **62**, 1393 (2001).
11. G. J. Hutchings, *Appl. Catal.* **72**, 1 (1991).
12. M. Dente, S. Pierucci, E. Tronconi, M. Cecchini, F. Ghelfi, *Chem. Eng. Sci.* **58**, 643 (2003).
13. J. C. Burnett, R. A. Keppel, W. D. Robinson, *Catal. Today* **1**, 537 (1987).
14. R. M. Contractor, *Chem. Eng. Sci.* **54**, 5627 (1999).
15. J. T. Gleaves, J. R. Ebner, T. C. Kuechler, *Catal. Rev. Sci. Eng.* **30**, 49 (1988).
16. Precursors prepared by different routes behaved identically in the experiments described in this paper. Therefore, we do not consider that our findings relate to a specific preparation of $VOHPO_4 \cdot 0.5H_2O$ or to a specific morphology, but we believe that our results have general applicability.
17. Additional data are available on *Science* Online.
18. F. Girgsdies *et al.*, poster presented at the XXXIX Jahrestreffen Deutscher Katalytiker meeting, Weimar, Germany, 15 to 17 March 2006 (http://edoc.mpg.de/display.epl?mode=doc&id=263374 and in the supporting online material).
19. T. Ressler *et al.*, *J. Catal.* **191**, 75 (2000).

20. We thank the Engineering and Physical Sciences Research Council for financial support.

Supporting Online Material

www.sciencemag.org/cgi/content/full/313/5791/1270/DC1
Materials and Methods
Figs. S1 to S10
Table S1
References
Scheme S1
Poster S1

25 May 2006; accepted 19 July 2006
10.1126/science.1130493

Fluorous Nanodroplets Structurally Confined in an Organopalladium Sphere

Sota Sato,[1] Junya Iida,[1] Kosuke Suzuki,[1] Masaki Kawano,[1] Tomoji Ozeki,[2] Makoto Fujita[1]*

The distinct properties of fluorous phases are practically useful for separation, purification, and reaction control in organic synthesis. Here, we report the formation of a liquid-like fluorous droplet, composed of 24 perfluoroalkyl chains confined in the interior of a 5-nanometer-sized, roughly spherical shell that spontaneously assembled in solution from 12 palladium ions and 24 bridging ligands. Crystallographic analysis confirmed the rigid shell framework and amorphous interior. Perfluoroalkanes can dissolve in this well-defined fluorous phase, whereas they can hardly dissolve in a surrounding polar organic solution, and their solubility (up to ~eight perfluoroalkane molecules per spherical complex) can be finely controlled by tuning the length of perfluoroalkyl chains tethered to the shell.

A fluorous phase manifests distinct solubilizing properties relative to aqueous and common organic phases and therefore proves useful for a range of separation (*1*–*3*), purification (*4*, *5*), and catalyst-immobilization (*6*–*8*) techniques. In particular, organic synthesis using the fluorous phase has developed rapidly in recent years (*9*) because of its high compatibility with environmentally benign chemistry. Nanometer-scale fluorous environments can be attained within vesicles, micelles, or dendrimers that in turn dissolve in aqueous or organic solvents; however, the phases are often poorly defined physically and structurally (*10*–*12*). We previously showed (*13*, *14*) that pyridine-capped banana-shaped bridging ligands spontaneously

assembled in solution with metal ions to form ~5-nm-diameter spherical shells. Here, we report that, by attaching a perfluoroalkyl group at the curvature point of the ligand, we obtained an $M_{12}L_{24}$ (where M represents a metal and L a ligand) spherical complex whose interior is filled with 24 perfluoroalkyl chains (Fig. 1). The interior of the complex can be regarded as a structurally well-confined, molecular-scale fluorous "droplet" (Fig. 1) that can selectively dissolve fluorocarbons, whereas a surrounding solution can hardly dissolve them.

Ligands **1a** to **1d** (Fig. 1) were prepared in high yield from the Mitsunobu or the Williamson reaction of the corresponding $R_FCH_2CH_2OH$ or $R_FCH_2CH_2I$ precursor, respectively, with 2,6-dibromophenol, followed by Sonogashira cross-coupling with 4-ethynylpyridine. When a mixture of ligand **1a** (11 μmol) and $Pd(NO_3)_2$ (9.1 μmol) in dimethyl sulfoxide (DMSO)–d_6 (0.70 ml) was heated at 70°C for 3 hours, the endofluorous $M_{12}L_{24}$ complex **2a** was quantitatively obtained, as indicated by nuclear magnetic resonance (NMR) spectroscopy (vide infra). Complexes **2b** to **2d** were quantitatively prepared by the same method.

After counterion exchange with triflate ion (OTf^-), the $M_{12}L_{24}$ stoichiometry of **2a** was confirmed by cold-spray ionization mass spectrometry (CSI-MS) (Fig. 2): From a series of prominent peaks of $[\mathbf{2a}\text{-}(OTf^-)_m + (DMSO)_n]^{m+}$ (with m values from 8 to 14 and n values of 0 or 1), the molecular weight was determined to be 20,276.5 (calculated as 20,272.2). In ^1H and ^{19}F NMR spectra, only one set of signals was observed for the ligand **1a** nuclei, consistent with the cuboctahedron symmetry of **2a** (Fig. 2). The observed large downfield shift of pyridine (Py) H_α and PyH_β protons [Δδ equal to 0.59 and 0.23 parts per million (ppm), respectively] is characteristic of pyridine-metal coordination. In ^{19}F NMR, signals for the C_6F_{13} chain were unambiguously assigned by ^{19}F-^{19}F nuclear Overhauser effect spectroscopy (NOESY) and correlation spectroscopy (COSY) experiments (*15*). In a similar manner, endofluorinated $M_{12}L_{24}$ spheres **2b** to **2d** were fully characterized. The diffusion coefficient of **2a** to **2d**, determined by diffusion-ordered NMR spectroscopy (DOSY) experiments using both ^1H and ^{19}F nuclei, was $D = 4.0 \times 10^{-11} \pm 0.5 \times 10^{-11}$ m^2 s^{-1}, consistent with the estimated diameter of 4.3 nm (*13*, *14*). We also obtained clear atomic force microscopy (AFM) images for **2a** to **2d** that indicated diameters of 4.9 ± 0.3 nm (fig. S8).

We expected that the fluorous core of **2a** could accommodate (or dissolve) fluorinated compounds through fluorophilic host-guest interaction. Thus, excess perfluorooctane, **3**, which is hardly soluble in DMSO, was suspended in a DMSO-d_6 solution of **2a** (0.43 mM), and the mixture was stirred vigorously at room temperature for 2 hours. Unencapsulated **3** was then separated by phase separation in a centrifuge, and the DMSO-d_6 solution was analyzed by ^{19}F NMR (Fig. 3). In addition to the signals from the C_6F_{13} chains of **2a**, we observed a set of four signals for included guests **3**. From the integral ratio, it was estimated that on average 5.8 molecules of **3** were accommodated by **2a**. This host-guest ratio remained almost unchanged even when the experiment was carried out at different concentrations (**2a** concentrations of 0.18, 0.37, or 0.54 mM). Detailed analysis of ^{19}F NMR spectra showed that the signals of the terminal fluorine atoms in the C_6F_{13} chain of **2a** were shifted further upfield than internal ones: Δδ ranged from 0.4 to 1.3 ppm for F^{d-f} and from 0.0 to 0.1 ppm for F^{a-c} (Fig. 3). On the basis of this finding, we assume that guest molecules accumulate at the core of the hollow complex. The guest signals are also shifted upfield relative to the signals of free perfluorooctane in $CDCl_3$ (Δδ from 1.3 to 2.3 ppm). The guest, **3**, can be drawn out from the interior of **2a** by addition of acetonitrile to the solution, because **3** can dissolve in the mixed solvent (Materials and Methods).

DOSY experiments afforded further evidence for the inclusion of **3** in **2a**. In ^{19}F DOSY NMR spectra, a single band consisting of signals from both **2a** and **3** was observed at $D = 3.2 \times 10^{-11}$ m^2 s^{-1} (Fig. 3B). Because the diffusion coefficient of free perfluorooctane is much larger ($D = 1.3 \times 10^{-9}$ m^2 s^{-1} in $CDCl_3$), the observed coincidence of diffusion coefficients indicates the association of **2a** with **3**.

Crystallography revealed that the complex, **2a**, possesses a raw egg–like structure, in which a rigid $M_{12}L_{24}$ shell framework encloses flexible, disordered perfluoroalkyl chains that resemble a liquid (Fig. 4). Single crystals of the **2a**•(**3**)$_n$ complex were obtained by slow vapor diffusion of ethyl acetate into a DMSO solution of **2a**•(**3**)$_n$ (n = 5.8). Although a conventional laboratory diffractometer afforded data with insufficient resolution to determine the structure, the use of synchrotron x-ray radiation provided impressive-

[1]Department of Applied Chemistry, School of Engineering, University of Tokyo, and Core Research for Evolutional Science and Technology (CREST), Japan Science and Technology Corporation (JST), 7-3-1 Hongo, Bunkyo-ku, Tokyo 113-8656, Japan. [2]Department of Chemistry and Materials Science, Tokyo Institute of Technology, 2-12-1 O-okayama, Meguro-ku, Tokyo 152-8551, Japan.

*To whom correspondence should be addressed. E-mail: mfujita@appchem.t.u-tokyo.ac.jp

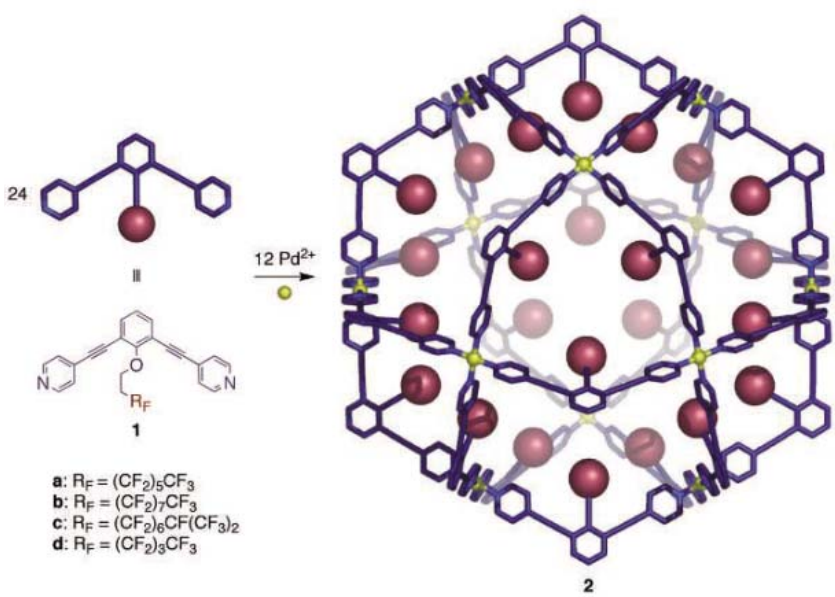

Fig. 1. Self-assembly of endofluorous $M_{12}L_{24}$ molecular spheres.

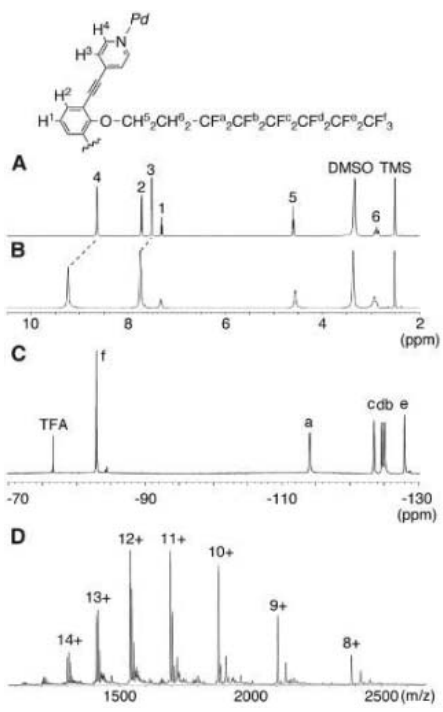

Fig. 2. (**A**) ^1H NMR spectrum of **1a**. (**B**) ^1H and (**C**) ^{19}F NMR spectra of **2a**. (**D**) CSI-MS spectrum of **2a** (CH_3CN:DMSO = 19:1, OTf^- salt).

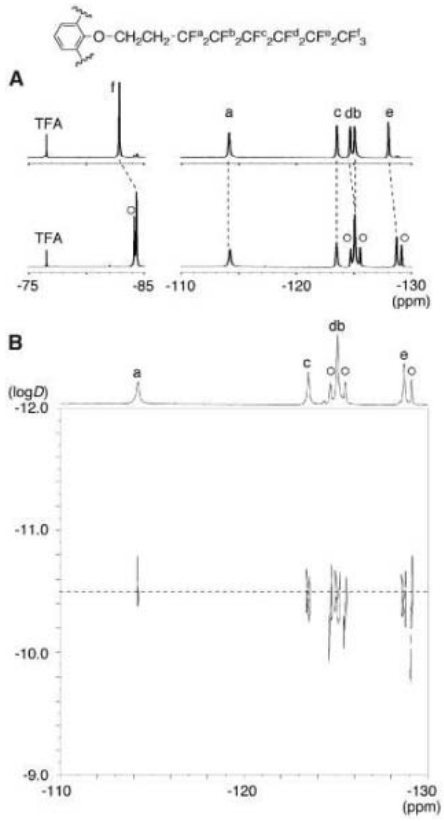

Fig. 3. (**A**) ^{19}F NMR spectra (470 MHz, DMSO-d_6) of (top) complex **2a** and (bottom) inclusion complex of **2a** and **3** (indicated in circles). (**B**) DOSY spectrum of inclusion complex of **2a** and **3**.

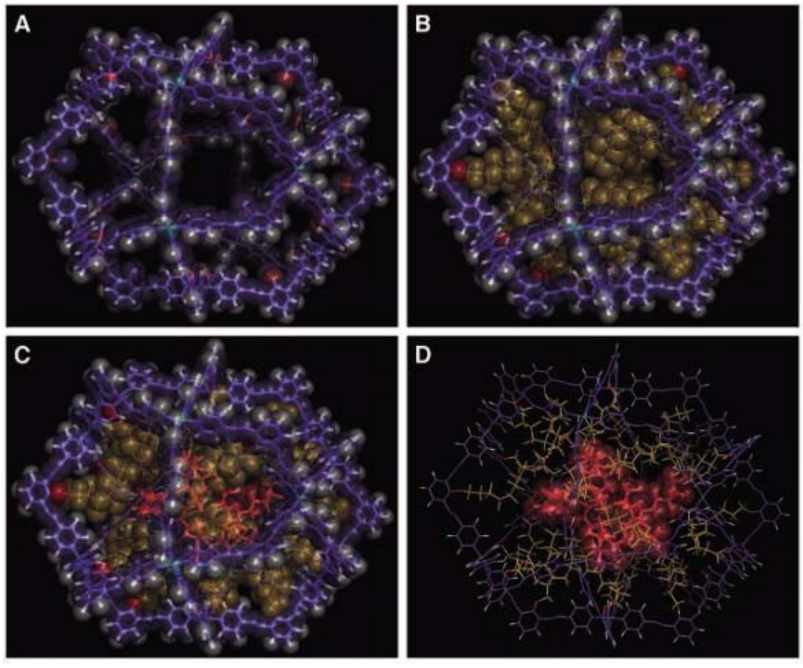

Fig. 4. Molecular structure of **2a**. (**A**) The *x*-ray crystal structure of the shell framework of **2a**. $C_6F_{13}CH_2$- side chains at the curvature point of the ligands are disordered and could not be located. (**B**) The $C_6F_{13}(CH_2)_2$- side chains (orange) are modeled, and only the chains are optimized, by force-field calculations. (**C** and **D**) Six molecules of perfluorooctane (**3**, red) were placed at the central void of **2a**, and structural annealing was conducted from 2000 to 300 K by molecular dynamics (MD) simulation. The images show one of the energy minimum structures obtained after MD simulation followed by force-field optimization. In (D), host **2a** is represented by wire frames, whereas the accommodated guest molecules are represented by space-filling models.

ly higher quality data, from which the $M_{12}L_{24}$ shell framework of **2a** could be refined (*16*). The fluorous chains and the included guest, **3**, are completely disordered and cannot be located in the crystallographic analysis. The shell framework is shown to be not spherical but oval, with a dimension of 4.9 nm by 4.2 nm (Fig. 4A). The distortion from the ideal spherical shape is probably induced by the aggregation of the fluorous chains in the shell.

To elucidate how the host, **2a**, accommodates the guest, **3**, we carried out force-field calculations: 24 $C_6F_{13}(CH_2)_2$- side chains were attached to the residual oxygen atoms of the ligand **1a** components in the crystal structure of **2a**, and only the side chains were optimized. The optimized structure shows that, despite the aggregation of the fluorous chains, a void remains at the core (Fig. 4B). Therefore, we added six perfluorooctane molecules to the void and minimized the whole structure by molecular dynamics simulation. Repeated, gradual annealing from 2000 to 300 K accumulated energy-minimized structures 30 times. All of these minimized structures converged almost identically to a structure in which the guest molecules interact with the terminal $CF_3CF_2CF_2$- portions of the perfluoroalkyl side chains (Fig. 4, C and D). This arrangement is consistent with the NMR spectra that show large upfield shifts of the signals from the terminal $CF_3CF_2CF_2$- groups. We emphasize that the guest molecules **3** are dissolved, rather than recognized, in a well-defined fluorous droplet composed of 24 C_6F_{13} side chains.

Because of the well-defined, precise structure of the $M_{12}L_{24}$ framework, the fluorous environment and the void space at the core are predictable and easily controlled by modifying the fluorinated side chain of the ligand. Sphere **2b** with $(CF_2)_7CF_3$ groups, or sphere **2c** with more bulky $(CF_2)_6CF(CF_3)_2$ groups, accommodated a smaller amount of perfluorooctane (circa 2.5 guest molecules per complexes), presumably due to reduced effective void volume at the core of the sphere. In contrast, sphere **2d**, with sterically less-demanding $(CF_2)_3CF_3$ side chains, evidenced no inclusion of perfluorooctane despite a larger void space in the sphere, perhaps because of insufficient fluorine density to define the fluorous atmosphere. Sphere **2a** included other fluorocarbons such as perfluorohexane (~8.0 molecules per **2a**) but not fluoroaromatics such as perfluorobenzene or perfluoronaphthalene, presumably because of better interaction with the external solvent. Further ligand tuning should enhance the viability of these fluorous droplets for mediating reaction chemistry.

References and Notes

1. A. Studer *et al.*, *Science* **275**, 823 (1997).
2. J. Yoshida, K. Itami, *Chem. Rev.* **102**, 3693 (2002).
3. J. A. Gladysz, D. P. Curran, I. T. Horváth, Eds., *Handbook of Fluorous Chemistry* (Wiley-VCH, Weinheim, Germany, 2004), chaps. 4 and 7.
4. A. Studer, P. Jeger, P. Wipf, D. P. Curran, *J. Org. Chem.* **62**, 2917 (1997).
5. W. Zhang, *Tetrahedron* **59**, 4475 (2003).
6. I. T. Horváth, J. Rábai, *Science* **266**, 72 (1994).
7. I. T. Horváth, *Acc. Chem. Rev.* **31**, 641 (1998).
8. R. H. Fish, *Chem. Eur. J.* **5**, 1677 (1999).
9. P. Kirsch, *Modern Fluoroorganic Chemistry* (Wiley-VCH, Weinheim, Germany, 2004), chap. 3.
10. M. P. Krafft, *Adv. Drug Delivery Rev.* **47**, 209 (2001).
11. J. G. Riess, *Tetrahedron* **58**, 4113 (2002).
12. K. C. Hoang, S. Mecozzi, *Langmuir* **20**, 7347 (2004).
13. M. Tominaga *et al.*, *Angew. Chem. Int. Ed. Engl.* **43**, 5621 (2004).
14. M. Tominaga, K. Suzuki, T. Murase, M. Fujita, *J. Am. Chem. Soc.* **127**, 11950 (2005).
15. J. L. Battiste, N. Jing, R. A. Newmark, *J. Fluorine Chem.* **125**, 1331 (2004).
16. X-ray crystallographic analysis of **2a**: The diffraction data were measured at 130 K [wavelength (λ) = 0.6890 Å] at Photon Factory–Advanced Ring for Pulse X-rays (PF-AR) of the High Energy Accelerator Research Organization (KEK). Space group *I*4/*m*, temperature (T) = 130 ± 2, a = 43.970 ± 0.006 Å, b = 43.970 ± 0.006 Å, c = 42.521 ± 0.009 Å, volume (V) = 82,208 ± 23 Å^3, atomic number (Z) = 1. Anisotropic least-squares refinement for the palladium atoms and isotropic refinement for the other atoms on 8023 independent merged reflections (R_{int} = 0.1329) converged at residual $wR_2(F^2)$ = 0.3243 for all data; residual $R_1(F)$ equals 0.2460 for 3472 observed data [$I > 2\sigma(I)$], and goodness of fit (GOF) equals 1.965. The successful refinement of the shell framework is remarkable because the framework crystallographically determined occupies only 13% of the extraordinary large cell volume (82,208 Å^3). The remaining volume of 87% is occupied by severely disordered

perfluoroalkyl chains, guest **5**, solvents, and counter ions. Hence the *R* value of 24.6% is quite reasonable given the size and complexity of the compound.

17. This work was financially supported by a Grant-in-Aid for Scientific Research (S) no. 14103014, from the Ministry of Education, Culture, Sports, Science, and Technology of Japan. Supplementary crystallographic data for compound **2a** can be obtained free of charge (under CCDC 602076) by contacting the Cambridge Crystallographic Data Centre, 12, Union Road, Cambridge CB2 1EZ, UK; via their Web site (www.ccdc.cam.ac.uk/data_request/cif), by e-mail (data_request@ccdc.cam.ac.uk), or by fax (+44 1223 336033). We thank K. Yamaguchi and H. Masu for CHNS elemental analyses.

Supporting Online Material
www.sciencemag.org/cgi/content/full/313/5791/1273/DC1
Materials and Methods
Figs. S1 to S8

11 May 2006; accepted 20 July 2006
10.1126/science.1129830

Triple-Bond Reactivity of Diphosphorus Molecules

Nicholas A. Piro, Joshua S. Figueroa, Jessica T. McKellar, Christopher C. Cummins*

We report a mild method for generating the diphosphorus molecule or its synthetic equivalent in homogeneous solution; the P_2 allotrope of the element phosphorus is normally obtained only under extreme conditions (for example, from P_4 at 1100 kelvin). Diphosphorus is extruded from a niobium complex designed for this purpose and can be trapped efficiently by two equivalents of an organic diene to produce an organodiphosphorus compound. Diphosphorus stabilized by coordination to tungsten pentacarbonyl can be generated similarly at 25°C, and in this stabilized form it still efficiently consumes two organic diene molecules for every diphosphorus unit.

A dichotomy exists in the chemistry of the group 15 elements: The stable molecular form of nitrogen is triply bonded dinitrogen, whereas the stable molecular form of phosphorus is the tetrahedral P_4 molecule, white phosphorus (*1*). Only upon heating white phosphorus to more than 1100 K does the P_4 = 2 P_2 equilibrium become important (*2*–*4*). Underlying this dichotomy is the tendency of nitrogen to engage in multiple bonding, as compared with phosphorus, for which the π-bond components of multiple bonds are relatively high in energy and quite reactive (*5*, *6*). Thus, the triple bond in the atmospherically abundant dinitrogen molecule is one of the strongest known chemical bonds (its bond dissociation enthalpy, D_e, is 226 kcal/mol), whereas that in the diphosphorus molecule is only about half as strong (D_e = 117 kcal/mol) (*7*, *8*). P_2 is therefore known principally as an exotic gas-phase species of astrophysical interest (*9*), as a reactive component of plasmas generated in the high-temperature deposition of III/V semiconductor materials (*10*), and in the context of matrix-isolation experiments (*11*–*14*). The use of P_2 in chemical synthesis requires a means to generate it in solution and under mild conditions of temperature and pressure. Accordingly, we describe a mild method that uses niobium chemistry as a vehicle for the generation of diphosphorus (or a synthetic equivalent) in solution, where it may be trapped by suitable organic acceptors.

Organic azides, molecules of formula N=N=N–R, where R is a variable organic substituent, are known to react with transfer of their nitrene moiety (N–R) to a group 5 metal through observable or isolable intermediates, in which an intact RN_3 molecule is complexed (*15*–*17*). The final products in such a nitrene transfer reaction are the group 5 metal imido and N_2 gas (Fig. 1A). Diphosphorus-substituted analogs of organic azides, of formula P=P=N–R, would be a useful addition to the library of low-coordinate phosphorus compounds (*5*), and we wondered whether they would react analogously with group 5 metals to transfer nitrene while extruding the desired P_2 molecule (Fig. 1B).

To synthesize such a solution-phase P_2-generating molecular system, we created the phosphorus-phosphorus bond within the protective coordination sphere of a niobium complex. Recently, we have used the terminal phosphide anion $[P{\equiv}Nb(N[Np]Ar)_3]^{1-}$ (where Np is neopentyl and Ar is 3,5-$C_6H_3Me_2$) as its sodium salt to great advantage in assembling phosphorus-element bonds atop the protective $Nb(N[Np]Ar)_3$ platform (*18*, *19*), and the present work is a logical extension of that methodology.

The system (η^2-Mes*NPP)$Nb(N[Np]Ar)_3$ (where Mes* is 2,4,6-*t*-$Bu_3C_6H_2$), **1**, containing the diphosphorus-substituted organic azide ligand bound through its P_2 unit to the niobium trisanilide platform, has been obtained in 60% isolated yield as an orange-red solid after an NaCl-elimination reaction between Niecke's chloroiminophosphane ClP=NMes* (*20*) and our terminal phosphide anion sodium salt, $Na[P{\equiv}Nb(N[Np]Ar)_3]$ (*21*). Complex **1** has been characterized by single-crystal x-ray crystallography (Fig. 2A); the structure so obtained is notable for its short P=P and P=N interatomic distances [2.0171(±0.0009) and 1.556 (±0.002) Å (where the error is estimated standard deviation), respectively], which suggest multiple bonding between these atoms. Characterization data for **1** obtained by nuclear magnetic resonance (NMR) spectroscopy (^{31}P, ^{13}C, and ^{1}H) in benzene-d_6 solution are consistent with the observed solid-state structure of the complex, with the ^{31}P data [doublets with a one-bond P-P coupling constant $^{1}J_{PP}$ = 650 Hz at a chemical shift, δ, of 334 and 315 parts per million (ppm)] being most diagnostic for the system. Alternative isomeric formulations of **1** may be similar in energy to the solid-state structure of **1**, and we considered them in our computational studies.

Heating a solution of complex **1** in neat 1,3-cyclohexadiene (1,3-CHD), the latter serving both as solvent and as trap for the P_2 unit, to 65°C for 3 hours gave smooth and quantitative conversion to niobium imido **2** together with a single phosphorus-containing product. This product (**3** in Fig. 2A) is characterized by a singlet in the ^{31}P NMR spectrum at δ = −80 ppm. Formulation of **3** as the double Diels-Alder (*22*) adduct of P_2 with two equivalents of 1,3-CHD was confirmed by its isolation in pure form, crystallization, and characterization by single-crystal x-ray crystallography (Fig. 2B). Although P=P double bonds, such as that of the *bis*-$Cr(CO)_5$ complex of diphosphene PhP=PPh (*23*), can react with a diene to form a Diels-Alder adduct, double diene addition to two π bonds of a P_2 unit has not been reported. We propose that this reaction occurs in two steps: (i) transfer of P_2 to the first 1,3-CHD

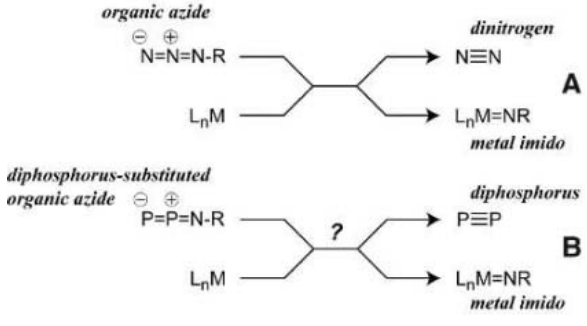

Fig. 1. (**A**) Reaction of an organic azide with a metal complex to extrude dinitrogen while delivering a metal imido unit and (**B**) the envisioned analogous process with diphosphorus extrusion.

Department of Chemistry, Massachusetts Institute of Technology, 77 Massachusetts Avenue, Cambridge, MA 02139–4307, USA.

*To whom correspondence should be addressed. E-mail: ccummins@mit.edu

molecule generating unobserved intermediate 2,3-diphosphabicyclo[2.2.2]octa-2,5-diene, depicted in brackets in Fig. 2A, and (ii) [4+2] cycloaddition of this intermediate to the second molecule of 1,3-CHD with endo stereoselectivity (selectivity such that the resulting C-C double bonds are proximal) (*22*, *24*). The tetracyclic structure of **3** with its cofacial pair of C=C π bonds is analogous to that of oligocondensed bicyclo[2.2.2]octenes studied as examples of laticyclic conjugation (*25*).

The use of excess 1,3-CHD is not required for thermal extrusion of P_2 from complex **1**. For example, at 50°C in toluene-d_8 solution, **1** was observed by ^{1}H NMR spectroscopy to decay to **2** with first-order rate constant $k = 4 \times 10^{-4}$ s^{-1}, with the appearance of imido **2** following the same kinetic profile. Under these conditions, however, no prominent signals were generated in the ^{31}P NMR spectrum of the reaction mixture, and the fate of the P_2 unit is not known. Also, pure **2** was obtained as golden yellow single crystals in 48% isolated yield following thermolysis of **1** in tetrahydrofuran (THF) solvent at 70°C for 45 min, and was characterized by x-ray diffraction (Fig. 2A). Notably, P_2 condensation is known to give the red modification of phosphorus, not the white phosphorus that is soluble and if formed would have been observed by ^{31}P NMR spectroscopy (*1*, *26*). Dimerization of two P_2 molecules to give P_4 is a process forbidden by orbital symmetry (*3*) and accordingly does not take place under mild conditions (*1*, *26*).

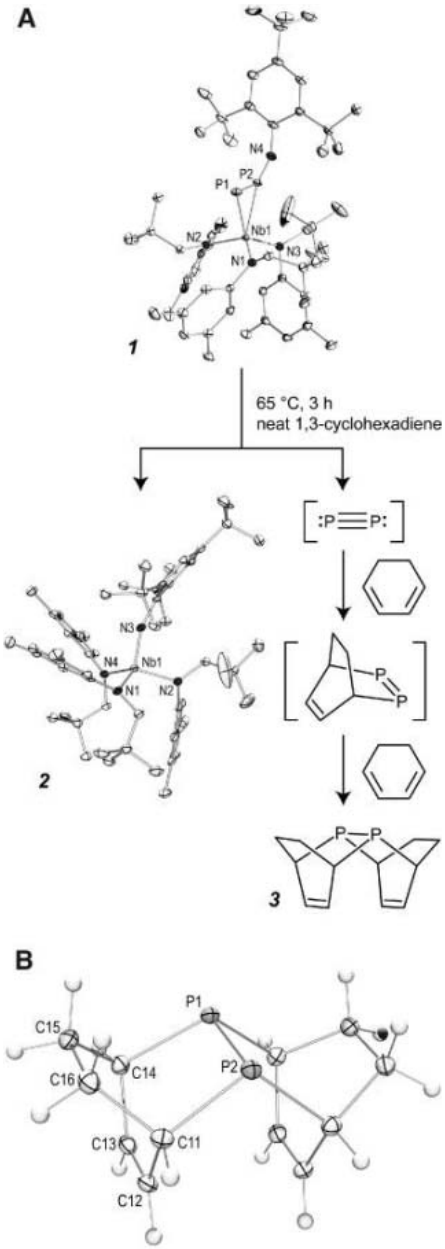

Fig. 2. (**A**) Heating a 1,3-CHD solution of niobium complex **1** results in P_2 extrusion and transfer into organodiphosphorus compound **3**. Thermal ellipsoid representations of **1** and **2** derived from x-ray diffraction studies are included. (**B**) Thermal ellipsoid rendering of organodiphosphorus compound **3**.

The combined observations are consistent with fragmentation of **1** to give **2** along with transient P_2 that subsequently can be trapped, as with 1,3-CHD. It is likely that **1** undergoes rearrangement from its solid-state structure **1**i (Fig. 3) to an alternative structure **1**ii or **1**iii, in which a Nb-N bond is formed, before loss of P_2. The proposed **1** → [**1**ii or **1**iii] → **2** + P_2 fragmentation is the simplest scenario consistent with all the available data and finds a close analogy in our recent description of C≡P triple-bond generation by unimolecular fragmentation of a niobium precursor (*27*) that has a metallacycle structure as in **1**ii.

Four possible isomeric forms of **1** (Fig. 3 and Table 1) have been investigated with the use of quantum chemical calculations. The lowest energy structure **1**i corresponds to the observed solid-state structure of **1** (Fig. 2A) and, on the basis of ^{31}P NMR shielding calculations, we also assign **1**i to be the structure adopted by **1** in solution. The next highest in energy is structure **1**iv, in which the PPNMes* ligand coordinates to niobium only through its terminal phosphorus atom; this structure is analogous to that of known tantalum and vanadium organic azide complexes (*15*–*17*). In addition, rearrangement of **1**i to **1**ii might be expected to take place through a structure such as **1**iv. The highest energy isomer is **1**iii, in which the PPNMes* ligand has migrated to an η^2-PN bonding mode and incorporates a one-coordinate phosphorus atom. Considering the energies of the computationally modeled isomers, a pathway passing through **1**ii as opposed to **1**iii is preferred. However, coordination of a Lewis acidic metal fragment, such as $W(CO)_5$, to the one-coordinate phosphorus atom of **1**iii might cause a pathway involving this isomer to become preferred. Notably, the computational study predicts, regardless of the microscopic pathway, that the fragmentation of **1** to **2** and P_2 is overall essentially thermoneutral.

In an effort to stabilize P_2 in solution after its extrusion from the $Nb(N[Np]Ar)_3$ platform, we investigated the possibility of its generation as a tungsten pentacarbonyl complex. Diphosphorus is already established as a ligand in transition-element chemistry, but as a rule it is found connected to two or more metal centers

Table 1. Model study of possible isomers of **1** and P_2 elimination. Calculations were performed at the BP86/TZ2P level of DFT theory using density functional theory methods. Ar^1 = 2,6-*t*-$Bu_2C_6H_3$, Me = CH_3, and Ph = C_6H_5. *E*(rel), the energy of **1**i to **1**iv relative to isomer **1**i. Δ*E*, the energy change for the fragmentation reaction of **1**i.

Model isomer or reaction	Complex	*E*(rel) or Δ*E* (kcal/mol)
(η^2-*PP*-Ar^{1}NPP)Nb(N[Me]Ph)$_3$	**1**i	0
(κ^2-*PN*-Ar^{1}NPP)Nb(N[Me]Ph)$_3$	**1**ii	+19
(η^2-*PN*-Ar^{1}NPP)Nb(N[Me]Ph)$_3$	**1**iii	+28
(η^1-*P*-Ar^{1}NPP)Nb(N[Me]Ph)$_3$	**1**iv	+6
1i → (Ar^{1}N)Nb(N[Me]Ph)$_3$ + P_2		0

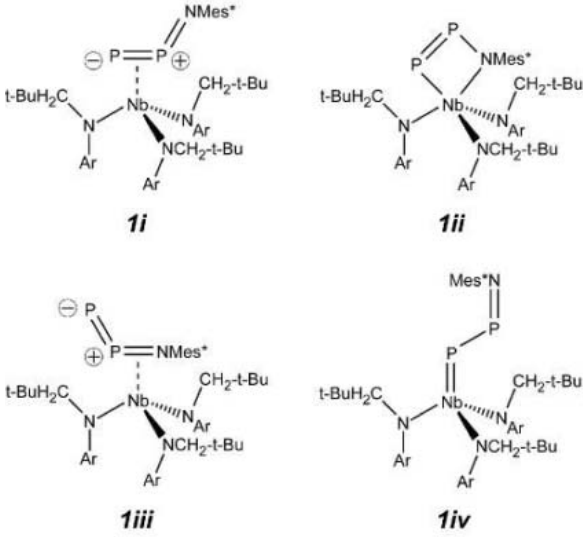

Fig. 3. Line drawings of four isomeric forms of **1** investigated using quantum chemical calculations. For simplicity, only a single resonance structure is drawn for each isomer.

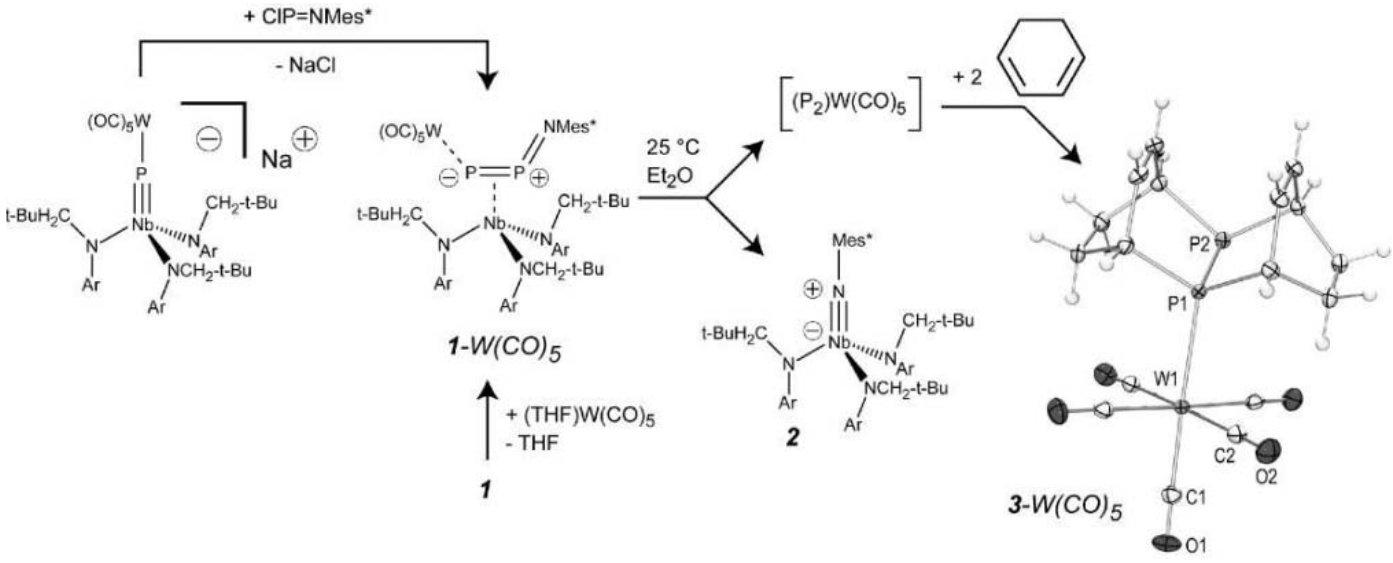

Fig. 4. Generation and trapping of a tungsten pentacarbonyl P_2 complex.

(*28*). Transition metal complexes of P_2 often are obtained as a result of P_4 activation (*29*), and white phosphorus is also known to serve as a P_2 source in organic reactions (*30*). We hoped that by binding P_2 to a single $W(CO)_5$ fragment, we would stabilize it sufficiently to extend its lifetime in solution but still retain triple-bond reactivity for the diphosphorus moiety. The targeted reactive intermediate—in this case, $(P_2)W(CO)_5$—has been the subject of a theoretical study concluding that, in contrast to N_2, the P_2 ligand preferentially binds side-on to the tungsten center (*31*).

The tungsten pentacarbonyl-capped phosphide anion $[(OC)_5W\text{-}P{\equiv}Nb(N[Np]Ar)_3]^{1-}$ was prepared by reaction of $W(CO)_6$ with phosphide anion $[P{\equiv}Nb(N[Np]Ar)_3]^{1-}$ and reacts with ClP=NMes* by means of salt elimination to generate **1**-$W(CO)_5$ (Fig. 4). The structure of this thermally unstable complex was confirmed spectroscopically. A pair of doublets at δ = 285 and 247 ppm with $^1J_{PP}$ = 730 Hz appear in the ^{31}P NMR spectrum of a benzene-d_6 solution at 20°C. Such a large coupling constant indicates the presence of substantial P-P multiple bonding in **1**-$W(CO)_5$. An alternative method for generation of **1**-$W(CO)_5$ exhibiting identical ^{1}H and ^{31}P NMR spectral properties was to add photochemically generated $(THF)W(CO)_5$ to a solution of **1** with liberation of THF (Fig. 4). The former method is preferred synthetically due to the relative ease of stoichiometry control.

At 10°C in toluene-d_8 solution, **1**-$W(CO)_5$ is seen to decay following clean first-order kinetics with a rate constant $k \approx 1.9 \times 10^{-4}$ s^{-1} in the presence of 0 to 80 equivalents of 1,3-CHD, as followed by ^{1}H NMR spectroscopy. The decay of **1**-$W(CO)_5$ under these conditions produces imido **2** together with the $W(CO)_5$ adduct of **3**. The insensitivity of the rate of this process to 1,3-CHD concentration strongly suggests that the rate-determining step is fragmentation to **2** and $(P_2)W(CO)_5$; subsequent sequential trapping of the latter by first one and then a second equivalent of 1,3-CHD (sequence not shown explicitly in Fig. 4) accounts for formation of **3**-$W(CO)_5$ (*32*). Diagnostic of **3**-$W(CO)_5$ are a pair of ^{31}P NMR doublets at $\delta = -34$ and -84 ppm with $^1J_{PP}$ = 340 Hz. The resonance at $\delta = -34$ ppm is assigned to the coordinated phosphorus in view of the flanking ^{183}W satellites it exhibits ($^1J_{WP}$ = 230 Hz). Confirming the formulation of **3**-$W(CO)_5$, identical spectral features were generated upon addition of (pyridine)$W(CO)_5$ to a sample of **3**. Additionally, **3**-$W(CO)_5$ was separated from **2**, and crystals grown from ether were subjected to a single-crystal x-ray diffraction study (Fig. 4).

The $W(CO)_5$-supported variant of the P_2 generation/transfer scheme is attractive for several reasons. The organic diene trap, 1,3-CHD, need not be used in excess for efficient interception of the putative $(P_2)W(CO)_5$ intermediate, and the fragmentation of **1**-$W(CO)_5$ takes place under ambient conditions without the need for heating. These features bode well for the extension of effective P_2 triple-bond reactivity to a wide substrate array, especially given the status of 1,3-CHD as a relatively unreactive Diels-Alder diene (*33*). As initial evidence that the trapping chemistry is not limited to 1,3-CHD as the organic partner, we found that both cyclopentadiene and 2,3-dimethylbutadiene serve as efficient traps for $(P_2)W(CO)_5$ with production, respectively, of corresponding tetra- and bicyclic organodiphosphorus compounds (*34*, *35*). Besides raising fundamental questions about the mechanism and scope of P_2 solution chemistry, the experimental observation of diphosphorus transfer into organic molecules creates the opportunity to test diphosphine structures such as **3** for utility as synthetic catalysts (*36*–*38*).

References and Notes

1. N. N. Greenwood, A. Earnshaw, *Chemistry of the Elements* (Butterworth-Heinemann, Boston, ed. 2, 1997).
2. D. P. Stevenson, D. M. Yost, *J. Chem. Phys.* **9**, 403 (1941).
3. H. Bock, H. Muller, *Inorg. Chem.* **23**, 4365 (1984).
4. O. J. Scherer, *Angew. Chem. Int. Ed. Engl.* **39**, 1029 (2000).
5. M. Regitz, O. J. Scherer, *Multiple Bonds and Low Coordination in Phosphorus Chemistry* (Thieme, Stuttgart, Germany, 1990).
6. K. B. Dillon, F. Mathey, J. F. Nixon, *Phosphorus: The Carbon Copy* (Wiley, Chichester, UK, 1998).
7. K. P. Huber, G. Herzberg, *Constants of Diatomic Molecules*, vol. IV of *Molecular Spectra and Molecular Structure* (Van Nostrand Reinhold, New York, 1979).
8. L. G. M. Pettersson, B. J. Persson, *Chem. Phys.* **170**, 149 (1993).
9. A. J. Sauval, J. B. Tatum, *Astrophys. J. Suppl. Ser.* **56**, 193 (1984).
10. N. Kobayashi, Y. Kobayashi, *Jpn. J. Appl. Phys.* **30**, L1699 (1991).
11. A. Kornath, A. Kaufmann, M. Torheyden, *J. Chem. Phys.* **116**, 3323 (2002).
12. M. McCluskey, L. Andrews, *J. Phys. Chem.* **95**, 2988 (1991).
13. L. Andrews, M. McCluskey, Z. Mielke, R. Withnall, *J. Mol. Struct.* **222**, 95 (1990).
14. Z. Mielke, M. McCluskey, L. Andrews, *Chem. Phys. Lett.* **165**, 146 (1990).
15. G. Proulx, R. G. Bergman, *J. Am. Chem. Soc.* **117**, 6382 (1995).
16. G. Proulx, R. G. Bergman, *Organometallics* **15**, 684 (1996).
17. M. G. Fickes, W. M. Davis, C. C. Cummins, *J. Am. Chem. Soc.* **117**, 6384 (1995).
18. J. S. Figueroa, C. C. Cummins, *Dalton Trans.* **2006**, 2161 (2006).
19. C. C. Cummins, *Angew. Chem. Int. Ed. Engl.* **45**, 862 (2006).
20. E. Niecke, J. Hombeuel, M. Blättner, V. Von Der Gönna, A. Ruban, in *Phosphorus, Arsenic, Antimony, and Bismuth*, H. H. Karsch, Ed., vol. 3 of *Synthetic Methods of Organometallic and Inorganic Chemistry*, W. A. Herrman, Ed. (Verlag, New York, 1996), pp. 28–30.

21. J. S. Figueroa, C. C. Cummins, *Angew. Chem. Int. Ed. Engl.* **43**, 984 (2004).
22. J. G. Martin, R. K. Hill, *Chem. Rev.* **61**, 537 (1961).
23. J. Borm, G. Huttner, O. Orama, L. Zsolnai, *J. Organomet. Chem.* **282**, 53 (1985).
24. R. Hoffmann, R. B. Woodward, *J. Am. Chem. Soc.* **87**, 4388 (1965).
25. W. Grimme *et al.*, *J. Chem. Soc., Perkin Trans. 2* 1893 (1998).
26. H. W. Melville, S. C. Gray, *Trans. Faraday Soc.* **32**, 271 (1936).
27. J. S. Figueroa, C. C. Cummins, *J. Am. Chem. Soc.* **126**, 13916 (2004).
28. O. J. Scherer, M. Ehses, G. Wolmershauser, *Angew. Chem. Int. Ed. Engl.* **37**, 507 (1998).
29. M. Ehses, A. Romerosa, M. Peruzzini, *Top. Curr. Chem.* **220**, 107 (2002).
30. C. Charrier, N. Maigrot, L. Ricard, P. LeFloch, F. Mathey, *Angew. Chem. Int. Ed. Engl.* **35**, 2133 (1996).
31. C. Esterhuysen, G. Frenking, *Chem. Eur. J.* **9**, 3518 (2003).
32. In the absence of 1,3-CHD, the rate constant for **1**-W(CO)$_5$ fragmentation is unchanged but the fate of (P_2)W(CO)$_5$ has not yet been determined.
33. J. Sauer, R. Sustmann, *Angew. Chem. Int. Ed. Engl.* **19**, 779 (1980).
34. Characterization data for the cyclopentadiene and 2,3-dimethylbutadiene reaction products are provided in the supporting online material text and figs. S7 and S8. For information on a structurally related diphosphorus bicycle synthesized by an unrelated method, see (*35*).
35. N. H. T. Huy, L. Ricard, F. Mathey, *J. Organomet. Chem.* **582**, 53 (1999).
36. X. F. Zhu, J. Lan, O. Kwon, *J. Am. Chem. Soc.* **125**, 4716 (2003).
37. J. E. Wilson, G. C. Fu, *Angew. Chem. Int. Ed. Engl.* **45**, 1426 (2006).
38. Experimental and computational details as well as x-ray diffraction data for **1**, **2**, **3**, and **3**-W(CO)$_5$ are provided as supporting material on *Science* Online.

39. We thank NSF for support of this research through grant CHE-0316823 and through a predoctoral fellowship to N.A.P. Complete crystallographic data were deposited in the Cambridge Crystallographic Database Centre (606636 to 606639).

Supporting Online Material

www.sciencemag.org/cgi/content/full/313/5791/1276/DC1
SOM Text
Figs. S1 to S13
Tables S1 to S3
References

8 May 2006; accepted 28 July 2006
10.1126/science.1129630

Discovery of a Young Planetary-Mass Binary

Ray Jayawardhana[1]* and Valentin D. Ivanov[2]

We have identified a companion to the young planetary-mass brown dwarf Oph 162225-240515. This pair forms a resolved binary consisting of two objects with masses comparable to those of extrasolar giant planets. Several lines of evidence confirm the coevality and youth of the two objects, suggesting that they form a physical binary. Models yield masses of ~14 and ~7 times the mass of Jupiter for the primary and the secondary object, respectively, at an age of ~1 million years. A wide (~240–astronomical unit) binary in the ultra-low-mass regime poses a challenge to some popular models of brown dwarf formation.

Brown dwarfs occupy the mass gap between dwarf stars and giant planets. Unlike stars, they are unable to fuse hydrogen because they have masses below the hydrogen-burning limit of ≈0.075 solar masses [≈75 times the mass of Jupiter ($M_{Jupiter}$)]. The distinction between brown dwarfs and planets is less clear. Some researchers draw the line at ≈13 $M_{Jupiter}$, because objects above that boundary can ignite deuterium, a less abundant isotope of hydrogen, for a short time early in their life, whereas those below ≈13 $M_{Jupiter}$ cannot. The vast majority of the hundreds of brown dwarfs identified since 1995 are free-floating objects, but a handful are in orbit around stars, further blurring the distinction between brown dwarfs and planets. Brown dwarfs and planets are often lumped together as substellar objects (*1*).

Among the most intriguing substellar objects identified to date are those with masses comparable to extrasolar giant planets (*2*, *3*). Unlike planets, these "planetary mass objects" ("planemos" for short), or "sub–brown dwarfs," as they are sometimes called, are not bound to stars. Because planemos represent the lowest mass free-floating objects known, determining whether they form the same way as stars and higher mass brown dwarfs will advance our understanding of the star-formation process. Some planemos appear to harbor accretion disks (*4*, *5*), just like stars and brown dwarfs at young ages (*6*–*8*). The existence of disks around all three classes of objects suggests that they have a common origin. Binary properties of planemos could provide a more definitive test, because some formation models predict a low binary frequency and a paucity of wide pairs at the lowest masses (*9*, *10*). Here, we report the identification of a wide binary system consisting of two planemos.

An optical *I*-band image of the young planetary-mass brown dwarf Oph 162225-240515 (hereafter Oph 1622-2405) (*5*, *11*, *12*), taken with the European Southern Observatory's (ESO's) New Technology Telescope using the ESO Multimode Instrument (EMMI), showed a candidate companion at a separation of ≤2″. Therefore, we obtained optical spectra of both objects with the Focal Reducer/low-dispersion Spectrograph-2 (FORS2) and near-infrared J_s-, H-, K_s-, and L'-band images with the Infrared Spectrometer and Array Camera (ISAAC) on ESO's Very Large Telescope UT2, under excellent seeing conditions (*13*).

The binary is well resolved in all of our imaging and spectroscopic data. It has a separation of 1.94″ ± 0.01″ (±SD) and a position angle of 182.2° ± 0.4° (table S1). At a distance of 125 pc (*11*), this corresponds to a projected separation of ≈242 astronomical units (AU). The colors of the secondary are slightly more red than those of the primary (Fig. 1), consistent with its being a somewhat cooler object. We measured a brightness difference of 1.4 ± 0.1 magnitudes (mag) between the two objects in the optical *I* band (*13*). In the near-infrared, we found J_s = 14.65 ± 0.05 (mag), H = 14.19 ± 0.05 (mag), K_s = 13.66 ± 0.06 (mag), and L' = 13.23 ± 0.05 (mag) for the primary, and J_s = 15.41 ± 0.05 (mag), H = 14.87 ± 0.05 (mag), K_s = 14.22 ± 0.06 (mag), and L' = 13.61 ± 0.06 (mag) for the secondary.

By examining a variety of features (e.g., TiO and VO absorption troughs) as well as the overall shapes of the spectra in comparison to those of cool field dwarfs (*14*), we derived best-match spectral types of M9 for the primary and M9.5-L0 for the secondary (Fig. 2) (*5*). These spectral types imply effective temperatures of 2400 and 2100 K, respectively (*15*), with an uncertainty of ±100 K. The infrared colors of the two components of the binary are also consistent with their having spectral types in the late M–early L range (*16*). Furthermore, the

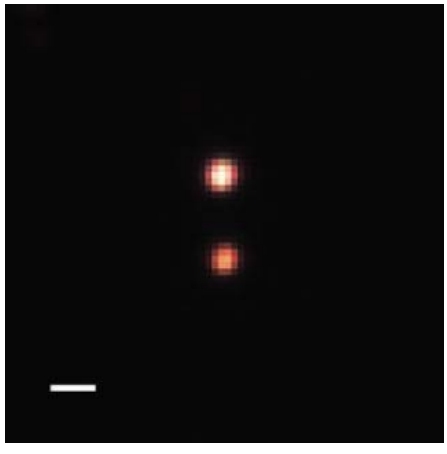

Fig. 1. A three-color J_s-H-K_s image of Oph 162225-240515AB. North is up, and East is to the left. The field of view is 10″ × 10″, and the scale bar indicates 1″. The apparent separation of the binary is 1.94″, corresponding to 242 AU at a distance of 125 pc.

[1]Department of Astronomy and Astrophysics, University of Toronto, Toronto, ON M5S 3H8, Canada. [2]European Southern Observatory, Avenida Alonso de Cordova 3107, Vitacura, Santiago 19001, Chile.

*To whom correspondence should be addressed. E-mail: rayjay@astro.utoronto.ca

flux ratios between the primary and the secondary are consistent with the difference in their spectral types, making a strong case that the two are at the same distance and thus almost certainly form a physical binary. Given that Allers *et al*. (*11*) found nine brown dwarf and planemo candidates in an area of 1700 square arc min in Oph, the likelihood of two such objects being within 2″ of each other by chance is $<2 \times 10^{-4}$, strengthening the case for physical association.

We plotted the two objects on Hertzsprung-Russell diagrams (Fig. 3). The absolute J_s, H, K_s, and L' magnitudes were derived from the apparent magnitudes, assuming a distance of 125 pc and a visual extinction $A_V = 0$ (mag) (*11*). We also show the 1-million-year-old and 5-million-year-old isochrones for very-low-mass objects from the widely used DUSTY00 evolutionary models (*17*). This comparison to models yields a mass of 13 to 15 $M_{Jupiter}$ for the primary and 7 to 8 $M_{Jupiter}$ for the secondary at an age of ≈1 million years [consistent with the age of Ophiuchus (*11*)]. Our mass estimate for the primary is slightly higher than that derived by Allers *et al*. (*11*), because we found somewhat lower J_s, H, and K_s magnitudes; ours were more consistent with those in the 2-Micron All Sky Survey (*2MASS*) catalog. The two objects indeed appear to be coeval, providing further evidence that they form a physical binary, and they have a mass ratio of ~0.5. The well-known uncertainties in the evolutionary models could affect the mass estimates, especially at the youngest ages and the lowest masses (*18*). However, regardless of their absolute masses, Oph 1622-2405AB is likely to be the lowest mass binary identified to date.

Neither component of Oph 1622-2405AB has a measurable excess at near-infrared wavelengths shorter than ≈4 μm in comparison to field M9-L0 dwarfs (*16*), consistent with the spectral energy distribution for the pair in Allers *et al*. (*11*). The system, however, does show a mid-infrared excess (at wavelengths longer than ≈6 μm), which is well modeled as thermal emission from a dusty disk in previous observations with the Spitzer Space Telescope (*11*). Given the poor angular resolution of Spitzer (≈3″ at 10 μm), it is not possible to determine whether the excess is associated with one or both planemos. We detected strong emission in the hydrogen Hα 6563 Å line, often seen in young stars and brown dwarfs, from both components (Fig. 4), possibly originating in material being accreted from the disk onto the planemo(s) (*5*). The Hα equivalent widths are 19 ± 1 and 65 ± 5 Å for the primary and the secondary, respectively. These values are well above those that are seen in quiescent-field M9-L0 dwarfs (*19*), which strongly suggests that both components of the binary are young and that neither is a foreground/background dwarf. The mid-infrared excess from the system, previously detected with Spitzer, taken together with the association with the Oph cloud and the shapes of the gravity-sensitive KI and NaI features (Fig. 2) in comparison to

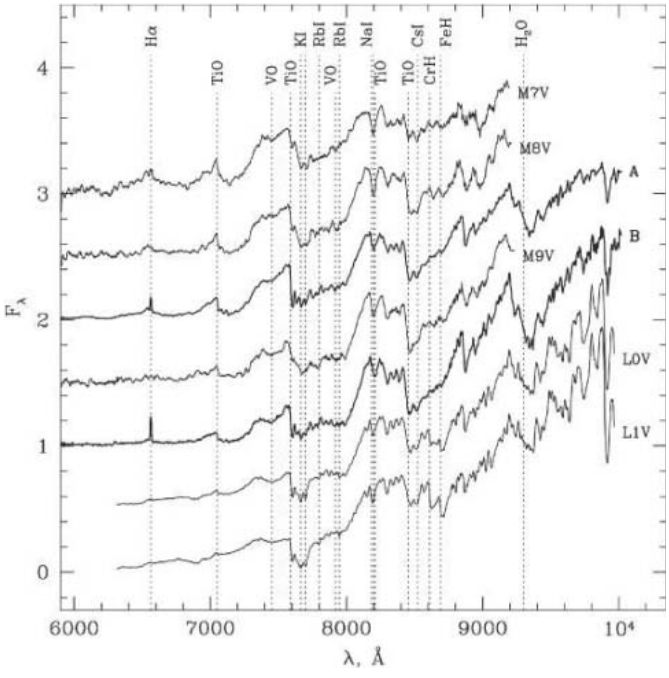

Fig. 2. Optical spectra of the primary (A) and the secondary (B) of Oph 162225-240515AB in comparison with spectra of cool field dwarfs (*16*). The spectral types and key features are marked. F_λ corresponds to flux in arbitrary units while λ refers to wavelength in Å.

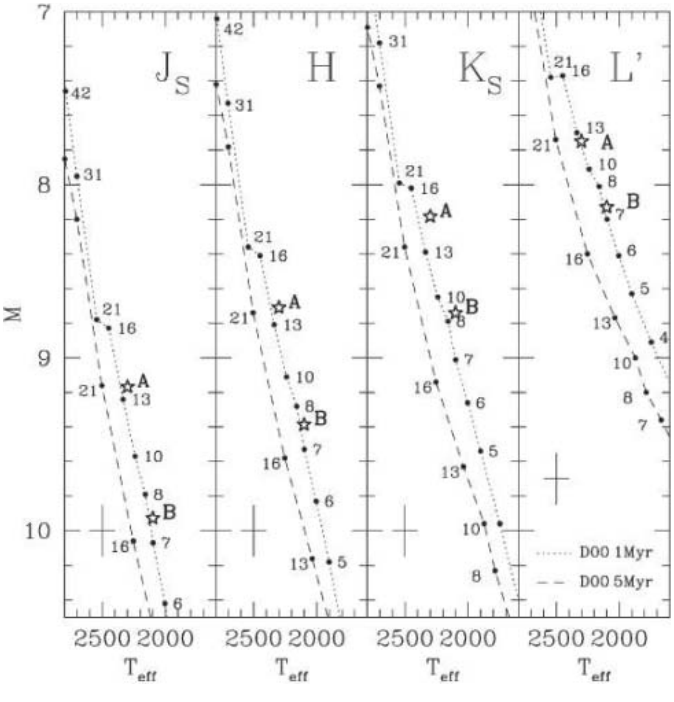

Fig. 3. The positions of Oph 162225-240515A and B (stars) on Hertzsprung-Russell diagrams. The *y* axis, *M*, corresponds to absolute magnitudes (scaled to a distance of 10 pc) in four near-infrared bands—J_s, H, K_s, and L'—derived from the apparent magnitudes, assuming a distance of 125 pc and visual extinction $A_V = 0$ (*11*). The *x* axis gives the effective temperature, T_{eff}, in kelvin. Also plotted are 1-million-year-old (dotted lines) and 5-million-year-old (dashed lines) isochrones for DUSTY00 evolutionary models (*17*). The numbers along the isochrones give masses in units of Jupiter mass. The typical error bars are shown as crosses at the bottom left corner of each panel. The *M* uncertainty combines the photometric errors with estimates of the errors in the extinctions (0.1 mag in *K*) and the distances (10%), added in quadrature. The typical error in T_{eff} is estimated to be ±100 K.

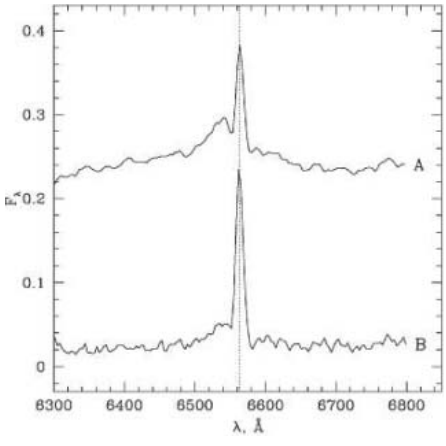

Fig. 4. Close-up of the Hα emission lines from Oph 162225-240515A and Oph 162225-240515B.

field dwarfs, strengthens the case for the youth of Oph 1622-2405AB.

There is no consensus yet on the origin of free-floating substellar objects. One possibility is that they form like higher mass stars, as a result of the turbulent fragmentation and collapse of molecular cloud cores (*20*). Another scenario, which has gained popularity in recent years, is that brown dwarfs are stellar embryos ejected from multiple protostellar systems (*9*, *10*). Recent observations have attempted to distinguish between these scenarios by comparing the physical properties of substellar objects with those of Sun-like stars. A variety of studies have shown that many young brown dwarfs and planemos exhibit infrared excesses (*4*, *6*, *7*, *11*) and spectroscopic signatures of accretion (*5*, *8*), indicative of disks. However, these diagnostics are only sensitive to the innermost portions of the disk and therefore cannot test whether brown dwarf disks are truncated, as expected in the ejection scenario, as a result of close dynamical encounters. Recently, Scholz *et al*. (*21*) found evidence for >10-AU disks among ~25% of Taurus brown dwarfs, contrary to predictions of certain ejection simulations (*10*), but the test is still somewhat indirect.

In this context, the binary properties of substellar objects could be among the most important diagnostics of their origin. In particular, ejection models predict a very low rate of binaries among brown dwarfs (<5%) and do not favor the formation of wide (>20-AU) binaries (*9*, *10*). Imaging surveys of (old) brown dwarfs in the solar neighborhood reveal that ~15% are in binaries with maximum separations of ≈20 AU (*22*, *23*). The same appears to hold true for brown dwarfs in star-forming regions and young open clusters (*24*, *25*), with a few notable exceptions (*26*–*28*). The dearth of wide binaries is consistent with ejection models, but the overall binary fraction is higher than predicted by some hydrodynamical simulations of that scenario (*10*).

Therefore, our identification of an ultra-low-mass binary with a projected separation of ≈242 AU is surprising. The high mass ratio of Oph 1622-2405AB is consistent with the bias toward approximately equal mass pairs seen in the substellar regime, but its wide separation is contrary to the general trend toward tighter binaries at the lowest masses. We propose that Oph 1622-2405AB is unlikely to have survived ejection from a multiple protostellar system because such a dynamical interaction would have torn apart a softly bound pair (*9*, *10*). Given its fragility, a future close encounter with a passing star or a brown dwarf could still disrupt this binary.

The lowest mass binary known previously is 2MASSW J1207334-393254, a young ~25 M_{Jupiter} brown dwarf with an ~8 M_{Jupiter} companion at a separation of ~55 AU (*28*). Given its high mass ratio and wide separation, several authors have argued that this pair most likely formed as a petite version of stellar binaries through cloud fragmentation, instead of the planetary companion forming by means of core accretion in a disk around the primary (*29*). The same arguments apply even more strongly to Oph 1622-2405AB, given that its mass ratio is higher and its separation is wider. This binary is analogous in some ways to 2MASS J11011926-7732383AB in Chamaeleon I with a mass ratio of 0.5 and a separation of 240 AU, although its components have higher masses of ~50 and ~25 M_{Jupiter} (*26*). Thus, a successful theory of star formation must account for wide binaries composed of brown dwarfs and even planemos. On the observational front, the key questions are whether such systems are common or rare and whether binary properties depend on the age or the environment. For example, wide binaries may be more frequent among young brown dwarfs, but more systematic surveys are needed to test this possibility.

References and Notes

1. G. Basri, *Annu. Rev. Astron. Astrophys.* **38**, 485 (2000).
2. M. R. Zapatero Osorio *et al.*, *Science* **290**, 103 (2000).
3. P. W. Lucas, P. F. Roche, *Mon. Not. R. Astron. Soc.* **314**, 858 (2000).
4. L. Testi *et al.*, *Astrophys. J.* **571**, L155 (2002).
5. R. Jayawardhana, V. D. Ivanov, *Astrophys. J.*, in press; preprint available online (http://arxiv.org/abs/astro-ph/0607152).
6. A. Natta *et al.*, *Astron. Astrophys.* **393**, 597 (2002).
7. R. Jayawardhana, D. R. Ardila, B. Stelzer, K. E. Haisch Jr., *Astron. J.* **126**, 1515 (2003).
8. R. Jayawardhana, S. Mohanty, G. Basri, *Astrophys. J.* **592**, 282 (2003).
9. B. Reipurth, C. J. Clarke, *Astron. J.* **122**, 432 (2001).
10. M. R. Bate, I. A. Bonnell, V. Bromm, *Mon. Not. R. Astron. Soc.* **332**, L65 (2002).
11. K. N. Allers, J. E. Kessler-Silacci, L. A. Cieza, D. T. Jaffe, *Astrophys. J.* **644**, 364 (2006).
12. It was pointed out to us after the *Science* Express publication that the companion was reported independently in K. N. Allers' Ph.D. thesis (*30*), but we note that it was not mentioned in the Allers *et al*. paper published subsequently in *Astrophysical Journal* (*11*).
13. Materials and methods are available as supporting material on *Science* Online.
14. The comparison spectra for field M and L dwarfs are from http://dwarfarchives.org, maintained by J. D. Kirkpatrick.
15. E. L. Martìn *et al.*, *Astron. J.* **118**, 2466 (1999).
16. S. K. Leggett *et al.*, *Astrophys. J.* **564**, 452 (2002).
17. G. Chabrier, I. Baraffe, F. Allard, P. Hauschildt, *Astrophys. J.* **542**, 464 (2000).
18. I. Baraffe, G. Chabrier, F. Allard, P. Hauschildt, *Astron. Astrophys.* **382**, 563 (2002).
19. S. Mohanty, G. Basri, *Astrophys. J.* **583**, 451 (2003).
20. P. Padoan, A. Nordlund, *Astrophys. J.* **617**, 559 (2004).
21. A. Scholz, R. Jayawardhana, K. Wood, *Astrophys. J.* **645**, 1498 (2006).
22. J. E. Gizis *et al.*, *Astron. J.* **125**, 3302 (2003).
23. H. Bouy *et al.*, *Astron. J.* **126**, 1526 (2003).
24. A. L. Kraus, R. J. White, L. A. Hillenbrand, *Astrophys. J.* **633**, 452 (2005).
25. E. L. Martìn, D. Barrado y Navascués, I. Baraffe, H. Bouy, S. Dahm, *Astrophys. J.* **594**, 525 (2003).
26. K. L. Luhman, *Astrophys. J.* **614**, 398 (2004).
27. H. Bouy *et al.*, *Astron. Astrophys.* **451**, 177 (2006).
28. G. Chauvin *et al.*, *Astron. Astrophys.* **425**, L29 (2004).
29. G. Lodato, E. Delgado-Donate, C. J. Clarke, *Mon. Not. R. Astron. Soc.* **364**, L91 (2005).
30. K. N. Allers, Ph.D. thesis, University of Texas, Austin (2005).

31. This paper is based on observations collected at the European Southern Observatory, Chile, under programs 276.C-5050 and 277.C-5012. We thank the ESO staff for carrying out the observations in service mode and making the data available to us quickly. This research was supported by a Natural Sciences and Engineering Research Council of Canada grant and University of Toronto startup funds to R.J.

Supporting Online Material

www.sciencemag.org/cgi/content/full/1132128/DC1
Materials and Methods
Table S1
References

5 July 2006; accepted 24 July 2006
Published online 3 August 2006;
10.1126/science.1132128
Include this information when citing this paper.

50-Ma Initiation of Hawaiian-Emperor Bend Records Major Change in Pacific Plate Motion

Warren D. Sharp[1]* and David A. Clague[2]

The Hawaiian-Emperor bend has played a prominent yet controversial role in deciphering past Pacific plate motions and the tempo of plate motion change. New ages for volcanoes of the central and southern Emperor chain define large changes in volcanic migration rate with little associated change in the chain's trend, which suggests that the bend did not form by slowing of the Hawaiian hot spot. Initiation of the bend near Kimmei seamount about 50 million years ago (MA) was coincident with realignment of Pacific spreading centers and early magmatism in western Pacific arcs, consistent with formation of the bend by changed Pacific plate motion.

The Hawaiian-Emperor chain consists of at least 129 volcanoes and stretches for more than 6000 km across the northern Pacific basin. The Hawaiian chain is the archetypal example of a hot spot track formed as the Pacific plate moved over a mantle magma source (*1*). One of the most distinctive features of the chain is the Hawaiian-Emperor bend (HEB) (Fig. 1), which has been widely interpreted to indicate a major change in the direction of Pacific plate motion based on a fixed–hot spot frame of reference (*2*). Features

expected to accompany such a shift in Pacific plate motion are lacking at 43 million years ago (Ma) (*3*), the previously accepted age of the HEB (*4*). Paleomagnetic observations show that the Hawaiian hot spot moved rapidly southward during formation of the Emperor chain and may have become nearly fixed thereafter (*5*, *6*). It has therefore been suggested that the HEB primarily reflects cessation of rapid hot spot motion rather than changed Pacific plate motion (*3*, *5*). Nonetheless, both hot spot motion and changed Pacific plate motion at the HEB are indicated by analysis of global plate circuits (*7*). We present new ages for Hawaiian-Emperor seamounts, suggest a revised position for bend initiation, and develop their implications for the origin of the HEB.

An extensive body of radioisotopic ages was developed for the islands and seamounts of the Hawaiian-Emperor chain during systematic dating campaigns in the 1960s to 1980s (*4*, *8*). These ages confirmed an important prediction of the hot spot hypothesis, showing that the volcanoes of the chain become progressively older with distance from the currently active hot spot under Hawaii. However, the early ages include many conventional K-Ar and $^{40}Ar/^{39}Ar$ total fusion analyses on whole rocks that lack internal reliability criteria, making their accuracy difficult to assess. Continuing improvements in $^{40}Ar/^{39}Ar$ extraction line-mass spectrometer systems and analytical protocols have reduced sample size requirements and increased reliability and precision. We have dated individual dredged pebbles and small pieces of drill core by the $^{40}Ar/^{39}Ar$ method via broad-beam laser incremental heating applied to plagioclase, anorthoclase, and amphibole. Even in cases where whole rocks are moderately to highly altered, the feldspars and amphiboles separated from them typically have little or no alteration (*4*); thus, the new dates provide reliable ages where, in some cases, none have previously been available (*9*).

The sample collection that we have drawn upon has been accumulated over many years and includes dredged samples from seven cruises (*9*) and core from Ocean Drilling Program Leg 55. To date former locations of the hot spot as closely as possible, we have analyzed samples that can be assigned on the basis of their chemical compositions, mineralogy, and mineral chemistry to distinctive stages in the development of Hawaiian-Emperor volcanoes (*4*). We report new $^{40}Ar/^{39}Ar$ ages for eight eruptive centers that have been measured on shield or postshield lavas with a single exception (Table 1). On the basis of geologic studies and modeling of volcanoes in the Hawaiian Islands, such lavas erupt while a volcano traverses the hot spot in ~1 million years (My) (*10*). The duration of shield and postshield magmatism may be greater than in the Hawaiian Islands at volcanoes formed in segments of the seamount chain characterized by slower plate–hot spot motion (e.g., the HEB) or more widely spaced volcanoes (e.g., the central Emperor chain). We therefore conservatively estimate that shield and postshield lavas were erupted at each volcano for up to 2 My. We assume that dredging or deep-sea drilling has accessed lavas only from the younger half of this interval. Accordingly, we assign a geological uncertainty of 1 My to shield and postshield lavas to reflect that they formed somewhat after passage over the hot spot's center. This geological uncertainty is asymmetric (occurring only on the older side of the measured age), is larger than the $^{40}Ar/^{39}Ar$ measurement errors, and was com-

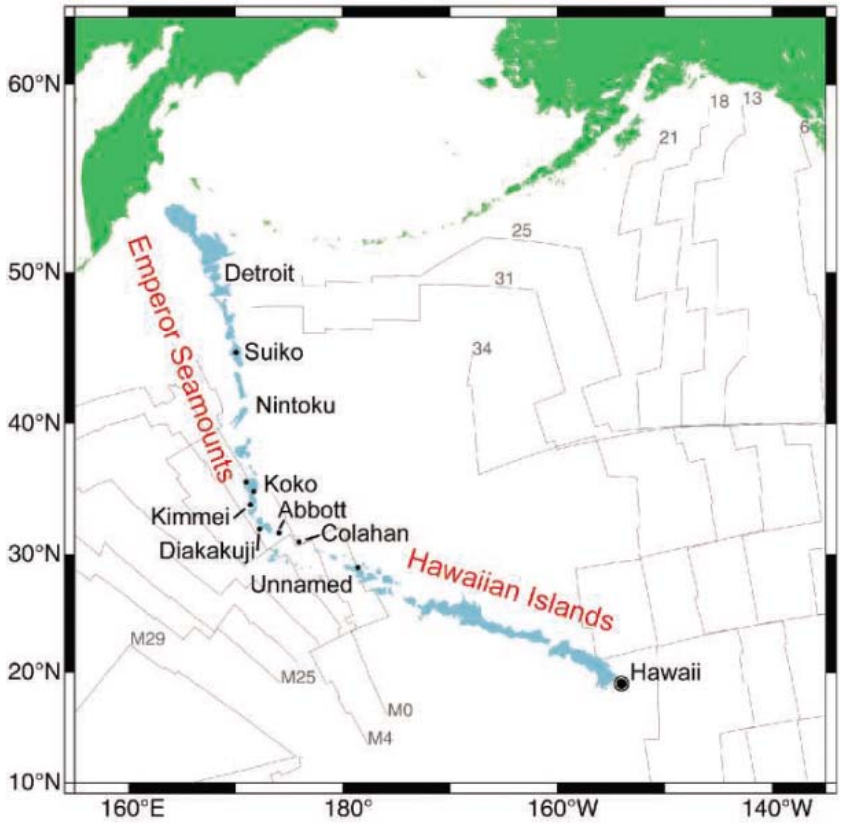

Fig. 1. Map of the northwestern Pacific basin. Seamounts and islands of Hawaiian-Emperor chain are shown in blue. Small circles show locations of samples dated in this study. Gray lines show seafloor magnetic anomalies labeled with chrons of the geomagnetic polarity time scale.

Table 1. Summary of weighted mean $^{40}Ar/^{39}Ar$ ages for Hawaiian-Emperor seamounts. *n* = number of reliable ages obtained for each eruptive center; stage refers to stage of volcanism dated by analogy with volcanoes of the Hawaiian Islands (*4*); distance is measured along the chain from Kilauea (*4*). Ages were calculated using an age of 28.02 Ma for the Fish Canyon sanidine standard; decay constants, isotopic abundances, and criteria for reliable ages are given in (*9*).

Seamount	Age ± 2σ (Ma)	*n*	Stage	Distance from Kilauea (km)
Suiko	60.9 ± 0.3	3	Shield and postshield	4860
Koko (north)	52.6 ± 0.8	1	Shield	3812
Koko (south)	50.4 ± 0.1	5	Postshield	3758
Kimmei	47.9 ± 0.2	1	Postshield	3668
Diakakuji	46.7 ± 0.1	3	Shield	3493
Abbott	41.5 ± 0.3	1	Shield	3280
Colahan	38.7 ± 0.2	4	Rejuvenated	3128
Unnamed	31.0 ± 0.2	1	Postshield	2600

[1]Berkeley Geochronology Center, 2455 Ridge Road, Berkeley, CA 94709, USA. [2]Monterey Bay Aquarium Research Institute, 7700 Sandholdt Road, Moss Landing, CA 95039, USA.

*To whom correspondence should be addressed. E-mail: wsharp@bgc.org

bined quadratically with measurement errors to give total uncertainties (table S1). The single rejuvenated-stage lava we have dated is readily distinguished from shield and postshield lavas (*4*) and has been assigned a geological uncertainty of 5 My.

Our new ages for Hawaiian-Emperor volcanoes plotted as a function of distance from the active Hawaiian hot spot at Kilauea further confirm a monotonic increase in age along the chain, although rates of migration of the volcanism vary considerably (Fig. 2). Such a monotonic age progression distinguishes the Hawaiian-Emperor chain from some other Pacific seamount chains such as the Line Islands and Gilbert Ridge, which have more complex age patterns and may have formed in response to local lithospheric extension (*11*, *12*). Mean volcanic migration rates increased along the Emperor seamounts from Detroit to Koko, slowed markedly north of the HEB, and remained slow and relatively uniform through the HEB and beyond. Rates in the southern Emperors greatly exceed the hot spot's mean southward motion from Detroit to Koko determined from paleomagnetic inclination changes (4.3 ± 2.3 to 5.8 ± 1.9 cm/year) (*6*, *13*). Accelerating motion of the Pacific plate, the hot spot, or both are required in the central Emperor chain, followed by slowing of the same at or before Koko. That these highly variable motions are not associated with deviations in the trend of the Emperor chain indicates that Pacific plate and hot spot motions must have been directed essentially along the trend of the chain. If so, the HEB cannot have been produced, as previously suggested (*3*, *5*), by slowing of the hot spot. Furthermore, if the HEB reflects primarily slower southward motion of the hot spot, the rate of volcanic migration should have slowed through the HEB as hot spot motion diminished. Contrary to this prediction, volcanic migration through the HEB is approximately constant within the limits of our data (Fig. 2). The alternative hypothesis—that the HEB formed primarily by Pacific plate motion change—is examined below in light of our new ages.

The age of the HEB is critical to assessing its relation to other events on and around the Pacific plate. An age of 43 Ma for the HEB (*4*, *14*) has long been accepted; however, our new $^{40}Ar/^{39}Ar$ dates indicate older ages for HEB volcanoes. Moreover, the new ages reveal that the HEB formed over a period of several million years; thus, the HEB's age is critically dependent on which part of it is considered. The 43 Ma date for the HEB was determined for its geometric apex near Diakakuji seamount. Initiation of the HEB occurred north of Diakakuji, near Kimmei seamount, where the chain's trend rotates from nearly due south to southeasterly (*4*). Postshield alkalic basalt from Kimmei seamount yields an age of 47.9 ± 0.2 Ma, providing a minimum age for HEB initiation. An age of 50.0 ± 0.9 Ma, our preferred estimate for HEB initiation, is obtained by interpolating Kimmei's shield formation age from dated shield-stage lavas at adjacent seamounts (e.g., Koko's northern eruptive center, Diakakuji, and Abbott seamounts) (Fig. 2).

HEB initiation at 50 Ma coincided with a major reorganization of northern Pacific spreading centers between seafloor magnetic anomalies 22 and 24 (*15*), corresponding to 49 to 53 Ma on the geomagnetic polarity time scale (*16*). Initiation of magmatism in the Izu-Bonin-Mariana (IBM) arc systems that extend for 2200 km along the western edge of the Pacific plate was likely marked by eruption of compositionally and mineralogically distinctive volcanic rocks with ages as old as 50 Ma (*9*, *17*, *18*). Geologic relations (*19*, *20*) and dynamic models (*21*, *22*) of IBM subduction initiation show that the IBM arcs likely originated by nucleation of subduction along northerly trending fracture or transform zones. This relation implies that a major shift in Pacific plate motion was associated with IBM initiation. If so, Pacific plate motion would have become more westerly upon development of self-sustaining subduction along the IBM arc system, consistent with the Hawaiian-Emperor track after the HEB (*23*). Reorganization of Pacific spreading centers and reconfiguration of western Pacific plate margins are expected features of a major shift in Pacific plate motion (*3*, *15*) but have previously been considered older than the HEB. Coincident inception of the HEB at 50 Ma therefore supports a causal link among onset of subduction beneath the IBM arc, reorganized spreading, Pacific plate motion change, and formation of the HEB.

Formation of the HEB by a change in Pacific plate motion has previously been considered too rapid to be caused by buoyancy forces generated from mantle convection (*24*, *25*), manifested primarily as slab pull (*23*). Until now, however, the time scale of HEB formation has not been well resolved. The new dates for HEB volcanoes show that formation of the HEB lasted for >8 My—that is, from HEB initiation (50.0 ± 0.9 Ma) to eruption of shield lavas at Abbott seamount near the HEB's terminus (41.5 ± 0.3 Ma). HEB formation, and by inference associated Pacific plate motion change, was therefore considerably slower than previously appreciated, making it compatible with evolution of plate buoyancy forces, particularly pull from negative slab buoyancy expected to develop in the first few million years after initiation of IBM subduction (*22*). Early Eocene initiation of the >2600-km Tonga-Kermadec arc in the southwestern Pacific may also have contributed to redirection of Pacific plate motion (*26*). In sum, the geometry, age, and tempo of formation of the HEB are broadly consistent with those expected from changes in Pacific plate motion induced by the onset of self-sustaining sub-

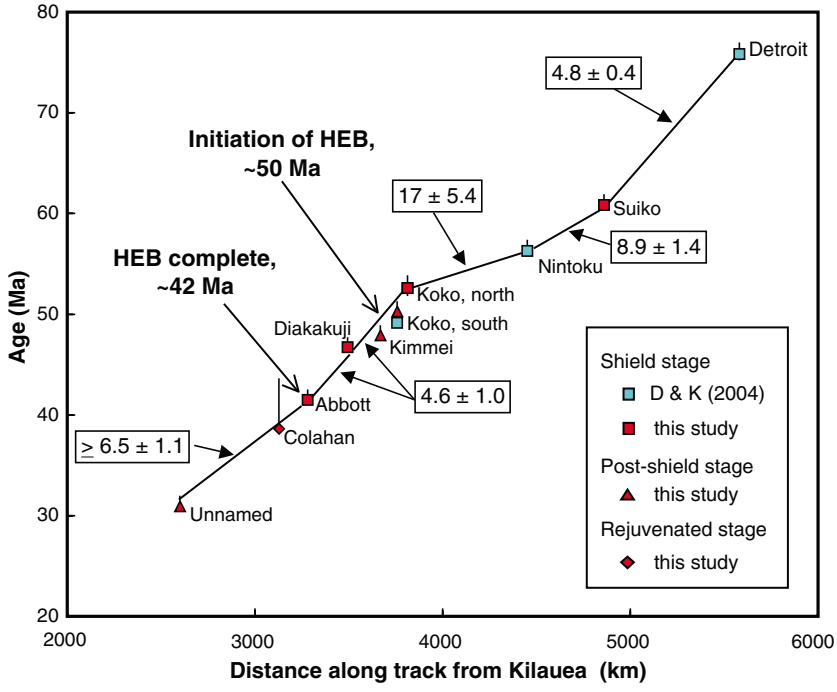

Fig. 2. $^{40}Ar/^{39}Ar$ ages of Hawaiian-Emperor volcanoes plotted against distance along the chain from the modern hot spot at Kilauea volcano. Age errors shown include geological uncertainties, as discussed in the text and (*9*). Boxed values are volcanic migration rates for respective segments of the Hawaiian-Emperor chain in cm/year. Previously published ages (blue symbols) are from Duncan and Keller (*29*).

duction in early Eocene nascent arcs of the western Pacific.

A key remaining question concerns the cause of forced convergence that modeling indicates was needed to kick-start IBM subduction (*21*). The straight track of the Hawaiian-Emperor chain from Suiko (60.9 ± 0.3 Ma) to Koko's southern summit (50.4 ± 0.1 Ma) does not record changes in the direction of Pacific plate motion; therefore, motion change in the Eurasian or Australian plates adjoining to the west may be indicated. Possible triggers for such change are the lockup of the India-Eurasia collision zone (*4*, *27*), which is approximately dated by the onset of major crustal shortening in that region at ~50 Ma (*28*), and rifting of Australia from Antarctica, leading to convergence between the Australian and Pacific plates (*23*).

References and Notes

1. J. T. Wilson, *Can. J. Phys.* **41**, 863 (1963).
2. W. J. Morgan, *Nature* **230**, 42 (1971).
3. I. O. Norton, *Tectonics* **14**, 1080 (1995).
4. D. A. Clague, G. B. Dalrymple, *U.S. Geol. Surv. Prof. Pap. 1350*, 5 (1987).
5. J. A. Tarduno, R. D. Cottrell, *Earth Planet. Sci. Lett.* **153**, 171 (1997).
6. J. A. Tarduno *et al.*, *Science* **301**, 1064 (2003); published online 24 July 2003 (10.1126/science.1086442).
7. B. Steinberger, R. Sutherland, R. J. O'Connell, *Nature* **430**, 167 (2004).
8. I. McDougall, *Bull. Geol. Soc. Am.* **75**, 107 (1964).
9. See supporting material on *Science* Online.
10. D. J. DePaolo, E. M. Stolper, *J. Geophys. Res.* **101**, 11643 (1996).
11. A. S. Davis, L. B. Gray, D. A. Clague, J. R. Hein, *Geochem. Geophys. Geosyst.* **3**, 10.1029/2001GC000190 (2002).
12. A. A. P. Koppers, H. Staudigel, *Science* **307**, 904 (2005).
13. P. V. Doubrovine, J. A. Tarduno, *Geochem. Geophys. Geosyst.* **5**, Q11L04 (2004).
14. G. B. Dalrymple, D. A. Clague, *Earth Planet. Sci. Lett.* **31**, 313 (1976).
15. T. M. Atwater, in *The Geology of North America, The Eastern Pacific Ocean and Hawaii*, E. Winterer *et al.*, Eds. (Geological Society of America, Boulder, CO, 1989), vol. N, pp. 21–72.
16. S. C. Cande, D. V. Kent, *J. Geophys. Res.* **97**, 13917 (1995).
17. M. A. Cosca, R. J. Arculus, J. A. Pierce, J. G. Mitchell, *Island Arc* **7**, 579 (1998).
18. J. A. Pearce *et al.*, in *Proceedings of the Ocean Drilling Program, Scientific Results*, P. Fryer *et al.*, Eds. (Ocean Drilling Program, College Station, TX, 1992), vol. 125, pp. 623–659.
19. T. W. C. Hilde, S. Uyeda, L. Kroenke, *Tectonophysics* **38**, 145 (1977).
20. R. J. Stern, S. H. Bloomer, *Geol. Soc. Am. Bull.* **104**, 1621 (1992).
21. C. E. Hall, M. Gurnis, M. Sdrolias, L. L. Lavier, R. D. Muller, *Earth Planet. Sci. Lett.* **212**, 15 (2003).
22. M. Gurnis, C. Hall, L. Lavier, *Geochem. Geophys. Geosyst.* **5**, Q07001 (2004).
23. R. G. Gordon, A. Cox, C. E. Harter, *Nature* **274**, 752 (1978).
24. M. A. Richards, C. Lithgow-Bertonelli, *Earth Planet. Sci. Lett.* **137**, 19 (1996).
25. D. Bercovici, *Earth Planet. Sci. Lett.* **205**, 107 (2003).
26. S. H. Bloomer *et al.*, in *Active Margins and Marginal Basins of the Western Pacific*, B. Taylor, J. Natland, Eds. (American Geophysical Union, Washington, DC, 1995), pp. 1–30.
27. P. Patriat, J. Ardache, *Nature* **3111**, 615 (1984).
28. A. Yin, T. M. Harrison, *Annu. Rev. Earth Planet. Sci.* **28**, 211 (2000).
29. R. A. Duncan, R. A. Keller, *Geochem. Geophys. Geosyst.* **5**, Q08L03 (2004).

30. Supported by NSF grant OCE-9911292. We thank T. Atwater, R. Duncan, M. Feinman, M. Richards, and J. Tarduno for discussions.

Supporting Online Material

www.sciencemag.org/cgi/content/full/313/5791/1281/DC1
Materials and Methods
Figs. S1 to S7
Tables S1 to S3
References

7 April 2006; accepted 26 June 2006
10.1126/science.1128489

Corridors Increase Plant Species Richness at Large Scales

Ellen I. Damschen,[1]*†‡ Nick M. Haddad,[1] John L. Orrock,[2]†‡ Joshua J. Tewksbury,[3] Douglas J. Levey[4]

Habitat fragmentation is one of the largest threats to biodiversity. Landscape corridors, which are hypothesized to reduce the negative consequences of fragmentation, have become common features of ecological management plans worldwide. Despite their popularity, there is little evidence documenting the effectiveness of corridors in preserving biodiversity at large scales. Using a large-scale replicated experiment, we showed that habitat patches connected by corridors retain more native plant species than do isolated patches, that this difference increases over time, and that corridors do not promote invasion by exotic species. Our results support the use of corridors in biodiversity conservation.

Loss of biological diversity is a leading threat to the sustainability of the biosphere (*1*) and is largely caused by habitat loss and fragmentation (*2*). Landscape corridors (strips of habitat connecting otherwise isolated habitat patches) are hypothesized to reduce the negative effects of fragmentation by facilitating gene flow and the movement of organisms, thereby preventing local extinctions and increasing species diversity (*3*). Corridors have become a central feature of ecological management plans worldwide, but evidence of their effectiveness has lagged behind the push for their implementation (*4*).

Although a number of experimental studies have demonstrated positive corridor effects on single species (*5*–*7*), few have examined corridor effects on entire communities. All of these studies were conducted at very small spatial scales (10 cm^2 to 10 m^2), and taken together they have yielded equivocal results (*8*–*11*).

We examined the long-term effect of corridors on plant species diversity by studying six ~50-ha experimental landscapes at the Savannah River Site in South Carolina, containing both isolated and connected habitat patches (Fig. 1A). Each landscape consisted of a central patch measuring 100 m by 100 m, four surrounding patches 150 m away, and a buffer area extending >150 m from these surrounding patches' furthest edges (Fig. 1A). One of the four surrounding patches was connected to the central patch by a corridor 150 m by 25 m (the "connected" patch). The other three surrounding patches were equal in area to the connected patch plus its corridor, but were unconnected. These unconnected patches were of two types: winged and rectangular. Rectangular patches were 100 m by 137.5 m; the additional 37.5 m relative to the 100-m–by–100-m central patch controlled for the increased area provided by the connected patch's corridor. Winged patches were 100 m by 100 m, with two 25-m–by–75-m projections off of opposite patch sides to control for the area of the connected patch's corridor and to allow examination of the elongation in patch shape associated with corridors. Winged and connected patches had equal edge-to-area ratios. Patch and corridor dimensions were chosen because they are within the range of typical U.S. Forest Service (USFS) management activities. Further explanation of the experimental design is provided elsewhere and in the supporting online material (*6*, *12*).

All plant species were surveyed in each patch from 2000 to 2005, except in 2004, when patches were burned by the USFS as part of restoration management (*12*). Our patches were open habitats with young longleaf pines

[1]Department of Zoology, North Carolina State University, Raleigh, NC 27695–7617, USA. [2]Department of Ecology, Evolution, and Organismal Biology, Iowa State University, Ames, IA 50010, USA. [3]Department of Biology, Box 351800, University of Washington, Seattle, WA 98195–1800, USA. [4]Department of Zoology, Post Office Box 118525, University of Florida, Gainesville, FL 32611–8525, USA.

*To whom correspondence should be addressed. E-mail: damschen@nceas.ucsb.edu
†Present address: National Center for Ecological Analysis and Synthesis, 735 State Street, Suite 300, Santa Barbara, CA 93101, USA.
‡Present address: Department of Biology, Box 1137, Washington University, St. Louis, MO 63130, USA.

(*Pinus palustris*) surrounded by dense pine plantations. There was a sharp contrast between the patch habitat, which had a rich herbaceous understory, and the surrounding pine plantation matrix, which was relatively depauperate. Longleaf pine forests historically dominated this region, covering >37 million ha (Fig. 1B) (*13*). Over 97% of these forests have been lost to agriculture, pine plantations, and the interruption of historical fire regimes (*13*, *14*). Native longleaf pine forests are characterized by an open, productive, and diverse understory, with a sparse canopy overhead (*13*, *14*). They are maintained by frequent low-intensity fires (*13*, *14*). Many species native to longleaf pine forests persisted inside our patch openings but were absent from the surrounding pine plantation matrix.

We detected no difference in the number of plant species in connected and unconnected patches immediately after the creation of our experimental landscapes (Fig. 2A). Over time, connected patches became more species-rich, containing 20% more plant species than unconnected patches by the end of the study (Fig. 2, A and B).

Our experimental design allowed us to link the beneficial effects of corridors on species richness directly to the connectivity provided by corridors. Specifically, it allowed us to reject four alternative hypotheses about what generated the higher species richness in connected patches. First, higher species richness was not caused by increased patch area or elongation, because connected patches had greater numbers of species than did unconnected patches (rectangular or winged) of equal area or equal patch elongation (winged patches). These results did not change when we removed species found in the corridor, wings, or the extra area of the rectangle and compared only the central areas (100 m by

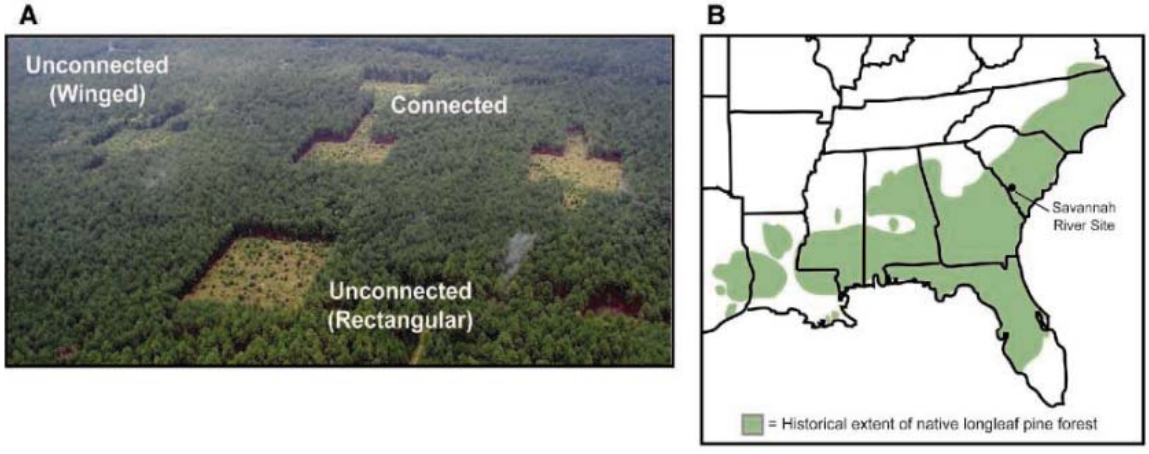

Fig. 1. (**A**) One of the six experimental study sites at the Savannah River Site, South Carolina, USA. Patches are connected or unconnected by a corridor. Unconnected patches are either rectangular or winged. (**B**) The location of the Savannah River Site relative to the historical distribution of native longleaf pine forest [after Outcalt and Sheffield (*25*)].

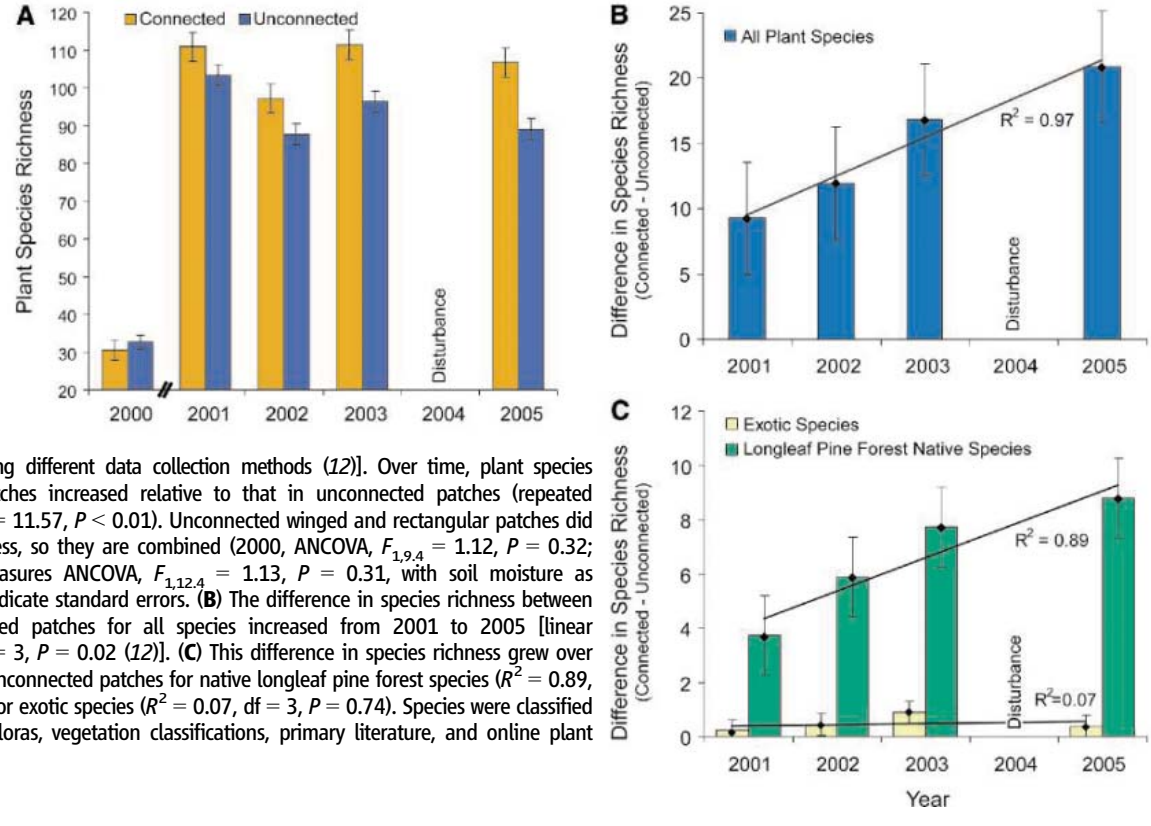

Fig. 2. (**A**) Plant species richness over time. In 2000, the first growing season after site creation, plant species richness did not differ between connected and unconnected patches (ANCOVA, $F_{1,9.4} = 0.36$, $P = 0.56$), indicating that subsequent changes were due to the experimental manipulation [species richness in 2000 is not directly comparable to 2001–2005, indicated with breaks on the *x* axis, because estimates were obtained using different data collection methods (*12*)]. Over time, plant species richness in connected patches increased relative to that in unconnected patches (repeated measures ANCOVA, $F_{1,12.5} = 11.57$, $P < 0.01$). Unconnected winged and rectangular patches did not differ in species richness, so they are combined (2000, ANCOVA, $F_{1,9.4} = 1.12$, $P = 0.32$; 2000–2005, repeated measures ANCOVA, $F_{1,12.4} = 1.13$, $P = 0.31$, with soil moisture as covariate). All error bars indicate standard errors. (**B**) The difference in species richness between connected and unconnected patches for all species increased from 2001 to 2005 [linear regression, $R^2 = 0.97$, df = 3, $P = 0.02$ (*12*)]. (**C**) This difference in species richness grew over time in connected versus unconnected patches for native longleaf pine forest species ($R^2 = 0.89$, df = 3, $P = 0.05$) but not for exotic species ($R^2 = 0.07$, df = 3, $P = 0.74$). Species were classified with the use of regional floras, vegetation classifications, primary literature, and online plant databases (*12*).

100 m) of each patch [analysis of covariance (ANCOVA), $F_{1,13.3} = 10.66$, $P < 0.01$ (*12*) (fig. S1 and table S1)], confirming that the area of the corridor was not driving the pattern.

Second, the increased species richness in connected patches was not generated by differences in patch shape that are independent of connectivity (such as variation in the proportion of edge, altering within-patch heterogeneity). Permanent vegetation plots distributed across all parts of all patches (fig. S1) did not differ in species richness (repeated measures ANCOVA, $F_{6,21.6} = 0.64$, $P = 0.70$) or evenness (repeated measures ANCOVA, $F_{6,34.5} = 1.32$, $P = 0.28$, table S2), and the degree of similarity among plots was not affected by patch shape [multi-variate analysis of variance (MANOVA), Pillai's trace, $F_{6,28} = 0.81$, $P = 0.57$, Bray-Curtis distance; MANOVA, Pillai's trace, $F_{6,28} = 1.14$, $P = 0.37$, Sorenson distance (*12*)].

Third, inputs to the plant community from the soil seed bank cannot account for increased plant species richness in connected patches. The plant community arising from the seed bank after the sites were created in 2000 was unaffected by corridors (Fig. 2A and table S1). Additionally, 3 years later, the number of species of seeds emerging from over 12,000 soil cores collected from 960 plots where plant communities were measured remained unaffected by corridors [ANCOVA, $F_{2,16.4} = 0.72$, $P = 0.50$ (*12*)]. This suggests that species in the seed bank were not limited by dispersal, were unaffected by corridors, and were not responsible for the increase in species richness we observed.

Fourth, local differences in soil moisture, an important driver of plant species richness in longleaf pine forests (*15*), were not responsible for the increased species richness in connected patches. Soil moisture was often a predictor of species richness in analyses, but after controlling for these within-patch differences, connectivity effects remained (*12*).

Corridor effects were apparent across the 5 years of our study despite environmental variation in successional stages, annual precipitation, and disturbance events. The influences of these other effects were apparent in the annual fluctuations in species richness across both connected and unconnected patches (Fig. 2A). For example, unusually high rainfall at the study area in 2003 [35% higher than the mean from 2000 to 2005 and 57% higher than in the previous year (2002)] and the prescribed burn in 2004 are plausible explanations for the increased species richness in 2003 and 2005, respectively. Our study shows that despite other factors that influence the number of plant species in any given year, a consistent effect of connectivity emerges.

Corridors are often championed as tools to help preserve species of conservation concern, largely on the basis of the untested assumption that increased connectivity benefits native species more than it benefits common "weedy," exotic, or invasive species. Our results support this assumption. Our experimental sites harbored many species that are native to longleaf pine forests (*16*, *17*), including 29 species of locally rare or uncommon flowering herbs and grasses that are a part of restoration efforts by the USFS (*17*). The species richness (repeated measures ANCOVA, $F_{1,11} = 6.62$, $P = 0.03$, Fig. 2C) and abundance (repeated measures ANCOVA, $F_{1,9.3} = 6.12$, $P = 0.04$, table S3) of these native species increased over time in connected versus unconnected patches.

Conversely, one of the major and untested concerns about using corridors is that they will increase the spread of exotic species (*18*, *19*). In our experiment, corridors had no detectable effect on the number of exotic species [repeated measures ANCOVA, $F_{1,23.5} = 2.32$, $P = 0.14$; our definition of exotic species included invasive exotics (*12*) (Fig. 2C and table S4)]. Corridors similarly did not affect the abundance (repeated measures ANCOVA, $F_{1,9.1} = 0.76$, $P = 0.41$) or proportion (repeated measures ANCOVA, $F_{1,14.8} = 0.15$, $P = 0.70$, table S4) of exotic species in the total species pool. In addition, native early-successional weeds that are not associated with historical longleaf pine forests were also not responsible for the increase in species richness we observed. Our results did not change when these species were removed (repeated measures ANCOVA, connectivity, $F_{1,11.9} = 9.36$, $P = 0.01$, table S3).

The most parsimonious explanation for the increased plant species richness we observed in connected patches is that corridors alter the balance among three important processes and interactions in ways that promote diversity. Corridors promote colonization by increasing seed deposition (*6*, *20*), promote within-patch recruitment by increasing pollen movement (*6*, *21*), and alter foraging by seed predators that could benefit species otherwise more likely to be excluded by seedling competition (*22*–*24*). Although individual plant species and their interactions will differ in their response to corridors, the results reported here show that across ~300 plant species and their countless interactions, connecting patches with corridors leads to a positive net effect on native plant species richness. By providing experimental evidence that corridors increase the number of native plant species in large-scale communities over a wide range of environmental conditions, we show that corridors are not simply an intuitive conservation paradigm; they are a practical tool for preserving biodiversity.

References and Notes

1. A. Balmford, W. Bond, *Ecol. Let.* **8**, 1218 (2005).
2. D. S. Wilcove, D. Rothstein, J. Dubow, A. Phillips, E. Losos, *Bioscience* **48**, 607 (1998).
3. E. O. Wilson, E. O. Willis, in *Ecology and Evolution of Communities*, M. L. Cody, J. M. Diamond, Eds. (Belknap Press, Cambridge, MA, 1975).
4. D. Simberloff, J. A. Farr, J. Cox, D. W. Mehlman, *Conserv. Biol.* **6**, 493 (1992).
5. P. Beier, R. F. Noss, *Conserv. Biol.* **12**, 1241 (1998).
6. J. J. Tewksbury *et al.*, *Proc. Natl. Acad. Sci. U.S.A.* **99**, 12923 (2002).
7. N. M. Haddad *et al.*, *Ecology* **84**, 609 (2003).
8. S. K. Collinge, *Ecology* **81**, 2211 (2000).
9. F. Gilbert, A. Gonzalez, I. Evans-Freke, *Proc. R. Soc. London Ser. B* **265**, 577 (1998).
10. A. Gonzalez, J. H. Lawton, F. S. Gilbert, T. M. Blackburn, I. Evans-Freke, *Science* **281**, 2045 (1998).
11. M. Hoyle, F. Gilbert, *Oikos* **105**, 359 (2004).
12. Materials and methods and supporting material are available on *Science* Online.
13. D. G. Brockway, K. W. Outcalt, *For. Ecol. Manage.* **106**, 125 (1998).
14. D. H. VanLear, W. D. Carroll, P. R. Kapeluck, R. Johnson, *For. Ecol. Manage.* **211**, 150 (2005).
15. L. K. Kirkman, R. J. Mitchell, R. C. Helton, M. B. Drew, *Am. J. Bot.* **88**, 2119 (2001).
16. C. C. Frost, paper presented at the Tall Timbers Fire Ecology Conference, Tall Timbers Research Station, Tallahassee, FL, 1993 (paper no. 18).
17. J. C. Kilgo, J. I. Blake, Eds., *Ecology and Management of a Forested Landscape* (Island Press, Washington, DC, 2005), pp. 99–102.
18. S. Proches *et al.*, *Science* **310**, 779 (2005).
19. D. Simberloff, J. A. Farr, J. Cox, D. W. Mehlman, *Conserv. Biol.* **6**, 493 (1992).
20. D. J. Levey, B. M. Bolker, J. J. Tewksbury, S. Sargent, N. M. Haddad, *Science* **309**, 146 (2005).
21. P. A. Townsend, D. J. Levey, *Ecology* **86**, 466 (2005).
22. J. L. Orrock, B. J. Danielson, M. J. Burns, D. J. Levey, *Ecology* **84**, 2589 (2003).
23. J. L. Orrock, E. I. Damschen, *Ecol. Appl.* **15**, 793 (2005).
24. J. L. Orrock, D. J. Levey, B. J. Danielson, E. I. Damschen, *J. Ecol.* **94**, 838 (2006).
25. K. W. Outcalt, R. M. Sheffield, *The Longleaf Pine Forest: Trends and Current Conditions* (U.S. Department of Agriculture Forest Service, Southern Research Station, Asheville, NC, 1998).

26. Funding was provided by NSF (grants DEB 9815834 and 9907365) and the USFS, Savannah River (a National Environmental Research Park), under Interagency Agreement DE-AI09-00SR22188 with the U.S. Department of Energy. We thank J. Blake, E. Olson, C. Hobson, D. Imm, J. Segar, and other members of the USFS who provided critical assistance in the experimental landscape construction and maintenance; and B. Danielson, S. Sargent, K. Rosenfeld, T. Wentworth, J. Stucky, A. Krings, F. Gould, and field technicians for their contributions to this project. This work was also supported by an NSF Biological Informatics Postdoctoral Fellowship (DIB 0532935) to E.I.D. This work was conducted while E.I.D. was a Center Associate and J.L.O. was a postdoctoral fellow at the National Center for Ecological Analysis and Synthesis, a center funded by NSF (DEB 0072909), the University of California, and the Santa Barbara campus of the University of California.

Supporting Online Material

www.sciencemag.org/cgi/content/full/313/5791/1284/DC1
Materials and Methods
Fig. S1
Tables S1 to S5
References

17 May 2006; accepted 4 July 2006
10.1126/science.1130098

Manipulation of Host Hepatocytes by the Malaria Parasite for Delivery into Liver Sinusoids

Angelika Sturm,[1]* Rogerio Amino,[2,3]* Claudia van de Sand,[1] Tommy Regen,[1] Silke Retzlaff,[1] Annika Rennenberg,[1] Andreas Krueger,[1] Jörg-Matthias Pollok,[4] Robert Menard,[2] Volker T. Heussler[1]†

The merozoite stage of the malaria parasite that infects erythrocytes and causes the symptoms of the disease is initially formed inside host hepatocytes. However, the mechanism by which hepatic merozoites reach blood vessels (sinusoids) in the liver and escape the host immune system before invading erythrocytes remains unknown. Here, we show that parasites induce the death and the detachment of their host hepatocytes, followed by the budding of parasite-filled vesicles (merosomes) into the sinusoid lumen. Parasites simultaneously inhibit the exposure of phosphatidylserine on the outer leaflet of host plasma membranes, which act as "eat me" signals to phagocytes. Thus, the hepatocyte-derived merosomes appear to ensure both the migration of parasites into the bloodstream and their protection from host immunity.

Infection of a mammalian host by the malaria parasite starts when the sporozoite stage delivered by the mosquito reaches the liver and invades hepatocytes (*1*, *2*). The intracellular sporozoite then differentiates and generates a new invasive and motile form, called the merozoite, which invades erythrocytes. To gain access to erythrocytes, the hepatic merozoite must reach the lumen of the liver sinusoids from hepatocytes through the space of Disse, a layer of extracellular matrix, and the sinusoid endothelium. It is not known how hepatic merozoites reach the blood and avoid phagocytosis by the numerous resident macrophages, called Kupffer cells, which patrol the liver sinusoids.

To address this issue, we first analyzed the terminal phase of parasite development inside hepatocytes in vitro. The complete development of *Plasmodium berghei*, a species that infects rodents, lasts 2 to 3 days in cultured hepatoma cells and in primary mouse hepatocytes. The process takes place inside a parasitophorous vacuole, which is formed upon parasite entry into the host cell, and involves the differentiation of a sporozoite into a large multinucleated schizont and eventually several thousands of merozoites. We first examined *P. berghei* maturation in vitro after incubation of sporozoites with the HepG2 hepatoma cell line. At 48 hours postinfection (hpi), parasites developed inside adherent HepG2 cells as exo-erythrocytic forms (EEFs) (fig. S1). However, at 63 to 70 hpi, the number of adherent cells containing parasites declined sharply to ~40% of their initial number, although the culture supernatants contained only small numbers of free merozoites that would be expected from rupturing of these cells. Instead, large numbers of parasite-filled, floating cells were observed (Fig. 1, A and B). Examination of these detached infected cells by transmission electron microscopy (TEM) (Fig. 1C and fig. S2) and scanning electron microscopy (SEM) (Fig. 1D) confirmed the presence of normal-shaped merozoites filling the whole volume of the host cells. The pattern of immunofluorescence staining (*3*) with polyclonal antibodies specific for the exported protein 1 (Exp1), a parasite protein that becomes inserted into the parasitophorous vacuole membrane (PVM), indicated disruption of the PVM (Fig. 1E) and liberation of merozoites into the host cell cytoplasm.

Unexpectedly, merozoites were also found within round, membrane-bound vesicles that were devoid of host cell nuclei and that we named merosomes (Fig. 1, F and G). Merosomes of various sizes were formed upon budding from the detached host cells (Fig.

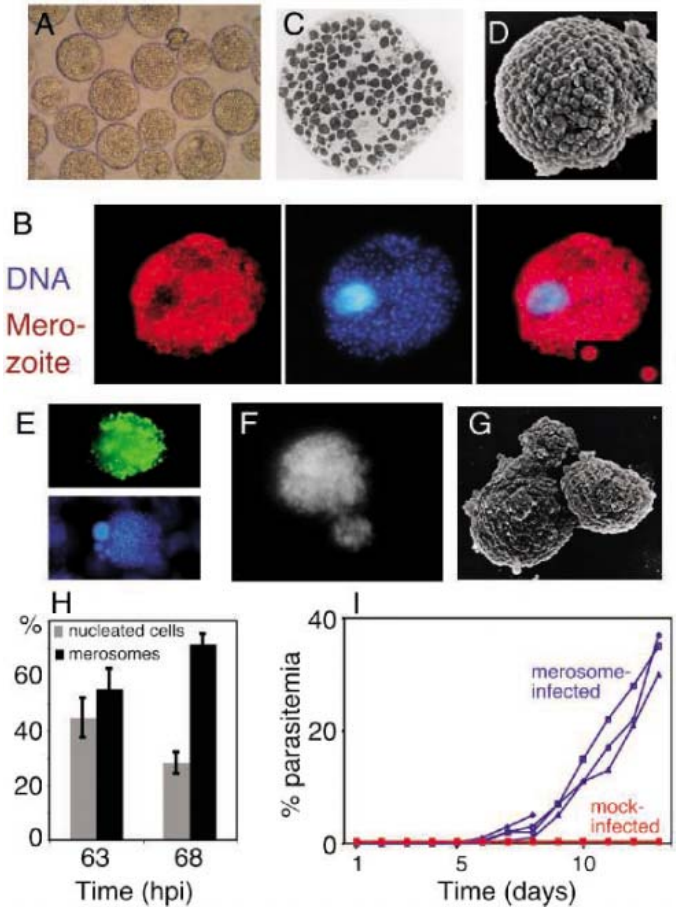

Fig. 1. Detached infected cells extrude merosomes, which contain infective merozoites. (**A**) Phase contrast image of infected HepG2 cells floating in the culture medium. (**B**) Immunofluorescence staining of a single floating cell with merozoite-specific antiserum (red); DNA is stained in blue (Hoechst 33258). Inset shows released merozoites at a higher magnification. (**C** and **D**) TEM and SEM of a single detached cell. (**E**) Disruption of the PVM during parasite merogony; green, Exp1; blue, Hoechst 33258. (**F**) Immunofluorescence image of living GFP-expressing parasites in a detached cell, demonstrating the budding of parasite-filled vesicles (merosomes). (**G**) SEM image of budding merosomes. (**H**) Merosome formation increases with time. Detached cells were collected after the indicated times, immobilized on poly-L lysine slides, fixed, and stained with the DNA dye Hoechst 33258. Nucleated cells and merosomes (devoid of host cell nucleus) were counted and the percentage (mean ± SD) of both populations was calculated from three independent experiments. (**I**) Infection of mice with detached cells. Four mice received culture supernatant containing 20 to 50 detached cells/merosomes (blue lines). Four control mice (red lines) received an equal amount of culture supernatant without detached cells, to exclude the possibility that previously liberated merozoites caused infection.

[1]Bernhard Nocht Institute for Tropical Medicine, Bernhard-Nocht-Strasse 74, 20359 Hamburg, Germany. [2]Department of Parasitology, Institut Pasteur, 28 Rue du Dr. Roux, 75724 Paris Cedex 15, France. [3]Department of Biochemistry, Federal University of Sao Paulo, Rua Tres de Maio, 04044-020, Sao Paulo, Brazil. [4]Department of Hepatobiliary Surgery, University Hospital Hamburg-Eppendorf, Martinistrasse 52, 20246 Hamburg, Germany.

*These authors contributed equally to this work.
†To whom correspondence should be addressed. E-mail: heussler@bni-hamburg.de

1H). To test whether merozoites inside detached cells and merosomes were infective, we injected them intravenously into mice. Parasites were detected in the blood of all injected mice (Fig. 1I), showing that the detached host cells could release infectious merozoites.

To examine if merosomes were also formed in vivo, we injected wild-type *P. berghei* sporozoites into C57/Bl6 mice and analyzed liver sections for the presence of detached infected cells and merosomes. At 40 hpi, most infected hepatocytes were still closely connected to neighboring hepatocytes (Fig. 2A, left), whereas at 46 hpi we detected predominantly detached cells, or parasite-filled cell extensions inside blood vessels (Fig. 2A, right). To obtain a real-time view of the process of merozoite release, we injected sporozoites from different *P. berghei* clones that express the green fluorescent protein (GFP) (*4*, *5*) into animals and monitored 45- to 53-hpi parasite-infected cells in the liver by time-lapse intravital imaging (*3*). EEFs appeared as large green fluorescent structures in the liver parenchyma. With time, however, fluorescent cell extensions, presumably corresponding to the merosomes seen in vitro, were observed budding from infected cells and reaching the blood circulation (Fig. 2, B to F, and movies S1 to S4). Based on the volume of individual merozoites and of released merosomes, it was estimated that merosomes can contain from just a few to several thousand merozoites. Once in the circulation, merosomes usually appeared to remain intact for extended periods of time (>1 hour) and drifted at a much slower speed than that of circulating erythrocytes, suggesting that the surface of merosomes might interact with that of liver sinusoid endothelial cells.

The process of merosome release from mature EEFs in the liver was next quantified in two distinct mouse strains (total number of mice, $n = 8$). On average, the percentage of budding EEFs increased between 42 and 50 hpi from ~39 to ~52% (Fig. 2D, $n = 88$ EEFs). During this time, 56% of merosomes were located inside sinusoids (Fig. 2, E and F), confirming the results of the histological examinations (Fig. 2A). The EEFs that were not seen emitting merosomes during the observation intervals were frequently still growing in size, suggesting that merosome budding might have followed the observation period. We conclude that merosome release from mature EEFs is a common phenomenon that occurs in most, if not all, mature *P. berghei* liver stages, and that merosomes can ensure

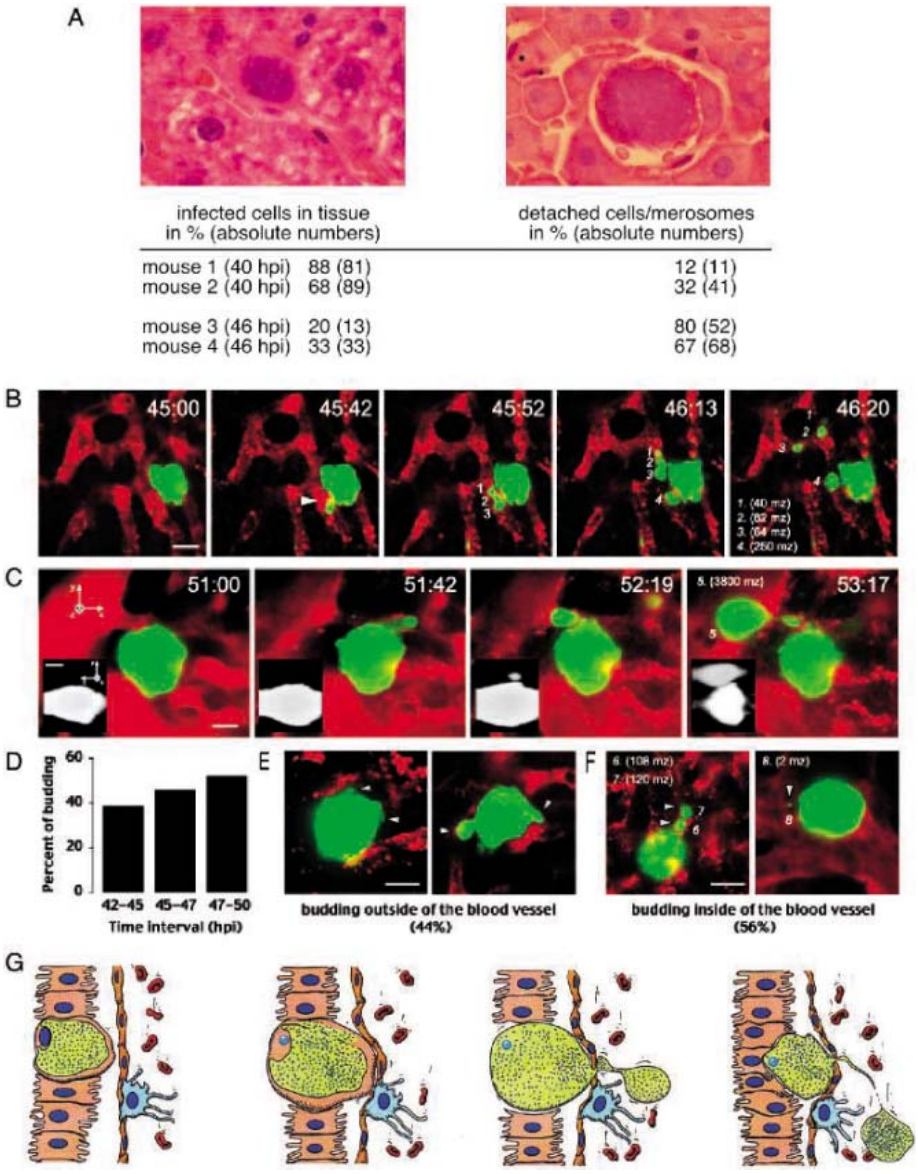

Fig. 2. Histological and real-time analysis of merozoite release in the liver of mice. (**A**) Histological sections showing EEFs at 40 to 46 hpi in the parenchyma (left) and in the sinusoids (right), respectively. Detached cells/merosomes and infected cells in the liver parenchyma of four different mice were counted and are presented as the percentage of infected cells counted (absolute numbers are in parentheses). (**B** to **F**) Intravital imaging of EEF budding and merosome release by confocal microscopy. The GFP-expressing parasite is shown in green and the blood circulation in red (red fluorescent bovine serum albumen injected intravenously). White arrowheads show host cell buds. The time postinfection (in hours) is shown in the upper-right corner. Bars, 15 μm. (B) Time-lapse sequence showing a green fluorescent EEF budding merosomes inside a small sinusoid. The merosomes are labeled with a number, and the estimated number of merozoites (mz), calculated as the merosome volume divided by the merozoite volume (2.66 μm^3), is shown in parentheses. (C) Each panel of the colored time-lapse sequence is a maximum projection of three images covering 8 μm in depth. The sequence shows a late EEF budding a large merosome, which is growing while moving toward the central vein. The insets show the EEF lateral view (90° counterclockwise rotation of *y* axis). As shown by the last two insets, the diameter of the blood vessel limits the size of the merosome and the transfer of merozoites from the EEF into the merosome. (D) Quantification of budding EEF in the liver of mice ($n = 88$ EEFs). (E and F) Percentage of parasites budding outside the nearby sinusoid versus those budding inside ($n = 46$ budding EEFs). The confocal images are representatives of each type of budding. (**G**) Hypothesis for the release of *Plasmodium* merozoite-filled vesicles (merosomes, green) from infected hepatocytes. Red blood cells (red) are separated from hepatocytes by endothelial cells (orange) and the space of Disse. Kupffer cell is in blue.

the direct delivery of merozoites in the blood circulation.

The molecular events during cell detachment and merosome formation were next analyzed in vitro. Staining of the infected HepG2 cells early after detachment with the nucleic acid stain Hoechst 33258 revealed condensation of the cell nuclei, suggesting that these cells were undergoing cell death (Fig. 3A, lower panels). Loss of mitochondria membrane potential (fig. S3) and the release of cytochrome c from mitochondria of infected cells (Fig. 3A) supported this assumption. In agreement with these observations, electron microscopy showed that detached cells did not contain normal-shaped mitochondria (fig. S4). However, host cell death did not occur by classic apoptosis or necrosis (Fig. 3B and Fig. 4, A, B, and D). Activation of cysteine proteases other than caspases induced cell death (Fig. 3B). Treatment of infected HepG2 cells with the general cysteine protease inhibitor E64 at 55 hpi completely inhibited PVM destruction and cytochrome c release (fig. S5), and no detached cells were detected in the culture medium. When infected cultures were treated with E64 at 61 hpi (1 to 2 hours before infected cells normally detach), most infected cells did not detach, but a proportion of infected cells were still floating in the culture medium (Fig. 3B). These cells exhibited a different phenotype compared with that of untreated detached cells. The PVM of E64-treated detached cells was still visible, and the host cell nucleus appeared less condensed than in untreated detached cells (Fig. 3C). Therefore, E64 appeared capable of blocking the ongoing processes of PVM and host cell nucleus destruction mediated by cysteine proteases. Other key differences between cell death observed in detached cells and apoptosis were that the DNA in condensed host cell nuclei was not fragmented (Fig. 4D and fig. S6) and that in the membrane of detached cells and merosomes, the asymmetric distribution of phosphatidylserine (PS) residues, which is normally a hallmark of viable cells, was maintained (Fig. 4, A and B, and fig. S7). The recognition of dead versus viable cells by phagocytes relies, at least in part, on exposure of PS on the outer leaflet of the membrane of dying cells (*6*–*8*), and we therefore analyzed how the parasite manipulates the host cell signaling machinery, resulting in the inhibition of the PS switch (*3*). In apoptotic cells, the PS switch is initiated by Ca^{2+} release from internal stores like mitochondria and the endoplasmic reticulum into the cytoplasm of the cell. Staining of detached, infected cells with a cell-permeable Ca^{2+}-indicator dye revealed that merozoites contained much higher levels of intracellular Ca^{2+} than host cells (Fig. 4B, upper panels). This suggests that like *P. falciparum* erythrocytic merozoites (*9*, *10*), hepatic merozoites actively accumulate intracellular Ca^{2+}, which is released from damaged internal stores of the dying host cell. Ca^{2+} uptake by merozoites keeps Ca^{2+} levels in the host cell low and inhibits the PS switch to the outer leaflet of the host cell membrane as long as the intracellular parasites are viable. However, forced Ca^{2+} influx in detached cells by treatment with the Ca^{2+} ionophore ionomycin induced the PS switch, indicating that there is not a general block of PS exposure in these cells (Fig. 4A).

Under in vitro conditions, merozoites in detached hepatocytes have a restricted lifetime. Parasite death is accompanied by DNA fragmentation (Fig. 4D) and Ca^{2+} release from the parasite back into the host cell cytoplasm, resulting in PS switch to the outer leaflet of the host cell membrane (Fig. 4, A and B, lower panel). In phagocytosis assays, ionomycin-treated PS-positive detached cells were more frequently engulfed by macrophages than PS-negative detached cells containing viable parasites (fig. S8).

In marked contrast to the induction of cell death observed during merozoite development, it has recently been shown that early *Plasmodium* liver stages even confer resistance to apoptosis to the host cell (*11*, *12*). However, dying EEFs were shown to provoke phagocyte infiltration in vivo, and it was suggested that these dead parasites cannot protect host cells from under-

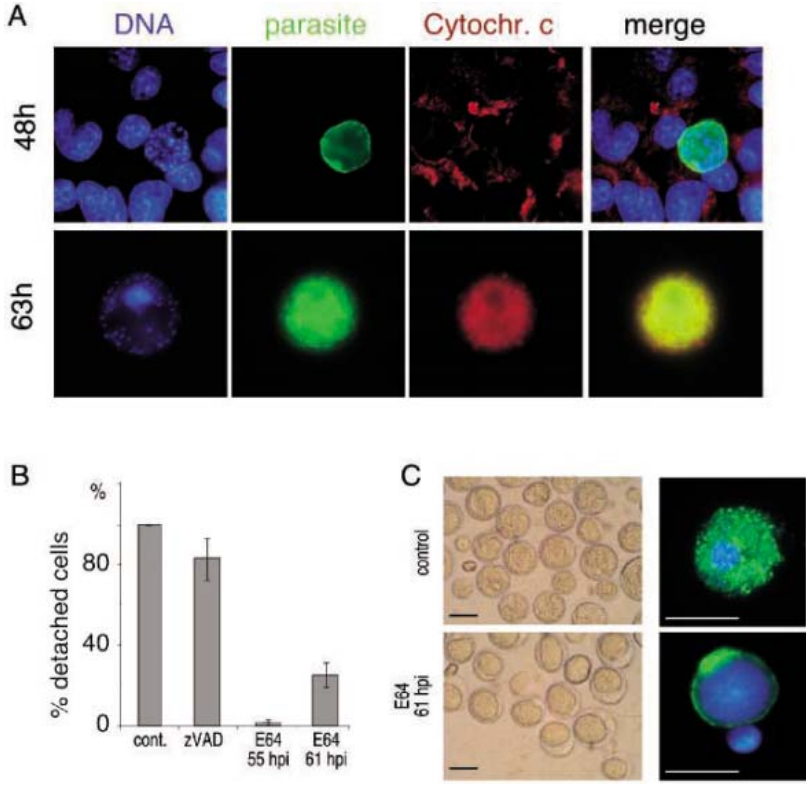

Fig. 3. Induction of host cell death during merozoite formation. (**A**) Cytochrome c release from mitochondria in floating cells. Infected HepG2 cells were fixed at 48 hpi (control, upper panels) or 63 hpi (lower panels) and stained with antibodies against PbExp1 or Pbhsp90 (green) and cytochrome c (red). (**B**) The general cysteine protease inhibitor E64, but not the caspase inhibitor zVAD-fmk, blocks the detachment of host cells. Cultures were left untreated (cont.) or treated with E64 at 55 or 61 hpi, or with zVAD-fmk (at 55 hpi). At 65 hpi, culture supernatants were collected and the number of floating cells was determined. Results are expressed as the percentage of control cells (mean ± SD). (**C**) Cultures were treated with E64 at 61 hpi for 4 hours. Treated detached cells (lower panels) exhibit a different phenotype from that of untreated control cells (upper panels). Immunofluorescent analysis with an antibody against the PVM protein Exp1 (right panels) shows the partly preserved PVM in E64-treated cells (lower right panel). The structure of the PVM was maintained in 76% (±12%) of detached cells treated with E64 from 61 to 65 hpi. DNA is stained with Hoechst 33258 (blue). Bars, 20 μm.

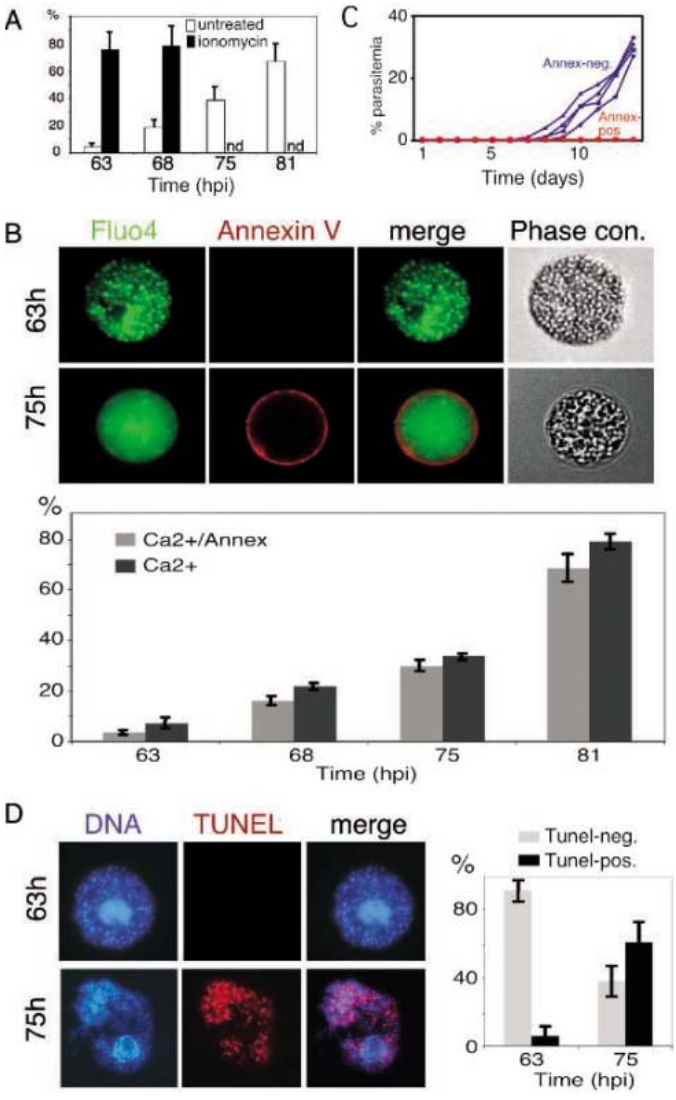

Fig. 4. Merosomes do not expose PS at their surface for several hours. (**A**) Detached cells were isolated at different time points and stained with Annexin-V—fluorescein isothiocyanate and propidium iodide (see also fig. S7). The percentage (mean ± SD) of Annexin-V–positive cells was calculated from three independent experiments (white bars). Detached cells treated for 1 (63 hpi) and 6 hours (68 hpi) with ionomycin (1 μg/ml) are represented by black bars (mean ± SD; nd, not done). (**B**) Merozoites accumulate Ca^{2+} and inhibit the PS switch in the host cell membrane. Floating cells at 63 hpi (upper panels) and 75 hpi (middle panels) were stained with Fluo-4/AM (green) and Annexin-V-Alexa 568 (red). Quantitative assessment of Ca^{2+} release and PS switch (bottom panel). For each time point, 100 to 300 cells were examined and the percentage (mean ± SD) of cells with released Ca^{2+} (dark bars) and cells with released Ca^{2+} and PS switch (gray bars) was calculated. (**C**) Detached, Annexin-V–stained cells at 63 or 75 hpi were isolated with a micropipette and transferred to 24-well plates; Annexin-V–positive or Annexin-V–negative floating cells were separated and subsequently injected into mice. Mouse parasitemia were determined daily for 2 weeks [four mice infected with Annexin-V–positive cells (red symbols); four mice infected with Annexin-V–negative cells (blue symbols)]. (**D**) TUNEL (terminal deoxynucleotidyl transferase–mediated dUTP nick-end labeling) staining of floating cells at 63 and 75 hpi. Red, TUNEL stain; blue, Hoechst 33258 stain. In three independent experiments, the total number of detached cells was determined and the number of TUNEL-positive cells was calculated and expressed as the percentage of all counted cells (mean ± SD). Gray bars represent TUNEL-negative detached cells, black bars TUNEL-positive detached cells.

going cell death (*12*). The results obtained by intravital imaging indicate that the remnants of infected cells left behind after merosome release could also contribute to the observed phagocyte infiltration.

In conclusion, we have shown that *Plasmodium* liver-stage parasites manipulate their host cells to guarantee the safe delivery of merozoites into the bloodstream (Fig. 2G). Merosomes bulge into liver sinusoids and appear to act as shuttles that ensure the release of living merozoites directly into the circulation, and by not presenting the PS signature of a dying cell, also act as shields that protect them from phagocytosis. This mechanism of merozoite release may increase erythrocyte invasion and parasite survival, because extracellular merozoites are readily recognized and engulfed by Kupffer cells and other phagocytic cells in the liver sinusoids (*13*). The proteases that control cell death and cell movement of the host cell, as well as the factors that mediate Ca^{2+} accumulation and prevent PS exposure, appear to be essential to parasite survival. They might become interesting targets for inhibiting the release of *Plasmodium* merozoites from hepatocytes and thus preventing erythrocyte infection and the onset of the disease.

References and Notes

1. U. Frevert *et al.*, *PLoS Biol.* **3**, e192 (2005).
2. R. Amino *et al.*, *Nat. Med.* **12**, 220 (2006).
3. Materials and methods are available as supporting material on *Science* Online.
4. R. Natarajan *et al.*, *Cell. Microbiol.* **3**, 371 (2001).
5. B. Franke-Fayard *et al.*, *Mol. Biochem. Parasitol.* **137**, 23 (2004).
6. B. Verhoven, R. A. Schlegel, P. Williamson, *J. Exp. Med.* **182**, 1597 (1995).
7. V. A. Fadok, A. de Cathelineau, D. L. Daleke, P. M. Henson, D. L. Bratton, *J. Biol. Chem.* **276**, 1071 (2001).
8. M. O. Li, M. R. Sarkisian, W. Z. Mehal, P. Rakic, R. A. Flavell, *Science* **302**, 1560 (2003).
9. M. Wasserman, J. P. Vernot, P. M. Mendoza, *Parasitol. Res.* **76**, 681 (1990).
10. G. A. Biagini, P. G. Bray, D. G. Spiller, M. R. White, S. A. Ward, *J. Biol. Chem.* **278**, 27910 (2003).
11. P. Leiriao *et al.*, *Cell. Microbiol.* **7**, 603 (2005).
12. C. van de Sand *et al.*, *Mol. Microbiol.* **58**, 731 (2005).
13. J. A. Terzakis, J. P. Vanderberg, D. Foley, S. Shustak, *J. Protozool.* **26**, 385 (1979).

14. We thank M. Lütgehetmann and S. Korton for technical advice and U. Froehlke for technical assistance. We also thank C. Schmetz for electron microscopy imaging, S. Shorte for intravital imaging, and T. Ishino, M. Yuda, C. Janse, B. Franke-Fayard, and A. Waters for providing the *P. berghei* fluorescent clones. G. Langsley, E. Tannich, and H. Lotter are thanked for critically reading the manuscript. This work was supported by grant HE 4497/1-1 from the Deutsche Forschungsgemeinschaft (to V.T.H.) and a Howard Hughes Medical Institute International Scholar Award (to R.M.)

Supporting Online Material

www.sciencemag.org/cgi/content/full/1129720/DC1
Materials and Methods
Figs. S1 to S8
Movies S1 to S4

9 May 2006; accepted 18 July 2006
Published online 3 August 2006;
10.1126/science.1129720
Include this information when citing this paper.

Exploiting the Reversibility of Natural Product Glycosyltransferase-Catalyzed Reactions

Changsheng Zhang,[1] Byron R. Griffith,[1] Qiang Fu,[2] Christoph Albermann,[1]* Xun Fu,[1] In-Kyoung Lee,[1]† Lingjun Li,[2] Jon S. Thorson[1]‡

Glycosyltransferases (GTs), an essential class of ubiquitous enzymes, are generally perceived as unidirectional catalysts. In contrast, we report that four glycosyltransferases from two distinct natural product biosynthetic pathways—calicheamicin and vancomycin—readily catalyze reversible reactions, allowing sugars and aglycons to be exchanged with ease. As proof of the broader applicability of these new reactions, more than 70 differentially glycosylated calicheamicin and vancomycin variants are reported. This study suggests the reversibility of GT-catalyzed reactions may be general and useful for generating exotic nucleotide sugars, establishing in vitro GT activity in complex systems, and enhancing natural product diversity.

Glycosyltransferases (GTs) constitute a superfamily of ubiquitous enzymes that attach carbohydrate moieties to biological molecules (*1*) and thus play a role in the biosynthesis of oligosaccharides (*2*), glycosaminoglycans (*3*), glycopeptides (*4*), and glycosylated anticancer and anti-infective agents (*5*). These enzymes are generally perceived as unidirectional catalysts that drive the formation of glycosidic bonds from nucleotide diphosphate sugar (NDP-sugar) donors and aglycon acceptors (*6*). In contrast, we report that GTs involved in the biosynthesis of anticancer (the enediyne calicheamicin, CLM) and antibiotic (the glycopeptide vancomycin, VCM) natural product–based drugs catalyze reversible, bidirectional reactions. Specifically, the four GTs tested (CLM CalG1 and CalG4 and VCM GtfD and GtfE) were found to catalyze three new reactions: (i) the synthesis of exotic NDP-sugars from glycosylated natural products, (ii) the exchange of native natural-product glycosides with exogenous carbohydrates supplied as NDP-sugars, and (iii) the transfer of a sugar from one natural product backbone to a distinct natural-product scaffold. As proof of the broader applicability of these new reactions, the GT-catalyzed production of >70 differentially glycosylated CLM variants and a VCM analog bearing both a handle for chemical diversification and a rare amino sugar are also reported.

The *calG1* gene was amplified from the genomic DNA of the CLM producer, *Micromonospora echinospora*, and overexpressed in *Escherichia coli*, and the recombinant CalG1 was purified to homogeneity (fig. S1) (*7*, *8*). Incubation of the aglycon **1** with the surrogate substrate thymidine diphosphate (TDP)-β-L-rhamnose (Fig. 1A) in the presence of CalG1

[1]Laboratory for Biosynthetic Chemistry, Pharmaceutical Sciences Division, School of Pharmacy, National Cooperative Drug Discovery Group Program, University of Wisconsin (UW)–Madison, 777 Highland Avenue, Madison, WI 53705–2222, USA. [2]School of Pharmacy and Department of Chemistry, University of Wisconsin, 777 Highland Avenue, Madison, WI 53705–2222, USA.

*Present address: Institute of Microbiology, University of Stuttgart, Allmandring 31, 70569 Stuttgart, Germany.
†Present address: Korea Research Institute of Bioscience and Biotechnology, Yuseong, Daejeon 305-333, Korea.
‡To whom correspondence should be addressed. E-mail: jsthorson@pharmacy.wisc.edu

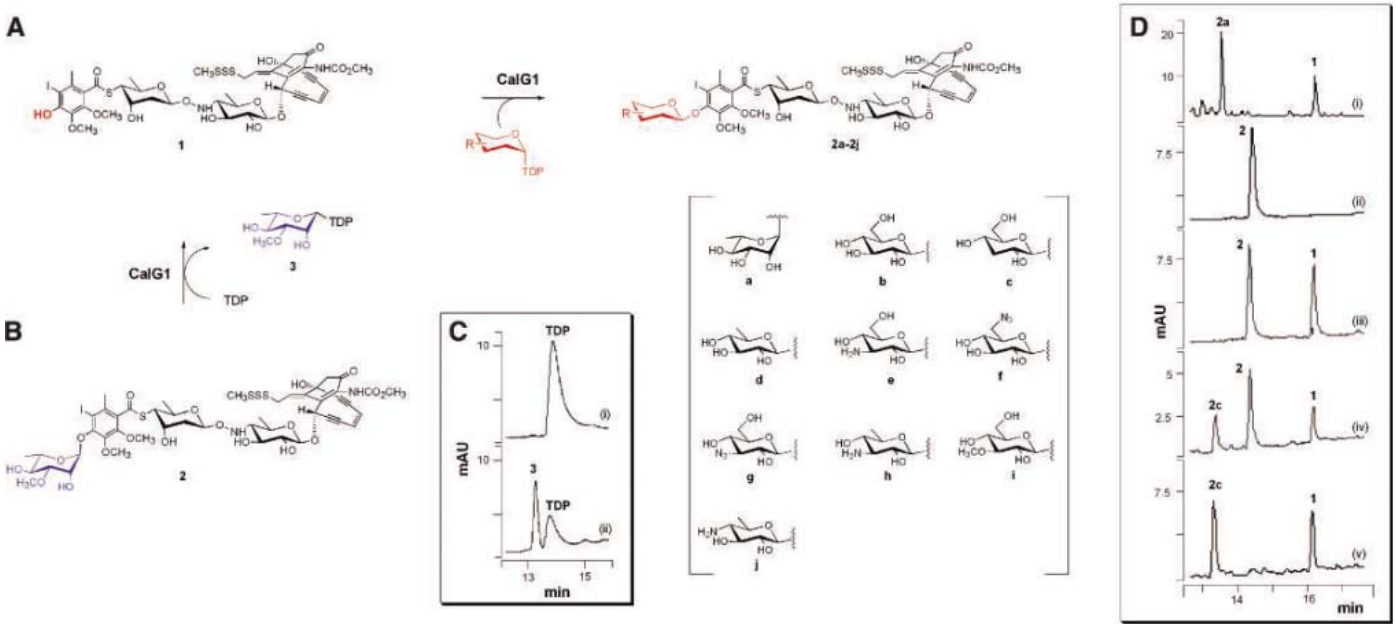

Fig. 1. In vitro CalG1-catalyzed reactions. (**A**) The CalG1-catalyzed transfer of unnatural sugars to the acceptor **1**. The TDP-sugars corresponding to glycosides **2c** to **2j** were enzymatically generated as previously described, TDP-β-L-rhamnose (for **2a**) was prepared via chemical synthesis, and TDP-α-D-glucose (for **2b**) was obtained from a commercial source. (**B**) CalG1-catalyzed reverse glycosyltransfer and sugar exchange reactions. In the first step, the terminal 3′-*O*-methylrhamnose unit of **2** (CLM α_3^I, 1 of 10 CLMs produced by *M. echinospora*) was transferred to TDP, yielding **1** and TDP-3-*O*-methyl-β-L-rhamose [**3**, see also (C) and (D)]. The subsequent sugar exchange involved the transfer of unnatural sugars (from exogenous NDP-sugars) to **1** to give compounds **2a** to **2j**. (**C**) Anion-exchange HPLC of CalG1-catalyzed **3** formation: (i) control with 50 μM **2** and 100 μM TDP [see also (D), ii] and (ii) 50 μM **2**, 100 μM TDP, and CalG1 [see also (D), iii]. The new peak at 13 min. was isolated and identified as **3** by MS/MS (fig. S5). AU, absorbance units. (**D**) Reverse-phase HPLC of CalG1-catalyzed reactions: (i) 50 μM **1**, 300 μM TDP-β-L-rhamnose, and CalG1; (ii) reverse glycosyltransfer control with 50 μM **2** and 100 μM TDP [see also (C), i]; (iii) 50 μM **2**, 100 μM TDP, and CalG1 [see also (C), ii]; (iv) 50 μM **2**, 300 μM TDP-3-deoxy-α-D-glucose, and CalG1 (sugar exchange); and (v) 50 μM **1**, 300 μM TDP-3-deoxy-α-D-glucose, and CalG1. All CalG1 assays were performed in a total volume of 100 μl in tris-HCl buffer (10 mM, pH = 7.5) containing 1 mM of $MgCl_2$ and 10 μM CalG1 with incubation at 30°C for 3 to 12 hours. HPLC parameters are described in the Materials and Methods.

led to the formation of a new product (Fig. 1D, i), characterized as **2a** by liquid chromatography–mass spectrometry (LC-MS). Consistent with CalG1 as the requisite rhamnosyltransferase in CLM biosynthesis, no product was observed when CalG1 was replaced with other GTs in this assay. Also, substitution of TDP-α-L-rhamnose for TDP-β-L-rhamnose in the CalG1 assay yielded no product, consistent with CalG1 functioning as a stereospecific inverting GT. A diverse library of 22 TDP sugars (Materials and Methods) was used to probe the NDP-sugar specificity of CalG1 (Fig. 1A and fig. S2). Nine additional TDP-sugar substrates were converted to their corresponding CLM glycosides, **2b** to **2j** (Fig. 1A), in percent conversions of 27 to 62% (fig. S3). LC coupled to tandem MS (LC-MS/MS) of products **2b** and **2d** revealed fragmentation patterns consistent with attachment of the sugar to the aromatic ring of the substrate and were highly consistent with the fragmentation of naturally occurring standard CLM variants α_3^I (**2**) and γ_1^I (**5**) (Fig. 2 and fig. S4). Cumulatively, these studies designated CalG1 as the CLM rhamnosyltransferase, capable of flexibility toward diverse TDP-D- and TDP-L-sugar donors.

In an experiment designed to further verify the regiospecificity of CalG1, CLM α_3^I (**2**) (Fig. 1B) and TDP-3-deoxy-α-D-glucose were co-incubated with CalG1 under standard conditions. Because the CalG1 glycosylation site in **2** is occupied by 3′-*O*-methylrhamnose (Fig. 1B), no reaction was expected. However, two new products were observed, subsequently identified by LC-MS as **1** and the corresponding 3-deoxyglucoside, **2c** (Fig. 1D, iv and v). Analysis of control reactions led to the conclusion that this transformation involved a TDP-dependent reverse glycosyltransfer. Specifically, co-incubation of **2** with TDP yielded **1** only in the presence of CalG1 (Fig. 1D, ii and iii, and fig. S5A), and analysis of the same "reverse" reaction by anion-exchange high performance liquid chromatography (HPLC) (Fig. 1C) unveiled the production of TDP-3-*O*-methyl-β-L-rhamnose (**3**) (Fig. 1B and fig. S5) in substantial quantity, which was absent in the control assay. Thus, CalG1 efficiently excised the native CLM 3′-*O*-methylrhamnosyl unit in the presence of TDP (to provide **1** and TDP sugar **3**) and, in the presence of a slight excess of exogenous TDP-3-deoxyglucose, ultimately catalyzed the formation of **2c**. Such CalG1-catalyzed in situ "sugar exchange" might offer an expeditious method for substituting the CLM 3′-*O*-methylrhamnose with other natural or unnatural sugars. To test this idea, we assayed CLM derivatives (Fig. 2) α_3^I (**2**), β_1^I (**4**), γ_1^I (**5**), and δ_1^I (**6**); dimethy hydrazide (DMH) Nac γ (**7**), γ_2^I (**8**), and Nac ε (**9**); and "fragment III" (**10**) (*9*) in CalG1-catalyzed reactions with the 10 established CalG1 TDP-sugar substrates. In every case, the desired sugar-exchanged product was observed by HPLC (figs. S6 and S10) with an average sugar exchange conversion of 60% for the eight CLM aglycons in the presence of purified TDP-α-D-glucose or TDP-β-L-rhamnose. Notably, this simple set of assays led to the CalG1-catalyzed production of a CLM library exceeding 70 members (**2a** to **2j**, **4a** to **4j**, **5a** to **5j**, **6a** to **6j**, **7a** to **7j**, **8a** to **8j**, **9a** to **9j**, and **10a** and **10b**) (figs. S7 and S8) and thereby highlights the combinatorial power of GT-catalyzed sugar exchange.

Given that GT-catalyzed sugar exchange activity proceeds via an established NDP-sugar intermediate, we hypothesized that GTs could also be used to harvest an exotic sugar from one natural-product scaffold and transfer it to a different

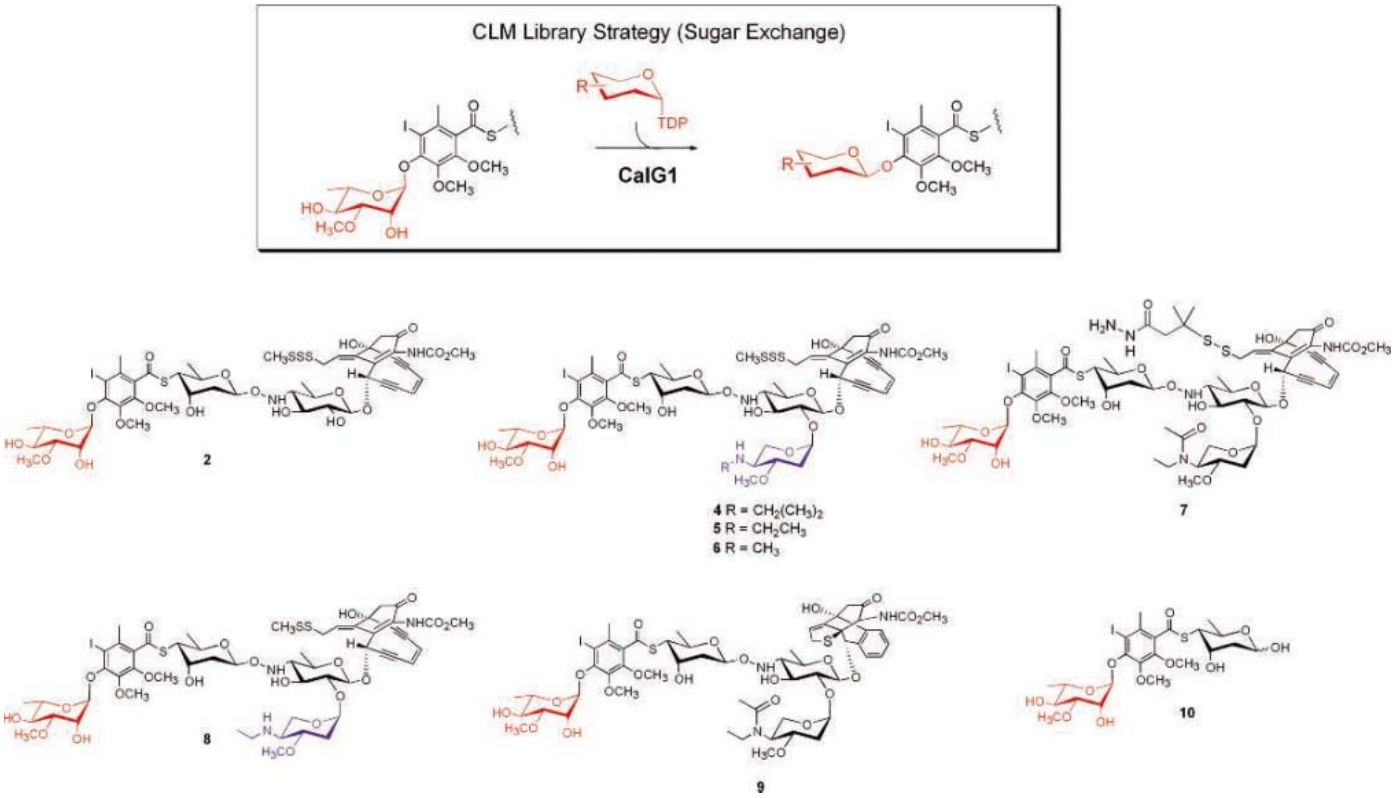

Fig. 2. Strategy for the construction of a CLM library by CalG1-catalyzed sugar exchange. The general strategy involved the CalG1-mediated exchange of the natural 3′-*O*-methylrhamnose (highlighted in red) in CLMs α_3^I (**2**), β_1^I (**4**), γ_1^I (**5**), and δ_1^I (**6**) and DMH Nac γ (**7**), γ_2^I (**8**), and Nac ε (**9**) with sugars supplied via the 10 established CalG1 NDP-sugar substrates (fig. S2A). In addition, fragment III (**10**) was also converted to the rhamnoside and glucoside to cumulatively provide 72 diversely functionalized CLM derivatives. For this study, CLMs **2** and **4**, **5**, and **6** are natural metabolites, whereas **7**, **8**, **9**, and **10** are chemically modified CLM derivatives. A typical CalG1 sugar exchange reaction contained 50 μM aglycon (**2** and **4** to **10**), 300 μM NDP sugar, and 10 μM CalG1 in a total volume of 100 μl in tris-HCl buffer (10 mM, pH = 7.5) containing 1 mM of $MgCl_2$ at 30°C for 3 hours. HPLC parameters are described in the Materials and Methods, and chromatograms for representative reactions are provided in fig. S6. The structures of all library members are illustrated in fig. S7, and conversion rates are provided in figs. S8 and S10. It should also be noted that CalG4 can excise the aminopentosyl units (highlighted in blue) from **4**, **5**, **6**, and **8** for sugar or aglycon exchange.

aglycon in a single reaction. This permutation of GT catalysis would avoid the often-complex synthesis of highly functionalized NDP-sugars (*10*). The assays designed to test this idea contained CalG1, a putative 3′-*O*-methylrhamnose donor—**4**, **5**, **6**, **7**, **8**, or **10** (Fig. 2)—TDP, and the representative acceptor **1**. In each case, the simultaneous excision and in situ transfer of 3′-*O*-methylrhamnose from each respective donor to **1** was observed, yielding the expected 3′-*O*-methylrhamnosylated product **2** (fig. S9). In comparison, controls lacking either CalG1 or TDP gave only starting materials. Thus, in situ aglycon exchange reactions can extend the potential diversity accessible by CalG1.

The reversibility of the CalG1-catalyzed sugar exchange and aglycon exchange transformations described above raised the question as to whether other GT systems would exhibit similar behavior. Thus, three additional GT-catalyzed reactions were examined for reversibility: those of CalG4 (the putative CLM aminopentosyltransferase), GtfD, and GtfE (the VCM vancosaminyl- and glucosyltransferase, respectively) (*7*, *11*–*13*). CalG4 was produced in a similar fashion as CalG1 (fig. S1) (*7*, *8*). In the presence of TDP, CalG4 catalyzed the excision of the aminopentose sugar moiety (Fig. 2, highlighted in blue) from sugar donor CLM derivatives **4**, **5**, **6**, and **8** (fig. S11). CalG4 also catalyzed in situ aglycon exchange, transferring the excised aminopentoses from donors **4**, **5**, **6**, and **8** to the exogenous aglycon acceptor **1** in the presence of TDP with conversions ranging from 19 to 69% (fig. S12). In comparison, controls lacking TDP (even in the presence of alternative NDPs) or CalG4 gave only starting materials. Besides identifying CalG4 as the aminopentosyltransferase involved in CLM biosynthesis, these results confirm that, in contrast to the previously proposed uridine diphosphate (UDP) sugar pathways (*14*), CLM aminopentose biosynthesis proceeds via a TDP-sugar pathway. Additionally, this study demonstrates that the reversibility of GT catalysis is not unique to the CalG1 reaction.

To extend these studies beyond enediyne scaffolds, we overexpressed and purified the VCM GTs GtfD and GtfE as previously described (*11*). Similar to the CLM GTs, GtfD catalyzed the excision of L-vancosamine from the parent sugar donor VCM (**11**) to form pseudoaglycon **13** (Fig. 3A). In a separate aglycon exchange reaction, GtfD catalyzed the transfer of L-vancosamine from **11** to the unnatural acceptor **14** (*13*) to give **15**, a VCM analog containing both a sugar-appended azido handle for chemoselective ligation and a vancosaminyl moiety (27% conversion) (Fig. 3A and fig. S13). Likewise, the glucosyltransferase GtfE could also catalyze sugar excision from both **13** and the unnatural sugar donor **14**. Consistent with an equilibrium only moderately favoring the glycoside product in the GtfE-catalyzed reaction, the equilibrium constant (K_{eq}) was determined to be 4.5 (fig. S14). GtfE could also participate in aglycon exchange, as revealed by the GtfE-catalyzed generation of unnatural NDP-sugar **16** for CalG1-catalyzed glycosyltransfer to the enediyne acceptor **1** in a tandem, one-pot, GtfE-CalG1-catalyzed aglycon exchange reaction (Fig. 3B). With an overall conversion of 48%, this transformation highlights the potential of two-GT systems to mediate aglycon exchange between compounds from different natural product classes (fig. S15).

The exploitation of GT-catalyzed reaction reversibility may facilitate the use of glycosylation as a tool to modulate the activity of

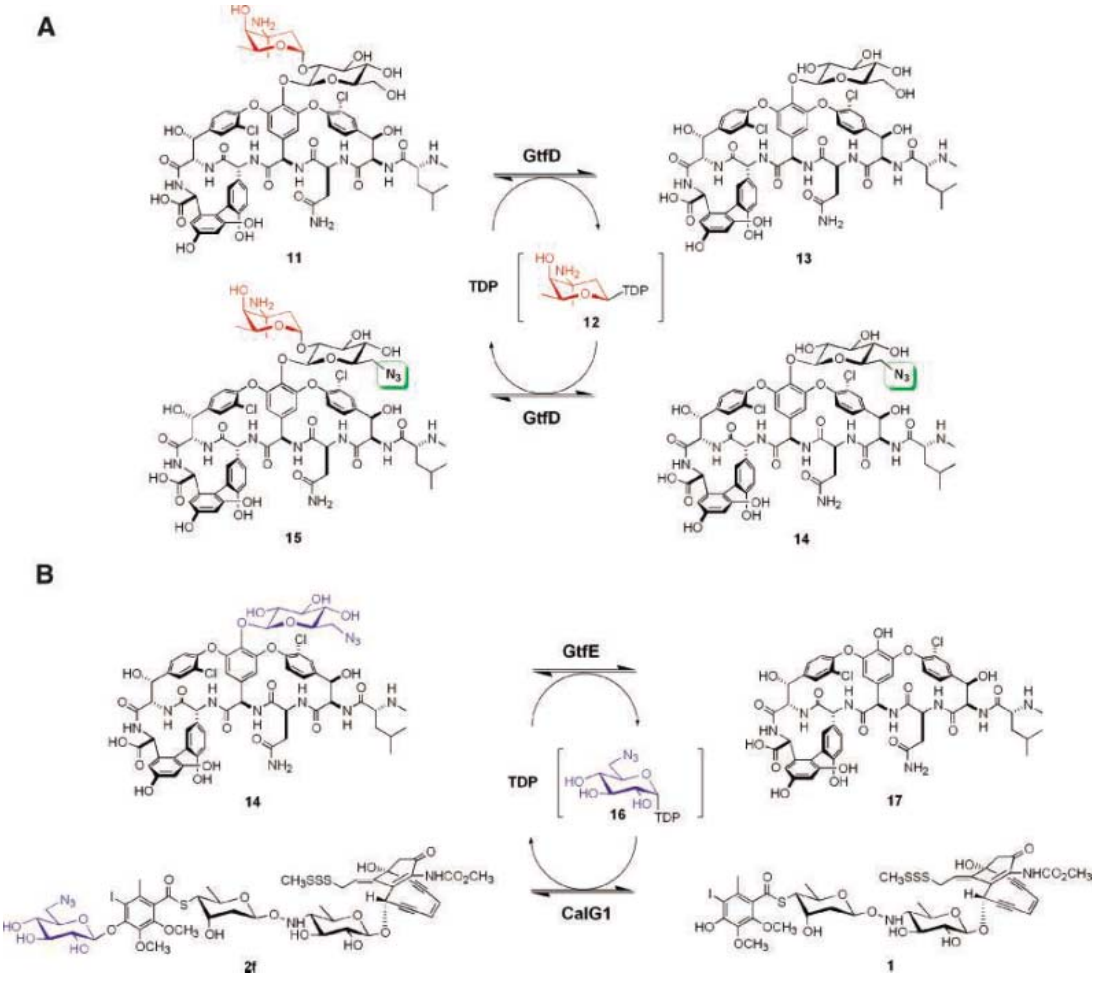

Fig. 3. VCM GT-catalyzed reverse and aglycon exchange reactions. (**A**) GtfD-catalyzed aglycon exchange reaction to provide 2′-vancosaminyl-6′-azidoglucosyl-VCM (**15**). The TDP-β-L-vancosamine (**12**) for this reaction was generated in situ by a GtfD-catalyzed reverse glycosyltransfer and subsequently transferred to the unnatural 6-azidoglucose–containing derivative **14** to give compound **15** in 27% conversion (fig. S13). The reaction was performed in a total volume of 100 μl in tricine-NaOH buffer [75 mM Tricine, pH = 9.0, 2.5 mM $MgCl_2$, 2.5 mM tris (2-carboxy ethel)-phosphine, and 1 mg/ml bovine serum albumin (BSA)] containing 100 μM **11**, 100 μM **14**, 1 mM TDP, and 12 μM GtfD. (**B**) A two-component GT-catalyzed aglycon exchange reaction using two diverse natural product scaffolds. In this one-pot reaction, TDP-6-azido-α-D-glucose (**16**, provided by GtfE-catalyzed reverse glycosyltransfer from sugar donor **14**) served as the NDP-sugar donor for the CalG1-mediated attachment of 6-azidoglucose to CLM **1**, yielding **2f** in 48% conversion (fig. S14). A typical reaction contained 100 μM **14**, 50 μM **1**, 100 μM TDP, 10 μM GtfE, and 10 μM CalG1 in a total volume of 100 μl in tris-HCl buffer (10 mM, pH = 7.5) containing 1 mM of $MgCl_2$ at 30°C for 3 hours. For Fig. 3, detailed assay and HPLC parameters and chromatograms are provided in the Materials and Methods.

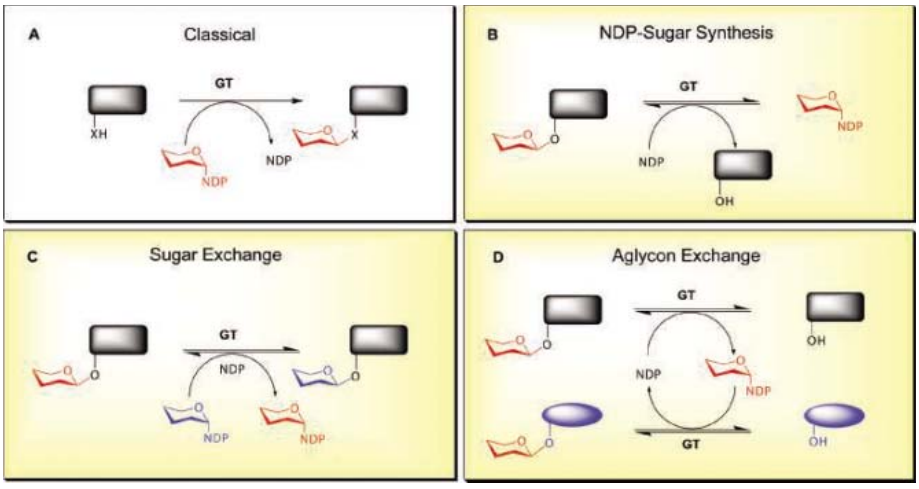

Fig. 4. Schematic of glycosyltransferase catalysis. **(A)** The classical GT-catalyzed sugar transfer from an NDP-sugar donor to an acceptor to form a glycosidic bond. Although the acceptor nucleophile in these reactions is most often oxygen (X=O), GTs are also known to catalyze the formation of *N*-, *S*- and even *C*-glycosidic bonds. **(B)** NDP-sugar synthesis via reverse glycosyltransfer. **(C)** The GT-catalyzed sugar exchange reaction to exchange native natural product sugar appendages with alternative sugars supplied as exogenous NDP-sugars. **(D)** A generalized scheme for an aglycon exchange reaction wherein a sugar is excised from one natural product (as an NDP-sugar) and subsequently attached to a distinct aglycon acceptor. In this reaction, the interchange of aglycons from a single natural product class is generally accomplished via one GT, whereas the interchange of aglycons from different compound classes requires multiple GTs.

therapeutically important natural products (*5*). For example, before this work, only two methods for differentially glycosylating CLMs were available: pathway engineering and total synthesis. Whereas the former has proven to be a powerful derivatization tool for certain natural products (*15*), the stringent genetic limitations of the CLM-producing *M. echinospora* has rendered this approach impractical (*7*). Alternatively, reworking previously reported CLM syntheses to provide efficient divergent routes to the >70 CLM analogs reported herein is also likely impracticable (*16*–*18*). With respect to rare NDP-sugars, the demonstrated in situ generation of TDP-β-L-vancosamine (**12**) (Fig. 3A) herein is an advance over reported synthetic methods that required seven linear steps to achieve an overall yield of less than 7%, originating from the same starting material, VCM (*10*). The CLM-derived TDP-3-*O*-methyl-β-L-rhamnose (**3**) (Fig. 1B) and the three TDP-*N*-alkylaminopentoses (derived from donors **4**, **5**, **6**, and **8**) (Fig. 2 and fig. S11) have not been previously synthesized, and therefore direct comparisons to other synthetic routes are not possible (*19*–*21*).

Although Glaser and Brown described the reversibility of the native chitin synthetase reaction in one of the first reports of in vitro GT activity (*22*), the perception of GT catalysis has remained one of unidirectionality, transforming NDP-sugar and aglycon substrates into glycoside products (Fig. 4A) (*23*–*28*). In contrast, this study uncovered reversibility in reactions catalyzed by both previously uncharacterized GTs (CalG1 and CalG4) and well-studied GTs (GtfD and GtfE) (*11*–*13*). Consistent with an equilibrium only moderately favoring glycoside formation (K_{eq} = 4.5 for GtfE), these model GT-catalyzed reactions could be modulated via simple adjustments in relative substrate concentrations. Glycosyltransfer reversibility could be exploited to synthesize valuable rare NDP-sugars (Fig. 4B), exchange one sugar on a core scaffold for another (Fig. 4C), or transfer sugars from one scaffold to another (Fig. 4D), suggesting GT catalysis to be of greater versatility and utility than was previously appreciated.

References and Notes

1. C. Breton, L. Snajdrova, C. Jeanneau, J. Koca, A. Imberty, *Glycobiology* **16**, 29R (2006).
2. P. Sears, C.-H. Wong, *Science* **291**, 2344 (2001).
3. P. L. Deangelis, L. C. Oatman, D. F. Gay, *J. Biol. Chem.* **278**, 35199 (2003).
4. M. Wacker *et al.*, *Science* **298**, 1790 (2002).
5. B. R. Griffith, J. M. Langenhan, J. S. Thorson, *Curr. Opin. Biotechnol.* **16**, 622 (2005).
6. K. M. Koeller, C. H. Wong, *Chem. Rev.* **100**, 4465 (2000).
7. J. Ahlert *et al.*, *Science* **297**, 1173 (2002).
8. Analysis of the CLM γ_1^I biosynthetic gene cluster revealed four putative GT-encoding genes, *calG1*, *calG2*, *calG3*, and *calG4*, implicating a distinct GT for each sugar attachment (*7*). The *calG1* and *calG4* genes were expressed and purified to near homogeneity (fig. S1), with overall yields of 10 to 15 mg per liter of culture, as described in the Materials and Methods.
9. S. Walker, R. Landovitz, W. D. Ding, G. A. Ellestad, D. Kahne, *Proc. Natl. Acad. Sci. U.S.A.* **89**, 4608 (1992).
10. M. Oberthür, C. Leimkuhler, D. Kahne, *Org. Lett.* **6**, 2873 (2004).
11. H. C. Losey *et al.*, *Biochemistry* **40**, 4745 (2001).
12. C. T. Walsh, H. C. Losey, C. L. Freel Meyers, *Biochem. Soc. Trans.* **31**, 487 (2003).
13. X. Fu *et al.*, *Nat. Biotechnol.* **21**, 1467 (2003); and references cited therein.
14. T. Bililign, E. M. Shepard, J. Ahlert, J. S. Thorson, *ChemBioChem* **3**, 1143 (2002).
15. S. Blanchard, J. S. Thorson, *Curr. Opin. Chem. Biol.* **10**, 263 (2006).
16. Nicolaou and co-workers achieved the enantioselective synthesis of CLM γ_1^I in 29 steps with an overall yield of 0.63% (*17*), whereas Danishefsky and co-workers achieved CLM γ_1^I in 17 steps with an overall yield of 0.67% (*18*).
17. K. C. Nicolaou *et al.*, *J. Am. Chem. Soc.* **115**, 7625 (1993).
18. S. A. Hitchcock, M. Y. Chumoyer, S. H. Boyer, S. H. Olson, S. J. Danishefsky, *J. Am. Chem. Soc.* **117**, 5750 (1995).
19. Advanced synthetic intermediates related to these NDP sugars have been reported. As a point of comparison, the simpler substrate TDP-β-L-rhamnose has been prepared by a five-step chemical synthesis with an overall yield of 27% or by a two-step enzymatic method with 62% yield (*20*). The most advanced intermediate corresponding to the aminopentoses found in the CLMs required 11 linear steps and provided an overall yield of <12% (*21*).
20. K. Marumo *et al.*, *Eur. J. Biochem.* **204**, 539 (1992).
21. S.-H. Kim, D. Augeri, D. Yang, D. Kahne, *J. Am. Chem. Soc.* **116**, 1766 (1994).
22. L. Glaser, D. H. Brown, *J. Biol. Chem.* **228**, 729 (1957).
23. Cardini *et al*. first demonstrated the reversibility of the native sucrose synthetase reaction (*24*), which has subsequently been exploited to prepare UDP glucose on large scale (*25*). However, this enzyme is unique among Leloir GTs in that it catalyzes the formation of an unusually high-energy sucrose glycosidic linkage [Gibbs free energy (ΔG°) of −29.3 kJ/mol] (*26*). The reversibility of a reaction catalyzed by macrolide resistance GT OleD was implicated by the measurement of its equilibrium constant (K_{eq} = 156) (*27*). Reversibility of the reaction catalyzed by macrolide GT VinC using a threefold molar excess of VinC was also recently reported (*28*). The reaction catalyzed by the unusually fast plant galactosyltransferase F3GalTase has also been shown to be readily reversible (*29*).
24. C. E. Cardini, L. F. Leloir, J. Chiriboga, *J. Biol. Chem.* **214**, 149 (1955).
25. C. Rupprath, T. Schumacher, L. Elling, *Curr. Med. Chem.* **12**, 1637 (2005).
26. E. F. Neufeld, W. Z. Hassid, *Adv. Carbohydr. Chem.* **18**, 309 (1963).
27. L. M. Quiros, R. J. Carbajo, A. F. Brana, J. A. Salas, *J. Biol. Chem.* **275**, 11713 (2000).
28. A. Minami, K. Kakinuma, T. Eguchi, *Tetrahedron Lett.* **46**, 6187 (2005).
29. K. D. Miller, V. Guyon, J. N. S. Evans, W. A. Shuttleworth, L. P. Taylor, *J. Biol. Chem.* **274**, 34011 (1999).

30. We thank the UW–Madison School of Pharmacy Analytical Instrumentation Facility for analytical support, S. Borisova and H.-w. Liu (University of Texas, Austin) for the gift of TDP-α-L-rhamnose and TDP-β-L-rhamnose, C. T. Walsh (Harvard Medical School, Boston, MA) for providing GtfD and GtfE expression clones, Wyeth Research for the generous gift of CLM analogs, and G. Williams and Y. Huang for many helpful discussions. B.R.G. is a postdoctoral fellow of the American Cancer Society (PF-05-016-01-CDD), and Q.F. acknowledges a graduate fellowship sponsored by Merck Research Laboratories, the Analytical Division of the American Chemical Society, and the DuPont Corporate Center for Analytical Sciences. This research was supported in part by NIH grant nos. AI52218, CA84374, and GM70637; National Cooperative Drug Discovery Group grant U19 CA113297 from the National Cancer Institute (to J.S.T.); the UW School of Pharmacy; Wisconsin Alumni Research Foundation; and a NSF CAREER Award (CHE-0449991 to L.L.). L.L. is an Alfred P. Sloan research fellow, and J.S.T. is an H. I. Romnes fellow. J.S.T. has served on the scientific advisory boards of zuChem and Kosan. J.S.T. dedicates this paper to P. G. Schultz on the occasion of Schultz's 50th birthday.

Supporting Online Material

www.sciencemag.org/cgi/content/full/313/5791/1291/DC1
Materials and Methods
Figs. S1 to S15
References

16 May 2006; accepted 11 July 2006
10.1126/science.1130028

Structural Asymmetry of AcrB Trimer Suggests a Peristaltic Pump Mechanism

Markus A. Seeger,[1,3]* André Schiefner,[2]*† Thomas Eicher,[1] François Verrey,[1] Kay Diederichs,[2] Klaas M. Pos[1]‡

The AcrA/AcrB/TolC complex spans the inner and outer membranes of *Escherichia coli* and serves as its major drug-resistance pump. Driven by the proton motive force, it mediates the efflux of bile salts, detergents, organic solvents, and many structurally unrelated antibiotics. Here, we report a crystallographic structure of trimeric AcrB determined at 2.9 and 3.0 angstrom resolution in space groups that allow asymmetry of the monomers. This structure reveals three different monomer conformations representing consecutive states in a transport cycle. The structural data imply an alternating access mechanism and a novel peristaltic mode of drug transport by this type of transporter.

Drug resistance during infection or cancer treatment is often caused by the overproduction of efflux transporters, leading to decreased levels of antibiotics or chemotherapeutics inside the cells (*1*, *2*). Drug-efflux transporters can be of the ABC type that use the free energy of adenosine triphosphate (ATP) hydrolysis, or they can be secondary transporters that use the proton motive force to energize the extrusion of drugs. ABC-type transporters are predominantly found in eukaryotes, whereas in prokaryotes the main drug-efflux systems function as H^+/drug exchangers. In Gram-positive bacteria, drug resistance is often conferred by members of the major facilitator superfamily (*3*). In Gram-negative bacteria, however, resistance-nodulation-cell division (RND) type efflux pumps play a dominant role (*1*, *4*). Structures of the primary membrane transport proteins bacteriorhodopsin (*5*–*7*) and the Ca^{2+}-ATPase (*8*) in different conformations allowed to establish hypotheses about a solute transport pathway. Transport of solutes by secondary carriers of the major facilitator superfamily [LacY (*9*) and GlpT (*10*)] and the glutamate transporter homolog Glt_{Ph} (*11*–*13*) is likewise expected to depend on major structural conversions (*14*).

The first structure of the RND pump AcrB was obtained at 3.5 Å resolution from crystals grown in a trigonal space group assigned as *R*32 (*15*–*18*). An AcrB monomer contains 12 transmembrane α helices (TM1 to TM12) (fig. S1). TM4 and TM10 are surrounded by the other transmembrane helices of the monomer and harbor the residues D407, D408 (TM4), and K940 (TM10), which appear to play an essential role in proton translocation (*16*, *19*). The periplasmic part of AcrB consists of the TolC

[1]Institute of Physiology and Zurich Centre for Integrative Human Physiology (ZIHP), University of Zurich, Winterthurerstrasse 190, Zürich, Switzerland. [2]Department of Biology, University of Konstanz, Universitätsstrasse 10, M647, D-78457 Konstanz, Germany. [3]Institute of Microbiology, Swiss Federal Institute of Technology (ETH), Zürich, Switzerland.

*These authors contributed equally to this work.
†Present address: Department of Molecular Biology, BCC206, The Scripps Research Institute (TSRI), 10550 North Torrey Pines Road, La Jolla, CA 92037, USA.
‡To whom correspondence should be addressed. E-mail: kmpos@access.unizh.ch

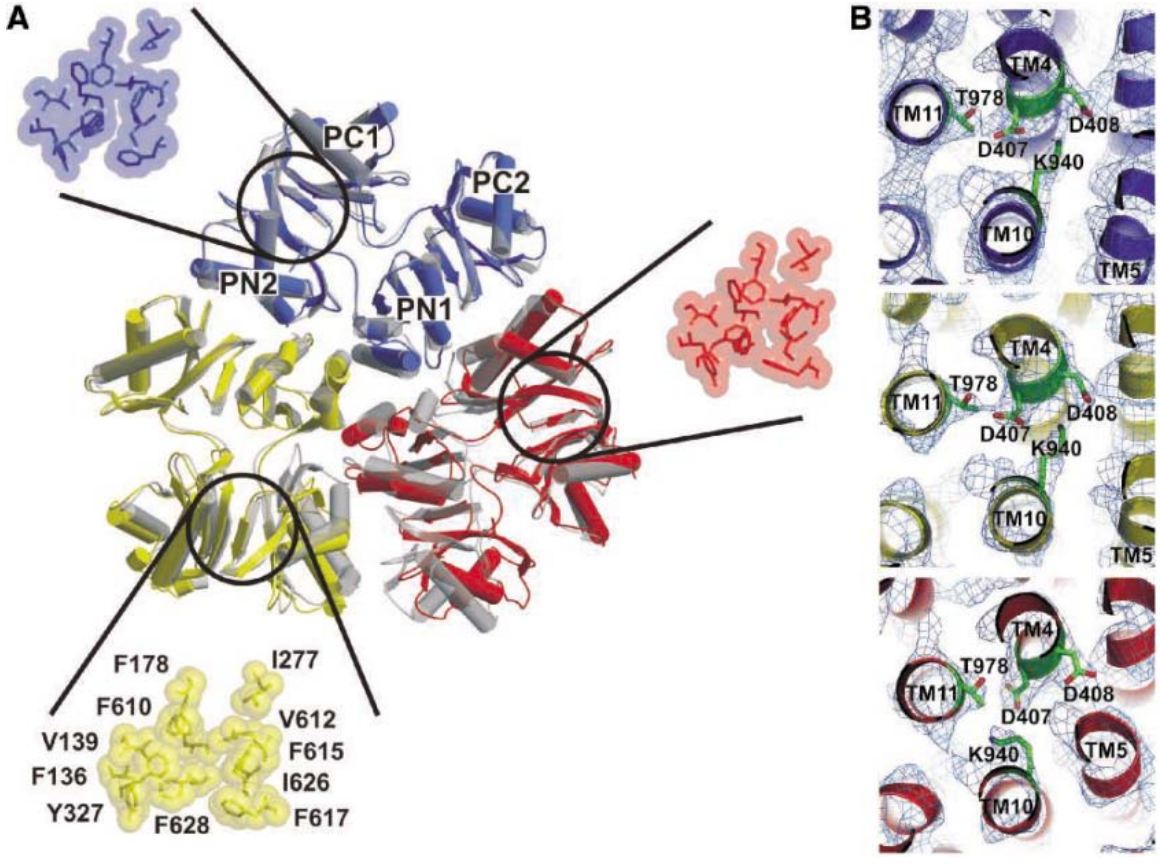

Fig. 1. Main structural differences of the AcrB monomers. (**A**) The three AcrB monomers shown in top view as cylinder presentation in blue (L), yellow (T), and red (O) are superimposed onto the symmetric AcrB trimer model depicted in transparent gray. In the T monomer (yellow), a hydrophobic pocket is defined by phenylalanines 136, 178, 610, 615, 617, and 628; valines 139 and 612; isoleucines 277 and 626; and tyrosine 327 at the PN2/PC1 interface. (**B**) Structural changes in the putative proton translocation site. Conserved residues D407, D408 (TM4), and K940 (TM10) in the three monomers (L, blue; T, yellow; O, red) are depicted with 2Fo-Fc electron density maps contoured at 0.5 σ (L) or 1 σ (T and O) as viewed from the cytoplasm. In the L and T monomers, the same conformation is observed, whereas in the O monomer, K940 forms a salt bridge with D407. This interaction seems to be stabilized by hydrogen bonding of T978 (TM11). To restore the geometry as it appears in the L monomer, proton uptake is anticipated.

docking domain (DN and DC subdomains), which is located farthest from the membrane plane, and the pore domain, composed of subdomains PN1, PN2, PC1, and PC2. The TolC docking domain, on which TolC has been shown to dock coaxially (*20*), exhibits a funnel-like structure narrowing to a central pore located in the pore domain. The central pore structure consists of three α helices (designated pore helices) donated by the PN1 subdomains of each AcrB monomer. Near the membrane plane, the central pore leads to a central cavity, and further to a 35 Å wide transmembrane hole defined by the ringlike arrangement of the TM helices of the trimer, which was proposed to be filled with phospholipids (*16*). Three vestibules at the monomer interfaces located just above the membrane plane lead toward the central cavity. The current hypothesis about the mechanism of transport envisions the diffusion of substrates via the transmembrane domains and vestibules into the central cavity and the opening of the central pore to allow the transport of the substrates through AcrB toward TolC (*21*) and export to the external medium (*16*, *22*). Large changes were postulated to be associated with this transport function, which was tentatively termed "elevator mechanism" (*17*), but remained elusive because of a lack of structural information.

Here, we define the structural changes that constitute the basis of solute transport by AcrB. To gain structural insight into the mechanism of transport by AcrB, crystals belonging to monoclinic (*C*2, 2.9 Å resolution) and triclinic (*P*1, 3.0 Å resolution) space groups were grown, and complete data sets with good statistics were measured (table S1). Previous functional interpretations (*16*–*18*, *23*) were based on the trigonal crystal form, which harbors a trimer with exact three-fold symmetry. In this crystal form, models with good geometry and low crystallographic *R* factor have not been reported so far. Our subsequent analysis revealed that those crystals that appeared to be *R*32 suffered from merohedral twinning and were in fact twinned *R*3 crystals with noncrystallographic symmetry (table S1). A high twinning fraction results in a blurred electron density, which cannot be computationally deconvoluted, and explains the difficulties encountered with the trigonal crystal form. We therefore analyzed the data from the untwinned *C*2 and *P*1 crystal forms containing three and six monomers corresponding to one and two nonsymmetric trimers, respectively.

The structures of these three independently obtained asymmetric trimers are very similar (table S2); distances given below refer to the asymmetric trimer from the well-diffracting *C*2 crystal form. Its atomic model (Fig. 1) was refined to R factors of R = 22.6 % (R_{free}, 26.7 %) (table S1). It is substantially more complete than the model based on the trigonal crystal form and contains one consecutive chain of amino acids 2 to 1033 in two monomers and of amino acids 2 to 1045 in the third monomer. The C-terminal amino acids 1034 to 1057 (1046 to 1057) are unassigned as a result of missing electron density.

At root mean square deviations (RMSD) between 2.1 and 3.1 Å (table S2), the monomers of a trimer structurally deviate from each other much more than can be expected from monomers obeying noncrystallographic symmetry (Fig. 1 and fig. S2). One monomer appears not to be constrained by interaction with its neighbors, and its conformation is therefore termed loose (L). Another exhibits an opening from the inside of the pore domain toward the funnel of the AcrB trimer, and its conformation is designated as open (O). In this monomer, the PN1 subdomain is tilted toward and tightly interacts with the neighboring monomer's PN1 and PN2 subdomains. This interaction imposes a constraint on the conformation of the neighboring monomer, which we label tight (T). The conformation of the L monomer is closest (RMSD of 0.9 Å) (table S2) to that of the symmetric AcrB monomer model, whereas the T and O monomers

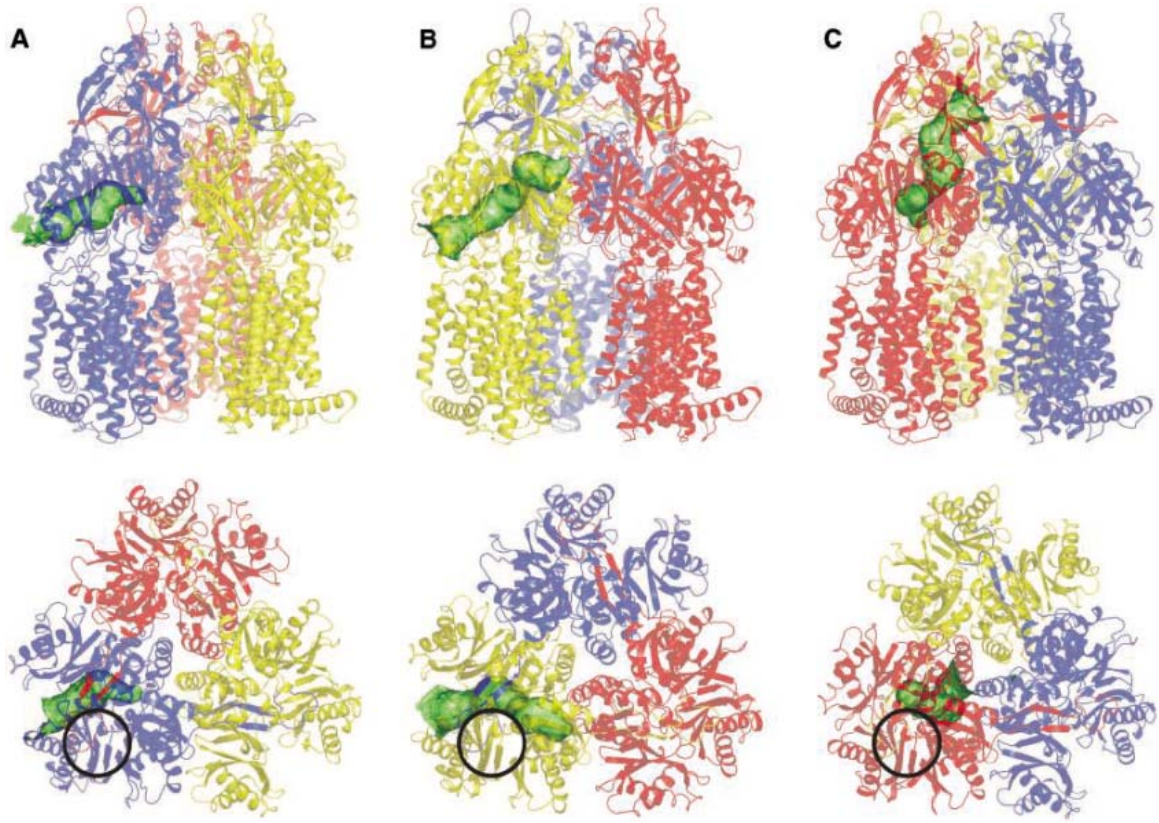

Fig. 2. Visualization of tunnels in the pore domain of the AcrB peristaltic drug efflux pump. Each monomer shows a tunnel penetrating the periplasmic part in a distinct manner. The tunnels are highlighted as green surfaces in a ribbon model of the AcrB trimer. The upper panels shows the side view and the lower panels the top view of the AcrB trimer. (**A**) In the L monomer (blue), the tunnel starts at the lateral cleft (PC1/PC2 interface) ~15 Å above the membrane plane extending halfway toward the center (pore) of the trimer. (**B**) In the T monomer (yellow), the tunnel extends diagonally upward through the pore domain (PN1/PN2 interface) toward the pore in the center of the trimer. (**C**) With the conversion from T to O, the PC1/PC2 cleft closes because of the conformational change of the PC2 subdomain and leads to complete closure of the tunnel laterally. Moreover, tilting of the PN1 subdomain in the O monomer creates an exit pathway toward the funnel and TolC. The location of the hydrophobic binding pocket in the T monomer (yellow) is indicated in each conformation by a black circle. Only in the T monomer is this binding pocket accessible for substrates.

differ significantly from it (RMSD of 1.8 and 3.0 Å, respectively) (table S2).

The largest structural changes are located in the pore domain of the trimer, whereas in the TolC docking domain, including the inter-monomer connecting loops, no major structural differences are detected (fig. S2). A prominent feature of the AcrB trimer is the periplasmic central "pore," composed of PN1 subdomain α helices (Fig. 1A). Compared with the orientation of the other PN1 subdomains, the PN1 subdomain of the O monomer is considerably tilted (~12°) toward the PN1 and PN2 subdomains of the T monomer (Fig. 1A). A synchronous reorientation of the PC2 subdomain mediated through an antiparallel β-sheet (Nβ2-Cβ13) interaction (fig. S1) in the O monomer reduces the distance between the PC2 subdomain and the membrane plane by more than 6.5 Å (figs. S2 and S3). A coil-to-helix transition and bending of the helical N-terminal part of TM8 appears to be associated with this large conformational change. This part of TM8 adopts a coil conformation in the L monomer and forms an intermediate conformation in the T monomer and a kinked helix in the O monomer (fig. S3B). In the T monomer, the PC2 subdomain does not change in comparison to the L-monomer conformation, most probably because the PN1 subdomain (and therefore the PC2 subdomain) is locked because of interaction with the O monomer's PN1 subdomain (Fig. 1A). A contraction of the T monomer is observed as a result of the movement of its TM helices (except TM2) of up to 3 Å toward its periplasmic part (fig. S2) and appears to be induced by the upshift of the PN1 subdomain of the T monomer because of interaction with the PN1 subdomain of the O monomer (Fig. 1). From the PN1 subdomain, the upshift is transduced to TM3 and TM4 by two parallel β sheets, Nβ1′ and Nβ16 (fig. S1).

The structural changes in the T monomer create a hydrophobic pocket in the PN2/PC1 subdomain interface (Fig. 1A), which is not present in the L and O monomers. We suggest that the hydrophobic pocket located on the T monomer may supply a substrate binding pocket inside the pore domain (Fig. 1A).

Visualization of cavities within the protein revealed large tunnels in the pore domain of all three monomers (Fig. 2). The width of these tunnels would be sufficient to accommodate solute molecules transported by AcrB. In the L and T monomers, a large, laterally accessible pathway is present about 15 Å above the membrane plane. In vivo, AcrA (*24*) is expected to protect the lateral exit against direct contact with the periplasm (*16*, *25*, *26*). In the T monomer, the tunnel leads to residues of the O monomer PN1 subdomain, which operates as a plug for the tunnel exit. In the O conformation, the tilting of the PN1 subdomain opens an exit pathway from the binding pocket toward the funnel of AcrB. Because of the simultaneous structural change of the PN1 and PC2 subdomains, the lateral entrance of the tunnel observed in the L and T monomer is completely closed in the O monomer and determines the direction of substrate transport toward the funnel (Fig. 2C).

The asymmetric structure of AcrB suggests that the three monomer conformations represent consecutive states of a transport cycle. A possible drug-transport mechanism can be proposed if a cycling of each monomer through the conformations L, T, O, and back to L is assumed. The PN1 subdomains, including the pore helices, might play the role of a ratchet pin that enforces the order of the conformational changes. The PN1 conformational change from O to the L monomer causes the loss of strong interaction with the PN1 and PN2 subdomains of the T monomer and enables the conversion of the PN1/PC2 subdomains from T to the O monomer conformation. Consequently, bound substrate in the T monomer would be squeezed out of the hydrophobic pocket located at the interface of the PN2/PC1 subdomains during the transition to the O monomer conformation. The conversion of the PN1 subdomain of the T monomer into the tilted conformation of the O monomer also reestablishes strong interaction with the PN2 subdomain of the L monomer and induces conformational changes leading to formation of the binding pocket at the PN2/PC1 interface (Fig. 1) and the change from the L to the T monomer conformation.

This sequence of events creates a pathway for the efflux of drugs through the tunnels with a transport mechanism that is analogous to that of a peristaltic pump and is schematically displayed in Fig. 3. Diffusion of substrate within the tunnel is limited by an occlusion site whose position migrates toward the funnel, effectively guiding the substrate toward TolC. The unspecific nature of transport implied by such a mechanism could account for the observed broad substrate specificity of the AcrA/AcrB/TolC

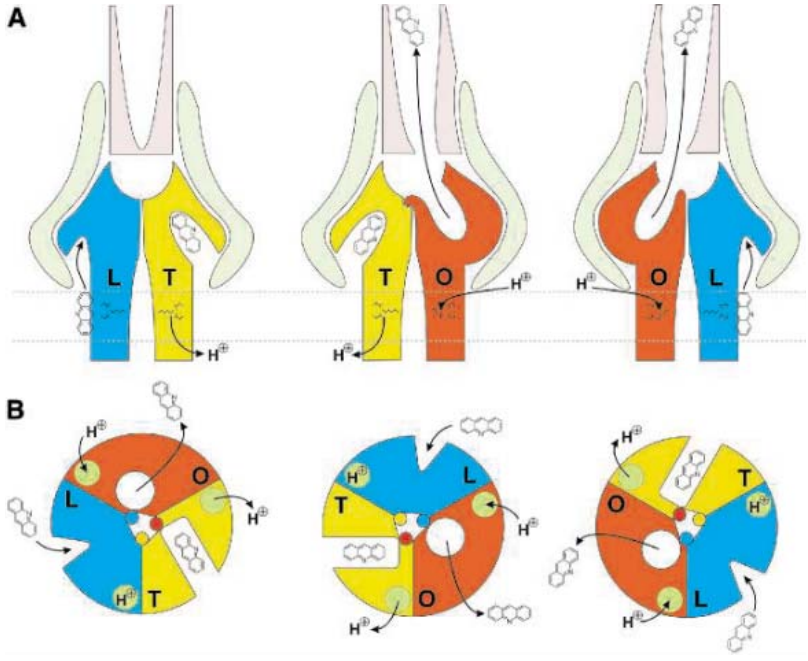

Fig. 3. Schematic representation of the AcrB alternating site functional rotation transport mechanism. The conformational states loose (L), tight (T), and open (O) are colored blue, yellow and red, respectively. (**A**) Side-view schematic representation of two of the three monomers of the AcrB trimer. AcrA and TolC are indicated in light green and light purple colors, respectively. The proposed proton translocation site (D407, D408, and K940) is indicated in the membrane part of each monomer. (**B**) The lateral grooves in the L and T monomer indicate the substrate binding sites. The different geometric forms reflect low (triangle), high (rectangle), or no (circle) binding affinity for the transported substrates. The PN1 subdomains (including the pore helices) located in the middle of the model are highlighted and form the corners of an asymmetric triangle (white) to indicate the communication between the monomers. In the first state of the cycle, a monomer binds a substrate (acridine) in its transmembrane domain (L conformation), subsequently transports the substrate from the transmembrane domain to the hydrophobic binding pocket (conversion to T conformation) and finally releases the substrate in the funnel toward TolC (O conformation). The conversion from the O-monomer to the L-monomer conformation is suggested to be the major energy-requiring (proton motive force–dependent) step in this functional rotation cycle and requires the binding of a proton to the proton translocation site (D407, D408, and K940) from the periplasm. The conversion from the T monomer to the O monomer is accompanied by the release of a proton from the proton translocation site to the cytoplasm. AcrA can be expected to participate in the transduction of the conformational changes from AcrB to TolC, which results in the opening of the TolC channel and the facilitation of drug extrusion to the outside of the cell.

pump as well as for the transport of small molecules such as hexane (*27*, *28*). It is therefore proposed that besides the specific binding in the hydrophobic pocket of the T monomer, unspecific diffusion of small substrates through the observed tunnels occurs. Substrate transport from the membrane domain to the periplasmic tunnel might be via a lateral pathway, including the TM8/TM9 groove and the AcrA/AcrB interface. Recent reports (*25*, *26*) substantiate the close interaction between AcrA and AcrB (or of the homolog proteins MexA and MexB) in the tripartite complex, and we therefore anticipate conformational changes of AcrA coupled to those of AcrB. On the other hand, our structure does not support substrate transport through the central pore, as implied by the elevator mechanism (*14*, *17*), because access of substrates from the central cavity to the funnel is prohibited by the small diameter of the pore.

As AcrB is energized by the proton-motive force, transient protonation of titratable groups within the transmembrane domain of the protein can be expected to be the mechanism that delivers the energy required for the conformational changes described above. Indeed, we observe a prominent K940 (TM10) side-chain reorientation away from D408 and toward D407 (both on TM4) in the O conformation (Fig. 1B) and a bulging of TM5 toward TM4 and TM10, strengthening the hypothesis that this part of the transmembrane domain is central to proton binding and release (*16*, *19*). As thoroughly investigated in the case of bacteriorhodopsin (*5*–*7*, *29*), side-chain rearrangements (Fig. 1B) can leverage global conformational changes of the magnitude we observed for TM8 (fig. S3), involving reversible tilts of helices and the transient change of kinks and bulges in the main chain. We speculate that, in the case of AcrB, subtle changes in the transmembrane part (TM4 and TM10) produce the large conformational changes in the pore domain ultimately resulting in drug efflux. Different from what has been suggested for LacY (*30*) and EmrE (*31*), the proton and substrate translocation in AcrB appear to be spatially separated.

We have proposed a possible transport mechanism that, based on a functional rotation of the trimer, creates a peristaltic pump mechanism in each monomer (Fig. 3). Our model merges Jardetzky's alternate access pump (*32*) with the rotating site catalysis of F_1F_0-ATPase (*33*, *34*) and suggests a working hypothesis for the transport mechanism of RND transporters.

References and Notes

1. X. Z. Li, H. Nikaido, *Drugs* **64**, 159 (2004).
2. S. V. Ambudkar, I. W. Kim, Z. E. Sauna, *Eur. J. Pharm. Sci.* **27**, 392 (2006).
3. P. N. Markham, A. A. Neyfakh, *Curr. Opin. Microbiol.* **4**, 509 (2001).
4. K. Poole, *Clin. Microbiol. Infect.* **10**, 12 (2004).
5. J. K. Lanyi, *Mol. Membr. Biol.* **21**, 143 (2004).
6. H. Luecke, *Biochim. Biophys. Acta* **1460**, 133 (2000).
7. R. Neutze *et al.*, *Biochim. Biophys. Acta* **1565**, 144 (2002).
8. C. Toyoshima, G. Inesi, *Annu. Rev. Biochem.* **73**, 269 (2004).
9. J. Abramson *et al.*, *Science* **301**, 610 (2003).
10. Y. Huang, M. J. Lemieux, J. Song, M. Auer, D. N. Wang, *Science* **301**, 616 (2003).
11. D. Yernool, O. Boudker, Y. Jin, E. Gouaux, *Nature* **431**, 811 (2004).
12. D. J. Slotboom, I. Sobczak, W. N. Konings, J. S. Lolkema, *Proc. Natl. Acad. Sci. U.S.A.* **96**, 14282 (1999).
13. M. Grunewald, B. I. Kanner, *J. Biol. Chem.* **275**, 9684 (2000).
14. I. Sobczak, J. S. Lolkema, *Curr. Opin. Microbiol.* **8**, 161 (2005).
15. K. M. Pos, K. Diederichs, *Acta Crystallogr. Biol. Crystallogr.* **D58**, 1865 (2002).
16. S. Murakami, R. Nakashima, E. Yamashita, A. Yamaguchi, *Nature* **419**, 587 (2002).
17. E. W. Yu, G. McDermott, H. I. Zgurskaya, H. Nikaido, D. E. Koshland Jr., *Science* **300**, 976 (2003).
18. K. M. Pos, A. Schiefner, M. A. Seeger, K. Diederichs, *FEBS Lett.* **564**, 333 (2004).
19. L. Guan, T. Nakae, *J. Bacteriol.* **183**, 1734 (2001).
20. N. Tamura, S. Murakami, Y. Oyama, M. Ishiguro, A. Yamaguchi, *Biochemistry* **44**, 11115 (2005).
21. V. Koronakis, A. Sharff, E. Koronakis, B. Luisi, C. Hughes, *Nature* **405**, 914 (2000).
22. S. Murakami, N. Tamura, A. Saito, T. Hirata, A. Yamaguchi, *J. Biol. Chem.* **279**, 3743 (2004).
23. E. W. Yu, J. R. Aires, G. McDermott, H. Nikaido, *J. Bacteriol.* **187**, 6804 (2005).
24. J. Mikolosko, K. Bobyk, H. I. Zgurskaya, P. Ghosh, *Structure* **14**, 577 (2006).
25. D. Nehme, K. Poole, *Antimicrob. Agents Chemother.* **49**, 4375 (2005).
26. T. Touze *et al.*, *Mol. Microbiol.* **53**, 697 (2004).
27. D. G. White, J. D. Goldman, B. Demple, S. B. Levy, *J. Bacteriol.* **179**, 6122 (1997).
28. X. Z. Li, L. Zhang, K. Poole, *J. Bacteriol.* **180**, 2987 (1998).
29. B. W. Edmonds, H. Luecke, *Front. Biosci.* **9**, 1556 (2004).
30. O. Mirza, L. Guan, G. Verner, S. Iwata, H. R. Kaback, *EMBO J.* **25**, 1177 (2006).
31. N. Gutman, S. Steiner-Mordoch, S. Schuldiner, *J. Biol. Chem.* **278**, 16082 (2003).
32. O. Jardetzky, *Nature* **211**, 969 (1966).
33. J. P. Abrahams, A. G. Leslie, R. Lutter, J. E. Walker, *Nature* **370**, 621 (1994).
34. P. D. Boyer, *Annu. Rev. Biochem.* **66**, 717 (1997).

35. We thank the beamline staff at the Swiss Light Source (SLS) of the Paul Scherrer Institut in Villigen (Switzerland), and at the European Synchrotron Radiation Facility (ESRF) in Grenoble (France). This work was supported by a grant of the Transregio-Sonderforschungsbereich Zurich-Konstanz to K.D. We thank P. A. Karplus and W. Welte for critical reading and discussion. The atomic coordinates and structure factors of the C2 and P1 crystal forms have been deposited at the Protein Data Bank with accession numbers 2GIF and 2HRT, respectively. This work is dedicated to Peter Dimroth on the occasion of his 65th birthday.

Supporting Online Material

www.sciencemag.org/cgi/content/full/313/5791/1295/DC1
Materials and Methods
Figs. S1 to S3
Tables S1 and S2
References

20 June 2006; accepted 1 August 2006
10.1126/science.1131542

CYK-4/GAP Provides a Localized Cue to Initiate Anteroposterior Polarity upon Fertilization

Noah Jenkins,* Jennifer R. Saam,* Susan E. Mango‡

The *Caenorhabditis elegans* anteroposterior axis is established in response to fertilization by sperm. Here we present evidence that RhoA, the guanine nucleotide–exchange factor ECT-2, and the Rho guanosine triphosphatase–activating protein CYK-4 modulate myosin light-chain activity to create a gradient of actomyosin, which establishes the anterior domain. CYK-4 is enriched within sperm, and paternally donated CYK-4 is required for polarity. These data suggest that CYK-4 provides a molecular link between fertilization and polarity establishment in the one-cell embryo. Orthologs of CYK-4 are expressed in sperm of other species, which suggests that this cue may be evolutionarily conserved.

Many organisms depend on sperm entry to polarize the one-cell embryo. In *C. elegans*, sperm establish the anteroposterior axis and lead to asymmetric distribution of PAR-3 and PAR-6 to the anterior cortex (*1*). The prevailing view is that sperm modulate actomyosin contractility, which induces cortical flow toward the nascent anterior pole, thereby pulling PAR-3 and PAR-6 anteriorly (*2*–*4*). Two models could account for how contractile forces become asymmetric. One possibility is that sperm entry generates a physical disruption in the actomyosin network, enabling the network to pull away from the site of sperm entry. Alternatively, a component of sperm could control actomyosin contractility while leaving the network physically intact. Here we describe a sperm-donated factor that controls the actomyosin cytoskeleton and anterior PAR localization.

Our previous studies demonstrated that the guanosine triphosphatase (GTPase)–activating protein (GAP) *cyk-4* was critical to polarize epithelia (*5*, *6*). To investigate the role of *cyk-4*

Department of Oncological Sciences, Huntsman Cancer Institute, University of Utah, Salt Lake City, UT 84112, USA.

*These authors contributed equally to this work.
‡To whom correspondence should be addressed. E-mail: susan.mango@hci.utah.edu

during polarization, we examined the fertilized embryo, a well-characterized model for polarity (*2*). Antibody staining revealed that CYK-4 was dramatically enriched in sperm (64 out of 64 embryos examined) (Fig. 1, A and B). Inactivation of *cyk-4* by RNA interference (RNAi) indicated that staining was specific and RNAi effective (fig. S1) (*7*). Upon fertilization, CYK-4 could be detected at the posterior cortex of the one-cell embryo of both wild-type embryos and embryos lacking maternal CYK-4 (Fig. 1, C to K, and figs. S2 and S3) (*7*). We observed paternal CYK-4 in punctate structures, derived from sperm membranous organelles (MOs) and often associated with the sperm pronucleus (*8*). Based on nuclear morphology, paternal CYK-4 remained associated with the cortex and MOs during meiosis and the onset of polarity, a period of about 30 min (Fig. 1, C to K) (*2*).

To determine whether *cyk-4* was important for polarity, we examined anterior PAR proteins using green fluorescent protein (GFP) reporters in *cyk-4(RNAi)* embryos (Fig. 2, A and B) (*7*). In wild-type embryos, PAR-6::GFP was confined to 47% of egg length at the time of pronuclear meeting. In *cyk-4(RNAi)* embryos, PAR-6::GFP expanded to 87% of egg length, and endogenous PAR-3 was observed throughout the cortex (table S1 and fig. S4). These data suggest that *cyk-4* is required to establish anterior polarity.

In other organisms, *cyk-4* orthologs function with the guanine nucleotide exchange factor (GEF) *ect-2* during cytokinesis (*9*), which prompted us to examine *ect-2*. Antibody staining revealed that ECT-2 was enriched with nonmuscle myosin NMY-2::GFP at the cell cortex ($n > 20$) (Fig. 3). Colocalization of these two proteins in multiple images suggested that ECT-2 moves anteriorly coincident with NMY-2::GFP. Reduction of *ect-2* by RNAi indicated that staining was specific and RNAi effective (13 out of 16) (fig. S1). Inactivation of *ect-2* led to distribution of PAR-6::GFP and PAR-3 throughout the cortex at the time of pronuclear meeting, in addition to pronounced cytokinesis defects (Fig. 2C, and table S1 and fig. S4) (*7*). Because *ect-2* and *cyk-4* polarity phenotypes were visible before the first cell division, mislocalization of anterior PAR proteins was not a secondary consequence of failed mitosis. We conclude that *cyk-4* and *ect-2* are critical to establish the anterior PAR domain.

ect-2 and *cyk-4* are predicted to control Rho family GTPases, which suggested a possible mechanism for controlling polarity. In vitro, *cyk-4* can function as a GAP for *rhoA*, *cdc-42*, or *rac*, and in vivo, it likely controls RhoA during cytokinesis (*10*). We found that in embryos with reduced RhoA [*rho-1(RNAi)*], PAR-6::GFP was dispersed throughout the cortex at pronuclear meeting (Fig. 2D and table S1). This phenotype resembled that of *ect-2(RNAi)*, which suggested that ECT-2 and RHO-1 function in a common pathway. The similarity of phenotypes contrasts with those associated with other *C. elegans* GTPases. For example, *cdc-42* is required for posterior PAR localization and spindle positioning, but not for initial anterior PAR localization (*11*). No early polarity defects have been noted for the three *C. elegans rac* genes *ced-10*, *mig-2*, and *rac-2*, even when they were inactivated together (*12*). These observations suggest that RHO-1/RhoA is a good candidate effector for ECT-2 and, by extension, CYK-4 during the initial stages of polarization. We propose that the regulatory cassette of *rho-1*, *cyk-4*, and *ect-2* that is used during cytokinesis is also deployed for polarity.

Normally, anterior PAR localization depends on a gradient of actomyosin toward the anterior pole (*3*, *4*). Because Rho proteins control the actomyosin cytoskeleton in many contexts, we examined the actomyosin cytoskeleton with nonmuscle myosin NMY-2::GFP. In wild-type embryos, NMY-2::GFP was present at the egg cortex, where it formed coalescing foci that advanced anteriorly (Fig. 4, A to C) (*7*). In 7 out of 10 *ect-2(RNAi)* and 6 out of 8 *rho-1(RNAi)* embryos, a lower proportion of NMY-2::GFP localized cortically, and this remaining protein failed to coalesce into large foci (Fig. 4, D to I) (*7*). These data suggest that *ect-2* and *rho-1* are critical to generate a contractile actomyosin network.

Conversely, *cyk-4* controlled relaxation or disassembly of the actomyosin network. Of 30 *cyk-4(RNAi)* embryos, 15 had a dynamic actomyosin network that remained evenly distributed over the cortex (Fig. 4, J to L) (*7*). In these embryos, initial contractility appeared wild type but sperm-induced asymmetry was lost. In 10 out of 30, asymmetric NMY-2::GFP occurred, but the global transition from foci to puncta was delayed until after pronuclear meeting, which suggested a temporal role for *cyk-4* (fig. S5) (*7*). The remaining 5 out of 30 embryos had an intermediate phenotype (fig. S6) (*7*). The variable *cyk-4(RNAi)* phenotypes could reflect incomplete inactivation by RNAi or the existence of additional polarity pathways.

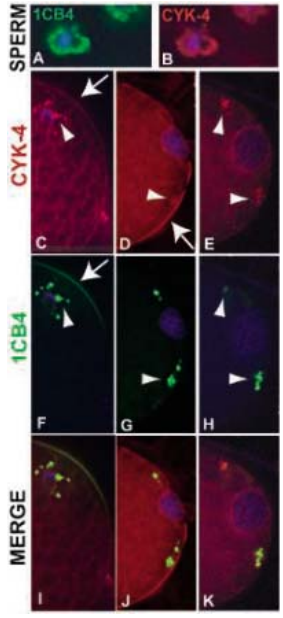

Fig. 1. CYK-4 is enriched in sperm. (**A** and **B**) Endogenous CYK-4 (red) localizes within sperm, which are costained with the membranous organelle marker 1CB4 (green) (*8*, *25*); DNA is blue. Paternal CYK-4 in embryos (**C** to **K**): embryos that are maternally *cyk-4(RNAi)* but paternally CYK-4+. [(C), (F), and (I)] before meiosis; [(D), (G), and (J)] undergoing meiosis II; [(E), (H), and (K)] post meiosis, with polarity initiation. Paternal CYK-4 is at the posterior cortex (arrows) and in membranous organelles (arrowheads). Anterior is left and embryos are ~50 μm long.

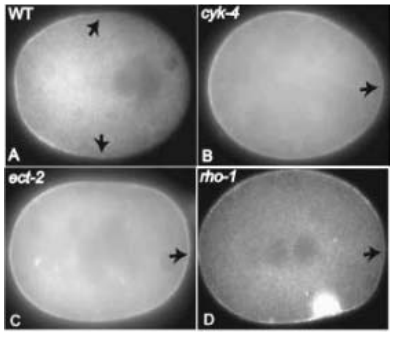

Fig. 2. Anterior localization of PAR-6::GFP depends on *cyk-4*/GAP, *ect-2*/GEF, and *rho-1*/RhoA. Compared with the wild type (WT) (**A**), PAR-6::GFP is expanded in *cyk-4(RNAi)* (**B**), *ect-2(RNAi)* (**C**), and *rho-1(RNAi)* (**D**) embryos. Arrows denote end points of PAR-6::GFP.

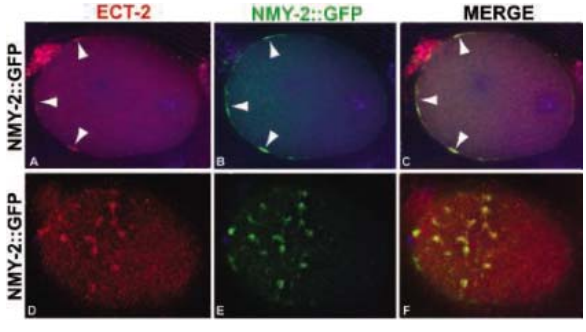

Fig. 3. ECT-2 localizes to the cortex and is coincident with NMY-2::GFP. (**A** and **D**) Endogenous ECT-2 (red) is enriched in puncta at the cell cortex. (**B** and **E**) These puncta colocalize with NMY-2::GFP (green); (**C** and **F**) merge is yellow. (A) to (C) are cross sections; (D) to (F) are surface shots. On the basis of nuclear morphology and position, embryos are undergoing pronuclear migration.

Supporting the former hypothesis, we detected CYK-4 protein in 39% of sperm after RNAi treatment (fig. S6) (*7*). These data suggest that *cyk-4* is required to down-regulate the actomyosin cytoskeleton posteriorly and, thereby, to induce asymmetric pulling forces.

One effector of RhoA is RhoA kinase, which phosphorylates myosin light chain (MLC) and MLC phosphatase, which leads to MLC activation and actomyosin contractility (*13*). In *C. elegans*, MLC-4 is required for anteroposterior polarity, actomyosin contractility, and anterior PAR localization (*14*). These observations suggested that RHO-1, ECT-2, and CYK-4 might control MLC-4. To test this idea, we monitored activated MLC using an antibody specific for phospho-MLC (*7*, *13*).

Phospho-MLC was located at the cell cortex of wild-type embryos, where it overlapped with foci of NMY-2::GFP (Fig. 5, A and B, and fig. S7) (*7*). We detected phospho-MLC associated with the anterior cortex and absent from the posterior after fertilization, indicating loss of active MLC (fig. S8) (*7*). Loss of immunoreactivity in *mlc-4*(–) embryos indicated that phospho-MLC staining was specific (fig. S9) (*7*). Phosphorylation of MLC required *ect-2* and *rho-1*, since neither *ect-2(RNAi)* ($n > 10$) nor *rho-1(RNAi)* ($n = 7$ out of 9) embryos had detectable phospho-MLC at the cell cortex (Fig. 5, C and G, and fig. S7) (*7*). As predicted, *cyk-4(RNAi)* embryos contained phospho-MLC, which colocalized with NMY-2::GFP in an extended domain ($n > 10$ one-cell embryos with meiotic defects) (Fig. 5E and fig. S8) (*7*). These findings suggest that ECT-2 and RHO-1 promote, whereas CYK-4 inhibits, activated MLC and, therefore, actomyosin contractility.

To address the importance of sperm-donated CYK-4, we examined embryos from *NMY-2::GFP* females mated with *cyk-4(RNAi)* males (*7*). As monitored by NMY-2::GFP, 29% lacked polarity altogether, whereas 17% had an intermediate phenotype ($n = 48$) (Fig. 6, D and E); the remainder looked wild type. By antibody staining, 42% of sperm had reduced or absent CYK-4 after RNAi ($n = 90$) (Fig. 6B). These data indicate that paternally endowed CYK-4 is required to polarize the embryo. Conversely, we showed CYK-4+ from male sperm could rescue polarity, but not meiotic cytokinesis, for fertilized *cyk-4(RNAi)* eggs (figs. S10 and S11).

We propose that the bolus of CYK-4 donated by sperm down-regulates the actomyosin network in the posterior, thereby generating a gradient of contractility (fig. S12) (*7*). The gradient of contractility depends on differential activation of MLC. There may be additional effectors, given that RhoA in other organisms influences the actin cytoskeleton in multiple ways. In addition to CYK-4, previous studies have shown that the sperm-donated centrosome is required for anteroposterior polarity (*1*, *15*, *16*). Currently, it is unclear whether CYK-4 acts in parallel to the centrosome or whether these two sperm cues function in a common pathway. We note that the requirement for a mature centrosome helps explain why polarity initiates after the completion of meiosis, despite the presence of paternal CYK-4 immediately after fertilization.

Consistent with the model that RhoA, CYK-4, and ECT-2 function during the earliest stage of polarization, we observed the strongest polarity defects during the first half of the first cell cycle (table S1) (*7*). Subsequently, anterior PAR proteins and CDC-42 contribute to actomyosin dynamics (*3*, *4*, *17*). PAR-2 may function even later or in parallel, because anterior PAR are localized normally in *par-2* mutant embryos (*18*). Thus, polarization during the first cell cycle involves multiple stages governed by distinct sets of factors.

Our studies may also have implications for the role of CYK-4 during cytokinesis. Although the spindle midzone is a target of CYK-4 (*9*), recent studies revealed that a visible spindle midzone is not essential for cytokinesis (*19*, *20*). We suggest that the cortical actomyosin cytoskeleton may be a focus of CYK-4 during cytokinesis as it is during polarization.

Organisms such as tunicates and teleosts undergo asymmetric actomyosin contraction upon fertilization, which contributes to polarization of the fertilized egg (*21*). In *P. mammillata*, contraction depends on an actomyosin basket with its opening located at the site of sperm entry. Thus, asymmetry in these embryos may

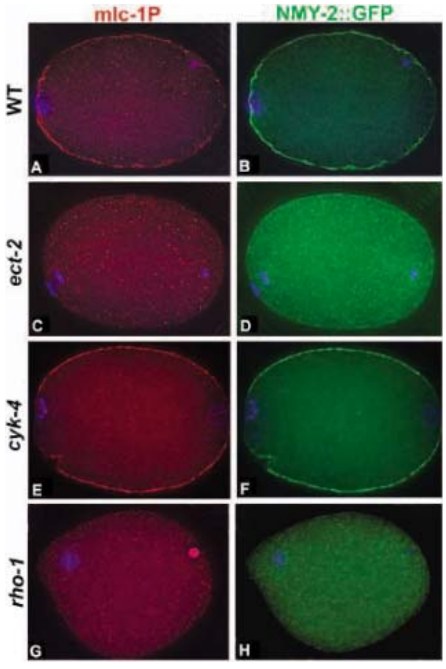

Fig. 5. Phospho-MLC localized at the cortex during polarization. (**A** and **B**) In wild-type (WT) embryos, antibodies that recognize phospho-MLC (mlc-1P, red) detect activated, endogenous MLC at the cell cortex, colocalized with NMY-2::GFP (green). In *ect-2(RNAi)* (**C** and **D**) and *rho-1(RNAi)* (**G** and **H**) embryos, phospho-MLC is rarely detected. (**E** and **F**) *cyk-4(RNAi)* embryos exhibit phospho-MLC throughout the cortex, with NMY-2::GFP. DNA is blue.

Fig. 4. *ect-2/GEF*, *rho-1/rhoA*, and *cyk-4/GAP* regulate the actomyosin wave. In wild-type (WT) embryos, a meshwork of nonmuscle myosin NMY-2::GFP (**A**, early) is enriched anteriorly during pronuclear migration (**B**, wave) and subsequently disperses into puncta at pronuclear meeting (**C**). In *ect-2(RNAi)* embryos (**D** to **F**) and *rho-1(RNAi)* embryos (**G** to **I**), contractile foci are rarely observed at any stage. In *cyk-4(RNAi)* embryos, 50% of embryos remain contractile over the entire embryo at all stages (**J** to **L**).

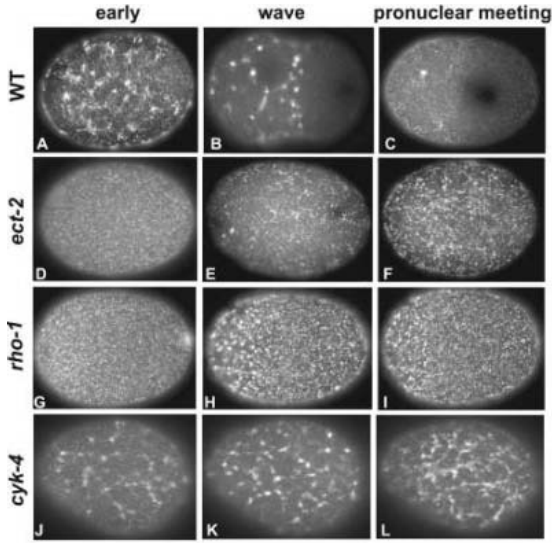

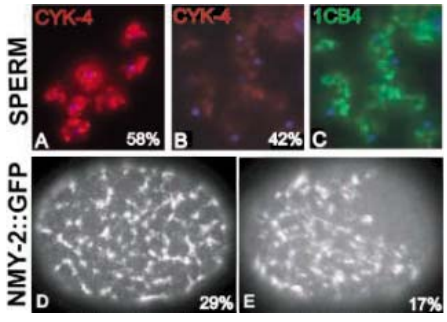

Fig. 6. Paternal *cyk-4* is required for polarity. Sperm from *cyk-4(RNAi); him-8* males exhibit reduced CYK-4 (**B**), while others appear unaffected (**A**). Sperm were counterstained for membranous organelles (1CB4) (**C**). Embryos from *NMY-2::GFP; fem-1* females and *cyk-4(RNAi); him-8* males exhibit loss of polarized NMY-2::GFP (**D**), or have a partial defect (**E**).

depend on the geometry of the actomyosin network rather than modulation of RhoA (*21*). On the other hand, animals with an even distribution of cortical actin may use orthologs of *rho-1*, *ect-2*, and *cyk-4* to modulate actomyosin configuration, analogous to *C. elegans*. Intriguingly, the *cyk-4* ortholog MgcRacGAP, is named for its enrichment in male germ cells in humans and *Drosophila* (*22*, *23*). In *Drosophila*, sperm entry is dictated by the position of the egg's micropyle, and therefore, a possible role for sperm in axis formation has not been addressed. One possibility is that *Drosophila* sperm contribute to embryonic polarity, and the stereotyped entry-point enables the egg and sperm to coordinate their polarizing activities. In mammals, there is debate regarding when polarity is established and the potential role of sperm (*24*). An exciting avenue for future investigation will be to determine whether other animals use CYK-4, RhoA, and ECT-2 to establish embryonic polarity in response to sperm.

References and Notes

1. B. Goldstein, S. N. Hird, *Development* **122**, 1467 (1996).
2. S. Q. Schneider, B. Bowerman, *Annu. Rev. Genet.* **37**, 221 (2003).
3. E. Munro, J. Nance, J. R. Priess, *Dev. Cell* **7**, 413 (2004).
4. R. J. Cheeks *et al.*, *Curr. Biol.* **14**, 851 (2004).
5. M. F. Portereiko, J. Saam, S. E. Mango, *Curr. Biol.* **14**, 932 (2004).
6. M. F. Portereiko, S. E. Mango, *Dev. Biol.* **233**, 482 (2001).
7. Materials and methods and additional data are available as supporting material on *Science* Online.
8. H. Okamoto, J. N. Thomson, *J. Neurosci.* **5**, 643 (1985).
9. M. Glotzer, *Science* **307**, 1735 (2005).
10. V. Jantsch-Plunger *et al.*, *J. Cell Biol.* **149**, 1391 (2000).
11. C. R. Cowan, A. A. Hyman, *Annu. Rev. Cell Dev. Biol.* **20**, 427 (2004).
12. E. A. Lundquist, P. W. Reddien, E. Hartwieg, H. R. Horvitz, C. I. Bargmann, *Development* **128**, 4475 (2001).
13. K. Riento, A. J. Ridley, *Nat. Rev. Mol. Cell Biol.* **4**, 446 (2003).
14. C. A. Shelton, J. C. Carter, G. C. Ellis, B. Bowerman, *J. Cell Biol.* **146**, 439 (1999).
15. P. L. Sadler, D. C. Shakes, *Development* **127**, 355 (2000).
16. C. R. Cowan, A. A. Hyman, *Nature* **431**, 92 (2004).
17. M. Gotta, M. C. Abraham, J. Ahringer, *Curr. Biol.* **11**, 482 (2001).
18. A. A. Cuenca, A. Schetter, D. Aceto, K. Kemphues, G. Seydoux, *Development* **130**, 1255 (2003).
19. K. J. Verbrugghe, J. G. White, *Curr. Biol.* **14**, 1755 (2004).
20. S. E. Encalada, J. Willis, R. Lyczak, B. Bowerman, *Mol. Biol. Cell* **16**, 1056 (2005).
21. F. Prodon, G. Pruliere, J. Chenevert, C. Sardet, *Med. Sci. (Paris)* **20**, 526 (2004).
22. A. Toure *et al.*, *J. Biol. Chem.* **276**, 20309 (2001).
23. M. Agnel, L. Roder, C. Vola, R. Griffin-Shea, *Mol. Cell. Biol.* **12**, 5111 (1992).
24. M. Zernicka-Goetz, *Nat. Rev. Mol. Cell Biol.* **6**, 919 (2005).
25. S. W. L'Hernault, in *C. elegans II*, D. L. Riddle, T. Blumenthal, B. J. Meyer, J. R. Priess, Eds. (Cold Spring Harbor Laboratory Press, Plainview, NY, 1997), vol. 1, pp. 271–294.

26. We thank M. Babst, M. Glotzer, J. Nance, J. Priess, B. Bowerman for reagents; and A. Schier, J. Rosenblatt, and laboratory members for reading the manuscript. Some strains were supplied by the *Caenorhabditis* Genetics Center, imaging was performed at the University of Utah Cell Imaging Facility. Oligo synthesis and DNA sequencing were supported by CCSG 2P30CA42014. This work was funded by K01DK02966-2 to J.R.S. S.E.M. was supported by NIH R01 GM056264, the Huntsman Cancer Institute, and Department of Oncological Sciences.

Supporting Online Material

www.sciencemag.org/cgi/content/full/1130291/DC1
SOM Text
Table S1
Figs. S1 to S12
Movies S1 to S5
References

22 May 2006; accepted 19 July 2006
Published online 27 July 2006;
10.1126/science.1130291
Include this information when citing this paper.

The Mevalonate Pathway Controls Heart Formation in *Drosophila* by Isoprenylation of Gγ1

Peng Yi,* Zhe Han,*† Xiumin Li, Eric N. Olson†

The early morphogenetic mechanisms involved in heart formation are evolutionarily conserved. A screen for genes that control *Drosophila* heart development revealed a cardiac defect in which pericardial and cardial cells dissociate, which causes loss of cardiac function and embryonic lethality. This phenotype resulted from mutations in the genes encoding HMG-CoA reductase, downstream enzymes in the mevalonate pathway, and G protein Gγ1, which is geranylgeranylated, thus representing an end point of isoprenoid biosynthesis. Our findings reveal a cardial cell–autonomous requirement of Gγ1 geranylgeranylation for heart formation and suggest the involvement of the mevalonate pathway in congenital heart disease.

Mutations in genes controlling heart development frequently cause fatal cardiac malformations, the most common type of birth defect in humans. Because many of the mechanisms involved in heart development are evolutionarily conserved, the fruit fly *Drosophila melanogaster* represents a powerful model for genetically dissecting this complex developmental process. The *Drosophila* heart, or dorsal vessel, which pumps bloodlike cells through an open circulatory system, is composed of parallel rows of contractile cardial cells (cardioblasts) tightly attached to pericardial cells; the latter perform supportive and secretory functions (Fig. 1A) (*1*).

We performed a P-element genetic screen (*2*) for *Drosophila* mutants with heart defects using transgenic flies harboring a green fluorescent protein (GFP) transgene under control of the *Hand* enhancer (*3*), which is specific for cardial cells, pericardial cells, and the lymph gland—a hematopoietic organ in fruit flies (Fig. 1B). The *Hand*-GFP transgene allows visualization of the developing heart at single-cell resolution. Among a collection of mutants with cardiac abnormalities, we observed a heart defect in which pericardial cells dissociated from cardioblasts in the dorsal vessel at the end of embryogenesis. We termed this phenotype "broken hearted" (bro). Here, we describe five such mutants of different genetic loci (Fig. 1, C to G). In contrast to the wild-type dorsal vessel in which the pericardial cells are intimately associated with cardioblasts, in each of these mutants, the relative positions of pericardial cells and cardioblasts changed with each heartbeat.

The P element in the *bro1* locus [l(3)01152] is located in the first exon of the *hydroxymethyl-*

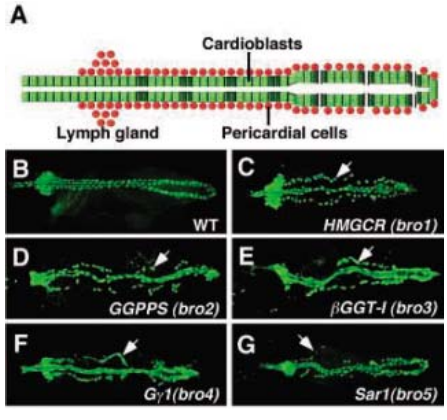

Fig. 1. Mutants in different genetic loci gave rise to a common broken hearted (bro) cardiac defect. (**A**) Schematic drawing of a late stage 17 embryonic heart (dorsal view, anterior to the left). (**B** to **G**) Stage 17 embryonic heart labeled by Hand-GFP (*3*) in wild-type embryo (B) or five bro homozygous mutants [(C) to (G)] (pericardial cells are indicated by arrows) (C) *HMGCR*, *bro1*, [l(3)01152]; (D) *GGPPS/qm*$^{L14.4}$, *bro2*; (E) *βGGT-I*$^{S-2554}$, *bro3*; (F) *Gγ1*, *bro4*, [l(2)k08017]. (G) *Sar1*, *bro5*, [l(2)k07408].

Department of Molecular Biology, University of Texas Southwestern Medical Center, 6000 Harry Hines Boulevard, Dallas, TX 75390–9148, USA.

*These authors contributed equally to this work.
†To whom correspondence should be addressed. E-mail: zhe.han@utsouthwestern.edu (Z.H.); eric.olson@utsouthwestern.edu (E.N.O.)

glutaryl (HMG)–coenzyme A (CoA) reductase gene (*HMGCR*) (Fig. 1C and fig. S1, A, C, and D), which is expressed in the dorsal vessel and the gonadal mesoderm, where it is required for migration of primordial germ cells (*4*). Mutants trans-heterozygous for $HMGCR^{01152}$ and a deficiency line Df(3R)Exel9013, in which the *HMGCR* gene is deleted, or two EMS mutants (*2*), $HMGCR^{clb26.31}$ and $HMGCR^{clb11.54}$ (*4*), showed similar, but more severe, cardiac defects than homozygous $HMGCR^{01152}$ mutants (Fig. 2, A and B, and fig. S1B). Expression of HMGCR in the heart, with the use of a Hand-GAL4 driver and a UAS-HMGCR transgene, rescued the cardiac defects in the $HMGCR^{01152}$ mutant (Fig. 2C).

HMGCR controls a rate-limiting step in the conversion of HMG-CoA into mevalonate, a precursor for the synthesis of cholesterol and isoprene derivatives that modify the C termini of proteins containing a CAAX motif (C, cysteine; A, aliphatic amino acid; X, any amino acid) (*5*) (Fig. 2E). In contrast to mammalian cells, *Drosophila* does not use the mevalonate pathway to synthesize cholesterol. Injection of embryos at the syncytial blastoderm stage with 0.1 μM mevinolin, a statin drug that lowers cholesterol level by inhibiting HMGCR activity, caused cardiac defects at stage 17 similar to those of the *HMGCR* mutants (Fig. 2D).

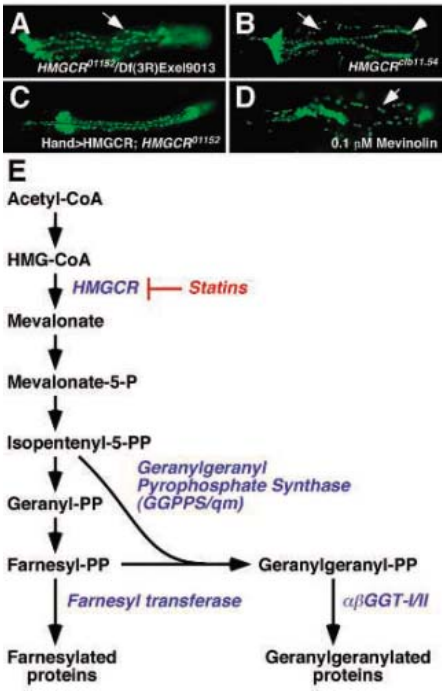

Fig. 2. HMGCR is required for *Drosophila* heart formation. **(A)** Trans-heterozygous mutant $HMGCR^{01152}$/Df(3R)Exel9013 showed a severe bro defect. **(B)** *HMGCR* EMS mutant $HMGCR^{clb11.54}$ showed a more severe cardiac defect in which the posterior region of the heart tube was abnormally dilated (arrowhead). **(C)** Expression of HMGCR specifically in the heart using Hand-GAL4 and UAS-HMGCR is sufficient to rescue the bro defect in $HMGCR^{01152}$ embryos. **(D)** Embryos injected with 0.1 μM mevinolin showed cardiac defects similar to those of *HMGCR* null mutants at stage 17. The dissociated pericardial cells in (A), (B), and (D) are indicated by arrows. **(E)** HMGCR regulated isoprenoid synthesis pathway in *Drosophila*.

To investigate whether either of the two major isoprenoids (Fig. 2E), farnesyl pyrophosphate (farnesyl-PP) and geranylgeranyl pyrophosphate (geranylgeranyl-PP), might be required for heart formation, we examined mutants in the genes encoding geranylgeranyl pyrophosphate synthase (GGPPS) and geranylgeranyl transferase type I β subunit (βGGT-I), which act downstream of HMGCR and are required for the biosynthesis of geranylgeranyl-PP or transfer of geranylgeranyl-PP to protein, to find out whether they also cause cardiac defects. Indeed, *GGPPS* (also called *qm*) mutant embryos showed 100% penetrance for the bro phenotype, just as *HMGCR* mutants did (Fig. 1D), and at least 30% of the β*GGT-I* mutants displayed the same phenotype (Fig. 1E). In contrast, two deficiency lines [Df(2L)Exel6010 or Df(3R)Exel6269] deleting either the farnesyl transferase α(CG2976) or β(CG17565) subunit did not display similar cardiac defects (fig. S2). These findings suggested that the cardiac defects of *HMGCR* mutant embryos resulted from a failure of geranylgeranylation of a target substrate protein required for the adhesion between cardioblasts and pericardial cells.

Analysis of another *bro* mutant (*bro4*) (Fig. 1F) suggested that the G protein γ subunit 1 (Gγ1), which contains a C-terminal CAAX motif, is the substrate of this geranylgeranylation modification required for heart formation. The P element in the *bro4* locus l(2)k08017 is inserted into the splice donor site after the first exon of the *Gγ1* gene (fig. S3A). Gγ1 expression level was reduced by more than 50% in homozygous l(2)k08017 embryos (fig. S3, B and C), which suggested that l(2)k08017 is a hypomorphic mutant allele of the *Gγ1* gene. Mutants trans-heterozygous for the l(2)k08017 insertion and a deficiency that deletes the *Gγ1* gene [Df(2R)H3E1] or for Df(2R)H3E1 and a *Gγ1* null allele (*6*) showed the same cardiac defects as the homozygous l(2)k08017 embryos (Fig. 3A and fig. S3D). Double mutants of the hypomorphic *HMGCR* and *Gγ1* alleles showed a more severe cardiac defect than either single mutant (Fig. 3B). A fifth bro mutation was mapped to the *Sar1* gene (Fig. 1G and fig. S4), which encodes a guanosine triphosphatase that controls budding of vesicles overlaid with coat protein complex II (COPII) from the endoplasmic reticulum (ER) to the Golgi network (*7*).

The developmental onset of cardiac defects was identical in the *HMGCR*, *Gγ1*, *GGPPS/qm*, β*GGT-I*, and *Sar1* mutants. Cardioblasts and pericardial cells were properly specified and aligned until stage 16 (fig. S5, A to D). However, at stage 17, pericardial cells began to dissociate from the dorsal vessel. These observations suggest that these genes are required to maintain cardiac integrity. The phenotypes of the dif-

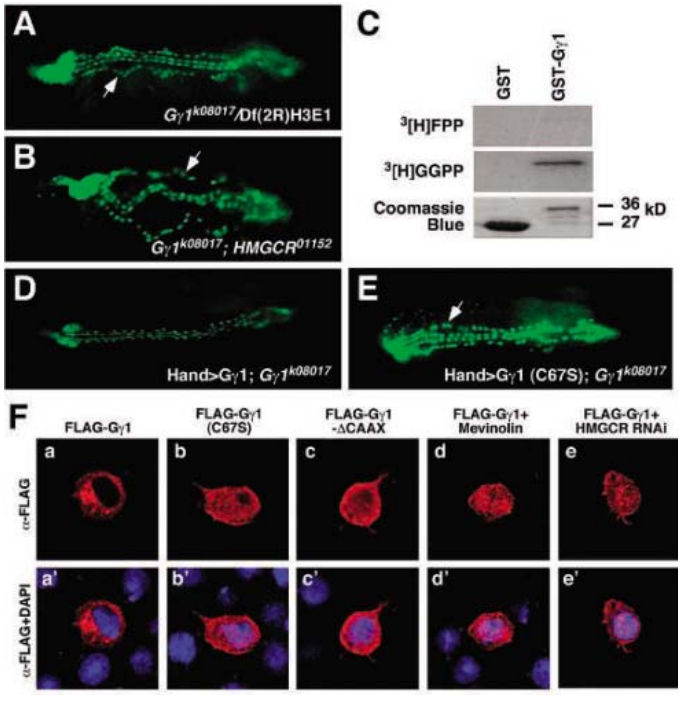

Fig. 3. Geranylgeranylation of Gγ1 is required for heart formation. **(A)** Trans-heterozygous mutant $Gγ1^{k08017}$/Df(2R)H3E1 shows the same bro defect as the $Gγ1^{k08017}$ mutant. **(B)** $Gγ1^{k08017}$; $HMGCR^{01152}$ double mutants show a much more severe bro defect than either single mutant. **(C)** Gγ1 can be efficiently geranylgeranylated, as labeled by ^{3}[H]GGPP, but cannot be farnesylated by ^{3}[H]FPP. Recombinant GST (27 kD) and GST-Gγ1 (36 kD) proteins are shown by Coomassie blue staining. **(D)** Expression of Gγ1 in the heart using Hand-GAL4 driving UAS-Gγ1 is sufficient to rescue the $Gγ1^{k08017}$ mutant cardiac defects. **(E)** Targeted expression of Gγ1 (C67S) in the heart failed to rescue the $Gγ1^{k08017}$ cardiac defects. The dissociated pericardial cells [(A), (B), and (E)] are indicated by arrows. **(F)** Subcellular localization of wild-type or mutant Gγ1 following exposure to mevinolin or HMCGR RNAi in S2R$^+$ cells. Gγ1 is localized to the cytosolic compartment (a and a′), whereas the two mutant forms show nuclear and cytoplasmic localization (b, b′, c, and c′). In the presence of mevinolin (d and d′) or HMGCR double-stranded RNA treatment (e and e′), Gγ1 shows a ubiquitous localization as seen with the two mutant forms.

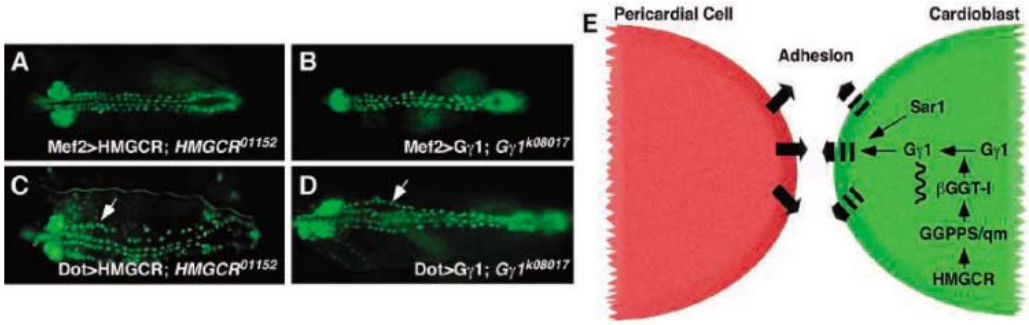

Fig. 4. HMGCR and Gγ1 are specifically required in cardioblasts to maintain cardiac integrity. (**A** and **B**) Expression of HMGCR or Gγ1 in cardioblasts is sufficient to rescue the *bro* defect in *HMGCR*^{01152} or *Gγ1*^{k08017} mutants, respectively. (**C** and **D**) Expressing HMGCR (C) or Gγ1 (D) in pericardial cells cannot rescue the bro defect in *HMGCR*^{01152} or *Gγ1*^{k08017} mutants. (**E**) A model summarizing the function of the mevanolate pathway, Gγ1, and Sar1 during *Drosophila* heart formation.

ferent mutants were also comparable, except for the two *HMGCR* EMS mutants or the *HMGCR*^{01152}/Df(3R)Exel9013 mutant, which was more severe and showed distortion of the shape of the dorsal vessel.

The final C-terminal residues of all G protein γ subunits contain a CAAX motif (*5*) in which the variable amino acid X determines the type of lipid modification: If X is serine, methionine, alanine, or glutamine, the cysteine is modified by farnesylation, whereas if X is leucine or valine, it is modified by geranylgeranylation (*8*, *9*). Using an in vitro prenylation assay, we found that *Drosophila* Gγ1 protein, which contains a CAAX motif of Cys-Thr-Val-Leu (CTVL), was modified by geranylgeranylation, but not by farnesylation (Fig. 3C), in agreement with the requirement of *GGPPS/qm* and *βGGT-I* for cardiac development.

To determine directly if geranylgeranylation of Gγ1 is essential for heart development, we tested whether wild-type and mutant forms of Gγ1 protein could rescue the cardiac defect of the Gγ1 mutant. Targeted expression of wild-type Gγ1 in the heart was sufficient to rescue the cardiac defects of *Gγ1* mutants (Fig. 3D), whereas mutant forms of Gγ1, in which geranylgeranylation was abolished by either a substitution of Ser for Cys^{67} (Gγ1-C67S) in the CAAX box or a deletion of the CAAX box (Gγ1-ΔCAAX), failed to rescue the cardiac defects in *Gγ1* mutants (Fig. 3E and fig. S3E). We conclude that geranylgeranylation of the CAAX motif of Gγ1 is required for its normal activity during *Drosophila* heart formation.

Lipid modification of the CAAX motif facilitates the association of proteins with membranes (*5*, *10*). To further explore how geranylgeranylation of Gγ1 affects its biological function, we examined the subcellular localization of the Gγ1 protein in *Drosophila* S2R^{+} cells. Wild-type Gγ1 protein was always excluded from the nucleus in S2R^{+} cells, whereas the two mutant forms of Gγ1, which were not geranylgeranylated, were located throughout the cytoplasm and nucleus (Fig. 3F, a to c and a′ to c′). Because Gγ1 is a small protein and can enter the nucleus freely, the specific localization of wild-type Gγ1 protein to the cytoplasm likely reflects its interaction with membranous structures, which requires modification by geranylgeranylation.

In S2R^{+} cells treated with three HMGCR inhibitors (atorvastatin, mevinolin, and simvastatin), as well as HMGCR double-stranded RNA, the wild-type Gγ1 protein displayed the same abnormal subcellular distribution as the two mutant forms of Gγ1 (Fig. 3F, d, e, d′, and e′, and fig. S3F). These findings suggest that abnormal subcellular localization of Gγ1 accounts for the cardiac defects in the mevalonate pathway mutants and *Gγ1* mutants. Gα has also been shown to be required at an earlier stage of heart development for proper alignment of cardioblasts (*11*), which is distinct from the function of Gγ1 revealed here.

Cardiac defects of *HMGCR* or *Gγ1* mutants could be completely rescued by targeted expression of UAS-HMGCR and UAS-Gγ1 transgenes, respectively, using a Hand-GAL4 driver (Figs. 2C and 3D), which directs expression in both cardioblasts and pericardial cells, or a Mef2-GAL4 driver, which is expressed in cardioblasts but not in pericardial cells (Fig. 4, A and B). In contrast, targeted expression of HMGCR or Gγ1 using Dot-GAL4, which only drives expression in pericardial cells, failed to rescue the cardiac defects in either mutant (Fig. 4, C and D). These results demonstrate that HMGCR and Gγ1 function specifically in cardioblasts to adhere with pericardial cells and exclude the possibility that the bro cardiac phenotype arises secondarily from general metabolic abnormalities.

HMGCR and downstream enzymes in the biochemical pathway leading to the synthesis of geranylgeranyl-PP are specifically required in cardioblasts to modify Gγ1 (Fig. 4E). We propose that geranylgeranylation, which is required for the proper intracellular localization of Gγ1, is in turn required for generating a signal for pericardial cells to adhere to cardioblasts throughout heart formation. Indeed, Gβγ has been shown to control Golgi apparatus organization and vesicle formation during exocytosis in mammalian cells (*12*, *13*). The finding that a mutation in *Sar1* causes the same cardiac phenotype as the *Gγ1* mutation further supports the possibility that this collection of mutations perturbs the secretion of a factor required for maintenance of cardiac integrity. Inhibition of this pathway with statins results in cardiac defects similar to those resulting from mutations in *HMGCR* and downstream genes required for isoprenoid biosynthesis, which raises the possibility that congenital heart defects reportedly associated with the use of statins (*14*), which are contraindicated during pregnancy, may reflect perturbation in a similar developmental pathway.

HMGCR has also been shown to be required for recruitment of primordial germ cells (PGCs) to the gonad in *Drosophila* (*4*), but the protein target(s) of the mevalonate pathway that mediate this process have not been identified. Perhaps Gγ1 functions in the gonad mesoderm to guide PGC migration. We speculate that lipid modifications mediated by the mevalonate pathway contribute to directed cell migration and subsequent cell-cell adhesion in diverse cell types. Given the conservation of cardiac developmental control mechanisms, it will be of interest to investigate the potential involvement of the mevalonate pathway in mammalian heart development and congenital heart disease.

References and Notes

1. R. M. Cripps, E. N. Olson, *Dev. Biol.* **246**, 14 (2002).
2. Materials and methods are available as supporting material on *Science* Online.
3. Z. Han, E. N. Olson, *Development* **132**, 3525 (2005).
4. M. Van Doren, H. T. Broihier, L. A. Moore, R. Lehmann, *Nature* **396**, 466 (1998).
5. D. E. Clapham, E. J. Neer, *Annu. Rev. Pharmacol. Toxicol.* **37**, 167 (1997).
6. Y. Izumi, N. Ohta, A. Itoh-Furuya, N. Fuse, F. Matsuzaki, *J. Cell Biol.* **164**, 729 (2004).
7. M. Aridor *et al.*, *J. Cell Biol.* **152**, 213 (2001).
8. B. T. Kinsella, R. A. Erdman, W. A. Maltese, *Proc. Natl. Acad. Sci. U.S.A.* **88**, 8934 (1991).
9. Y. Reiss, S. J. Stradley, L. M. Gierasch, M. S. Brown, J. L. Goldstein, *Proc. Natl. Acad. Sci. U.S.A.* **88**, 732 (1991).
10. K. H. Muntz, P. C. Sternweis, A. G. Gilman, S. M. Mumby, *Mol. Biol. Cell* **3**, 49 (1992).
11. F. Fremion *et al.*, *J. Cell Biol.* **145**, 1063 (1999).
12. C. Jamora *et al.*, *Cell* **91**, 617 (1997).
13. M. Ohashi, W. B. Huttner, *J. Biol. Chem.* **269**, 24897 (1994).
14. R. J. Edison, M. Muenke, *N. Engl. J. Med.* **352**, 2759 (2005).
15. We thank M. Brown and J. Goldstein for comments on the manuscript, the Bloomington stock center for fly stocks, R. Lehmann for reagents, and A. Tizenor for graphics. Z.H. is supported by the National Scientist Development Grant from the American Heart Association. E.N.O. is supported by grants from the NIH, the Donald W. Reynolds Cardiovascular Clinical Research Center, and the Robert A. Welch Foundation (1-0025).

Supporting Online Material

www.sciencemag.org/cgi/content/full/1127704/DC1
Materials and Methods
Figs. S1 to S5
References

21 March 2006; accepted 12 July 2006
Published online 20 July 2006;
10.1126/science.1127704
Include this information when citing this paper.

Human Lineage–Specific Amplification, Selection, and Neuronal Expression of DUF1220 Domains

Magdalena C. Popesco,[1,2,3]* Erik J. MacLaren,[1,2,3]*† Janet Hopkins,[1,2,3] Laura Dumas,[1,3] Michael Cox,[1,2,3] Lynne Meltesen,[1,4] Loris McGavran,[1,4] Gerald J. Wyckoff,[5] James M. Sikela[1,2,3]‡

Extreme gene duplication is a major source of evolutionary novelty. A genome-wide survey of gene copy number variation among human and great ape lineages revealed that the most striking human lineage–specific amplification was due to an unknown gene, *MGC8902*, which is predicted to encode multiple copies of a protein domain of unknown function (DUF1220). Sequences encoding these domains are virtually all primate-specific, show signs of positive selection, and are increasingly amplified generally as a function of a species' evolutionary proximity to humans, where the greatest number of copies (212) is found. DUF1220 domains are highly expressed in brain regions associated with higher cognitive function, and in brain show neuron-specific expression preferentially in cell bodies and dendrites.

Extreme gene duplication in a species-specific manner, followed by divergence and functional specialization, can be an important factor in the evolution of phenotypic traits unique to that species (*1*). Copy number variations between human and chimpanzee have been discovered with the use of a draft sequence of the chimpanzee genome (*2*), although primate outgroup information is currently limited to draft sequence from only one other species, the macaque (*3*). Draft sequences are prone to misassembly of recently duplicated sequences (*4*), a limitation that is the most severe for the most evolutionarily recent (i.e., similar) duplications. A complementary approach is cDNA array–based comparative genomic hybridization (aCGH) (*5*). We previously used cDNA aCGH to carry out genome-wide gene copy number comparisons between human and great ape species (*5*), and identified 134 genes showing human lineage–specific (HLS) increases and six genes showing HLS decreases.

To obtain an independent estimate of the copy number of each HLS gene, we determined the full insert sequences of the cDNAs (table S1) and used these as BLAT (http://genome.ucsc.edu) queries to search a recent human genome assembly (Build 35) (*6*) as well as available genome draft sequences from chimp (*2*) and macaque (*3*). The great majority (86.4%) of genes predicted by cDNA aCGH to have an HLS increase in copy number produced more BLAT hits (score >200) in the human genome than in either chimp or macaque (table S2), and 44 of these (31%) had more than five BLAT hits in the human genome (Fig. 1A).

After removal of all BLAT hits predicted to be intronless, one gene, *MGC8902* (cDNA IMAGE clone 843276), showed the most striking human-specific increase, with 49, 10, and 4 hits found in human, chimp, and macaque, respectively (Fig. 1A). All human hits associated with *MGC8902* (49/49) were predicted to be nonretroposed copies. It was also ranked as the fifth highest HLS aCGH signal out of the 134 genes predicted to have HLS increases in copy number (*7*), and contains six predicted DUF1220 domains (Fig. 1B). The genomic sequences predicted to encode DUF1220 domains typically show a unique signature of an evenly spaced two-exon repeat unit (Fig. 1B). A recent report treats this exon pair as a new repeat that is part of a gene family termed NBPF (*8*). The repeat is inclusive of the DUF1220 domain but also contains additional protein-coding sequences that may not share all the biological and evolutionary characteristics of DUF1220.

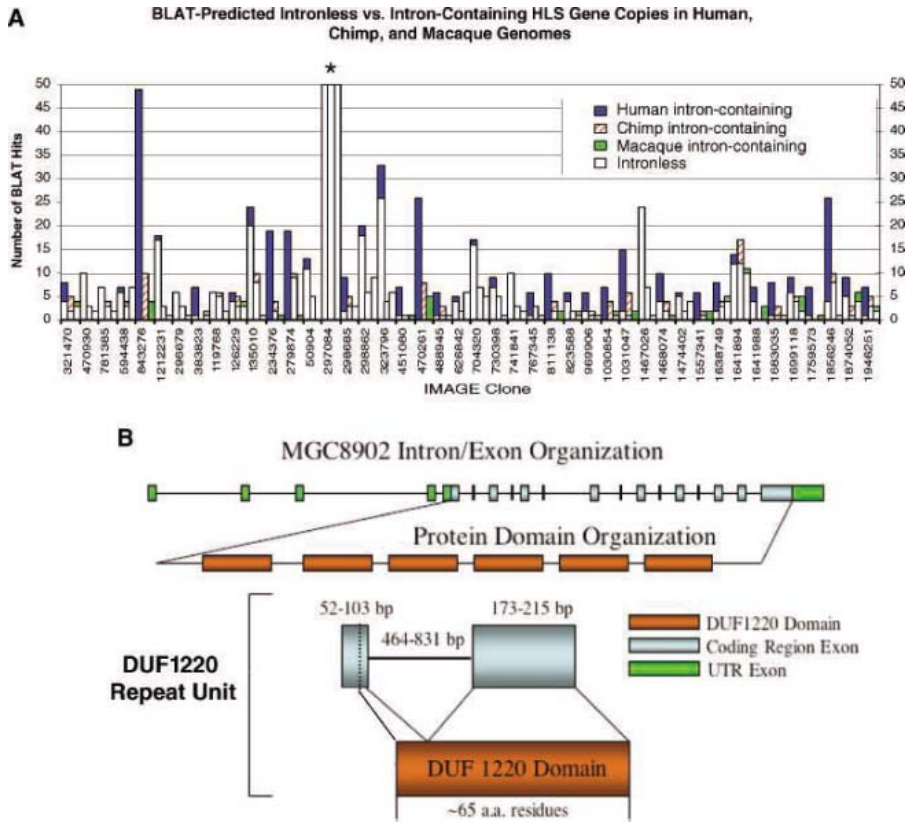

Fig. 1. Cross-species BLAT survey of HLS cDNAs and organization of the *MGC8902* gene. (**A**) BLAT searches were performed using full cDNA insert sequences for 140 HLS genes (*5*) as queries. The IMAGE clones (http://image.llnl.gov/) that yielded >5 BLAT hits in the human genome are shown. BLAT hits with span sizes exceeding the size of the cDNA query were scored as potentially containing introns. Potentially "intronless" BLAT hits are shown in white. The asterisk denotes BLAT hits associated with the ribosomal protein gene *RLP23AP7*, which had hit totals of 150, 144, and 133 for human, chimp, and macaque, respectively. All of these were intronless. (**B**) The genomic exon/intron organization of *MGC8902* and the predicted domain structure of the translated protein. A representative DUF1220 genomic repeat unit is also shown.

[1]Human Medical Genetics and [2]Neuroscience Programs, [3]Department of Pharmacology, [4]Department of Pathology, University of Colorado at Denver and Health Sciences Center, Aurora, CO 80045, USA. [5]Division of Molecular Biology and Biochemistry, University of Missouri, Kansas City, MO 64110, USA.

*These authors contributed equally to this work.

†Present address: Wellcome Trust Sanger Institute, Wellcome Trust Genome Campus, Hinxton, Cambridgeshire CB10 1SA, UK.

‡To whom correspondence should be addressed. E-mail: james.sikela@uchsc.edu

It has been estimated that 34 different human genes encode DUF1220 domains (table S3) (www.ncbi.nlm.nih.gov/IEB/Research/Acembly). Pfam (Version 17.0) (*9*) predicts that 60 human DUF1220-containing proteins exist, containing a total of 271 DUF1220 domains (fig. S1) derived from 11 seed domains (*10*) (fig. S2A). Estimates based on cDNA sequences indicated that 22 genes exist, including six pseudogenes (*8*). None of these cDNAs showed perfect identity to human genomic sequences, raising the possibility that this count is an underestimate. Recent additional sequencing of chromosome 1 identified at least 15 gene sequences that encode DUF1220 domains, although several sequence gaps still remain in DUF1220-encoding regions (*11*).

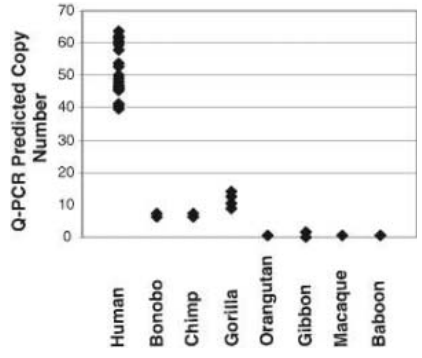

Fig. 2. QPCR-based estimation of the number of DUF1220 domains found within different species. QPCR was carried out to survey the frequency of DUF1220 domain (Q8IX62 17-33) sequences in various primate species. Corresponding numerical values can be found in table S6.

The amino acid sequences of each of the 11 DUF1220 seed domains were next used as BLAT queries against genome sequences from several species (table S4). The 11 seed domains showed no matches outside of mammals, and 10 of the 11 were primate-specific, with the highest number of copies always found in human (fig. S2B). The remaining seed domain (O75042) was found in primate and nonprimate mammals, usually as a single domain encoded by a single-copy gene [*Myomegalin*/*PDE4DIP* (*12*)] that also encodes a spindle-associated domain (fig. S2C). The most human BLAT hits were obtained with three domains found in one predicted protein, Q8IX62. One of these (Q8IX62_Human/17-83) had 90 hits in human but only 16 and 11 in chimp and macaque, respectively. Of the human hits, 37 (41%) were 100% matches (fig. S2B), by far the highest frequency of identical human matches found for any of the 11 seed domains. For macaque, a similar number of BLAT hits was obtained whether the January 2005 or January 2006 sequence assembly was used (table S5).

To provide an independent estimate of the frequency of this domain, we carried out quantitative polymerase chain reaction (QPCR) analysis on multiple individuals from each of several species, using a primer and probe set with sequences that are identical to sequences in the human and chimp genomes (Fig. 2 and table S6). Consistent with BLAT results and previously reported aCGH data, QPCR analysis also found that the human genome had significantly more copies than that of any other species ($P < 0.01$) and, generally, the evolutionarily closer the species was to human, the more DUF1220 domains were encoded in its genome. Interhominoid cDNA aCGH data reported previously (*5*) for cDNA IMAGE 843276 [average $\log_2$ ratio: bonobo (3) = –1.79; chimpanzee (4) = –1.98; gorilla (3) = –1.19; orangutan (3) = –2.74] are in very close agreement ($r = 0.9886$) with the cross-species QPCR data presented in Fig. 2. Taken together, aCGH, BLAT, and QPCR data indicate that the number of DUF1220 copies is highly expanded in humans, reduced in African great apes, further reduced in orangutan and Old World monkeys, single-copy in nonprimate mammals, and absent in nonmammalian species. Some intraspecies copy number variability was apparent, although a survey of a limited number of individuals (22 individuals from diverse human populations) revealed no population-specific trends (table S6).

Human genomic locations predicted from the BLAT analysis using the 11 seed domains (fig. S3, A and B) were in general agreement with fluorescence in situ hybridization (FISH) analysis (fig. S4) and two recent reports (*8*, *11*), positioning the majority of DUF1220 (NBPF) sequences at 1q21.1, a complex genomic region immediately adjacent to the pericentromeric C-band 1q12. Additional sequences are found at 1p36 and 1p13.3. After eliminating redundant (overlapping) positions, we identified 212, 37, and 30 unique DUF1220-positive BLAT hits in human, chimp, and rhesus, respectively, along with only one each for mouse and rat.

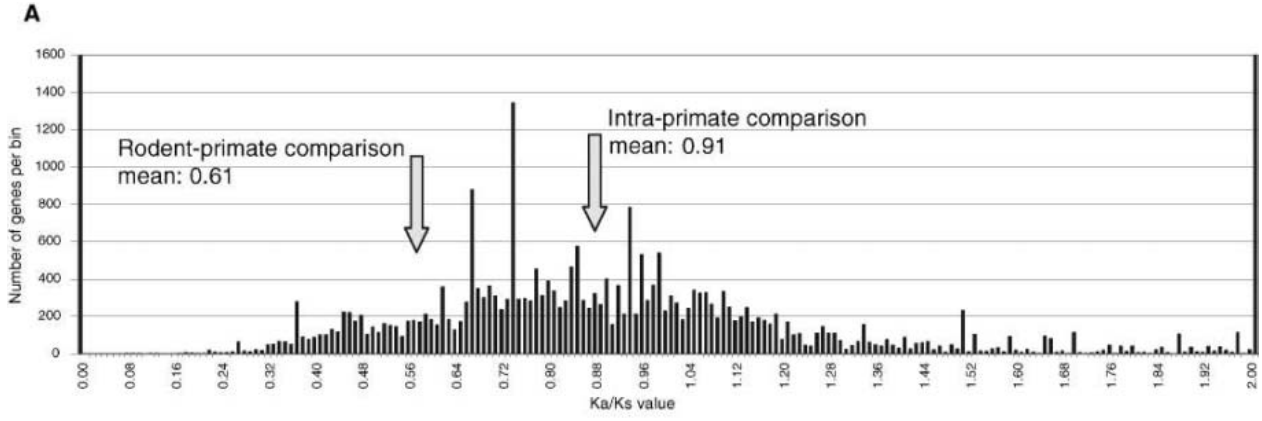

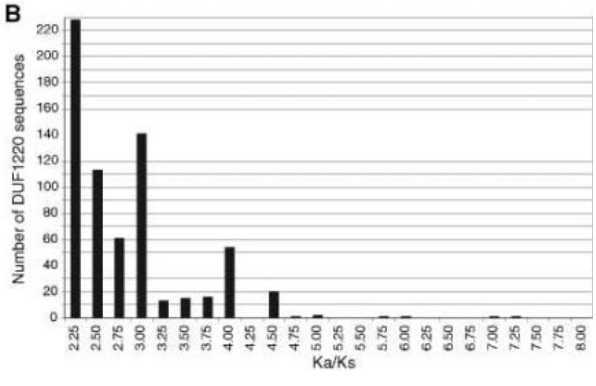

Fig. 3. Ka/Ks values of DUF1220-encoding sequences. (**A**) Sequences with Ka/Ks values 0 through 2.0. Rodent-primate and primate-primate comparison means are shown (arrows); human-specific comparisons produce an even higher mean. Of these comparisons, 3106 have a Ka/Ks value of 0, and 2035 have a Ka/Ks value of 2.0 or greater; the scale here is limited so that the major patterns can be seen. (**B**) Sequences with Ka/Ks values 2.25 through 8.0; all of these comparisons are primate homologous comparisons, and most are human-human pairwise comparisons.

Evolutionary analysis (*13*) was performed with a nonredundant set of the human, chimp, rhesus, mouse, and rat DUF1220 nucleotide sequences derived from the BLAT searches described above (table S7). These sequences were filtered for frame-shift insertions and aligned, and the resulting 256 sequences were used for construction of a phylogenetic tree (fig. S5). In addition, Ka/Ks ratios (ratios of the rate of amino acid substitution to silent substitution) were determined for each pairwise combination of sequences (Fig. 3, A and B, and table S8). The domain that is found as a single copy in nonprimate mammals, O75042, is the likely ancestral domain, consistent with a phylogenetic analysis of the 11 DUF1220 seed domains (www.sanger.ac.uk/cgi-bin/Pfam/getacc?PF06758), with the primate-specific domains appearing more recently. The ladder-like nature of the phylogenetic tree suggests that serial domain amplification and subsequent divergence are the rule in this large set of repeats. Also, 33% (10,583/32,131) of pairwise comparisons showed a Ka/Ks ratio of 1 or greater—a traditional signature of positive selection (*14*).

On average, primate-primate homologous comparisons had a higher ratio of nonsynonymous to synonymous changes (Ka/Ks mean = 0.91) than did rodent-primate homologous comparisons (Ka/Ks mean = 0.61), indicative of either a higher level of positive selection or a relaxation of functional constraint (Fig. 3A). The average Ka/Ks value for primate homologous comparisons was unusually high (0.91) relative to general estimates of primate evolutionary rate (*15*), with two human-versus-rhesus comparisons producing the highest values (>7.1) (Fig. 3B). In contrast, Ka/Ks analysis of non-DUF1220 sequences from a DUF1220-containing gene did not appear to show evidence of positive selection (*8*).

Western blot analysis was carried out on a panel of normal adult human tissues, using an affinity-purified antibody directed against a 20–amino acid peptide derived from a primate-specific DUF1220 domain. A heavy band was visible at ~36 kD in heart, brain, spleen, skeletal muscle, and small intestine (Fig. 4A), which was blocked in all tissues, except in the skeletal muscle, by the adsorption control (fig. S6A). This same band was faintly present in kidney, lung, stomach, colon, and rectum. In addition, other heavy bands were visible between 25 and 40 kD throughout the tissue panel. The same ~36 kD band was highly expressed in frontal lobe, temporal lobe, parietal lobe, occipital lobe, and cerebellum, whereas it was absent in placenta (Fig. 4B).

Using double-label immunofluorescence, we analyzed normal adult brain regions from several individuals with the same affinity-purified DUF1220 antibody. DUF1220 sequences were consistently found in neurons but not in glia. In the cerebellum, preferential expression was observed in Purkinje cells, where signals were restricted to cell bodies (cytoplasm) and dendrites (Fig. 4, C to E, and fig. S6, B to D). In addition to labeling in the cerebellum, neuron-specific DUF1220 signals were present in the cortical layers of the hippocampus (Fig. 4, F and G). DUF1220 domains were also abundantly expressed in neurons within the neocortex (frontal, parietal, occipital, and temporal lobes), thought to be critical to higher cognitive functions (Fig. 4, H to K).

Although the precise function of genes encoding DUF1220 domains and the domains themselves is at present unknown, the pattern of amplification and location of expression have led us to speculate that the domains and the genes that encode them may be important to cognitive function. In light of the strong DUF1220 expression we observed in neurons of the neocortex, it is intriguing that multiple independent evolutionary processes [brain enlargement, neocortex expansion (*16*), gene duplication, and domain amplification] can be seen as having individually and cumulatively contributed to increasing the

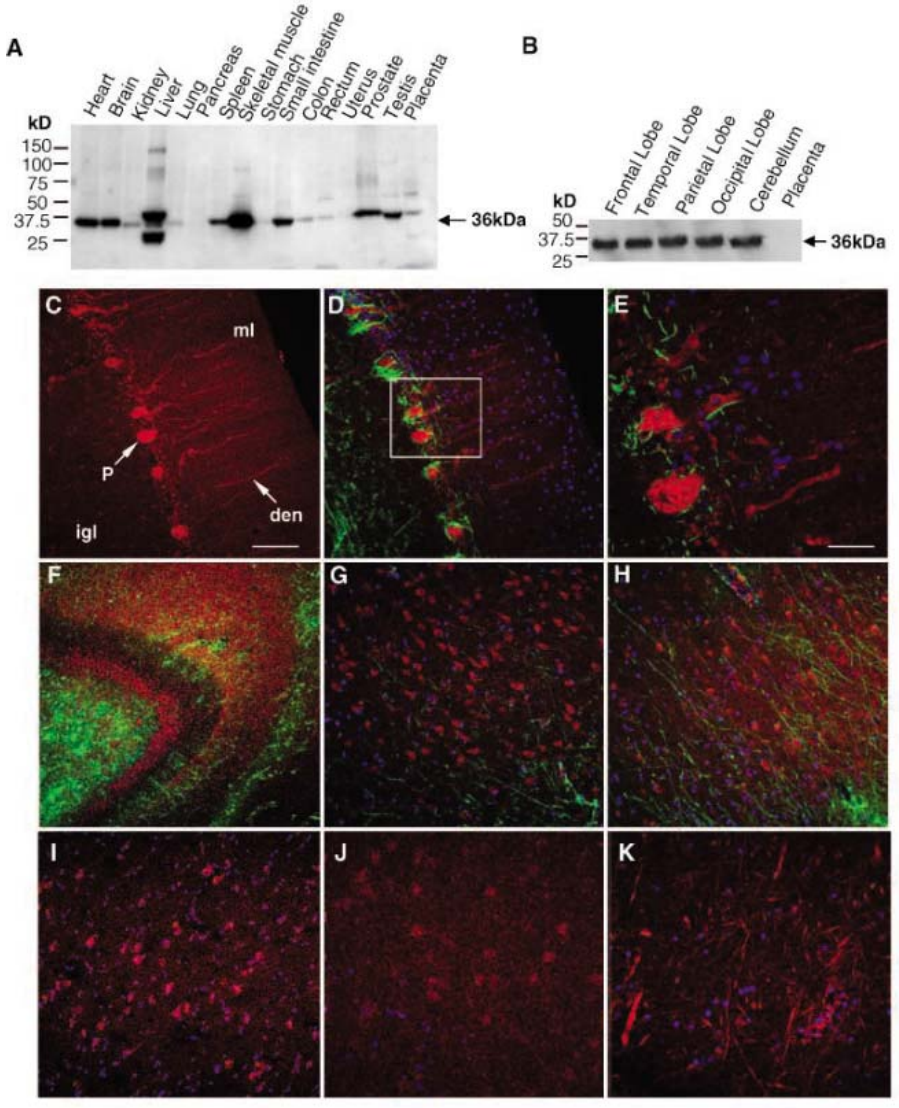

Fig. 4. Western and immunofluorescence analysis of normal adult human tissues with antibody to a peptide derived from a primate-specific DUF1220 domain. (**A** and **B**) Western blot analysis of total protein lysates (50 μg) from normal adult human tissues (male and female; ages ranging from 22 to 82 years). Lysates were electrophoresed on 4 to 20% denaturing SDS–polyacrylamide gel electrophoresis gels, transferred to polyvinylidene difluoride membranes, and probed with DUF1220 affinity-purified antibody (A). Further blotting analysis was performed on adult human brain regions with DUF1220 affinity-purified antibody (B). (**C** to **E**) Double-label immunofluorescence of DUF1220 antibody in the human cerebellum (30-year-old white female). (C) DUF1220 affinity-purified antibody; Purkinje cells and dendrites were detected. (D) Double labeling with DUF1220 affinity-purified antibody and neurofilament 160 kD; (E) higher magnification of inset in (D). Double labeling with DUF1220 affinity-purified antibody and glial fibrillary acidic protein (GFAP) in (**F**) hippocampus, (**G**) cortical regions of the hippocampus, and (**H**) frontal lobe. (**I** to **K**) Neuron-specific DUF1220 signals in (I) temporal lobe, (J) parietal lobe, and (K) occipital lobe. Nuclei are labeled with 4′,6′-diamidino-2-phenylindole (DAPI). P, Purkinje cell; den, dendrite; igl, internal granule layer; ml, molecular layer. Scale bars, 100 μm [(C), (D), and (F) to (I)], 50 μm [(E), (J), and (K)].

DUF1220-coding potential of the human brain, suggesting that such an increase may have conferred strong selective advantages.

The genomic regions that harbor DUF1220 sequences appear to be particularly complex and, as a result, different genome assemblies differ with respect to the predicted number of DUF1220-encoded sequences. However, two recent genome-wide BAC aCGH cross-species studies (*17*, *18*) independently support the findings reported here that DUF1220-encoding genes show human lineage–specific increases in copy number and appeared with remarkable rapidity. If they indeed are the result of strong positive selection, they may play an important role in human lineage–specific traits (*19*) and serve to illustrate how certain regions of the genome can undergo episodes of "punctuated" evolution (*20*).

References and Notes

1. S. Ohno, *Evolution by Gene and Genome Duplication* (Springer, Berlin, 1970).
2. Chimpanzee Sequencing and Analysis Consortium, *Nature* **437**, 69 (2005).
3. Rhesus Monkey Genome Project, Baylor College of Medicine Human Genome Sequencing Center (www.hgsc.bcm.tmc.edu/projects/rmacaque).
4. J. Cheung *et al.*, *Genome Biol.* **4**, R25 (2003).
5. J. R. Pollack *et al.*, *Nat. Genet.* **23**, 41 (1999).
6. Human Genome Sequencing Consortium, *Nature* **431**, 931 (2004).
7. A. Fortna *et al.*, *PLoS Biol.* **2**, e207 (2004).
8. K. Vandepoele, N. Van Roy, K. Staes, F. Speleman, F. van Roy, *Mol. Biol. Evol.* **22**, 2265 (2005).
9. A. Bateman *et al.*, *Nucleic Acids Res.* **32**, D138 (2004).
10. E. L. L. Sonnhammer, S. R. Eddy, R. Durbin, *Proteins* **28**, 405 (1997).
11. S. G. Gregory *et al.*, *Nature* **441**, 315 (2006).
12. I. Verde *et al.*, *J. Biol. Chem.* **276**, 11189 (2001).
13. D. L. Swofford, *PAUP: Version 4* (Sinauer Associates, Sunderland, MA, 1998).
14. M. Kreitman, *Annu. Rev. Genomics Hum. Genet.* **1**, 539 (2000).
15. C. M. Malcom, G. J. Wyckoff, B. T. Lahn, *Mol. Biol. Evol.* **20**, 1633 (2003).
16. M. Goodman, *Am. J. Hum. Genet.* **64**, 31 (1999).
17. V. Goidts *et al.*, *Hum. Genet.* **119**, 185 (2006).
18. G. M. Wilson *et al.*, *Genome Res.* **16**, 173 (2006).
19. J. M. Sikela, *PLoS Genet.* **2**, e80 (2006).
20. J. E. Horvath *et al.*, *Genome Res.* **15**, 914 (2005).

21. We thank S. Burgers, J. Chang, A. Blackler, A. Fortna, A. Solidar, J. Smith, and B. Carstens for technical help; D. Manchester, M. Churchill, J. Pollack, Y. Kim, and J. Kent for helpful discussions; L. Jorde for providing genomic DNAs from diverse human populations; the Macaque Genome Sequencing Consortium for generating genome sequence assemblies and making data available before publication; B. K. DeMasters and C.-I. Sze for providing postmortem human brain tissue; R. Levinson for immunocytochemical expertise and for use of light microscopy facilities; and J. Caldwell for assistance with interpretation of immunofluorescence results. Supported by a Butcher Foundation grant and NIH grant AA11853 (J.M.S.) and the University of Missouri Research Board (G.J.W.).

Supporting Online Material

www.sciencemag.org/cgi/content/full/313/5791/1304/DC1
Materials and Methods
Figs. S1 to S6
Tables S1 to S8
References

5 December 2005; accepted 6 July 2006
10.1126/science.1127980

Reducing the Racial Achievement Gap: A Social-Psychological Intervention

Geoffrey L. Cohen,[1]* Julio Garcia,[2]* Nancy Apfel,[2] Allison Master[2]†

Two randomized field experiments tested a social-psychological intervention designed to improve minority student performance and increase our understanding of how psychological threat mediates performance in chronically evaluative real-world environments. We expected that the risk of confirming a negative stereotype aimed at one's group could undermine academic performance in minority students by elevating their level of psychological threat. We tested whether such psychological threat could be lessened by having students reaffirm their sense of personal adequacy or "self-integrity." The intervention, a brief in-class writing assignment, significantly improved the grades of African American students and reduced the racial achievement gap by 40%. These results suggest that the racial achievement gap, a major social concern in the United States, could be ameliorated by the use of timely and targeted social-psychological interventions.

The drive for self-integrity—seeing oneself as good, virtuous, and efficacious—is a fundamental human motivation (*1*–*3*). Membership in valued social groups is often a major source of individuals' sense of self-integrity (*4*, *5*). Consequently, negative characterizations of one's group can prove threatening, especially in chronically evaluative environments.

Because people subjected to widely known negative stereotypes impugning the intelligence of their group are aware of these negative characterizations, they may worry that performing poorly could confirm the stereotype of their group (*6*–*8*). This situation can create chronic stress at school and work, by burdening people with an extra psychological threat not experienced by those outside their group. If too severe, stress can undermine performance (*6*–*10*). Indeed, simply observing a group member who might confirm a negative stereotype about one's group can induce threat, undermining performance (*5*).

One potentially effective way to buffer people against threat and its consequences, we suggest, is to allow them to reaffirm their self-integrity (*2*, *3*). Self-affirmations, by buttressing self-worth, can alleviate the stress arising in threatening performance situations (*11*). They can take the form of reflections on personally important, overarching values, such as the importance of family or a self-defining skill (*2*, *3*).

The research reported here tested whether a self-affirmation intervention designed to lessen threat would enhance the academic achievement of negatively stereotyped minority students. The intervention rested on three assumptions: First, people are motivated to maintain self-integrity; second, because group memberships are an important source of self-integrity, negative group characterizations can pose a chronic threat to self-integrity; third, such threat, if too severe, can undermine performance.

School settings can be stressful to almost all students regardless of race. However, for African American students, the academic environment involves an extra degree of threat not experienced by nonminority students, due to the negative stereotype about the intelligence of their race. This threat, on average, raises stress to levels that are debilitating to performance (*6*–*9*). Accordingly, we expect that a self-affirmation intervention would be particularly effective at improving their academic performance. We would, in fact, expect this intervention to improve the performance of all groups of individuals subjected to a threat sufficiently pervasive and intense to impede that entire group's average performance.

This prediction was tested in two randomized double-blind field experiments (*12*). The second, a replication study, occurred a year after the first and involved a different cohort of students. Participants were seventh-graders from middle- to lower-middle-class families at a suburban northeastern middle school whose student body was divided almost evenly between African Americans and European Americans. The experiments involved 119 African American students and 124 European American students distributed roughly evenly across the two studies. All the teachers who participated taught the same academic subject (one not typically related to gender stereotypes). This subject was the intervention-targeted course in both studies; it was the one in which the intervention was administered.

In the fall term of each year, students were randomly assigned, at the level of the individual student, to the affirmation condition or the control condition. For each teacher and classroom period, there were approximately equal numbers of participants in each condition. Teachers were blind to students' condition assignment and unaware of the

[1]Department of Psychology, University of Colorado, Muenzinger Psychology Building, Boulder, CO 80309–0345, USA. [2]Department of Psychology, Yale University, 2 Hillhouse Avenue, New Haven CT 06520, USA.

*To whom correspondence should be addressed. E-mail: cohen.geoff@gmail.com (G.L.C.); jpmex@gmail.com (J.G.)
†Present address: Department of Psychology, Stanford University, Stanford, CA 94305, USA.

specific research hypothesis. The experimental treatment occurred as close to the start of the fall term as possible, when evaluative stress was assumed to be high. Teachers distributed closed envelopes, each containing an exercise packet, to all students in their class. Each envelope was marked with the name of the student who was to receive it. The exercise was presented as a regular class assignment and took approximately 15 min to complete. Students opened their envelopes, removed the packet, and were guided through the procedure via written instructions in the packet. Students completed the exercise independently and in silence, providing written responses to the tasks contained in the packet.

Following standard procedures, the affirmation and control exercises presented a list of values (such as relationships with friends or family or being good at art) (*12*). In experiment 1, treatment students were asked to indicate their most important value, control students their least important value. In the replication study, treatment students were asked to indicate their two or three most important values, control students their two or three least important values.

Treatment students in both studies then wrote a brief paragraph about why their selected value(s) were important to them. Control students wrote about why the chosen value(s) might be important to someone else. To reinforce the manipulation, students indicated their level of agreement with statements concerning their chosen value(s) (such as "I care about these values," in the treatment condition versus "some people care about these values," in the control condition). Upon completion, students placed the exercise packet in its envelope, sealed it, and returned it. Envelopes were collected and forwarded to the researchers. Teachers immediately resumed their lesson plan. One exercise was completed during the academic term in the first study, two in the replication study.

Multiple regression was used to test treatment effects (*12*). Based on their official transcripts, African Americans in the affirmation condition earned higher fall-term grades in the targeted course than did those in the control condition. On a grade metric ("A" = 4.0, "B" = 3.0, etc.), the treatment effect was 0.26 grade points in study 1 [regression coefficient $B = 0.26$, $t(41) = 2.44$, $P < 0.02$] and 0.34 grade points in the replication [$B = 0.34$, $t(60) = 2.69$, $P < 0.01$]. The likelihood of observing two effects of this magnitude by chance is approximately 1 in 5000. No treatment effect occurred for European Americans in either experiment [$|B$'s$| < 0.16$, $|t$'s$| < 1.1$, NS]. The race × experimental condition interaction was significant in both experiments [$B = 0.29$, $t(98) = 2.00$, $P < 0.05$; $B = 0.52$, $t(119) = 2.80$, $P < 0.01$, respectively]. Tables S1 and S2 present the regression coefficients, standard errors, and t values for each term in the full regression model for experiments 1 and 2, respectively (*12*).

This treatment effect was not limited to a small number of students performing poorly or well before the intervention. Figure 1, displaying the treatment effect at varying levels of preintervention performance (averaged over both studies), illustrates the generality of the impact of the treatment. It benefited nearly 70% of African Americans. The treatment benefit was equally strong for previously poorly performing students [$t(31) = 2.74$, $P = 0.01$] and for students in the moderate range [$t(30) = 2.40$, $P = 0.02$]. The highest performing students benefited less from the intervention than did low- or moderate-performing students, but covariate-adjusted results continued to show a marginally significant trend toward a positive effect of the intervention [$t(31) = 1.72$, $P < 0.10$].

The average performance gap between African Americans in the control condition and European Americans overall in the fall term of the targeted course was 0.75 grade points (0.68 in the first experiment, 0.82 in the second). The average treatment effect for African Americans was 0.30 points, roughly a 40% reduction in the racial achievement gap.

Combining the data from both studies provides a sufficiently large sample to permit meaningful analysis of the rate of poor performance (the percentage of students receiving a D or below) (*12*). For African American students, this rate was 20% in the control condition and 9% in the treatment condition, a significant difference in logistic regression [Wald (1) = 8.14, $\Delta\chi^2$ (1) = 11.40, $P < 0.01$]. European Americans did not vary by condition (6% versus 7%, respectively). The race × experimental condition interaction was significant [Wald (1) = 3.96, $\Delta\chi^2$ (1) = 4.39, $P < 0.05$]. Figure S1 shows that the poor performance rate of African Americans in the control condition did not differ from that of African Americans in the fall term of the targeted course in the three previous years ($z < 1$, NS). In contrast, the poor performance rate of African Americans in the affirmation condition was significantly lower ($z = -2.73$, $P < 0.01$) (*12*). That is, the control condition showed no effect on performance, whereas the affirmation condition did.

An exploratory issue concerns whether, if the affirmation reduced feelings of threat, its impact extended to other courses. African American students in the affirmation condition earned a higher grade point average (GPA) in these nontargeted courses than did those in the control condition [experiment 1: $B = 0.31$, $t(40) = 2.63$, $P < 0.02$; experiment 2: $B = 0.21$, $t(58) = 1.70$, $P < 0.10$ two-tailed test, $P < 0.05$ one-tailed test]. Pooling data from both experiments yielded a significant effect [$B = 0.23$, $t(108) = 2.51$, $P < 0.02$]. European Americans again displayed no condition effect in either experiment [$|B$'s$| < 0.13$, $|t$'s$| < 1$, NS]. The race × experimental condition interaction was significant in experiment 1 [$B = 0.45$, $t(97) = 2.75$, $P < 0.01$], marginal in experiment 2 by a two-tailed test [$B = 0.30$, $t(117) = 1.74$, $P < 0.09$], significant by a one-tailed test ($P < 0.05$), and significant over both studies [$B = 0.30$, $t(228) = 2.42$, $P < 0.02$]. Because of these effects, the treatment effect on overall GPA was virtually as significant as it was on grade in the targeted course.

We obtained data related to how the affirmation process played out in vivo. The replication study provided data on performance over time. Figure 2 displays average in-class performance (proportion of total points earned) for each of 10 chronological performance blocks during the academic term

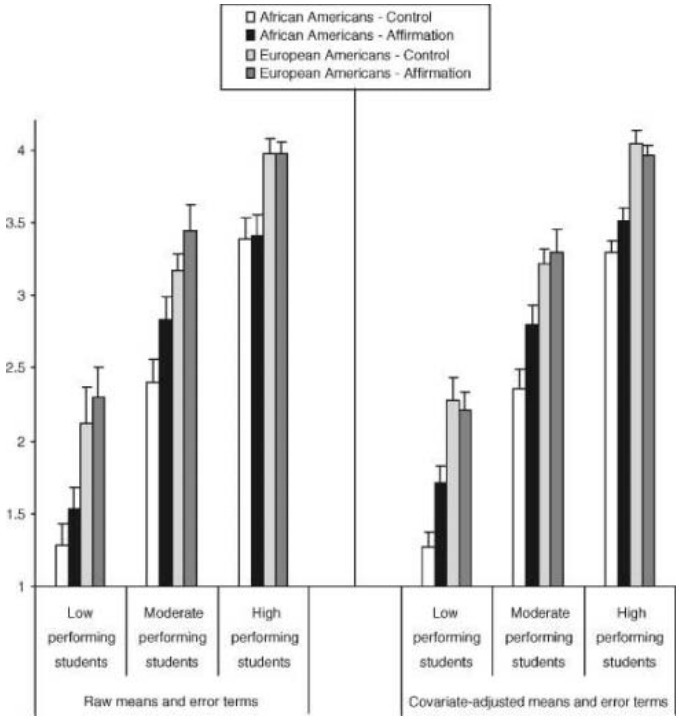

Fig. 1. Mean grade point average in the targeted class as a function of student race, experimental condition, and preintervention level of performance (an average of the prior year's GPA and preintervention in-class performance). Students were categorized into low-, moderate-, and high-performance categories on the basis of tertiary splits done separately within each racial group; the categorization represents students' relative standing within their race. (**Left**) Raw means and error terms. (**Right**) Means and error terms adjusted for baseline covariates. The scale reflects the grade metric, ranging from 0 (= F) to 4.33 (= A+). Error bars represent standard errors.

(*12*). These data suggest that the intervention buffered African American students against the impact of an early decline in performance by interrupting a downward trend. The performance pattern of African Americans in the affirmation condition, unlike that of the remaining groups, was a "sideways S" pattern, well-fitted by a cubic function [$F(1, 29) = 9.53$, $P < 0.01$], not a downward linear trend ($F < 1$, NS). In contrast, African American students in the control condition showed a significant downward linear trend; their performance continued to fall as the term progressed [repeated measures analysis, $F(1, 33) = 10.45$, $P < 0.01$]. European Americans showed a similar, although somewhat less steep, downward trend in both conditions [$F(1, 30) = 4.86$, $F(1, 25) = 7.30$, respectively, P values < 0.05] (*13*).

We also obtained evidence of another psychological process that may play a role in the intervention's efficacy by having students complete a measure of cognitive activation of the racial stereotype presented as a classroom exercise. This validated measure consisted of 34 word fragments (*5*, *6*). Seven (such as _ACE) could be completed with either a stereotype-irrelevant word (such as FACE) or a stereotype-relevant word (such as RACE). Because the experiments yielded similar effects on the primary outcome of course performance and because condition effects on the activation measure did not vary by experiment (F's $<$ 1.7, NS), data were combined to increase statistical power in this ancillary analysis (*12*). African American students generated fewer stereotype-relevant words in the affirmation condition (mean = 2.79, SD = 0.98) than in the control condition (mean = 3.25, SD = 0.91) [$t(105) = -2.56$, $P < 0.02$]. European American students showed no condition effect (means = 3.07 and 2.79; SDs = 1.08 and 1.28, respectively) ($t < 1.3$, NS). The control condition thus replicated the established pattern of African Americans' displaying higher racial-stereotype activation than European Americans in intellectually evaluative situations (*6*) [$t(111) = 2.20$, $P = 0.03$]; the affirmation condition eliminated it ($|t| < 1.5$, NS). The race × condition interaction was significant [$F(1, 218) = 6.61$, $P < 0.02$]. Activation was not generally associated with performance; however, this may have occurred because the measure was assessed several months after the original intervention and the critical performance variable (*12*).

How did our seemingly small intervention produce such large effects? First, in normal school settings, a negative recursive cycle can occur, where psychological threat and poor performance feed off one another, leading to ever-worsening performance. This downward spiral effect is indicated by (i) the relatively steep linear decline in African Americans' performance in the control condition (Fig. 2) and (ii) an ancillary analysis that showed, after controlling for level of preintervention performance, that African Americans in the control condition who saw their performance sinking early in the term (that is, who showed a relatively large preintervention drop from block 1 to block 2) performed worse later in the term (earned lower mean performance across blocks 3 to 10) (partial $r = -0.52$, $P < 0.01$) (*12*). This was not seen with European Americans in either condition (partial $r = +0.24$, $P < 0.08$). Because a recursive process depends on a continual feedback cycle, any interruption of that cycle could have long-term effects (*14*).

Second, a small reduction in psychological threat can set off another recursive cycle by leading to a slight improvement in subsequent performance, which in turn can further lessen performance-inhibiting threat, etc., leading to sustained or improving performance over time. Two of our results support this notion: (i) The intervention interrupted African Americans' downward trend and deflected it upward (Fig. 2), and (ii) an early drop in performance in this group did not predict worse performance later (partial $r = 0.02$, NS). The difference in correlations between the African American conditions was significant ($z = -2.06$, $P < 0.05$).

Third, small interventions can generate large effects if those effects accumulate across multiple trials (such as the multiple performance opportunities observed here) (*15*). Even if the intervention produced only a small improvement on each assignment, the sum of those improvements can translate into a large effect on final grades.

Fourth, as past research suggests, the psychological availability of mental concepts can affect the encoding and interpretation of social experience (*16*). Consistent with this possibility, our intervention reduced the psychological availability of the stereotype. This then could have changed African Americans' perception of the level of bias in the environment, and their interpretations of academic success and defeat, over the long term.

Finally, our apparently disproportionate results rested on an obvious precondition: the existence in the school of adequate material, social, and psychological resources and support to permit and sustain positive academic outcomes. Students must also have had the skills to perform significantly better. What appear to be small or brief events in isolation may in reality be the last element required to set in motion a process whose other necessary conditions already lay, not fully realized, in the situation. The flicking of a switch viewed in isolation may seem a quick and minor physical movement, seemingly out of proportion with the effect of having a room or a city block flooded with light.

Our findings demonstrate that alleviating psychological threat can improve intellectual achievement in a real-world environment (*8*). Our intervention is among the first aimed purely at altering psychological experience to reduce the racial achievement gap, a major problem in the United States. Unlike other interventions, it benefits the targeted students, including those most at risk, reducing group-based inequality while not adversely affecting nontargeted students (*17*). This research highlights the importance of situational threats linked to group identity in understanding intellectual achievement in real-world, chronically evaluative settings. Our results challenge conventional and scientific wisdom by demonstrating that a psychological intervention, although brief, can help reduce what many view as an intractable disparity in real-world academic outcomes.

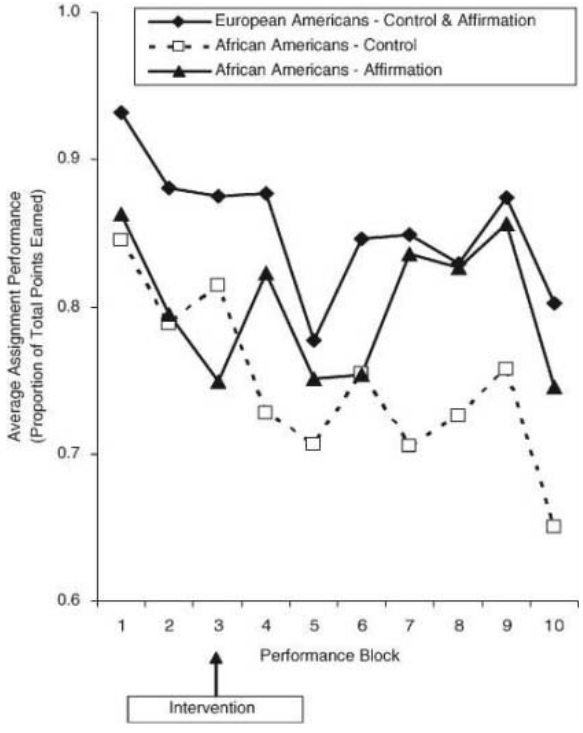

Fig. 2. Mean academic performance as a function of chronological performance block, student race, and experimental condition. Blocks 1 and 2 represent preintervention performance; blocks 3 to 10 represent postintervention performance. The data on European Americans in both conditions were combined, because they did not differ significantly.

References and Notes

1. S. E. Taylor, J. D. Brown, *Psychol. Bull.* **103**, 193 (1988).
2. C. M. Steele, in *Advances in Experimental Social Psychology*, L. Berkowitz, Ed. (Academic Press, New York, 1988), pp. 261–302.
3. D. K. Sherman, G. L. Cohen, in *Advances in Experimental Social Psychology*, M. P. Zanna, Ed. (Academic Press, San Diego, CA, 2006), pp. 183–242.

4. H. Tajfel, J. C. Turner, in *The Psychology of Intergroup Relations*, S. Worchel, W. G. Austin, S. Worchel, Eds. (Nelson Hall, Chicago, IL, 1986), pp. 7–24.
5. G. L. Cohen, J. Garcia, *J. Pers. Soc. Psychol.* **89**, 566 (2005).
6. C. M. Steele, J. Aronson, *J. Pers. Soc. Psychol.* **69**, 797 (1995).
7. C. M. Steele, S. J. Spencer, J. Aronson, in *Advances in Experimental Social Psychology*, M. P. Zanna, Ed. (Academic Press, San Diego, CA, 2002), pp. 379–440.
8. J. Aronson, C. B. Fried, C. Good, *J. Exp. Soc. Psychol.* **38**, 113 (2002).
9. R. B. Zajonc, in *Psychology of Group Influence*, P. B. Paulus, Ed. (Erlbaum, Hillsdale, NJ, 1980), pp. 35–60.
10. E. Zigler, E. C. Butterfield, *Child Dev.* **39**, 1 (1968).
11. J. D. Creswell *et al.*, *Psychol. Sci.* **16**, 846 (2005).
12. Materials and methods are available as supporting material on *Science* Online.
13. Repeated measures analyses (with teacher and gender controlled) indicated that the downward linear trend varied by condition for African Americans [$F(1, 59) = 7.30$, $P < 0.01$], but not for European Americans ($F < 1$, NS). The race × condition × performance block interaction was also significant [$F(1, 112) = 4.57$, $P < 0.05$].
14. T. D. Wilson, P. W. Linville, *J. Pers. Soc. Psychol.* **49**, 287 (1985).
15. R. P. Abelson, *Psychol. Bull.* **97**, 129 (1985).
16. S. T. Fiske, S. E. Taylor, *Social Cognition* (McGraw-Hill, New York, 1991).
17. S. J. Ceci, P. B. Papierno, *Am. Psychol.* **60**, 149 (2005).
18. We are grateful to the student participants and their parents and to the teachers and administrators of the school district for their involvement in the project. We also thank J. Sherwin, P. Brzustoski, V. Purdie-Vaughns, C. Steele, E. Zigler, D. Green, E. Uhlmann, G. Walton, and S. Cole for their guidance and feedback. This research was supported by grants from the Nellie Mae Education Foundation and from the Institute for Social and Policy Studies (Yale University).

Supporting Online Material

www.sciencemag.org/cgi/content/full/313/5791/1307/DC1
Materials and Methods
SOM Text
Fig. S1
Tables S1 and S2
References

4 April 2006; accepted 6 July 2006
10.1126/science.1128317

A Role for the Macaque Anterior Cingulate Gyrus in Social Valuation

P. H. Rudebeck,* M. J. Buckley, M. E. Walton, M. F. S. Rushworth

Complex human social interaction is disrupted when the frontal lobe is damaged in disease, and in extreme cases patients are described as having acquired sociopathy. We compared, in macaques, the effects of lesions in subdivisions of the anterior cingulate and the orbitofrontal cortices believed to be anatomically homologous to those damaged in such patients. We show that the anterior cingulate gyrus in male macaques is critical for normal patterns of social interest in other individual male or female macaques. Conversely, the orbitofrontal cortex lesion had a marked effect only on responses to mildly fear-inducing stimuli. These results suggest that damage to the anterior cingulate gyrus may be the cause of changes in social interaction seen after frontal lobe damage.

Normal patterns of human social interaction are disrupted after ventromedial frontal lobe damage (*1*). The absence of normal social behavior may be so extreme that patients are described as suffering from acquired sociopathy (*2*). The lesions are not restricted to ventromedial frontal cortex but encompass laterally adjacent orbitofrontal cortex and medially adjacent anterior cingulate cortex (ACC). Damage to just one anatomical subdivision may explain the patients' impaired social cognition. We assessed how selective lesions of ACC gyrus (ACC_G), ACC sulcus (ACC_S), or lateral orbital and ventral prefrontal cortex (PFv+o) affect the way macaques value social information.

The possibility that orbitofrontal damage underlies impaired social interaction has received attention not just as a result of patient studies but because, in macaques, circumscribed orbitofrontal lesions lead to altered emotional responsiveness to stimuli that normally induce mild fear (*3*, *4*). The deficit may be due to an inability to predict the reinforcement consequences of a stimulus or of another individual. Orbitofrontal lesions impair visual discrimination reversal learning, which requires the modification of associations between stimuli and primary reinforcers (*5*). It has been argued that the flexible assignment of reinforcement values to stimuli is a prerequisite for emotion and social behavior (*6*). Patients with ventromedial frontal lesions also perform poorly on visual discrimination reversal tasks (*7*). On the other hand, neuroimaging studies have shown that the ACC is active when human participants engage in social interaction, although its contribution has been unclear (*8*–*11*). Despite their proximity, the connections of ACC and orbitofrontal cortex are distinct in both man and monkey, and so their roles in social behavior may be correspondingly distinct (*12*–*14*).

The three lesions are summarized in Fig. 1 (and figs. S1 to S3). The PFv+o lesion was similar to one previously used to remove the principle target region of visual connections within the frontal lobe (*15*). The ventromedial region, which has connections with both PFv+o and ACC_G regions (*13*), was excluded to better assess each area's independent contribution to social behavior and emotion. Three animals received each lesion, and performances were compared with those of four unoperated controls.

Measurements were made of latencies to pick up food items in the presence of fear-inducing stimuli (toy snakes) in experiment 1, social stimuli (short films of other macaques) in experiment 2, or neutral control objects (fig. S4b). The latencies indexed the macaques' assessment of the value of obtaining further information about the stimulus before reaching and reflected their relative valuation of the stimulus in contrast to the incentive value of

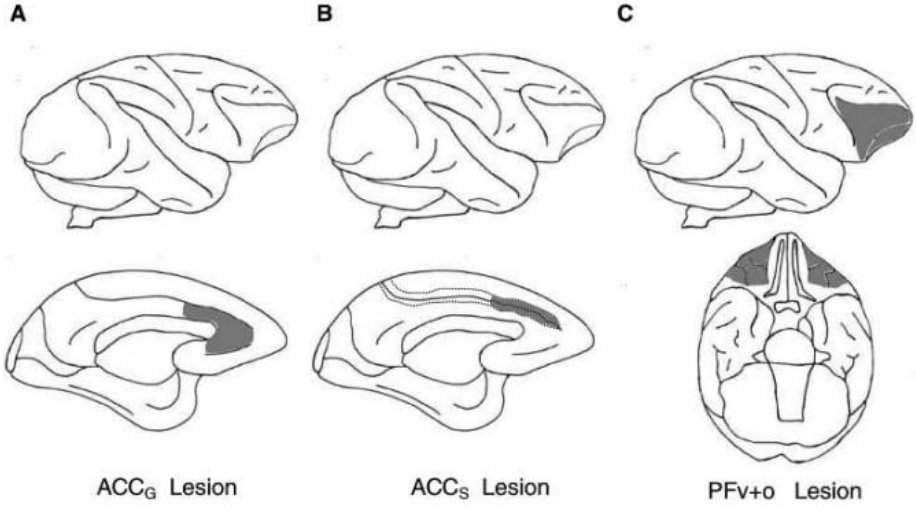

Fig. 1. Summary of (**A**) intended ACC_G lesion, (**B**) intended ACCs lesion (in both cases medial and lateral views of the brain are shown in top and bottom images, respectively), and (**C**) intended PFv+o lesion (ventral and lateral views are shown in top and bottom images, respectively). Lesion locations are shown on views adapted from the atlas of Paxinos *et al*. (*29*).

Department of Experimental Psychology, University of Oxford, Oxford, OX1 3UD, UK.

*To whom correspondence should be addressed. E-mail: peter.rudebeck@psy.ox.ac.uk

the food. Normally macaques react fearfully to snake stimuli even in the absence of prior experience (*16*), but such responses to the type of stimuli used in experiment 1 have been shown to be disrupted by lesions of more-medial orbitofrontal cortex (*3*, *4*). Male macaques prefer to view images of females or males of high social status, similar to those used in experiment 2, and will forgo small food rewards to do so (*17*, *18*). Macaques may estimate dominance of even unknown males from their appearance because of its correlation with size, age, and maturity (*19*).

Animals were tested in the Wisconsin General Testing Apparatus (WGTA) (fig. S4a). On each trial, they were given 30 s to pick up a small food item. A 30-s intertrial interval preceded the onset of the next trial. On each day, animals were exposed to five different stimuli of possible social or emotional importance and 10 neutral objects that were placed in a plastic box beneath the food. The test was repeated for 4 days with the same stimuli and for 4 further days with a new stimulus set.

The four groups did not respond in the same way to the mild fear stimuli in experiment 1 (Fig. 2A). A three-way analysis of variance (ANOVA) comparing reaching latencies of the four groups to the two snake stimuli during four presentations of each revealed significant differences [group by stimulus interaction: $F(3, 9) = 9.725$, $P = 0.003$]. Although control animals were not always fearful of a static rubber snake, they were consistently reluctant to take food from above a moving toy snake, but the case was significantly different for both the PFv+o group [stimulus by group interaction (control or PFv+o): $F(1, 5) = 31.141$, $P = 0.003$] and the ACCs group [stimulus by group interaction (control or ACC_S): $F(1, 5) = 18.953$, $P = 0.007$]. The ACC_G animals varied in their responsiveness to the moving snake, with one individual, G2, within the control range, so there were no significant differences between ACC_G and controls ($P > 0.1$). The difference between the ACC_G and PFv+o group reached borderline significance [$F(1, 4) = 7.548$, $P = 0.052$].

The four groups also differed in responsiveness to the social stimuli in experiment 2, but now the effect was due to the distinctive pattern of behavior in the ACC_G group. There was agreement among normal male controls as to which social stimuli of other macaques were more interesting (*17*); reaching latencies varied significantly depending on stimulus [$F(1, 4) = 17.493$, $P = 0.018$] (Fig. 2B). They were slower to pick up food in the presence of a large staring male, a female macaque with visible sexual perineal swellings, and a midsized macaque making affiliative lip-smacking gestures (Fig. 2B, right) than was the case with other less socially salient images. The same effect was not, however, seen in all groups [main effect of group: $F(1, 5) = 14.113$, $P = 0.013$] (Fig. 2B). The ACC_G group remained uninterested in any of the images of

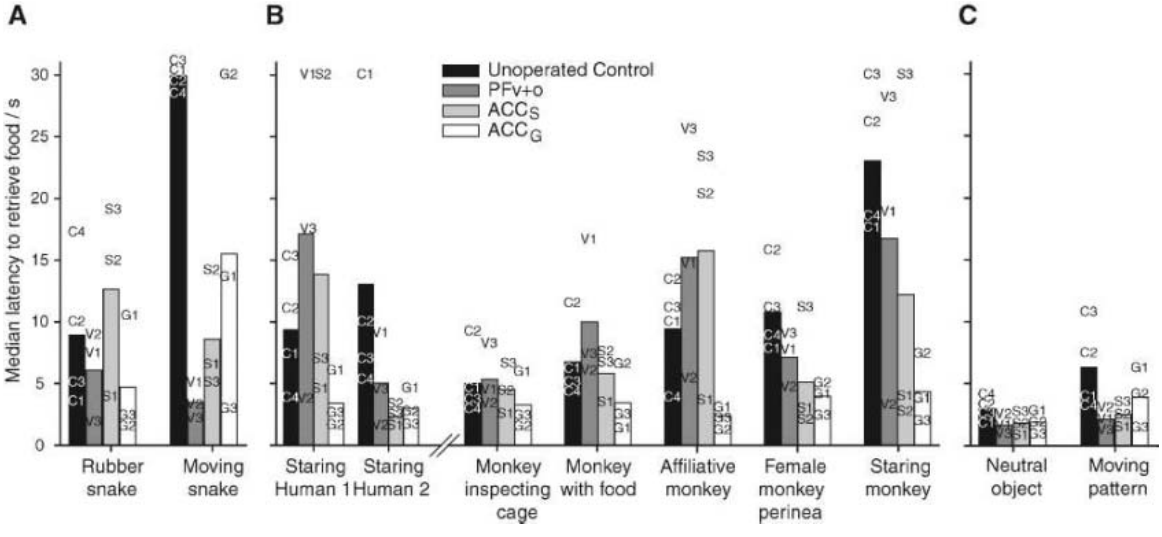

Fig. 2. Response to mild fear and social stimuli in experiment 1. **(A)** Median latency to retrieve food in the presence of a mild fear-inducing stimulus (static or moving snake). **(B)** Median latency to retrieve food in the presence of social stimuli in experiment 2, either unknown human actors (left) or macaques (right). **(C)** Median latency to retrieve food in the presence of neutral control stimuli. Symbols indicate scores for each individual.

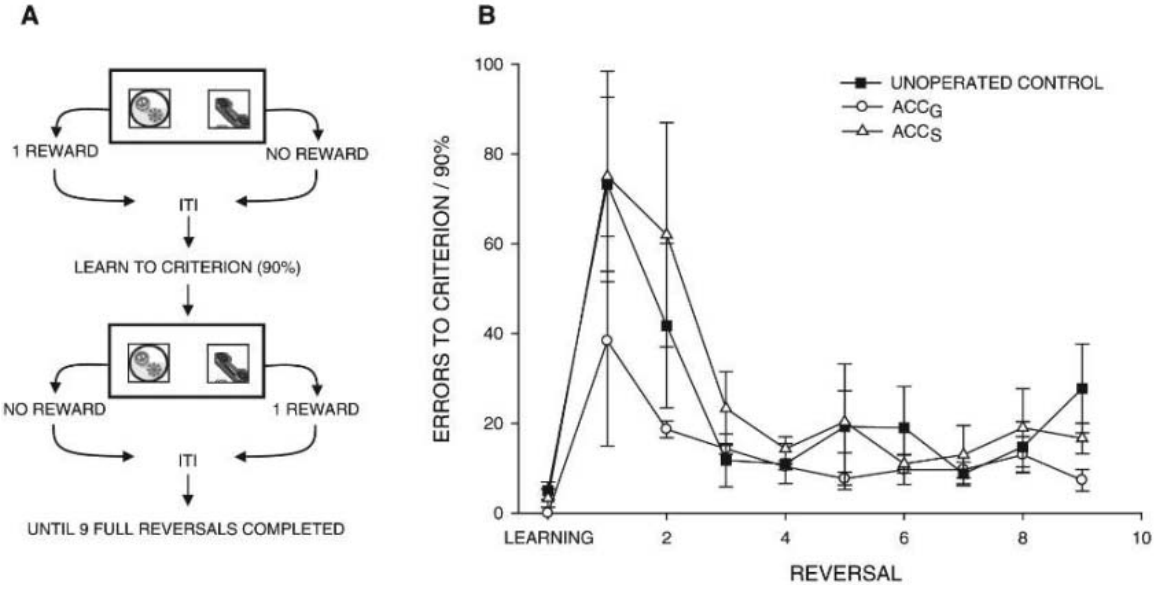

Fig. 3. Visual discrimination reversal learning task. **(A)** Animals were presented with two images on the screen. Selection of one stimulus led to a reward, whereas selection of the other did not. Animals learned the task until they performed above a criterion of 90% correct performance. The reward contingencies were then reversed, and animals had to relearn the new stimulus reward association to a criterion of 90%. Animals completed nine full reversals after initial learning. **(B)** Mean (±SEM) number of errors to criterion per reversal.

other macaques, and the patterns of change in interest with stimulus type seen in the control group were absent (Fig. 2B). ACC_G performance was significantly different to both that of controls [main effect of group: $F(1, 5) = 14.113$, $P = 0.013$] and that of the PFv+o group [main effect of group: $F(1, 4) = 8.651$, $P = 0.042$], although the contrast with the ACC_S group did not reach significance ($P > 0.1$). By contrast, comparable modulations of reaching latencies were seen in PFv+o and ACC_S groups as in the controls, and there were no significant differences between any of these three groups ($P > 0.1$). A complementary analysis of the expression of social behaviors found that ACC_G animals produced fewer social responses than either control, PFv+o, or ACC_S animals (Materials and Methods and fig. S5). Previous investigations have assessed macaques' emotional and social responsiveness by exposure to unfamiliar humans (*5*). Although PFv+o latencies were generally comparable to those of control animals, they were sometimes shorter in response to one of the two unfamiliar humans, and this prevented ANOVAs involving this group from reaching significance (Fig. 2B). Nevertheless a comparison of the ACC_G and control groups once again revealed significant differences [main effect of group: $F(1, 5) = 7.030$, $P = 0.045$].

To further test the robustness of the distinction drawn between ACC_G and PFv+o group's diminished responsiveness to mild fear and social stimuli, respectively, we used a four-way ANOVA to compare the two groups' latencies for the two exemplars of fear stimuli and the two most effective exemplars of social stimuli (female macaque and dominant male macaque) across the four presentations. A highly significant interaction between stimulus category, stimulus exemplar, and group was found on comparing ACC_G and PFv+o groups [$F(1, 4) = 23.494$, $P = 0.008$]. The difference was only marginally significant [$F(1, 4) = 4.954$, $P = 0.09$] when ACC_G and ACC_S groups were directly compared.

Significant reductions in ACC_G reaching latency were only observed on trials involving social stimuli but not when control objects were presented (Fig. 2C). Although group differences were found in responses to the first set of neutral junk objects and moving inanimate visual patterns [$F(9, 27) = 2.817$, $P = 0.046$], these transpired to be due to quicker latencies in the PFv+o group in comparison with those of controls [$F(1, 5) = 30.075$, $P = 0.003$] and not quicker latencies in the ACC_G group ($P > 0.1$). Significant interactions [$F(1, 5) > 6.686$, $P < 0.05$] between group (ACC_G versus control) and stimulus (neutral versus each of the four most effective social stimuli) confirmed the specificity of the ACC_G effect to social stimuli.

The orbitofrontal involvement in emotional responses to stimuli, such as those that induced mild fear (Fig. 2A), may be related to its role in representing expectations about the reinforcement outcomes associated with stimuli because lesions also impair visual discrimination reversal learning (*3*–*7*, *20*). Unlike the orbitofrontal cortex, the ACC_G contribution to social behavior may be unrelated to the representation and learning of outcome expectations. Indeed, both ACC_G and ACC_S groups were unimpaired on a reversal learning test similar to the one previously used with orbitofrontal lesions ($P > 0.1$) (Fig. 3).

It has previously been observed that macaques spend less time in proximity with one another after large ACC lesions (*21*). The present results suggest that this may be a consequence of a lowered valuation of social information. The specificity of the ACC_G lesion was apparent when its effects were compared with those of the PFv+o lesion on several tests involving fear and social stimuli. The ACC region critical for mediating the valuation of social stimuli appears to be the ACC_G immediately rostral and dorsal to the genu of the corpus callosum and includes areas 32 and rostral area 24. The ACC_G lesion did not include subcallosal area 25 ventral to the genu of the corpus callosum (Fig. 1 and fig. S2), which has been linked with mood change and depression (*22*). The ACC_G lesions sometimes disrupted parts of ACC_S, but the damage was neither complete nor bilateral. Moreover, it is difficult to attribute the deficit to the ACC_S because complete ACC_S lesions only affected the mild fear task significantly and not the social task; a pattern of change opposite to that seen in the ACC_G group. A note of caution is warranted; although ACC_G and ACC_S groups exhibited opposite patterns of change when contrasted with controls, often only marginally significant differences were found when the two groups were directly compared with one another, perhaps because of the small group sizes and some interindividual variability that might be related to damage to adjacent white matter. Despite these caveats, the absence of consistent impairment after ACC_S lesions should not be overlooked. The ACC_S lesion is not simply ineffective and is known to cause clear changes in reward guided choice and decision-making (*23*).

Signal changes have been recorded in a homologous area when human subjects perform tasks requiring consideration of other individuals or engagement in social interaction (*8*–*11*). The prisoner's dilemma game, ultimatum game, and theory of mind tasks used in neuroimaging studies are complex, and changes are recorded beyond the ACC_G, making it difficult to ascertain its particular importance. ACC_G changes have also been correlated with autistic social interaction impairments (*24*). The present results demonstrate an essential and causal role for ACC_G in valuing social information when the implications of another individual's presence must be taken into account before acting.

Normal emotion and social behavior is dependent on the integrated interactions of several brain areas, including orbitofrontal cortex and amygdala (*25*, *26*), but the present study suggests the ACC_G has an important complementary role. Orbitofrontal cortex may be essential for emotion and social behavior as a consequence of its involvement in the representation of the outcome expectancies that guide choice and learning (*4*, *5*, *20*) and its general role in encoding the relative economic values of a wide range of both social and nonsocial stimuli (*4*, *27*). Damage to any one of these interconnected areas early in development may lead to widespread neurobiological and behavioral changes (*28*).

References and Notes

1. A. Bechara, H. Damasio, A. R. Damasio, *Cereb. Cortex* **10**, 295 (2000).
2. J. L. Saver, A. R. Damasio, *Neuropsychologia* **29**, 1241 (1991).
3. A. Izquierdo, E. A. Murray, *J. Neurophysiol.* **91**, 2023 (2004).
4. A. Izquierdo, R. K. Suda, E. A. Murray, *J. Neurosci.* **25**, 8534 (2005).
5. A. Izquierdo, R. K. Suda, E. A. Murray, *J. Neurosci.* **24**, 7540 (2004).
6. E. T. Rolls, *The Brain and Emotion* (Oxford Univ. Press, Oxford, 1999), p. 367.
7. L. K. Fellows, M. J. Farah, *Brain* **126**, 1830 (2003).
8. C. D. Frith, U. Frith, *Science* **286**, 1692 (1999).
9. J. Rilling *et al.*, *Neuron* **35**, 395 (2002).
10. J. K. Rilling, A. G. Sanfey, J. A. Aronson, L. E. Nystrom, J. D. Cohen, *Neuroimage* **22**, 1694 (2004).
11. T. Singer *et al.*, *Science* **303**, 1157 (2004).
12. P. L. Croxson *et al.*, *J. Neurosci.* **25**, 8854 (2005).
13. D. Ongur, J. L. Price, *Cereb. Cortex* **10**, 206 (2000).
14. G. W. Van Hoesen, R. J. Morecraft, B. A. Vogt, in *Neurobiology of Cingulate Cortex and Limbic Thalamus*, B. A. Vogt, M. Gabriel, Eds. (Birkhauser, Boston, 1993), pp. 249–284.
15. T. J. Bussey, S. P. Wise, E. A. Murray, *Behav. Neurosci.* **115**, 971 (2001).
16. S. Mineka, in *Theoretical Foundations of Behaviour Therapy*, H. J. Eysenck, I. Martin, Eds. (Plenum, New York, 1987), pp. 81–111.
17. R. O. Deaner, A. V. Khera, M. L. Platt, *Curr. Biol.* **15**, 543 (2005).
18. S. V. Shepherd, R. O. Deaner, M. L. Platt, *Curr. Biol.* **16**, R119 (2006).
19. D. S. Sprague, *Am. J. Phys. Anthropol.* **105**, 511 (1998).
20. G. Schoenbaum, M. Roesch, *Neuron* **47**, 633 (2005).
21. K. A. Hadland, M. F. S. Rushworth, D. Gaffan, R. E. Passingham, *Neuropsychologia* **41**, 919 (2003).
22. H. S. Mayberg *et al.*, *Neuron* **45**, 651 (2005).
23. S. W. Kennerley, M. E. Walton, T. Behrens, M. J. Buckley, M. F. S. Rushworth, *Nat. Neurosci.* **9**, 940 (2006).
24. T. Ohnishi *et al.*, *Brain* **123**, 1838 (2000).
25. J. Bachevalier, K. A. Loveland, *Neurosci. Biobehav. Rev.* **30**, 97 (2006).
26. N. H. Kalin, S. E. Shelton, R. J. Davidson, *J. Neurosci.* **24**, 5506 (2004).
27. C. Padoa-Schioppa, J. A. Assad, *Nature* **441**, 223 (2006).
28. R. C. Saunders, B. S. Kolochana, J. B. Bachevalier, D. R. Weinberger, *Nature* **393**, 169 (1998).
29. G. Paxinos, X. F. Huang, A. Toga, *The Rhesus Monkey Brain in Stereotaxic Coordinates* (Academic Press, San Diego, CA, 2000).

30. This work was supported by the Medical Resarch Council (P.R., M.J.B., M.E.W., and M.F.S.R) and the Royal Society (M.J.B. and M.F.S.R.). We thank G. Daubeny for assistance with histology and D. Gaffan for advice and encouragement.

Supporting Online Material

www.sciencemag.org/cgi/content/full/313/5791/1310/DC1
Materials and Methods
Figs. S1 to S5
References

31 March 2006; accepted 3 July 2006
10.1126/science.1128197

SEM Technology

New WETSEM technology enables scanning electron microscopes to image and analyze wet samples such as cells, tissue biopsies, and foods in their native environments. Eliminating the need for time-consuming preparation procedures, the technology ensures that sample integrity is not compromised by artifacts and solves the problem of preparing wet samples for high-resolution imaging. The technology closes the resolution gap between conventional electron microscopy and light microscopy and offers the convenient sample preparation of light microscopy.

Electron Microscopy Sciences For information 215-412-8400 www.emsdiasum.com

Handheld Dispensers

The Repeater stream and Xstream are easy-to-use, ergonomic handheld dispensers that offer speed, precision, and flexibility as well as the ability to dispense liquids with high vapor pressure and/or high viscosity, while also preventing cross-contamination. They feature a motorized piston, intuitive programming, and a simple one-button tip ejection system. When these dispensers are used with the Eppendorf Combitips Plus tip system, the tip is automatically recognized and its volume displayed. Both models perform all standard pipetting and dispensing functions; the Xstream can also perform titrations, supernatant removal, and sequential dispensing.

Eppendorf North America For information 800-645-3050 www.eppendorfna.com

Mass Spectrometer

The Q-Tof Premier is a quadrupole, orthogonal acceleration time-of-flight (TOF) tandem mass spectrometer designed to offer enhanced levels of flexibility, sensitivity, specificity, and speed of acquisition. The Q-Tof Premier, when combined with Ultra Performance LC, provides high quality data in a wide variety of applications, including metabolite profiling, biomarker discovery, and quantitative proteomics. The system's LockSpray source automates the acquisition of exact mass measured data.

Waters For information 800-252-4752 www.waters.com

Hepatocyte Cell Transfection

A powerful cationic polyethylenimine (PEI)–derived transfection reagent optimized for the delivery of genes to primary human hepatocytes and hepatocyte-like cells is available. Compatible with serum and antibiotics, jetPEI-Hepatocyte DNA transfection reagent has demonstrated transfection efficiencies greater than 50% in primary hepatocytes. Similar transfection efficiencies have been shown in popular hepatocyte-derived cell lines such as BNL-CL.2 and HepG2. The jetPEI-Hepatocyte is a galactose-bearing linear polyethylenimine designed to enhance the transfection of cells expressing galactose-specific membrane lectins.

Polyplus-transfection For information 760-481-4918 www.polyplus-transfection.com

Charged Aerosol Detector

The Corona Charged Aerosol Detector offers all-in-one performance benefits to the high-performance liquid chromatography market that refractive index, low wavelength, evaporative light scattering, and chemiluminescent nitrogen detector methods lack. Already in use by major pharmaceutical companies, it has been enhanced for greater compatibility with solvents used in industrial, chemical, and polymer analyses. The new Corona Plus is designed to address the needs of laboratory personnel who use THF (tetrahydrofuran) as a mobile-phase component in the chromatographic separations and sample analyses.

ESA Biosciences For information +44 1844-239381 www.esainc.com

Increased Transformation Efficiency

DNA transformation can be difficult to achieve in many bacterial strains due to the presence of restriction/modification (R-M) systems that cleave unmodified DNA that is recognized as "foreign." TypeOne Restriction inhibitor provides a powerful method for increasing transformation efficiencies in bacterial strains with type I R-M systems. TypeOne Inhibitor is readily electroporated into cells along with transforming DNA. In vivo, the protein acts as a molecular decoy that inhibits DNA cleavage, leaving the transforming DNA intact.

Epicentre Biotechnologies For information 800-284-8474 www.EpiBio.com

Sealing Tape Roll

The Nunc Sealing Tape Roll Dispenser conveniently provides researchers with the means to protect plate wells from contaminants, dust, and evaporation. Each dispenser contains a roll of 1000 clear, polyester tapes with self-sealing acrylic adhesive backing that firmly adheres to plate wells. Each tape is 121 mm by 78.33 mm and is suitable for use with all microplates, including those constructed of polypropylene, polystyrene, and other popular resins. A tab enables easy removal of the adhesive backing. Unlike heat seal tapes, Nunc adhesive sealing tapes do not require a separate instrument to use. The tapes accommodate a temperature range of –20°C to +120°C.

Nalge Nunc International For information 585-586-8800 www.nuncbrand.com

Newly offered instrumentation, apparatus, and laboratory materials of interest to researchers in all disciplines in academic, industrial, and government organizations are featured in this space. Emphasis is given to purpose, chief characteristics, and availability of products and materials. Endorsement by *Science* or AAAS of any products or materials mentioned is not implied. Additional information may be obtained from the manufacturer or supplier by visiting www.science.labvelocity.com on the Web, where you can request that the information be sent to you by e-mail, fax, mail, or telephone.

HUPO

Human Proteome Organisation

HUPO 5th Annual World Congress

October 28 – November 1, 2006
Long Beach, CA

The HUPO 5th Annual World Congress, "Translating Proteomics from Bench to Bedside," will take place in the Long Beach Convention Center. The center occupies a waterside location surrounded by a variety of hotels, restaurants, and shops, all within an easy walk. Long Beach is centrally located in the heart of Southern California, approximately 25 miles south of Los Angeles, on the Pacific Coast.

HUPO 2006 Mission

- To facilitate the exchange of scientific ideas, knowledge, and information
- To promote the application of proteomic based novel prognostic, diagnostic, and therapeutic tools
- To advance our understanding of the proteomic basis underlying human diseases

http://www.hupo2006.com

Go on-line to:

Submit abstract (select "abstract submission")

Register (select "Registration")

Book hotel room (Select "Hotel reservations")

View program (select "Congress Program")

View exhibitors

Photo courtesy of Destinations Long Beach Magazine

Photo courtesy of Destinations Long Beach Magazine

PRE-CONGRESS PROGRAM

Saturday, October 28 and Sunday, October 29

• Education Program • Clinical Day

CONGRESS PROGRAM

Sunday evening, October 29:
Exhibition Opening and Reception

Monday - Wednesday, October 30 – November 1, 2006:
Over 20 symposia, oral sessions, and poster sessions on the topics of:

- Bioinformatics in Proteomics
- C. Elegans Proteomics
- Diabetics and Metabolic Disorders
- Glycoproteomics
- Human Disease Proteomics
- Mass Spectrometry
- Membrane Proteins and Proteomics
- Metabolomics
- Nanotechnology and Single Molecular Imaging
- Novel Technologies in Protein Separations
- Post-Translational Modifications
- Protein Arrays
- Proteomics and Therapeutics
- Single Molecular Detection
- Stem Cell Proteomes
- Systems Biology and Networks
- The Mitochondrial Proteome
- The UPS-Proteasome Complexes

Plus: workshops, panel discussions, and corporate symposia

EXHIBITS. The Long Beach Congress provides many opportunities for companies to exhibit and promote products and services to an elite group of scientists. Exhibit booths, scientific posters, Internet access and refreshment breaks will be located in the exhibit hall. Details are available on the Congress web site.

Congress Co-Chairs:
Professor Peipei Ping, UCLA
Professor John Yates, Scripps Research Institute

For information, call the Congress Management Office: 505-989-4876

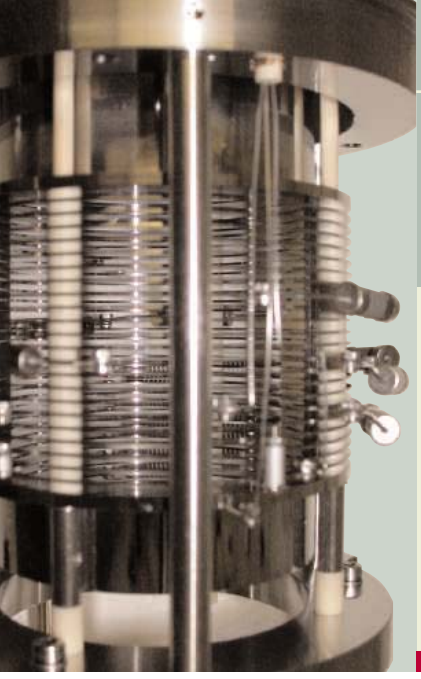

Life Science Technologies

Mass Spectrometry in Drug Discovery and Development: FROM PHYSICS TO PHARMA

Long a quintessential tool of physicists, mass spectrometry has emerged as a critical technology for the pharmaceutical field. It gives researchers greater sensitivity, higher throughput, and extra information about molecules with druggable potential. **by Peter Gwynne and Gary Heebner**

Drug discovery and development projects can generate hundreds of thousands of compounds that scientists must analyze to characterize structures and identify impurities. Once they have identified a drug target and have run bioassays to understand better how it functions, they can focus their efforts on finding small organic molecules that alter the target's function. To characterize these small entities, as well as larger biomolecules, life scientists increasingly rely on mass spectrometry (MS).

Originating in physics labs, MS has gradually gained a significant spot in the pharmaceutical world. "Its latest impact will be on the rational approach to drug design, via its capability to elucidate protein posttranslational modifications," says Emmanuel Raptakis, product manager of **Shimadzu Biotech**. "It gives an excellent view of molecules and their modifications." The technology's application has also begun to spread beyond small-molecule drugs. "With the more modern techniques, it also applies to biomolecules such as proteins, glycoconjugates, or oligonucleotides," explains Christoph Menzel, global product manager for mass spectrometry at **Qiagen**. Beyond that, adds Jasmine Gray, marketing director for protein sciences at **GE Healthcare**, "Biomarker discovery is the buzzword that everybody's using. MS is one of the critical parts of the identification and characterization of proteins."

'Ubiquitous and Indispensable'

Douglas Mautz, senior director of pharmacology (discovery absorption, distribution, metabolism, and excretion [ADME] and drugs and pharmacology metabolism) for contract research organization **MDS Pharma Services**, summarizes the situation. "I saw mass spectrometry was amazingly powerful in life science 15 years ago," he recalls. "Now I view it as nearly ubiquitous and indispensable." Lester Taylor, product manager for life science mass spectrometry at **Thermo Electron**, outlines the technology's clinical potential. "The development of drugs with higher potency that you can take once a day rather than more often has presented a challenge of analytical detection of low levels in plasma and urine," he says. "MS facilitates that."

Inclusion of companies in this article does not indicate endorsement by either AAAS or *Science*, nor is it meant to imply that their products or services are superior to those of other companies.

The technology's value spans the entire drug pipeline. "In clinical trials, where you can generate thousands of samples, you need to be able to quantify drugs and metabolites quickly and accurately," points out Joe Anacleto, senior director of the small molecule business for **Applied Biosystems**. "MS is the method of choice for that." Indeed, says Robert Plumb, pharmaceutical application and development manager for **Waters Corporation**, "It has become almost a cornerstone of modern drug discovery and development, from target identification and validation up to combinatorial chemistry and parallel synthesis chemistry." Victor Fursey, assistant vice president for sales and marketing at **Bruker Daltonics**, echoes that thought. "You see mass spectrometry in everything from new chemical entities to formula determination to target profiling and preclinical work," he says. "Now, you even see it at the far end, in manufacturing. And many researchers are working to bring mass spectrometry into diagnostics."

Mass spectrometry doesn't stand alone. Pharmaceutical researchers routinely team it up with other techniques to obtain synergistic effects. "Liquid chromatography/mass spectrometry (LC/MS) is now the de facto technique for providing quantitative data for drug evaluation and submission for drug approval," Taylor explains.

Taylor makes another key point. "Instruments no longer have dedicated mass spectroscopists running them," he says. "Now, in many of the biological applications, biologists are using the tools. Vendors need to ensure the highest standards of performance in a way that's much more robust and easy to obtain on a routine basis."

Flavors and Configurations

Biological molecules produce several fragments when subjected to mass spectrometry. The technique does not yield the fragments' actual masses. Rather, it determines their mass-to-charge ratio; if scientists know an ion's charge, they can then calculate its mass. The fragments produce a mass spectrum that scientists continued ›

IN THIS ISSUE:

Life Science Technologies: MASS SPECTROMETRY IN DRUG DISCOVERY AND DEVELOPMENT

can use to identify each molecule uniquely. Because biomolecules' mass spectra differ little from instrument to instrument, the information can be stored in a database and unfamiliar spectra searched against known ones.

Mass spectrometers typically include three components: an ionization device, a mass analyzer, and a detector. Since almost any ionization method can be coupled to any mass analyzer, commercially available mass spectrometers come in what Alan Millar, Waters's Synapt product manager, calls "several different flavors and configurations."

Life scientists usually rely on two ionization methods: matrix-assisted laser desorption ionization (MALDI) and electrospray ionization (ESI). MALDI is a solid phase technique that can analyze a digested protein sample from a 2-D polyacrylamide gel. ESI, a liquid methodology, is compatible with high pressure liquid chromatography (HPLC) and capillary electrophoresis (CE).

Mass analyzers commonly used for biochemical applications include ion trap, time-of-flight (TOF), triple-quadrupole, and quadrupole-TOF instruments. Ion trap systems capture ions in a small volume and then eject specific ranges of masses toward a detector. Their advantages include compact size and the ability to increase the signal-to-noise ratio of a measurement. In TOF systems, each ion has the same kinetic energy but moves at a speed that varies with its mass. Time-of-flight analyzers are highly compatible with very fast ionization methods such as MALDI. Quadrupole (or quad) analyzers permit only ions with specific mass-to-charge ratios to pass through an electrical field to the detector. Varying the field allows users to analyze different ions.

After they travel through any analyzer, ion species strike an ion detector. This ejects electrons that cause a voltage proportional to the number of ions that passed through the analyzer.

Researchers often couple quadrupole analyzers to ESI devices, and frequently use them in tandem configurations (referred to as MS/MS). Vendors now offer combinations of mass analyzers as solutions to specific problems in drug discovery and development. "We see a proliferation of hybrid instruments, ending up as one plus one equals three," Applied Biosystems' Anacleto notes.

Mother Nature's Cruel Way

The major barrier to productive MS analysis is not the instrumentation, but successful purification of biomolecules suitable for analysis. "The most important proteins in biomarker discovery are the low-abundant proteins; that's Mother Nature's cruel way of treating us," GE Healthcare's Gray explains. "That puts pressure on the front end – sample preparation – and the back end – mass spectrometry and data analysis. To look at low-abundant proteins, you need increasingly more sensitive techniques on the MS end and increasingly better fractionation on the front end. Sample preparation is the most critical phase of the whole process. Any sins you commit here cannot be recovered by even the most sophisticated mass spectrometer."

That's why sample preparation has become the most critical and challenging task in MS analysis. It involves purifying, storing, and recovering proteins, peptides, and other biomolecules and removing such contaminating species as buffers, salts, and detergents prior to MS analysis. "You're not looking to filter one protein away from the others; you're trying to reduce the complexity of a sample," Gray points out. "It's still a mixture that you want to enrich."

EMD Biosciences, **Pierce**, and **Sigma-Aldrich**, among other companies, offer a wide range of products and kits for purifying proteins and other biological molecules for MS analysis. GE Healthcare, which has long produced chromatography columns and systems, protein purification kits, and reagents, now offers specialized kits for use with MS studies. Those include its Ettan CAF MALDI Sequencing Kit for peptide-mass fingerprinting using MALDI-TOF mass spectrometry. "Chemically, it's a process that results in more reproducible fragmentation of the peptides in MALDI ionization," Gray explains.

Another preparatory method involves liquid chromatography. Termed Ultra Performance LC by Waters, the method takes advantage of the performance abilities of sub–two-micron particles. Used as front ends for mass spectrometry, UPLC systems can improve resolution by a factor of two, sensitivity by a factor of three, and separations by 10 times.

Chip-based Products

Qiagen also offers kits and reagents for sample preparation prior to MALDI-MS, including two chip-based products released this year. "Our Mass·Spec·Focus Chips are engineered for higher sensitivity and purification of samples from, for example, 2-D gel separation," Menzel says. "Their functionalities such as phosphopeptide enrichment derive from different zones on the chip's surface that retain particular peptides and simultaneously guide the droplet for a concentration in the analysis zone. This gives up to one thousand times the sensitivity compared with conventional targets."

The company's Mass·Spec·Turbo Chips, meanwhile, offer higher throughput and particular LC-MALDI applications. Each chip consists of a dense array of very homogenous matrix spots deposited by vacuum sublimation on an ultraphobic surface. "This allows simple, reproducible LC-MALDI applications with increased sensitivity without interfering with established protocols" Menzel says.

Further in preparation for mass spectrometry Qiagen's Qproteome series of protein fractionation kits is designed to "reduce

Look for these upcoming Life Science Technology articles

Functional Genomics . . . . . 29 September
Aging and Neuroscience . . . . . 6 October
Nanobiotechnology . . . . . 3 November

Or, access past articles at http://www.sciencemag.org/products/articles.dtl

Laboratory Automation . . . . . 13 January
Combinatorial and Computational Chemistry . . . . . 17 March
Cell Signaling in Cancer Research . . . . . 24 March
Proteomics . . . . . 14 April
Biochips and Lab-on-a-Chip Devices . . . . . 5 May
Pharmacogenomics . . . . . 28 July

Video Features from *Science*

As part of its continuing service to readers, *Science* announces two new video features. A new documentary complements the report on AIDS in Latin America and the Caribbean that appeared in the 28 July issue of this publication. Prepared by Biocompare and *Science*, it features interviews with notable scientists, physicians, and activists who help to treat and prevent HIV/AIDS in the region. You can find the presentation at:

HTTP://WWW.SCIENCEMAG.ORG/AIDSVIDEO

Another new feature comes from *Science* Online Seminars. The editors of *Science* select an author of a breakthrough paper to discuss the application of the research and/or the methods and protocol in an audio/slideshow presentation. Produced by the Office of Publishing and Member Services, the show is free and requires no registration. Just go to *Science* Online at:

HTTP://WWW.SCIENCEMAG.ORG/ONLINESEMINAR

the overwhelming complexity in biological systems," as Menzel explains. To supplement the pure fractionation kits, the company offers depletion kits that sort out high abundant proteins and total protein extraction kits that allow gentle but effective lysis of mammalian or bacterial cells.

GE Healthcare has recently released three new separation technologies. "Ettan nanoLC and Ettan MDLC give researchers flexibility in their peptides' separation methods upstream of MS. And nanoCOLLECT interfaces with the chromatography systems as a microfraction collector or spotting of fractions onto MALDI slides," Gray says. "We have created different chromatography solutions that interface to the different types of mass spectrometry. That's useful because you will tend to identify different proteins depending on what type of mass spectrometry technique you use – whether electrospray or MALDI; you have to choose your weapon." Since only a small proportion of identified proteins overlaps the different MS methods of upstream separation methods such as 2D electrophoresis and chromatography, she continues, "Researchers try to arm themselves with as many methods as possible to identify as many low-abundant proteins as possible."

No Standing Pat

Suppliers of mass analyzers refuse to stand pat on their technology. Several have recently introduced MS systems or enhancements that can provide additional data for researchers working in both drug discovery and life science research.

Waters recently introduced the first mass spectrometer to employ new ion-mobility technology and software, which it calls the Synapt High Definition MS System. "It's a new category of mass spectrometry," Millar explains. "It has a very innovative performance and functionality. It introduces an additional dimension of ion separation: Ions are separated according to size, shape, and charge prior to mass spectrometry. That results in more specificity, which means that we can extract more information."

A key feature of this new system is the patented Waters Triwave technology, a method for combining highly efficient measurement and separations based on ions' mobility with high performance quadrupole/TOF mass spectrometry. "This is the enabling technology that powers the Synapt system," Millar says. "It permits the high-efficiency ion mobility, which is very important. It also enables us to combine the ion mobility with the tandem MS. It's not just about performing the ion mobility but being able to combine it into a solution." Operational control and data acquisition and processing are performed through the company's MassLynx Software.

Shimadzu Biotech's AXIMA-TOF^2, launched in June, represents the next generation in MALDI collision-induced dissociation (CID) MS/MS. A TOF-TOF mass spectrometer with high energy MS/MS, it delivers information-rich spectra with greater sensitivity and higher confidence in identification. "It uses electron technology licensed from Johns Hopkins University that allows high-energy CID without the need to accelerate the ions; that gives better transmission," Raptakis says. "It's a very versatile tool – the highest energy collision-induced dissociations you can get. It has the ability to look at complex structures like peptides and lipids, which will break very effectively in a number of highly informative pathways. It is the most efficient way to discover, for example, double bond localization in lipid research and to generate cross-linked cleavage in oligosaccharides structural elucidation experiments."

Applied Biosystems recently launched another system aimed at drug discovery, that it calls the LightSight Software for Metabolic Identification. "It's a new piece of software especially for metabolite discoveries in the drug discovery phase," Anacleto explains. "We worked very closely with over a hundred scientists to understand their work flows in identifying metabolites quickly and easily. It's focused primarily on productivity for fairly routine work finding key metabolites." Scientists can use the system with the Applied Biosystems 4000 Q TRAP mass spectrometer, as well as other triple quadrupole and hybrid linear ion trap mass spectrometers from Applied Biosystems/MDS SCIEX.

Dealing with More Data

As a consequence of their increased sensitivity and higher throughput, MS technologies generate significantly more data than in the past. "You might acquire a mass spec in 20 to 30 seconds and find yourself looking at 20–30 megabytes of data," says Ian Brookhouse, development manager for MALDI mass spectrometers at Shimadzu Biotech. To manage this increase, companies such as **Agilent**, **Ciphergen**, **PerkinElmer**, and Waters offer software for data management and analysis, often integrated into the MS **continued ›**

system. "We've been working on application managers – dedicated software tools that permit you to put a particular focus on specific tasks such as proteomics or metabolic identification, or food safety," Waters's Plumb reports. "We also have the ability to store an archive and retrieve it, and to combine data from different projects, such as MS and X-ray crystallography."

Thermo Electron has introduced what it calls QuickQuan for automating high-throughput LC-MS/MS assays in early drug discovery. "This is a software and hardware solution that allows users to analyze multiple sets of compounds in an automated fashion without having to optimize and tune for a particular compound," Taylor says. "You can automatically set up to run for each compound you're checking on. The system tunes itself automatically and analyzes assay samples overnight without needing to have people on hand. It works in combination with our triple quadrupole system."

Last year, GE Healthcare launched its DeCyder MS differential analysis software. "It creates a three-dimensional plot of the retention time and m/z ratio," Gray says. "Instead of traditional peaks, you have a signal intensity spot map like a 2-D electrophoresis map. It basically helps you to compare the different peptides between different runs and tease apart all the nuances and find that needle in the haystack."

Fursey of Bruker Daltonics highlights an emerging field facilitated by MS. "Metabolomics is gaining a lot of momentum in the effort to understand the pharmaceutical world," he says. "Much of what's going on in metabolomics stems from nuclear magnetic resonance [NMR] technology. We're finding that mass spectrometric data can be very complementary to NMR." His company and Bruker BioSpin offer the Metabolic Profiler, an integrated platform for metabolic studies and analyzing complex mixtures. It features an HPLC-microTOF ESI-TOF system and an optional Avance NMR spectrometer and integrated software for data acquisition, evaluation, and statistical analysis in such applications as assessing the metabolic profile of a living organism to distinguish between normal and altered states and studying the mechanism of drug-induced toxicity. Fursey notes that the Metabolic Profiler is fully integrated into the Bruker Compass OA software environment.

The CRO Connection

Although vendors have made their MS systems increasingly user-friendly, some drug discovery and development groups – particularly in small and medium-sized pharmas – prefer to keep the technology at a distance. They turn to contract research organizations (CROs) such as **Covance**, MDS Pharma Services, **PPD**, and **Quintiles** for MS and related services.

MDS, for example, provides a full spectrum of resources, including mass spectrometry, to meet the pharmaceutical and biotechnology industries' drug discovery and development needs. "While access to capacity is certainly one advantage," Mautz says, "we find that our sponsors value access to expertise and our experience in handling compounds with less than ideal biophysical properties."

While multiple lines of business in MDS use mass spectrometry, Mautz's team has a particular focus on discovery ADME. "We offer standard quantitative work," he says. "And because we are an ADME group, we move from quantitative into qualitative aspects of mass spectrometry. When we ask what are the metabolites, fragmentation analysis by mass spectrometry is the most powerful tool to provide an answer."

In addition, Mautz's team is working on MALDI imaging/profiling for analysis of tissues. "MALDI imaging represents a new and exciting technique for improving our understanding of distribution while still in discovery," Mautz explains. "If the ADME sciences can provide a better distribution picture earlier on, discovery teams may choose compounds that are more likely to get to the site of actions or to avoid those going somewhere they don't want them to go. This may in turn improve the clinical failure rates."

Mass spectrometry has rapidly found a new home in drug discovery and development. Manufacturers who have already developed a wide range of capable systems will continue to focus on integrating different components and streamlining upstream sample preparation steps.

Peter Gwynne (pgwynne767@aol.com) is a freelance science writer based on Cape Cod, Massachusetts, U.S.A. Gary Heebner (gheebner@cell-associates.com) is a marketing consultant with Cell Associates in St. Louis, Missouri, U.S.A.

Featured Companies

Agilent Technologies
MS software,
http://www.agilent.com

Applied Biosystems
mass spectrometry systems,
http://appliedbiosystems.com

Bruker Daltonics, Inc.
mass spectrometry systems,
http://www.bdal.com

Ciphergen Biosystems, Inc.
MS software,
http://www.ciphergen.com

Covance, Inc.
contract research organization,
http://www.covance.com

EMD Biosciences (an affiliate of Merck KGaA)
protein purification products,
http://www.emdbiosciences.com

GE Healthcare
MS software, protein purification products,
http://www.gehealthcare.com

MDS Pharma Services
contract research organization,
http://www.mdsps.com

PerkinElmer Life and Analytical Sciences
MS software,
http://las.perkinelmer.com

Pierce
protein purification products,
http://www.piercenet.com

PPD, Inc.
contract research organization,
http://www.ppdi.com

Qiagen GmbH
high density MS chips,
http://www.qiagen.com

Quintiles Transnational Corporation
contract research organization,
http://www.quintiles.com

Shimadzu Biotech
mass spectrometry systems,
http://www.shimadzu-biotech.net

Sigma-Aldrich Corporation
protein purification products,
http://www.sigmaaldrich.com

Thermo Electron Corporation
mass spectrometry systems,
http://www.thermo.com

Waters Corporation
mass spectrometry systems,
http://www.waters.com

POSITIONS OPEN

TENURE-TRACK ASSISTANT PROFESSOR
Microbiology and Molecular Genetics

The Department of Microbiology and Molecular Genetics in the Medical School of the University of Texas Health Science Center, Houston (UTHSC-H), seeks an exceptional scientist for a tenure-track position at the Assistant Professor level. Candidates must have a Ph.D. and/or M.D. and several years of postdoctoral experience. Demonstrated excellence in research is more significant than the area of research. The successful candidate will join faculty using diverse microbial systems to study cell biology, regulatory biology, signal transduction, development, and pathogenesis by bacteria, fungi, and viruses. In addition to directing an extramurally funded research program, the successful candidate will be expected to participate in teaching graduate and medical students. The position affords a competitive salary, start-up package, and unparalleled opportunities to interact with basic scientists as well as clinical and translational researchers. As part of the Texas Medical Center, departmental faculty collaborate and interact with the other academic and health components including Baylor College of Medicine, M.D. Anderson Cancer Center, Rice University, the Texas A&M Institute of Bioscience and Technology, and the UTHSC-H Institute for Molecular Medicine. The breadth and quality of biomedical science in the Texas Medical Center rivals that of any academic medical center in the world. Applicants should submit curriculum vitae, a statement of research interests and plans, and contact information for at least three referees. For full consideration, completed applications should be submitted by November 1, 2006.

Applications should be directed to:

Samuel Kaplan, Ph.D.
Microbiology and Molecular Genetics
The University of Texas Medical School
6431 Fannin Street, MSB 1.206
Houston, TX 77030-1501
E-mail: carolyn.love@uth.tmc.edu.

The University of Texas Health Science Center at Houston is an Equal Opportunity/Affirmative Action Employer. Minorities/Females/Persons with Disabilities/Veterans. Women and minorities are encouraged to apply. This position is subject to Texas Education Code § 51.215. A background check will be required for the final candidate.

ASSISTANT IN
Department of Pharmacology and Therapeutics
University of Florida

The Department of Pharmacology and Therapetuics invites well-trained, doctorate-level individuals, to apply for a nontenure-track Assistant In faculty position. The successful candidates will perform basic science related to the effect of angiotensin II and glial cell derived neurotrophic factor on catecholamine biosynthesis with hypertension, obesity, and aging in rats. Salary is commiserate with experience. Applicants should apply online at **website: http://jobs.ufl.edu** (position number 00022993) and send their curriculum vitae and three letters of recommendation to: **Dr. Philip Scarpace, Department of Pharmacology and Therapeutics, P.O. Box 100267, Gainesville, FL 32610-0267.** Application deadline is October 2, 2006, with an anticipated start date on or after October 20, 2006. *The University of Florida is an Equal Opportunity Institution.*

POSTDOCTORAL ASSOCIATE, 05769

Job description: Postdoctoral Associate position available in our infectious disease modeling group. Qualifications: A Ph.D. in mathematical biology or related area and experience in mathematical modeling are expected. A working knowledge of Matlab and similar programs is preferable. Submit a resume with names of three references to: **Dr. Ynte Schukken** or **Yrjo Grohn, e-mail: yhs2@cornell.edu** or **ytg1@cornell.edu**. *Cornell University is an Affirmative Action/Equal Opportunity Employer and Educator.*

POSITIONS OPEN

FACULTY POSITIONS, PRINCIPAL INVESTIGATORS
Asia-Pacific International Molecular Biology Network Insitiute of Biochemistry and Cell Biology Professorship Program

The Asia-Pacific International Molecular Biology Network (A-IMBN) is dedicated to promoting the development of molecular biology and biotechnology throughout the Asia-Pacific region. Institute of Biochemistry and Cell Biology (IBCB) is one of the leading research institutions in biochemistry, molecular, and cell biology in China. A-IMBN-IBCB Professorship was created and has functioned since 2006. A unit laboratory of electronic International Molecular Biology Laboratory was established in IBCB this year. We invite applications for two positions of Principal Investigators for this Professorship program in unit laboratory.

We seek one with world-class research records in the field of molecular immunology, and the other with proven capability in the area of the modernization of traditional oriental medicines. The latter should have an indepth understanding in traditional medicine areas, and also have strong backgrounds in molecular biology areas, evidenced by publication records. Both should be willing to be involved in the drug (or functional biomaterials) development program. Previous experience in drug development research beyond the laboratory bench is preferred.

Candidates should have a Ph.D. or equivalent degrees and will be expected to develop vigorous, independently funded research programs and to contribute to graduate and postdoctoral training programs. The positions come with excellent laboratory space and substantial startup funds. Competitive salary plus a salary subsidy supported by A-IMBN-IBCB Professorship, housing subsidy, and fringe benefit package will be commensurate with experience.

Applicants should send curriculum vitae with a complete list of publications, a concise summary of past research accomplishments and future research plans, and three letters of references to: **Mr. Banghe Mao, Faculty Search Committee, Institute of Biochemistry and Cell Biology, SIBS, CAS, 320 Yue-Yang Road, Shanghai 200031, China,** or electronically to **e-mail: bhmao@sibs.ac.cn (Telephone: 086-21-54921006** and **fax: 086-21-54921011).** Applications will be accepted until positions are filled. Interviews may be conducted at any time upon arrangement.

Details please see **websites: http://www.a-imbn.org, http://www.embl.org,** and **http://www.sibcb.ac.cn.**

PROFESSOR IN ISOTOPE GEOCHEMISTRY
Yale University

The Department of Geology and Geophysics at Yale University invites applications for a professorship, at either the junior or senior level, for research in radioactive, radiogenic, or light stable isotopes.

We seek a candidate with outstanding prospects for research and scholarly leadership who will complement the existing strengths of the Department. A successful applicant must be willing to develop and implement independent, externally funded research programs, advise students, and facilitate interdisciplinary research.

Applicants should submit curriculum vitae, a statement of research and teaching interests, and a list of publications, plus the names, addresses, and e-mail addresses for four references to: **Professor David Bercovici, Chair, Department of Geology and Geophysics, Yale University, P. O. Box 208109, New Haven, CT 06520-8109.** Applications that arrive before September 30, 2006, will receive full consideration.

For full information regarding Yale Geology and Geophysics, visit our **website: http://www.yale.edu/geology.** *Yale University is an Equal Opportunity/Affirmative Action Employer. Applications from women and minority scientists are strongly encouraged.*

Chief, Laboratory of Bacterial Diseases
National Institute of Allergy and Infectious Diseases
National Institutes of Health

The National Institute of Allergy & Infectious Diseases (NIAID), Division of Intramural Research (DIR) is seeking an outstanding individual to head the newly established Laboratory of Bacterial Diseases (LBD) in Bethesda, Maryland. The laboratory is to be located in the new C.W. Bill Young Center for Biodefense and Emerging Pathogens located on the NIH campus in Bethesda, Maryland.

The mission of the LBD will be to study basic and applied aspects of bacterial diseases related to biodefense or emerging and re-emerging pathogens, focusing on pathogenic bacteria. Exceptional scientists with research interests in basic, translational or clinical aspects of bacterial pathogenesis are encouraged to apply. The long-term goals of the Institute include supporting research that enables the development of new diagnostics, vaccines, and therapeutics.

This position requires an M.D., Ph.D. or equivalent with proven leadership abilities and a strong independent research program. Preference will be given to candidates with a documented record of accomplishment in bacterial disease research, and those whose program(s) are consistent with the mission of the NIAID.

The Laboratory Chief will have independent resources to conduct basic and clinical research and will supervise other Principal Investigators with independent research programs. The successful candidate is expected to lead a strong research program in laboratory and/or clinical research. Committed resources include space, support personnel and an allocated annual budget to cover service, supplies, animals and related resources and salaries. A Laboratory Chief in the DIR is equivalent to a Department Chair in a University or Medical School. Applicants must be U.S. citizens or permanent residents and be eligible for the appropriate security clearance under the CDC Select Agent Program. Salary will be commensurate with experience and qualifications.

Interested candidates may contact **Dr. Karyl Barron, Deputy Director, DIR, NIAID at 301/402-2208 or email (kbarron@niaid.nih.gov)** for additional information about the position and/or infectious diseases research at the NIH.

To apply for the position, candidates must submit curriculum vitae, bibliography, a detailed statement of research interests, and reprints of up to three selected publications, preferably via Email to: Lynn Novelli at novelly@niaid.nih.gov. In addition, the names of three potential references must be sent to **Dr. Steven M. Holland, Chair, NIAID Search Committee, c/o Ms. Lynn Novelli, DIR Committee Manager, 10 Center Drive, MSC 1356, Building 10, Room 4A26, Bethesda, Maryland 20892-1356.** Completed applications **MUST** be received by **Monday, September 25, 2006**. Please refer to **AD#004** on all correspondence. Further information on this position and guidance on submitting your application is available on our website at: **http://healthresearch.niaid.nih.gov**

Chief, Laboratory of Human Bacterial Pathogenesis
National Institute of Allergy and Infectious Diseases
National Institutes of Health

The National Institute of Allergy & Infectious Diseases (NIAID), Division of Intramural Research (DIR) is seeking an outstanding individual to head the Laboratory of Human Bacterial Pathogenesis (LHBP) in Hamilton, Montana.

The mission of the LHBP is to study human bacterial diseases related to emerging and re-emerging pathogens. The research to be conducted in the LHBP is to include; 1) the molecular basis of host-pathogen interactions, 2) the genetic basis of bacterial virulence and pathogenesis, 3) the use of animal modeling to define host defense mechanisms and biology and immunology of host-pathogen interactions, and 4) development of novel and improved intervention strategies to control bacterial infectious diseases. The ultimate goal is to develop diagnostics, vaccines, and therapeutics for emerging and re-emerging infectious diseases.

This position requires a Ph.D. and/or M.D. or equivalent with proven leadership abilities and a strong independent research program. Preference will be given to candidates with a documented record of accomplishment in bacterial disease research, and especially to those whose program(s) are consistent with the mission of the NIAID to study emerging and re-emerging bacterial pathogens.

The Laboratory Chief will have independent resources to lead and conduct laboratory research and translational/clinical research, as appropriate. Mechanisms are available to conduct clinical studies at the Bethesda campus and/or to obtain clinical samples through contract mechanisms at non-NIH institutions. The individual will supervise other Principal Investigators with independent research programs investigating the pathogenicity of Staphylococcus and Streptococcus species. Committed resources include space, support personnel, animal resources and an allocated annual budget to cover service, supplies and salaries. A Laboratory Chief in the DIR is equivalent to a Department Chair in a University or Medical School. Salary is dependent on experience and qualifications.

Interested candidates may contact **Dr. Karyl Barron, Deputy Director, DIR, NIAID at (301) 402-2208 or email (kbarron@niaid.nih.gov)** for additional information about the position. To apply for the position, candidates must submit a curriculum vitae, bibliography, a detailed statement of research interests, and reprints of up to three selected publications preferably via email to: **Felicia Braunstein at braunsteinf@niaid.nih.gov or by US Mail to: Ms. Felicia Braunstein, DIR Committee Manager, 10 Center Drive MSC 1349, Building 10, Rm. 4A-30, Bethesda, Maryland 20892-1349**. In addition, the names of three referees must be sent to **Dr. Tom Schwan, Chairperson, NIAID Search Committee, c/o Ms. Felicia Braunstein, DIR Committee Manager, 10 Center Drive MSC 1349, Building 10, Rm. 4A-30, Bethesda, Maryland 20892-1349**. Please note search **#005** when sending materials. Completed applications **MUST** be received by **October 6, 2006**. Further guidance on submitting your application is available on our website at: **http://healthresearch.niaid.nih.gov**.

WWW.NIH.GOV

I want to help find a cure for cancer

Not worry about my student loans

If you're interested in a biomedical research career, you should know that the National Institutes of Health Loan Repayment Programs may repay up to $35,000 per year of your qualified educational loan debt.

Deadline for Applications is December 1

For more information, visit www.lrp.nih.gov or call 1–866–849–4047

The NIH Loan Repayment Programs | ***Healthier Futures Through Research***

Positions @ NIH

THE NATIONAL INSTITUTES OF HEALTH

Tenured/Tenure-Track Position
Neuroimmunology (Basic/Translational)
Division of Intramural Research

The Division of Intramural Research of the National Institute of Neurological Disorders and Stroke is recruiting an individual for a tenured or tenure-track position in the area of Neuroimmunology. The applicant should have a special interest and experience in translational research relating to multiple sclerosis or other immune mediated disease of the central nervous system. The individual would direct an independent research program on molecular, biological or immunological aspects of immune mediated diseases of the nervous system and especially multiple sclerosis. The program would conduct its work in conjunction with the Neuroimmunology Branch (NIB) which was established to study the cause and treatment of immunological mediated diseases of the central nervous system. The individual should have a demonstrated background and knowledge in research focused on immune mediated disease of the nervous system and with expertise in the use of animal models or in human immunology. The candidate will have a Ph.D. and/or M.D. degree with excellent scientific skills in structuring an original and productive research program using outstanding communication and collaborative abilities. Candidates for a tenured position must have an international reputation and well-documented evidence of ongoing independent accomplishments. An individual selected for a tenure-track position is expected to build a dynamic and productive research group. Laboratory facilities, start-up and sustained research funds and salary will be competitive with premier academic institutions. Applicants should send curriculum vitae, bibliography, statement of research interests, and names of references to: **Dr. Story Landis, Director, National Institute of Neurological Disorders and Stroke, c/o Peggy Rollins, Office of the Scientific Director, Division of Intramural Research, Building 35 Room GA908, NIH, Bethesda, MD 20892 (301-435-2232)**. Applications will be reviewed upon receipt.

Tenured/Tenure-Track Position
Neuroimmunology (Clinical)
Division of Intramural Research

The Division of Intramural Research of the National Institute of Neurological Disorders and Stroke is recruiting an individual for a tenured or tenure-track position in the area of neuroimmunology with a focus on clinical research. The applicant should have a special interest and experience in translational clinical research relating to multiple sclerosis or other immune mediated disease of the central nervous system. The individual would direct an independent research program on immune mediated diseases of the nervous system and especially multiple sclerosis. The program would conduct its work in conjunction with the Neuroimmunology Branch (NIB) which was established to study the cause and treatment of immunological mediated diseases of the central nervous system. The individual should have a demonstrated background and knowledge in research focused on immune mediated disease of the nervous system and with expertise in human immunology and/or the application of clinical trial methodology to the study of disease mechanisms and testing new therapies. The candidate will have earned a M.D. degree and will have excellent scientific skills in structuring an original and productive research program using outstanding communication and collaborative abilities. The candidate will have a medical license in the United States and preference will be given to a candidate who has completed training in an accredited training program in neurology and is either board eligible or board certified in Neurology. Candidates for a tenured position must have an international reputation and well-documented evidence of ongoing independent accomplishments. An individual selected for a tenure-track position is expected to build a dynamic and productive research group. Laboratory facilities, start-up and sustained research funds and salary will be competitive with premier academic institutions. Applicants should send curriculum vitae, bibliography, statement of research interests, and names of references to: **Dr. Story Landis, Director, National Institute of Neurological Disorders and Stroke, c/o Peggy Rollins, Office of the Scientific Director, Division of Intramural Research, Building 35 Room GA908, NIH, Bethesda, MD 20892**. Applications will be reviewed upon receipt.

National Institutes of Health
Center for Scientific Review

NIH SCIENTIFIC REVIEW ADMINISTRATOR: LUNG BIOLOGIST
(Health Scientist Administrator)
Vacancy #'s: CSR-06-140166-DE and CSR-06-140166-MP

We are seeking exceptionally qualified scientists, with doctorate level training and independent research and administrative experience in lung biology and pathology to join a team of Scientific Review Administrators (SRAs) to help shape the future of scientific review. SRAs are responsible for taking a leadership role in providing scientific, administrative, and logistical oversight of the peer review process. The incumbent(s) will be responsible for the initial administrative and scientific review of NIH research grant applications in bioengineering sciences and technology and will possess an M.D. or Ph.D. degree (or have equivalent training and experience), have independent research experience, and strong records of publication or other productivity in academia or industry. These positions are in the Respiratory Sciences Integrated Review Group (IRG). The IRG is responsible for the merit evaluation of grant applications focused on the mechanism(s) of lung injury, repair and remodeling in non-vascular pulmonary tissues or cells including areas such as lung development, pulmonary fibrosis and lung toxicology. A broad knowledge of one or more of these scientific areas is desirable. For additional information on the IRG please see our web site, at: http://cms.csr.nih.gov/PeerReviewMeetings/CSRIRGDescription/RESIRG/

Salary is commensurate with research experience and accomplishments, and a full Civil Service package of benefits (including retirement, health, life and long-term care insurance, Thrift Savings Plan participation, etc.) is available.

For additional information on this position and for instructions on submitting your application, please visit our website at: **http://jobsearch.usajobs.opm.gov/a9nih.asp**

RAPID ACCESS TO PREVENTIVE INTERVENTION DEVELOPMENT "RAPID" PROGRAM
National Cancer Institute

The National Cancer Institute announces the ongoing initiative: Rapid Access to Preventive Intervention Development (RAPID). RAPID will make available to academic investigators the preclinical and early clinical drug development contract resources of NCI's Division of Cancer Prevention. In some instances resources will be provided to the investigator. The goal of RAPID is the rapid movement of novel molecules and concepts from the laboratory to the clinic for clinical trials of efficacy. RAPID will assist investigators who submit successful requests by providing any (or all) of the pre-clinical and phase 1 clinical developmental requirements for phase 2 clinical efficacy trials. These include, for example, preclinical pharmacology, toxicology, and efficacy studies; bulk supply, GMP manufacturing, and formulation; and regulatory and IND support and phase 1 clinical studies. Suitable types of agents for RAPID may range from single chemical or biological entities to defined complex mixtures with the potential to prevent, reverse, or delay carcinogenesis. For more detailed information, visit the web site, **http://cancer.gov/prevention/RAPID**

Requests for RAPID resources are to be submitted as described in the web site. Written requests will be evaluated by a specially constituted RAPID panel, consisting of outside experts from academia and industry. Requests must be received on or before **November 1, 2006**. Applications should be submitted directly to the office listed below. Inquiries are encouraged, and the opportunity to clarify issues or questions is welcome. Please contact:

RAPID Program Official, Executive Plaza North, Room 2117, 6130 Executive Blvd., Bethesda, MD 20892, Rockville, MD 20852 (for express/courier service), Telephone: (301) 435-5011, Email: kapetani@mail.nih.gov, Or Telephone: (301) 594-0459, Email: jc94h@nih.gov, Fax: (301) 402-0553.

WWW.NIH.GOV

Tenure Track Position in the Laboratory of Immunology

National Institute of Allergy and Infectious Diseases
National Institutes of Health

The Laboratory of Immunology (LI), Division of Intramural Research, National Institute of Allergy and Infectious Diseases, National Institutes of Health invites applications for a tenure track position in immunology.

LI strongly encourages scientists with an interest in any area of biomedical research related to immunology to apply. Candidates should have a Ph.D., M.D. or equivalent degree and an outstanding record of post-doctoral accomplishment. LI wishes to recruit a highly creative individual who will establish an independent research program that takes full advantage of the special opportunity afforded by the stable long-term funding of the Intramural Research Program at NIH. She/he should be interested in developing and applying novel approaches to the study of problems of major biological and /or medical importance, efforts that may be enhanced through participation in emerging trans-NIH initiatives involving technology development, translational investigation, and multidisciplinary science. Generous ongoing support for salary, technical personnel, post-doctoral fellows, equipment, and research supplies will be provided, as well as access to existing or planned core facilities / collaborative centers for projects involving RNAi screening, microarrays, production of transgenic and gene manipulated mice, advanced imaging, and computational biology. In addition to an outstanding international post-doctoral community, a superior pool of graduate and undergraduate students is also available to the successful applicant.

LI has a distinguished history of accomplishment in immunology and is seeking to appoint an outstanding early career investigator who can continue and enhance this record of achievement. Current LI Principal Investigators are Ronald Germain, Michael Lenardo, Rose Mage, David Margulies, William Paul, Ethan Shevach and Tsan Xiao.

Applicants should send a CV and bibliography and an outline of a proposed research program (no more than two pages) electronically to **Mrs. Lynn Novelli (novelly@niaid.nih.gov)**. Three letters of reference should also be sent either electronically or by mail to **Mrs. Lynn Novelli, Committee Manager, 10 Center Drive, MSC 1356, Building 10, Room 4A26, Bethesda, Maryland 20892-1356**. Please refer to **Ad #011** on all communications. Further information about this position may be obtained by contacting **Dr. William Paul (301 496-5046; wpaul@niaid.nih.gov). Applications must be received by October 14, 2006**.

A full package of benefits (including retirement, health, life and long term care insurance, Thrift Savings Plan participation, etc.) is available. Women and minorities are especially encouraged to apply. U.S. citizenship is not required.

National Human Genome Research Institute

Investigator Recruitment in Cancer Genetics
National Human Genome Research Institute

The Cancer Genetics Branch (CGB) of the National Human Genome Research Institute (NHGRI) is seeking to recruit an outstanding tenure-track investigator to pursue innovative, independent research in cancer genetics. General areas of interest include, but are not limited to:

- Cancer Gene Therapy
- Comparative Cancer Genomics
- Genetic Epidemiology
- Molecular Profiling of Tumors
- Functional Genomics of Cancer
- Genome Instability in Cancer
- Markers for Early Detection
- Genetics of Tumor Progression

The successful candidate will be able to take advantage of interactions with a highly collegial group of scientists within NHGRI and the NIH campus as a whole. In addition, they will have access to NHGRI's outstanding core laboratories.

Candidates must have a Ph.D., M.D., or equivalent degree, as well as comprehensive, advanced training and a record of accomplishment in one of the targeted areas. This position includes generous start-up funds, an ongoing commitment of research space, laboratory resources, and positions for personnel and trainees.

Interested applicants should submit a curriculum vitae, a three-page description of their proposed research, and three letters of recommendation through our online application system at **http://research.nhgri.nih.gov/apply**.

The closing date is **November 17, 2006**.

For more information on CGB and NHGRI's Intramural Program, please see **http://www.genome.gov/Research**. Specific questions regarding the recruitment may be directed to **Dr. William Pavan (Search Chair) at bpavan@mail.nih.gov or by fax at (301-402-2036)**. Questions may also be directed to **Dr. Elaine Ostrander, Chief of the Cancer Genetics Branch, at eostrand@mail.nih.gov or by FAX (301-480-0472)**.

MICHIGAN STATE UNIVERSITY

International Environmental Law and Policy Assistant Professor, Tenure Stream

James Madison College (residential undergraduate liberal arts college with an emphasis on public and international affairs) and the Department of Fisheries and Wildlife in the College of Agriculture and Natural Resources at Michigan State University, seek a colleague in international environmental law with an emphasis on the governance of renewable natural resources especially as it relates to fisheries, wildlife and water resources. This tenure stream position is a joint academic year appointment to the two units, at the Assistant Professor level.

The ideal candidate for this position would have a background in biology and international environmental institutions and be prepared to teach undergraduate and graduate classes in international environmental law. We would expect the candidate's research interests and graduate course offerings to focus on environmental law, particularly as that relates to the sustainability and use of fisheries, wildlife and/or water resources globally. This colleague would also be expected to play a role in the undergraduate specialization in Science, Technology, Environment and Public Policy (**http://www.fw.msu.edu/undergraduates/specializations/STEPPS/index.htm**) and be active in the Environmental Science and Policy Program (**http://environment.msu.edu**). This individual would also actively interact with partner agencies such as the Michigan Department of Natural Resources, US Fish and Wildlife Service and Great Lakes Fishery Commission.

The Department of Fisheries and Wildlife offers both undergraduate and graduate degree programs. The faculty's cutting-edge theoretical and applied research focuses on natural resource and ecosystem management (for details, see: **http://www.fw.msu.edu**). James Madison College provides undergraduates a liberal education in public and international affairs and is dedicated to the highest standards of excellence in undergraduate teaching and engagement (for details, see **http://www.jmc.msu.edu/**).

The successful candidate should possess a Ph.D. or a Ph.D. and J.D. and training or experience with international environmental institutions and law. Additionally, the successful candidate would likely have a research agenda that involves international environmental law as it relates to the governance of renewable natural resources. This is an innovative, interdisciplinary appointment and we seek an individual who can interact successfully with natural resources (related to fish, wildlife, and water) and public affairs (related to international relations, global governance, international law, and public policy) professionals.

Applicants should submit a letter describing how their research and teaching interests relate to the research and teaching foci noted above. Supporting materials should include a vita, at least three confidential letters of recommendation, and samples of scholarship and teaching materials.

Minority and women candidates are strongly encouraged to apply. The deadline for receipt of applications is **October 1, 2006**. Completed files should be sent by that date to: **International Environmental Law and Policy Search Committee, Department of Fisheries and Wildlife, Michigan State University, East Lansing, Michigan 48824-1222 or millenba@msu.edu (Subject Line = IEL2006)**. Questions about the position should be directed to **Dr. Kelly Millenbah (517-353-4802, millenba@msu.edu)**. Position to begin August 16, 2007. Late submissions will be considered if a suitable candidate pool is not identified by the deadline.

MSU IS AN AFFIRMATIVE ACTION, EQUAL OPPORTUNITY INSTITUTION.

Advanced Proteome Therapeutics Inc.

"Advancing the field of Protein-site Targeting"

Advanced Proteome Therapeutics Inc. (APTI) is a new, Boston-based company that is applying a bold platform technology geared toward the rapid commercialization of protein therapeutics. We are seeking skilled experimentalists who thrive on providing innovative solutions to challenging problems and are both independent and strongly interactive.

APTI exploits a proprietary technology that is chemoselective and has the potential for rapidly producing complementary molecules, either noncovalently or covalently, to macromolecular therapeutic targets. The technology and science underlying our approach to therapeutics should appeal to scientists who are interested in pioneering an entirely new approach to drug discovery and development that is broadly based on underutilized chemical principles, as applied to protein-site targeting.

There are a number of positions available that call for skills and demonstrated expertise in the areas of:

(1) protein modification and purification, cloning and phage display techniques, and assay development.
(2) combinatorial chemistry and related automation: scientists capable of automated assay formatting and validation studies who will perform data analysis and confirmatory follow-up assays.
(3) solid phase organic synthesis and peptide chemistry
(4) conjugation chemistry and organic synthesis

Knowledge of protein structure determinations and molecular modeling are a definite plus.

APTI offers a dynamic work environment as well as an excellent salary and stock option package. If the prospect of shaping the direction and culture of a new company excites your interest, e-mail your resume and a cover letter to **jobs@aptbiotech.com**.

Faculty Position
Cell Biology: Neuroscience

The Department of Biology, Skidmore College, invites applications for a tenure track Assistant Professor position in **cell biology**, beginning in the Fall of 2007. The successful candidate will contribute to our general biology curriculum and a successful and growing interdisciplinary Neuroscience Program. Area of specialization is open.

Applicants must have a Ph.D. in biology or a related discipline, teaching experience, a successful independent research program, and a primary interest in teaching undergraduates at a liberal arts and sciences institution; postdoctoral experience is required. Yearly course load will be selected from among foundation courses in biology and neuroscience, exploration courses for non-majors and specialty courses in the candidate's area of expertise. Establishment of a strong research program that involves undergraduates is expected. Excellent teaching, research, and imaging facilities are available. Send curriculum vitae, statements of teaching and research interests, and three letters of recommendation to:

Corey R. Freeman-Gallant, Chair, Department of Biology
Skidmore College
815 North Broadway
Saratoga Springs, New York 12866
Cell Biology Search

Review of applications will begin on **October 13, 2006**. Skidmore College encourages applicants from women and men of diverse racial, ethnic, and cultural backgrounds.

www.skidmore.edu/academics/biology

Skidmore College is committed to being an inclusive campus community and, as an Equal Opportunity Employer, does not discriminate in its hiring or employment practices on the basis of gender, race or ethnicity, color, national origin, religion, age, disability, family or marital status, or sexual orientation.

Faculty Positions in Molecular Recognition and Bioinformatics

THE UNIVERSITY AT BUFFALO'S STRATEGIC PLANNING PROCESS, *UB 2020*, HAS IDENTIFIED BIOINFORMATICS AND MOLECULAR RECOGNITION IN BIOLOGICAL SYSTEMS AS AREAS WHERE MORE THAN 30 NEW HIRES ARE PROJECTED, WITH A SIGNIFICANT INVESTMENT OF RESOURCES, OVER THE NEXT THREE YEARS.

POSITION DESCRIPTIONS

In the first phase of our multi-year recruiting plan, several positions are available immediately at all ranks in the Schools of Medicine and Biomedical Sciences, Dental Medicine, Arts and Sciences, Pharmacy, and Engineering at the University at Buffalo, The State University of New York, with concomitant appointment in its New York State Center of Excellence in Bioinformatics and Life Sciences.

Successful candidates will have research interests in Bioinformatics and/or Molecular Recognition, in areas such as computational biology, genomics, molecular recognition in biology, signal transduction, and analysis of biological networks using experimental approaches ranging from *in silico* through *in vivo*.

Successful applicants will receive tenured or tenure-track appointments in departments appropriate to their interests. These include, but are not restricted to, Biochemistry, Biological Sciences, Chemical and Biological Engineering, Microbiology and Immunology, Oral Biology, Pharmacology and Therapeutics, Physiology and Biophysics, and Structural Biology. A history of collaborative research will be a key consideration in evaluation of applicants for senior positions, as will their potential to provide academic leadership and thereby facilitate future recruitments. Additional information on departmental programs may be obtained on specific home pages, accessible via www.buffalo.edu, or at www.bioinformatics.buffalo.edu.

STATE-OF-THE-ART FACILITIES

Ample laboratory space exists in the new Center of Excellence building, which opened in June 2006 and is situated adjacent to the Hauptman-Woodward Medical Research Institute and the Roswell Park Cancer Institute's Center for Genetics and Pharmacology in the Buffalo Niagara Medical Campus. When fully staffed, these three facilities will be home to over 500 biomedical scientists. The Center itself maintains a modern, state-of-the-art experimental infrastructure in biomedical sciences, and houses a major computational facility and high-quality confocal microscopy. Cutting-edge genomics and proteomics facilities are located immediately adjacent to the Center, as well as on the two local campuses of the University at Buffalo.

CANDIDATE REQUIREMENTS

Applicants should have Ph.D., M.D., D.V.M., D.D.S., or equivalent degree with postdoctoral and professional experience appropriate to the rank of appointment, e.g., a minimum of two years of postdoctoral experience for the rank of Assistant Professor. Research experience should be in molecular, cellular, genetic and/or computational approaches to signaling networks, molecular/microbial pathogenesis, development and differentiation or the basis of human disease. A well-established research program is essential for established candidates. Duties include teaching undergraduate, graduate and professional students, research training of students and postdoctoral fellows, and conduct of biomedical research.

APPLICATIONS

Applications in electronic format should include a C.V., brief statement of research interests, and the names and email addresses of three references, and should be directed to Bioinformatics/Molecular Recognition Search at ub-mrbs@buffalo.edu. Consideration of applications will continue until all available positions are filled.

University at Buffalo *The State University of New York*

The University at Buffalo is an Equal Opportunity Employer/Recruiter and strongly encourages applications from members of protected groups.

UNIVERSITY OF ALBERTA
EDMONTON, ALBERTA, CANADA

100 New Positions in the Faculty of Engineering

Since its inception, the Faculty of Engineering has been on the frontier of research and innovation. The Faculty educates outstanding engineers and conducts the research that makes Alberta a world leader in areas that range from oil sands technology to microsystems and nanotechnology.

The Faculty of Engineering at the University of Alberta intends to expand significantly its role as a leader in the provision of engineering education and the conduct of leading, internationally-recognized research. Toward this end, we will be seeking candidates to fill 100 new positions at the Assistant, Associate and Full Professor ranks, as well as a number of Canada Research Chairs and Endowed Chairs.

The Faculty of Engineering is focusing the advancement of its scholarship and research efforts in four major areas:

- Energy and Natural Resources Engineering
- Nanotechnology and Interfacial Engineering
- Biomedical and Bioengineering
- Information and Communications Technologies

We encourage applications from candidates with interest and expertise in these areas, especially those with interdisciplinary experience that involves several of these areas, and those who have combined their engineering background with work in the physical and life or medical sciences.

Engineering faculty members at the University of Alberta work in an integrated, collaborative environment, where a strong focus on fundamentals is combined with extensive industrial interactions and ample opportunity for novel collaborations.

Our staff members also collaborate with the National Research Council National Institute for Nanotechnology—an integrated, multi-disciplinary institution involving researchers in engineering, science, medicine and other disiplines, that is located on the University of Alberta campus in our engineering precinct.

The Faculty of Engineering has over 3500 undergraduate and 1100 graduate students, placing it in the top 5% by size of over 400 engineering schools in North America. In recent years, the Faculty has undergone significant expansion of its physical infrastructure with the addition of over one million sq. ft. of outstanding new teaching, research and personnel space.

Successful candidates will be expected, in due course, to become licensed Professional Engineers in the Province of Alberta.

For more information about faculty positions in the four major areas of interest, and for application deadlines, go to: **www.engineering.ualberta.ca** or **www.careers.ualberta.ca.**

Interested candidates also may wish to contact one of the following:

J Fraser Forbes, Chair
Chemical & Materials Engineering
E-mail: fraser.forbes@ualberta.ca
http://www.engineering.ualberta.ca/cme

JJR Cheng, Chair
Civil & Enviromental Engineering
(including School of Mining and Petroleum Engineering)
E-mail: roger.cheng@ualberta.ca
http://www.engineering.ualberta.ca/civil

Horacio Marquez, Chair
Electrical & Computer Engineering
E-mail: marquez@ece.ualberta.ca
http://www.engineering.ualberta.ca/ece

Larry Kostiuk, Chair
Mechanical Engineering
E-mail: larry.kostiuk@ualberta.ca
http://www.engineering.ualberta.ca/mece

The University of Alberta is one of Canada's foremost research-intensive universities, with over $400 million annually in external research funding and undergraduate and graduate enrollment exceeding 35,500. With a population of over one million people, the greater Edmonton area offers a diverse array of cultural and sporting activities year-round, with a strong focus on the arts and a vibrant community spirit. Located only a few hours away from the spectacular Canadian Rockies, Edmontonians have quick and easy access to some of the finest skiing, kayaking, cycling, camping, backpacking and fishing in the world. For more information about the University of Alberta go to www.ualberta.ca.

All qualified candidates are encouraged to apply; however, Canadians and permanent residents will be given priority. If suitable Canadian citizens and permanent residents cannot be found, other individuals will be considered. The University of Alberta hires on the basis of merit. We are committed to the principle of equity in employment. We welcome diversity and encourage applications from all qualified women and men, including persons with disabilities, members of visible minorities, and Aboriginal persons.

THE UNIVERSITY OF TEXAS
MD ANDERSON CANCER CENTER
Making Cancer History™

Executive Vice President and Chief Academic Officer

The University of Texas M. D. Anderson Cancer Center seeks an experienced, decisive, and imaginative academic leader, with a distinguished record of innovation in research, to fill the position of Executive Vice President and Chief Academic Officer.

Celebrating more than six decades of Making Cancer History®, The University of Texas M. D. Anderson Cancer Center is located in Houston on the campus of the Texas Medical Center, the country's largest collection of hospitals and academic medical institutions. It is one of the world's most respected institutions devoted exclusively to cancer patient care, research, education and prevention.

M. D. Anderson Cancer Center was created by the Texas Legislature in 1941 as a component of The University of Texas System. The faculty (M.D. and Ph.D.) has grown to 1056. M. D. Anderson is one of the nation's original three Comprehensive Cancer Centers designated by the National Cancer Act of 1971 and is one of 39 Comprehensive Cancer Centers today. M. D. Anderson has ranked among the nation's top two cancer hospitals in U.S. News & World Report's "America's Best Hospitals" survey since the survey's inception in 1990 and has ranked number one four times in the last seven years. It receives more research funding from the National Cancer Institute than any other academic institution. Ten thousand patients are placed on therapeutic clinical trials each year.

The Executive Vice President and Chief Academic Officer is a member of the executive management team consisting of the President, the Chief Academic Officer, the Physician in Chief and the Chief Business Officer. Working closely with the president and faculty, the EVP and CAO has primary responsibility for the academic and educational missions of MDACC and oversight of clinical and laboratory research across the organization. He or she will play a pivotal role in strengthening existing academic programs, developing innovative strategies for expanding the Center's research and educational activities, recruiting outstanding new faculty and advocating for strong academics as a critical factor in realizing the Center's strategic objectives in research and patient care.

The successful candidate will have an M.D., Ph.D., or both, with academic achievements commensurate with tenure, experience or interest in cancer research and care, and significant administrative experience in an academic setting. The candidate must be a strong leader and a capable motivator, and able to develop the talents of others in support of the Center's mission. His or her engagement in the broader community must be over-arching and robust.

Korn/Ferry International is assisting the University of Texas M. D. Anderson Cancer Center with this important search. Please forward, as soon as possible, nominations of appropriate candidates or expressions of interest to: **Warren E. Ross, M.D. (warren.ross@kornferry.com), Korn/Ferry International, 1835 Market Street, Suite 2000, Philadelphia, PA 19103.**

The University of Texas M. D. Anderson Cancer Center is an Equal Opportunity/ Affirmative Action Employer and Educator.

Faculty Positions Boyce Thompson Institute for Plant Research at Cornell University

BTI, an independent not-for-profit research organization, invites applications for up to three tenure-track faculty positions at any level. We seek candidates whose research addresses important questions in biology using plant, plant-microbe, or plant-herbivore systems. Research topics should be complementary to current research at BTI and Cornell. Particular areas of interest include plant metabolism, small molecule biochemistry, enzymology, ecology, and plant interactions with other organisms. Applications from scientists using model systems not currently represented at BTI are encouraged. BTI is located on the central Cornell campus and has a research-oriented environment with state-of-the-art facilities and family-friendly policies. Our location offers superb opportunities for interactions and formal links to appropriate Cornell departments. We encourage applications from women and minorities.

Applicants should submit a *curriculum vitae*, a statement of research interests, and a concise description of research plans (2-3 pages). Please submit applications and have letters from three references sent to: **Gary Blissard, Search Committee Chair, Boyce Thompson Institute, Tower Road, Ithaca, New York 14853, fax (607-254-1217), e-mail: ee54@cornell.edu**. Review of applications will begin on **November 1, 2006** and will continue until the positions are filled. Additional information about BTI can be obtained at **http://bti.cornell.edu**.

We encourage applications from women and minorities. EEO/AA/M/F/D/V.

Department Head Department of Zoology

The Department of Zoology at Oklahoma State University (OSU) invites applications for the position of Department Head. We recently reorganized and seek a dynamic and visionary leader to help us increase our national prominence in our selected research areas: **(1) Ecology and Evolutionary Biology** and **(2) Environmental Stress**. The starting date will be on or after 1 August 2007 and is flexible.

The ideal candidate will have the academic rank of Professor, a nationally recognized research program consistent with our research foci, demonstrated success in obtaining extramural grant support, significant administrative experience, a commitment to supporting innovative teaching, and a vision for curricular reform that will produce students highly qualified for careers in research, teaching, and other professional positions.

OSU is a land-grant institution with 24,000 students located in north-central Oklahoma, 70 miles from Oklahoma City and Tulsa. Currently, the Department of Zoology has approximately 400 undergraduate and 50 graduate students, 4 staff, and 11 faculty with a long history of democratic governance.

Applicants should submit a letter of application, statements of research, teaching, and administrative philosophies, a curriculum vitae, and four letters of reference testifying to the applicant's leadership and administrative skills to: **Dr. Robert V. Miller, Chair, Department Head Search Committee, Department of Zoology, 430 LSW, Oklahoma State University, Stillwater, OK 74078-3052. Telephone: 405/744-6243; E-mail: bob.miller@okstate.edu.** Informal inquiries to **Dean Peter M. A. Sherwood** of the College of Arts and Sciences are welcome (Telephone: **405/744-5663**; email: **peter.sherwood@okstate.edu**). Application review will begin **1 November 2006** and will continue until the position is filled. For further information about the position, Department, and OSU, please see **http://zoology.okstate.edu**.

Oklahoma State University encourages applications from qualified women, minorities, and persons with disabilities.

Editor-in-Chief SEARCH

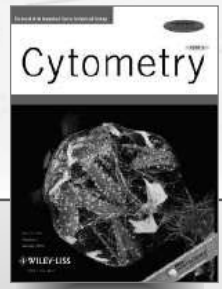

The **International Society for Analytical Cytology** is searching for a new Editor-in-Chief of *Cytometry Part A*. Individuals interested in this part-time position should direct inquiries to Fred Waldman:

waldman@cc.ucsf.edu
415.476.3821

All applications must be received by September 15, 2006

ISAC International Society for Analytical Cytology

WILEY

National Center for Design of Biomimetic Nanoconductors

Postdoctoral Research Positions

The National Center for Design of Biomimetic Nanoconductors, an NIH Roadmap Nanomedicine Development Center, is seeking applicants for a number of computational and experimental postdoctoral research positions. The model computational systems are native and mutant biological channels and other ion transport proteins and synthetic channels, and heterogenous membranes containing channels and transporters. The model experimental systems are engineered protein channels and synthetic channels in isolation, and in self-assembled membranes supported on nanoporous silica scaffolds. The ultimate goal is to understand how biomimetic nanoscale design can be utilized in devices to achieve the functions that membrane transport accomplish in biological systems: a) Electrical and electrochemical signaling, b) generation of osmotic pressures and flows, c) generation of electrical power, and d) energy transduction. The Center is highly multi-disciplinary and includes senior researchers at the following institutions...

University of Illinois at Urbana Champaign	Eric Jakobsson (Director)
	Narayan R. Aluru
	Umberto Ravaioli
Illinois Institute of Technology	H. Larry Scott
	Marco Saraniti
Oxford University	Hagan Bayley
Purdue University	Gerhard Klimeck
	Mark Lundstrom
	Michael McLennan
Sandia National Laboratories	Susan B. Rempe
	Steven J. Plimpton
	Kevin Leung
Argonne National Laboratory	Millie Firestone
University of California at Davis	Atul N. Parikh
University of Chicago	Benoit Roux
University of New Mexico	C. Jeffrey Brinker
Wabash College	Scott E. Feller
Yale University	David A. LaVan

For more information on the specific work going on in each of these labs and application instructions, please go to http://www.nanoconductor.org or e-mail Dave Mattson at dmattson@uiuc.edu.

POST-DOCTORAL ASSOCIATE POSITION in Behavioral Neuroendocrinology in the School of Life Sciences at Arizona State University to study the neuroendocrine mechanisms of aggressive behavior. Please see **www.public.asu.edu/~aomcm/** for more information on our research program. Salary supported from a funded NIMH grant with three years remaining. Candidates must have earned a Ph.D. in Biology, Neuroscience, Psychology or a related field at the time of appointment. Experience with neuroendocrine techniques desired. Starting time for the position is negotiable.

Send cover letter summarizing your qualifications, experience and interests, curriculum vitae, up to three representative reprints, and have two letters of recommendation sent to: **Dr. Michael Moore, School of Life Sciences, Arizona State University, P.O. Box 874501, Tempe, AZ 85287-4501**. Email submissions are acceptable (**Michael.C.Moore@asu.edu**). Application deadline is **October 1, 2004**; if not filled biweekly thereafter until search is closed.

Arizona State University is an Affirmative Action/Equal Opportunity Employer.

DEPARTMENT OF
NATURAL RESOURCES & ENVIRONMENTAL SCIENCE
COLLEGE OF
AGRICULTURE, BIOTECHNOLOGY AND NATURAL RESOURCES

TWO TENURE TRACK FACULTY POSITIONS: WILDLIFE CONSERVATION ECOLOGIST AND LARGE MAMMAL ECOLOGIST

To be filled at the Assistant/Associate level

The Department of Natural Resources and Environmental Science (NRES) seeks two tenure-track Assistant/Associate Professors to begin July 1, 2007. For the Wildlife Conservation Ecologist Position we seek candidates with strong quantitative skills and a broad range of interests, especially applied to birds or mammals. For the Large Mammal Ecology position, we will consider candidates with a broad range of interests, including nutrition, population biology or behavior.

Candidates are expected to develop a competitively funded research program, a dynamic graduate training program, and to play an integral role in the advising and development of our Wildlife Ecology and Conservation curriculum. Post doctoral or equivalent experience in teaching and the procurement of extramural funding are preferred. Candidates capable of developing a sound basic and applied research program with interests in working in arid and montane ecosystems, especially the Great Basin, and interacting with state and federal agencies are especially encouraged to apply.

Applicants should apply on-line at: **www.unrsearch.com/** and will be asked to attach a cover letter, statements of research and plans, statement of teaching philosophy and a current CV by **October 1, 2006**. Additionally, you may attach any Teaching Evaluations or Samples of Written Work. Either attach or send unofficial transcripts and three letters of reference to: **Ms. Heidi McConnell, hmc@cabnr.unr.edu, Search Committee Secretary, Dept. of Natural Resources & Environmental Science, University of Nevada, Reno/MS 186, 1000 Valley Road, Reno, NV 89512-0013**.

EEO/AA Women and under-represented groups are encouraged to apply.

University of Massachusetts Medical School

TENURE-TRACK NEUROSCIENCE POSITION

The Brudnick Neuropsychiatric Research Institute (BNRI), established as part of the unprecedented research expansion at the University of Massachusetts Medical School, invites applications for a tenure-track position at the level of Assistant/Associate Professor. The BNRI was established in 2000 as a division of the Department of Psychiatry and is committed to broad based research investigating basic neurobiological principles underlying psychiatric disorders. Faculty interests focus on a variety of neurobiological problems and psychiatric disorders, with a common theme in the neurobiology of addiction. Applicants whose interests focus on addiction are especially welcomed, particularly those with a strong behavioral component. The BNRI is integrated into the Interdepartmental Neuroscience Program, which provides opportunities for graduate training and interactions with a large group of multidisciplinary neuroscientists. The BNRI is housed in a state-of-the-art laboratory facility, which includes magnets for high resolution functional brain imaging. The successful candidate is expected to establish an independent research program and play an integral role in new program initiatives. The position is highly competitive with regard to salary, start-up funds, and laboratory space.

Applicants should send a CV, statement of research interests, and names and addresses of three references to:

Dr. Steven Treistman, Director
Brudnick Neuropsychiatric Research Institute
University of Massachusetts Medical School
303 Belmont Street
Worcester, MA 01604
E-mail: bnri@umassmed.edu
www.umassmed.edu/bnri

An Equal Opportunity/Affirmative Action Employer.

ÉCOLE POLYTECHNIQUE
FÉDÉRALE DE LAUSANNE

Faculty Positions in Chemistry

at Ecole Polytechnique Fédérale de Lausanne (EPFL)

The EPFL anticipates making several faculty appointments at the level of tenure track assistant professor in its Institute of Chemical Sciences and Engineering (ISIC). Outstanding scientists with recognized accomplishments in any field of chemistry will be considered. We particularly encourage applications in the fields of inorganic chemistry and theoretical chemistry. Exceptional candidates seeking a higher-level appointment may also be considered.

The successful candidate will establish and lead a vigorous, independent research program, interact with existing projects and be committed to excellence in teaching at both the undergraduate and graduate levels. Significant start-up resources and research infrastructure will be available.

Applications including curriculum vitae, publication list, concise statement of research and teaching interests as well as the names and addresses (including email) of at least five references should be submitted in PDFformat via the website http://sb.epfl.ch/ chemsearch **by October 15, 2006.**

For additional information, please contact **Professor Hubert Girault** (hubert.girault@epfl.ch) or consult the following websites: http://www.epfl.ch/Eplace.html, http://sb.epfl.ch/en and http://isic.epfl.ch

The EPFL is an equal opportunity employer.

ÉCOLE POLYTECHNIQUE
FÉDÉRALE DE LAUSANNE

Faculty Positions in Organic Chemistry

at Ecole Polytechnique Fédérale de Lausanne (EPFL)

The EPFL anticipates making several faculty appointments at the level of tenure track assistant professor in its Institute of Chemical Sciences and Engineering (ISIC). Outstanding scientists with recognized accomplishments in any field of chemistry will be considered. We particularly encourage applications in the field of organic chemistry. Exceptional candidates seeking a higher-level appointment may also be considered.

The successful candidate will establish and lead a vigorous, independent research program, interact with existing projects and be committed to excellence in teaching at both the undergraduate and graduate levels. Significant start-up resources and research infrastructure will be available.

Applications including curriculum vitae, publication list, concise statement of research and teaching interests as well as the names and addresses (including email) of at least five references should be submitted in PDF format via the website http://sb.epfl.ch/chemsearch by **October 31, 2006.**

For additional information, please contact Professor Hubert Girault (hubert.girault@epfl.ch) or consult the following websites: http://www.epfl.ch/Eplace.html, http://sb.epfl.ch/en and http://isic.epfl.ch

The EPFL is an equal opportunity employer.

The Program in Science Technology and Environmental Policy at Princeton University 2006-2008
Fellowship Program for Distinguished Faculty, Senior Scholars, and Practitioners

The Program in Science, Technology and Environmental Policy (**STEP**) at Princeton University's Woodrow Wilson School of Public and International Affairs (Michael Oppenheimer, director) announces its 2006-2008 Senior Fellowship program. STEP will award fellowships accompanied by one-half year support at full salary or full year at half salary to eligible, distinguished faculty, scholars and practitioners. These awards are designed to promote advanced policy research in any of these areas: global climate change, global environmental governance, energy policy, global air pollution, conservation biology and ecology, bioethics and biotechnology, environmental health and disease, risk assessment, global science and security policy and information security. We seek candidates whose interests complement those of STEP faculty. Outstanding faculty, independent scholars, and practitioners anywhere in the world are eligible to apply. The fellows program is open to all regardless of citizenship.

STEP fellows will have the opportunity to interact and collaborate with STEP faculty, other fellows, researchers and students and to participate in the various activities of the STEP program including faculty graduate seminars, colloquia, and public lectures. As part of the fellowship experience, STEP fellows will be involved in some of the following activities: participation on a university sponsored research project, collaboration with STEP faculty on projects of mutual interest, attendance at STEP seminars, and participation in meetings with STEP students, faculty, and postdocs.

Salaries vary according to individual circumstances, but will not exceed a maximum that is set each fall. Rank is contingent upon qualifications. Applicants not on leave from other positions will be eligible for employee benefits; others will be eligible for health insurance only. Applicants interested in teaching a seminar at Princeton University during their visit should so indicate.

Applicants should send a CV and cover letter (no more than 1,000 words) describing their proposed activities while at Princeton. On a separate sheet of paper, applicants should submit a confidential statement indicating (1) their salaries (not including summer research support) for the current academic year and (2) financial support available to them from their home institutions, other grantors, and any other sources during their time at Princeton. Send all materials via email to **Charles Crosby** at **ccrosby@princeton.edu**. The review process will begin immediately and continue until positions are filled.

Program in Science Technology and Environmental Policy at Princeton University - 2006-2008 Postdoctoral Fellowship Program

The Program in Science, Technology and Environmental Policy (**STEP**) at Princeton University's Woodrow Wilson School of Public and International Affairs (Michael Oppenheimer, Director) announces its 2006-2008 Postdoctoral Fellowship Program. STEP will award one-year research positions (with the possibility of renewal for a second year) to eligible, talented researchers. These awards are designed to promote basic policy-relevant research under the supervision of one or more STEP faculty members in the broad areas of global climate change, global air pollution, energy policy, global environmental governance, conservation biology and ecology, bioethics and biotechnology, environmental health and disease, risk assessment, global science and security policy and information security. The Postdoctoral Fellows Program is open to all regardless of citizenship, but requires a completed doctorate and does not support work towards the completion of a degree. STEP fellows will be eligible for salary and full employee benefits in accordance with University guidelines.

Applicants should send a CV and a cover letter describing their areas of expertise and interest via email to **Charles Crosby** at **ccrosby@princeton.edu**. The review process will commence immediately and continue until positions are filled.

For more information about applying to Princeton please link to:
http://web.princeton.edu/sites/dof/ApplicantsInfo.htm

Candidates may choose to complete the "Invitation to Self-Identify" form **http://web.princeton.edu/sites/dof/forms/PSoftSelfID.pdf**. Providing the self-identification information is completely voluntary and declining to submit the information will not adversely affect your candidacy.

Princeton University is an Equal Opportunity/ Affirmative Action Employer.

The Ruth & Bruce Rappaport Faculty of Medicine, Technion – Israel Institute of Technology, Haifa, Israel invites candidates to apply for tenure-track positions in Cell Biology, Pharmacology, Biochemistry, Immunology, Genetics, Neurosciences, Physiology and Microbiology. A Ph.D. and/or M.D. degree followed by a successful post-doctoral training is required. Applicants, with proven excellence in research, will be expected to establish an independent research program, obtain extramural funds and teach medical and graduate students.

Generous laboratory space, start-up funds and technical assistance will be available to successful candidates.

Applications (hard copy or electronic), including curriculum vitae, list of publications, a short (2-3 pages) summary describing future research plans and names and contact information of four referees should arrive no later than November 30, 2006. Please send to:

Dr. Orly Avni
Search Committee Coordinator
Rappaport Faculty of Medicine
POB 9649, Haifa, Israel 31096

Email: **naomic@tx.technion.ac.il**

Georgia Tech College of Sciences

Chair, School of Applied Physiology

The School of Applied Physiology invites nominations and applications for the position of Chair. We are seeking an outstanding scholar and educator with a national presence to lead a vibrant and growing program (www.ap.gatech.edu). The successful candidate will have an active funded research program and excellent administrative and leadership skills.

Existing research programs use a systems physiology approach to study movement and mobility at all levels, from molecule to organism. Research areas include muscle and exercise physiology, neural control, biomechanics, and prosthetics and orthotics. We have an internationally recognized M.S. in Prosthetics and Orthotics and a new Ph.D. program. Opportunities for collaboration exist on campus and with the Emory School of Medicine, Georgia State University and the Atlanta VA Medical Center. Georgia Tech is one of the nation's top 10 public research universities and is situated on an attractive 400 acre campus in the heart of Atlanta, a culturally-rich and dynamic city.

Review of applications will begin October 1st and will continue until the position is filled. Interested parties should submit a curriculum vitae and names and addresses of five references.

Submit by email to: science@cos.gatech.edu.

Or, by regular mail, to: Chair of Applied Physiology Search Committee, College of Sciences Dean's Office, Georgia Institute of Technology, Atlanta, GA 30332-0365.

Georgia Tech, a unit of the University System of Georgia, is an equal education and employment opportunity institution.

TENURE-TRACK FACULTY POSITIONS
University of Missouri-Columbia
School of Medicine
Center for Cellular and Molecular Immunology

The newly established Center for Cellular and Molecular Immunology (CCMI) at the University of Missouri-Columbia, School of Medicine is seeking highly qualified applicants for Faculty positions at the Assistant, Associate, and Full Professor level. Candidates with interests in the molecular mechanisms of autoimmunity, hypersensitivity, and transplantation immunology are encouraged to apply, but strong applicants from other areas such as tumor immunology and immunity to infectious diseases will also be considered. Salary and startup packages are highly competitive. All applicants must have a Ph.D. and/or M.D. and an outstanding track record in research. The appointee will be expected to develop a competitive, independently funded research program or if appointed at the Associate or Full Professor level, to have a proven ability to attract external funds. Appointees will also be expected to fulfill modest service and teaching duties. Good communication skills are required. Academic appointment will be either in the Department of Molecular Microbiology and Immunology or in the Department of Surgery depending upon programmatic fit. The CCMI is being established under a new leadership and will be located in newly renovated space in the Medical Sciences Building. Review of applications will begin **October 1, 2006** and will continue until the positions are filled.

Applicants should submit a two page personal statement describing his/her research interests, a curriculum vitae, and names, addresses, telephone numbers, and e-mail of at least three references to: **CCMI Search Committee, c/o Ms Shelly Crawford, M616 Medical Sciences Building, Department of Molecular Microbiology and Immunology, University of Missouri-Columbia, School of Medicine, Columbia, MO 65212; (573) 882-8989**,

The University of Missouri is an AA/EOE. Women and minorities under-represented in biomedical research are encouraged to apply.

Immunology Faculty Position at the Sloan-Kettering Institute

The Immunology Program at the Sloan-Kettering Institute (SKI) is seeking innovative investigators for tenure-track positions at the Assistant, Associate, and Member levels who wish to address basic problems in immunology with possible relevance to cancer. Applicants should have a doctoral-level degree and the potential to develop a strong independent research program or a proven record of accomplishments, depending on the level of appointment. Qualified applicants with an M.D. degree may be offered a joint appointment in an appropriate department in Memorial Hospital. Candidates will join a faculty with a broad range of research interests, including transplantation, T and NK cell development and function, gene regulation, antigen presentation, infectious disease and tumor immunology. The program has recently moved into contiguous space on 3+ floors in a new 23 story laboratory building. Faculty will also be eligible for appointments in the newly established Gerstner Sloan-Kettering Graduate School of Biomedical Sciences, as well as the Weill Graduate School of Medical Sciences of Cornell University.

SKI offers a highly interactive, supportive and exciting research environment with programs in Immunology, Cancer Biology & Genetics, Cell Biology, Molecular Pharmacology & Chemistry, Molecular Biology, Developmental Biology, Computational Biology and Structural Biology, as well as unparalleled clinical programs in cancer research, treatment and prevention.

Candidates should e-mail their application, preferably in PDF format, to **immuno@mskcc.org.** The application should include a CV, a description of past research, a description of proposed research, and copies of three representative publications. Candidates should arrange to have three signed letters of reference sent by e-mail to **immuno@mskcc.org** or regular mail to: **Dr. James P. Allison, Chairman, Immunology Program, C/o Kathleen Driscoll, Memorial Sloan-Kettering Cancer Center, 1275 York Avenue, Box 494, New York, NY 10021.** Application Deadline: October 15, 2006. For more information please visit our website at **www.ski.edu.** Memorial Sloan-Kettering Cancer Center is an affirmative action, equal opportunity employer.

Memorial Sloan-Kettering Cancer Center
The Best Cancer Care. Anywhere.
www.mskcc.org

MBL Biological Discovery in Woods Hole

Founded in 1888 as the Marine Biological Laboratory

Assistant/Associate and Senior Scientists

Josephine Bay Paul Center for Comparative Molecular Biology and Evolution

Positions in Ecological Genomics and Molecular Evolution

The Josephine Bay Paul Center for Comparative Molecular Biology and Evolution at the Marine Biological Laboratory invites applications for Assistant, Associate, and Senior Scientists in the areas of molecular microbial ecology and evolution, comparative genomics and bioinformatics. Preference will be given but not restricted to individuals whose research centers on 1) evolution of microbial communities, 2) microbial genomes, and 3) analysis/management of biodiversity data. Candidates who employ theoretical and experimental approaches to understand evolutionary processes in Bacteria, Archaea, Protists and/or viral systems are encouraged to apply. The successful candidates will establish productive research programs in a highly collaborative environment, and they will have the opportunity to join the faculty of the MBL/Brown graduate program. Applicants must hold a Ph.D. in Biology or a related field, and have a strong record of scientific publication and ability to attract extramural funding.

The Bay Paul Center and the Marine Biological Laboratory have considerable strengths in molecular evolution, functional genomics, microbial diversity and ecology, and advanced imaging. The Center maintains state-of-the-art facilities for high-throughput molecular and computational analysis. As part of our expansion at the Bay Paul Center we offer competitive start-up and salary packages. Initial review of applications will begin immediately and continue until appropriate candidates are identified.

For fullest consideration, please apply by **October 15, 2006**. Applicants should submit curriculum vitae, statement of research interests and list of five references to:

Mitchell L. Sogin
c/o Phyllis Doheny
Positions in Ecological Genomics and Molecular Evolution
Josephine Bay Paul Center
MBL
7 MBL Street
Woods Hole, MA 02543

The MBL is an Equal Opportunity/Affirmative Action Employer/Non-smoking workplace.

USA UNIVERSITY OF SOUTH ALABAMA MITCHELL CANCER INSTITUTE

The Vincent F. Kilborn, Jr. Cancer Research Fellowship

An endowment has been established in memory and honor of Mr. Vincent F. Kilborn, Jr., to support cancer research at the Mitchell Cancer Institute (MCI), University of South Alabama. Annual revenues generated from the endowment will help fund the early career development of an outstanding individual who has recently earned a doctoral degree with a focus on cancer research. The selected candidate will receive an annual stipend and support for research expenses for up to 3 years. The recipient will hold the title of "Vincent F. Kilborn, Jr. Cancer Research Fellow" (Kilborn Fellow). The Kilborn Fellow will receive extensive mentoring from the senior professional research faculty of the MCI, and will be a significant contributor to the cancer research workforce of the Institute. He/she will participate in one or more multidisciplinary research programs focusing on new drug, immunotherapeutic, and diagnostic discovery and development, with an emphasis on fundamental mechanisms of cancer metastasis and drug resistance. The Kilborn Fellow also is expected to actively compete for extramural grant funding. The highly successful Kilborn Fellow who succeeds in winning significant grant support for his/her research, may be eligible for consideration for an additional 3-year term of support under the Kilborn Fellowship, and/or a tenure-track faculty appointment.

The MCI is ideally located in Mobile Alabama, a progressive, mid-sized port city of rich cultural history, in the beautiful upper Gulf coastal region. Moderate climate, abundant outdoor recreational opportunities, low cost-of-living and a "college-town" atmosphere all contribute to a high "quality of life" opportunity.

Individuals wishing to be considered for this position should submit a letter outlining their research interests and a *curriculum vitae*, to: **Dr. Øystein Fodstad, Barbara Colle Chair and Scientific Director, USA/MCI, 307 N. University Blvd., MSB 2015, Mobile, AL 36688; or e-mail ofodstad@usouthal.edu**.

Yale University

LUX ET VERITAS

DEAN OF ENGINEERING

Yale University invites applications and nominations for the position of Dean of Engineering. The Dean will provide leadership to the Faculty of Engineering, which includes five departments and one program; Applied Physics, Biomedical, Chemical, Environmental, Mechanical and Electrical Engineering, within the Faculty of Arts and Sciences. Additional ladder appointments will be made in the near future to support recent initiatives in environmental engineering, biomedical engineering and nanoscale science and technology, and to sustain ongoing programs. The new Dean would be expected to play a key role in these recruitments and in planning future research and educational initiatives. Yale engineering faculty have strong collaborations with colleagues in the mathematical, physical, and biological sciences in the Faculty of Arts and Sciences, as well as with faculty in the school of medicine, forestry and environmental studies, and management. At the undergraduate level, Yale engineering places particular emphasis on providing a broad and balanced curriculum with a view to training future leaders.
Letters of application should be addressed to:

Provost Andrew D. Hamilton, P.O. Box 208365,
Yale University, Warner House, 1 Hillhouse Avenue,
New Haven, CT 06520-8365.

Yale University is an affirmative action, equal opportunity employer and particularly welcomes applications and nominations of women and members of underrepresented minorities.

A TRADITION OF EXCELLENCE

ASSOCIATE DIRECTOR AND ENDOWED CHAIR FOR CLINICAL RESEARCH THE METHODIST HOSPITAL RESEARCH INSTITUTE

The Methodist Hospital Research Institute of The Methodist Hospital, Houston, Texas, seeks an exceptional physician scientist to lead its effort in clinical research. The Methodist Hospital System consists of 1,450 beds, including 950 located in the Texas Medical Center in Houston. Together with our partners at Weill Cornell Medical College and New York-Presbyterian Hospital in New York City, there are 3,500 beds available for clinical investigation and clinical trials. The successful candidate will be responsible for organizing and leading the Institute's clinical research in Houston and collaborating with our Cornell and NYP colleagues. We encourage applications from individuals who currently lead substantial programs conducting clinical research. The hospital is in an unprecedented expansion phase, which includes building a new 590,000 SF outpatient facility and 340,000 SF research building. These state-of-the-art facilities are designed to foster extensive collaboration between clinical and basic scientists.

The successful applicant will hold an endowed chair and receive a generous salary, fringe benefits, and a relocation package. Individuals interested in this unique career opportunity should send via e-mail a curriculum vitae, including grant funding information and the names of five references to:

Michael W. Lieberman, M.D., Ph.D.
c/o Ms. Elizabeth Al-Ateeqi
Director, The Methodist Hospital Research Institute
6565 Fannin, Mail Stop B490
Houston, TX 77030
EAAL-Ateeqi@tmh.tmc.edu

Methodist The Methodist Hospital Research Institute

LEADING MEDICINE℠

VCU Medical Center

Virginia Commonwealth University

CARDIOLOGY

Heart Failure Research and Clinical Specialist

Division of Cardiology
MCV Physicians
Richmond, Virginia

Associate Professor/Assistant Professor/Professor: BC/BE faculty member is sought for continued expansion of the VCU Pauley Heart Center of Virginia Commonwealth University. The VCU Pauley Heart Center is a regional referral center with a reputation for excellence in routine, as well as complex patient management. The Heart Center's faculty are leaders in diagnostics, interventional cardiology, cardiovascular research and cardiac surgery. Expanding cardiac services is a key strategic initiative of the VCU Health System.

Heart Failure Specialist: VCUHS is seeking to expand science and research in Heart Failure management. To devote 50-75% effort to research endeavors. We are seeking candidates with an established research base. In addition, candidates should possess a strong clinical background in heart failure as well as experience with transplant and device management. The successful candidate will also participate in Total Artificial Heart studies and have access to a new state of the art Cardiovascular research lab open in 2007. Generous support to facilitate program recognition will be available.

The position offers clinical care, teaching and research opportunities.

Interested candidates should forward their curriculum vitae to: **George W. Vetrovec, M.D., Chairman, Division of Cardiology, Department of Internal Medicine, Virginia Commonwealth University, P.O. Box 980036, Richmond, VA 23298; Phone 804-628-1215; Fax 804-828-8321; email gvetrove@hsc.vcu.edu.**

Virginia Commonwealth University is an Affirmative Action, Equal Opportunity Employer. Women and minorities are encouraged to apply.

WPI

Assistant Professor Chemistry & Biochemistry

The Department of Chemistry and Biochemistry invites applications for a tenure-track position starting in August 2007. The candidate is expected to develop a vigorous, externally-funded research program at the interface of chemistry and biochemistry. This position is part of a new life science research initiative at WPI supported by a state-of-the-art research facility scheduled to open in spring 2007. This $40M facility will host life science related departments and the Bioengineering Institute. Candidates should have a Ph.D. degree with postdoctoral experience, proven research ability, and an interest in teaching in the inorganic/bioinorganic chemistry area.

The Department offers undergraduate and graduate (Ph.D.) degrees in chemistry and biochemistry. WPI is a private, selective technological university with an undergraduate student body of 2800 and 1000 full-time and part-time graduate students. Worcester, New England's third largest city, offers ready access to diverse economic, cultural and recreational resources of the region. Further information about WPI and the department can be accessed at **http://www.wpi.edu.**

The application should consist of a detailed curriculum vita, a proposal describing plans for future research, a statement of teaching interests, and three letters of reference. These materials should be sent to **Dr. Robert E. Connors, Chair, Search Committee, Department of Chemistry and Biochemistry, Worcester Polytechnic Institute, 100 Institute Road, Worcester, MA 01609.** Review of applications will begin immediately and will continue until a suitable candidate is identified.

WPI offers a smoke free environment, competitive compensation and an excellent benefits package including health insurance, family tuition reimbursement and generous vacations.

To enrich education through diversity, WPI is an affirmative action, equal opportunity employer.

A place of discovery…

PRINCIPAL INVESTIGATOR

The Systems Biology Group at the Samuel Lunenfeld Research Institute invites applications for a **Principal Investigator** position (assistant to full professor equivalent, according to experience) in the area of integrative cell biology. Areas of interest include, but are not limited to, mathematical modeling of dynamic cellular systems, chemical biology, imaging of cellular processes, and high-throughput biology. Our group has an international reputation in signal transduction, cell cycle, cell polarity, differentiation, and cell metabolism.

You hold a PhD or PhD/MD with postdoctoral experience and a strong publication record. Candidates are expected to develop innovative and highly competitive independent research programs. The Samuel Lunenfeld Research Institute is affiliated with Mount Sinai Hospital and the University of Toronto (**http://www.mshri.on.ca**). The Institute is a leading centre for molecular and cellular biology with particular strengths in cancer and development and stem cell biology, and is part of a vibrant research community in Toronto. The position will include the opportunity of cross-appointment with the University of Toronto. We offer competitive salary and startup packages commensurate with experience and qualifications. Applications should include a current CV, summary of research interests and goals, most relevant publications, and contact information for three referees. Applications should be submitted, preferably by e-mail, by October 15, 2006 to: **Chair, Systems Biology Search Committee, Samuel Lunenfeld Research Institute, 600 University Avenue, Room 850A, Toronto, ON M5G 1X5**
e-mail: SystemsBiol@mshri.on.ca

We thank all candidates for applying. Only those selected for an interview will be contacted. We are a fully accredited hospital and an equal opportunity employer.

MOUNT SINAI HOSPITAL | Samuel Lunenfeld Research Institute

A WORLD CLASS FACILITY IN THE HEART OF TORONTO

University of Virginia Health System

2 POSITIONS AVAILABLE

Instructor of Research of Internal Medicine - Digestive Health Center of Excellence

Position 1 (Biology): Ph.D. required in biology with relevant post-doctoral experience and quality publications. Qualified candidates will have research interests in immunology related to inflammatory bowel disease, experience with animal models of chronic and acute inflammation required. Knowledge of adoptive transfer, isolation of intestinal/epithelial/endothelial cells, live-cell confocal microscopy, FACS, qPCR, cell cycle progression and transcription factor signaling mechanisms. Salary commensurate with experience.

Position 2 (Biomedical Science): Ph.D. in a biomedical science, preferably with post-doctoral experience. Editorial experience and training are required. Demonstrated ability to rapidly grasp unfamiliar research areas is preferred as role involves working with a wide variety of clinicians and researchers. Experience in publishing is essential as the individual will be expected to take the lead in the preparation of a wide variety of publications as well as being invaluable for the integration of electronic submission processes. The candidate should have a high degree of computer literacy and enjoy working with others in a highly interactive research environment. Salary commensurate with experience.

Submit CV and two letters of reference and indicate the position to which you are applying, to:

University of Virginia DHC, Box 800708
Charlottesville, VA 22908
attn: Martha Dudley

The University of Virginia is an Equal Opportunity/ Affirmative Action Employer.

Duke University Medical Center

Tenure-track Faculty Position (Assistant/ Associate Professor) in the Department of Molecular Genetics and Microbiology, Duke University Medical Center

Applications are invited for a tenure track position. We are interested in individuals who will develop an outstanding research program in Virology, preferably focusing on DNA tumor viruses or factors governing viral pathogenesis.

The Department currently has 21 tenure-track faculty working in virology, microbial pathogenesis, DNA repair and animal and human genetics and genomics. Multiple interdisciplinary programs at Duke University afford a rich environment for scientific interactions. The facilities and start-up support are excellent.

Applications should include a curriculum vitae, a brief description of research accomplishments, a short description of plans for future research, teaching experience, and the names and contact information for three individuals who can provide references. The deadline for applications is **January 15, 2007**. Applications should be e-mailed as a single pdf to: **MGMFacultySearch@mc.duke.edu**. Non-electronic applications will not be accepted.

Women and minorities are encouraged to apply. Duke University is An Equal Opportunity/Affirmative Action Employer.

UNIVERSITY OF MARYLAND

THE DEPARTMENT OF CHEMISTRY AND BIOCHEMISTRY

Biomolecular X-ray Crystallographer

All Levels Tenure-track or Tenured Position
(Assistant Professor, Associate Professor, and Professor)

As part of major university initiatives in the life sciences and biophysics, the Department of Chemistry and Biochemistry seeks to appoint a biomolecular x-ray crystallographer to a tenured or tenure-track position. The successful candidate will add to a program in biomolecular crystallography that was initiated this past year with the hire of one individual at the Assistant Professor level. We seek outstanding scientists whose research interests complement existing strengths in the department and across the university and who are committed to developing outstanding programs in research and teaching. One of four departments within the College of Chemical and Life Sciences, members of the Department of Chemistry and Biochemistry participate in university centers and initiatives that include the Center for Biomolecular Structure and Organization, the Center for Bioinformatics and Computational Biology, the Institute for Physical Science and Technology, as well as a university-wide initiative in biophysics. The University of Maryland, College Park is the flagship campus of the University of Maryland System and is ideally situated in close proximity to Washington, D.C., Baltimore, and Maryland's I-270 Technology Corridor. Candidates should submit a curriculum vitae, a three-page summary of research plans, a statement of educational interests, and contact information for three persons from whom letters of recommendation can be requested. Please submit applications via the department web site (**http://www.chem.umd.edu/Employment/index.php**).

Qualifications: We seek scholars who will build or have highly visible, widely acclaimed research programs and who are capable of excellence in undergraduate and graduate education. Candidates are expected to have a Ph.D. degree, demonstrated accomplishments in independent research, and promise as an effective educator.

Salary: Commensurate with qualifications.

Deadline: Review of applications will begin **October 11, 2006**, but we will continue to accept applications until the position is filled.

AN EQUAL OPPORTUNITY, AFFIRMATIVE ACTION EMPLOYER. APPLICATIONS FROM WOMEN AND MINORITIES ARE ENCOURAGED.

The **Midwest Regional Center of Excellence for Biodefense and Emerging Infectious Diseases (MRCE)** headquarters at **Washington University** is seeking a **Project Manager**. The MRCE is one of 10 NIAID funded centers devoted to research on emerging infectious diseases and potential agents of bioterrorism. This position oversees many of the varied non-financial activities of a multi-institution research consortium with an annual budget of $6.5 million and more than 25 ongoing projects. Coordinates and oversees 2 grant competitions and 2 fellowship competitions each year, communicates with scientific advisory committee members reviewing grants, and assists in the writing and preparation of the center's yearly progress report to NIH. Interacts frequently with center's financial manager and staff to discuss fiscal issues. Coordinates center's annual meeting and guest lecture series and assists to varying degrees with some of the more than 30 projects funded by the center. Serves as spokesperson for the center by traveling, writing, and speaking at meetings as needed. Supervises 2 staff members and reports to center Director.

Requirements: Advanced degree (PhD, MD, DVM) preferably in life sciences. Excellent writing skills, experience with NIH grant applications and progress reports, familiarity with NIH guidelines and ability to communicate effectively with both researchers and their administrators. Attention to detailed human and animal research compliance regulations, documentation and record keeping and ability to multitask. Ability to plan and budget new projects, prioritize tasks, and superior organizational skills.

For consideration, please submit C.V. and cover letter to: **biodefense@id.wustl.edu**

UCI
University of California, Irvine

FACULTY POSITION IN PHARMACOLOGY

The Department of Pharmacology at the University of California, Irvine (UCI) invites applications for a tenure-track faculty position at the level of Associate or Full Professor. We seek a scholar with a proven record of research accomplishments. He/she should have specific interest in the mechanisms governing gene expression and their functional links to metabolism and neuronal responses. Special consideration will be given to candidates with expertise and experience in integrating genetic, biochemical and physiological approaches. Other qualifications include an M.D. and/or Ph.D. in pharmacology or a related field and an interest and talent for teaching.

Curriculum vitae, names of references, and a summary of research interests should be sent to: **Janet Deshaw, Academic Personnel Coordinator, Department of Pharmacology, School of Medicine, University of California, Irvine, Irvine, CA 92697-4625**.

The University of California, Irvine has an active career partner program and an NSF ADVANCE Program for Gender Equity and is an Equal Opportunity Employer committed to excellence through diversity.

UNIVERSITY OF MASSACHUSETTS AMHERST
PHYSICS DEPARTMENT
GLUCKSTERN PROFESSORSHIP

The Physics Department at the University of Massachusetts Amherst is extending its search for a senior faculty member with an outstanding record of research accomplishments to fill the endowed Robert L. Gluckstern Distinguished Professorship in Physics. The Physics Department anticipates substantial new hiring in several areas over the next five years. We plan a major expansion in the area of biological physics during the next several years and a major priority is to hire a leader in this field, either theorist or experimentalist, who will help us to build an internationally recognized program. Substantial opportunities exist for collaborations within the Physics Department and with other departments including Biology, Biochemistry, Microbiology, Chemical Engineering, and Polymer Science. Although biological physics is our priority, we also encourage applications from outstanding candidates in other fields of physics. Communications from established scientists will be held in confidence and no references will be sought without approval. Applicants should send a vitae and a statement of research and teaching interests to: **Gluckstern Faculty Search, Department of Physics, University of Massachusetts, Amherst, MA 01003**. Priority deadline is **October 25, 2006**; however, applications will be accepted until the position is filled. *The University of Massachusetts is an Affirmative Action/Equal Opportunity employer committed to enhancing the diversity and gender balance of its faculty, staff, and students in the sciences. Women and members of minority groups are encouraged to apply.*

POSITIONS OPEN

NAVAL RESEARCH LABORATORY
Computational Mechanics

The **COMPUTATIONAL SCIENTIST** selected for this employment opportunity will join a diverse research group consisting of experimental and theoretical Physicists, Mathematicians, and Engineers. The group's research interests include the study of mechanical and acoustic properties of complex fluid-structure systems, interaction of elastic and acoustic waves with fluid-structure systems at various length scales, and flow-induced structural-acoustics.

This position will be filled at Level IV ($76,554 to $118,957). Salary will be determined based upon selectee's background, experience, and market considerations.

Candidates who have a strong background and interest in the area of computational mechanics should apply, particularly as related to the development of scalable and efficient numerical algorithms for modeling and solution of large-scale problems in elasticity, elasto-dynamics, elasto-acoustics and wave-structure interactions. Problems of current interest include: radiation, scattering and propagation of acoustic waves from submerged visco-elastic structures; sound transmission and interior pressure levels associated with aircraft and automotive bodies; radiation and scattering of sound from turbulent flows around submerged and floating structures; acoustic scattering in littoral environments; wave propagation in heterogeneous, anisotropic and near incompressible elastic structures with applications to MRI-based elastography and nondestructive parameter identification; and the structural acoustics of micro and nano-scale systems.

Announcement opens 1 September 2006, and closes 30 September 2006. To apply, visit the **website: https://chart.donhr.navy.mil** and click on jobs, type in vacancy announcement number DM-NRL-06-0571-NR and press enter to obtain qualification information and instruction on how to apply.

The Naval Research Laboratory is an Equal Opportunity Employer.

ASSISTANT PROFESSOR
Molecular Genetics

The Department of Biology at East Carolina University invites applications for a full-time, tenure-track position in molecular genetics at the rank of Assistant Professor beginning August 20, 2007. We seek an Experimental Biologist who studies fundamental molecular processes and mechanisms. Individuals able to contribute to the Department's programs and strengths in biotechnology, evolution, and developmental biology are especially encouraged to apply. Qualifications for the position include a Ph.D. in molecular genetics, or a related field, and postdoctoral research experience. The successful candidate will be expected to establish a vigorous, well-funded research program, contribute to undergraduate and graduate teaching, and mentor graduate students participating in Master's and interdisciplinary Ph.D. programs. Appropriate service to the University, community, and profession is also expected.

Applicants must complete a candidate profile and submit a cover letter, curriculum vitae, statements of research and teaching interests, and the names and contact information for three references online at **website: http://www.jobs.ecu.edu.** For further information, **e-mail J. Bond (e-mail: bondja@ecu.edu)** or write to: **Dr. Jason E. Bond, Chair, Molecular Genetics Search Committee, East Carolina University, Department of Biology, Greenville, NC 27858. Website: http://www.ecu.edu/biology.** Review of applications will begin on 15 October 2006. *East Carolina University (ECU), is an Equal Opportunity/Affirmative Action Employer that accommodates individuals with disabilities. Individuals requesting a disability accommodation should call the* ***ECU Office of Disability Support Services*** *at* ***telephone: 252-737-1016 (voice/TTY/relay).*** *Proper documentation of identity and employment are required at the time of employment. Official transcript required upon employment.*

CAREERS IN BIOENGINEERING AND NANOTECHNOLOGY

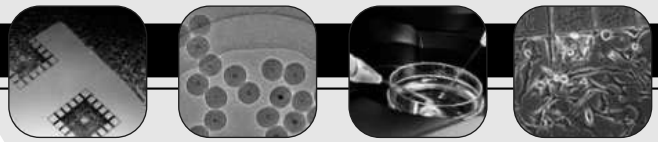

The **Institute of Bioengineering and Nanotechnology** in Singapore is seeking highly motivated individuals who are interested in making an impact in advancing research and development in the following areas:

DELIVERY OF DRUGS, PROTEINS AND GENES

Where the controlled release of various therapeutics involves the use of nanoparticles with functionalized moieties for targeting diseased cells and organs, or for responding to specific biological stimuli.

CELL AND TISSUE ENGINEERING

Where sophisticated materials architecture is employed to design and fabricate living replacement devices for surgical reconstruction and transplantation.

ARTIFICIAL ORGANS AND IMPLANTS

Where multifunctional systems and devices are engineered as biomimetic structures for use as organ replacement.

NANOBIOTECHNOLOGY

Which encompasses the efficient catalytic synthesis and separation of chiral pharmaceuticals, as well as the sensing and detection of biologics and biomolecules using nanostructured materials.

MEDICAL AND BIOLOGICAL DEVICES

Which involve nanotechnology and microfabricated systems for the detection and treatment of diseases.

BIOLOGICAL AND BIOMEDICAL IMAGING

Which comprises the imaging of cells, tissues, small animals and biomaterials using advanced techniques and novel imaging tags.

Positions are available for **Senior Group Leader, Group Leader, Principal Research Scientist, Senior Research Scientist, Research Scientist, Postdoctoral Fellow, Research Officer and Lab Officer** in IBN's six research areas.

We provide competitive salaries as well as attractive benefits that include medical and dental coverage, housing subsidy, shipping and settling-in allowance, air passage for staff and family, paid home leave at the end of contract, and a substantial non-contributory gratuity payment on completion of the contract. Remuneration will commensurate with qualification and experience.

If you are interested in joining a multi-disciplinary research institute at the cutting edge of bioengineering and nanotechnology, please forward a cover letter, your curriculum vitae, and a list of three references to:

Prof. Jackie Y. Ying
Executive Director
Institute of Bioengineering and Nanotechnology
31 Biopolis Way, The Nanos, #04-01
Singapore 138669
Email enquiries may be directed to
recruit@ibn.a-star.edu.sg
Website: www.ibn.a-star.edu.sg

Institute of Bioengineering and Nanotechnology
A*STAR

Head-Department of Integrative Biology and Physiology University of Minnesota Medical School

The University of Minnesota Medical School invites applications from exceptional leaders to be considered for the position of Head of the Department of Integrative Biology and Physiology (IBP). As Head of the Department, the successful candidate will establish and lead the research and teaching missions of the unit as well as recruit outstanding faculty in basic and translational aspects of physiology to the University. We seek candidates whose scientific expertise complements existing strengths in the Department and Medical School. Particular interest will be given to those investigators who work at the systems level to study human disease and/or model systems; but investigators in all areas of physiology are encouraged to apply. The candidate must also have an outstanding record of scholarly accomplishment, educational experience and executive leadership as well as excellent interpersonal, team building and communications skills. For details about the Department please consult: **http://physiology.med.umn.edu**.

All candidates must have a PhD and/or MD degree and qualify for appointment as a tenured professor of the University. We will begin reviewing applications immediately and until the position is filled. Please send a curriculum vitae and the names of three references to:

Dr. David A. Bernlohr
Chair, IBP Search Committee
Department of Biochemistry
Molecular Biology and Biophysics
University of Minnesota
6-155 Jackson Hall
321 Church Street S.E.
Minneapolis, MN 55455

or as an attachment to **swans143@umn.edu**. Confidential inquiries are welcomed.

The University of Minnesota is an Equal Opportunity Educator and Employer.

THE UNIVERSITY OF CALIFORNIA, BERKELEY Faculty Positions in Department of Chemistry

The Department of Chemistry solicits applications for three faculty positions beginning in the Fall 2007. Applications should include a curriculum vitae including list of publications and a 2-3 page description of proposed research. We seek creative and energetic candidates who show extraordinary promise or accomplishment in research and teaching. Although focused on specific research areas, exceptional candidates in any area of chemistry will also be considered. Junior-level applicants should have three letters of recommendations sent on their behalf. For the UC Statement of Confidentiality see **http://apo.chance.berkeley.edu/evalltr.html**. The deadline for receipt of applications is **October 31, 2006**. Application review will begin with receipt of applications. Applications and letters should be sent to the address provided below. Mail materials to:

Faculty Search (ID #_____)
Department of Chemistry
University of California, Berkeley
Berkeley, CA 94720-1460

Chemical Biology (Search ID #821C)
Both senior-level and junior-level applicants will be considered in the field of chemical biology with a focus on chemical approaches to probe biology. Teaching assignments could be in both the undergraduate chemical biology major and graduate level instruction.

Materials Chemistry (Search ID #1018B)
Junior-level applicants will be considered in any area of materials chemistry. This appointment represents continued growth of this area in the department including a new undergraduate major in materials chemistry. Teaching assignment at both the undergraduate and graduate levels is expected.

Inorganic Chemistry (Search ID #1117)
Junior-level applicants will be considered in any area of inorganic chemistry ranging from biological to materials approaches. Teaching assignment at both the undergraduate and graduate levels is expected.

The University of California is an Equal Opportunity/ Affirmative Action Employer.

POSITIONS OPEN

The Department of Chemistry and Biochemistry at Denison University is seeking to expand its faculty with a tenure-track position at the **ASSISTANT PROFESSOR** level in physical or analytical chemistry. Successful candidates will have a strong commitment to teaching at the undergraduate level and the capacity to develop an active research program that involves undergraduates. The Department particularly welcomes applications from candidates with interdisciplinary research interests such as at the interface of biology or environmental science.

Our American Chemical Society-accredited Department has well-developed programs in both chemistry and biochemistry, excellent classroom and laboratory facilities, extensive computer resources, and a broad range of instrumentation which is used in both teaching and research: spectroscopy (400 MHz nuclear magnetic resonance, fourier transform infrared, ultraviolet and visible spectroscopy), separations (gas chromatography/mass spectometry and other gas chromatography methods, high performance liquid chromatography, electrophoresis), electrochemistry, and biochemistry (bioseparations, high speed centrifugation and PCR). A Ph.D. is required and postdoctoral experience is preferred. Applicants should submit curriculum vitae, undergraduate and graduate transcripts, a statement of teaching philosophy, and a summary of research plans. These materials and three letters of recommendation should be sent to: **Dr. Jordan L. Fantini, Department of Chemistry and Biochemistry, Ebaugh Laboratories, Denison University, Granville, OH 43023.** Denison University is located in central Ohio, 30 minutes east of Columbus and about two and a half hours from Cleveland, Cincinnati, Ohio, and Pittsburgh, Pennsylvania. Visit us at our **website: http://www.denison.edu/chem/.** Informal inquiries may be made via **e-mail: fantinij@denison.edu.** Our review of completed applications will begin October 15, 2006, and continue until the position is filled. *Denison University, an Equal Opportunity and Affirmative Action Employer, is committed to enhancing the diversity of its faculty, staff, and students and encourages applications from women, minorities, veterans, and disabled persons.*

BASIC SCIENCE RESEARCHER
Stress/Pain Neurobiology

The Department of Anesthesiology and Critical Care at the University of Pennsylvania's School of Medicine seeks candidates for an **ASSISTANT** or **ASSOCIATE PROFESSOR** position in either the tenure-track or the nontenure research track. Track and rank will be commensurate with experience. The successful applicant will have experience in the field of stress neurobiology with a focus on stress and/or pain research. Applicants must have a Ph.D. or equivalent degree and have demonstrated excellent qualifications in research.

Applicants to the tenure-track must demonstrate qualifications and experience in teaching. For either track the individual's research will complement ongoing research in the Center which includes elucidating the neural substrates linking stress and pain, neurobiological mechanisms by which stress leads to psychiatric and medical disorders, identifying genetic, developmental and environmental determinants of stress and/or pain sensitivity, cellular mechanisms of substance abuse, and mechanisms by which the brain processes visceral information. The Stress Neurobiology Center is located at the Children's Hospital of Philadelphia (CHOP).

Please submit curriculum vitae, a letter of interest, and three reference names to:

Dr. Rita J. Valentino
Director, Center for Stress Neurobiology
The Children's Hospital of Philadelphia
34th Street and Civic Center Boulevard
Abramson Research Center, Suite 4399
Philadelphia, PA 19104
E-mail: valentino@e-mail.chop.edu.

The University of Pennsylvania is an Equal Opportunity, Affirmative Action Employer. Women and minority candidates are strongly encouraged to apply.

POSITIONS OPEN

RESEARCH SCIENTIST 4
(Entomology)

The New York State Department of Health (NYSDOH) is recruiting for a Research Scientist 4 (RS4) in Ithaca, New York, to oversee laboratory and field operations for the Department's Arthropod-borne Disease Program activities located at Cornell University. Minimum qualifications: Bachelor's degree and five years of professional scientific vector-borne or zoonotic disease research experience; or a Master's degree and four years of such experience; or a scientific doctorate degree and two years of such experience. Preferred qualifications: Experience in medical entomology, vector-borne disease risk assessment, zoonotic and/or vector-borne disease research and study design, molecular biology, or epidemiology. Experience with vector-borne disease surveillance, data collection methods, and data analysis using epidemiological principles and methodologies; and with statistical software, relational database, geographic information systems applications, and graphical software packages. Experience managing a laboratory and supervising staff conducting vector surveillance and/or research. Strong publication record in recognized peer-reviewed scientific literature. Duties: The RS4 will act as program liaison with local health departments, other state agencies, and health care providers in the region, by providing technical expertise and consultation in arthropod-borne disease surveillance, prevention and applicable interpretation of research activities. The RS4 will demonstrate strong independent research within Departmental policies and procedures; coordinate and conduct all phases of scientific investigations; supervise field and laboratory work conducted by lower-level regional research staff, entomological Assistants and/or students; determine geographic areas for targeted research; supervise specimen collection, identification and testing; and compile and publish reports of the data collected. The selected candidate will report to the program director in Albany and maintain an academic link with Cornell University and the University at Albany School of Public Health, support the NYSDOH Tick Identification Service, and provide laboratory and classroom resources for local health department vector-borne disease staff. Salary $71,229. Application procedure: Submit resume to: **Human Resources Management Group, RS4/JC Room 2276, Corning Tower Building, Empire State Plaza, Albany, NY 12237-0012,** or by **e-mail: resume@health.state.ny.us,** with a subject line of RS4/JC or by **fax: 518-474-6771.** Applications accepted until position filled.

An Affirmative Action/Equal Opportunity Employer. Women, minorities, and people with disabilities are encouraged to apply.

POSTDOCTORAL AND RESEARCH ASSOCIATE POSITIONS for molecular and neurobiological studies. We focus on regulatory mechanisms for expression of neuronal proteins triggered by nutrients, hormones, and neuronal activity. We investigate chromatin remodeling events, RNA transport and localized translational control. Various modern technologies based upon molecular, cellular, proteomic and array approaches are used (*EMBO-Journal* **25:** 3203, 2006; *Mol. Cell* **19:** 643, 2005; *J. Neurosci.* **25:** 3350, 2005; *Molecular Cellular Proteomics* **4:** 300 and 975, 2005). A Ph.D. in biological sciences or biophysics is required. Interested applicants should send curriculum vitae and statement of research interests to: **Dr. Li-Na Wei, Department of Pharmacology, University of Minnesota Medical School, 6-120 Jackson Hall, 321 Church Street S.E., Minneapolis, MN 55455, U.S.A. E-mail: weixx009@umn.edu, telephone: 612-625-9402.** For details please go to **website: http://www.pharmacology.med.umn.edu/staffwei.html.** *The University of Minnesota is an Equal Opportunity Educator/Employer.*

POSITIONS OPEN

ASSISTANT PROFESSOR
Developmental Biology

The Department of Natural Sciences invites applications for a tenure-track Assistant Professor with a focus on developmental biology, beginning in fall 2007. Teaching duties include upper division undergraduate courses and laboratories in developmental biology, comparative anatomy of vertebrates, histology, and participation in introductory biology. Creating a specialty class is also possible. The successful applicant is expected to develop and maintain an active research program leading to peer-reviewed publications. The area of research is not specified, but may reflect molecular and cellular processes that regulate organismal and developmental processes. This individual will complement our existing faculty and programs in biology, microbiology, and biochemistry. A research laboratory, modest startup funds, and teaching release time are available. Doctorate and commitment to both teaching and research required. We encourage the Assistant Professor to engage students in supervised research. Send letter of application including statement of teaching philosophy and research plan, curriculum vitae, and names of three references to: **Developmental Biology Search Committee, Department of Natural Sciences, University of Michigan-Dearborn, 4901 Evergreen Road, Dearborn, MI 48128.** Review of applications will begin December 1, 2006. The University of Michigan, Dearborn, Department of Natural Sciences includes biology, chemistry, physics, and specialized programs in biochemistry, earth sciences, environmental science, and microbiology **(website: http://casl.umd.umich.edu/natsci/).** *The University of Michigan, Dearborn is dedicated to the goal of building a culturally diverse and pluralistic faculty committed to teaching and working in a multicultural environment and strongly encourages applications from minorities and women. The University of Michigan, Dearborn is an Equal Opportunity, Affirmative-Action Employer.*

TENURE-TRACK ASSISTANT PROFESSOR, EXCITABLE MEMBRANE/ION CHANNEL BIOPHYSICIST. The Department of Biomedical Sciences (BMS) seeks to fill a tenure-track position at the rank of **ASSISTANT PROFESSOR** in the area of excitable membrane biophysics. The successful candidate is expected to develop an independent, extramurally funded research program and contribute to undergraduate and graduate teaching. Information about the BMS Department can be found at **website: http://www.cvmbs.colostate.edu/bms.** Applicants must have a Ph.D., D.V.M., M.D., or equivalent degree and postdoctoral research experience. A cover letter, curriculum vitae, statements of research and teaching interests, and names of three references, who may be contacted when appropriate, should be sent to: **Michael Tamkun, Chair of the Search Committee, Neuroscience Division, Department of Biomedical Sciences, 1617 Campus Delivery, Colorado State University, Fort Collins, CO 80523.** Application materials can be submitted to **e-mail: tamkunmm@lamar.colostate.edu.** Review of applications will begin October 1, 2006, and continue until a successful candidate is identified.

Colorado State University is an Equal Opportunity/Affirmative Action Employer.

FACULTY POSITION
Biological Chemistry

The Department of Chemistry of the University of Kentucky invites applications for a tenure-track position in the area of biological chemistry, directed at the **ASSISTANT PROFESSOR** level. We are seeking candidates who will develop a strong, nationally competitive research program and who are dedicated to excellence in teaching at both the graduate and undergraduate levels. Please see our website **(website: http://www.chem.uky.edu/facultysearch)** for a complete description of the position and application details. Initial consideration of applications will begin October 15, 2006, with an anticipated starting date of August 2007. *The University of Kentucky is an Equal Opportunity Employer and strongly encourages applications from women and underrepresented minorities.*

Does your next career step need direction?

There's only one place to go for career advice if you value the expertise of *Science* and the long experience of AAAS in supporting career advancement - ScienceCareers.org. The pages of *Science* and our website ScienceCcareers.org offer:

- Thousands of job postings
- Funding information
- Career advice articles and tools
- Networking opportunities

www.sciencecareers.org

POSITIONS OPEN

ASSISTANT PROFESSOR
Harvard University
Plant Evolutionary Biology

The Department of Organismic and Evolutionary Biology at Harvard University invites applications for a tenure-track faculty position in evolutionary biology. We seek to appoint an individual whose research on plants makes use of tools and approaches drawn from genomics, ecology, systematics, biomechanics, development, physiology, and/or systems biology to address fundamental questions regarding the origin and maintenance of diversity in plant lineages and/or communities. Applicants will be expected to develop an innovative research program and contribute to teaching at the graduate and undergraduate levels. Initial appointment is for a term of five years, with possibility of promotion, including to tenure. Applications from or information about female and minority candidates are encouraged.

Applicants should submit the following as electronic PDF files: curriculum vitae, statements of research and teaching interests, representative publications, and arrange for three references to be sent via e-mail to: **N. Michele Holbrook, Charles Bullard Professor of Forestry, c/o Allison Schellhammer, e-mail: aschellhammer@oeb.harvard.edu.** Letters of nomination from third parties are also welcome. Review of applications will begin on October 15, 2006.

Further information about Organismic and Evolutionary Biology is available at **website: http://www.oeb.harvard.edu;** information about plant biology at Harvard can be found at **website: http://www.pbi.fas.harvard.edu.**

Harvard University is an Affirmative Action/Equal Opportunity Employer.

FACULTY POSITION IN MOLECULAR BIOPHYSICS
Johns Hopkins University School of Medicine

The Department of Biophysics and Biophysical Chemistry **(website: http://biophysics.med.jhmi.edu)** seeks outstanding candidates for the position of **ASSISTANT PROFESSOR.** Applications are sought in all areas of molecular biophysics and biophysical chemistry, including, but not limited to, enzymology, structural biology, single molecule studies, computational biophysics, biological spectroscopy, and mechanistic chemical biology. Priority will be given to applications received by November 1, 2006. Please submit paper copies of curriculum vitae, a summary of current and proposed research, and arrange to have three letters of recommendation sent to:

Search Committee
Department of Biophysics and Biophysical Chemistry
Johns Hopkins University School of Medicine, WBSB 713
725 North Wolfe Street
Baltimore, MD 21205-2185
Fax: 410-502-6910

The Johns Hopkins University is an Equal Opportunity Employer.

ASSISTANT/ASSOCIATE PROFESSOR

One long-term contract **FACULTY POSITION.** Begin January 2007 preferably, otherwise August 2007. Ph.D. required, primary teaching responsibility anatomy/physiology along with freshman biology courses. Experience in small college preferred. Liberal arts environment. Responsibilities include academic advising, committee work, expected to engage in research with undergraduates, to write grants and to publish. Strong record of teaching excellence and scholarship desirable. Send letter stating interest, complete resume, transcripts, and three letters of reference to: **Sr. John Karen Frei, Dean, School of Natural and Health Sciences, Barry University, 11300 N.E. Second Avenue, Miami Shores, FL 33161** by November 15, 2006.

POSITIONS OPEN

FACULTY POSITION
The Institute for Behavioral Medicine Research (IBMR) Jointly with the College of Dentistry

The Ohio State University College of Dentistry is seeking to fill a position in the College of Dentistry and the Institute for Behavioral Medicine Research (IBMR) to study the mind/body axis and behavioral medicine with a focus on the impact of psychological stress on the immune system. This person will be part of a large multidisciplinary research group within the IBMR and the College of Dentistry. For this position, the person should have a significant research track record in the fields of psychobiology and/or immunology.

The IBMR at the Ohio State University Medical Center is a research institute. Significant interactions between the IBMR and the College of Dentistry have been initiated and the applicant for this position will play an important role in bridging these units. Applicants should submit curriculum vitae, three letters of reference to: **Dr. John Sheridan, Associate Dean for Research, The Ohio State University College of Dentistry, 3143 Postle Hall, 305 West 12th Avenue, Columbus, OH 43218.** *The Ohio State University is an Equal Employment Opportunity/Affirmative Action Employer. Women, minorities, veterans, and individuals with disabilities are encouraged to apply.*

FACULTY OPENINGS
Boston College
Chemistry Department

The Department of Chemistry at Boston College invites applications for two Faculty positions to be effective in the fall of 2007: chemical biology and biochemistry and all related interdisciplinary chemistry fields (bioorganic, biophysical, and bioinorganic chemistry); experimental physical chemistry, all branches thereof and all related interdisciplinary chemistry fields (materials, soft condensed matter).

Applicants are sought at the **ASSISTANT PROFESSOR** level; however, outstanding applicants at the senior level are also welcome. Successful applicants are expected to establish a prominent, externally funded research program, and will join a Department of approximately 125 doctoral students, 25 postdoctoral fellows, 40 undergraduate majors, and an internationally recognized faculty. Boston College, located in a residential community bordering the city of Boston, is within 20 minutes of the major universities and medical centers in the Boston/Cambridge area. For application details, please refer to **website: http://chemserv.bc.edu.** Due date for all applications: 15 October 2006. *Boston College, a university of eight schools and colleges, is an Equal Opportunity Employer and supports Affirmative Action.*

The Department of Oncological Sciences of the Mount Sinai School of Medicine is seeking **ACADEMIC TRACK FACULTY** at all levels. Candidates can be Ph.D. or M.D./Ph.D., must have a strong research background, and will be expected to establish a robust externally funded research program within the Department's highly interactive environment. Each position comes with a generous startup package, state-of-the-art laboratory space, and protected time for research-related activities.

We encourage applicants with research programs in the following topics: innovative mouse models of solid tumors; tumor microenvironment; developmental therapeutics.

Applicants should submit curriculum vitae, including contact details for at least three references, and a summary of research accomplishments and plans for future research directions no later than November 15, 2006. Applications may be submitted by **e-mail: oncsci.search@mssm.edu,** or by mail to: **Search Committee, Department of Oncological Sciences, Mount Sinai School of Medicine, One Gustave L. Levy Place, P.O. Box 1130, New York, NY, 10029.**

Website: http://www.mssm.edu/oncological_sciences.

POSITIONS OPEN

FACULTY POSITION IN BIOCHEMISTRY
University of Alaska, Fairbanks

The University of Alaska, Fairbanks, Department of Chemistry and Biochemistry and the Program in Biochemistry and Molecular Biology invites applications for a tenure-track position at the **ASSISTANT PROFESSOR** level in neuroscience, toxicology, pharmacology, or related areas. The candidate will establish an externally funded research program in their area of interest focusing on molecular mechanisms. Mentoring of graduate and undergraduate students in research projects is expected. Teaching duties include undergraduate and graduate core courses in biochemistry, and advanced courses in neuroscience, toxicology, pharmacology or related areas. A Ph.D. in biochemistry or related discipline is required, postdoctoral experience is highly preferred. For information about the Department of Chemistry and Biochemistry at the University of Alaska, Fairbanks, please visit **website: http://www.uaf.edu/chem/.** To apply, fill in an online application including as attachments a cover letter with the names and complete contacts of at least three references, curriculum vitae, a statement of proposed research, and a statement of teaching philosophy and student mentoring. This online application may be found at **website: http://www.uakjobs.com/applicants/Central?quickFind=56148.** In addition to the online application, please arrange to have sent graduate transcripts to: **Thomas B. Kuhn, Chair Biochemistry Search Committee, Department of Chemistry and Biochemistry, University of Alaska, Fairbanks, P.O. Box 756160 Fairbanks, AK 99775-6160.** Review of applications begins on October 23, 2006. *The University of Alaska is an Equal Opportunity / Affirmative Action Employer and Educational Institution. Minorities and women are encouraged to apply.*

FACULTY POSITION
ASSISTANT PROFESSOR (TENURE TRACK)
Department of Psychiatry

The Department of Psychiatry at the Uniformed Services University of the Health Sciences, Bethesda, Maryland, is seeking to fill an Assistant Professor, tenure-track, teaching and research position with particular emphasis on biological psychiatry. The Department is comprised of 20 full-time faculty and has active research interests in the neurobiology and behavior of stress, post-traumatic stress disorder, anxiety, depression, and substance abuse. The successful candidate will be responsible for developing a funded research program and will participate in medical student and resident education and clinical care. Individuals who hold an M.D., have completed an approved psychiatric residency and are Board-eligible/certified are invited to apply. Send curriculum vitae, description of current and anticipated research interests, and the names and addresses of four references to: **Robert J. Ursano, M.D., Chairman, Department of Psychiatry, Uniformed Services University, 4301 Jones Bridge Road, Bethesda, MD 20814 (e-mail: rursano@usuhs.mil).** Review of applications is ongoing. *The University is an Affirmative Action/Equal Opportunity Employer.*

NATIONAL UNIVERSITY OF SINGAPORE
Department of Chemical and Biomolecular Engineering

The Department of Chemical and Biomolecular Engineering at National University of Singapore invites applications for **TENURE-TRACK FACULTY** positions at all levels. The Department is one of the largest internationally with excellent in-house infrastructure for experimental and computational research. A Ph.D. in chemical engineering or related areas and a strong research record with excellent publications are required. Please refer to **website: http://www.chbe.nus.edu.sg/** for more information on the areas of interest and for application details. Applicants should send full curriculum vitae (including key publications), a detailed research plan, a statement of teaching interest, and a list of names of at least three references to: **Professor Raj Rajagopalan, Head of Department (Attention: Ms. Nancy Chia, e-mail: nancychia@nus.edu.sg).**

Targeting the Kinome

December 4 – 6, 2006
Basel, Switzerland

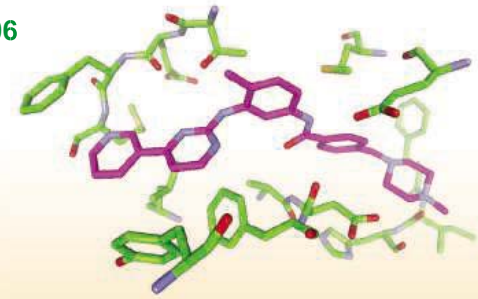

Confirmed speakers:

Kari Alitalo (Helsinki), David Baltimore (Pasadena), Mariano Barbacid (Madrid), David Barford (London), Philip Cohen (Dundee), Sara Courtneidge (La Jolla), George Demetri (Boston), Doriano Fabbro (Basel), Jim Fagin (Cincinnati), Pascal Furet (Basel), Carlos Garcia-Echeverria (Basel), Susan Gasser (Basel), Mike Hall (Basel), Carl-Henrik Heldin (Uppsala), Tony Hunter (La Jolla), Nancy Hynes (Basel), Sandra Jacob (Basel), Heidi Lane (Basel), Alexander Levitzki (Jerusalem), David Livingston (Boston), Nick Lydon (Wilson), Paul Manley (Basel), Alex Matter (Singapore), Adrian Merlo (Basel), Peter Parker (London), Tony Pawson (Toronto), Thomas Roberts (Boston), Joseph Schlessinger (New Haven), William Sellers (Boston), Radek Skoda (Basel), Michael Stratton (Hinxton), George Thomas (Cincinnati), Axel Ullrich (Martinsried), Victor Velculescu (Baltimore), Jürgen Wagner (Basel), Owen Witte (Los Angeles), Michael Yaffe (Cambridge)

In addition to the plenary lectures we will also have poster sessions. We particularly encourage doctoral students, postdoctoral fellows and young investigators to actively participate at the Meeting.

For registration please visit our website at http://www.targeting-the-kinome.org/. Application deadline: November 1, 2006

For further questions, please contact baselkinome@fmi.ch

Assistant/Associate Professor in SYSTEMS BIOLOGY

The Department of Systems Biology at Harvard Medical School invites applications for the position of Assistant or Associate Professor. Areas of particular interest to the Department include spatial organization and homeostasis in tissues and embryos, and the effects of drugs on biological networks. Technology research areas of special interest include methods for tracking the state or abundance of specific molecules in single cells or in living tissues, or for integrating high-dimensional data sets with mechanistic models.

The Department is a supportive and congenial environment for researchers originally trained in quantitative or theoretical disciplines who are now interested in important biological or medical problems, as well as for biologists with strong interests in modeling approaches or quantitative measurement. We place particular emphasis on mentoring young faculty, supporting risky or innovative research programs, and helping young faculty address the challenges of balancing family life with work.

Applications should include a CV and a research proposal and should be sent to: **Timothy J. Mitchison, PhD, Chair, Systems Biology Search Committee, Harvard Medical School, 200 Longwood Ave, WAB-536, Boston, MA 02115.**

Please arrange for three letters of reference to be sent to the same address. PDF submissions are also acceptable and should be e-mailed to: **SystemsBiology_Search@hms.harvard.edu**

Harvard University is an Affirmative Action/Equal Opportunity Employer. Women and minorities are particularly encouraged to apply.

ANIMAL PHYSIOLOGIST

The **Department of Biological Sciences** at the **University of South Carolina** invites applications for a tenure track position at the rank of Assistant Professor in Animal Physiology. While the interests of the candidate need to be in some aspect of animal physiology, preference will be given to individuals dealing in areas of research that complement existing strengths in the department. These areas include sensory systems and neurobiology, cell physiology and signaling, metabolic regulation, development and evolution of organ systems, and cellular and organismal responses to the environment. The successful candidate should have post-doctoral experience and will be expected to establish an independent extramurally funded research program and to teach physiology at the undergraduate and graduate levels. Additional departmental information can be found at the following website: **http://www.biol.sc.edu/**.

Review of applicants will begin **November 1, 2006** and will continue until the position has been filled. Applicants should send a curriculum vitae, a summary of their research accomplishments, a description of future research plans, a statement of teaching interests, and copies of representative publications to: **Dr. David Reisman, Animal Physiologist Search Committee, Department of Biological Sciences, University of South Carolina Columbia, SC 29208**.

In addition, applicants must arrange to have three letters of reference that can be sent by email to: **animalphys@biol.sc.edu**.

The University of South Carolina is an Affirmative Action, Equal Opportunity Employer. Minorities and women are encouraged to apply.

POSITIONS OPEN

ANIMAL EVOLUTIONARY ECOLOGIST ASSISTANT PROFESSOR

The Department of Biology at Willamette University invites applications for a tenure-track position at the level of Assistant Professor for an Evolutionary Ecologist to begin August 2007. Proficiency with molecular techniques is required. Preference will be given to candidates who research whole animal level questions and whose interests complement our existing field-based strengths. Specific areas of interest include, but are not limited to, comparative morphology, population genetics, adaptation, speciation, and the evolution of species interactions. Teaching duties include introductory biology, an intermediate course in evolution, and a research methods course including molecular techniques and/or strong computational skills. The successful applicant will be expected to develop a fundable research program that involves undergraduates. Ph.D. and teaching experience required; postdoctoral training and publications strongly preferred. Applicants should submit a letter of application, curriculum vitae, a concise description of teaching and research interests, and three letters of reference to: **Barbara Stebbins-Boaz, Ph.D., Chair, Department of Biology, Willamette University, 900 State Street, Salem, OR 97301.** Applications should be received by October 13, 2006. Please visit our website for more information at **website: http://www.willamette.edu/go/jobs/.** *Willamette maitains a strong institutional commitment to diversity and strives to recruit and retain candidates from communities of color and ethnic groups.*

TENURE-TRACK FACULTY POSITION ECOSYSTEMS ECOLOGIST

The Department of Biology, Villanova University, invites Ecosystem Ecologists to apply for a tenure-track position at the **ASSISTANT PROFESSOR** level to begin August 2007. The successful candidate will contribute to teaching of undergraduate and graduate offerings in general biology and ecosystems ecology, develop an active research program, seek external funding, and mentor undergraduate and graduate student research. For more information, see **website: http://www.biology.villanova.edu/ecosys.html.** Ph.D. and postdoctoral experience required. Submit application letter, curriculum vitae, research plans, statement of teaching philosophy, and official undergraduate and graduate transcripts, and have three letters of recommendation sent to: **Ecosystems Ecology Search Committee, Department of Biology, Villanova University, Villanova, PA 19085.** Review of completed applications begins October 31, 2006. Villanova University is a Roman Catholic University sponsored by the Augustinian Order. *An Affirmative Action/Equal Employment Opportunity Employer, Villanova seeks a diverse faculty committed to scholarship, service, and especially teaching, who understand, respect, and contribute to the University's mission and values. Faculty diversity is an educational mission of the Department.*

Faculty position for Ph.D. level, basic or translational researcher in Division of Nephrology, Department of Medicine. Positions are nontenure-track as **INSTRUCTOR/ASSISTANT PROFESSOR.** Collaboration with existing genetic epidemiology laboratory in the division highly desirable. Genetic epidemiology laboratory focuses on ischemia reperfusion injury during kidney transplantation; chronic kidney allograft dysfunction; and cardiovascular disease; and pharmacogenetics. *Not a J-1 or H1B opportunity.* Please submit curriculum vitae to **Human Resources** at:

Minneapolis Medical Research Foundation
600 Shapiro Building; 914 So. 8th Street
Minneapolis, MN 55404
Telephone: 612-347-5954
Fax: 612-373-1817
E-mail: hr@hfa-mn.org
Websites: http://www.hcmc.org/depts/medicine/medresearch.htm
and
www.mmrf.org.

Equal Opportunity Employer.

POSITIONS OPEN

The Department of Biological Sciences at Murray State University is seeking candidates for two full-time, tenure-track faculty appointments at level in the general area of cellular biology to the **ASSISTANT PROFESSOR** beginning August 2007. Applicants must have a Ph.D., research interests at the cellular level, and a strong commitment to establishing a research program involving undergraduate and graduate students. Preference will be given to candidates with postdoctoral research and teaching experience, a record of quality publications, and evidence of the ability to attract extramural funding. Specific research areas are open, but preference will be given to individuals with interests in any of the following areas: mechanisms of gene expression, cellular bioinformatics, cell signaling, and cell differentiation. Teaching responsibilities will include undergraduate and graduate level courses commensurate with Departmental needs and the individual candidates' expertise. The Department of Biological Sciences has faculty with graduate program concentrations in cell and molecular biology, physiology, ecology and organismal biology. Application deadline: October 6, 2006. To apply: submit a letter of interest, curriculum vitae, statements of teaching interests and philosophy, description of research, relevant reprints, copies of transcripts, and three letters of recommendation to: **Dr. Timothy Johnston, Search Committee Chair, Department of Biological Sciences, 334 Blackburn Sciences Building, Murray State University, Murray, KY 42071.** *Women and minorities are encouraged to apply. Murray State University is an Equal Education and Employment Opportunity, Minorities/Females/Persons with Disabilities, Affirmative Action Employer.*

NEURAL/GLIAL STEM CELL NEUROSCIENCE FACULTY
Department of Neuroscience
University of Connecticut Health Center

The University of Connecticut Health Center Department of Neuroscience, in conjunction with the State of Connecticut Stem Cell Research Program, seeks applicants for a tenure-track faculty position at the **ASSISTANT PROFESSOR** level. Applicants should have research focusing on the use of stem cells for the treatment of neurodegenerative diseases and/or neurological disorders. The study of both approved human cell lines and contributions to the creation and study of nonapproved lines is anticipated. Applicants are expected to have a Ph.D., M.D. or equivalent, with appropriate training in basic and translational science. We are particularly interested in applicants who will work independently, but who would also establish productive collaborations with our existing core group of cellular and molecular neurobiologists, to move basic research from the "bench to the bedside." We envision this faculty member as a catalyst, promoting collaborative efforts that would be synergistic in nature. A generous startup package is available. Applicants should send their curriculum vitae, statement of research interests, teaching goals and plans, electronic versions of two representative publications, and three letters of reference to **e-mail: neurosciencejob@uchc.edu.** Applications will be accepted until October 31, 2006.

The University of Connecticut is an Equal Opportunity/Affirmative Action Employer. Women and people from diverse racial, ethnic, and cultural backgrounds are strongly encouraged to apply.

CIRCADIAN BIOLOGY

Postdoctoral positions are available immediately for highly motivated individuals interested in pursuing the molecular and cellular basis of circadian rhythms in mammals and/or insects. Candidates should have a strong background in molecular biology and biochemistry. A working knowledge of circadian biology is desirable. Please send curriculum vitae and contact information for three references to: **Dr. Steven M. Reppert, Department of Neurobiology, University of Massachusetts Medical School, LRB – 7th Floor, 364 Plantation Street, Worcester, MA 01605. E-mail: steven.reppert@umassmed.edu. Website: http://www.umassmed.edu/neurobiology/.**

An Equal Opportunity/Affirmative Action Employer.

POSITIONS OPEN

CHAIR, DEPARTMENT OF BIOLOGY
Emory University
Search Continued

The Department of Biology in Emory College of Emory University invites applications for the position of Department Chair and Professor of Biology. Emory is a nationally and internationally known research university and has recently begun a comprehensive fundraising campaign to strengthen its research and teaching programs. The Biology Department is currently composed of 23 tenure-track faculty and 7 Senior Lecturers and Lecturers. The successful candidate for this position will have a distinguished record of extramurally funded research and scholarly activity sufficient to merit appointment at the rank of tenured Full Professor in Emory College. Applicants must have a doctoral degree or its equivalent in biology, or other appropriate discipline, and should have a research focus in one of the three areas of research strength in the Department: population biology, ecology and evolution; computational neuroscience; genetics, cell, and developmental biology. Applicants should have excellent communication, leadership, and administrative skills, and should have a strong commitment to undergraduate and graduate teaching. The successful candidate will oversee the continued growth of the Department via the hiring of new faculty, the continued development of the undergraduate curriculum, and the possible reconfiguration of the Departmental graduate program.

Please submit a cover letter, curriculum vitae, statement of research interests, experience, and future plans, teaching philosophy, and departmental leadership philosophy. Materials should be submitted to: **Chair - Search Committee, Department of Biology, 1510 Clifton Road, Emory University, Atlanta, GA 30322.** Documents may be submitted electronically to **e-mail: george.h.jones@emory.edu.** Applications will be reviewed on receipt and the review process will continue until a suitable candidate is identified. Please visit the Departmental **website: http://www.biology.emory.edu,** to learn more about biology at Emory. *Emory University is an Equal Opportunity Affirmative Action Employer. Women and underrepresented minority candidates are encouraged to apply for this position.*

UNIVERSITY OF ROCHESTER. The Department of Chemistry invites applications for positions in all areas of experimental chemistry at the **ASSISTANT, ASSOCIATE**, and **FULL PROFESSOR** levels. Candidates with research interests in organic chemistry, broadly defined, are especially encouraged to apply. Candidates are expected to establish an outstanding program of original research and be effective teachers at the graduate and undergraduate levels. Applicants should send curriculum vitae, a statement of research plans, teaching interests, and arrange for three letters of recommendation to be sent, preferably in electronic form, to **Ms. Karen Dean, e-mail: dean@chem.rochester.edu**, or mail to: **Chemistry Faculty Search Committee, c/o Ms. Karen Dean, Department of Chemistry, University of Rochester, RC Box 270216, Rochester, New York 14627-0216.** Review of applications will begin on October 16, 2006. *The University of Rochester is an Equal Opportunity Employer. Women and minority candidates are strongly encouraged to apply.*

PROTEIN CHEMIST
The Ohio State University Comprehensive Cancer Center

Seeking a Ph.D. Protein Biochemist, with at least three years of experience in protein purification and analysis desired, in the laboratory of **Dr. Richard Fishel.** Familiarity with routine PAGE/Western analysis, high performance liquid chromatography purification, cellular overexpression, and at least a fundamental understanding of mass spectrometry, surface plasmon resonance, fluorescence anisotropy, and stop-flow/quench-flow kinetic studies. To apply, please go to **website: http://www.jobsatosu.edu** requisition 319514. *Equal Employment Opportunity/Affirmative Action Employer.*

COURSE

EIGHTH ADVANCED VACCINOLOGY COURSE
ADVAC 8
Les Pensières, Veyrier-du-Lac
(near Annecy, French Alps) 14 - 25 May 2007

Organized by Fondation Mérieux and University of Geneva
With the co-sponsorship of European Commission, Bill and Melinda Gates Foundation, NIH/NIAID and Fogarty, Johns Hopkins Bloomberg, Institut Pasteur, ESPID, NFID, NVPO, Vaccine Industry.

Scientific Direction
Paul-Henri Lambert, MD, Geneva , Director of the Course.
Stanley Plotkin, MD, Philadelphia, Senior Advisor.

Objective of the course
To facilitate critical decision-making in vaccinology. Top-level lectures, practical exercises. English language.

Who should apply?
Scientists and decision-makers from the public and private sectors.

Application deadline
15 November 2006

Information and application forms
www.fondation-merieux.org and www.advac.org
contact: advac@medecine.unige.ch or
katia.mielczarek@fondation-merieux.org

Programme Fees
1- Standard registration fee, incl. full attendance in the course (2 weeks) and course material: EUR 3 500, VAT incl.; Reduced registration fee for academic & governmental sector, NGOs : EUR 1400, VAT incl.
2- Accommodation fee (lodging and meals) : EUR 2 050, VAT incl.

Fellowships (travel, accommodation and registration costs) will be available for participants from Developing Countries, new EU members and East-European countries. Also offered to selected ESPID members whereas NFID provides fellowships to young American vaccinologists.

CONFERENCE

POSITIONS OPEN

FACULTY POSITION IN ENVIRONMENTAL / ANALYTICAL CHEMISTRY
University of Alaska, Fairbanks

The University of Alaska, Fairbanks, Department of Chemistry and Biochemistry invites applications for a tenure-track position at the **ASSISTANT** or **ASSOCIATE PROFESSOR** level in the area of environmental/analytical chemistry. Teaching duties include undergraduate and graduate courses in environmental / analytical chemistry, and advanced courses in the candidate's field of expertise. The candidate is expected to establish an externally funded research program in an area related to environmental chemistry. The candidate is expected to mentor graduate and undergraduate students in research projects. A Ph.D. in chemistry or related discipline is required, postdoctoral experience is highly preferred. For information about the Department of Chemistry and Biochemistry at the University of Alaska, Fairbanks, please visit **website: http://www.uaf.edu/chem/.** To apply, fill in an online application that includes a cover letter with the names of three references, curriculum vitae, statement of proposed research, and a statement of teaching philosophy. This online application may be found at **website: http://www.uakjobs.com/applicants/Central?quickFind=56149.** In addition to the online application, please arrange to have at least three letters of reference and graduate transcripts sent to: **William R. Simpson, Environmental / Analytical Search Committee Chair, Department of Chemistry, University of Alaska, Fairbanks, P.O. Box 756160 Fairbanks, AK 99775-6160.** Review of applications begins on October 23, 2006. *The University of Alaska is an Equal Opportunity/Affirmative Action Employer and Educational Institution. Minorities and women are encouraged to apply.*

Faculty positions in (1) evolutionary and functional genomics and (2) microbiology. The Department of Biology at Clark University, Worcester, Massachusetts **(website: http://www.clarku.edu/departments/biology/)**, invites applications for two tenure-track appointments at the rank of **ASSISTANT PROFESSOR,** to begin fall 2007. Successful candidates will have research space in the newly constructed Lasry Center for Biosciences and will be expected to develop externally funded research programs involving Ph.D. and undergraduate students. Postdoctoral experience and evidence of success in obtaining extramural funding are desired. Promise of teaching excellence at undergraduate and graduate levels is expected. Evolutionary and functional genomics: The candidate will conduct research in comparative genomics and contribute to the evolutionary and molecular biology components of our curriculum. Microbiology: The candidate will conduct research in any area of microbiology, will teach microbiology, and contribute to the pre-health curriculum. Applicants should submit curriculum vitae, a summary of research interests, a statement of teaching interests, and three key publications, and should arrange to have three letters of reference submitted electronically to the: **Search Committee for Evolutionary and Functional Genomics (e-mail: genomics@clarku.edu)** or **Microbiology (e-mail: micro@clarku.edu).** Follow up hardcopy is not required. Letters can also be mailed to the **Chair** of the appropriate **Search Committee, Clark University, 950 Main Street, Worcester, MA 01610-1477.** E-mail enquiries may be directed to **e-mail: sfoster@clarku.edu.** Review of applications begins October 15, 2006. *Affirmative Action/Equal Opportunity Employer. Minorities and women are especially encouraged to apply.*

POSTDOCTORAL POSITION available to study toll-like receptor and other receptors-mediated cell signaling in *Plasmodium falciparum* GPI/antigens-induced cytokine responses using gene knockout macrophages, and dendritic and T cells, and regulation of innate immune responses. Experience in immunological techniques is required. Send curriculum vitae to: **Dr. D.C. Gowda, Biochemistry and Molecular Biology, Penn State College of Medicine, Hershey, PA 17033** at **e-mail: gowda@psu.edu.** *Penn State is committed to Affirmative Action, Equal Opportunity and to the diversity of its work force.*

POSITIONS OPEN

THE UNIVERSITY OF CHICAGO

The Department of Neurobiology, Pharmacology, and Physiology seeks to recruit new faculty in the tenure track. Appointments can be made at any level in the broad area of neurobiology. Interested persons should send their application to: **S. Murray Sherman, Chairman, Department of Neurobiology, Pharmacology and Physiology, The University of Chicago, 947 East 58th Street, Chicago, IL 60637.** Applications can also be sent via e-mail with attachments to **e-mail: npp@bsd.uchicago.edu.** The application should include a cover letter, curriculum vitae, a statement of research objectives, and the names and contact information of three academic references. Applicants are also responsible for arranging to have the reference letters sent. Applications will be accepted until the positions are filled. Application review will begin November 1, 2006. *The University of Chicago is an Equal Opportunity/Affirmative Action Employer.*

ASSISTANT PROFESSOR
Molecular Biology
Illinois State University, Normal

A tenure-track faculty position in molecular biology is available in the Department of Biological Sciences **(website: http://www.bio.ilstu.edu).** The faculty member will be part of an interdisciplinary Biochemistry and Molecular Biology (BMB) program offered between Biological Sciences and Chemistry. Interest in at least one of the following areas is desirable: virology, developmental biology, or cell biology. Investigators pursuing questions pertaining to nucleic acid structure and function are especially encouraged to apply. The successful candidate is expected to develop a competitive, extramurally funded research program involving B.S., M.S., and Ph.D. students. Ph.D. and postdoctoral experience required. To assure full consideration, send cover letter, curriculum vitae, three recommendation letters, and a brief statement of research goals to: **Dr. Craig Gatto, Biochemistry and Molecular Biology Search Committee, Campus Box 4120, Illinois State University, Normal, IL 61790-4120.** Review of applications will begin on October 15, 2006. Preferred start date of August 16, 2007. *Illinois State University is an Equal Opportunity University encouraging diversity.*

Early-stage biotech company in Burlingame, California, is looking to hire a **RESEARCH ASSOCIATE II** or **III** with experience in intravital microscopy of the microcirculation of animals. Candidate must make at least a two-year commitment. Candidate must have a bachelor's degree and two to four years of experience with intravital microscopy and general computer skills. Further training will be provided by company and expert consultant at nearby university. Animal handling, animal surgery, and biochemical assay skills are desireable. Send resumes or curricula vitae to **e-mail: nmatsui@trfpharma.com.**

University of Idaho, College of Natural Resources, seeks a **LIMNOLOGIST** for an academic-year, tenure-track **ASSISTANT PROFESSOR** position to begin fall 2007. Candidates must have Ph.D. in limnology, must demonstrate research productivity through refereed publications and grants, and must demonstrate a commitment to teaching excellence. Teaching will include an undergraduate course in limnology and two graduate courses. Expected to develop a strong, externally funded research program. For details visit **website: http://www.cnrhome.uidaho.edu/fishwild.** Apply at **website: http://www.hr.uidaho.edu.** Review of applications will begin October 31, 2006. *Affirmative Action/Equal Opportunity Employer.*

POSITIONS OPEN

POSTDOCTORAL FELLOW or **RESEARCH ASSISTANT PROFESSOR** in neuroscience (multiphoton imaging of the brain) is now available at the Medical University of South Carolina (MUSC). The successful candidate will work in the laboratory of **Dr. Prakash Kara** using two-photon calcium imaging and multi-electrode recording techniques in vivo to examine how (i) neural connections and functional maps from eye to brain are refined during the critical periods of postnatal development, and (ii) the functional micro-architecture of disparity tuning in the visual cortex. The Kara laboratory is outfitted with a state-of-the-art two-photon imaging system, designed specifically for functional imaging in the intact brain of any mammalian species. Prior research experience and expertise in sensory systems neuroscience, fluorescence microscopy and electrophysiological recording in vivo, optics, quantitative analysis of neural signals, and programming in Matlab, ImageJ, or IDL is required. Please e-mail curriculum vitae, a brief statement of research interests, and names of three references (preferably by e-mail) to: **Dr. Prakash Kara, Department of Neurosciences, Room 403 BSB, 173 Ashley Avenue, Charleston, SC 29425; e-mail: kara@musc.edu; website: http://neurosciences.musc.edu/faculty/full_time/kara.html.** *MUSC is an Affirmative Action/Equal Opportunity Employer.*

POSTDOCTORAL POSITION
Developmental and Stem Cell Biology
Mount Sinai School of Medicine, New York

Two NIH-funded Postdoctoral positions are available to study regulation of hematopoietic and vascular development using genetically manipulated mice and embryonic stem (ES) cell lines (see *Development* **128**(10)**:**1717, 2001; *Blood* **107**(8)**:**3122, 2006; *Development Dynamics* **235**(9)**:** 2549, 2006; **Fraser et al.,** *Blood*, in press, published online June 2006). Strong background in molecular and cell biology required. Preference will be given to applicants seeking first postdoctoral position. Please e-mail/fax curriculum vitae, names of three references to: **Margaret H. Baron, M.D., Ph.D., fax: 212-849-2442. E-mail: margaret.baron@mssm.edu**. *Equal Opportunity Employer.*

MARKETPLACE